

INTERNATIONAL CONFERENCE ON
METALLURGICAL COATINGS & THIN FILMS

39th ICMCTF

April 23–27, 2012

Town & Country Resort Hotel and Convention Center
San Diego, California, USA

Program
Technical Sessions
Abstracts
Exhibition

Sponsored by:

Advanced Surface Engineering Division of AVS



WELCOME TO ICMCTF 2012!

On behalf of the Advanced Surface Engineering Division of the AVS and the 2012 Organizing Committee, I am pleased to welcome you to the 39th annual International Conference on Metallurgical Coatings and Thin Films, ICMCTF 2012. Since its inception in 1974, the ICMCTF has grown into a premier meeting in its field. This year's program continues the strong tradition of promoting a global exchange of the latest information among scientists, technologists, and manufacturers involved in the science and engineering of metallurgical coatings and thin films.

The ICMCTF 2012 comprises a full week of exciting activities along with a strong technical program consisting of seven (7) technical symposia, four (4) topical symposia, and a large Thursday evening poster session, technical sessions are presented through Friday noon. The conference opens Monday morning at 8:00 am with a **Plenary Lecture by Prof. Peter Fratzl from the Max Planck Institute, Potsdam, Germany. His talk is entitled "How Interfaces Control the Mechanical Behavior of Biological Materials."** We continue to cover the broad field of thin films and coatings including those used for optical, biomedical, energy storage, and tribological applications. We revise our technical program year after year to reflect the latest trends in the field. This year's Topical Symposia on Graphene and 2D Nanostructures; Energetic Materials and Microstructures for Nanomanufacturing are some of the prime examples of our concerted efforts to expand into new and emerging fields where surface engineering and coating technologies can play a major role. An outstanding technical program for 2012 has been organized by the Program Chair, Paul Mayrhofer, as well as the program committees' Symposium and Session Chairs.

The Advanced Surface Engineering Division of AVS recognizes individual scientists and engineers for outstanding research or technological innovation through the R. F. Bunshah Award and ICMCTF Lecture. This year's recipient, **Prof. Sture Hogmark of Uppsala University, Sweden, is being recognized for his pioneering work in surface engineering for friction and wear control; his honorary lecture is entitled: "Tribological Coatings: Novel Concepts and Conditions For Successful Application".** The Bunshah Award and the Graduate Student Awards convocation will take place on Wednesday at 5:45 pm. Please join us for the Awards Buffet Reception beside the Tiki Pavilion following the Awards Convocation. Please note that nominations for 2013 are already being accepted by the awards committee.

The Exhibition is open on Tuesday and Wednesday. The vendor exhibits not only offer an opportunity to obtain information about the latest products and services available, it also provides a unique networking opportunity for the exchange of ideas on equipment, materials, and services. Last year, we inaugurated an Industrial Keynote Lecture series as part of the opening ceremonies of our exhibit program. This year's **Industrial Keynote Lecturer is Prof. Roger De Gryse from Ghent University, Belgium. His talk is entitled "Rotatable Magnetrons, Today and Tomorrow" and is being presented on Tuesday at 9:40 am.**

The papers submitted to ICMCTF are processed through the "Elsevier Editorial System," thus guaranteeing a very high level of review and refereeing for ICMCTF 2012 Proceedings with the same rigorous quality as regular issues of **"Thin Solid Films"** and **"Surface and Coatings Technology"**. During the week, the five Proceedings Editors will work with the publishers, authors, and reviewers to continue the task of ensuring your submitted manuscripts are peer-reviewed and ready for publication. Your help in providing timely reviews to the Editors is essential. Please contact the Proceedings Editors to provide help with a review; the editors are always in need of qualified reviewers.

A dedicated team of volunteers has devoted a significant amount of their time and effort over the past year to make this meeting a success and I would like to thank everyone involved with creating, running, and evolving this conference. I wish to particularly acknowledge the Program Chair, Paul Mayrhofer, who has worked tirelessly to assemble this year's technical program with the Program Committee. I would also like to thank Phyllis Greene, the Conference Manager, and Melani Muratore, the Conference Secretary, for their dedication and personal commitment to making this conference a success. I also acknowledge Jeanette DeGennaro for her successful efforts as the Exhibits Manager. ICMCTF acknowledges the generous support of the many outstanding companies who sponsor our conference. Their support is very much appreciated, and we encourage more companies to join these fine enterprises in lending support for this premier meeting in our field.

Planning for ICMCTF 2013 is already underway. The organizing committee solicits your suggestions regarding how we may continue to improve our conference in the future. Please offer your suggestions to next year's General Chair, Paul Mayrhofer, and Program Chair, Yip-Wah Chung, during the week. Plan to attend the Thursday ICMCTF 2013 Planning Meeting at 12:00–1:15 pm in the Pacific Salon 1 and 2. It has been a pleasure serving you as the General Chair and working with such an outstanding team of people. Have an enjoyable and productive week at ICMCTF 2012.

Ali Erdemir
ICMCTF 2012, General Chair

**ICMCTF issues special thanks and acknowledgment to the following persons
for their contributed research images used to create the ICMCTF 2012 banner:**

Denis Music, RWTH, Aachen, Germany
Andre Anders, Lawrence Berkeley National Laboratory, USA

Manfred Schloegl, Montanuniversitaet Leoben, Austria
Reza Yazdi, Linköping University, Sweden

TABLE OF CONTENTS

Welcoming Remarks	Inside Front Cover
Conference Overview and Schedule of Events.....	ii–iii
Executive Organizing Committee	iv
Symposium and Session Chairs	v–vii
Plenary Session	viii
Exhibitor Keynote Lecture	ix
Focused Topic Sessions	x–xiii
ASED/ICMCTF Awards Invitation	xiv
R.F. Bunshah Award and Lecture	xv–xvi
ICMCTF Graduate Student Award Finalists	xvii
Sponsors	xviii–xxiv
Short Courses and Announcements	xxv
Room Matrix and Planning Grid.....	xxvi–xxvii
Daily Technical Session Schedule	TS-1–TS-42
Exhibitors	E-1–E-28
Abstracts (Arranged by Day)	1–135
Author Index	136–144
Awards, Nominations and Protocols.....	146–149
Diagrams of Conference Facility	152–153
Call for Award Nominations	154
2013 ICMCTF information	Inside back Cover

ASED EXECUTIVE COMMITTEE

Jochen Schneider, Chair 2012, RWTH Aachen University, Germany

Ali Erdemir, Past Chair, Argonne National Laboratory, USA

Christian Mitterer, Chair Elect, Montanuniversitaet Leoben, Austria

Andrey Voevodin, Treasurer, Air Force Research Laboratory, USA

Yip Wah Chung, Secretary, Northwestern University, USA

Joe Greene, University of Illinois, USA

Andre Anders, Lawrence Livermore National Laboratory, USA

Jolanta Klemberg-Sapieha, Ecole Polytechnique de Montreal, Canada

Christopher Muratore, Air Force Research Laboratory, USA

Michael Stueber, Forschungszentrum Karlsruhe, Germany

Steve J. Bull, Newcastle University, UK

Claus Rebholz, University of Cyprus, Cyprus

Jeffrey Lince, The Aerospace Corporation USA



Ali Erdemir
General Chair

Argonne National Laboratory, USA



Paul Mayrhofer
Program Chair

Montanuniversitaet Leoben, Austria



Yip Wah Chung

Program Chair 2013

Northwestern University, USA

THIS BOOK BELONGS TO:

ICMCTF 2012 CONFERENCE OVERVIEW

Registration: (Golden Foyer)	Sunday, April 22 4:30 pm – 6:30 pm Monday, April 23 7:30 am – 3:30 pm Tuesday, April 24 7:30 am – 3:30 pm Wednesday, April 25 7:30 am – 3:30 pm Thursday, April 26 7:30 am – 3:30 pm Friday, April 27 7:30 am – 10:30 am
Plenary Session:	Monday, April 23, 8:00 am – 9:45 am in the Golden Ballroom room. The Plenary Lecturer, Prof. Peter Fratzl , Director of the Max Planck Institute of Colloids and Interfaces, Potsdam (DE), his Plenary presentation is entitled: <i>“How Interfaces Control the Mechanical Behavior of Biological Materials.”</i>
Technical Sessions:	All technical sessions are held at the Town and Country Hotel. Consult the Room Matrix for a session's time of day (AM or PM) and room assignment. View the maps in this program book to see the room locations. The poster session for all symposia is held in the Golden Ballroom Thursday afternoon, 5:00 – 7:00 pm.
Exhibitor Keynote:	Tuesday, April 24, 9:40 am in the Golden Ballroom. Prof. Roger de Gryse , Emeritus of Ghent University (BE) is presenting a keynote lecture entitled <i>“Rotatable Magnetrons, Today and Tomorrow.”</i>
Exhibition:	The Exhibition is Tuesday, April 24, 11:00 am – 7:00 pm, and Wednesday, April 25 10:00 am – 2:00 pm. Tuesday's reception begins at 5:30 pm in the Exhibit Hall, (T&C). Complimentary light luncheon refreshments will be served in the Exhibit Hall (T&C): Tuesday and Wednesday 12:15 pm.
Awards & Reception:	The ASED/ICMCTF Awards Convocation: lecture by the R.F. Bunshah Award Recipient, Dr. Sture Hogland , entitled: <i>“Tribological Coatings: Novel Concepts and Conditions for Successful Application,”</i> Golden Ballroom, 5:45 pm. Awards Buffet Reception follows at 7:30 pm poolside near the Tiki Pavilion.
Conference Proceedings:	The Proceedings for ICMCTF 2012 will be posted electronically on the Journals' websites: <i>Surface and Coatings Technology</i> (Symposiums A, B, E, G, and TS 1 & 3) or <i>Thin Solid Films</i> (Symposiums C, D, F, and TS 2 & 4). All attendees will receive an email notice when the Proceedings are posted and complimentary open access is available.
Editorial Office:	The Editorial Office is the Terrace Salon Three Room. Monday-Thursday: 8:30 am – 5:00 pm and Friday: 8:30 am – 12:00 pm.
Focused Topic Sessions:	1) CSM Instruments: FTS, Monday, April 23, 12:15 pm – 1:15 pm, Pacific Salon 1-2 2) VAMAS TWA 22, Monday, April 23, 5:30 – 6:30 pm, Royal Palm 1-3 3) Bruker-Nano Inc.: FTS, Wednesday, April 25, 4:30 – 5:30 pm, Pacific Salon 1-2 4) Elsevier, FTS, Thursday, April 26, 12:15 – 1:15 pm, Royal Palm 1-3 5) Oerlikon Leybold Vacuum, April 26, 4:10 – 5:10 pm, Pacific Salon 1-2 6) Elsevier Workshop, Friday, April 27, 8:30 am – 1:00 pm, Towne
Audio-Visual Room:	The Audio-visual Prescreening Room is the Dover Room, near the Tiki Pavilion. Sunday: 3:30 – 6:30 pm, and Monday – Thursday: 8:00 am – 5:30 pm.
Cyber Cafe & Wi-Fi:	The ICMCTF Cyber Café sponsored by ELSEVIER is available to all ICMCTF attendees & Exhibitors. The Wi-Fi broad band signal can be found in the Golden Foyer, most meeting rooms, the Exhibition Hall, and the adjacent Lion Fountain Patio. The complimentary Wi-Fi service is LIMITED to 200 ICMCTF users at a time, Sunday – Friday: noon.

5 Short Courses Sunday – Thursday: On-site registration is available at the ICMCTF Registration Counters
Please see Melani or Phyllis. For more course details and descriptions see the website: <http://www2avs.org/conferences/icmctf>

Sunday: Andre Anders, LBNL, “Ionized PVD: From Arcs to HIPIMS”
Monday: Joe Greene, University of Illinois, “Thin Film Nucleation, Growth, and Microstructural Evolution”
Tuesday: Steve Bull, Newcastle University, “Nanomechanical Assessment of Thin Films and Coatings”
Wednesday: Ivan Petrov, University of Illinois, “Advanced thin Film Characterization”
Thursday: Joe Greene, University of Illinois, “Reactive Sputter Deposition: Mechanisms and Operation”

2012 ICMCTF SCHEDULE OF EVENTS

DAY	TIME	EVENT	LOCATION
SUNDAY	4:30 pm – 6:30 pm	Conference Registration	Golden Foyer
	8:30 am – 5:00 pm	Short Course	Towne in Meeting House
MONDAY	7:30 am – 3:30 pm	Conference Registration	Golden Foyer
	8:00 am – 9:45 am	Plenary Session	Golden Ballroom
	8:30 am – 5:00 pm	Short Course	Towne in Meeting House
	10:00 am – 5:30 pm	Technical Sessions	Various Rooms – See Matrix
	12:15 pm – 1:15 pm	CSM Instruments: Focused Topic Session	Pacific Salon 1-2
	5:30 pm – 6:30 pm	VAMAS - TWA 22	Royal Palm 1-3
	6:00 pm – 7:30 pm	Welcome Mixer	Golden Foyer & Lion Patio
TUESDAY	7:30 am – 3:30 pm	Conference Registration	Golden Foyer
	8:00 am – 5:30 pm	Technical Sessions	Various Rooms – See Matrix
	8:30 am – 5:00 pm	Short Course	Towne in Meeting House
	9:40 am – 10:40 am	Exhibitor Keynote Lecture	Golden Ballroom
	11:00 am – 7:00 pm	Exhibition Hall Open	T&C - Exhibit Hall
	12:15 pm	Light Luncheon Refreshments	T&C - Exhibit Hall
	5:30 pm – 7:00 pm	Exhibits Reception	T&C - Exhibit Hall
WEDNESDAY	7:30 am – 3:30 pm	Conference Registration	Golden Foyer
	8:00 am – 5:30 pm	Technical Sessions	Various Rooms – See Matrix
	8:30 am – 5:00 pm	Short Course	Towne in Meeting House
	9:30 am – 10:00 am	Breakfast Forum: Exhibitors Only	T&C - Exhibit Hall
	10:00 am – 2:00 pm	Exhibition Hall Open	T&C - Exhibit Hall
	12:15 pm	Light Luncheon Refreshments	T&C - Exhibit Hall
	4:30 pm – 5:30 pm	Bruker Nano: Focused Topic Session	Pacific Salon 1-2
	5:45 pm – 7:15 pm	Awards Convocation	Golden Ballroom
THURSDAY	7:30 pm – 10:00 pm	Awards Buffet Reception	Poolside near Tiki Pavilion
	7:30 am – 3:30 pm	Conference Registration	Golden Foyer
	8:00 am – 5:30 pm	Technical Sessions	Various Rooms – See Matrix
	8:30 am – 5:00 pm	Short Course	Towne in Meeting House
	12:00 pm – 1:15 pm	2013 ICMCTF Planning Meeting	Pacific Salon 1-2
	12:15 pm – 1:15 pm	Elsevier: Focused Topic Session	Royal Palm 1-3
	4:10 pm – 5:10 pm	Oerlikon Leybold Vacuum: Foc. Top. Sess.	Pacific Salon 1-2
	5:00 pm – 7:00 pm	Poster Session	Golden Ballroom
	6:00 pm – 7:00 pm	Poster Reception	Golden Ballroom
FRIDAY	7:30 pm – 10:00 pm	2012 Conference Committee Dinner	Meet at the Restaurant
	7:30 am – 10:30 am	Conference Registration	Golden Foyer
	8:00 am – 12:00 pm	Technical Sessions	Various Rooms – See Matrix
	8:30 am – 1:00 pm	Elsevier Reviewer/Referee Workshop	Towne in Meeting House
	12:30 pm – 1:30 pm	Thank You & See You in 2013 Party	Trellis Courtyard, near pool

1. The ICMCTF Editorial Office is located in the Terrace Salon Three Room: Monday – Thursday 8:30 am – 5:00 pm, and Friday 8:30 am – 12:00 pm (noon). Authors will be notified of the editorial decision concerning their paper/s via email. Referees should return their reports, via the EES electronic system, to the Editorial Office as soon as possible. During the conference week, Symposium and Session Chairs, please stop at the Editorial Office to inquire as to the status of the papers presented in your sessions; offer assistance to the Editors with the refereeing process.
2. The Audio-Visual Prescreening and Presenter's Preparation Room is located in the Dover Room. Hours: Sunday, 3:30 pm – 6:30 pm and Monday – Thursday, 8:00 am – 5:30 pm.
3. This year the Cyber Café sponsored by ELSEVIER is located in the Golden Foyer. The Cyber Café is available to all ICMCTF Attendees and Exhibitors at no charge Sunday – Friday, noon.
4. Bring your laptops: Wi-Fi is accessible throughout the conference week at no charge to all ICMCTF participants. The broad band is available in the Golden Foyer, most meeting rooms, the Exhibition Hall, and the Lion Fountain Patio.
5. Short Courses are available Sunday – Thursday. For On-site Registration, please see Melani or Phyllis

Sunday: Andre Anders, LBNL, "Ionized PVD: From Arcs to HIPIMS"

Monday: Joe Greene, University of Illinois, "Thin Film Nucleation, Growth, and Microstructural Evolution"

Tuesday: Steve Bull, Newcastle University, "Nanomechanical Assessment of Thin Films and Coatings"

Wednesday: Ivan Petrov, University of Illinois, "Advanced Thin Film Characterization"

Thursday: Joe Greene, University of Illinois, "Reactive Sputter Deposition: Mechanisms and Operation"

ICMCTF 2012

2012 Executive Organizing Committee

GENERAL CHAIR

Ali Erdemir
Argonne National Laboratory
Building 212, Room D-222
9700 South Cass Avenue
Argonne, IL 60439
USA
630-252-6571, Fax: 630-252-5568
erdemir@anl.gov

PROGRAM CHAIR

Paul Mayrhofer
Montanuniversitaet Leoben
Dept. of Physical Metallurgy & Materials Testing
Franz Josef Strasse 18
Leoben 8700, Austria
+43-384-2402-4211, Fax: +43-384-2402-4202
paul.mayrhofer@unileoben.ac.at

PROCEEDINGS EDITORS

Gregory Abadias
University of Poitiers
Lab de Physique des Matl, CNRS
SP2MI, Teleport 2
Bd Marie et Pierre Curie
86962 Chasseneuil-Futuroscope, France
+33-5-4949-6748, Fax: +33-5-4949-6692
Gregory.abadias@univ-poitiers.fr

Michael Stüber
Forschungszentrum Karlsruhe
Hermann-von-Helmoltz-Platz 1
Eggenstein-Leo, D-76344, Germany
+49-727-608-23889, Fax: +49-721-608-24567
Michael.stueber@kit.edu

Samir Aouadi
Department of Physics
Southern Illinois University Carbondale
Neckers 483A
Carbondale, IL 62901-4401, USA
Tel: (618) 453-3659
saouadi@physics.siu.edu

Stan Veprek
Dept of Chemistry
Technical University Munich
Lichtenbergstrasse 4
D-85747 Garching, Germany
Tel.: +49 (89) 289 13624
Fax: +49 (89) 289 13626
stan.veprek@lrz.tu-muenchen.de

Claus Rebholtz
University of Cyprus
Mechanical & Manufacturing Engineering
75 Kallipoleos
Nicosia 1678, Cyprus
+357-22-892-282, Fax: +357-22-892-254
claus@ucy.ac.cy

EXHIBITS MANAGER

Jeannette DeGennaro
AVS
125 Maiden Lane, 15th Floor
New York, NY 10038, USA
212-248-0200 ext 229, Fax: 212-248-0245
cell: 201-961-248-5268
jeannette@avs.org

TREASURER

Andrey Voevodin
Air Force Research Laboratory
2941 Hobson Way Room 106
WPAFB, OH 45433, USA
937-255-4651, Fax: 877-350-9964
a.voevodin@woh.rr.com

PAST CHAIR

Steve J. Bull
Newcastle University
Merz Court
Newcastle Upon Tyne NE1 7RU
United Kingdom
+44-191-222-7913, Fax: +44-191-222-5292
s.j.bull@ncl.ac.uk

CONFERENCE MANAGER

Phyllis Greene
3090 S. Bridle Drive; Rafter J
Jackson, WY 83001-9124, USA
307-734-8009
pgreene@mrl.uiuc.edu

CONFERENCE SECRETARY

Melanie Muratore
2516 Hilton Drive
Dayton, OH 45409, USA
937-901-2497
icmctf@icmctf.org

ICMCTF 2012

Symposium and Session Chairs

SYMPOSIUM A Coatings for Use at High Temperature

Don Lipkin
GE Research, USA
lipkin@ge.com

Ann Bolcavage
Rolls-Royce Corporation, USA
ann.bolcavage@rolls-royce.com

A1. Coatings to Resist High Temperature Oxidation, Corrosion and Fouling

Lars-Gunnar Johansson
Chalmers University of Technology, Sweden
lg@chalmers.se

Dmitry Naumenko
Forschungszentrum Juelich, Germany
d.naumenko@fz-juelich.de

Francisco J Perez Trujillo
Universidad Complutense, Spain
fjperez@quim.ucm.es

Brian Hazel
Pratt & Whitney, USA
brian.hazel@pw.utc.com

A2. Thermal and Environmental Barrier Coatings

Richard Wellman
Cranfield University, UK
r.wellman@cranfield.ac.uk

David Litton
Pratt & Whitney, USA
david.litton@pw.utc.com

Rodney Trice
Purdue University, USA
rtrice@purdue.edu

A3/F8. Coatings for Fuel Cells & Batteries

Eileen Yu
Newcastle University, UK
eileen.yu@ncl.ac.uk

Gayatri V. Dadheech
General Motors, USA
gayatri.dadheech@gm.com

SYMPOSIUM B Hard Coatings and Vapor Deposition Technology

Andre Anders
Lawrence Berkeley National Laboratory, USA
aanders@lbl.gov

Yip-Wah Chung
Northwestern University, USA
ywchung@northwestern.edu

Claus Rebholz
University of Cyprus, Cyprus
claus@ucy.ac.cy

B1. PVD Coatings and Technologies

Per Eklund
Linköping University, Sweden
perek@ifm.liu.se

Joerg Vetter
Sulzer Metaplas GmbH, Germany
joerg.vetter@sulzer.com

Jia-Hong Huang
National Tsing Hua University, Taiwan
jhhuang@mx.nthu.edu.tw

B2. CVD Coatings and Technologies

Sakari Rupp
Walter AG, Germany
sakari.ruppi@walter-tools.com

Francis Maury
CIRIMAT, France
francis.maury@ensiacet.fr

B3. Ion-Surface Interactions in Film Growth and Post-Growth Processes

Kostas Sarakinos
Linköping University, Sweden
kostas@ifm.liu.se

Steven B. Fairchild
Air Force Research Laboratory, USA
steven.fairchild@wpafb.af.mil

B4. Properties and Characterization of Hard Coatings and Surfaces

Jianliang Lin
Colorado School of Mines, USA
jlin@mines.edu

Bo Zhao
Exxon Mobil, USA
bozhao2009@u.northwestern.edu

Christopher P. Mulligan
US Army ARDEC, Benet Laboratories, USA
c.mulligan@us.army.mil

B5. Hard and Multifunctional Nano-Structured Coatings

Joerg Paulitsch
Montanuniversitaet Leoben, Austria
joerg.paulitsch@unileoben.ac.at

Rosendo Sanjines
Ecole Polytechnique Federale de Lausanne
EPFL, Switzerland
rosendo.sanjines@epfl.ch

Petr Zeman
University of West Bohemia, Czech Republic
zemanp@kfy.zcu.cz

B6. Coating Design and Architectures

Christian Mitterer
Montanuniversitaet Leoben, Austria
christian.mitterer@unileoben.ac.at

Michael Stueber
Karlsruhe Institute of Technology, Germany
michael.stueber@kit.edu

B7. Computational Design and Experimental Development of Functional Thin Films

Bjoern Alling
Linköping University, Sweden
bjoal@ifm.liu.se

David Holec
Montanuniversitaet Leoben, Austria
david.holec@unileoben.ac.at

Aram Amassian
KAUST, Saudi Arabia
aram.amassian@kaust.edu.sa

Panos Patsalas
University of Ioannina, Greece
ppats@cc.uoi.gr

SYMPOSIUM C Fundamentals and Technology of Multifunctional Thin Films: Towards Optoelectronic Device Applications

Marco Cremona
Pontificia Universidade Catolica do Rio de Janeiro, Brazil
cremona@fis.puc-rio.br

Tetsuya Yamamoto
Kochi University of Technology, Japan
yamamoto.tetsuya@kochi-tech.ac.jp

C1. Recent Advances in Optical Thin Films

Kumar Khajurivala
Janos Technology, Inc., USA
kumar@janostech.com

Rob Sczupak
Reynard Corporation, USA
rsczupak@reynardcorp.com

C2/F4. Thin Films for Photovoltaics and Active Devices: Synthesis and Characterization

Tomoaki Terasako
Ehime University, Japan
terasako.tomoaki.mz@ehime-u.ac.jp

Marco Cremona
Pontificia Universidade Catolica do Rio de Janeiro, Brazil
cremona@fis.puc-rio.br

C3. Optical Characterization of Thin Films, Surfaces and Devices

Eva Schubert
University of Nebraska-Lincoln, USA
evaschub@engr.unl.edu

Joerg Krueger
BAM Berlin, Germany
joerg.krueger@bam.de

C4. Transparent Conductive Films: Inorganic Oxides, Organic Materials, Metals

Peter Kelly
Manchester Metropolitan University, UK
peter.kelly@mmu.ac.uk

Sunnie Lim
Lawrence Berkeley National Laboratory, USA
sunnielim@lbl.gov

C5/F7. Polarisation Phenomena in Thin Films and Devices

Shelly Moram
University of Cambridge, UK
mam65@cam.ac.uk

David Holec
Montanuniversitaet Leoben, Austria
david.holec@unileoben.ac.at

SYMPOSIUM D Coatings for Biomedical and Healthcare Applications

Roland Hauert
EMPA, Switzerland
roland.hauert@empa.ch

Jeffrey Piascik
RTI International, RTP, NC, USA
jpiascik@rti.org

D1. Bioactive and Biocompatible Coatings and Surface Functionalization of Biomaterials

Sandra E. Rodil Posada
Institute de Investigaciones en Materials, UNAM, Mexico
ser42@iim.unam.mx

Dmitry V. Shtansky
National University of Science and Technology Moscow, Russia
shtansky@shs.misis.ru

D2. Coatings for Biomedical Implants

Roland Hauert
EMPA, Switzerland
roland.hauert@empa.ch

Jeffrey Piascik
RTI International, RTP, NC, USA
jpiascik@rti.org

D3. Coatings for Mitigating Bio-corrosion, Tribo-corrosion and Bio-fouling

Margaret Stack
Univeristy of Strathclyde, UK
Margaret.stack@strath.ac.uk

Mathew Mathew
Rush University, USA
mathew_t_mathew@rush.edu

SYMPOSIUM E Tribology & Mechanical Behavior of Coatings and Engineered Surfaces

Nigel Jennett
National Physical Laboratory, UK
nigel.jennett@npl.co.uk

Thomas W. Scharf
University of North Texas, USA
thomas.Scharf@unt.edu

E1. Friction, Wear, Lubrication Effects & Modeling

Juan-Carlos Sánchez Lopez
CSIC-University Sevilla, Spain
jcslopez@icmse.csic.es

Samir Aouadi
Southern Illinois University, Carbondale, USA
saouadi@physics.siu.edu

Vincent Fridrici
Ecole Centrale de Lyon, France
vincent.fridrici@ec-lyon.fr

Osman L. Eryilmaz
Argonne National Laboratory, USA
eryilmaz@anl.gov

E2. Mechanical Properties and Adhesion

Richard Chromik
McGill University, Canada
richard.chromik@mcgill.ca

David F. Bahr
Washington State University, USA
dbahr@wsu.edu

Ming-Tzer Lin
National Chung Hsing University, Taiwan
mingtlin@dragon.nchu.edu.tw

William Clegg
University of Cambridge, UK
wjc1000@cam.ac.uk

E3/G2. Development, Characterization, and Tribology of Coatings for Automotive and Aerospace Applications

Helmut Rudigier
OC Oerlikon Balzers AG, Liechtenstein
helmut.rudigier@oerlikon.com

Satish Dixit
Plasma Technologies Inc. CA, USA
sdixit@ptise.com

Ryan Evans
Timken Company, USA
ryan.evans@timken.com

E4/G4. Coatings for Machining Advanced Materials and for Use in Advanced Manufacturing Methods

Mirjam Arndt
OC Oerlikon Balzers AG, Liechtenstein
mirjam.arndt@oerlikon.com

Xueyuan Nie
University of Windsor, Canada
xnie@uwindsor.ca

SYMPOSIUM F New Horizons in Coatings and Thin Films

Ulf Helmersson
Linköping University, Sweden
ulfhe@ifm.liu.se

Jeff Zabinski
Air Force Research Laboratory, USA
jeffrey.zabinski@wpafb.af.mil

Sanjay V. Khare
University of Toledo, USA
khare@physics.utoledo.edu

F1. Nanomaterials, Nanofabrication, and Diagnostics

Suneel Kodambaka
University of California at Los Angeles, USA
kodambaka@ucla.edu

Yolanda Aranda Gonzalvo
Hiden Analytical, UK
gonzalvo@hiden.co.uk

F2. High Power Impulse Magnetron Sputtering

Ralf Bandorf
Fraunhofer IST, Germany
ralf.bandorf@ist.fraunhofer.de

Jolanta Sapieha
Ecole Polytechnique de Montreal, Canada
jolanta-ewa.sapieha@polymtl.ca

Daniel Lundin
Linköping University, Sweden
daniel.lundin@liu.se

F3. New Boron, Boride and Boron Nitride Based Coatings

Hans Hoegberg
Linköping University, Sweden
hanho@ifm.liu.se

Aharon Inspektor
Kennametal Incorporated, USA
aharon.inspektor@kennametal.com

F4/C2. Thin Films for Photovoltaics and Active Devices: Synthesis and Characterization

Tomoaki Terasako
Ehime University, Japan
terasako.tomoaki.mz@ehime-u.ac.jp

Marco Cremona
Pontificia Universidade Catolica do Rio de Janeiro, Brazil
cremona@fis.puc-rio.br

F6. Coatings for Compliant Substrates

Ben Beake
Micromaterials Co., UK
ben@micromaterials.co.uk

Roberto M. Souza
Polytechnic School of the University of Sao Paulo, Brazil
roberto.souza@poli.usp.br

F7/C5. Polarisation Phenomena in Thin Films and Devices

Shelly Moram
University of Cambridge, UK
mam65@cam.ac.uk

David Holec
Montanuniversitaet Leoben, Austria
david.holec@unileoben.ac.at

F8/A3. Coatings for Fuel Cells & Batteries

Eileen Yu
Newcastle University, UK
eileen.yu@ncl.ac.uk

Gayatri V Dadheech
General Motors, USA
gayatri.dadheech@gm.com

SYMPOSIUM G Applications, Manufacturing and Equipment

Daphne Pappas
Army Research Laboratory, USA
daphne.pappas@arl.army.mil

Kenji Yamamoto
Kobe Steel, Japan
yamamoto.kenji1@kobelco.com

G1. Innovations in Surface Coatings and Treatments

Ladislav Bardos
Uppsala University, Sweden
ladislav.bardos@angstrom.uu.se

Rainer Cremer
KCS Europe GmbH, Germany
cremer@kcs-europe.de

G2/E3. Development, Characterization, and Tribology of Coatings for Automotive and Aerospace Applications

Helmut Rudigier
OC Oerlikon Balzers AG, Liechtenstein
helmut.rudigier@oerlikon.com

Satish Dixit
Plasma Technologies Inc. CA, USA
sdixit@ptise.com

Ryan Evans
Timken Company, USA
ryan.evans@timken.com

G3. Atmospheric and Hybrid Plasma Technologies

Roland Gesche
Ferdinand-Braun Institut Berlin, Germany
roland.gesche@fbh-berlin.de

Hana Barankova
Uppsala University, Sweden
hana.barankova@angstrom.uu.se

G4/E4. Coatings for Machining Advanced Materials and for Use in Advanced Manufacturing Methods

Mirjam Arndt
OC Oerlikon Balzers AG, Liechtenstein
mirjam.arndt@oerlikon.com

Xueyuan Nie
University of Windsor, Canada
xn timer@uwindsor.ca

G5. Coatings Pre-treatment, Post-treatment and Duplex Technology

Nazlim Bagcivan
RWTH Aachen, Germany
bagcivan@iot.rwth-aachen.de

Sudhir Brahmandam
Kennametal Inc., USA
sudhir.brahmandam@kennametal.com

G6. Advances in Industrial PVD & CVD Deposition Equipment

Markus Rodmar
Sandvik Tooling, USA
markus.rodmar@sandvik.com

Kirsten Bobzin
RWTH Aachen, Germany
bobzin@iot.rwth-aachen.de

SYMPOSIUM TS1 Surface Engineering for Thermal Transport, Storage and Harvesting

Christopher Muratore
Air Force Research Laboratory, USA
chris.muratore@wpafb.af.mil

Baratunde Cola
Georgia Technical Institute, USA
cola@gatech.edu

SYMPOSIUM TS2 Advanced Characterization of Coatings and Thin Films

Peter Schaaf
TU Ilmenau, Germany
peter.schaaf@tu-ilmenau.de

Finn Giuliani
Imperial College London, UK
f.giuliani@imperial.ac.uk

Sandra Korte
University of Cambridge, UK
sk511@cam.ac.uk

SYMPOSIUM TS3 Energetic Materials and Micro-Structures for Nanomanufacturing

Claus Rebholz
University of Cyprus, Cyprus
claus@ucy.ac.cy

Charalabo C. Doumanidis
National Science Foundation, USA
cdoumani@ucy.ac.cy

Teichi Ando
Northeastern University, USA
tando@coe.neu.edu

SYMPOSIUM TS4 Graphene and 2D Nanostructures

Manish Chhowalla
Rutgers University, USA
manish1@rci.rutgers.edu

Christian Teichert
Montanuniversitaet Leoben, Austria
christian.teichert@unileoben.ac.at

Post Deadline Session

Wolfgang Kalss
OC Oerlikon Balzers AG, Liechtenstein
wolfgang.kalss@oerlikon.com

Sven Ulrich
Karlsruhe Institute of Technology, Germany
sven.ulrich@kit.edu

Plenary Session

Monday, April 23, 2012, 8:00 am
Golden Ballroom

How Interfaces Control the Mechanical Behavior of Biological Materials

Professor Peter Fratzl

Director of the Max Planck Institute of Colloids and Interfaces, Potsdam, Germany



Peter Fratzl is director at the Max Planck Institute of Colloids and Interfaces in Potsdam, Germany, and honorary professor of physics at Humboldt University, Berlin, and at Potsdam University. He received an engineering degree from the Ecole Polytechnique in Paris, France (1980), and a doctorate in Physics from the University of Vienna, Austria (1983). Before moving to Potsdam in 2003, he has been holding professor positions in materials physics at the Universities of Vienna and Leoben in Austria and been director of the Erich Schmid Institute of Materials Science of the Austrian Academy of Sciences.

Peter Fratzl's lab studies the relation between (hierarchical) structure and mechanical behaviour of biological materials, such as mineralized tissues, extracellular matrix, or plant cell walls, as well as bio-inspired composite materials. This is complemented by medically oriented research on osteoporosis and bone regeneration. Peter Fratzl has published more than 350 papers in journals and books, mostly on interdisciplinary materials science topics. He received several international awards for his work including the Max Planck Research Award 2008 from the Humboldt Foundation (together with Robert Langer, MIT) and the Leibniz Award 2010 of the German Science Foundation. In 2010, he was awarded an honorary doctorate from the University of Montpellier, France, and since 2007 he is foreign member of the Austrian Academy of Sciences.

ABSTRACT

Biological materials, such as wood, grasses, protein fibres, bone, sea shells or glass sponges are generally composites of different types of polymers as well as mineral. These materials are able to adapt to the mechanical requirements of the environment by growing and assembling structural components in a hierarchical fashion. This implies the existence of various types of interfaces at all levels of hierarchy. From a mechanical viewpoint, interfaces may be considered as defects but, in many natural materials, interface structures emerged which improve rather than deteriorate the overall mechanical properties of the composite. Bone, for example, consists in about equal amounts of a collagen-rich matrix and calcium-phosphate nano-particles. These components are joined in a complex hierarchy of fibres and lamellar structures to a material with exceptional fracture resistance. Similarly, tendon collagen consists of an assembly of fibrils which partly deform by shearing the interface between them. An example for self-healing properties due to molecular-scale interfaces is the byssus fibre used by mussels to attach to rocks. These fibres combine large deformation with stiffness and abrasion resistance. Finally, plant cell walls generate internal stresses and even complex movements upon changes of environmental humidity. This force generation and actuation capabilities are based on water swelling of hemicellulose-rich interfaces between cellulose microfibrils arranged in complex architectures. Unravelling the structural principles of these unexpected material properties may indicate ways towards new types of composite materials with adaptive capabilities.

Exhibitor Keynote Lecture

Tuesday, April 24, 2012, 9:40 am - 10:40 am
Golden Ballroom

Rotable Magnetrons, Today and Tomorrow

Dr. Roger De Gryse

Ghent University, Belgium



Dr. De Gryse obtained an M.S. in electronic engineering in 1964 from the Ghent University and his Ph.D in Applied Science in 1976 with a study on the influence of surface States on the frequency behaviour of MIS (Metal-Insulator-Semiconductor) structures. In the same year he became a research fellow at the department of Solid State Sciences of the Ghent University. During that period, he was essentially responsible for the development of Ultra High Vacuum systems; first generation quadrupole SIMS, low energy ion scattering (LEIS) equipment, Wien velocity filters and energy selectors such as CMA's and 127° analysers which he used for the study of catalytic systems.

From his LEIS experience grew his interest in the interaction between ion beams and solids which in turn triggered his interest in magnetron sputtering as a technology and as a process for the growth of high quality coatings, especially by using rotatable magnetrons.

In 1991 he became a lecturer at the department of Solid State Sciences and in 1999 full Professor at the same department of the Ghent University. He retired and became Emeritus in 2007 but is still active within the research group DRAFT (Design, Research and Feasibility of Thin Films) headed by Prof. D. Depla.

In 1988 he founded, together with some colleagues one of the first spin off companies at the Ghent University. This company, SINVACO, specialised in the development and production of rotatable magnetrons, cylindrical cathodes, and the design of dedicated vacuum equipment became world wide the largest manufacturer of rotatable magnetrons for the web coating and glass coating industry. In 2000, SINVACO was acquired by a Belgian company, Bekaert N.V. and Dr De Gryse was at the origin of a new Bekaert division called Bekaert Advanced Materials. This division is worldwide still the largest manufacturer of rotatable magnetrons for both the web and glass coating industry. Since then, he has been a member of the board of Bekaert Advanced Materials.

ABSTRACT

The continuously increasing demand for a higher quality of life needs the fabrication of products with improved functionality at ever decreasing prices. Moreover, environmental awareness requires that these products are manufactured with so called “clean technologies.” These demands have led to a rapid technological progress within the thin film industry. Physical Vapor Deposition (PVD) has proven to be able to cope with these requirements and within the PVD family, magnetron sputtering in all its varieties is probably the best known and widespread used deposition technology. This success finds its cause in the thin film quality, the reproducibility, flexibility, and scalability of the sputtering process. The concept of magnetron sputtering has been used under many different forms. Probably the best known implementation of magnetically assisted sputtering is to be found in the “classics” such as in the planar magnetrons, either circular or rectangular. However, magnetically assisted sputtering is also used in many other forms such as inverted magnetrons, cylindrical-post magnetrons, cylindrical hollow cathode magnetrons, facing target magnetrons and rotatable cathode magnetrons. This last variety, the rotatable magnetron, is maybe the least known to the general public but most intensively used in large area coating applications like in web coating and glass coating. In this contribution, we will focus on rotatable magnetrons, their benefits and drawbacks and peculiarities. For example it turns out that in reactive sputtering their behavior is quite different as compared to a rectangular magnetron of similar dimensions. Also, new trends in rotatable magnetron sputtering will be discussed, as well from a technological point of view as from the viewpoint of market demands.

ICMCTF 2012 Focused Topic Sessions

Monday, April 23, 2012, 12:15 – 1:15 pm

Pacific Salon 1-2



Coating Quality Control Solutions

Nicholas Randall, Gregory Favato, and Bo Shou

For more than 30 years, CSM Instruments has been developing dedicated instruments for measuring the mechanical properties of PVD and CVD coatings. The Revetest scratch tester has become the industry standard for measuring the adhesion and scratch resistance of hard coatings. With our extensive experience gained over the years, we have recently developed a new line of instruments which are intended for routine Quality Control (QC) inspection of hard coatings. Such machines are affordable, robust, and simple to operate, therefore allowing even the smallest coating manufacturer to be able to quantify coating mechanical properties to standard methods (ISO, ASTM, JIS, etc.).

CSM Instruments has also worked tirelessly to increase the sensitivity and resolution of our already industry leading instrumentation. This can best be seen by looking at the development of the new Nanoindentation Tester 2 (NHT2) and the Nanotribometer 2 (NTR2). These instruments allow for more accurate measurement of hardness and frictional properties respectively by not only increasing the resolution of measurement but also by becoming a more user-friendly measurement platform.

This tutorial will focus on our most recent innovations in the indentation, scratch, and tribology testing of thin films and coatings. Specific focus will be placed on recent research into the optimization of the progressive load scratch test for investigating the mechanical integrity of hard coatings. Based on nanoindentation measurements obtained from a coating-substrate system, the scratch test can be dimensioned with respect to load range and indenter geometry. The measured data from this scratch test is used to simulate spatial stress profiles and to calculate the von Mises stress characteristics and the maximum tensile stresses in the scratch direction. This can increase sensitivity of the test for specific depth regions in the coating and allow improved analysis of critical interfaces, transition layers and surface-near substrate regions.

FOOD & REFRESHMENTS WILL BE PROVIDED
VISIT BOOTH #203

Monday, April 23, 2012, 5:30 – 6:30 pm

Royal Palm 1-3

VAMAS TWA22 Annual General Meeting **Mechanical Property Measurements of Thin Films and Coatings**

Nigel Jennett¹, Nicholas Randall², Junhee Hahn³

¹National Physical Laboratory, UK

²CSM Instruments Inc., ³Korea Research Institute of Standards and Science

This is an open meeting that will report on the projects undertaken by VAMAS Technical Working Area 22 in
(continued)

2011/12, discuss ideas and priorities for future work, and generate new co-operative action. Current projects include evaluation of the performance of scratch testing and indentation testing and results will be reported that are being fed into International Standards (ISO) for those tests.

All are warmly welcomed, especially those interested in co-operative action to generate data that would support new methods and standards in this field.

VAMAS Technical Working Area 22 addresses pre-standardization needs in the general area of test method development and evaluation for the measurement of the mechanical properties of small volumes of materials, in particular thin films and coatings on substrates. Activities cover nano-mechanical measurement methods to determine the mechanical properties of surfaces, and the films or coatings themselves, as well as larger scale test methods to evaluate the performance of coating/substrate systems as a whole. Membership is open to all and the adopted activities are those that attract sufficient international partners willing to work together for the common goal.

Wednesday, April 25, 2012, 4:30 – 5:30 pm

Pacific Salon 1-2



**Advanced 3-D Nano and Micro Scratch Testing of
Thin Films with In-line Imaging**

Dr. Norm Gitis

STLE Fellow and Chair of STLE Committee on Tribotesting

Vice President of Bruker Nano Inc.

Advanced 3-D scratch-adhesion tests are proposed, based on synchronization of X and Y stages and implementation of 3-D sensors that monitor simultaneously the normal load and lateral forces in all directions, while the software automatically calculates the actual friction coefficient in real time. The scratch depth is continuously monitored with an integrated capacitance sensor. The in-line imaging is performed via optical microscope with a digital camera, producing panoramic photos in the same file with friction, load, and acoustic data. Optionally, it is done with an advanced optical profiler (for micro-scratches) or AFM (for nano-scratches), all fully integrated in the CETR-APEX world-leading testing platform. All the motions of the test specimen between the microscope, profiler, and AFM are done automatically, based on the precision factory calibration of distances.

Examples of impressive test results are presented and discussed for ultra-thin and relatively-thick films of various hard and soft materials.

This session is intended to deepen the audience's knowledge of the thin-film and coatings high-end metrology.

Please visit Bruker Nano Inc. Booth #212 in the Exhibit Hall.



Elsevier Authors Workshop: How to get published

Presented by Jan Willem Wijnen

Elsevier is the world's leading publisher of science and health information and publishes a number of journals that are highly relevant for ICMCTF attendees, such as "Thin Solid Films", "Surface and Coatings Technology" and "Vacuum."

Publisher of these journals, Jan Willem Wijnen, will present a workshop that will provide insight into the publishing process and explain the fundamental components and guidelines that authors should adhere to in preparing manuscripts and submitting them to scientific journals for publication. The workshop will cover each step of the submission, review, and revision processes; attendees will hear the Do's and Don'ts of getting published.

Selected editors will attend and present their perspectives on what they consider to be the basic elements of top quality articles that are published in their respective journals.

The workshop is aimed at new authors, but also at more experienced authors who want to hear how to bypass common publishing hurdles or discuss with the editors.

Please visit the Elsevier Booth #210 in the Exhibition Hall.

Thursday, April 26, 2012, 4:10 – 5:10 pm

Pacific Salon 1-2



Vacuum and Applications for Thin Film Coating Systems

Sang Hyun Park

Oerlikon Leybold Vacuum

There are many different types of material-controlling techniques such as PVD, sputtering, CVD, etch, etc in modern industry. One of the most important things with these techniques is the vacuum that controls the environment for material transfer and changes in isolated systems. The vacuum created by different types of vacuum pumps has been used in these technologies thanks to several advantages over competing techniques where the vacuum is not required to control the environment-such as printing technology. Regardless of whether coating systems will be built by users themselves or purchased from commercial system makers, the proper selection of vacuum and pumps along with application requirements will be the first step of system design.

(continued)

At the focus topic, from the experience of Oerlikon Leybold Vacuum in vacuum technology, components and a wide range of coating systems for more than 162 years, general aspects of vacuum and applications for thin film coatings will be reviewed. Requirements for different coating applications from the process point of view and vacuum roles for various thin film coating systems and applications will be discussed. The advantages and disadvantages of different vacuum techniques will be explained for thin film coatings and systems. Material handling and safety at coating systems will be reviewed with process materials. Some system examples from Oerlikon Leybold Vacuum with vacuum selections will be presented.

For coating system and pump discussions during the ICMCTF Exhibition, visit our Booth #219.

Friday, April 27, 2012, 8:30 am – 1:00 pm

Towne Room



ELSEVIER

Elsevier Referee and Reviewer Workshop

Professor Allan Matthews

Editor of the *Journal Surface & Coatings Technology*

Jan Willem Wijnen

Publisher Elsevier

Writing papers and getting published is an essential part of scientific research and scientific journals are the backbone of science. But besides authors, reviewers play a key role in building scientific knowledge, because they advise journal editors whether or not to publish a paper.

Being a reviewer is not just acting as inspector, it is also helping your colleagues to publish a better paper, by pointing out weaknesses in the manuscript, suggesting additional views, strengthen the argument and spot errors. As a reviewer for a journal you are in a position to help fellow-researchers and play an important role in the advancing science. Moreover, you will learn a lot from reviewing papers and may be the first to hear about important new findings.

Do you want to become a reviewer for journals?

The workshop consists of a presentation about the publishing process and the fundamentals of the review process. During the second part of the workshop a real manuscript will be reviewed and the outcome will be discussed.

The workshop is intended for young scientists who have the ambition to become a regular reviewer for journals. They should have recently obtained their PhD-degree (or be close to graduating with their degree) and have (co-)authored at least three refereed journal papers.

Interested candidates should send their CV, (expected) date of graduation and publication list to Jan Willem Wijnen (j.wijnen@elsevier.com). There will be a maximum number of participants (based on first-come-first-serve) and qualified candidates will be notified immediately after they have applied.

Very limited spaces are available, please contact Jan Willem Wijnen for any additional information and to register.

Please visit the Elsevier Booth #210 in the Exhibition Hall.

Your Personal Invitation
**ASED/ICMCTF Annual Awards
Convocation and Reception**

**You are invited to the ICMCTF Lecture
by Dr. Sture Hogmark
2012 R.F. Bunshah Award Recipient**

**Wednesday, April 25
Golden Ballroom, 5:45 pm.**



**Graduate Student Award
Winners will be announced.**

**Awards Buffet Reception
following the Convocation,
Poolside, 7:30 pm.**

**Come raise a toast to
our ICMCTF Awardees.**



2012 R.F. Bunshah Annual Award & ICMCTF Lecture

Sture Hogmark

Materials Science and Tribology, Ångström Laboratory, Uppsala University, Sweden

This Award is intended to recognize outstanding research or technological innovation in the areas of interest to the Advanced Surface Engineering Division (ASED) of the AVS, with emphasis on the fields of surface engineering, thin films, and related topics.



Sture Hogmark began working on materials science aspects of tribology, which continued to be the focus of his career, as a graduate student in Uppsala University, Sweden, in the early 1970s. With a background in engineering physics, he obtained his PhD in 1976 based on his research into the mechanisms of tool steel wear. In 1980, Hogmark initiated the Tribomaterials Group at the Ångström Laboratory, and in 1998 he was appointed Professor of Materials Science and Tribology at Uppsala University, a chair he occupied until his retirement in 2010. He is presently an Emeritus Professor of Materials Science and Tribology.

Sture widened his research to include many kinds of tools and critical mechanical components. This work was carried out in collaboration with Swedish companies including Uddeholm, Sandvik, Erasteel, Volvo, and Scania. The science of tribology was initially very descriptive, and development of reliable tests and test methodologies was an early priority. Energy savings and materials and environmental conservation are global research targets.

Materials properties are linked to practical performance with the aim to design materials and surfaces that can generate low friction and, hence, exhibit high wear resistance. FIB, SEM, TEM, ESCA, AES, AFM, and nanoindentation are examples of important research tools.

In the late 1970s, Hogmark was one of the first to investigate the use of coatings on cutting tools to reduce wear, and later on forming tools and mechanical components for which the combination of low friction, low wear, and excellent galling resistance are essential. Today, his coatings research includes active “smart” materials that respond mechanically, chemically, or with lubricants during tribological loading to reduce friction and wear.

Among Hogmark’s achievements are the following: developing the relationship between surface properties and sliding friction (1979), deriving a model for hardness measurements in thin films (1984), synthesizing the first nanocrystalline diamond coatings (1996), introducing wear-resistant multilayered coatings (1998), developing an understanding of residual stresses in thin coatings (1999), elucidating the role of lubricant additives for protection of steel/diamond-like carbon film contacts (2003), and explaining the superior tribological behaviour of stellite in heavily-loaded tribological contacts (2009). Hogmark and his PhD students have launched several companies based on the results of their tribological research. These include TiSurf International, Nova Diamant, Applied Nano Surfaces, and Primateria.

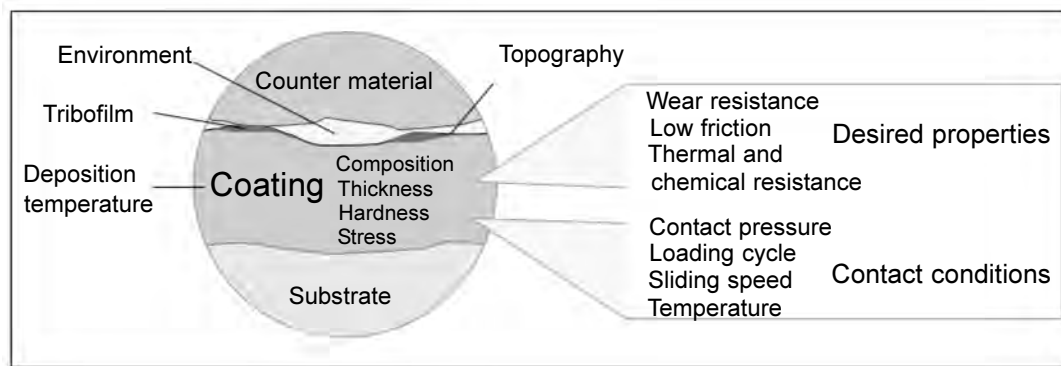
Hogmark has graduated more than 50 PhD students, published 180 papers, and presented more than 200 conference lectures. Currently, he is engaged in research on the surfaces of skis for optimum glide and, together with colleagues, has recently uncovered the “mystery” of the curling of curling stones. Another recent interest is the development of heat- and corrosion-resistant materials and thin film coatings for generation-IV nuclear reactors

Abstract: Tribological Coatings: Novel Concepts and Conditions for Successful Application

The expectations for tribological coatings are very high. On a global scale, they should help preserve the environment by minimizing materials consumption and energy waste, while offering wear protection and low friction. In addition, coated tools and components are expected to function as designed throughout long lifetimes. A large number of excellent coating materials have been developed that have high hardness and wear resistance, and simultaneously exhibit very low friction. However, a good coating material is not sufficient; a number of additional conditions must be fulfilled. This talk has two aims: to guide in the selection and practical use of tribological coatings in order to enjoy their full potential, and to demonstrate some current trends in coating development for low friction applications.

There are a number of parameters, as shown below, that determine whether a coated tool or mechanical component will function successfully during its entire expected lifetime. Depending on the application, the external conditions that the coating experiences will have a stronger or weaker influence.

(continued)



To avoid premature coating failure due to cracking and fragmentation, the hardness of the substrate has to be at least as high as that of the counter surface. If a coating is applied to a substrate material that is softer than the counter surface, it either must be very thick or very ductile.

One has also to ensure that the substrate will withstand the deposition temperature without softening. Unfortunately, this limits the number of candidate substrate materials for many promising coatings. For example, the common ball-bearing steel AISI 52100 softens at temperatures below 200°C. For Al and Mg alloys, the number of potential coatings is even more limited.

Another important issue is adhesion of the coating to the substrate. One of the most important factors to consider for hard and brittle coatings is the presence of internal stresses. Tensile stresses are usually detrimental, but reasonably high compressive stresses are beneficial since they improve coating cohesion and increase its hardness and wear resistance. However, they may deteriorate the adhesion. The combined influence of compressive stresses in the coating and substrate geometry on practical adhesion has been estimated using simple geometrical models. Excessively high compressive stresses in combination with unfavourable geometry may cause spontaneous flaking.

In sliding applications for tools or mechanical components, not only are friction and wear resistance important; it is also necessary to avoid adhesion of the counter material to the coating surface. This phenomenon is often termed galling. Modern development of forming and cutting tools aims at the highest possible galling resistance. An important question arises; is galling related to chemical or topographical properties or both? It is well known that certain materials like austenitic stainless steels or Ti-, Al-, or Ni-alloys are difficult to machine and deform plastically because of their strong tendency to adhere to the tool surface. This also makes them poor materials in sliding components. Thus, special effort is required for the development of surfaces to use against these “difficult” counter materials. Generally, the smoother the surface of a tool or component, the better is its galling resistance.

In on-going *in situ* experiments in the SEM, the galling resistance of finely polished tool steel surfaces are compared with equally finely polished surfaces of DLC coatings by repeatedly sliding against a tip of austenitic stainless steel. For the DLC coatings, the friction coefficient remains ~0.15 for the entire series of 10 consecutive sliding passes, whereas for the tool steels, the coefficient increases from 0.15 during the first pass to ~0.8 after only 4 passes. Intentional scratches in a DLC coating affect friction only during two passes; the coefficient returns to 0.15 at the third pass as the scratches become partially filled and their ridges worn off. In this example, the DLC coatings act to preserve the low initial friction level by avoiding galling while, in addition, inhibiting local scratch damage.

One track in the current development of *active coatings* involves the design of coatings whose wear resistance and/or friction properties improve *during* use. A way of achieving this is to design materials and conditions in which the coating, the surrounding medium, and/or the counter material react chemically or combine mechanically to form tribofilms with the desired properties. The prerequisites for low friction in dry or boundary-lubricated sliding contact combine high hardness with low shear resistance. Well-known materials with these properties are diamond in humid atmosphere or water, MoS₂, WS₂, and ZnO in dry sliding.

Another approach is coatings that change composition during tribological loading. For example, TiC_x-based coatings alloyed with excess amounts of Al or Ni lose graphitic carbon when loaded in tribological contact. In addition, the graphite aligns with crystallographic easy shear planes parallel to the sliding direction.

Finally, there is a trend today to design tribological materials and coatings such that they, together with the surrounding medium and/or the counter material, will form new materials in the form of *tribofilms* that can lower the friction.

ICMCTF 2012 Graduate Student Awards

The Graduate Student Awards were established by the Advanced Surface Engineering Division (ASED) of the AVS in 2006 to honor and encourage outstanding graduate students carrying out research in areas of interest to ASED, with emphasis in the fields of surface engineering, thin films, and related topics. The ASED seeks to recognize students of exceptional ability who show promise for significant future achievement.

The ASED is pleased to announce the three finalists for 2012, chosen based upon the quality of their written research summaries, resumes, and evaluation letters. The selection of the winners will take into consideration the above listed application materials in addition to the quality and professionalism of their oral presentations and discussion at the 2012 ICMCTF.

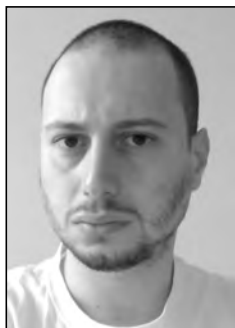


Jessica Krogstad

University of California, Santa Barbara, USA

“New Perspectives on the Phase Stability Challenge
in Zirconia-Based TBCs”

(Paper A2. 18, Tuesday 10:20 am, Room: Sunrise)



Davide G. Sangiovanni

Linköping University, Sweden

“Toughness Enhancement in Transition Metal Nitride Thin
Films by Alloying and Valence Electron Concentration Tuning”

(Paper B7.1-10, Tuesday 11:00 am pm, Room: Royal Palm 1-3)



Moritz To Baben

RWTH Aachen University, Germany

“The Effect of Nitrogen Content on Stability and Elastic Properties
of TiAlN Studied by ab Initio Calculations and Combinatorial
Reactive Magnetron Sputtering”

(Paper B7.2-1, Tuesday 1:50 pm, Room: Royal Palm 1-3)

**** Please plan to attend the ICMCTF Awards Convocation
Wednesday, 5:45 pm in the Golden Ballroom ****

**ICMCTF 2012 extends a very
special thank you to Oerlikon
Balzers for their generous
support of conference activities.**

oerlikon
balzers



**Please attend and enjoy the
Welcome Mixer, 6 pm, Monday,
April 23, Golden Foyer.
Lift your glass in appreciation to
ICMCTF sponsor Oerlikon Balzers.**

**ICMCTF 2012 thanks Plansee
for their generous donation in
providing complimentary drinks
to each attendee at the
Exhibits Reception.**



PLANSEE

Booth 323

**Please visit the Plansee
Composite Materials Booth
323 in the Exhibition Hall to
express your appreciation for
their conference sponsorship
and support.**

**Thank you Elsevier for sponsoring
the Cyber Café.**



Booth 210

**Please visit Elsevier, publisher of the
ICMCTF Proceedings, in the Exhibit
Hall at Booth 210.**

**Attend the Elsevier Author's
Workshop: Thursday 12:15 pm,
Royal Palm 1-3.**

**Inquire to register for the Friday
Referee/Reviewer Workshop
8:30 am - 1:00 pm Towne Room
email: j.wijnen@elsevier.com**

**ICMCTF 2012 thanks AJA
International for their generous
support in providing conference
tote bags to each attendee.**



**Please visit AJA International
at Booth 202 in the Exhibition Hall
to express your appreciation for
their conference sponsorship.**

**ICMCTF 2012 thanks Refining
Systems Inc. for their generous
support of conference and
exhibition activities.**



Booth 101

**Please visit them at Booth 101
in the Exhibition Hall to say
thank you for their conference
donation in support of ICMCTF.**

**We hope you enjoy the
Conference Notebooks provided
by Refining Systems Inc.**

ICMCTF 2012 thanks CemeCon for their generous support of the Conference Program and activities.



Please visit CemeCon at Booth 313 in the Exhibition Hall to express your appreciation for their generosity in support of ICMCTF 2012.

ICMCTF thanks Hauzer Techno Coating for their generous support.



Please visit Hauzer at Booth 320 in the Exhibition Hall to express your appreciation for their conference sponsorship in support of ICMCTF 2012.



PLANSEE

ELSEVIER

oerlikon
balzers



Thanks to our generous ICMCTF 2012 sponsors. Please visit their booths in the Exhibit Hall.



PLASMATERIALS, Inc.



KRATOS
ANALYTICAL
A SHIMADZU GROUP COMPANY



Kurt J. Lesker
Company

Hauzer TECHNO COATING
PVD / PACVD TECHNOLOGY

AMERICAN
ELEMENTS



World's Leading Manufacturer of Engineered and Advanced Material Products

ICMCTF 2012 Short Courses

April 22 – 26, 2012, Sunday – Thursday

Five Short Courses are being presented by leading experts in their respective fields:

Sunday, April 22: **Ionized PVD: From Arcs to HIPIMS**, André Anders, LBNL, Berkeley, CA

Monday, April 23: **Thin Film Nucleation, Growth, and Microstructure Evolution**, Joe Greene, University of Illinois, IL

Tuesday, April 24 **Nanomechanical Assessment of Thin Films and Coatings**, Steve Bull, Newcastle University, UK

Wednesday, April 25: **Advanced Thin Film Characterization**, Ivan Petrov, University of Illinois, IL

Thursday, April 26: **Reactive Sputtering Deposition: Mechanisms and Operation**, Joe Greene, University of Illinois, IL

Courses are one day from 8:30 am – 5:00 pm. Each of the of the four courses cost \$480 per participant and \$125 per graduate student. A \$200 discount is granted if three courses at \$480 are taken. For all courses, extensive course notes will be provided.

Limited On-site registration is available at the conference registration desk. Please see Melani or Phyllis.

View the detailed Short Course descriptions on the web: <http://www2.avs.org/conferences/icmctf/pages/shortcourses.html>

ATTENDEE ROOM

The Devonshire Room in the hotel's Executive Conference Center (the old Meeting House) has been set aside as a "no-host" gathering room during the ICMCTF 2012. The room will provide space for attendees to mingle with exhibitors, family members and companions.

We hope you enjoy the Conference, and take some time to experience the attractions of San Diego.

USE OF VIDEO EQUIPMENT PROHIBITED

The use of video recording equipment, cameras, cell phone cameras, or audio equipment is prohibited at any AVS Symposium, Short Course, or Topical Conference without prior written approval of the Society. The Society reserves the right to reproduce, by any means selected, any or all of these presentations and materials.

REMINDER: Please turn off CELL PHONES and PAGERS when you are attending Technical Sessions.

ICMCTF 2012 Room Matrix- Program at a Glance

Room Day	Golden Foyer	TC/Exhibit Hall	Golden Ballroom	Esquire/ Towne	Pacific Salon 1-2	Pacific Salon 3	Royal Palm Salon 1-3	Royal Palm Salon 4-6	Sunrise	Sunset	Tiki Pavilion
Sunday Afternoon	Registration 4:30 -6:30 pm			Short Course in progress Anders				AVS BoD 8:00 am			
Monday Morning	Registration 7:30am-3:30 pm		Fratzl PLENARY 8:00 -9:45 am		Attend the Plenary Lecture at 8:00am in the Golden Ballroom.						
Monday Morning	Registration continues		Today's technical sessions start at 10:00am	Short Course in progress Greene	E1.1 FTS/CSM Instruments 12:15-1:15pm	C1.1	F6.1	B1.1	TS2.1	D1.1	C2.1/F4.1
Monday Afternoon	Welcome Mixer 6:00 -7:30 pm	Exhibitor Setup noon	Today:Afternoon technical sessions start at 1:30pm	Short Course continues	E3.1/G2.1	C3.1	F1.1 VAMAS 5:30 pm	B1.2	TS2.2	D3.1	C2.2/F4.2
Tuesday Morning	Registration 7:30am-3:30 pm	Exhibitor Setup 8:00-10:00 am	DeGryse Exhibit Keynote 9:40am	Short Course in progress Bull	E1.2	C4.1	B7.1	B1.3	A2.1	F2.1	C2.3/F4.3
Tuesday Afternoon	Registration continues	Exhibits 11:00 am-7:00 pm Opens Today	Today:Afternoon technical sessions start at 1:50pm	Short course continues	E3.2/G2.2		B7.2	B4.1	A2.2	F2.2	G5.1
Wednesday Morning	Registration 7:30 am-3:30 pm	Exhibits 10:00 am -2:00 pm Closes Today		Short Course in progress Petrov	E1.3		B5.1	B4.2	A1.1	TS4.1	G1.1
Wednesday Afternoon	Registration continues	Exhibitor Breakdown 2:00-6:00 pm	Today:Afternoon technical sessions start at 1:50pm	Short Course continues	E4.1/G4.1 FTS Bruker-Nano 4:30-5:30pm		B5.2	B4.3	A1.2	TS1.1	G3.1
Wednesday Evening			Awards Convocation Hogmark 5:45-7:00pm		Attend the Honorary Lecture at 5:45 pm in the Golden Ballroom.						
Thursday Morning	Registration 7:30 am-3:30 pm		Poster Set-up Noon Posting of Materials	Short Course in progress Greene	E4.2/G4.2 2013 Planning MITG 12:00-1:15pm		B6.1 FTS-Elsevier 12:15-1:15pm	B2.1	A1.3 A3.1/F8.1	TS3.1	E2.1
Thursday Afternoon	Registration continues	Today:Afternoon technical sessions start at 1:30pm	Poster Session 5:00-7:00 pm	Short course continues	PD FTS:Orlikon Leybold Vacuum 4:10-5:10 pm		B6.2	B2.2	A3.2/F8.2	C5.1/ F7.1	E2.2
Friday Morning	Registration 7:30 - 10:30 am			Elsevier Reviewer/ Referee Workshop 8:30am-1pm			F3.1	B3.1	G6.1	D2.1	E2.3

Editorial Ofc: Terrace Salon 3; Mo-Th, 8:30am-5:00pm; Fr 8:30am- 12:00pm

AV Pre-Screen: Dover; Su., 3:30-6:30pm; Mo-Th, 8:00am-5:30pm

CyberCafé/Wi-Fi: Golden Foyer-no charge for attendees, Su-Fr noon

Light Refreshments: in the Exhibit Hall/TC; Tu & We, 12:15 pm

Sun - Thurs, Short Courses: in Towne Room 8:30am-5:00pm

Mon: Welcome Mixer: 6:00-7:30pm, Golden Foyer & Patio

Tues: Exhibits Reception: 5:30-7:00pm, TC-Exhibit Hall

Wed: Awards Reception: 7:30pm, Poolside near Tiki Pavilion

Thurs: Poster Reception: 6:00-7:00pm, Golden Ballroom

Fri: Thank you, See You Next Year 2013 Party:

12:30-1:30pm, Trellis Courtyard near pool

ICMCTF 2012 Planning Grid

We provide this form to help you plan your week at the ICMCTF 2012.
Keep in mind that invited presentations are scheduled for 40 minutes, while contributed presentations are scheduled for 20 minutes

Time	Monday		Tuesday		Wednesday,		Thursday		Friday	
	Paper	Room	Paper	Room	Paper	Room	Paper	Room	Paper	Room
8:00										
8:20										
8:40										
9:00										
9:20										
9:40										
10:00										
10:20										
10:40										
11:00										
11:20										
11:40										
12:00										
Lunch										
1:30										
1:50										
2:10										
2:30										
2:50										
3:10										
3:30										
3:50										
4:10										
4:30										
4:50										
5:10										

Suggested room abbreviations:

DO-Dover- Pre-Screening DV-Devonshire GB – Golden Ballroom GF-Golden Foyer PSL-2 – Pacific Salon 1-2 PS3 – Pacific Salon 3
 RPI-Royal Palm Salon 1-3 RP4 – Royal Palm Salon 4-6 SR-Sunrise SS-Sunset TP Tiki Pavilion EX – Exhibit Hall/TC

NOTES

Key to Session/Paper Numbers

- A** Coatings for Use at High Temperature
- B** Hard Coatings and Vapor Deposition Technology
- C** Fundamentals and Technology of Multifunctional Thin Films: Towards Optoelectronic Device Applications
- D** Coatings for Biomedical and Healthcare Applications
- E** Tribology & Mechanical Behavior of Coatings and Engineered Surfaces
- F** New Horizons in Coatings and Thin Films
- G** Applications, Manufacturing, and Equipment
- PD** Post Deadline Discoveries and Innovations
- PL** Plenary Talk
- TS1** Surface Engineering for Thermal Transport, Storage and Harvesting
- TS2** Advanced Characterization of Coatings and Thin Films
- TS3** Energetic Materials and Micro-Structures for Nanomanufacturing
- TS4** Graphene and 2D Nanostructures

Presentation numbers are listed in the program as follows: Symposium letter first, followed by session number, followed by a dash, then a secondary section number for that session, and finally a number for the scheduled presentation. So E2-3-5 would be symposium E, session number 2, section number 3, paper number 5.

Symposium scheduling pointers:

- All morning sessions begin at 8:00 am except for Monday where the sessions begin at 10:00 am following the 8:00 am Plenary Session.
- Afternoon sessions on Monday and Thursday begin at 1:30 pm following the lunch break starting at 12:10 pm. Afternoon sessions on Tuesday and Wednesday begin at 1:50 pm.
- Invited speakers (marked as such in the program) are allotted 40 minutes. Contributed speakers are allotted 20 minutes.

If you are making an oral presentation:

All technical session rooms are equipped with computers, LCD projectors, screens, laser pointers and microphones. Please test presentation materials to be certain that they are compatible with the equipment being provided in the technical session rooms. The room used for the Presenter's Preview will be the Dover. Please allow ample time for the test, preferably the day before the presentation. The Preview Room's hours of operation are Sunday, 3:30-6:30 pm and Monday – Thursday 8:00 am – 5:30 pm.

If you are making a poster presentation:

Boards are available for posting materials at approximately noon on Thursday, April 26. Prior to entering the Golden Ballroom, authors presenting a poster will check in at a table located in the doorway. Please be prepared to show photo identification as well as your registration badge. These forms of identification must match the name of the **presenter of the poster in the ICMCTF program**. A sign listing the paper number, title, and presenting author will aid each presenter in locating the correct board where their poster is to be displayed. The board provided is approximately four feet by four feet. All poster materials **MUST** be posted by 4:50 pm. All presenters are required to be at their presentation during the entire session; this is in order to promote discussion and for the author to answer attendee questions. All poster materials will be discarded if not removed from the boards by 9:00 pm Thursday evening.

Monday Morning, April 23, 2012

Plenary Lecture
8:00-9:45
Golden Ballroom

Hard Coatings and Vapor Deposition Technology
Room: Royal Palm 4-6 - Session B1-1

PVD Coatings and Technologies
Moderators: P. Eklund, Linköping University, Sweden, J.H. Huang, National Tsing Hua University, Taiwan, J. Vetter, Sulzer Metaplas GmbH, Germany

10:00 am	<p>Plenary Lecture Session 8:00 – 9:45</p> <p>Professor Peter Fratzl</p> <p>Director of the Max Planck Institute of Colloids and Interfaces, Potsdam, Germany</p> <p>Abstract:</p> <p>"How Interfaces Control the Mechanical Behavior of Biological Materials"</p> <p>Please see full abstract on the Plenary Session Page</p> <p>Golden Ballroom</p>	<p>B1-1-1 Properties of nanocrystalline Al-Cu-O films reactively sputtered by dc pulse dual magnetron, J. BLAZEK, J. MUSIL, P. STUPKA, R. CERSTVY, J. HOUSKA, University of West Bohemia, Czech Republic</p>
10:20 am		<p>B1-1-2 Reactive cathodic arc-evaporation of corundum structured crystalline (Al,Cr)₂O₃, J. PAULITSCH, Christian Doppler Laboratory for Application Oriented Coating Development at the Department Of Phys. Metal. And Mater. Testing, Montanuniversität, Austria, J. RAMM, M. LECHTHALER, OC Oerlikon Balzers AG, Liechtenstein, P. POLCIK, PLANSEE Composite Materials GmbH, Germany, M. POHLER, Christian Doppler Laboratory for Advanced Hard Coatings at the Dep. Of Phys. Metal. And Mater. Testing, Montanuniversität, Austria, D. HOLEC, P.H. MAYRHOFER, Montanuniversität Leoben, Austria</p>
10:40 am		<p>B1-1-3 Invited Wear mechanism of coated cutting tools and improvement of their cutting performance, T. ISHIKAWA, Hitachi Tool Engineering, Ltd., Japan</p>
11:00 am		<p>Invited talk continued.</p>
11:20 am		<p>B1-1-5 Phase Transformations in Face Centered Cubic (Al,Cr)₂O₃ Thin Films, KHATIBI, J. LU, J. JENSEN, P. EKLUND, L. HULTMAN, Linköping University, Sweden</p>
11:40 am		<p>B1-1-6 Influence of Fe-Impurities in AlCr-Targets on Arc Evaporation Process and Film Properties, M. MÜHLBACHER, R. FRANZ, Montanuniversität Leoben, Austria, M. LECHTHALER, OC Oerlikon Balzers AG, Liechtenstein, P. POLCIK, PLANSEE Composite Materials GmbH, Germany, C. MITTERER, Montanuniversität Leoben, Austria</p>
12:00 pm	<p>CSM Instruments Focused Topic Session: "Coating Quality Control Solutions" 12:15 – 1:15 pm Pacific Salon 1-2</p>	

Monday Morning, April 23, 2012

Fundamentals and Technology of Multifunctional Thin Films: Towards Optoelectronic Device Applications Room: Pacific Salon 3 - Session C1-1 Recent Advances in Optical Thin Films Moderators: K. Khajurivala, Janos Technology Incorporated, US, R. Sczupak, Reynard Corporation, US		Fundamentals and Technology of Multifunctional Thin Films: Towards Optoelectronic Device Applications Room: Tiki Pavilion - Session C2-1/F4-1 Thin Films for Photovoltaics and Active Devices: Synthesis and Characterization Moderators: T. Terasako, Graduate School of Science and Engineering, Ehime University, Japan, M. Cremona, Pontificia Universidade Católica do Rio de Janeiro	
10:00 am	C1-1-1 Invited Manipulation of Photons by Photonic Crystals, S. NODA, T. ASANO, Kyoto University, Japan		C2-1/F4-1-1 The Degradation of Ti_xN_{1-x}/HfO_2 p-channel MOSFETs under Hot Carrier Stress, J.Y. TSAI, National Sun Yat-Sen University, Taiwan
10:20 am	Invited talk continued.		C2-1/F4-1-2 Investigation of Random Telegraph Signal with High-K/Metal Gate MOSFETs, C.E. CHEN, National Chiao Tung University, Taiwan
10:40 am	C1-1-3 Phase transformation, structures and properties of pure and carbon containing titania thin films annealed in air and in hydrogen, W.C. LEE, M. WONG, National Dong Hwa University, Taiwan		C2-1/F4-1-3 Enhancement of Resistive Switching Characteristics in SiO_2 -based RRAM by High Temperature Forming Process, Y.T. CHEN, National Sun Yat-Sen University, Taiwan
11:00 am	C1-1-4 Effect of Laser Power on the Microstructure and Photoluminescence of Silicon-rich Nitride Thin Films by Magnetron Sputtering, C.K. CHUNG, C.H. LI, T.S. CHEN, Y.T. LIN, National Cheng Kung University, Taiwan		C2-1/F4-1-4 The Impact of Strain on Gate-Induced Floating Body Effect for PD SOI p-MOSFETs, W.H. LO, T.C. CHANG, C.H. DAI, NSYSU, Taiwan
11:20 am	C1-1-5 Invited ZnO light-emitting diodes and laser diodes, X.W. SUN, Nanyang Technological University, Singapore		C2-1/F4-1-5 Invited Plasma deposited ZnO layers for thin film photovoltaics: synthesis, characterization and growth mechanism, M. CREATORE, Eindhoven University of Technology, Netherlands
11:40 am	Invited talk continued.		Invited talk continued.
12:00 pm	C1-1-7 The deposition of metal oxide coatings for electro-catalytic and photo-active applications by closed field unbalanced magnetron sputter ion plating, X. ZHANG, K. COOKE, Teer Coatings Limited, Miba Coating Group, UK, G. EITZINGER, High Tech Coatings GmbH, Miba Coating Group, Austria, J. HAMPSHIRE, Z. ZHANG, Teer Coatings Limited, Miba Coating Group, UK	CSM Instruments Focused Topic Session “Coating Quality Control Solutions” 12:15 – 1:15 pm Pacific Salon 1-2	

Monday Morning, April 23, 2012

Coatings for Biomedical and Healthcare Applications Room: Sunset - Session D1-1 Bioactive and Biocompatible Coatings and Surface Functionalization of Biomaterials Moderators: D.V. Shtansky, National University of Science and Technology "MISIS", Russian Federation, S. Rodil Posada, Universidad Nacional Autonoma de Mexico, Mexico		Tribology & Mechanical Behavior of Coatings and Engineered Surfaces Room: Pacific Salon 1-2 - Session E1-1 Friction Wear Lubrication Effects & Modeling Moderators: Lopez, CSIS-University Sevilla, S. Aouadi, Southern Illinois University, US, V. Fridrici, Ecole Centrale de Lyon, O.L. Eryilmaz, Argonne National Laboratory, US	
10:00 am	D1-1-1 The effect of the surface treatment of Ti alloy on the nanomechanical response of bone grown on Ti6Al4V in vitro, J. CHEN, MA. BIRCH, S.J. BULL, S. ROY, Newcastle University, UK	E1-1-1	Assessment of factors influencing the behaviour of MoS ₂ coatings by means of factorial design, J. YANG, V. FRIDRICI, PH. KAPSA, Ecole Centrale de Lyon, France
10:20 am	D1-1-2 A comparative study on bactericidal efficiency of nano structured pure TiO ₂ thin films and Al-TiO ₂ composite thin films, A.B. PANDA, Mesra, INDIA, SK. MAHAPATRA, P.K. BARHAI, I. BANERJEE, Birla Institute of Technology, India	E1-1-2	Application of the friction energy density approach to quantify the fretting wear endurance of DLC hard coatings: influence of temperature and frequency, S. FOUVRY, G. BLONDY, Ecole Centrale de Lyon, France
10:40 am	D1-1-3 Invited Surface Engineering and Modification of Biomaterials, P. CHU, City University of Hong Kong, Hong Kong Special Administrative Region of China	E1-1-3 Invited	Atomic-Scale Friction of Surfaces and Coatings, A. MARTINI, University of California, Merced, US
11:00 am	Invited talk continued.		Invited talk continued.
11:20 am	D1-1-6 Surface modification of zirconia nanofiber coatings for biomedical applications, J. PIASCIC, B. STONER, RTI International, US, D. SURMAN, Kratos Analytical Inc., UK, A. CHAROENPANICH, E. LOBOA, North Carolina State University, US	E1-1-5	Imaging Dynamic of Polishing Technology for Digital Surfacing Of Ophthalmic Plastics, S. MEZGHANI, M. EL MANSORI, Arts et Métiers ParisTech, France
11:40 am	D1-1-7 Immobilization of pamidronates on the nanotube surface of titanium discs and their interaction with bone cells, Z.C. XING, T.H. KOO, Kyungpook National University, Republic of Korea, S. MOON, Y. JEONG, Korea Institute of Materials Science, Republic of Korea, I.K. KANG, Kyungpook National University, Republic of Korea	E1-1-6	A study on friction coefficient and wear coefficient of coated systems submitted to micro-scale abrasion tests, R. COZZA, Centro Universitário da FEI – Fundação Educacional Inaciana "Padre Sabóia de Medeiros", Brazil
12:00 pm	CSM Instruments Focused Topic Session: "Coating Quality Control Solutions" 12:15 – 1:15 pm Pacific Salon 1-2		

Monday Morning, April 23, 2012

<p>New Horizons in Coatings and Thin Films Room: Royal Palm 1-3 - Session F6-1</p> <p>Coatings for Compliant Substrates Moderators: B. Beake, Micro Materials Ltd, UK, R.M. Souza, Mechanical Engineering Department, Universidade de São Paulo</p>		<p>Advanced Characterization of Coatings and Thin Films Room: Sunrise - Session TS2-1</p> <p>Advanced Characterization of Coatings and Thin Films Moderators: P. Schaaf, TU Ilmenau, Germany, F. Giuliani, Imperial College London - South Kensington Campus, UK, S. Korte, University of Erlangen-Nürnberg, Germany</p>	
10:00 am	<p>F6-1-1 Invited Deformation and Delamination in Polymer Metal Thin Film Structures, N.R. MOODY, E.D. REEDY, E. CORONA, D. ADAMS, Sandia National Laboratories, US, M. KENNEDY, Clemson University, US, M. CORDILL, Montanuniversität Leoben, Austria, J. YEAGER, Los Alamos National Laboratory, US, D. BAHAR, Washington State University, US</p>	<p>TS2-1-1 Invited 3D Microstructure Analysis of Thin Films and Coatings in the Micro, Nano and Atomic Scale, F. MÜCKLICH, Saarland University and Materials Engineering Center, Germany</p>	
10:20 am	Invited talk continued.	Invited talk continued.	
10:40 am	<p>F6-1-3 Extracting mechanical properties of coatings on compliant substrates using nanoindentation, S.J. BULL, Newcastle University, UK</p>	<p>TS2-1-3 Atom probe tomography of self-organized nanostructuring in Zr-Al-N thin films, L. JOHNSON, N. GHAFOR, Linköping University, Sweden, M. THUVANDER, K. STILLER, Chalmers University of Technology, Sweden, M. ODÉN, L. HULTMAN, Linköping University, Sweden</p>	
11:00 am	<p>F6-1-4 Organic ultrathin film adhesion on compliant substrate using scratch test technique, X. BODDAERT, Ecole Nationale Supérieure des Mines de Saint Etienne, France, G. COVAREL, Laboratoire de Physique et Mécanique Textiles, Université de Haute Alsace, France, B. BENSARD, M. MATTEI, P. BENABEN, J. BOIS, Ecole Nationale Supérieure des Mines de Saint Etienne, France</p>	<p>TS2-1-4 3D FIB/SEM imaging and 3D EBSD analysis of compressed MgO micropillars, M. RITTER, Hamburg University of Technology, Germany, S. KORTE, W.J. CLEGG, P.A. MIDGLEY, University of Cambridge, UK</p>	
11:20 am	<p>F6-1-5 Flexibility and electrical stability of ITO-coated polyethylene terephthalate (PET) and polyethylene naphthalate (PEN) under monotonic and cyclic bending, G. POTOCZNY, S. ABELL, University of Birmingham, UK, K. SIERROS, D. CAIRNS, West Virginia University, US, S. KUKUREKA, University of Birmingham, UK</p>	<p>TS2-1-5 Recent Advances in XPS for the Characterization of Thin Films, D. SURMAN, Kratos Analytical Inc., UK, C. BLOMFIELD, A. ROBERTS, S. HUTTON, S. PAGE, Kratos Analytical Ltd., UK</p>	
11:40 am	<p>F6-1-6 Compliant metallic electrodes for Electroactive Polymer Actuators, F. HABRARD, G. KOVACS, J. PATSCHEIDER, Empa, Switzerland</p>		
12:00 pm	<p align="center">CSM Instruments Focused Topic Session: “Coating Quality Control Solutions” 12:15 – 1:15 pm Pacific Salon 1-2</p>		

Monday Afternoon, April 23, 2012

Hard Coatings and Vapor Deposition Technology Room: Royal Palm 4-6 Session B1-2/PVD Coatings and Technologies Moderators: P. Eklund, Linköping University, Sweden, J.H. Huang, National Tsing Hua University, Taiwan, J. Vetter, Sulzer Metaplas GmbH, Germany		Fundamentals and Technology of Multifunctional Thin Films: Towards Optoelectronic Device Applications Room: Tiki Pavilion Session C2-2/F4-2 Thin Films for Photovoltaics and Active Devices: Synthesis and Characterization Moderators: T. Terasako, Graduate School of Science and Engineering, Ehime University, Japan, M. Cremona, Pontificia Universidade Católica do Rio de Janeiro	
1:30 pm	B1-2-1 Effect of vacuum arc plasma state on the property of nitride coatings deposited by conventional and new arc cathode., S. TANIFUJI , K. YAMAMOTO, H. FUJII, Y. KUROKAWA, Kobe Steel Ltd., Japan	C2-2/F4-2-1	Reactive Deposition of Aluminum-doped Zinc Oxide films using Asymmetric Linked Dual Rotatable Magnetron, M. AUDRONIS , V. BELLIDO-GONZALEZ, Genco Ltd, UK
1:50 pm	B1-2-2 Industrial-scale sputter deposition of Cr _{1-x} Al _x N coatings with various compositions from segmented Cr and Al targets, T. WEIRATHER , C. SABITZER, S. GRASSER, Montanuniversität Leoben, Austria, C. CZETTL, Ceratizit Austria GmbH, Austria, P. POLCIK, PLANSEE Composite Materials GmbH, Germany, M. KATHREIN, Ceratizit Austria GmbH, Austria, C. MITTERER, Montanuniversität Leoben, Austria	C2-2/F4-2-2	Influence of the Kind and Content of Doped Impurities on Impurity-Doped ZnO Transparent Electrode Applications in Thin-Film Solar Cells, J. NOMOTO, T. HIRANO, T. MIYATA, T. MINAMI, Kanazawa Institute of Technology, Japan
2:10 pm	B1-2-3 Invited Preparation of Superhard Tetrahedral Amorphous Carbon, Nano-crystalline Diamond and Cubic Boron Nitride Films with Low Internal Stress by Means of Excimer Laser Ablation and Annealing, S. WEISSMANTEL , G. REISSE, K. GUENTHER, R. BERTRAM, H. GRUETTNER, M. NIEHER, University of Applied Sciences Mittweida, Germany, D. ROST, Roth & Rau MicroSystems GmbH, Germany	C2-2/F4-2-3	Comparative physical properties of Ga-, In-, Zr- and Sn-doped ZnO semiconductor thin films fabricated via sol-gel method, C.Y. TSAY , W.C. LEE, S.S. LO, C.J. CHANG, C.K. LIN, Feng Chia University, Taiwan
2:30 pm	Invited talk continued.	C2-2/F4-2-4	Temperature Dependence of Electrical Properties of Ga-Doped ZnO Films Deposited by Ion-Plating with DC Arc Discharge, T. TERASAKO , Graduate School of Science and Engineering, Ehime University, Japan, H.-P. SONG, H. MAKINO, Kochi University of Technology, Japan, S. SHIRAKATA, Graduate School of Science and Engineering, Ehime University, Japan, T. YAMAMOTO, Kochi University of Technology, Japan
2:50 pm	B1-2-5 Ion-assisted epitaxial sputter-deposition and properties of metastable Zr _{1-x} Al _x N(001) (0.05 < x < 0.25) alloys, A. MEI , B.M. HOWE, University of Illinois at Urbana-Champaign, US, N. GHAFOR, M. ODEN, H. FAGER, E. BROITMAN, Linköping University, Sweden, M. SARDELA, University of Illinois at Urbana-Champaign, US, L. HULTMAN, Linköping University, Sweden, A. ROCKETT, J.E. GREENE, I. PETROV, University of Illinois at Urbana-Champaign, US	C2-2/F4-2-6	Doped Cadmium Oxide as a High Performance Transparent Conductive Oxide, R. MENDELSBERG, K.M. YU, Y. ZHU, D. SPEAKS, S. LIM, Lawrence Berkeley National Laboratory, US, S. ZHAO, University of California, Berkeley, US, J. REICHERTZ, S. MAO, W. WALUKIEWICZ, A. ANDERS, Lawrence Berkeley National Laboratory, US
3:10 pm	B1-2-6 The influence of deposited surface structures on mechanical properties, M.C. FUCHS , N. SCHWARZER, Saxonian Institute of Surface Mechanics, Germany	C2-2/F4-2-7 Invited	Current Status and Future Prospects of the CIGS PV Technology, S. NIKI , S. ISHIZUKA, H. KOMAKI, S. FURUE, K. MATSUBARA, H. SHIBATA, A. YAMADA, Research Center for Photovoltaic Technologies, AIST, Japan, N. TERADA, Kagoshima University, Japan, T. SAKURAI, K. AKIMOTO, Tsukuba University, Japan
3:30 pm	B1-2-7 High Rate Magnetron Sputtering of Chromium Coatings for Tribological Applications, K. NYGREN , Uppsala University, Angstrom Laboratory, Sweden, M. SAMUELSSON, Linköping University, Sweden, Å. KASSMAN-RUDOLPHI, Uppsala University, Angstrom Laboratory, Sweden, U. HELMERSSON, Linköping University, Sweden, U. JANSOON, Uppsala University, Angstrom Laboratory, Sweden	Invited talk continued.	
3:50 pm	B1-2-8 Behavior of DLC Coated Low-Alloy Steel under Tribo-Corrosion: Effect of Top Layer and Interlayer Variation, K. BOBZIN, N. BAGCIVAN, S. THEISS, R. WEIB , Surface Engineering Institute - RWTH Aachen University, Germany, U. DEPNER, T. TROBMAN, J. ELLERMEIER, M. OECHSNER, Institute for Materials Technology - TU Darmstadt, Germany	C2-2/F4-2-9	Reactive magnetron sputtering of precursors for CZTS solar cells, T. KUBART , T. ERICSON, J.J. SCRAGG, C. PLATZER-BJÖRKMAN, The Angstrom Laboratory, Uppsala University, Sweden
4:10 pm	B1-2-9 Integration of the Larco®-technology for ta-C-coatings in an industrial hard material batch system, M. HOLZHERR , M. FALZ, T. SCHMIDT, VTD Vakuumtechnik Dresden GmbH, Germany, H.-J. SCHEIBE, M. LEONHARDT, C.-F. MEYER, Fraunhofer-Institut für Werkstoff- und Strahltechnik, IWS, Germany	C2-2/F4-2-10	Investigation of resistive switching characteristic and mechanism on InGaO _x film, J.B. YANG , National Sun Yat-Sen University, Taiwan
4:30 pm	B1-2-10 Invited Ion-assisted PVD growth of carbon-transition metal nanocomposite thin films, G. ABRASONIS , Helmholtz-Zentrum Dresden-Rossendorf, Germany	C2-2/F4-2-11	Influence of forming process on resistance switching characteristics of In ₂ O ₃ /SiO ₂ bi-layer, J.J. HUANG , National Sun Yat-Sen University, Taiwan
4:50 pm	Invited talk continued.	C2-2/F4-2-12	Investigating the multiple high resistance states after ac and dc reset methods for resistance switching memory application, H.C. TSENG , National Sun Yat-Sen University, Taiwan
5:10 pm	B1-2-12 The effect of hydrogen addition on the residual stress of cubic boron nitride film prepared by R.F. magnetron sputtering of B ₄ C target, J.K. PARK , J.-S. KO, W.-S. LEE, Y.J. BAIK, Korea Institute of Science and Technology, Republic of Korea	Welcome Mixer 6:00 – 7:30 pm Golden Foyer and the Lion Fountain Patio Sponsored by Oerlikon Balzers	

Monday Afternoon, April 23, 2012

Fundamentals and Technology of Multifunctional Thin Films: Towards Optoelectronic Device Applications Room: Pacific Salon 3 - Session C3-1 Optical Characterization of Thin Films, Surfaces and Devices Moderators: J. Krueger, BAM Berlin, Germany, E. Schubert, University of Nebraska-Lincoln, US		Coatings for Biomedical and Healthcare Applications Room: Sunset - Session D3-1 Coatings for Mitigating Bio-Corrosion, Tribo-Corrosion and Bio-Fouling Moderators: Stack, University of Strathclyde, UK, M.T. Mathew, Rush University Medical Center, US	
1:30 pm	C3-1-1 Invited Terahertz Ellipsometry Materials Characterization, T. HOFMANN, University of Nebraska-Lincoln, US	D3-1-1 Invited	Significance of Tribocorrosion and Bio-Tribocorrosion in the Oral Environment: The Case of Dental Implants, L.A. ROCHA, Universidade do Minho, Departamento de Engenharia Mecânica, Campus de Azurém, Portugal
1:50 pm	Invited talk continued.	Invited talk continued.	
2:10 pm	C3-1-3 Modeling the optical properties of 2D colloidal crystals, S. PORTAL-MARCO, E. CABRERA, University of Barcelona, Spain, J. FERRE-BORRULL, Rovira i Virgili University, Spain, O. ARTEAGA, New York University, E. PASCUAL, E. BERTRAN, University of Barcelona, Spain	D3-1-3	Surface modification using PVD to apply silver-copper-mixed layers, G. GOTZMANN, C. WETZEL, Fraunhofer Institut für Elektronenstrahl- und Plasmatechnik, Medizinische Applikationen, Germany, L. ACHENBACH, N. ÖZKUCUR, R.H. FUNK, Medizinische Fakultät, Institut für Anatomie, TU Dresden, Germany, C. WERNER, Leibniz-Institut für Polymerforschung Dresden e.V., Research Division Biofunctional Polymer Materials, Germany
2:30 pm	C3-1-4 Confocal 2D Photoluminescence Mapping of Porous Silicon, A. ABUSOGLU, T. KARACALI, H. EFEGLU, Ataturk University, Turkey	D3-1-4	Studies on Corrosion and Tribocorrosion Behaviour of Electrodeposited CoW-WC Nanocomposites, S.K. GHOSH, BARC, India, J.P. CELIS, KUL, Belgium
2:50 pm	C3-1-5 Structure, electronic properties and electron energy loss spectra of transition metal nitride films, L. KOUTSOKERAS, M. MATENOGLU, P. PATSALAS, University of Ioannina, Greece	D3-1-5	An Electrochemical Investigation of TMJ Implant Metal Alloys in a Synovial Fluid-Like Environment: The influence of pH variation, D. ROYHMAN, University of Illinois at Chicago, College of Dentistry, US, R. RADHAKRISHNAN, M.T. MATHEW, M. WIMMER, Rush University Medical Center, US, C. SUKOTJO, University of Illinois at Chicago, College of Dentistry, US
3:10 pm	C3-1-6 Fabrication and characterization of a $V_2O_5/V/V_2O_5$ multilayer thin films for uncooled microbolometers, D. KAUR, V. GOYAL, Indian Institute of Technology Roorkee, India	D3-1-7 Invited	Fretting corrosion with proteins: the role of organic coating about the synergistic mechanisms, J. GERINGER, J. PELLIER, B. FOREST, ENSM-SE, France, D. MACDONALD, CEST-PSU, US
3:30 pm	C3-1-7 Gaschromic Properties of IrO_2 Thin Films Grown by Pulsed Laser Deposition Technique, C.H. HSU, C.C. CHANG, Institute of Physics, Academia Sinica, Nankang, Taiwan, M.H. WEN, Institute of Physics, Academia Sinica, Nankang, Taiwan, Y.R. WU, Y.T. HSIEH, W.H. CHAO, Institute of Physics, Academia Sinica, Nankang, Taiwan, C.K. LIN, Feng Chia University, Taipei, Taiwan, M.J. WANG, M.K. WU, Institute of Physics, Academia Sinica, Nankang, Taiwan	Invited talk continued.	
3:50 pm	C3-1-8 Formation of nanoscale pyramids on polycrystalline silicon by self-mask etching to improve the solar cell efficiency, H.H. LIN, W.H. CHEN, F.C.N. HONG, C.J. WANG, National Cheng Kung University, Taiwan	D3-1-10	Optimisation of Pulsed Bipolar Plasma Electrolytic Oxidation of Magnesium Alloy for Biological Applications, Y. GAO, A. YEROKHIN, A. MATTHEWS, University of Sheffield, UK
4:10 pm	C3-1-9 Production and Characterization of Copper Indium Disulfide Thin Film, Y.R. WU, C.C. CHANG, M.H. WEN, C.H. HSU, Y.T. HSIEH, W.H. CHAO, J.Y. LUO, M.K. WU, Institute of Physics, Academia Sinica, Nankang, Taiwan, H.S. KOO, Ming-Hsin University of Science and Technology, Taiwan	D3-1-11	Micro-textured CoCrMo Alloy for MoM joints: An Electrochemical Investigation, C. NAGELLI, M.T. MATHEW, Rush University Medical Center, US, RP. POURZAL, F. LIEDTKE, A. FISCHER, University of Duisburg-Essen, Germany, M. WIMMER, Rush University Medical Center, US
4:30 pm	C3-1-10 Invited Studying matter with laser driven x-ray sources, J. SPIELMANN, Institute of Optics and Quantumelectronics, Friedrich Schiller University Jena, Germany	<div style="text-align: center;"> <h2>Welcome Mixer</h2> <p>6:00 – 7:30 pm</p> <p>Golden Foyer and the Lion Fountain Patio</p> <p>Sponsored by</p> <h2>Oerlikon Balzers</h2> </div>	
4:50 pm	Invited talk continued.		
5:10 pm	C3-1-12 Synthesizes of Mesoporous Tantalum Oxide Films by Sol-Gel Process for the Applications in All-Solid-State Electrochromic Devices, Z.Z. TSAI, C.L. WU, C.K. WANG, Department of Materials Science and Engineering, National Cheng Kung University, Taiwan, S.C. WANG, Department of Mechanical Engineering, Southern Taiwan University, Taiwan, J.L. HUANG, Department of Materials Science and Engineering, National Cheng Kung University, Taiwan		
5:30 pm	C3-1-13 Fabrication and characterization of $ZnO/NiTi/ZnO$ multilayers for optoelectronic applications, D. KAUR, N. CHOUDHARY, Indian Institute of Technology Roorkee, India	VAMAS TWA 22 Annual General Meeting Mechanical Property Measurements of Thin Films and Coatings Royal Palm 1-3 5:30 – 6:30 pm	

Monday Afternoon, April 23, 2012

Tribology & Mechanical Behavior of Coatings and Engineered Surfaces Room: Pacific Salon 1-2 - Session E3-1/G2-1 Development, Characterization, and Tribology of Coatings for Automotive and Aerospace Applications Moderators: R. Evans, Timken Company, S. Dixit, Plasma Technology Inc., US, H. Rudigier, OC Oerlikon Balzers AG, Liechtenstein		New Horizons in Coatings and Thin Films Room: Royal Palm 1-3 - Session F1-1 Nanomaterials, Nanofabrication, and Diagnostics Moderators: Y. Gonzalvo, Hiden Analytical Ltd., S. Kodambaka, University of California, Los Angeles, US	
1:30 pm	E3-1/G2-1-1 The effective Indenter concept, its uses in measurement analysis and its extension into the time domain, N. SCHWARZER, N. BIERWISCH, SIO, Germany	F1-1-1 Invited Diagnostics in Low Pressure Plasmas and Characterisation of Films Properties in HIPIMS Technology, A.P. EHIASARIAN, Sheffield Hallam University, UK Invited talk continued.	
1:50 pm	E3-1/G2-1-2 Effect of BIAS and hydrogen on arc activated high ionization N ₂ -Ar plasma nitrided maraging steel grade 300, E. ALMANDOZ, J. FERNANDEZ, J.A. GARCIA, G.G. FUENTES, R.J. RODRIGUEZ, Asociacion de la Industria Navarra, Spain		
2:10 pm	E3-1/G2-1-3 Invited Requirements for Broad Acceptance of DLC Coatings for Tribological Applications in the Commercial Aerospace Market, L. PINGREE, The Boeing Company, US	F1-1-3 Design of new coating materials for neutron detector applications, the example TM _{1-x} Gd _x N, B. ALLING, Linköping University, Sweden, C. HÖGLUND, R. HALL-WILTON, ESS, Sweden, L. HULTMAN, Linköping University, Sweden	
2:30 pm	Invited talk continued.	F1-1-4 Hierarchical ZnO Nanorod array Films with Enhanced Photocatalytic Performance, C.J. CHANG, M.H. HSU, C.Y. TSAY, C.K. LIN, Feng Chia University, Taiwan	
2:50 pm	E3-1/G2-1-5 Influence of HVOF spraying parameters on the wear resistance of Al-SiC composites coatings deposited on ZE41 magnesium alloy, A. LOPEZ, J. RAMS, B. TORRES, P. RODRIGO, M. CAMPO, Rey Juan Carlos University, Spain	F1-1-5 ZnO Nanostructures Synthesized by CO ₂ Supercritical Fluid at Low-Temperature Treatment, K.C. CHANG, T.M. TSAI, T.C. CHANG, Y.E. SYU, H.C. HUANG, D.S. GAN, T.F. YOUNG, National Sun Yat-Sen University, Taiwan	
3:10 pm	E3-1/G2-1-6 Influence of deposition process parameters on durability and residual stresses in highly oriented MoS ₂ films, B. VIERNEUSEL, S. TREMMEL, S. WARTZACK, Friedrich-Alexander-University Erlangen-Nuremberg, Germany	F1-1-6 One-step hybrid pulse anodization for nanoporous anodic aluminum oxide synthesis of aluminum thin films sputtered on Si(100) substrate, C.K. CHUNG, M.W. LIAO, O.K. KHOR, H.C. CHANG, National Cheng Kung University, Taiwan	
3:30 pm	E3-1/G2-1-8 Numerical analysis of the influence of film thickness and properties on the stress state of thin film-coated piston rings under contact loads., L.G.D.B.S. LIMA, L.C.S. NUNES, Universidade Federal Fluminense, Brazil, R.M. SOUZA, N.K. FUKUMASU, Universidade de São Paulo, Brazil, A. FERRARESE, Mahle Metal Leve S/A, Brazil	F1-1-7 Nanostructured mesoporous surfaces produced by phase separation in Al-Si thin films, P. MARTIN, A. BENDAVID, K-H. MULLER, L. RANDENIYA, CSIRO Materials Science and Engineering, Australia	
3:50 pm	E3-1/G2-1-9 Numerical analysis of wear and failure zones of coated piston skirt and piston rings under scuffing conditions, N.K. FUKUMASU, University of São Paulo, Brazil, L.G.D.B.S. LIMA, Universidade Federal Fluminense, Brazil, A. FERRARESE, Mahle Metal Leve S/A, Brazil, R.M. SOUZA, University of São Paulo, Brazil	F1-1-9 Invited Structural and Electronic Properties of Epitaxial Silicene, Y. YAMADA-TAKAMURA, JAIST, Japan	
4:10 pm	E3-1/G2-1-10 Effect of chromium on the wear mechanisms of self-adaptive WSC-Cr sputtered coatings, T. POLCAR, University of Southampton, UK, F. GUSTAVSSON, Uppsala University, Angstrom Laboratory, Sweden, M. DANEK, Czech Technical University in Prague, Czech Republic, A. CAVALEIRO, University of Coimbra, Portugal	Invited talk continued.	
4:30 pm	E3-1/G2-1-11 Performance impact of honing dynamics on surface finish of precoated cylinder bores, M. EL MANSORI, Arts et Métiers ParisTech, France, B. GOELDEL, L. SABRI, Renault sas, France	F1-1-11 Carbon-Nanotube-Templated Metallic Microstructures for MEMS: Preparation and Characterization, R. HANSEN, Brigham Young University, US, R. BADGER, Utah Valley University, US, D. MCKENNA, B. JENSEN, R. VANFLEET, R. DAVIS, D. ALLRED, Brigham Young University, US	
4:50 pm	E3-1/G2-1-12 Macroscopic simulation of the liner honing process, B. GOELDEL, Renault SAS, France, M. EL MANSORI, Arts et Métiers ParisTech, France, L. SABRI, Renault SAS, France	F1-1-12 Nanocomposite-based wear sensor materials for in-situ process control in cutting applications, S. ULRICH, C. KLEVER, H. LEISTE, K. SEEMANN, M. STUEBER, Karlsruhe Institute of Technology, Germany	
5:10 pm	E3-1/G2-1-13 Friction and adhesion of Si and F incorporating diamond-like carbon (DLC) coatings sliding against aluminum, F.G. SEN, X. MENG-BURANY, University of Windsor, Canada, M.J. LUKITSCH, Y. QI, General Motors Research and Development Center, US, A.T. ALPAS, University of Windsor, Canada		
5:30 pm		VAMAS TWA 22 Annual General Meeting Mechanical Property Measurements of Thin Films and Coatings Royal Palm 1-3 5:30 – 6:30 pm	

Monday Afternoon, April 23, 2012

Advanced Characterization of Coatings and Thin Films
Room: Sunrise - Session TS2-2

Advanced Characterization of Coatings and Thin Films

Moderators: F. Giuliani, Imperial College London - South Kensington Campus, UK, S. Korte, University of Erlangen-Nürnberg, Germany, P. Schaaf, TU Ilmenau, Germany

1:30 pm	TS2-2-1 Testing of mechanical thin film properties by vibrating Micro-Electromechanical Systems (MEMS), P. SCHAAF, R. GRIESLER, J. KLAUS, M. STUBENRAUCH, K. TONISCH, J. PEZOLDT, S. MICHAEL, TU Ilmenau, Germany	
1:50 pm	TS2-2-2 A New FIB-DIC Material Removal Method for Poisson's Ratio and Residual Stress Measurement in thin films, M. SEBASTIANI, University of Rome "Roma Tre", Italy, E. BEMPORAD, F. CARASSITI, University of Rome "Roma Tre", Italy	
2:10 pm	TS2-2-3 Low temperature deformation in complex crystals, V. SCHNABEL, University of Cambridge, UK, S. KORTE, Gordon Laboratory, Department of Materials Science and Metallurgy, University of Cambridge, UK, C. WALTER, R. STEARN, W. CLEGG, University of Cambridge, UK	
2:30 pm	TS2-2-4 Carbon-Based Coating for Flexible Fabric Heater Prepared by Arc Ion Plating, C.C. HSU, C.M. CHEN, J.L. HE, Feng Chia University, Taiwan	
2:50 pm	TS2-2-5 Invited Kinetics of Thin Film Growth and Gas-Solid Reactions using <i>in situ</i> High-Temperature Scanning Tunneling Microscopy, S. KODAMBAKA, Y. MURATA, University of California, Los Angeles, US, V. PETROVA, I. PETROV, University of Illinois at Urbana-Champaign, US	
3:10 pm	Invited talk continued.	
3:30 pm	TS2-2-7 In-situ AFM studies of crack initiation in ultra-thin SiO _x films on polymer substrates., B. OZKAYA, University of Paderborn, Germany, S. STEVES, Ruhr Universität Bochum, Germany, C.N. LIU, O. OZCAN, University of Paderborn, Germany, P. AWAKOWICZ, Ruhr Universität Bochum, Germany, G. GRUNDMEIER, University of Paderborn, Germany	
3:50 pm	TS2-2-8 High Frequency Characterization of Screen-printed Silver Circuits with an Environmental Reliability Test, K.S. KIM, W.R. MYUNG, S.B. JUNG, Sungkyunkwan University, Republic of Korea	
4:10 pm	TS2-2-10 The Bipolar Resistance Switching Behavior with a Pt/CoSiO _x /TiN Structure of Nonvolatile Memory Device, Y.E. SYU, National Sun Yat-Sen University, Taiwan, G.W. CHANG, National Chiao Tung University, Taiwan	
4:30 pm	TS2-2-11 A low-temperature method to improve the performance of Ni: SiO ₂ - based nonvolatile memory by supercritical CO ₂ fluid, S.L. CHUANG, National Sun Yat-Sen University, Taiwan	
4:50 pm	TS2-2-12 Resistive switching characteristics induced by doping of Sn in SiO ₂ -based nonvolatile memory, T.M. TSAI, K.C. CHANG, T.C. CHANG, Y.E. SYU, D.S. GAN, National Sun Yat-Sen University, Taiwan	
5:10 pm	<p style="text-align: center;"> Welcome Mixer 6:00 – 7:30 pm Golden Foyer and the Lion Fountain Patio Sponsored by Oerlikon Balzers </p>	<p style="text-align: center;"> VAMAS TWA 22 Annual General Meeting Mechanical Property Measurements of Thin Films and Coatings Royal Palm 1-3 5:30 – 6:30 pm </p>

Tuesday Morning, April 24, 2012

Exhibitors Keynote Lecture 9:40 – 10:40 am Room: Golden Ballroom		Coatings for Use at High Temperature Room: Sunrise - Session A2-1 Thermal and Environmental Barrier Coatings Moderators: R. Wellman, Cranfield University, UK, D. Litton, Pratt & Whitney, US, R. Trice, Purdue University, US
8:00 am	<div style="text-align: center;"> Exhibitors Keynote Session Professor Emeritus Roger De Gryse Ghent University, Belgium “Rotatable Magnetrons, Today and Tomorrow” See Keynote Lecture Page for abstract Golden Ballroom 9:40 – 10:40 am </div>	A2-1-1 Progress in Measuring and Understanding the Delamination Toughness of Zirconia Coatings, E. DONOHUE, N. PHILIPS, M. BEGLEY, C.G. LEVI, University of California, Santa Barbara, US
8:20 am		A2-1-2 Monitoring Delamination of Thermal Barrier Coatings by Combined Photoluminescence Piezospectroscopy Imaging and Upconversion Luminescence Imaging Techniques, J.I. ELDRIDGE, NASA Glenn Research Center, US, B. HEEG, Lumium, Netherlands
8:40 am		A2-1-3 Invited The influence of transient thermal gradients and substrate constraint on the delamination of thermal barrier coatings, HUTCHINSON, School of Engineering and Applied Sciences, Harvard University, US Invited talk continued.
9:00 am		
9:20 am		A2-1-5 Raman Spectroscopy and Neutron scattering of Ferroelastic Switching in Ceria Stabilized Zirconia, A. BOLON, M. GENTLEMAN, Texas A&M University, US
9:40 am		A2-1-6 Thermo-mechanical properties of lanthanide added zirconia film deposited by EB PVD, Y.S. OH, K.H. KWAK, H.T. KIM, S.W. KIM, S.M. LEE, Korea Institute of Ceramic Engineering and Technology, Republic of Korea, B.K. JANG, National Institute for Materials Science, Japan
10:00 am		A2-1-7 Effect of post heat treatment on thermal durability of thermal barrier coatings in thermal fatigue tests, S. MYOUNG, H. KIM, M. KIM, S. LEE, Y. JUNG, Changwon National University, Republic of Korea, S. JUNG, T. WOO, Sung Il Co., Ltd. (SIM), Republic of Korea
10:20 am		A2-1-8 New Perspectives on the Phase Stability Challenge in Zirconia-based TBCs, J. KROGSTAD, S. KRÄMER, University of California, Santa Barbara, US, R. LECKIE, Los Alamos National Laboratory, US, M. LEPPLE, Karlsruhe Institute of Technology, Germany, Y. GAO, D. LIPKIN, GE Global Research, US, C.G. LEVI, University of California, Santa Barbara, US STUDENT AWARD FINALIST
10:40 am		A2-1-9 Invited Influence of the mechanical behaviour of the under layer in coating spallation, V. MAUREL, A. KOSTER, Mines-ParisTech, UMR CNRS 7633, France, L. RÉMY, Mines-ParisTech, UMR CNRS 7633, France Invited talk continued.
11:00 am		
11:20 am		A2-1-11 Inhibiting High Temperature Densification Through Multi-Phase TBCs, J.S. VAN SLUYTMAN, C.G. LEVI, University of California, Santa Barbara, US, V.K. TOLPYGO, Honeywell Aerospace, Phenix, AZ, US
11:40 am	Exhibition opens in TC-Exhibit Hall 11:00 am – 7:00 pm	

Tuesday Morning, April 24, 2012

Hard Coatings and Vapor Deposition Technology Room: Royal Palm 4-6 - Session B1-3 PVD Coatings and Technologies Moderators: P. Eklund, Linköping University, Sweden, J.H. Huang, National Tsing Hua University, Taiwan, J. Vetter, Sulzer Metaplas GmbH, Germany		Hard Coatings and Vapor Deposition Technology Room: Royal Palm 1-3 - Session B7-1 Computational Design and Experimental Development of Functional Thin Films Moderators: B. Alling, Linköping University, Sweden, A. Amassian, KAUST, P. Patsalas, University of Ioannina, D. Holec, Montanuniversität Leoben, Austria	
8:00 am	B1-3-1 Invited Preparation and characterization of anti-wear and anti-bacteria TaN-Cu, TaN-Ag, TaN(Ag,Cu) nanocomposite thin films, J.H. HSIEH, Ming Chi University of Technology, Taiwan	B7-1-1	Time domain effect on growth kinetics of thin silver films, D. MAGNFÄLT, Linköping University, IFM-Material Physics, Plasma and Coatings Physics Division, Sweden, G. ABADIAS, Université de Poitiers-CNRS-ENSMA, France, U. HELMERSSON, K. SARAKINOS, Linköping University, Sweden
8:20 am	Invited talk continued.	B7-1-2	Analysis of the particle velocity range for deposition and the optimum velocity of cold sprayed particles using smoothed particle hydrodynamics method, A.M. MANAP, T. OKABE, K. OGAWA, Tohoku University, Japan
8:40 am	B1-3-3 Effects of sputtering gas for the preparation of CN _x films by RF reactive sputtering, T.S. SHIROYA, Graduate School, Chiba Institute of Technology, Japan, Y. SAKAMOTO, Chiba Institute of Technology, Japan	B7-1-3 Invited	Molecular Dynamics Studies of Grain Boundaries in Mazed-bicrystal Thin Films, M. ASTA, University of California, Berkeley; Lawrence Berkeley National Laboratory, US, D. OLMSTED, University of California, Berkeley, US, C. OPHUS, Lawrence Berkeley National Laboratory, US, T. RADETIC, Lawrence Berkeley National Laboratory, US; University of Belgrade, Serbia, U. DAHMEN, University of Belgrade, Serbia
9:00 am	B1-3-4 Zirconium carbonitrides: study of tribological properties with deposition parameters, J. BARRIGA, L. MENDIZABAL, U. RUIZ DE GOPEGUI, Tekniker, Spain	Invited talk continued.	
9:20 am	B1-3-5 Comparison of sputter deposited WC coatings from alternative sources, H. ALAGOZ, E. UZUN, M. UGRAS, N. UDDIN, E. BENGU, Bilkent University, Turkey	B7-1-5	A non-equilibrium thermodynamic model for the formation of a Cu-Sn intermetallics film on a Cu substrate, F.D. FISCHER, Montanuniversität Leoben, Austria, J. SVOBODA, Academy of Sciences, Czech Republic
9:40 am	B1-3-6 The influence of the magnetic field strength on the poisoning behavior of Tantalum, R. HOLLERWEGER, Montanuniversität Leoben, Austria, M. LECHTHALER, OC Oerlikon Balzers AG, Liechtenstein, P. POLCIK, PLANSEE Composite Materials GmbH, Germany, J. PAULITSCH, P.H. MAYRHOFFER, Montanuniversität Leoben, Austria	B7-1-6	Epitaxially Grown V _x Mo _{1-x} N/MgO(001) Thin Films by Reactive Magnetron Sputtering, H. KINDLUND, J. LU, E. BROITMAN, J. BIRCH, Linköping University, Sweden, I. PETROV, J.E. GREENE, University of Illinois at Urbana-Champaign, US, L. HULTMAN, Linköping University, Sweden
10:00 am	B1-3-8 Cavitation and abrasion resistance of Ti-Al-Y-N coatings prepared by the PIII&D technique from filtered vacuum-arc plasma, V. BELOUS, V. VASYLIEV, A. LUCHANINOV, V. MARININ, E. RESHETNYAK, V. STREL'NITSKIY, National Science Center "Kharkov Institute of Physics and Technology", Ukraine, S. GOLTVYANYTSYA, V. GOLTVYANYTSYA, Real Ltd., Ukraine	B7-1-7	Atomistic study of crack formation in strained thin films, A. OILA, S.J. BULL, Newcastle University, UK
10:20 am	B1-3-9 Synthesis and Tribological Properties of W _x N _y Coatings, H. ALAGOZ, M. UGRAS, E. UZUN, M.F. GENISEL, E. BENGU, Bilkent University, Turkey	B7-1-8	Classical Molecular Dynamics Studies of Initial Nucleation Kinetics during TiN Thin Films Growth, D. SANGIOVANNI, D. EDSTRÖM, V. CHIRITA, L. HULTMAN, Linköping University, Sweden, I. PETROV, J.E. GREENE, University of Illinois at Urbana-Champaign, US
10:40 am	B1-3-10 Excellent thermal stability of Cu films containing insoluble Ru, RuN _x and ReN _x for advanced barrierless Cu metallization, W. DIATMIKA, J. CHU, National Taiwan University of Science and Technology, Taiwan, C. LIN, Asia-Pacific Institute of Creativity, Taiwan	B7-1-9	Do nitride alloys exhibit Vegard's-like linear behaviour?, D. HOLEC, P.H. MAYRHOFFER, Montanuniversität Leoben, Austria
11:00 am	B1-3-11 Microstructural features and thermal stability of AlN:Ag and Al-Si-N:Ag nanostructured films, A. SIOZIOS, D. ANAGNOSTOPOULOS, P. PATSALAS, University of Ioannina, Greece	B7-1-10	Toughness Enhancement in Transition Metal Nitride Thin Films by Alloying and Valence Electron Concentration Tuning, D. SANGIOVANNI, V. CHIRITA, L. HULTMAN, Linköping University, Sweden STUDENT AWARD FINALIST
11:20 am	B1-3-12 <i>Hard yet Tough Ceramic Coatings via Magnetron Sputtered Multilayers Nanocomposite and Polycrystalline Architecture.</i> , Y. WANG, S. ZHANG, Nanyang Technological University, Singapore, J.W. LEE, Ming Chi University of Technology, Taiwan, W. LEW, Nanyang Technological University, Singapore	B7-1-11 Invited	Bridging atomic structure with properties in III-Nitride heterostructures, KOMNINOI, Aristoteles University of Thessaloniki, Greece
11:40 am	Exhibition opens in TC-Exhibit Hall 11:00 am – 7:00 pm		Invited talk continued.

Tuesday Morning, April 24, 2012

Fundamentals and Technology of Multifunctional Thin Films: Towards Optoelectronic Device Applications Room: Tiki Pavilion - Session C2-3/F4-3 Thin Films for Photovoltaics and Active Devices: Synthesis and Characterization Moderators: T. Terasako, Graduate School of Science and Engineering, Ehime University, Japan, M. Cremona, Pontificia Universidade Católica do Rio de Janeiro, Brazil		Fundamentals and Technology of Multifunctional Thin Films: Towards Optoelectronic Device Applications Room: Pacific Salon 3 - Session C4-1 Transparent Conductive Films: Inorganic Oxides, Organic Materials, Metals Moderators: P. Kelly, Manchester Metropolitan University, UK, S. Lim, Lawrence Berkeley National Laboratory, US	
8:00 am	C2-3/F4-3-1 The I-V transfer characteristics of a-IGZO TFTs deteriorated owing to the copper diffusion in the process of the source/drain metal, H.L. CHIU, Y.H. TAI, L.S. CHOU, C.M. LI, National Chiao Tung University, Taiwan	C4-1-1	ZnO films deposited from a filtered cathodic vacuum arc: characterization and device applications, J.G. PARTRIDGE, E.H. MAYES, M.R. FIELD, D.G. MCCULLOCH, RMIT University, Australia, H-S KIM, R. HEINHOLD, S. ELZWAWI, G.C. TURNER, R.J. REEVES, M.W. ALLEN, University of Canterbury, New Zealand
8:20 am	C2-3/F4-3-2 Light-accelerated instability mechanism depending on bias and environment in amorphous Indium-Gallium-Zinc-Oxide Thin Film Transistors, Y.C. CHEN, National Sun Yat-Sen University, Taiwan	C4-1-2	Filtered cathodic arc deposited ZnO:Al assisted by a high-flux low-energy constricted gas plasma source, S. LIM, R. MENDELSBERG, Lawrence Berkeley National Laboratory, US, N. FRIEDERICHSEN, RWTH Aachen University, Germany, Y.K. ZHU, Harbin Institute of Technology, China, K.M. YU, A. ANDERS, Lawrence Berkeley National Laboratory, US
8:40 am	C2-3/F4-3-3 Suppressed Temperature-dependent Sub-threshold Leakage Current of amorphous Indium-Gallium-Zinc-Oxide Thin Film Transistors by Nitrous Oxide Plasma Treatment, G.W. CHANG, National Chiao Tung University, Taiwan, Y.E. SYU, National Sun Yat-Sen University, Taiwan	C4-1-3 Invited	The material challenges in oxide electronics: Recent progress in oxide films for electronic applications, B. SZYSZKA, Fraunhofer IST, Germany, C. ELSAESSER, FhG-IWM, Germany, B. MALIC, JSI, Slovenia, G. KIRIAKIDIS, FORTH, Crete, L. PEREIRA, R. MARTINS, UNINOVA, Portugal, K. GEHRKE, Osram, Germany, N. YOUNG, Phillips Research, UK, V. LAMBERTINI, Fiat CRF, Italy, U. WEIMAR, EKUT, Germany
9:00 am	C2-3/F4-3-4 Investigating of Negative Bias Stress Induced Temperature-Dependence Degradation for InGaZnO TFTs under Dark and Light Illumination, M.C. CHEN, T.C. CHANG, S.Y. HUANG, M.H. WU, National Sun Yat-Sen University, Taiwan, K.H. YANG, University of Toronto, Canada, M.C. YANG, T.C. CHEN, F.Y. JIAN, National Sun Yat-Sen University, Taiwan	Invited talk continued.	
9:20 am	C2-3/F4-3-5 Invited Optimising OLED devices for solid state lighting applications using optical spectroscopy, P. MONKMAN, Durham University, UK	C4-1-5	Enhanced stability performance for Ga-doped ZnO films by indium co-doping, H.-P. SONG, H. MAKINO, N. YAMAMOTO, T. YAMAMOTO, Research Institute, Kochi University of Technology, Japan
9:40 am	Invited talk continued.	C4-1-6	Temperature dependence of electrical properties in polycrystalline Ga-doped ZnO films deposited on oxide nanosheet seed layer, H. MAKINO, Kochi University of Technology, Japan, T. SHIBATA, National Institute for Materials Science, Japan, H.-P. SONG, N. YAMAMOTO, Kochi University of Technology, Japan, T. SASAKI, National Institute for Materials Science, Japan, T. YAMAMOTO, Kochi University of Technology, Japan
10:00 am	C2-3/F4-3-7 New rare-earth quinolate complexes for organic light-emitting devices, H. CAMARGO, M. CREMONA, Pontificia Universidade Católica do Rio de Janeiro, Brazil, T. PAOLINI, H. BRITO, Universidade de São Paulo, Brazil	C4-1-7	Optical and Electrical Characterization of Ga-doped ZnO Thin Films Grown by Atmospheric Spray Pyrolysis, K. YOSHINO, N. KAMIYA, M. OSHIMA, University of Miyazaki, Japan
10:20 am	C2-3/F4-3-8 Effect of the deposition process and substrate temperature on the microstructure defects and electrical conductivity of thin Mo films, H. KÖSTENBAUER, Plansee SE, Austria, D. RAFAJA, U. MÜHLE, G. SCHREIBER, TU Bergakademie Freiberg, Germany, M. KATHREIN, J. WINKLER, Plansee SE, Austria	C4-1-8	Investigation of different techniques for achieving high quality p-type doping in transparent conductive zinc oxide by a sequential codoping approach, A. POPEL, N. M. K. S. DE SOUZA, University of Sydney, Australia, S. LIM, Lawrence Berkeley National Laboratory, US, B. ABENDROTH, TU Bergakademie Freiberg, Germany
10:40 am	C2-3/F4-3-9 Study of the electrical performance of rf magnetron sputtered TiO ₂ source and CuO drain split gate transistor, S. GOPIKISHAN, P. LAHA, A.B. PANDA, P.K. BARHAI, Birla Institute of Technology, India, AK. DAS, Bhabha Atomic Research Center, India, I. BANERJEE, SK. MAHAPATRA, Birla Institute of Technology, India	C4-1-9 Invited	Electrical Transport in ZnO and ZnMgO Films: A Comparison, K. ELLMER, A. BIKOWSKI, T. WELZEL, Helmholtz-Zentrum Berlin für Materialien und Energie, Germany
11:00 am	C2-3/F4-3-10 Characteristics and photocatalytic reactivity of TiO ₂ beads synthesized using a microwave-assisted hydrothermal method, W. WU, Y. TSOU, S. HUANG, MingDao University, Taiwan	Invited talk continued.	
11:20 am	C2-3/F4-3-11 Effect of growth parameters and annealing on some properties of sputtered ZnO thin films, R. CHANDER, GPC Bhikhiwind, India	C4-1-11	Study of reactively Co-sputtered Sb-Sn oxide, G. DING, M. LE, F. HASSAN, Z. SUN, M. NGUGEN, Intermolecular Inc, US
11:40 am	Exhibition opens in TC-Exhibit Hall 11:00 am – 7:00 pm		C4-1-12 Investigation of p-type conducting Cu-Al-O mixtures, C. SCHULZ, C. BALMER, B. SZYSZKA, Fraunhofer IST, Germany

Tuesday Morning, April 24, 2012

Tribology & Mechanical Behavior of Coatings and Engineered Surfaces Room: Pacific Salon 1-2 - Session E1-2 Friction Wear Lubrication Effects & Modeling Moderators: Lopez, CSIS-University Sevilla, S. Aouadi, Southern Illinois University, US, V. Fridrici, Ecole Centrale de Lyon, O.L. Eryilmaz, Argonne National Laboratory, US		New Horizons in Coatings and Thin Films Room: Sunset - Session F2-1 High Power Impulse Magnetron Sputtering Moderators: D. Lundin, Université Paris-Sud 11, France, J. Sapieha, Ecole Polytechnique de Montreal, Canada, R. Bandorf, Fraunhofer Institute for Surface Engineering and Thin Films IST, Germany	
8:00 am	E1-2-1 Friction induced evolution of mechanical properties of engineered surfaces, T. LISKIEWICZ , J. KUBIAK, Leeds University, UK	F2-1-1 Invited Energetic aspects of thin film growth in HiPIMS and in other pulsed plasmas, L. MARTINU , J. CAPEK, M. HALA, O. ZABEIDA, J.E. KLEMBERG-SAPIEHA, École Polytechnique de Montréal, Canada Invited talk continued.	
8:20 am	E1-2-2 Frictional Behavior of Silver Nano-pattern Fabricated by Thermal Dewetting, H.-J. KIM , D.E. KIM, Yonsei University, Republic of Korea		
8:40 am	E1-2-3 Scaling effects between micro- and macro-tribology for a Ti-MoS ₂ coating, P. STOYANOV , R. CHROMIK , H. STRAUSS, McGill University, Canada	F2-1-3 Unique Property of Our Brand New Technology Based On High Power Pulse Sputtering., S. HIROTA , K. YAMAMOTO, Kobe Steel Ltd., Japan, R. CREMER, KCS Europe GmbH, Germany	
9:00 am	E1-2-4 Mechanisms responsible for compositional variations of films sputtered from a WS ₂ target, E. SARHAMMAR , J. SUNDBERG, H. NYBERG, Uppsala University, Angstrom Laboratory, Sweden, T. KUBART, The Angstrom Laboratory, Uppsala University, Sweden, S. JACOBSON, U. JANSSON, T. NYBERG, Uppsala University, Angstrom Laboratory, Sweden	F2-1-4 Influence of pulse shape and peak current on the resulting properties of Ti-Si-C composite films deposited by HIPIMS, R. BANDORF , M. SCHOLTALBERS, G. BRÄUER, Fraunhofer IST, Germany	
9:20 am	E1-2-5 Tribological characteristics of carbon nitride synthesized using MW-PCVD, I. TANAKA , Graduate School, Chiba Institute of Technology, Japan, Y. SAKAMOTO, Chiba Institute of Technology, Japan	F2-1-5 Highly ionized carbon plasmas for the growth of diamond-like carbon thin films with magnetron sputtering, A. AJAZ , K. SARAKINOS, D. LUNDIN, U. HELMERSSON, Linköping University, Sweden	
9:40 am	E1-2-6 The Role of Planar Defects in Achieving Low Friction and Wear in Lubricious Oxide Coatings, V. AGEH , H. MOHSENI, T. SCHARF, The University of North Texas, US	F2-1-6 Characterization of hard coatings deposited by HIPIMS system and their cutting performance, T. SASAKI , Hitachi Tool Engineering, Ltd., Japan	
10:00 am	E1-2-7 Invited Structure and properties of nanocomposite DLC coatings on hard and soft substrates, J.T. DEHOSSON , University of Groningen, Netherlands	F2-1-7 Properties of Ti _{1-x} Al _x N films grown by HIPIMS and in hybrid HIPIMS-DCMS configuration: a comparative study, G. GRECZYNSKI , J. LU, J. JENSEN, Linköping University, Sweden, M. JOHANSSON, Seco Tools AB, Linköping University, Sweden, I. PETROV, J.E. GREENE, University of Illinois at Urbana-Champaign, US, W. KÖLKER, O. LEMMER, CemeCon AG, Germany, L. HULTMAN, Linköping University, Sweden	
10:20 am	Invited talk continued.	F2-1-8 (Cr _{1-x} Al _x)N: A Comparison of Direct Current, Middle Frequency Pulsed and High Power Pulsed Magnetron Sputtering for Injection Molding Components, K. BOBZIN , N. BAGCIIVAN, S. THEISS , Surface Engineering Institute - RWTH Aachen University, Germany	
10:40 am	E1-2-9 Synthesis and Tribological Behavior of MoS ₂ -Au Nanocomposite Films, R. GOEKE , Sandia National Laboratories, US, T. SCHARF, The University of North Texas, US, P. KOTULA, S. PRASAD, Sandia National Laboratories, US	F2-1-9 Structure evolution in TiAlCN/VCN nanoscale multilayer coatings deposited by reactive High Power Impulse Magnetron Sputtering technology., P. HOVSEPIAN , A. EHIAZARIAN, G. KAMATH, Sheffield Hallam University, UK, I. PETROV, University of Illinois at Urbana-Champaign, US	
11:00 am	E1-2-10 Electrodeposited of gold-multiwalled carbon nanotube to improve lubrication of composite films, P.-A. GAY , Haute Ecole ARC Ingenierie, Switzerland	F2-1-10 Structure and properties of thick CrN/AlN multilayer coatings deposited by the hybrid modulated pulsed power and pulsed dc magnetron sputtering, J. LIN , Colorado School of Mines, US, W. SPROUL, Reactive Sputtering, Inc., US, Z. WU, M. LEI, Dalian University of Technology, China, J. MOORE, Colorado School of Mines, US	
11:20 am	E1-2-11 A systematic study of suberlubricity potential of ta-C coatings, v. WEIHNACHT , S. MAKOWSKI, G. ENGLBERGER, A. LESON, Fraunhofer IWS, Germany	F2-1-11 The uniformity in thickness and microstructure of CrN films fabricated using plasma ion implantation-deposition based on high power pulsed magnetron sputtering, X.B. TIAN , Z.Z. WU, C.Z. GONG, Harbin Institute of Technology, China, P. CHU, City University of Hong Kong, Hong Kong Special Administrative Region of China	
11:40 am	E1-2-12 The wear resistance of boride layers in the four-ball lubricant test, E. GARCIA-BUSTOS , M.A. FIGUEROA-GUADARRAMA, G.A. RODRIGUEZ-CASTRO , E. GALLARDO-HERNANDEZ, I. CAMPOS-SILVA, Instituto Politecnico Nacional, Mexico	F2-1-12 Characterization of chromium and chromium nitride obtained by DC and HIPIMS sputtering techniques, A. FERREC , IMN – Nantes, France, A. TRICOTEAUX, C. NIVOT, LMCPA-Maubeuge, France, F. SCHUSTER , Laboratoire Commun MATPERF CEA-Mecachrome, France, M. GANCIU, National Institute for Laser, Plasma and Radiation Physics, Romania, P.-Y. JOUAN, A. DJOUADI, IMN – Nantes, France	
Exhibition opens in TC-Exhibit Hall 11:00 am – 7:00 pm			

Tuesday Afternoon, April 24, 2012

Coatings for Use at High Temperature Room: Sunrise - Session A2-2		Hard Coatings and Vapor Deposition Technology Room: Royal Palm 4-6 - Session B4-1	
Thermal and Environmental Barrier Coatings Moderators: R. Wellman, Cranfield University, UK, D. Litton, Pratt & Whitney, US, R. Trice, Purdue University, US		Properties and Characterization of Hard Coatings and Surfaces Moderators: J. Lin, Colorado School of Mines, US, C. Mulligan, U.S. Army ARDEC, Benet Laboratories, US, B. Zhao, Exxon Mobile, US	
1:50 pm	A2-2-1 Invited Process and Equipment for Advanced Thermal Barrier Coating Systems, A. FEUERSTEIN , C. PETORAK, L. LI, T.A. TAYLOR, Praxair Surface Technologies, Inc., US	B4-1-1 Epitaxial growth of sputtered TiO ₂ films on α -Al ₂ O ₃ , C. MITTERER , Montanuniversität Leoben, Austria, M. MÜHLBACHER, Materials Center Leoben Forschung GmbH, Austria, C. WALTER, J. KECKES, Montanuniversität Leoben, Austria, M. POPOV, J. SPITALER, Materials Center Leoben Forschung GmbH, Austria, C. AMBROSCH-DRAXL, Montanuniversität Leoben, Austria	
2:10 pm	Invited talk continued.	B4-1-2 Cu-dependent thermal transformations in hard Al-Cu-O coatings, P. ZEMAN , S. PROKSOVA, J. BLAZEK, R. CERSTVY, J. MUSIL, University of West Bohemia, Czech Republic	
2:30 pm	A2-2-3 Calcium-Magnesium-Alumino-Silicate (CMAS) degradation of EB-PVD thermal barrier coatings: solubility of different oxides from ZrO ₂ -Y ₂ O ₃ and ZrO ₂ -Nd ₂ O ₃ systems in the molten model CMAS, N. CHELLAH , M.H. VIDAL-SÉTIF, Thermal and Environmental Barrier Coatings, France	B4-1-3 Invited Multicomponent nanostructured coatings with high thermal stability, corrosion-, oxidation resistance, and improved lubrication, D.V. SHTANSKY , K.A. KUPTSOV, National University of Science and Technology "MISIS", Russian Federation, PH.V. KIRUYKHANTSEV-KORNEEV, A.N. SHEVEIKO, National University of Science and Technology "MISIS", Russian Federation, E.A. LEVASHOV, National University of Science and Technology "MISIS", Russian Federation	
2:50 pm	A2-2-4 Bond Coat Cavitation under CMAS-Infiltrated TBCs, K. WESSELS , University of California, Santa Barbara, US, D. KONITZER, GE Aviation, US, C.G. LEVI, University of California, Santa Barbara, US	Invited talk continued.	
3:10 pm	A2-2-5 Assessing the Delamination Behavior of CMAS Infiltrated TBCs under a Thermal Gradient, R.W. JACKSON , E. ZALESKI, C.G. LEVI, University of California, Santa Barbara, US	B4-1-5 Influence of residual stresses on the spinodal decomposition of metastable Ti _{1-x} Al _x N coatings, N. SCHALK , Materials Center Leoben Forschung GmbH, Austria, C. MITTERER, Montanuniversität Leoben, Austria, C. MICHOTTE, M. PENOY, Ceratizit Luxembourg S.à.r.l., Luxembourg	
3:30 pm	A2-2-6 CMAS infiltration of YSZ thermal barrier coatings and potential protection measures, V. KUCHENREUTHER , V. KOLARIK, M. JUEZ LORENZO, Fraunhofer ICT, Germany, W. STAMM, Siemens Power Generation, Germany, H. FIETZEK, Fraunhofer ICT, Germany	B4-1-6 <i>In-situ</i> small angle X-ray scattering and phase field study on the microstructural evolution at isothermal annealing of TiAlN thin films, A. KNUTSSON , J. ULLBRAND, L. ROGSTRÖM, Linköping University, Sweden, J. ALMER, Advanced Photon Source, US, B. JANSSON, Seco Tools AB, Linköping University, Sweden, M. ODÉN, Linköping University, Sweden	
3:50 pm	A2-2-7 Invited Overview of Environmental Barrier Coatings for Ceramic Matrix Composites, K. LEE , Rolls Royce, US	B4-1-7 Towards an Improved Stylus Geometry for the Scratch Test and Superficial Rockwell Hardness, G. FAVARO , CSM Instruments SA, Switzerland, N.M. JENNETT , National Physical Laboratory, UK	
4:10 pm	Invited talk continued.	B4-1-8 Surface Characterization of Optimized TiSiN Coating Deposited Via A Combination of DC and RF Magnetron Sputtering, A.R. BUSHROA , ABDUL RAZAK , University of Malaya, Malaysia, T. ARIGA, Tokai University, Japan, S. SINGH, M. HAJI HASAN, University of Malaya, Malaysia, M.R. MUHAMMAD, Multimedia University, Malaysia	
4:30 pm	A2-2-9 Progress In Depositing Solution Precursor Plasma Spray Thermal Barrier Coatings, M. GELL , E. JORDAN, J. ROTH, University of Connecticut, US	B4-1-9 Surface Analysis of TiAlON and CrAlN Coatings Deposited by Means of HPPMS, C. KUNZE , C. GNÖTH, University of Paderborn, Germany, M. TO BABEN, S. THEISS, N. BAGCIVAN, K. BOBZIN, J. SCHNEIDER, RWTH Aachen University, Germany, G. GRUNDMEIER, University of Paderborn, Germany	
4:50 pm	A2-2-10 Thermoelastic characteristics in thermal barrier coatings with graded layer between the top and bond coats, GO , S. MYOUNG, J. LEE, Y. JUNG, S. KIM, Changwon National University, Republic of Korea, U. PAIK, Hanyang University, Republic of Korea	B4-1-10 Nanoprobe measurements of anisotropy in thin-film nanocrystalline coatings, A. JANKOWSKI , H. AHMED, Texas Tech University, US	
5:10 pm	A2-2-11 Invited Stability of Silicates for Environmental Barrier Coatings, E. OPILA , University of Virginia, US, N. JACOBSON, NASA Glenn Research Center, US	B4-1-11 TaSiN Thin Films: Si Influence on the Optical and Electrical Properties, G. RAMÍREZ , Universidad Nacional Autónoma de México - Instituto de Investigaciones en Materiales, Mexico, S.E. RODIL, Instituto de Investigaciones en Materiales, Universidad Nacional Autónoma de México, México, S. MUHL, Universidad Nacional Autónoma de México - Instituto de Investigaciones en Materiales, Mexico, M. RIVERA, Instituto de Física - Universidad Nacional Autónoma de México, México, D. OEZER, R. SANJINES , EPFL, Switzerland	
5:30 pm	Invited talk continued.	<h2 style="text-align: center;">Exhibits Reception</h2> <h3 style="text-align: center;">TC- Exhibit Hall 5:30 – 7:00 pm</h3>	

Tuesday Afternoon, April 24, 2012

Hard Coatings and Vapor Deposition Technology Room: Royal Palm 1-3 - Session B7-2 Computational Design and Experimental Development of Functional Thin Films Moderators: B. Alling, Linköping University, Sweden, A. Amassian, KAUST, D. Holec, Montanuniversität Leoben, Austria, P. Patsalas, University of Ioannina, Greece		Tribology & Mechanical Behavior of Coatings and Engineered Surfaces Room: Pacific Salon 1-2 - Session E3-2/G2-2 Development, Characterization, and Tribology of Coatings for Automotive and Aerospace Applications Moderators: R. Evans, Timken Company, US, H. Rudigier, OC Oerlikon Balzers AG, Liechtenstein, S. Dixit, Plasma Technology Inc., US	
1:50 pm	B7-2-1 The effect of nitrogen content on stability and elastic properties of TiAlN studied by ab initio calculations and combinatorial reactive magnetron sputtering, M. TO BABEN , J. EMMERLICH, L. RAUMANN, J. SCHNEIDER, Materials Chemistry, RWTH Aachen university, Germany STUDENT AWARD FINALIST	E3-2/G2-2-1 <i>In situ</i> tribology of cold spray-deposited pure aluminum and Al-Al ₂ O ₃ composite coatings, J.M. SHOCKLEY , R. CHROMIK, H. STRAUSS, McGill University, Canada, E. IRISSOU, J.-G. LEGOUX, National Research Council, Canada	
2:10 pm	B7-2-2 First principle molecular dynamics simulations of high temperature properties in transition metal nitrides, P. STENETEG , I. ABRIKOSOV, B. ALLING, Linköping University, Sweden	E3-2/G2-2-2 Thermal Spray Lubricious Oxide Coatings, S. DIXIT , Plasma Technology Inc., US, O.L. ERYILMAZ, A. ERDEMIR, Argonne National Laboratory, US	
2:30 pm	B7-2-3 Invited Simulating the slow structural evolution of materials using Accelerated Molecular Dynamics, D. PEREZ , Los Alamos National Laboratory, US	E3-2/G2-2-3 Tribological properties of plasma sprayed AISi coatings reinforced by nano-diamond particles, M.D. BAO , Ningbo University of Technology, China, C. ZHANG, D. LAHIRI, A. ARGARWAL, Florida International University, US	
2:50 pm	Invited talk continued.	E3-2/G2-2-4 High temperature abrasive systems, J. DAVENPORT , R. STEARN, University of Cambridge, UK, M. HANCOCK, Rolls Royce, US, W. CLEGG, University of Cambridge, UK	
3:10 pm	B7-2-5 Stabilization of cubic AlN in TiN/AlN and CrN/AlN bi-layer systems by combined FEM and ab initio analysis, V. CHAWLA , D. HOLEC, P.H. MAYRHOFER, Montanuniversität Leoben, Austria	E3-2/G2-2-5 Invited Customized Surface Technology for Innovative Automotive and Industrial Products, T. HOSENFELDT , Y. MUSAYEV, Schaeffler Technologies GmbH & Co. KG, Germany	
3:30 pm	B7-2-6 Structural and elastic properties of polycrystalline Al _{1-x} Cr _x N alloys : multiscale computations versus experiments, T. PHAM , Institut P ⁺ - Université de Poitiers, France, K. BOUAMAMA, Ferhat Abbas University, Algeria, P. DJEMIA , University Paris 13, France, L. BELLARD, UPMC, France, D. FAURIE, University Paris 13, France, E. LE BOURHIS, P. GOUDEAU, Institut P ⁺ - Université de Poitiers, France	Invited talk continued.	
3:50 pm	B7-2-7 Theoretical spectroscopy investigation of hard TiN/SiNx interfaces, W. OLOVSSON , B. ALLING, L. HULTMAN, I. ABRIKOSOV, Linköping University, Sweden	E3-2/G2-2-7 Ultra-fast Synthesis of Superhard Borides: A Paradigm Shift in Surface Engineering for Tooling and Automotive Applications, A. ERDEMIR , O.L. ERYILMAZ, Argonne National Laboratory, US, S. TIMUR, Istanbul Technical University, Turkey, O. KAHEVCIOGLU, Argonne National Laboratory, US, G. KARTAL, Istanbul Technical University, Turkey, V. SISTA, Argonne National Laboratory, US	
4:10 pm	B7-2-8 Elasticity in TiAlN alloys: the significant elastic anisotropy and the dependence on the SQS model, F. TASNADI , M. ODÉN, I. ABRIKOSOV, Linköping University, Sweden	E3-2/G2-2-8 A study on tribological behavior of arc-coated Ti-Al-N films on AISI 4340 alloy steel for automotive application, C. HSU , Tatung University, Taiwan, C. LIN , Feng Chia University, Taiwan, D.W. LAI, Tatung University, Taiwan, K. OU, Taipei Medical University, Taiwan	
4:30 pm	B7-2-9 Improving thermal stability of hard coating films via a concept of multicomponent alloying., H. LIND , R. FORSÉN, B. ALLING, N. GHAFOR, F. TASNADI, M. JOHANSSON, I. ABRIKOSOV, M. ODÉN, Linköping University, Sweden	E3-2/G2-2-9 Predicting lifetime of silver and gold coating depending on their thickness, stress and environmental conditions, O.P. PERRINET , LTDS, France	
4:50 pm	B7-2-10 Packing structure and optical properties of functionalized pentacene, U. SCHWINGENSCHLOGL , N. SINGH , Y. SAEED, KAUST, Saudi Arabia	E3-2/G2-2-10 Understanding durability of lubricant/DLC coating interface, L. AUSTIN , T. LISKIEWICZ, A. NEVILLE , Leeds University, UK, R. TIETEMA, Hauzer Techno Coating, BV, Switzerland	
5:10 pm		E3-2/G2-2-11 From DLC to Si-DLC based layer systems with optimized properties for tribological applications, D. HOFMANN , S. KUNKEL, AMG Coating Technologies GmbH, Germany, K. BEWLOGUA, R. WITTORF, Fraunhofer IST, Germany	
5:30 pm	Exhibits Reception TC- Exhibit Hall 5:30 – 7:00 pm		

Tuesday Afternoon, April 24, 2012

New Horizons in Coatings and Thin Films Room: Sunset - Session F2-2 High Power Impulse Magnetron Sputtering Moderators: R. Bandorf, Fraunhofer Institute for Surface Engineering and Thin Films IST, J. Sapieha, Ecole Polytechnique de Montreal, D. Lundin, Université Paris-Sud 11, France		Applications, Manufacturing, and Equipment Room: Tiki Pavilion - Session G5-1 Coatings, Pre-Treatment, Post-Treatment and Duplex Technology Moderators: N. Baggivan, RWTH Aachen University, Germany, S. Brahmandam, Kennametal Incorporated, US	
1:50 pm	F2-2-1 HIPIMS Discharge Dynamics: Evolution and Origin of Plasma Instabilities, A. HECIMOVIC , Institut for Experimental Physics II, Research Department Plasma, Ruhr-Universität Bochum, Germany, T. DE LOS ARCOS, Ruhr Universität Bochum, Germany, V. SCHULZ-VON DER GATHEN, M. BOKE, J. WINTER, Institut for Experimental Physics II, Research Department Plasma, Ruhr-Universität Bochum, Germany	G5-1-1	Invited Ion treatment and duplex coatings by arc plasma immersion surface engineering processes., V. GOROKHOVSKY , Vapor Technologies, Inc., US
2:10 pm	F2-2-2 Modes of operation in HiPIMS: Understand and optimize the discharge pulse, D. LUNDIN , C. VITELARU, Université Paris-Sud 11, France, N. BRENNING, Royal Institute of Technology, U. HELMERSSON, Linköping University, Sweden, T. MINEA, Université Paris-Sud 11, France	Invited talk continued.	
2:30 pm	F2-2-3 High-rate reactive deposition of multifunctional Ta-O-N films using high power impulse magnetron sputtering, J. VLCEK , J. REZEK, J. HOUSKA, R. CERSTVY, University of West Bohemia, Czech Republic	G5-1-3	Growth kinetics of electrochemical boriding of titanium, G. KARTAL , S. TIMUR, Istanbul Technical University, Turkey
2:50 pm	F2-2-4 Variation of high power pulsed / modulated pulsed power magnetron sputtering based on oscillatory voltage wave forms for the deposition of carbon and aluminum oxide coatings, W. SPROUL , Reactive Sputtering, Inc., US, J. LIN, Colorado School of Mines, US, B. ABRAHAM, Zond, Inc. / Zpulser, LLC, US, J. MOORE, Colorado School of Mines, US, R. CHISTYAKOV, Zond, Inc. / Zpulser, LLC, US	G5-1-4	Improvement of Electrical Properties of Silicon Oxide Film with Ultraviolet and Organic Gas Assisted Annealings, T. ITO , T. MATUMOTO, K. NISHIOKA, University of Miyazaki, Japan
3:10 pm	F2-2-5 The development and the application of a high power impulse inverted cylindrical magnetron sputtering system for the elaboration of nanomaterials on wires or fibers., A. CHOQUET , D. DUDAY, A. LEJARS, O. VOZNIY, T. WIRTZ, CRP Gabriel Lippmann, Luxembourg	G5-1-5	Enhancement of gas barrier properties of polypropylene by surface treatment before DLC coating, H. TASHIRO , A. HOTTA, Keio University, Japan
3:30 pm	F2-2-6 Invited Low pressure High Power Impulse Magnetron Sputtering systems for deposition of biomedical functional thin films, V. STRANAK , University of Greifswald, Germany, M. CADA, Z. HUBICKA, Academy of Sciences, Czech Republic, S. DRACHE, A.P. HERRENDORF, H. WULFF, R. HIPPLER, University of Greifswald, Germany	G5-1-6	Invited Cathodic Arc Plasma Treatment for Surface Alloying and Modification, M. URGEN , Istanbul Technical University, Turkey
3:50 pm	Invited talk continued.	Invited talk continued.	
4:10 pm	F2-2-8 Material properties of Aluminum Metal (Titanium/Chromium) Nitride coatings deposited by High Power Impulse Magnetron Sputtering (HIPIMS ⁺) technology., F. PAPA , A. CAMPICHE, R. TIETEMA, T. KRUG, Hauzer Techno Coating, BV, Netherlands, T. SASAKI, T. ISHIKAWA, Hitachi Tool Engineering, Ltd., Japan	G5-1-8	Microstructure and tribological properties of laser textured PVD coatings on tool materials, M. ADAMIAK , Silesian University of Technology, Poland
4:30 pm	F2-2-10 On the Influence of superimposed MF and HPPMS/HIPIMS pulsed packages on the deposition rate and properties of TiN, J. ALAMI , Z. MARIC, INI Coatings Ltd., Germany, M. MALZER, M. FENKER, FEM Forschungsinstitut Edelmetalle & Metallchemie, Germany, M. MARK, J. LÖFFLER, E. PARRA MAZA, G. MARK, MELEC GmbH, Germany	G5-1-11	Evaluation of Electrochemical Boriding of Inconel alloys, V. SISTA , Argonne National Laboratory, US, O. KAHVECIOGLU, Istanbul Technical University, Turkey, G. KARTAL, Technical University of Istanbul, Turkey, Q.Z. ZENG, Xian Jiaotong University, China, O.L. ERYILMAZ, A. ERDEMIR, Argonne National Laboratory, US, S. TIMUR, Istanbul Technical University, Turkey
4:50 pm	F2-2-11 Angle-resolved energy flux measurements of a HIPIMS-powered rotating cylindrical magnetron in reactive and non-reactive atmosphere., S. KONSTANTINIDIS , University of Mons, Belgium, W. LEROY, Ghent University, Belgium, R. SNYDERS, University of Mons, Belgium, D. DEPLA, Ghent University, Belgium	G5-1-12	Electrochemical Boriding of Molybdenum, O. KAHVECIOGLU , Istanbul Technical University, Turkey, V. SISTA, O.L. ERYILMAZ, A. ERDEMIR, Argonne National Laboratory, US, S. TIMUR, Istanbul Technical University, Turkey
5:10 pm		G5-1-13	Mechanical and Microstructural Characterization of Nitrided AISI 4140 steel with Electroless NiP Coating, R. TORRES , P. SOARES, Universidade Católica do Paraná, Brazil, M. SOARES, IFSC, R.M. SOUZA, Mechanical Engineering Department, Universidade de São Paulo, Brazil, P. SOUZA, Universidade Católica do Paraná, Brazil, C. LEPIESNSKI, UFPR, Brazil
5:30 pm	<h2 style="text-align: center;">Exhibits Reception</h2> <h3 style="text-align: center;">TC- Exhibit Hall 5:30 – 7:00 pm</h3>		

Wednesday Morning, April 25, 2012

	Coatings for Use at High Temperature Room: Sunrise - Session A1-1 Coatings to Resist High Temperature Oxidation, Corrosion and Fouling Moderators: D. Naumenko, Forschungszentrum Jülich GmbH, Germany, L-G. Johansson, Chalmers University of Technology, Sweden, B. Hazel, Pratt and Whitney, US, J. Pérez, Universidad Complutense de Madrid, Spain	Hard Coatings and Vapor Deposition Technology Room: Royal Palm 4-6 - Session B4-2 Properties and Characterization of Hard Coatings and Surfaces Moderators: J. Lin, Colorado School of Mines, US, C. Mulligan, U.S. Army ARDEC, Benet Laboratories, US, B. Zhao, Exxon Mobile, US
8:00 am	A1-1-1 Invited Hot corrosion of NiAl diffusion coatings by gaseous Na ₂ SO ₄ , K. STILLER, H. LAI, P. KNUTSSON, L-G. JOHANSSON, Chalmers University of Technology, Sweden	B4-2-1 Invited Design and plasma synthesis of tribological surfaces for titanium, A. LEYLAND, University of Sheffield, UK, G. CASSAR, University of Sheffield, UK; University of Malta, Malta, A. MATTHEWS, University of Sheffield, UK
8:20 am	Invited talk continued.	Invited talk continued.
8:40 am	A1-1-3 Early Stages during Exposure of Uncoated and Coated HK40 Steel to Carburizing Atmospheres, D. MELO-MÁXIMO, TRAMES, S.A de C.V, Mexico, O. SALAS, J. OSEGUERA, Instituto Tecnológico y de Estudios Superiores de Monterrey-CEM, Mexico, R. REICHELT, Institut fuer Medizinische Physik und Biophysik Westfaelische Wilhelms-Universitaet, Germany	B4-2-3 Study of the environment effect on the tribological behavior of TiN, TiAlN and CrN coatings deposited by Reactive Magnetron Sputtering, J.S. RESTREPO, S. MUHL, Universidad Nacional Autónoma de México - Instituto de Investigaciones en Materiales, Mexico, M.F. CANO, F. SEQUEDA, J.M. GONZALEZ, Universidad Del Valle, Colombia
9:00 am	A1-1-4 New results and improvements of the catalytical poisoning concept against metal dusting, C. GEERS, M. GALETZ, M. SCHÜTZE, Dechema e.V., Frankfurt am Main, Germany	B4-2-4 Wear behaviour of plasma sprayed Cu-Ni coatings on Al7075, M.J. GHAZALI, Universiti Kebangsaan, Malaysia, E. MAT KAMAL, Universiti Teknikal, Malaysia, S. ABDULLAH, J. SHENG, Universiti Kebangsaan, Malaysia
9:20 am	A1-1-5 Structural Evolution of Candidate Coatings for Protection against Corrosion at High Temperature, L. MELO, Instituto Politécnico Nacional, Mexico, O. SALAS, J. OSEGUERA, Instituto Tecnológico y de Estudios Superiores de Monterrey-CEM, Mexico, V. LOPEZ-HIRATA, Instituto Politécnico Nacional, Mexico, R. TORRES, Pontificia Universidade Católica do Paraná, Brazil, R.M. SOUZA, Universidade Federal de Sao Paulo, Brazil	B4-2-6 Abrasive wear properties of AlCrN, AlTiN and CrN coatings, J.L.M. MO, M.H. ZHU, Southwest Jiaotong University, China, A. LEYLAND, A. MATTHEWS, University of Sheffield, UK
9:40 am	A1-1-6 Invited Fundamental Approaches to Optimizing the Hot-Corrosion Resistance of Coatings, B. GLEESON, University of Pittsburgh, US, Z. TANG, Iowa State University, US	B4-2-7 Annealing-induced structural and mechanical property changes of CVD-(Si)-B-C coatings, C. PALLIER, G. CHOLLON, P. WEISBECKER, F. TEYSSANDIER, LCTS-CNRS, France
10:00 am	Invited talk continued.	B4-2-8 Thermal evolution of thermal, electrical and optical properties of Ti-Al-N coatings, R. RACHBAUER, OC Oerlikon Balzers AG, Liechtenstein, J.J. GENGLER, Air Force Research Laboratory, Thermal Sciences and Materials Branch, US, A. VOEVODIN, Air Force Research Laboratory, US, K. RESCH, Materials Science and Testing of Plastics, Montanuniversitaet Leoben, Austria, P.H. MAYRHOFER, Montanuniversität Leoben, Austria
10:20 am	A1-1-8 High temperature oxidation studies of Detonation-Gun sprayed NiCrAlY+0.4wt%CeO ₂ coating on Fe and Ni -Based Superalloys in air under cyclic condition at 900 °C, S. KAMAL, Sharda University, India, D. MUDGAL, R. JAYAGANTHAN, S. PRAKASH, I.I.T-Roorkee, India	B4-2-9 Pressure and Temperature Effects on the Decomposition of Arc Evaporated Ti _{1-x} Al _x N Coatings During Metal Machining, N. NORRBY, M. JOHANSSON, Linköping University, Sweden, R. M'SAOUBI, Seco Tools AB., Sweden, M. ODÉN, Linköping University, Sweden
10:40 am	A1-1-9 High temperature oxidation studies of D-gun sprayed Cr ₃ C ₂ -25(NiCr) and Cr ₃ C ₂ -25(NiCr) + 0.2wt%Zr coatings on Ni and Co based superalloys in air at 900 °C, D. MUDGAL, Indian Institute of Technology Roorkee, India, S. KAMAL, Sharda University, India, S. SINGH, S. PRAKASH, Indian Institute of Technology Roorkee, India	B4-2-10 Understanding the deformation kinetics of Ti _{1-x} Al _x N ceramics at moderately elevated temperatures, C. CIUREA, V. BHAKHRI, N. NI, Imperial College London - South Kensington Campus, UK, P.H. MAYRHOFER, Montanuniversität Leoben, Austria, F. GIULIANI, Imperial College London - South Kensington Campus, UK
11:00 am	A1-1-10 Oxidation behavior of Hf-modified aluminide coatings on Haynes-188 at 1050°C, Y. WANG, M. SUNESON, SIFCO Minneapolis, US	B4-2-11 The Influence of Bias Voltage on Residual Stresses and Tribological Behavior of Ti/TiAlN and Cr/CrAlN Multilayer Systems, W. TILLMANN, T. SPRUTE, F. HOFFMANN, Technische Universität Dortmund, Germany
11:20 am		B4-2-12 The effect of Yttrium addition on TiAlN coating, L. ZHU, M. HU, Shanghai University, China, W. NI, Y. LIU, Kennametal Incorporated, US
11:40 am	<h2>Exhibition Closes today at 2:00 pm</h2>	

Wednesday Morning, April 25, 2012

Hard Coatings and Vapor Deposition Technology Room: Royal Palm 1-3 - Session B5-1 Hard and Multifunctional Nano-Structured Coatings Moderators: J. Paulitsch, Christian Doppler Laboratory for Application Oriented Coating Development at the Department of Physical Metallurgy and Materials Testing, Montanuniver, R. Sanjines, Ecole Polytechnique Fédérale de Lausanne, P. Zeman, University of West Bohemia, Czech Republic		Tribology & Mechanical Behavior of Coatings and Engineered Surfaces Room: Pacific Salon 1-2 - Session E1-3 Friction Wear Lubrication Effects & Modeling Moderators: Lopez, CSIS-University Sevilla, V. Fridrici, Ecole Centrale de Lyon, O.L. Eryilmaz, Argonne National Laboratory, US, S. Aouadi, Southern Illinois University, US	
8:00 am	B5-1-1 A study of microstructures and mechanical properties of cathodic arc deposited CrCN/ZrCN multilayer coatings, C.Y. TONG, J.W. LEE, Ming Chi University of Technology, Taiwan, S.H. HUANG, National Chiao Tung University, Taiwan, Y.B. LIN, C.C. KUO, Ming Chi University of Technology, Taiwan, T.E. HSIEH, Gigastorage Corporation, Taiwan, Y.C. CHAN, H.W. CHEN, J.G. DUH, National Tsing Hua University, Taiwan	E1-3-1 Invited Solid Lubrication Processes of Diamond-Like Carbon Coatings, J. FONTAINE, Ecole Centrale de Lyon, France	Invited talk continued.
8:20 am	B5-1-2 Effect of Zr content on structural, mechanical and phase transformation properties of magnetron sputtered TiNiZr shape memory alloy thin films, D. KAUR, N. KAUR, Indian Institute of Technology Roorkee, India		
8:40 am	B5-1-3 Self-Organized nano-Labyrinth Structure in Magnetron Sputtered $Zr_{0.6}Al_{0.4}N(001)$ Thin Films on $MgO(001)$, N. GHAFOR, L. JOHNSON, Linköping University, Sweden, D. KLENOV, FEI Company, B. ALLING, Linköping University, Sweden, I. PETROV, J.E. GREENE, University of Illinois at Urbana-Champaign, US, L. HULTMAN, M. ODÉN, Linköping University, Sweden	E1-3-3 Tribological behaviour at high temperature of hard CrAlN coatings doped with Y or Zr, J.C. SÁNCHEZ-LÓPEZ, A. CONTRERAS, Instituto de Ciencia de Materiales de Sevilla, Spain, A. GARCÍA-LUIS, M. BRIZUELA, Tecnalia, Spain	
9:00 am	B5-1-4 Wear/erosion behavior of TiN-based nanocomposite coatings on SS304 and a synchrotron radiation assisted coating failure investigation, Y. LI, Q. YANG, A. HIROSE, University of Saskatchewan, Canada, R. WEI, Southwest Research Institute, US	E1-3-4 High Temperature Tribometer Investigations of Oxide Coatings Synthesized by Cathodic Arc Evaporation, G. FAVARO, CSM Instruments SA, Switzerland, N. BIERWISCH, Saxonian Institute of Surface Mechanics, Germany, N.X. RANDALL, CSM Instruments SA, Switzerland, J. RAMM, OC Oerlikon Balzers AG, Liechtenstein, N. SCHWARZER, Saxonian Institute of Surface Mechanics, Germany, B. WIDRIG, OC Oerlikon Balzers AG, Liechtenstein	
9:20 am	B5-1-5 Invited Erosion Mechanisms of Hard Nanocomposite Coatings, E. BOUSSER, L. MARTINU, J.E. KLEMBERG-SAPIEHA, École Polytechnique de Montréal, Canada	E1-3-5 Adaptive Nitride Coatings With Lubricious Behavior From 25 to 1000 °C, S. AOUADI, S. STONE, A. HARBIN, Southern Illinois University, US, C. MURATORE, A. VOEVODIN, Air Force Research Laboratory, Thermal Sciences and Materials Branch, US	
9:40 am	Invited talk continued.	E1-3-7 High temperature tribological properties of Ti-Si-C-N coatings, D.J. KIM, J.Y. KIM, B.S. KIM, S.Y. KIM, Korea Research Institute of Chemical Technology, Republic of Korea, J.J. LEE, Seoul National University, Republic of Korea	
10:00 am	B5-1-7 Effects of structure and phase transformation on fracture toughness and mechanical properties of CrN/AlN multilayers, M. SCHLÖGL, J. PAULITSCH, J. KECKES, C. KIRCHLECHNER, P.H. MAYRHOFER, Montanuniversität Leoben, Austria	E1-3-8 Mechanical and Tribological Properties of Ti-Si-C-N Nanocomposite Coatings Deposited using a Plasma Enhanced Magnetron Sputtering (PEMS) Process, A.M. ABD EL-RAHMAN, Sohag University, Egypt, R. WEI, Southwest Research Institute, US	
10:20 am	B5-1-8 Nanoindentation and fatigue properties of magnetron sputtered AlN/NiTi multilayer thin films, D. KAUR, N. CHOUDHARY, Indian Institute of Technology Roorkee, India	E1-3-9 Invited Atomic Scale Origins of Friction in Metallic Contacts, M. CHANDROSS, S. CHENG, Sandia National Laboratories, US	
10:40 am	B5-1-9 Hardness of CrAlSiN nanocomposite coatings at elevated temperatures, S. LIU, S. KORTE, Gordon Laboratory, Department of Materials Science and Metallurgy, University of Cambridge, UK, X.Z. DING, X.T. ZENG, Singapore Institute of Manufacturing Technology, Singapore, W. CLEGG, Gordon Laboratory, Department of Materials Science and Metallurgy, University of Cambridge, UK	Invited talk continued.	
11:00 am	B5-1-10 Hard nanocrystalline Zr-B-C-(N) films prepared by pulsed magnetron sputtering, J. KOHOUT, P. STEIDL, J. VLCEK, R. CERSTVY, University of West Bohemia, Czech Republic	E1-3-11 Tribological study of PVD and CVD coated tool surfaces sliding on PA-6, PET and PTFE polymer substrates, G.G. FUENTES, A. SCANO, J. OSÉS, J. RODRIGO, R.J. RODRIGUEZ, Center of Advanced Surface Engineering - AIN, Spain, C. HARTL, Fachhochschule Köln, Germany, Y. QIN, University of Strathclyde, UK, J. HOUSDEN, Tecvac, UK	
11:20 am	B5-1-11 Magnetron co-sputtered hard and ductile TiB2/Ni coatings, H. WANG, Anhui University of Technology, China, F. GE, Ningbo Institute of Materials Technology and Engineering, China, P. ZHU, S. LI, Anhui University of Technology, China, F. HUANG, Ningbo Institute of Materials Technology and Engineering, China	E1-3-12 Au-ZnO Nanocomposite Coatings for Wear-Resistant Electrical Contacts, S. PRASAD, R. GOEKE, P. KOTULA, Sandia National Laboratories, US	
11:40 am	B5-1-12 Comparative investigation of boride and boronitride hard coatings produced by magnetron sputtering of MeB _x (Me: Mo, Cr, Ti) SHS-targets, P. KIRYUKHANTSEV-KORNEEV, A. SHEVEYKO, National University of Science and Technology "MISIS", Russian Federation, B. MAVRIN, Institute of Spectroscopy of RAS, Russian Federation, E.A. LEVASHOV, D.V. SHTANSKY, National University of Science and Technology "MISIS", Russian Federation	E1-3-13 The Effect of Ag Content on Friction Behavior of MoN-Ag and Mo ₂ N-Ag Nanocomposite Coatings, K. EZIRMIK, Ataturk University, Turkey, O. ERYILMAZ, Argonne National Laboratory, US, K. KAZMANLI, Istanbul Technical University, Turkey, A. ERDEMIR, Argonne National Laboratory, US, M. ÜRGEN, Istanbul Technical University, Turkey	

Wednesday Morning, April 25, 2012

Applications, Manufacturing, and Equipment Room: Tiki Pavilion - Session G1-1		Graphene and 2D Nanostructures Room: Sunset - Session TS4-1	
Innovations in Surface Coatings and Treatments Moderators: R. Cremer, KCS Europe GmbH, Germany, L. Bardos, Uppsala University, Sweden		Graphene and 2D Nanostructures Moderators: M. Chhowalla, Rutgers University, US, C. Teichert, Montanuniversität Leoben, Austria	
8:00 am	G1-1-1 Mathematical modeling of metal dusting during initial stages., F. CASTILLO-ARANGUREN, J. OSEGUERA-PEÑA, ITESM-CEM, Mexico	TS4-1-1 <i>Invited</i> Intercalation compounds and cluster superlattices: graphene based 2D composites, T. MICHELY, University of Cologne, Germany	
8:20 am	G1-1-2 A Dip soldering process for three dimensional integration, M. RAO, J.C. LUSTH, S.L. BURKETT, The University of Alabama, US	Invited talk continued.	
8:40 am	G1-1-3 <i>Invited</i> Coatings for Aerospace Applications, C. LEYENS, Technische Universität Dresden, Germany	TS4-1-3 Growth Kinetics of Monolayer and Multilayer Graphene on Pd(111), H.S. MOK, Y. MURATA, University of California, Los Angeles, US, S. NIE, N. BARTELT, K. MCCARTY, Sandia National Laboratories, US, S. KODAMBAKA, University of California, Los Angeles, US	
9:00 am	Invited talk continued.	TS4-1-4 <i>Invited</i> Self-assembled monolayer nanodielectrics for low-power graphene electronics, T. ANTHOPOULOS, F. COLLEAUX, C. MATTEVI, Imperial College London - South Kensington Campus, UK, M. CHHOWALLA, Rutgers University, US	
9:20 am	G1-1-5 Solid particle erosion resistance of thick coating deposited by new AIP (Arc Ion Plating) cathode., J. MUNEMASA, K. YAMAMOTO, H. FUJII, Kobe Steel Ltd., Japan, Y. IWAI, University of Fukui, Japan	Invited talk continued.	
9:40 am	G1-1-6 Combination of Hardness and Toughness of CVD HARDIDE Coatings Provides Enhanced Protection against Wear and Erosion., N. ZHUK, Hardide Plc, UK	TS4-1-6 Characterization of graphene on Cu and SiC surfaces, A. VOEVODIN, Air Force Research Laboratory, US, A. KUMAR, R. PAUL, D. ZEMLYANOV, D. ZAKHAROV, Purdue University, US, J. REMMERT, I. ALTFEDER, Air Force Research Laboratory, US, T.S. FISHER, Purdue University, US	
10:00 am	G1-1-7 Improvement of the adhesion force between DLC and polymers by CVD method with photografting polymerization, J. TAKAHASHI, A. HOTTA, Keio University, Japan	TS4-1-9 Rapid synthesis and in-situ nitrogen doping of few-layer graphene using microwave plasma chemical vapor deposition (MPCVD), A. KUMAR, Purdue University, US, A. VOEVODIN, Air Force Research Laboratory, US, R. PAUL, D. ZEMLYANOV, D. ZAKHAROV, Purdue University, US, J. REMMERT, I. ALTFEDER, Air Force Research Laboratory, US, T.S. FISHER, Purdue University, US	
10:20 am	G1-1-8 Electrophoretic deposition of carbon nanotube films on silicon substrates, A. SARKAR, D. HAH, Louisiana State University, US	TS4-1-10 <i>Invited</i> Soft Carbon Sheets: Synthesis, Processing and Applications in Organic Photovoltaics, J. HUANG, Northwestern University, US	
10:40 am	G1-1-9 <i>Invited</i> Implementation of Advanced Inorganic Coatings on Military Aircraft, B.D. SARTWELL, Department of Defense, US, G. KILCHENSTEIN, Office of Secretary of Defense, US, V. CHAMPAGNE, B. GABRIEL, Army Research Laboratory, US, M. DUFFLES, MDS Coating Technologies Corp., Canada	Invited talk continued.	
11:00 am	Invited talk continued.	TS4-1-12 Growth and characterization of dense CNT Forests on oxide-free copper foil surfaces for charge storage application, G. ATTHIPALLI, K. STRUNK, J. SOPCISAK, J. GRAY, University of Pittsburgh, US	
11:20 am	G1-1-11 The Wear behavior of Manganese Phosphate coatings applied to AISI D2 steel subjected to different heat treatments, s. SIVAKUMARAN, Sri Venkateswara College of Engineering,Pennalur, India, A. ALANGARAM, Sri Venkateswara College of Engineering, India	TS4-1-13 Growth of organic semiconductor films on graphene, G. HLAWACEK, F. KHOKHAR, R. VAN GASTEL, B. POELSEMA, H. ZANDVLIET, University of Twente, Netherlands, C. TEICHERT, Montanuniversität Leoben, Austria	
11:40 am	G1-1-12 Deposition of low melting point metals by Cold Dipping - Fluidized Bed Coating (CD - FBC), M. BARLETTA, Università degli Studi di Roma Tor Vergata, Italy, A. GISARIO, S. VENETTACI, Università degli Studi di Roma La Sapienza, Italy, S. VESCO, Università degli Studi di Roma Tor Vergata, Italy		
12:00 pm	Exhibition Closes today at 2:00 pm		

Wednesday Afternoon, April 25, 2012

Coatings for Use at High Temperature Room: Sunrise - Session A1-2 Coatings to Resist High Temperature Oxidation, Corrosion and Fouling Moderators: J. Pérez, Universidad Complutense de Madrid, Spain, B. Hazel, Pratt and Whitney, US, L-G. Johansson, Chalmers University of Technology, Sweden, D. Naumenko, Forschungszentrum Jülich GmbH, Germany		Hard Coatings and Vapor Deposition Technology Room: Royal Palm 4-6 - Session B4-3 Properties and Characterization of Hard Coatings and Surfaces Moderators: J. Lin, Colorado School of Mines, US, C. Mulligan, U.S. Army ARDEC, Benet Laboratories, US, B. Zhao, Exxon Mobile, US	
1:50 pm	A1-2-1 Microstructure degradation of simple, Pt- and Pt+Pd-modified aluminide coatings on CMSX-4 superalloy under cyclic oxidation conditions, R. SWADZBA, Silesian University of Technology, Poland	B4-3-1	Structure and composition of TiSiCN coatings synthesized by reactive arc evaporation: implications for cutting tool applications., E. GÖTHELID, L. LÖWENBERG, A. GENVALD, B. ERICSSON, M. AHLGREN, Sandvik Tooling, Sweden
2:10 pm	A1-2-2 Influence of vacuum parameters during heat treatment on surface composition of MCrAlY coatings, I. KELLER, D. NAUMENKO, L. SINGHEISER, W.J. QUADAKKERS, Forschungszentrum Jülich GmbH, Germany	B4-3-2	Influence of Process Parameters on the Properties of Low Temperature (Cr _{1-x} Al _x)N Coatings Deposited via Hybrid PVD DC-MSIP/HPPMS, K. BOBZIN, N. BAGCIVAN, M. EWERING, R.H. BRUGNARA, Surface Engineering Institute - RWTH Aachen University, Germany
2:30 pm	A1-2-3 Effect of Water Vapor on Thermally Grown Alumina Scales on Bond Coatings, K. UNOCIC, B. PINT, Oak Ridge National Laboratory, US	B4-3-3	Invited Development of a new type micro slurry-jet erosion (MSE) test method for evaluation of surface strength of hard thin coatings, Y. IWAI, University of Fukui, Japan, T. MATSUBARA, Palmeco Co., Ltd, Japan, K. YAMAMOTO, Kobe Steel Ltd., Japan Invited talk continued.
2:50 pm	A1-2-4 Effect of Water Vapor on the 1100°C Oxidation Behavior of Plasma-Sprayed TBCs with HVOF NiCoCrAlX Bond Coats, J. HAYNES, B. PINT, Oak Ridge National Laboratory, US		
3:10 pm	A1-2-5 Invited High Temperature Oxidation of Mo(Si,Al) ₂ Based Materials, M. HALVARSSON, A. INGEMARSSON, J.-E. SVENSSON, S. CANOVIC, A. JONSSON, A. HELLSTRÖM, L-G. JOHANSSON, Chalmers University of Technology, Sweden	B4-3-5	Investigation of structural ,mechanical and tribological properties of TiAlN/CrN multilayer films deposited by CFUBMS technique, C. LALOGLU, Turkey, Ö. BARAN, Erzincan University, Turkey, Y. TOTIK, İ. EFEÖGLU, Turkey
3:30 pm	Invited talk continued.	B4-3-6	The Phase Transition and Corrosion Resistance of ZrO ₂ (N) Thin Films on AISI 304 Stainless Steel Deposited by Ion Plating, J.H. HUANG, P.H. HUANG, G.P. YU, National Tsing Hua University, Taiwan
3:50 pm	A1-2-8 Microstructural damage criterion for Ni based single crystal superalloy coated with NiAlPt, P. SALLOT, V. MAUREL, L. RÉMY, Mines-ParisTech, France	B4-3-7	Synthesis and Characterization of Boron/Nitrogen Incorporated Diamond-Like-Carbon Thin Films, L.L. ZHANG, Y. LI, Y. TANG, Q. YANG, A. HIROSE, University of Saskatchewan, Canada
4:10 pm	A1-2-9 Compositional and Microstructural Changes in MCrAlY Coatings due to Interdiffusion with the Base Material, D. NAUMENKO, V. SHEMET, A. CHYRKIN, L. SINGHEISER, W.J. QUADAKKERS, Forschungszentrum Jülich GmbH, Germany	B4-3-8	Hardness Percolation in Plasma Enhanced Chemical Vapor Deposited a-SiC:H Thin Films, S. KING, Intel Corporation, US
4:30 pm	A1-2-10 Effects of Hf and Zr additions on the properties and oxidation resistance of β-NiAl+Cr overlay coatings, P. ALFANO, L. WEAVER, University of Alabama, US	B4-3-9	Tungsten-modified hydrogenated amorphous carbon coatings providing tailored friction properties, H. HETZNER, S. TREMMEL, S. WARTZACK, Friedrich-Alexander-University Erlangen-Nuremberg, Germany
4:50 pm	A1-2-11 The application of nanocrystalline NiCrAlY layer in thermal barrier coatings for industrial gas turbines, M.S. HUSSAIN, M. DAROONPARVAR, Universiti Teknologi, Malaysia	B4-3-10	Characterization of Plasma Electrolytic Oxidation (PEO) Coatings on 6082 Aluminium Alloy, A. JARVIS, A. YEROKHIN, University of Sheffield, UK, P. SHASHKOV, Cambridge Nanolytic, Ltd., UK, A. MATTHEWS, University of Sheffield, UK
5:10 pm		B4-3-11	The microstructure and mechanical properties of Cr-Si-Ti-Al-N coatings, Y.C. KUO, National Taiwan University of Science and Technology, Taiwan, J.W. LEE, C.J. WANG, Ming Chi University of Technology, Taiwan
5:30 pm	Bruker Nano Inc.: Focused Topic Session “Advanced 3-D Nano and Micro Scratch Testing of Thin Films with In-line Imaging” Today in Pacific Salon 1-2 4:30 – 5:30 pm		
5:50 pm	Awards Convocation – 5:45 pm Golden Ballroom Honorary Lecturer Sture Hogmark		

Wednesday Afternoon, April 25, 2012

Hard Coatings and Vapor Deposition Technology Room: Royal Palm 1-3 - Session B5-2 Hard and Multifunctional Nano-Structured Coatings Moderators: J. Paulitsch, Christian Doppler Laboratory for Application Oriented Coating Development at the Department of Physical Metallurgy and Materials Testing, Montanuniversität Leoben, R. Sanjines, Ecole Polytechnique Fédérale de Lausanne, P. Zeman, University of West Bohemia, Czech Republic		Tribology & Mechanical Behavior of Coatings and Engineered Surfaces Room: Pacific Salon 1-2 - Session E4-1/G4-1 Coatings for Machining Advanced Materials and for use in Advanced Manufacturing Methods Moderators: M. Arndt, OC Oerlikon Balzers AG, Liechtenstein, X. Nie, University of Windsor, Canada	
1:50 pm	B5-2-1 Tribological properties of $\text{Cr}_{0.65}\text{Al}_{0.35}\text{N}$ -Ag self-lubricating hard coatings from room temperature to 550 °C, C. MULLIGAN, U.S. Army ARDEC, Benet Laboratories, US, P. PAPI, Rensselaer Polytechnic Institute, J. LIN, W. SPROUL, Colorado School of Mines, US, D. GALL, Rensselaer Polytechnic Institute, US	E4-1/G4-1-1 Invited Development of Coating Technology Platforms for Wear Component Applications, I. SPITSBERG, S. BRAHMANDAM, D. SIDDLE, Kennametal Incorporated, US	
2:10 pm	B5-2-2 Invited Mechanical, tribological and thermal properties of sputtered a-C:H:N:Nb coatings, M. FENKER, H. KAPPL, FEM Forschungsinstitut Edelmetalle & Metallchemie, Germany	Invited talk continued.	
2:30 pm	Invited talk continued.	E4-1/G4-1-3 Oxygen Plasma Etching of Diamond-Like Carbon Coated Mold-Die for Micro-Texturing, T. AIZAWA, Shibaura Institute of Technology, Japan, T. AIZAWA, Mitsue Mold Engineering, Co. Ltd., Japan	
2:50 pm	B5-2-4 DLC-MoS ₂ Composite Coatings by Hybrid Technique of Ion Beam Deposition and Sputtering, H. NIAKAN, J.A. SZPUNAR, Q. YANG, University of Saskatchewan, Canada	E4-1/G4-1-5 Tensile properties of magnetron sputtered aluminum-scandium and aluminum-zirconium freestanding thin films: a comparative study, J. KOVAC, H-R. STOCK, B. KÖHLER, H. BOMAS, H-W. ZOCH, Stiftung Institut fuer Werkstofftechnik Bremen, Germany	
3:10 pm	B5-2-5 Growth of Amorphous Hf-Al-Si-N Thin Films by DC Magnetron Sputtering, H. FAGER, Linköping University, IFM, Thin Film Physics Division, Sweden, A. MEI, University of Illinois at Urbana-Champaign, US, B.M. HOWE, Air Force Research Laboratory, US, J.E. GREENE, I. PETROV, University of Illinois at Urbana-Champaign, US, L. HULTMAN, Linköping University, IFM, Thin Film Physics Division, Sweden	E4-1/G4-1-6 Near frictionless based on W-S-X magnetron sputtering coatings for Micromouldings., A. MANAIA, M.T. VIEIRA, R. ALVES, Coimbra University, Portugal	
3:30 pm	B5-2-6 Nanocomposite coatings in the Al-Ge-N system: synthesis, structure and mechanical and optical properties, E. LEWIN, M. PARLINSKA-WOJTAN, J. PATSCHEIDER, Empa, Switzerland	E4-1/G4-1-7 Tribological contact analysis of a CrN coated surface under inclined impact-sliding wear tests against steel and WC balls, J.F. SU, X. NIE, H. HU, University of Windsor, Canada	
3:50 pm	B5-2-7 Shape- Recovery of Thin Film Metallic Glasses Upon Annealing, C. RULLYANI, C. LI, J. CHU, National Taiwan University of Science and Technology, Taiwan	E4-1/G4-1-8 PVD coating development for advanced metal cutting, J. KOHLSCHIEHN, Kennametal, Essen, Germany	
4:10 pm	B5-2-8 Invited Thin Film Metallic Glasses: Unique Properties and Potential Applications, J. CHU, National Taiwan University of Science and Technology, Taiwan		
4:30 pm	Invited talk continued.	Bruker Nano Inc.: FTS Advanced 3-D Nano and Micro Scratch Testing of Thin Films with In-line Imaging, NORM GITIS, Bruker Nano Inc.	
4:50 pm	B5-2-10 Improving the corrosion resistance and hardness of TaN films by silicon addition, G. RAMÍREZ, S.E. RODIL, S. MUHL, G. GALICIA, Universidad Nacional Autónoma de México - Instituto de Investigaciones en Materiales, Mexico, E. CAMPS, L. ESCOBAR-ALARCÓN, Instituto Nacional de Investigaciones Nucleares de México, México, D. SOLIS-CASADOS, Universidad Autónoma del Estado de México - Centro de Investigación en Química Sustentable, Mexico		
5:10 pm	B5-2-11 Combinatorial studies of co-sputtered chromium-titanium oxide composite films, Y. SUN, J. CHANG, M. WONG, National Dong Hwa University, Taiwan		
5:30 pm	Bruker Nano Inc. : Focused Topic Session “Advanced 3-D Nano and Micro Scratch Testing of Thin Films with In-line Imaging” Today in Pacific Salon 1-2 4:30 – 5:30 pm		
5:50 pm	Awards Convocation – 5:45 pm Golden Ballroom Honorary Lecturer Sture Hogmark		

Wednesday Afternoon, April 25, 2012

<p>Applications, Manufacturing, and Equipment Room: Tiki Pavilion - Session G3-1</p> <p>Atmospheric and Hybrid Plasma Technologies Moderators: H. Barankova, Uppsala University, Sweden, R. Gesche, Ferdinand Braun Institut, Germany</p>		<p>Surface Engineering for Thermal Transport, Storage and Harvesting Room: Sunset - Session TS1-1 Surface Engineering for Thermal Transport, Storage and Harvesting Moderators: B. Cola, Georgia Technical Institute, US, C. Muratore, Air Force Research Laboratory, Thermal Sciences and Materials Branch, US</p>	
1:50 pm	<p>G3-1-1 Atmospheric plasma-assisted deposition of antimicrobial coatings on textiles, M. FLEISCHMAN, V. RODRIGUEZ-SANTIAGO, L. PIEHLER, D. PAPPAS, US Army Research Laboratory, US, J. LEADORE, United States Army Research Laboratory, US</p>	TS1-1-1	<p>Textured CrN Thin Coatings Enhancing Heat Transfer in Nucleate Boiling Processes, E.M. SLOMSKI, M. OECHSNER, S. FISCHER, P. STEPHAN, H. SCHEERER, T. TROBMANN, Technische Universität Darmstadt, Germany</p>
2:10 pm	<p>G3-1-2 Cold Atmospheric Plasma Inside Water, H. BARÁNKOVÁ, L. BARDOS, Uppsala University, Sweden</p>	TS1-1-2	<p>Effects of strain on thermal conductivity in amorphous thin films, M.T. ALAM, M.P. MANOHARAN, Penn State University, Mechanical & Nuclear Engineering Department, S.V. SHENOGIN, UES/Air Force Research Laboratory, Materials and Manufacturing Directorate, Thermal Sciences and Materials Branch, US, A. VOEVODIN, A.K. ROY, C. MURATORE, Air Force Research Laboratory, Materials and Manufacturing Directorate, Thermal Sciences and Materials Branch, US, M.D. HAQUE, Penn State University, Mechanical & Nuclear Engineering Department, US</p>
2:30 pm	<p>G3-1-3 Invited Deposition of DLC Films by Nanopulse plasma CVD at atmospheric pressure, N. OHTAKE, Tokyo Institute of Technology, Japan</p>	TS1-1-3	<p>Surface engineering for improved thermal transport at metal/carbon interfaces, S.V. SHENOGIN, UES/Air Force Research Laboratory, Materials and Manufacturing Directorate, Thermal Sciences and Materials Branch, US, J.J. GENGLER, Spectral Energies, LLC/Air Force Research Laboratory, Thermal Sciences and Materials Branch, US, J.J. HU, J.E. BULTMAN, UDRI/Air Force Research Laboratory, Thermal Sciences and Materials Branch, US, A.N. REED, A. VOEVODIN, A.K. ROY, C. MURATORE, Air Force Research Laboratory, Materials and Manufacturing Directorate, Thermal Sciences and Materials Branch, US</p>
2:50 pm	Invited talk continued.	TS1-1-4 Invited	<p>Heat flow across heterojunctions: Toward useful nanoscale thermal interface materials, T.S. FISHER, S.L. HODSON, A. KUMAR, Purdue University, US, A. VOEVODIN, Air Force Research Laboratory, US</p>
3:10 pm	<p>G3-1-5 A study of the interactive effects of hybrid current modes on the tribological properties of a PEO Plasma Electrolytic Oxidation coated AM60B Mg-alloys., R. HUSSEIN, D. NORTHWOOD, X. NIE, University of Windsor, Canada</p>	Invited talk continued.	
3:30 pm	<p>G3-1-6 Insight into Plasma Discharge in PEO: <i>In-situ</i> Impedance Spectroscopy Study, A. YEROKHIN, C.-J. LIANG, University of Sheffield, UK, E. PARFENOV, Ufa State Aviation Technical University, Russian Federation, A. MATTHEWS, University of Sheffield, UK</p>	TS1-1-6	<p>Factorial increases in interfacial thermal conductance using a monolayer, P. O'BRIEN, S.V. SHENOGIN, J. LIU, M. YAMAGUCHI, P. KEBLINSKI, G. RAMANATH, Rensselaer Polytechnic Institute, US</p>
3:50 pm	<p>G3-1-7 Control of ion distribution functions in capacitive sputter sources, D. EREMIN, S. GALLIAN, D. SZEREMLEY, R.P. BRINKMANN, T. MUSSENBRÖCK, Ruhr Universität Bochum, Germany</p>	TS1-1-7	<p>Ruthenium organometallic complexes with photo-switchable wettability for boiling heat transfer applications, N. HUNTER, Air Force Research Laboratory, Materials and Manufacturing Directorate, Thermal Sciences and Materials Branch, US, B. TURNER, Universal Technology Corporation, US, R. GLAVIN, Air Force Research Laboratory, Materials and Manufacturing Directorate, Thermal Sciences and Materials Branch, US, M. JESPERSEN, University of Dayton Research Institute, US, M. CHECK, S. PUTNAM, Universal Technology Corporation, US, A. VOEVODIN, Air Force Research Laboratory, Materials and Manufacturing Directorate, Thermal Sciences and Materials Branch, US</p>
4:10 pm	<p>G3-1-8 Tandem of DBD and ICP RF Atmospheric Plasma Systems for Yttrium Oxide Nanocoating of Consumable Semiconductor Parts, Y. GLUKHOY, A. RYABOY, T. KERZNER, Nanocoating Plasma Systems Inc., US</p>	TS1-1-8	<p>From hard coatings to thermoelectrics: effects of nanostructure on fundamental physical properties of transition metal nitride, oxide, and oxynitride thin film alloys, B.M. HOWE, Air Force Research Laboratory, US</p>
4:30 pm		TS1-1-9	<p>Modified Lithium Alanate for High-Capacity Thermal Energy Storage, A. AMAMA, Air Force Research Laboratory, US, J. GRANT, UDRI/Air Force Research Laboratory, Thermal Sciences and Materials Branch, US, P. SHAMBERGER, A. VOEVODIN, Air Force Research Laboratory, US, T.S. FISHER, Purdue University, US</p>
4:50 pm		TS1-1-10	<p>Heat reduction of concentrator photovoltaic module using high radiation coating, K. NISHIOKA, Y. OTA, University of Miyazaki, Japan, K. TAMURA, K. ARAKI, Daido Steel Co., Ltd., Japan</p>
5:10 pm	<p>Bruker Nano Inc. : Focused Topic Session “Advanced 3-D Nano and Micro Scratch Testing of Thin Films with In-line Imaging” Today in Pacific Salon 1-2 4:30 – 5:30 pm</p>		<p>Awards Convocation – 5:45 pm Golden Ballroom Honorary Lecturer Sture Hogmark</p>

Thursday Morning, April 26, 2012

Coatings for Use at High Temperature Room: Sunrise - Session A1-3 Coatings to Resist High Temperature Oxidation, Corrosion and Fouling Moderators: D. Naumenko, Forschungszentrum Jülich GmbH, Germany, B. Hazel, Pratt and Whitney, US, F. Perez Trujillo, Universidad Complutense de Madrid, Spain, L-G. Johansson, Chalmers University of Technology, Sweden		Coatings for Use at High Temperature Room: Sunrise - Session A3-1/F8-1 Coatings for Fuel Cells & Batteries Moderators: G. Dadheech, General Motors, US, E. Yu, Newcastle University, UK	
8:00 am	A1-3-1 Invited Development of high-temperature oxidation resistant coatings by electrodeposition, X. PENG, Institute of Metal Research, Chinese Academy of Sciences, China		
8:20 am	Invited talk continued.		
8:40 am	A1-3-3 Producing high temperature multifunction coatings on the basis of micro-sized spherical aluminum particles, R. ROUSSEL, M. JUEZ LORENZO, V. KUCHENREUTHER, V. KOLARIK, Fraunhofer ICT, Germany		
9:00 am	A1-3-4 Thermal barrier coatings on γ -TiAl protected by the halogen effect, s. FRIEDLE, M. SCHÜTZE, Dechema e.V., Frankfurt am Main, Germany, N. NIEBEN, R. BRAUN, DLR - Deutsches Zentrum für Luft- und Raumfahrt, Germany		
9:20 am	A1-3-5 High Temperature Protection of Ferritic Steels by Nano-Structured Coatings: Supercritical Steam Turbines Applications, S. MATO, P. HIERRO, I. CASTAÑEDA, A. ALCALÁ, I. LASANTA, Universidad Complutense de Madrid, Spain, M. TEJERO, Universidad Complutense de Madrid, Spain, J. SÁNCHEZ, Instituto de Ciencia de Materiales de Sevilla, Spain, M. BRIZUELA, Tecnalia, Spain, J. PÉREZ, Universidad Complutense de Madrid, Spain		
9:40 am			
10:00 am		A3-1/F8-1-7 Invited Oxidation of SOFC Interconnects, M. UEDA, K. KAWAMURA, T. MARUYAMA, Tokyo Institute of Technology, Japan	
10:20 am		Invited talk continued.	
10:40 am		A3-1/F8-1-9 Microstructural Investigation of Co- and RE-nanocoatings on FeCr Steels, S. CANOVIC, J. FROITZHEIM, R. SACHITANAND, M. NIKUMAA, M. HALVARSSON, L-G. JOHANSSON, J.-E. SVENSSON, Chalmers University of Technology, Sweden	
11:00 am		A3-1/F8-1-10 Nafion membrane surface coated with self-assembly membrane containing nanometer-sized Pt-Sn particles to mitigate methanol crossover, C.H. LIN, National Chung Hsing University, Taiwan, C.H. WAN, MingDao University, Taiwan, M.T. LIN, W. WU, National Chung Hsing University, Taiwan	
11:20 am		A3-1/F8-1-11 Suppression of methanol crossover with self-assembly membrane containing Pt ₃₅ -Ru ₆₅ catalyst particles coated on Nafion membrane surface, C.H. WAN, MingDao University, Taiwan, M.T. LIN, National Chung Hsing University, Taiwan, Y. JHENG, MingDao University, Taiwan	
11:40 am		A3-1/F8-1-12 Supercapacitance of Bamboo-Type Anodic Titania Nanotubes Array, Z. ENDUT, M.H. ABD SHUKOR, Center of Advanced Manufacturing and Material Processing, Malaysia, W.J. BASIRUN, University of Malaya, Malaysia	
12:00 pm	ELSEVIER FTS: How to Get Published Royal Palm 1-3 12:15 – 1:15 pm	2013 ICMCTF Planning Meeting Pacific Salon 1-2 12:00 – 1:15 pm All interested attendees are welcome	

Thursday Morning, April 26, 2012

Hard Coatings and Vapor Deposition Technology Room: Royal Palm 4-6 - Session B2-1 CVD Coatings and Technologies Moderators: F. Maury, CIRIMAT, France, S. Ruppi, Walter AG, Germany		Hard Coatings and Vapor Deposition Technology Room: Royal Palm 1-3 - Session B6-1 Coating Design and Architectures Moderators: C. Mitterer, Montanuniversität Leoben, Austria, M. Stueber, Karlsruhe Institute of Technology, Germany	
8:00 am	B2-1-1 AlTiN-CVD coatings - a new coating family for cast iron cutting with a high productivity, P. IMMICH, U. KRETZSCHMANN, U. SCHUNK, M. ROMMEL, LMT Fette Werkzeugtechnik, Germany, R. PITONAK, R. WEIBENBACHER, Böhlerit, Austria	B6-1-1 Invited	Combinatorial Development of Transition Metal Nitride Thin Films for Wear Protection, R. CREMER, KCS Europe GmbH, Germany
8:20 am	B2-1-2 C ₂ H ₆ as precursor for low pressure chemical vapour deposition of TiCNB hard coatings, C. CZETTL, Ceratizit Austria GmbH, Austria, C. MITTERER, Montanuniversität Leoben, Austria, M. PENOY, C. MICHOTTE, Ceratizit Luxembourg S.à.r.l., Luxembourg, M. KATHREIN, Ceratizit Austria GmbH, Austria	Invited talk continued.	
8:40 am	B2-1-3 Invited The Effects of Microstructure and Thermal Stresses on the Hardness of CVD Deposited α -Al ₂ O ₃ and TiC _x N(1-x) Coatings, H. CHIEN, Carnegie Mellon University, US, Z. BAN, P. PRICHARD, Y. LIU, Kennametal Incorporated, US, S. ROHRER, Carnegie Mellon University, US	B6-1-3	Compositional and Structural Evolution of Sputtered Ti-Al-N Thin Films as a Function of the used Target, P.H. MAYRHOFER, B. GROSSMANN, R. RACHBAUER, OC Oerlikon Balzers AG, Liechtenstein, P. POLCIK, PLANSEE Composite Materials GmbH, Germany
9:00 am	Invited talk continued.	B6-1-4	Deposition of TiAlN based coatings combined with subsequent electron beam surface treatment, K. WEIGEL, M. KEUNECKE, K. BEWLOGUA, Fraunhofer IST, Germany, R. ZENKER, TU Bergakademie Freiberg; Zenker Consult, Germany, S. SCHMIED, TU Bergakademie Freiberg, Germany
9:20 am	B2-1-5 3D EBSD analysis of CVD ceramics coatings, M. IGARASHI, A. OSADA, Mitsubishi Materials Corporation, Japan, C. SCHUH, Massachusetts Institute of Technology, US	B6-1-5	Influence of the plasma characteristic on the structure, properties and cutting performance of the (Ti,Al)N coatings deposited by cathodic arc evaporation, D. KURAPOV, S. KRASSNITZER, T. BACHMANN, J. HAGMANN, M. ARNDT, W. KALSS, H. RUDIGIER, OC Oerlikon Balzers AG, Liechtenstein
9:40 am	B2-1-6 TiSiN and TiSiCN hard coatings by CVD, I. ENDLER, M. HÖHN, J. SCHMIDT, S. SCHOLZ, M. HERRMANN, Fraunhofer IKTS, Germany, M. KNAUT, TU Dresden, Germany	B6-1-6	Effect of the interlayer coating architecture on the optimization of diamond deposition, A. POULON-QUINTIN, A. HODROJ, C. FAURE, L. TEULE-GAY, J-P. MANAUD, ICMCB-CNRS, France
10:00 am	B2-1-7 High temperature chemical vapor deposition of highly crystallized and textured silicon on metals for solar conversion, O. GOURMALA, R. BENABOUD, G. CHICHIGNOUD, E. BLANQUET, C. JIMENEZ, B. DOISNEAU, K. ZAIDAT, M. PONS, Grenoble INP, France	B6-1-7 Invited	Application Oriented Design of PVD-Coatings for Tools and Components, K. BOBZIN, Surface Engineering Institute - RWTH Aachen University, Germany, N. BAGCIVAN, RWTH Aachen University, Germany, M. EWERING, Surface Engineering Institute - RWTH Aachen University, Germany
10:20 am	B2-1-8 In-line Deposition of Silicon-based Films by Hot-Wire Chemical vapor Deposition, L. SCHÄFER, T. HARIG, M. HÖFER, A. LAUKART, Fraunhofer IST, Germany, D. BORCHERT, KEIPERT-COLBERG, Fraunhofer ISE, Germany, J. TRUBE, Leybold Optics GmbH, Germany	Invited talk continued.	
10:40 am	B2-1-9 Oxidation Resistance of Graphene Coated Metal Films: A Protective Coating, PRAMODAKUMAR. NAYAK, CHAN-JUNG. HSU, National Cheng Kung University, Taiwan, S.C. WANG, Southern Taiwan University, Taiwan, JAMESC. SUNG, KINIK Company, Taiwan, JOW-LAY. HUANG, National Cheng Kung University, Taiwan	B6-1-9	Structural model for the spinodal decomposition of Nb-Si-N nanocomposites based on ellipsometric results., G. RAMÍREZ, S.E. RODIL, S. MUHL, Universidad Nacional Autónoma de México - Instituto de Investigaciones en Materiales, México, M. RIVERA, Instituto de Física - Universidad Nacional Autónoma de México, México
11:00 am	B2-1-10 Highly chemically reactive AP-CVD coatings: Influence of the deposition parameters and application for thermally reversible interfacial bonding., M. MORENO-COURANJOU, A. MANAKHOV, N.D. BOSCHER, Centre de Recherche Public - Gabriel Lippmann, Luxembourg, J.J. PIREAUX, University of Namur (FUNDP), Belgium, A. CHOQUET, Centre de Recherche Public - Gabriel Lippmann, Luxembourg	B6-1-10	Characterization of the tribological and abrasive wear behaviour of carbon fibre reinforced epoxy composites in contact with a diamond-like carbon layer, H.-J. SCHEIBE, Fraunhofer IWS, Germany, M. ANDRICH, W. HUFENBACH, K. KUNZE, Technische Universität Dresden, Germany, J. BIJWE, Indian Institute of Technology, India, A. LESON, M. LEONHARDT, Fraunhofer IWS, Germany
11:20 am	B2-1-11 Optical properties of the ZnO thin films grown on glass substrates using catalytically generated high-energy H ₂ O, E. NAGATOMI, S. SATOMOTO, M. TAHARA, T. KATO, K. YASUI, Nagaoka University of Technology, Japan	B6-1-11 Invited	Direct current magnetron sputtering of ZrB ₂ from a compound target, H. HÖGBERG, Linköping University, Sweden
11:40 am	B2-1-12 Efficiency of indium oxide with doped tin by thermal evaporation and their optoelectronic properties, K.Y. PAN, National Tsing Hua University, Taiwan, L.D. LIN, Chinese Culture University, Taiwan, L.W. CHANG, H.C. SHIH, National Tsing Hua University, Taiwan	Invited talk continued.	
12:00 pm	2013 ICMCTF Planning Meeting Pacific Salon 1-2 12:00 – 1:15 pm All interested attendees are welcome		ELSEVIER FTS: How to Get Published Royal Palm 1-3 12:15 – 1:15 pm

Thursday Morning, April 26, 2012

Tribology & Mechanical Behavior of Coatings and Engineered Surfaces Room: Tiki Pavilion - Session E2-1 Mechanical Properties and Adhesion Moderators: M.T. Lin, National Chung Hsing University, Taiwan, D. Bahr, Washington State University, US, R. Chromik, McGill University, Canada, W. Clegg, University of Cambridge, UK		Tribology & Mechanical Behavior of Coatings and Engineered Surfaces Room: Pacific Salon 1-2 - Session E4-2/G4-2 Coatings for Machining Advanced Materials and for use in Advanced Manufacturing Methods Moderators: M. Arndt, OC Oerlikon Balzers AG, Liechtenstein, X. Nie, University of Windsor, Canada	
8:00 am	E2-1-1 Strain hardening behavior in multilayer thin films, D. BAHR, RL. SCHOEPPNER, S. LAWRENCE, I. MASTORAKOS, H. ZBIB, Washington State University, US	E4-2/G4-2-1	New Coating Systems for Temperature Monitoring in Turning Processes, M. KIRSCHNER, K. PANTKE, D. BIERMANN, Institute of Machining Technology, Germany, J. HERPER, W. TILLMANN, Institute of Materials Engineering, Germany
8:20 am	E2-1-2 Adhesion of tetrahedral amorphous carbon (ta-C) coatings deposited on different substrates: Simulations and experimental verification, N. BIERWISCH, Saxonian Institute of Surface Mechanics, Germany, G. FAVARO, CSM Instruments SA, Switzerland, J. RAMM, OC Oerlikon Balzers AG, Liechtenstein, N. SCHWARZER, Saxonian Institute of Surface Mechanics, Germany, M. SOBIECH, B. WIDRIG, OC Oerlikon Balzers AG, Liechtenstein	E4-2/G4-2-2	Hybrid TiSiN, CrCx/a-C:H PVD Coatings Applied to Cutting Tools, w. HENDERER, F. XU, Kennametal Incorporated, US
8:40 am	E2-1-3 Invited Analysis on the stress transfer and the interfacial strength of carbon coatings on metallic substrate using in-situ tensile and nanobending experiments in SEM and Raman spectroscopy., K. DURST, University Erlangen-Nuernberg, Germany	E4-2/G4-2-3	Effect of the Cutting Edge Entry Impact Duration on the Coated Tool's Wear in Down and Up Milling, K.-D. BOUZAKIS, Aristoteles University of Thessaloniki; Fraunhofer Project Center Coating in Manufacturing, Greece, G. KATIRTZOGLU, E. BOUZAKIS, S. MAKRIMALLAKIS, G. MALIARIS, Aristoteles University of Thessaloniki; Fraunhofer Project Center Coatings in Manufacturing, Greece
9:00 am	Invited talk continued.	E4-2/G4-2-4	Cutting performance of PVD coatings during dry drilling of sustainable austempered ductile iron (ADI), A. MEENA, M. EL MANSORI, Arts et Métiers ParisTech, France
9:20 am	E2-1-5 Study of adhesion and cracking of TiO ₂ coatings on a Ti alloy using an impact-sliding testing instrument, X. NIE, University of Windsor, Canada	E4-2/G4-2-5 Invited	Process design for the machining of high-strength steels, F. FELDERHOFF, Robert Bosch GmbH, Germany
9:40 am	E2-1-6 Influence of oxide film properties on the adhesion performance of epoxy-coated aluminium, O. ÖZKANAT, Delft University of Technology, Netherlands; Materials innovation institute (M2i), Netherlands, J.M.C. MOL, J.H.W. DE WIT, Delft University of Technology, Netherlands, H. TERRYN, Vrije Universiteit Brussel, Materials innovation institute (M2i), Belgium	Invited talk continued.	
10:00 am	E2-1-7 Adhesion and fatigue properties of TiB ₂ -MoS ₂ composite coatings deposited by closed-field unbalanced magnetron sputtering, F.B. BIDEV, O. BARAN, E. ARSLAN, Y. TOTIK, I. EFEUGLU, Ataturk University, Turkey	E4-2/G4-2-7	A nanostructured cutting edge, J. RECHBERGER, J. MAUSHART, Fraisa SA, Switzerland
10:20 am	E2-1-8 Coating thickness and interlayer effects on CVD-diamond film adhesion to cobalt-cemented tungsten carbides, P. LU, The University of Alabama, US, H. GOMEZ, University of South Florida, US, X. XIAO, M.J. LUKITSCH, A. SACHDEV, General Motors, US, D. DURHAM, A. KUMAR, University of South Florida, US, K. CHOU, The University of Alabama, US	E4-2/G4-2-9	Application of thick PVD coating deposited by new AIP cathode SFC for machining of automotive component, K. YAMAMOTO, S. TANIFUJI, Kobe Steel Ltd., Japan, G. FOX-RABINOVICH, McMaster University, Canada
10:40 am	E2-1-9 On the effect of pressure induced change of Young's modulus, hardness and yield strength, N. SCHWARZER, Saxonian Institute of Surface Mechanics, Germany	E4-2/G4-2-10	Evaluation of the Abrasive Wear Resistance of Nitride, Oxynitride and Oxide PVD Coatings at High Temperatures, P. DESSARZIN, P. KARVANKOVA, M. MORSTEIN, Platit AG, Switzerland, J. NOHAVA, CSM Instruments SA, Switzerland
11:00 am	E2-1-10 Invited A review of claims for ultra hardness in nanocomposite coatings, A. FISCHER-CRIPPS, Fischer-Cripps Laboratories Pty Ltd, Australia	E4-2/G4-2-11	Application-oriented coating and post-treatment for high performance broad band drilling operations, T. MICHALKE, Oerlikon Balzers Germany GmbH, Germany, S. STEIN, M. ARNDT, OC Oerlikon Balzers AG, Liechtenstein
11:20 am	Invited talk continued.		
11:40 am	ELSEVIER FTS: How to Get Published Royal Palm 1-3 12:15 – 1:15 pm		2013 ICMCTF Planning Meeting Pacific Salon 1-2 12:00 – 1:15 pm All interested attendees are welcome

Thursday Morning, April 26, 2012

Energetic Materials and Micro-Structures for Nanomanufacturing Room: Sunset - Session TS3-1 Energetic Materials and Micro-Structures for Nanomanufacturing Moderators: C. Rebholz, University of Cyprus, Cyprus, C. Doumanidis, University of Cyprus, Cyprus, T. Ando, Northeastern University, US		
8:00 am	TS3-1-1 Invited Recent ADvances in Nanolaminate Energetic Materials, c. ROSSI, 1CNRS; LAAS, France	
8:20 am	Invited talk continued.	
8:40 am	TS3-1-3 Comparison of engineered nanocoatings on the combustion of aluminum and copper oxide nanothermites, E. COLLINS, M. PANTOYA, A. VIJAYASAI, T. DALLAS, Texas Tech University, US	
9:00 am	TS3-1-4 Study of the reactive dynamics of nanometric Ru/Al multilayers using molecular dynamics, D. H. CHOI, J. A. P. M. D. BARAS, Université de Bourgogne - CNRS, France <div style="position: absolute; top: 50%; left: 50%; transform: translate(-50%, -50%) rotate(-45deg); font-weight: bold; font-size: 2em; color: black;">WITHDRAWN</div>	
9:20 am	TS3-1-5 Invited Exothermic metal-metal multilayers: Pulsed laser ignition thresholds, reaction modes and effects of environment, D. ADAMS, R. REEVES, P. MCDONALD, D. JONES, JR., M. RODRIGUEZ, Sandia National Laboratories, US	
9:40 am	Invited talk continued.	
10:00 am	TS3-1-7 Time-Resolved Emission Spectroscopy Of Electrically Heated Energetic Ni/Al Laminates, C. MORRIS, U.S. Army Research Laboratory, US, P. WILKINS, C. MAY, Lawrence Livermore National Laboratory, US, T. WEIHS, Johns Hopkins University, US	
10:20 am	TS3-1-8 Numerical simulations of self-propagating reactions and analysis of reacted microstructures in Ru/Al multilayers, K. WOLL, Functional Materials, Dept of Materials Science and Engineering, Saarland University, Germany, I. GUNDUZ, C. REBHOLZ, Dept. of Mechanical and Manufacturing Engineering, University of Cyprus, Cyprus, F. MÜCKLICH, Functional Materials, Dept of Materials Science and Engineering, Saarland University, Germany	
10:40 am	TS3-1-9 Fabrication, Characterization and Applications of Novel Nanoheater Structures, Z. GU, Q. CUI, J. CHEN, J. BUCKLEY, University of Massachusetts Lowell, US, T. ANDO, D. ERDENIZ, Northeastern University, US, P. WONG, Tufts University, US, C. REBHOLZ, A. HADJIAFEXENTI, I. GUNDUZ, C. DOUMANIDIS, University of Cyprus, Cyprus	
11:00 am	TS3-1-10 Effect of Mechanical Activation on SHS and Structure Formation in Nanostructured Geterogenous Reaction Systems, N. SHKODICH, VADCHENKO, ROGACHEV, SACHKOVA, Institute of Structural Macrokineitics and Materials Science RAS, Russia, NEDER, MAGERL, Institute of Crystallography and Structural Physics, University of Erlangen-Nürnberg, Germany	
11:20 am	<div style="text-align: center;"> 2013 ICMCTF Planning Meeting Pacific Salon 1-2 12:00 – 1:15 pm All interested attendees are welcome </div>	ELSEVIER FTS: How to Get Published Royal Palm 1-3 12:15 – 1:15 pm
11:40 am		

Thursday Afternoon, April 26, 2012

Coatings for Use at High Temperature Room: Sunrise - Session A3-2/F8-2		Hard Coatings and Vapor Deposition Technology Room: Royal Palm 4-6 - Session B2-2	
Coatings for Fuel Cells & Batteries Moderators: E. Yu, Newcastle University, UK, G. Dadheech, General Motors, US		CVD Coatings and Technologies Moderators: S. Ruppi, Walter AG, Germany, F. Maury, CIRIMAT, France	
1:30 pm	A3-2/F8-2-1 A Study on the high temperature charge-discharge characteristics of Si-xAl thin film anode for Li-ion batteries, Y.T. SHIH, C.H. WU, F.Y. HUNG, T.S. LUI, L.H. CHEN, National Cheng Kung University, Taiwan	B2-2-1 Invited CVD – Opportunities and Challenges, H. HOLZSCHUH, SuCoTec AG, Switzerland	
1:50 pm	A3-2/F8-2-2 Pseudo-capacitive performance of the Manganese oxide/Carbon Nanocapsules (CNC) electrode by Sol-gel technique, C. LIN, C.H. WU, C.W. WANG, C.Y. CHEN, Feng Chia University, Taichung, Taiwan, LEE, National Cheng Kung University, Taiwan	Invited talk continued.	
2:10 pm	A3-2/F8-2-3 Invited Electrified Vehicles for Personal Transportation and the Critical Role of Surface Coatings for Lithium Ion Batteries, M. VERBRUGGE, X. XIAO, General Motors Research and Development Center, US, R. DESHPANDE, J. LI, Y.T. CHENG, University of Kentucky, US	B2-2-3 SiC coatings grown by liquid injection chemical vapor deposition using single source metalorganic precursors., G. BOISSELIER, F. MAURY, CIRIMAT, France, F. SCHUSTER, CEA, France	
2:30 pm	Invited talk continued.	B2-2-4 Multilayer Diamond Coatings: Theory, Implementation in Production and Results in different Applications, J.C. BAREISS, W. KOELKER, C. SCHIFFERS, M. WEIGAND, O. LEMMER, CemeCon AG, Germany	
2:50 pm	A3-2/F8-2-5 Comparison of corrosion behaviors between AISI 304 stainless steel and Ti substrate s coated with TiZrN/TiN thin films as bipolar plate for unitized regenerative fuel cell, M.T. LIN, National Chung Hsing University, Taiwan, C.H. WAN, MingDao University, Taiwan, W. WU, National Chung Hsing University, Taiwan	B2-2-5 Adhesion of the DLC film on iron based materials as a function of gradient interlayer properties, D. BAQUIÃO, G. FARIA, L. SILVA JUNIOR, Institute for Space Research, Brazil, L. BONETTI, Clorovale Diamantes S.A., Brazil, E. CORAT, V. TRAVA-AIROLDI, Institute for Space Research, Brazil	
3:10 pm	A3-2/F8-2-6 Progress towards, thin, cost-effective coatings for PEMFC metallic Bipolar Plates by closed field unbalanced magnetron sputter ion plating., H. SUN, K. COOKE, Teer Coatings Limited, Miba Coating Group, UK, G. EITZINGER, High Tech Coatings GmbH, Miba Coating Group, Austria, P. HAMILTON, B. POLLET, University of Birmingham, UK	B2-2-6 Effect of the carrier gas flow rate on boron-doped diamond synthesis using mode-conversion type microwave plasma CVD, H.S. SHIMOMURA, Y. SAKAMOTO, Chiba Institute of Technology, Japan	
3:30 pm	A3-2/F8-2-7 Silica-Based Hydrophilic Bipolar Plate Coatings for PEM Fuel Cells, G. DADHEECH, BLUNK, General Motors, US	B2-2-7 Low temperature chemical vapor deposition of boron-carbon films for use in neutron detectors, H. PEDERSEN, Linköping University, Sweden, C. HÖGLUND, European Spallation Source ESS AB/ Linköping University, Sweden, J. BIRCH, J. JENSEN, A. HENRY, Linköping University, Sweden	
3:50 pm	A3-2/F8-2-8 Surface morphology and catalyst activity of Sn-Pt nanoparticles coated on anodizing aluminum oxide, C.C. CHEN, C.L. CHEN, Y.S. LAI, National United University, Taiwan	B2-2-8 Synthesis of diamond/carbon nanotube composite thin films by chemical vapor deposition, L. YANG, Q. YANG, Y. LI, Y. TANG, C. ZHANG, L.L. ZHANG, University of Saskatchewan, Canada	
4:10 pm		B2-2-9 Effects of ammonia/acetylene mixtures on the properties of carbon films prepared by thermal chemical vapor deposition, L.H. LAI, S.T. SHIUE, National Chung Hsing University, Taiwan	
4:30 pm		B2-2-10 Hollow-Cathode Deposition of Thin Films Via Metal Hydride Formation and Decomposition, S. MUHL, Universidad Nacional Autónoma de México - Instituto de Investigaciones en Materiales, Mexico, . LOPEZ, IIM-UNAM, Mexico, Y. PENA-RODRIGUEZ, Autonomous University of Madrid, Spain	
4:50 pm	Poster Session 5:00 – 7:00 pm Golden Ballroom Reception begins at 6:00 pm	Oerlikon Leybold Vacuum Focused Topic Session Vacuum and Applications for Thin Film Coating Systems Pacific Salon 1-2 4:10-5:10 pm	
5:10 pm			

Thursday Afternoon, April 26, 2012

Hard Coatings and Vapor Deposition Technology Room: Royal Palm 1-3 - Session B6-2 Coating Design and Architectures Moderators: C. Mitterer, Montanuniversität Leoben, Austria, M. Stüber, Karlsruhe Institute of Technology, Germany		Fundamentals and Technology of Multifunctional Thin Films: Towards Optoelectronic Device Applications Room: Sunset - Session C5-1/F7-1 Polarisation Phenomena in Thin Films and Devices Moderators: D. Holec, Montanuniversität Leoben, Austria, S. Moram, University of Cambridge, UK	
1:30 pm	B6-2-1 Invited A Knowledge-Based Approach for Optimized Coating Architecture, R. DANIEL, J. KECKES, C. MITTERER, Montanuniversität Leoben, Austria	C5-1/F7-1-1 Invited Recent Advances in the Thin Film Electro-Acoustic Technology, I. KATARDJIEV, V. YANTCHEV, Uppsala University, Angstrom Laboratory, Sweden	
1:50 pm	Invited talk continued.	Invited talk continued.	
2:10 pm	B6-2-3 Gradient chemical composition in layered pulsed reactive sputtered coatings for decorative purposes, A. CAVALEIRO, N.M.G. PARREIRA, University of Coimbra, Portugal, T. POLCAR, University of Southampton, UK, T. KUBART, Uppsala University, Angstrom Laboratory, Sweden, M. VASILEVSKIY, University of Minho, Portugal	C5-1/F7-1-3 Asymmetric electrical properties for dual-gate InGaZnO TFT under gate bias and light illumination, T.C. CHEN, NSYSU, Taiwan	
2:30 pm	B6-2-4 Investigation of the nucleation behavior of oxides synthesized by reactive arc evaporation from Al, Cr and Al-Cr targets, M. DÖBELI, ETH, Zürich, Switzerland, J. RAMM, H. RUDIGIER, OC Oerlikon Balzers AG, Liechtenstein, J. THOMAS, Leibniz-Institut für Festkörper- und Werkstofforschung, Germany, B. WIDRIG, OC Oerlikon Balzers AG, Liechtenstein	C5-1/F7-1-4 A systematic <i>ab-initio</i> study of the piezoelectricity in wurtzite nitride alloys: ScAlN, ScGaN, ScInN, YAlN, YInN, C. THOLANDER, F. TASNADI, I. ABRIKOSOV, Linköping University, Sweden	
2:50 pm	B6-2-5 Invited Phase stability of TiAlNO, M. TO BABEN, J. SCHNEIDER, Materials Chemistry, RWTH Aachen university, Germany	C5-1/F7-1-5 Investigation of the bias illumination stress for an InGaZnO TFT with and without Al ₂ O ₃ passivation layer, S.Y. HUANG, T.C. CHANG, National Sun Yat-Sen University, Taiwan	
3:10 pm	Invited talk continued.	C5-1/F7-1-6 Invited Control and Engineering of Spontaneous and Piezoelectric Polarisation in Nitride-based Nanostructures, E. O'REILLY, Tyndall National Institute; University College Cork, Ireland, S. SCHULZ, Tyndall National Institute, Ireland, M. CARO, Tyndall National Institute; University College Cork, Ireland	
3:30 pm	B6-2-7 On the formation of cubic and corundum structured (Al,Cr) ₂ O ₃ coatings synthesized by cathodic arc evaporation, H. NAJAFI, A. KARIMI, EPFL, Switzerland, P. DESSARZIN, M. MORSTEIN, Platit AG, Switzerland	Invited talk continued.	
3:50 pm	B6-2-8 Parametric Study on the Effect of Reactive Nitrogen on the Growth, Morphology and Optical Constants of ZrO _x N _y Thin Films, V. RAMANA, M. HERNANDEZ, University of Texas at El Paso, US, L. CAMPBELL, Air Force Research Laboratory, US	C5-1/F7-1-8 Growth and characterization of magnetron sputtered wurtzite Y _x Al _{1-x} N thin films, A. ZUKAUSKAITE, G. WINGQVIST, C. THOLANDER, F. TASNADI, J. BIRCH, L. HULTMAN, Linköping University, Sweden	
4:10 pm	B6-2-9 Stage-gate approach for the development of corrosion and erosion resistant PVD multilayer coatings, J. ELLERMEIER, U. DEPNER, T. TROßMANN, M. OECHSNER, Zentrum für Konstruktionswerkstoffe - TU Darmstadt, Germany, K. BOBZIN, N. BAGCIVAN, S. THEISS, R. WEIB, Surface Engineering Institute - RWTH Aachen University, Germany	C5-1/F7-1-9 Investigating Degradation Behavior of InGaZnO Thin-Film Transistors induced by Charge-Trapping Effect under DC and AC Gate-Bias Stress, T.Y. HSIEH, T.C. CHANG, T.C. CHEN, M.Y. TSAI, Y.T. CHEN, National Sun Yat-Sen University, Taiwan, F.Y. JIAN, National Chiao Tung University, Taiwan, W.S. LU, National Sun Yat-Sen University, Taiwan	
4:30 pm	B6-2-10 Biomimetics in thin film design – Enhanced properties by multilayer coatings and nanostructured surfaces, J.M. LACKNER, W. WALDHAUSER, Joanneum Research Forschungsges.m.b.H., Institute of Surface Technologies and Photonics, Functional Surfaces, Austria, L. MAJOR, Polish Academy of Sciences, Institute for Metallurgy and Materials Science, Poland, C. TEICHERT, Montanuniversität Leoben, Austria, P. HARTMANN, Joanneum Research Forschungsges.m.b.H., Institute of Surface Technologies and Photonics, Functional Surfaces, Austria	C5-1/F7-1-10 Piezoelectric Response During Nanoindentation in Scandium Aluminum Nitride Alloy Thin Films, E. BROITMAN, A. ZUKAUSKAITE, G. WINGQVIST, P. SANDSTRÖM, L. HULTMAN, Linköping University, Sweden	
4:50 pm		C5-1/F7-1-11 Investigating the degradation behavior under Hot Carrier Stress for InGaZnO TFT with symmetric and asymmetric structure, M.Y. TSAI, NSYSU, Taiwan	
5:10 pm	Poster Session 5:00 – 7:00 pm Golden Ballroom Reception begins at 6:00 pm		Oerlikon Leybold Vacuum Focused Topic Session Vacuum and Applications for Thin Film Coating Systems Pacific Salon 1-2 4:10-5:10 pm
5:30 pm			

Thursday Afternoon, April 26, 2012

Tribology & Mechanical Behavior of Coatings and Engineered Surfaces Room: Tiki Pavilion - Session E2-2 Mechanical Properties and Adhesion Moderators: M.T. Lin, National Chung Hsing University, Taiwan, W. Clegg, University of Cambridge, R. Chromik, McGill University, D. Bahr, Washington State University, US		Post Deadline Discoveries and Innovations Room: Pacific Salon 1-2 - Session PD-1 Post Deadline Discoveries and Innovations Moderators: W. Kalss, OC Oerlikon Balzers AG, Liechtenstein, S. Ulrich, Karlsruhe Institute of Technology, Germany
1:30 pm	E2-2-1 Micromechanical testing at up to 700 °C and in vacuum, S. KORTE, University of Erlangen-Nürnberg, Germany, L. SHIYU, R. STEARN, W. CLEGG, University of Cambridge, UK	PD-1-1 The Multi Beam Sputtering: a new thin film deposition approach, P. SORTAIS, T. LAMY, J. MÉDARD, Laboratoire de Physique Subatomique et Cosmologie de Grenoble (LPSC), France
1:50 pm	E2-2-2 Characterization of a self assembled monolayer using a MEMS tribogauge, A. VIJAYASAI, T. DALLAS, G. SIVAKUMAR, C. ANDERSON, R. GALE, G. RAMACHANDRAN, Texas Tech University, US	PD-1-2 Molecular dynamics simulation and experimental validation of nanoindentation measurements of silicon carbide coatings., A.-P. PRSKALO, Universität Stuttgart, Germany, S. ULRICH, Karlsruhe Institute of Technology, Germany, S. SCHMAUDER, J. LICHTENBERG, C. ZIEBERT, Kit, Iam-Awp, Germany
2:10 pm	E2-2-3 Invited In-situ SEM mechanical testing for adhesion energy mapping of multilayered Cu wiring structures in integrated circuits, S. KAMIYA, N. SHISHIDO, H. SATO, K. KOIWA, Nagoya Institute of Technology, JST CREST, Japan, M. OMIYA, Keio University, JST CREST, Japan, C. CHEN, Nagoya Institute of Technology, Japan, M. NISHIDA, Nagoya Institute of Technology, JST CREST, Japan, T. NAKAMURA, T.S. SUZUKI, Fujitsu Laboratories Limited, Japan, T. NOKUO, T. NAGASAWA, JEOL Limited, JST CREST, Japan	PD-1-3 Anatase TiO ₂ Beads Having Ultra-fast Electron Diffusion Rates for use in Low Temperature Flexible Dye-sensitized Solar Cells, J.-M. TING, KE, National Cheng Kung University, Taiwan
2:30 pm	Invited talk continued.	PD-1-4 MOCVD nano-structured TiO ₂ coatings for corrosion protection of stainless steels, H. HERRERA-HERNÁNDEZ, M. PALOMAR-PARDAVÉ, Universidad Autónoma Metropolitana- Azcapotzalco, Mexico, J.A. GALAVIZ-PÉREZ, J.R. VARGAS-GARCÍA, Departamento de Ingeniería, Metalúrgica, ESIQIE-IPN, Mexico
2:50 pm	E2-2-5 Preparation and Characterization of Super- and Ultrahard Nanocomposites, S. VEPREK, M. VEPREK-HEIJMAN, Technical University Munich, Germany, A.S. ARGON, Massachusetts Institute of Technology, US	PD-1-5 Improvement on the mechanical and corrosion properties of nanometric HfN/VN superlattices, P. PRIETO, Excellence Center for Novel Materials, CENM, Cali, Colombia, C.A. ESCOBAR, Universidad del Valle, Colombia, J.C. CAICEDO, Universidad del Valle, Colombia, W. APERADOR, Universidad Militar Nueva Granada, Colombia, J. ESTEVE, M.E. GOMEZ, Universitat de Barcelona, Spain
3:10 pm	E2-2-6 An expression to determine the Vickers indentation fracture toughness of Fe ₂ B layers obtained by the finite element method, A. MENESES-AMADOR, Instituto Politécnico Nacional, Mexico, I. CAMPOS-SILVA, SEPI ESIME Zacatenco, Mexico, J. MARTINEZ-TRINIDAD, Instituto Politécnico Nacional, Mexico, S. PANIER, Ecole des Mines de Douai, France, G.A. RODRIGUEZ-CASTRO, A. TORRES-HERNÁNDEZ, Instituto Politécnico Nacional, Mexico	PD-1-6 Characterization of High Temperature Instrumented Indentation System and Initial Results, D. JARDRET, Michalex, USA, M. FAJFROWSKI, Michalex, France
3:30 pm	E2-2-7 Mechanical properties of FeB and Fe ₂ B layers estimated by Berkovich nanoindentation on tool borided steels, G.A. RODRIGUEZ-CASTRO, Instituto Politécnico Nacional, Mexico, I. CAMPOS-SILVA, SEPI ESIME Zacatenco, Mexico, E. CHÁVEZ-GUTIÉRREZ, J. MARTINEZ-TRINIDAD, I. ARZATE-VÁZQUEZ, A. TORRES-HERNÁNDEZ, Instituto Politécnico Nacional, Mexico	
3:50 pm	E2-2-8 Measurement of Fracture Toughness on TiN thin film, A.N. WANG, G.P. YU, J.H. HUANG, National Tsing Hua University, Taiwan	Poster Session from 5:00 – 7:00 pm Golden Ballroom Reception begins at 6:00 pm
4:10 pm	E2-2-9 Bi-phase Ceramic Composite through Interpenetrating Network, E.H. KIM, J. LEE, Y. JUNG, Changwon National University, Republic of Korea	Oerlikon Leybold Vacuum Focused Topic Session Vacuum and Applications for Thin Film Coating Systems Pacific Salon 1-2 4:10-5:10 pm
4:30 pm	E2-2-10 Invited Probing the origin and evolution of strength in small volumes with in situ TEM nanomechanical testing, A. MINOR, University of California, Berkeley; National Center for Electron Microscopy, Lawrence Berkeley National Laboratory, US	
4:50 pm	Invited talk continued.	

Thursday Afternoon Poster Sessions

Coatings for Use at High Temperature Room: Golden Ballroom - Session AP

Symposium A Poster Session 5:00 pm

AP-1

Contact Corrosion propriety between Carbon Fiber Reinforced Composite Materials and Typical Metal alloys in an aggressive environment, **Z.J. PENG**, University of Windsor, Canada, **Z.J. WANG**, Univeristy of Windsor, Canada, **X. NIE**, University of Windsor, Canada

AP-2

Influence of native oxide scales on the mechanical properties of polycrystalline nickel substrates, **M. TATAT**, **P. GADAUD**, **C. COUPEAU**, **X. MILHET**, Institut P', CNRS – ENSMA - Université de Poitiers – UPR 3346, France, **P. RENAULT**, Institut P' - Université de Poitiers, France, **J. BALMAIN**, Laboratoire d'Etude des Matériaux en Milieux Agressifs - Université de La Rochelle, France

AP-3

Evaluation of galvanic and corrosion behaviour of some commercial aluminium-based coatings deposited by various methods, **O. FASUBA**, **A. YEROKHIN**, **A. MATTHEWS**, **A. LEYLAND**, University of Sheffield, UK

AP-4

High Temperature Diffusion Barriers for InSb based IR Detector, **A. LE PRIOL**, **E. LE BOURHIS**, **P. RENAULT**, Institut P' - Université de Poitiers, France, **H. SIK**, **P. MULLER**, SAGEM Défense Sécurité, France

AP-5

Improvement on the mechanical and corrosion properties of nanometric HfN/VN superlattices, **P. PRIETO**, Excellence Center for Novel Materials, CENM, Colombia, **C. ESCOBAR**, **J. CAICEDO**, Thin Film Group, Universidad del Valle, Colombia, **W. APERADOR**, Ingeniería Mecatrónica, Universidad Militar Nueva Granada, Colombia, **J. ESTEVE**, Universitat de Barcelona, Spain, **M. GÓMEZ**, Thin Film Group, Universidad del Valle, Colombia

AP-6

Study of the effect of densification on the mechanical properties of porous coatings after nano-indentation, **X.J. LU**, **P. XIAO**, **H. LI**, **A. FOK**, The University of Manchester, UK

AP-8

Oxygen incorporation in Cr₂AlC, **M. TO BABEN**, **L. SHANG**, **J. EMMERLICH**, **J. SCHNEIDER**, Materials Chemistry, RWTH Aachen university, Germany

AP-9

Multicomponent Coatings in Cr-Al-Si-B-(N) System Produced by Magnetron Sputtering of Composite SHS-Targets, **P. KIRYUKHANTSEV-KORNEEV**, **YU. POGOZHEV**, **D.V. SHTANSKY**, National University of Science and Technology "MISIS", Russian Federation, **J. VLCEK**, University of West Bohemia, Czech Republic, **E.A. LEVASHOV**, National University of Science and Technology "MISIS", Russian Federation

AP-10

Performance of Advanced Turbocharger Alloys and Coatings at 850-950°C in Air with Water Vapor, **J. HAYNES**, **B. ARMSTRONG**, **B. PINT**, Oak Ridge National Laboratory, US

AP-11

Oxidation Behavior of Ni-Ru Films under Glass Hot Pressing, **C.K. CHANG**, **K.Y. LIU**, **Y.C. HSIAO**, **F.B. WU**, National United University, Taiwan

AP-12

Wear characteristics of Zr-Al-Ni based PVD nanocomposite thin films deposited on non-ferrous alloy substrates, **J. LAWAL**, **A. MATTHEWS**, **A. LEYLAND**, University of Sheffield, UK

AP-13

The microstructure, mechanical properties and oxidation resistance of CrAlSiN coatings, **Y.C. KUO**, National Taiwan University of Science and Technology, Taiwan, **J.W. LEE**, **C.J. WANG**, Ming Chi University of Technology, Taiwan

AP-14

Improvement of interface adhesion and thermal stability in thermal barrier coatings through plasma heat treatment, **S. MYOUNG**, **J. JANG**, **K. LEE**, **Z. LU**, **Y. JUNG**, **J. LEE**, Changwon National University, Republic of Korea, **U. PAIK**, Hanyang University, Republic of Korea

Coatings for Use at High Temperature Room: Golden Ballroom - Session AP

Symposium A Poster Session 5:00 pm

AP-15

On Machining of Hardened AISI D2 Steel with Coated Tools, **W. MATTES**, **C. VIANA**, Brazil

AP-16

Microstructure characterization of diffusion aluminide coatings obtained by gas phase aluminizing on direct solidification Ni base superalloys Rene 142 and Rene 108, **B.W. WITALA**, **L.S. SWADZBA**, Silesian University of Technology, Poland, **L.K. KOMENDERA**, AVIO Polska Sp. z o.o., Poland, **M.H. HETMANCZYK**, **B.M. MENDALA**, **R. SWADZBA**, **G.M. MOSKAL**, Silesian University of Technology, Poland

AP-17

Degradation and thickness evaluation of thermal barrier coatings using nondestructive 3D scanning method, **G.M. MOSKAL**, **R. SWADZBA**, **L.S. SWADZBA**, **M.H. HETMANCZYK**, **B.M. MENDALA**, **B.W. WITALA**, Silesian University of Technology, Poland

Thursday Afternoon Poster Sessions

Hard Coatings and Vapor Deposition Technology

Room: Golden Ballroom - Session BP

Symposium B Poster Session

5:00 pm

BP-1

Trends in elasticity of binary and ternary transition metal aluminium nitrides, P. WAGNER, Montanuniversität Leoben, Austria, M. FRIAK, Max-Planck-Institut für Iron Research, Germany, P.H. MAYRHOFFER, D. HOLEC, Montanuniversität Leoben, Austria

BP-2

Investigation of the mechanical properties of ternary metal nitrides $Ti_xMo_{1-x}N$ and $Ti_xW_{1-x}N$ with $Ti=Ti, Zr, V, Nb, Ta$ and Cr , K. BOUAMAMA, Ferhat Abbas University, Algeria, P. DJEMIA, D. FAURIE, University Paris 13, France, G. ABADIAS, Institut P² - Université de Poitiers, France

BP-3

Structural and elastic properties of ternary metal nitrides $Ti_xTa_{1-x}N$ alloys: first-principles calculations versus experiments, M. BENHAMIDA, Laboratoire Optoélectronique et Composants, Ferhat Abbas University, Algeria, K. BOUAMAMA, Ferhat Abbas University, Algeria, P. DJEMIA, University Paris 13, France, L. BELLARD, UPMC, France, D. FAURIE, University Paris 13, France, G. ABADIAS, Institut P² - Université de Poitiers, France

BP-4

Growth of Zirconium Oxide by Heat Treatment of Zirconium Nitride Film under Controlled Atmosphere and Vacuum, J.W. SHINE, G.P. YU, J.H. HUANG, National Tsing Hua University, Taiwan

BP-5

Microstructure and Characterization of Sputtered Ni-based Films Codeposited with Ru and P, K.Y. LIU, Y.C. HSIAO, C.K. CHANG, F.B. WU, National United University, Taiwan

BP-7

Optimizing the PVD TiN thin film coating's parameters on AL 7075-T6 alloy for higher coating adhesion and better surface quality, E. ZALNEZHAD, University of Malaya, Malaysia

BP-8

Analysis of damaging phenomena of coated cutting tools using hardened die steels, K. MORISHITA, Hitachi Tool Engineering, Ltd., Japan

BP-9

Annealing effects on nanostructure and mechanical properties of laminated Ta-Zr coatings, Y.I. CHEN, S.M. CHEN, National Taiwan Ocean University, Taiwan

BP-10

Influence of thickness on mechanical and corrosion properties of Ti-Si-N coatings on D2 steel by unbalanced magnetron sputtering, Y.K. CHENG, G.P. YU, J.H. HUANG, National Tsing Hua University, Taiwan

BP-11

Effect of Nitrogen Flow Rate on The Structure And Mechanical Properties of TiZrN Thin Films by Unbalanced Magnetron Sputtering, C.W. LU, J.H. HUANG, G.P. YU, National Tsing Hua University, Taiwan

BP-12

Ternary d- $Ti_xTa_{1-x}N$: An addition to superhard materials?, L. KOUTSOKERAS, University of Ioannina, Greece, A. SKARMOUTSOU, National Technical University of Athens, Greece, G. ABADIAS, University of Poitiers, France, P. PSYLLAKI, Technological Education Institute of Piraeus, Greece, C. CHARITIDIS, National Technical University of Athens, Greece, C. LEKKA, P. PATSALAS, University of Ioannina, Greece

BP-13

Paramagnetic centers in hard graphite-like amorphous carbon, A. VIANA, C. MARQUES, Universidade Estadual de Campinas, Brazil

BP-14

Effects of sputtering gases on the preparation of boron nitride films using RF sputtering, M. IMAMIYA, Graduate School, Chiba Institute of Technology, Japan, Y. SAKAMOTO, Chiba Institute of Technology, Japan

Hard Coatings and Vapor Deposition Technology

Room: Golden Ballroom - Session BP

Symposium B Poster Session

5:00 pm

BP-15

Influence of Silicon-doping on MSIP Al_2O_3 coatings, K. BOBZIN, Surface Engineering Institute - RWTH Aachen University, Germany, N. BAGCIVAN, RWTH Aachen University, Germany, M. EWERING, Surface Engineering Institute - RWTH Aachen University, Germany

BP-16

3-dimensional DLC coating on microgear by bipolar PBII & D and plasma analysis, W.S. PARK, J.H. CHOI, T. KATO, The University of Tokyo, Japan, W.S. LEE, Korea Institute of Industrial Technology, Republic of Korea

BP-17

Mechanical properties and oxidation resistance of TiSiN/CrAIN films synthesized by a cathodic arc deposition process, Y.Y. CHANG, National Formosa University, Taiwan, Y.Y. LIOU, MingDao University, Taiwan

BP-18

Structural, Mechanical and Tribological Properties of TiTaBN Composite Graded Coatings Deposited by CFUBMS Technique, Ö. BARAN, Erzincan University, Turkey, İ. EFEOGLU, Ataturk University, Turkey, B. PRAKASH, Lulea Technical University, Sweden

BP-19

Effect of Si⁺ kinetic energy on the physical properties of Ti-Si-N thin films deposited by RCBPLD, L. ESCOBAR-ALARCON, E. CAMPS, V. MEDINA, National Institute for Nuclear Research, Mexico, D. SOLIS-CASADOS, Autonomus University of Mexico State, Mexico, I. CAMPS, Mexican National Autonomous University, Mexico

BP-20

The Role of Aluminium for the Nanostructure and Mechanical Properties of Sputtered Ti-B Films, P. EPAMINONDA, University of Cyprus, Cyprus, K. POLYCHRONOPOULOU, Northwestern University, US, K. FADENBERGER, Robert Bosch GmbH, Germany, M. BAKER, University of Surrey, UK, P. GIBSON, Joint Research Centre, Italy, A. LEYLAND, A. MATTHEWS, University of Sheffield, UK, P.H. MAYRHOFFER, Montanuniversität Leoben, Austria, C. REBHOLZ, University of Cyprus, Cyprus

BP-21

Microstructural characteristics of Cr7TiN coatings synthesized by unbalanced magnetron sputtering, S. Y. LEE, S. Y. LEE, K. KIM, S. Y. LEE, Korea Aerospace University, Republic of Korea

BP-22

Synthesis and characterization of Cr7TiN coatings synthesized by unbalanced magnetron sputtering, S. Y. LEE, S. Y. LEE, K. KIM, B. S. KIM, S. Y. LEE, Korea Aerospace University, Republic of Korea

BP-23

Mechanical Performance and Nanoscaled Deformation of Bias-Sputtered (AlCrTaTiZr)N_{Cy} Multi-component Coatings, S.Y. LIN, S.Y. CHANG, Y.C. HUANG, F.S. SHIEU, National Chung Hsing University, Taiwan

BP-24

Effects of Substrate Temperature and Bias-Voltage on Mechanical Properties and Oxidation Resistance of TiAlN Films, N. HATTORI, Keio University, Japan, T. TAKAHASHI, Yungalay Corporation, Japan, M. NOBORISAKA, T. MORI, M. TAKAHASHI, T. SUZUKI, Keio University, Japan

BP-26

Characterization of laser ablation bismuth and iron oxide plasmas used for deposition of bismuth-iron-oxide thin films, E. CAMPS, D. CARDONA, L. ESCOBAR-ALARCON, National Institute for Nuclear Research, Mexico, S. E. RODIL, Mexican National Autonomous University, Mexico

BP-27

A study of W/DLC/WSC composite films fabricated by magnetron sputtering method, M. DAI, C. WEI, S. LIN, H. HOU, K. ZHOU, Guangdong General Research Institute of Industrial Technology, China

BP-28

Comparison of the wear characteristics of TiN Coating with Manganese Phosphate Coating, S. SIVAKUMARAN, A. ALANGARAM, Sri Venkateswara College of Engineering, India

Thursday Afternoon Poster Sessions

Hard Coatings and Vapor Deposition Technology

Room: Golden Ballroom - Session BP

Symposium B Poster Session

5:00 pm

BP-29

Exotic mechanical properties of Cu-doped nano-columnar DLC coating, s. YUKAWA, T. AIZAWA, Shibaura Institute of Technology, Japan

BP-30

A Fem Supported Method for the Fast Determination of Nanoindenter's Tip Geometrical Deviations, K.-D. BOUZAKIS, M. PAPPA, G. MALIARIS, MICHAELIDIS, Aristoteles University of Thessaloniki; Fraunhofer Project Center Coatings in Manufacturing (PCCM), Greece

BP-31

An analysis of the effect of local environments on vacancy formation and diffusion energy barriers in $\text{Ti}_{0.5}\text{Al}_{0.5}\text{N}$ alloy, F. TASNÁDI, M. ODÉN, I. ABRIKOSOV, Linköping University, Sweden

BP-32

First-principles study of the local environment effects on surface diffusion in multicomponent nitrides, C. THOLANDER, F. TASNÁDI, B. ALLING, L. HULTMAN, Linköping University, Sweden

BP-33

Effects of electroless Ni and PVD-TiAlZrN duplex coatings on corrosion and erosion behavior of ductile iron, C.H. HSU, K.H. HUANG, Y.H. CHENG, Tatung University, Taiwan, C. LIN, Feng Chia University, Taiwan, K. OU, Taipei Medical University, Taiwan

BP-34

Microstructure and phase analysis of Cr-Mo-N composite film including different interlayer by hybrid PVD, Y.S. OH, Y.H. YANG, Korea Institute of Ceramic Engineering and Technology, Republic of Korea, I.W. LYO, Hyundai-Kia Motor Company, Korea, Republic of Korea, S.J. PARK, Hyundai Hysco, Korea, Republic of Korea

BP-35

Structure and properties of TiBCN coatings synthesized using unbalanced magnetron sputtering, C.H. HSIEH, C.H. TSAI, W.Y. HO, Department of Materials Science and Engineering, MingDao University, Taiwan, C.H. HSU, Department of Materials Science and Engineering, Tatung University, Taiwan, C.A. LIN, Department of Materials Science and Engineering, MingDao University, Taiwan, C.L. LIN, Department of Electro-Optical and Energy Engineering, MingDao University, Taiwan

BP-36

Low Temperature Plasma Nitriding of F51 Duplex Stainless Steel, A. TSCHIPTSCHIN, L.B. VARELA, University of São Paulo, Brazil, C. PINEDO, Heat Tech Technology for Heat Treatment and Surface Engineering Ltd, Brazil

BP-37

Residual stress on nanocomposite thin films using $\sin^2\Psi$ method, G. RAMÍREZ, S.E. RODIL, J.G. GONZÁLEZ-REYES, Universidad Nacional Autónoma de México - Instituto de Investigaciones en Materiales, Mexico

BP-38

Stress signature of an amorphous- to- crystalline transition into the β -phase during Ta thin film growth on Si., A. FILLON, J.J. COLIN, C. SZALA, A. MICHEL, G. ABADIAS, C. JAOUEN, Institut P' - Université de Poitiers, France

BP-39

Influence of Bias Voltage on Residual Stresses and Mechanical Properties of Multicomponent TiSiCrAlN Coatings, Y.Y. CHANG, National Formosa University, Taiwan, C.Y. TSAI, MingDao University, Taiwan

Hard Coatings and Vapor Deposition Technology

Room: Golden Ballroom - Session BP

Symposium B Poster Session

5:00 pm

BP-40

Effect of degree of ionization on preferred orientation and properties of TiN thin films deposited by high power impulse magnetron sputtering, C.Y. CHEN, G.P. YU, National Tsing Hua University, Taiwan, J.Y. WU, Institute of Nuclear Energy Research, Taiwan, J.H. HUANG, National Tsing Hua University, Taiwan

BP-41

Microstructures and mechanical properties of titanium carbide coating obtained by Thermo-reactive deposition process, X.S. FAN, Z.G. YANG, C. ZHANG, Tsinghua University, China

BP-42

Enhanced Glow Discharge Plasma Immersion Ion Implantation Using an Insulated Tube, Q.Y. LU, P. CHU, City University of Hong Kong, Hong Kong Special Administrative Region of China, L. H. LI, City University of Hong Kong; Beijing University of Aeronautics and Astronautics, Beijing, China, R. FU, City University of Hong Kong, Hong Kong Special Administrative Region of China

BP-43

Electrical transport properties in $\text{ZrN-SiN}_x\text{-ZrN}$ structures investigated by I-V measurements, D. OEZER, C.S. SANDU, EPFL, Switzerland, R. SANJINES, Ecole Polytechnique Fédérale de Lausanne, Switzerland

Thursday Afternoon Poster Sessions

Fundamentals and Technology of Multifunctional Thin Films: Towards Optoelectronic Device Applications

Room: Golden Ballroom - Session CP - Symposium C Poster Session - 5:00 pm
CP-1

Investigation on Physical Properties of CuInSe_2 Films Prepared by Pulsed Laser Deposition, M.H. WEN, J.Y. LUO, Y.T. HSIEH, C.C. CHANG, C.H. HSU, Y.R. WU, W.H. CHAO, M.K. WU, Institute of Physics, Academia Sinica, Nankang, Taiwan, H.S. KOO, Ming-Hsin University of Science and Technology, Taiwan

CP-2

Electro-optical properties and damp heat stability of Al-doped ZnO thin films prepared by laser induced high current pulsed arc deposition, J.B. WU, C.Y. CHEN, C.C. SHIH, J.J. CHANG, M.S. LEU, Material and Chemical Research Laboratories, Industrial Technology Research Institute, Taiwan, H.Y. TSENG, Y.C. LU, BeyondPV Co., Ltd, Taiwan

CP-3

Effect of Dopants and Thermal Treatment on Properties of Ga-Al-ZnO Thin Films Fabricated by Hetero Targets Sputtering System, K.H. KIM, Department of Electrical Engineering, Gachon University Republic of Korea, J.S. HONG, N. MATSUSHITA, Materials and Structures Laboratory, Tokyo Institute of Technology, Japan, H.W. CHOI, Department of Electrical Engineering, Gachon University, Korea

CP-4

Ellipsometry Study of a Reactively Sputtered Transparent Conductive Oxide(TCO), G. DING, M. LE, F. HASSAN, Z. SUN, M. NGUGEN, Intermolecular Inc, US

CP-5

Application-Specific Transparent Conductive Oxide Development using High Productivity Combinatorial Methods, M.A. NGUYEN, M. LE, Intermolecular Inc, US

CP-6

To Properties of Ga-Al doped ZnO films prepared on the polymer substrate, K.H. KIM, H.W. CHOI, K.H. KIM, Kyungwon University, Republic of Korea

CP-7

Charge trapping in indium zinc oxide thin film transistors with active channel fabricated by two-step deposition method, W. KIM, S.H. LEE, H.S. UHM, J.S. PARK, Hanyang University, Republic of Korea

CP-8

Fabrication and characterization of transparent thin film transistors with boron-doped silicon zinc oxide channel, H.S. UHM, S.H. LEE, W. KIM, J.S. PARK, Hanyang University, Republic of Korea

CP-9

Investigation on High-Performance Aluminum Zinc Tin Oxide Thin Film Transistors, L.F. TENG, P.T. LIU, C.S. FUH, National Chiao Tung University, Taiwan, Z.Z. LI, Ming-Hsin University of Science and Technology, Taiwan

CP-10

A Magnetization Study of Cobalt Oxide Films Deposited at Different Temperatures by Pulsed Injection MOCVD Using a β -Diketone Complex of Cobalt as the Precursor, L. APATIGA, J. ESPINDOLA, N. MENDEZ, Universidad Nacional Autónoma de México - Centro de Física Aplicada y Tecnología Avanzada, Mexico

CP-11

Investigating the Illuminated Hot-Carrier Effect under DC and AC operations for InGaZnO Thin-Film Transistors, T.Y. HSIEH, T.C. CHANG, T.C. CHEN, M.Y. TSAI, Y.T. CHEN, National Sun Yat-Sen University, Taiwan, F.Y. JIAN, National Chiao Tung University, Taiwan

CP-12

High Supercapacitive Performance of Sol-Gel ZnO-Added Manganese Oxide Coatings, C.-Y. CHEN, C.-Y. CHIANG, Feng Chia University, Taiwan, S.-J. SHIH, National Taiwan University of Science and Technology, Taiwan, C.Y. TSAY, C.K. LIN, Feng Chia University, Taiwan

CP-13

Characterization of dye sensitized solar cells with growth of ZnO passivating layer by Electron-beam evaporation, S.W. RHEE, K.H. KIM, H.W. CHOI, Kyungwon University, Republic of Korea

CP-15

Preparation of $\text{Zn}_x\text{Cd}_{1-x}\text{S}$ thin film by chemical bath deposition and application for dye-sensitized solar cell, C.C. CHANG, Institute of Physics, Academia Sinica, Nankang, Taiwan, C.S. HSU, Feng Chia University, Taiwan, C.H. HSU, M.K. WU, Institute of Physics, Academia Sinica, Nankang, Taiwan, C.C. CHAN, Feng Chia University, Taiwan

Fundamentals and Technology of Multifunctional Thin Films: Towards Optoelectronic Device Applications

Room: Golden Ballroom - Session CP - Symposium C Poster Session - 5:00 pm
CP-16

Effect of Thermal Treatment on Physical and Electrical Properties of porogen-containing and porogen-free ultralow- k plasma-enhanced chemical vapor deposition dielectrics, W.Y. CHUNG, National Chi-Nan University, Taiwan, Y.M. CHANG, J.I.M. LEU, National Chiao Tung University, Taiwan, T.J. CHIU, Y.L. CHENG, National Chi-Nan University, Taiwan

CP-17

Effects of UV Light Treatment for Low- k $\text{SiOC}(\text{-H})$ Ultra Thin Films Deposited by Using PEALD, C.K. CHOI, C.Y. KIM, J.W. KO, J.K. WOO, K.M. LEE, Jeju National University, Republic of Korea, W.Y. JEUNG, Korea Institute of Science and Technology, Republic of Korea

CP-18

The Impact of Heterojunction Formation Temperature on Obtainable Conversion Efficiency in n-ZnO/p- Cu_2O Solar Cells, Y. NISHI, T. MIYATA, T. MINAMI, Kanazawa Institute of Technology, Japan

CP-19

Effect of Thickness of Atomic Layer Deposition HfO_2 Film on Electrical and Reliability Performance, Y.L. CHENG, C.Y. HSIEH, Y.L. CHANG, National Chi-Nan University, Taiwan

CP-20

Growth, Structure and Optical Properties of 20%-Ti Doped WO_3 Thin Films, V. RAMANA, G. BAGHMAR, University of Texas at El Paso, US

CP-21

Gate Bias Dependence on Threshold Voltage Instability in $\text{HfO}_2/\text{Ti}_x\text{N}_{1-x}$ p-MOSFETs, W.H. LO, NSYSU, Taiwan, T.C. CHANG, National Sun Yat-Sen University, Taiwan, C.H. DAI, NSYSU, Taiwan

CP-22

Enhanced heating effect of SiO_2 -Ag and TiO_2 -Ag multi-layered and co-doped thin films, J.H. HSIEH, Y.T. SU, J.L. CHANG, S.J. LIU, Ming Chi University of Technology, Taiwan

CP-23

The Electrical Properties Correlated with Redistributed Deep States of a-Si:H TFTs on Flexible Substrates with Mechanical Bending, M.H. LEE, National Taiwan Normal University, Taiwan, B.F. HSIEH, National Chung Hsing University, Taiwan

CP-25

Effects of RF power on the properties of Si thin films deposited by an ICP CVD system with internal antennas, J.H. HSIEH, YAN-LIANG. LAI, Ming Chi University of Technology, Taiwan, YUICHI. SETSUHARA, Osaka University, Japan

CP-27

The different radio-frequency powers on characteristics of boron-doped amorphous carbon films prepared by reactive radio-frequency chemical vapor deposition, T.S. CHEN, S.E. CHIOU, S.T. SHIUE, National Chung Hsing University, Taiwan

CP-28

InN/GaN Quantum Well Heterostructures: Structural Characteristics and Strain Induced Modifications of the Electronic Properties, -. KIOSEOGLU, KALESKI, Aristoteles University of Thessaloniki, Greece, KOMNINO, Aristoteles University of Thessaloniki, Greece, KARAKOSTAS, Aristoteles University of Thessaloniki, Greece

CP-29

Optical properties of AlN:Ag and Al-Si-N:Ag nanostructured films and the effect of thermal annealing, A. SIOZIOS, E. LIDORIKIS, P. PATSALAS, University of Ioannina, Greece

CP-30

Investigation of photoluminescence and refractive index optical properties of thin film zinc silicate based on manganese, K.H. YOON, J.H. KIM, Chungbuk National University, Republic of Korea

CP-31

Er:Si Silicide Formation and Temperature Dependence of Barrier Inhomogeneity, H. EFEGLU, Turkey, Y. BABACAN, Erzincan University, Turkey

Thursday Afternoon Poster Sessions

Coatings for Biomedical and Healthcare Applications

Room: Golden Ballroom - Session DP

Symposium D Poster Session

5:00 pm

DP-1

Characterization and antibacterial performance of biocompatible Ti-Zn-O coatings deposited on titanium implants, M.T. TSAI, Hungkuang University, Taiwan, Y.Y. CHANG, National Formosa University, Taiwan, Y.C. CHEN, MingDao University, Taiwan, H.L. HUANG, J.T. HSU, China Medical University, Taichung, Taiwan

DP-2

Anti-bacterial Performance of Zirconia Coatings on Titanium Implants, H.L. HUANG, China Medical University, Taichung, Taiwan, Y.Y. CHANG, National Formosa University, Taiwan, J.C. WENG, Y.C. CHEN, MingDao University, Taiwan, C.H. LAI, T.M. SHIEH, China Medical University, Taichung, Taiwan

DP-3

Diffusion mechanism and Ag⁺ release kinetics on ZrCN - Ag NPs antimicrobial coatings, S. CALDERON V., Universidade do Minho, Dept. Física, Portugal, R. ESCOBAR GALINDO, Instituto de Ciencia de Materiales de Madrid (ICMM -CSIC), Spain, A. CAVALEIRO, University of Coimbra, Portugal, S. CARVALHO, Universidade do Minho, Dept. Física, Portugal

DP-4

Controlling the drug release from biocompatible polymers by changing plasma-treated area, K. HAGIWARA, Keio University, Japan, T. HASEBE, Toho University Sakura Medical center, Japan, R. ASAKAWA, Keio University, Japan, A. KAMIJO, Yokohama City University Hospital, Japan, T. SUZUKI, A. HOTTA, Keio University, Japan

DP-5

Ex-situ and in-situ techniques to study protein adsorption: fibrinogen and albumin adsorption on metal oxide thin films, P. SILVA-BERMEDEZ, Instituto de Investigaciones en Materiales, Universidad Nacional Autónoma de México, México, M. RIVERA, Instituto de Física - Universidad Nacional Autónoma de México, México, S. MUHL, S.E. RODIL, Instituto de Investigaciones en Materiales, Universidad Nacional Autónoma de México, México

DP-6

Biocompatibility of the Plasma-polymerized Para-xylene Films, C.M. CHOU, Feng Chia University; Taichung Veterans General Hospital, Taiwan, C.M. YEH, Taichung Hospital, Department of Health, Executive Yuan, Taiwan, C.J. CHUNG, Central Taiwan University of Science and Technology, Taiwan, J.L. HE, Feng Chia University, Taiwan

DP-7

Bioactive coating on anodized titanium substrate by a combination of micro-arc oxidation and electrophoretic deposition, P. SOARES, J.R. NEGRELLI, C.A.H. LAURINDO, Mechanical Engineering Department, Pontificia Universidade Catolica do Parana, Brazil, R. TORRES, Mechanical Engineering Department, Pontificia Universidade Católica do Paraná, Brazil

DP-10

Influence of Unipolar and Bipolar Voltage Modes on Corrosion Resistance of Cp-Ti Alloy coated by using Micro-arc Oxidation Process, E. DEMIRCI, Ataturk University, Turkey, E. ARSLAN, College of Erzurum, Turkey, V.K. EZIRMIK, Ataturk University, Turkey, Y. TOTIK, Turkey, İ. EFEGLU, Ataturk University, Turkey

DP-11

Improvement of Corrosion Resistance and Biocompatibility of Ti-6Al-7Nb Alloy Using Electrochemical Anodization Treatment, H.H. HUANG, C.P. WU, Y.S. SUN, National Yang-Ming University, Taiwan

DP-12

Corrosion based failure of silicon containing interfaces in diamond-like carbon coated Co-Cr-Mo joint implants, K. THORWARTH, U. MÜLLER, Empa, Switzerland, G. THORWARTH, Synthes GmbH, Switzerland, M. STIEFEL, C. FLAUB, R. HAUERT, Empa, Switzerland

Coatings for Biomedical and Healthcare Applications

Room: Golden Ballroom - Session DP

Symposium D Poster Session

5:00 pm

DP-13

Tribocorrosion resistance of CoCrMo alloys coated with TiAlN/TiAl Multilayers in simulated body fluid, M. FLORES, G. ALEMON, A. ALEMAN, Universidad de Guadalajara, Mexico, E. ANDRADE, UNAM, R. ESCOBAR, Instituto de Ciencia de Materiales de Madrid (ICMM - CSIC), Spain

DP-15

Electrochemical and Morphological Analysis on the Titanium Surface Modified by Shot Blasting and Anodic Oxidation Processes, E.M.S. SZESZ, Neoortho/Research Institute, Brazil, B.L. PEREIRA, C.E.B. MARINO, Universidade Federal do Paraná, Brazil, G.B. SOUZA, Universidade Estadual de Ponta Grossa, Brazil, P. SOARES, Pontificia Universidade Católica do Paraná, Brazil, N.K. KUROMOTO, Universidade Federal do Paraná, Brazil

DP-16

Morphological and mechanical characterization of the titanium anodic film obtained with a mixture of sulphuric and phosphoric acid under potentiostatic mode, A. ROSSETTO, S. BLUNK, Universidade Federal do Paraná, Brazil, C.E. FOERSTER, Universidade Estadual de Ponta Grossa, Brazil, P. SOARES, Pontificia Universidade Católica do Paraná, Brazil, B.L. PEREIRA, C. LEPIENSKI, N.K. KUROMOTO, Universidade Federal do Paraná, Brazil

DP-17

Investigation of Wear, Corrosion and Tribocorrosion Properties of AZ91 Mg Alloy Coated by Micro arc Oxidation Process in the Different Electrolyte Solution, E. DEMIRCI, Ataturk University, Turkey, E. ARSLAN, College of Erzurum, Turkey, V.K. EZIRMIK, Ataturk University, Turkey, O. BARAN, Erzincan University, Turkey, Y. TOTIK, Turkey, İ. EFEGLU, YILDIZ, Ataturk University, Turkey

DP-18

Effect of Nitrogen Plasma Immersion Ion Implantation Treatment on Corrosion Resistance and Cell Responses of Biomedical Ti and Ti-6Al-4V Metals, H.H. HUANG, S. WANG, C.H. YANG, National Yang-Ming University, Taiwan, W.F. TSAI, C.F. AI, Institute of Nuclear Energy Research, Taiwan

Thursday Afternoon Poster Sessions

Tribology & Mechanical Behavior of Coatings and Engineered Surfaces

Room: Golden Ballroom - Session EP

Symposium E Poster Session

5:00 pm

EP-1

About the identification of generic tribological parameters, M.C. FUCHS, N. SCHWARZER, Saxonian Institute of Surface Mechanics, Germany

EP-2

Gradient of tribological and mechanical properties of diamond-like carbon films grown on Ti6Al4V alloy with different condition of interlayer preparation, G. MARTINS, Clorovale Diamantes S.A., Brazil, C. SILVA, J. MACHADO, E. CORAT, V. TRAVA-AIROLDI, Institute for Space Research, Brazil

EP-3

Synthesis and characterization of high flatness diamond-like carbon films deposited by filtered cathodic arc deposition, D.Y. WANG, S.W. LIN, W.C. CHEN, MingDao University, Taiwan

EP-4

Effect of oxygen and nitrogen content on mechanical and tribological properties of Mo-N-O thin films, M. HRONADKA, P. NOVAK, J. MUSIL, R. CERSTVY, Z. SOUKUP, University of West Bohemia, Czech Republic

EP-5

The effective Indenter concept applied to a comprehensive 3D infinitesimal wear model, N. BIERWISCH, N. SCHWARZER, Saxonian Institute of Surface Mechanics, Germany

EP-6

Mechanical Characterization of RF-DC Plasma Nitrided Tool Steels, T. AIZAWA, Shibaura Institute of Technology, Japan, Y. SUGITA, YS Electric Industry, Co. Ltd., Japan

EP-7

Patterned Film Effects on the Adhesion of Al/TiN Barrier using Fracture-Energy Based Finite Element Analysis, C.C. LEE, Department of Mechanical Engineering, Chung Yuan Christian University, Chungli, Taiwan, C. S. WU, Department of Mechanical Engineering, Chung Yuan Christian University, Taiwan, B.F. HSIEH, S.T. CHANG, Department of Electrical Engineering, National Chung Hsing University, Taiwan

EP-8

Cyclic Creep and Fatigue Testing of Nanocrystalline Copper Thin Films, Y.T. WANG, C.J. TONG, W.T. TSENG, M.T. LIN, National Chung Hsing University, Taiwan

EP-9

On the determination of coating toughness during nanoindentation, J. CHEN, Newcastle University, UK

EP-10

Scratch Test of Optimized TiSiN Coating Deposited Via A Combination of DC and RF Magnetron Sputtering, A.R.BUSHROA, ABDUL RAZAK, University of Malaya, Malaysia, B. BEAKE, Micro Materials Ltd, UK, M. HAJI HASAN, University of Malaya, Malaysia, M.R. MUHAMMAD, Multimedia University, Malaysia

EP-11

Evaluation of Adhesion of TiAlN/CrN Multilayer Coatings Deposited by CFUBMS, H. ÇİÇEK, Ataturk University, Turkey, Ç. LALOĞLU, Turkey, Ö. BARAN, Erzinan University, Turkey, E. DEMIRCI, V. EZİRMİK, İ. EFEÖĞLU, Ataturk University, Turkey

EP-13

Adhesion tendency of polymers to hard coatings, M. REBELO DE FIGUEIREDO, C. BERGMANN, C. GANSER, C. TEICHERT, C. MITTERER, Montanuniversität Leoben, Austria

EP-14

Effect of Nitrogen content on the Microstructure and Residual Stress of Ternary Ta-Ti-N Thin Films Using Magnetron Sputtering, C.K. CHUNG, Y.R. LU, T.S. CHEN, C.H. LI, Y.T. LIN, National Cheng Kung University, Taiwan

EP-15

A study of microstructures and mechanical properties of cathodic arc deposited ZrSiN coatings with different Ti content, C. TSENG, National Chiao Tung University, Taiwan, T.C. TSENG, National Chiao Tung University, Taiwan, T.E. HSIEH, Gigastorage Corporation, Taiwan, J.G. DUH, H.W. CHEN, National Tsing Hua University, Taiwan

Tribology & Mechanical Behavior of Coatings and Engineered Surfaces

Room: Golden Ballroom - Session EP

Symposium E Poster Session

5:00 pm

EP-16

Effect of micro-droplets and surface morphology on the local residual stress field in thin hard coatings, E. BEMPORAD, M. SEBASTIANI, M. PICCOLI, F. CARASSITI, University of Rome "Roma Tre", Italy

EP-17

Tribological Behaviour of Electrodeposited CoW-WC Nanocomposite Coatings, S.K. GHOSH, A.K. SURI, BARC, India, J.P. CELIS, KUL, Belgium

EP-18

Duplex coating of DLC films for Al and Al alloys, Y. SAKAMOTO, Chiba Institute of Technology, Japan

EP-20

The effect of grooved surface texture on friction-induced vibration and noise, J.L.M. MO, H.L.D. DAN, G.X. CHEN, M.H. ZHU, Southwest Jiaotong University, China, T.M. SHAO, Key Laboratory of Tribology, Tsinghua University, China, Z.R. ZHOU, Southwest Jiaotong University, China

EP-21

Adhesion enhancement of polymers by an intermediate layer through photografting polymerization, J. TAKAHASHI, A. HOTTA, Keio University, Japan

EP-22

Tool life and surface characterization of four commercial drills, S. MUHL, Universidad Nacional Autónoma de México - Instituto de Investigaciones en Materiales, Mexico, D. GARCIA, A. FIGUEROA, SEPI, ESIME-Zacatenco, Instituto Politécnico Nacional, Mexico

EP-23

Surface modification of cast iron substrates using radical nitriding, I. SUGIURA, Graduate School, Chiba Institute of Technology, Japan, Y. SAKAMOTO, Chiba Institute of Technology, Japan

EP-24

Mechanical and Tribological Properties of Duplex Stainless Steels Submitted to P13 Nitriding at Low Temperatures, C.E. FOERSTER, Universidade Estadual de Ponta Grossa, Brazil, C. LEPIENSKI, S. BLUNK, A.M.C. OLIVEIRA, Universidade Federal do Paraná, Brazil, A. KOLITSCH, Institute of Ion Beam Physics and Material Research, Germany

EP-26

Characterisation of TiCN and TiCN/ZrN Coatings for Cutting Tool Application, P.C. SIOW, J. ABDUL GHANI, M.J. GHAZALI, Universiti Kebangsaan, Malaysia, T. RIA JAAFAR, Advanced Materials Research Centre SIRIM Berhad, Malaysia, C.H. CHE HARON, Universiti Kebangsaan, Malaysia

EP-27

Quantification of tool coating effects on surface finish while dry cutting of glass/epoxy composite, A. BEN-SOUSSIA, A. MKADDEM, M. EL MANSORI, A. MEENA, Arts et Métiers ParisTech, France

Thursday Afternoon Poster Sessions

New Horizons in Coatings and Thin Films Room: Golden Ballroom - Session FP

Symposium F Poster Session 5:00 pm

FP-1

Pseudocapacitive Performance of Vertical Copper Oxide Nanoflakes, Z. ENDUT, M.H. ABD SHUKOR, Center of Advanced Manufacturing and Material Processing, Malaysia, W.J. BASIRUN, University of Malaya, Malaysia

FP-2

Structural and Optical Properties of CdO Nanostructures Prepared by Atmospheric-pressure CVD, T. TERASAKO, T. FUJIWARA, Graduate School of Science and Engineering, Ehime University, Japan, Y. NAKATA, M. YAGI, Kagawa National College of Technology, Japan, S. SHIRAKATA, Graduate School of Science and Engineering, Ehime University, Japan

FP-3

Substrate texturing effect on the microstructural and electrochemical performance of the rf sputtered LiCoO₂ film cathodes, J. KUMAR, J. BABU, Sri Venkateswara University, Thin Films Laboratory, India, C. V. University of Texas at El Paso, US, O.M. HUSSAIN, Sri Venkateswara University, Thin Films Laboratory, India

FP-4

The Grain Evaluation and Electrochemical properties of RF sputtered LiMn₂O₄ thin films., J. BABU, J. KUMAR, O. MAHAMMAD, Sri Venkateswara University, Thin Films Laboratory, India, V. RAMANA, University of Texas at El Paso, US

FP-5

Electrochemical Properties of V₂O₅ Thin Films Grown on Flexible Substrates using Plasma Assisted Activated Reactive Evaporation, K. HARI KRISHNA, University of Calabria, Italy, O.M. HUSSAIN, Sri Venkateswara University, India

FP-6

Bismuth thin films deposited by DC Magnetron Sputtering for electrochemical analysis electrodes, S.E. RODIL, P. SILVA-BERMEDEZ, J. BARON, O. GARCIA-ZARCO, Instituto de Investigaciones en Materiales, Universidad Nacional Autónoma de México, México

FP-7

SnO₂-cored heteronanowires sheathed with metal shells and their application to gas sensors, H.W. KIM, Hanyang University, Republic of Korea

FP-8

Enhancement of electron-emission and long-term stability in tip-type carbon nanotube field emitters by lithium coating, J.S. PARK, B.J. KIM, J.P. KIM, J.S. PARK, Hanyang University, Republic of Korea

FP-9

Electron emission properties of carbon nanotubes grown on polymer substrates with high absorbency, B.J. KIM, H.B. CHANG, J.S. PARK, Hanyang University, Republic of Korea

FP-10

Structure and Electronic Properties of Sputter-Deposited LiFePO₄ Thin Films, V. RAMANA, M. MARES, G. BAGHMAR, University of Texas at El Paso, US

FP-11

Development of thin film cathodes for lithium-ion batteries in the materials system Li-Mn-O by r.f. magnetron sputtering, J. FISCHER, C. ZIEBERT, C. ADELHELM, J. YE, M. RINKE, J. DESAIGUES, M. STUBER, S. ULRICH, H. SEIFERT, Kit, Iam-Awp, Germany

FP-12

The resistive switching characteristics in TaON films for nonvolatile memory applications, M.C. CHEN, T.C. CHANG, National Sun Yat-Sen University, Taiwan, Y.C. CHIU, National Chiao Tung University, Taiwan, S.C. CHEN, National Tsing Hua University, Taiwan, S.Y. HUANG, National Sun Yat-Sen University, Taiwan, S. SZE, National Chiao Tung University, Taiwan, F.S. YEH(HUANG), National Tsing Hua University, Taiwan, M.J. TSAI, Indian Institute of Science Bangalore, India

New Horizons in Coatings and Thin Films Room: Golden Ballroom - Session FP

Symposium F Poster Session 5:00 pm

FP-13

Switching mechanism transition induced by annealing treatment in ZnO/Ru/ZnO resistive memory, L.C. CHANG, Y.H. WEI, Ming Chi University of Technology, Taiwan, K.H. LIU, Chang Gung University, Taiwan

FP-14

Bismuth Oxide thin films grown by RF reactive magnetron sputtering, P. LUNCA POPA, P. EKLUND, Linköping University, Sweden

FP-15

Electromechanical reliability of ITO-coated polymer substrates after exposure to acrylic acid, K. BURROWS, University of Birmingham, UK, A. HOOVER, D. CAIRNS, K. SIERROS, West Virginia University, US, S. KUKUREKA, University of Birmingham, UK

FP-16

Observation of amorphous to crystalline phase transformation in Te substituted Sn-Sb-Se chalcogenide thin films for memory applications, R. CHANDER, R. THANGARAJ, GNDU, India

FP-17

Investigating the degradation behavior under Hot Carrier Stress for InGaZnO TFT with symmetric and asymmetric structure, M.Y. TSAI, NSYSU, Taiwan

FP-18

Investigating the Drain Bias stress of InGaZnO TFTs under Dark and Light Illumination for AMOLED application, S.Y. HUANG, T.C. CHANG, L.W. LIN, M.C. YANG, National Sun Yat-Sen University, Taiwan, K.H. YANG, University of Toronto, Canada, M.H. WU, M.C. CHEN, National Sun Yat-Sen University, Taiwan, F.Y. JIAN, National Tsing Hua University, Taiwan

FP-19

Properties of Ge • SiC nanodots / SiC stacked structure, Y. ANEZAKI, T. OOTANI, Nagaoka University of Technology, Japan, K. SATOU, Department of Electrical, Electronic and Information Engineering, Japan, T. KATO, Nagaoka University of Technology, Japan, A. KATO, Department of Electrical, Electronic and Information Engineering, Japan, K. YASUI, Nagaoka University of Technology, Japan

FP-20

Oxygen-Graded TiO_x (x=1.5-1.9) Produced by High Power Impulse Magnetron Sputtering and Its Thin Film Solar Cell Application, Y.H. CHEN, W.C. YAN, M.C. LAI, J.L. HE, Feng Chia University, Taiwan

FP-21

Time Evolution and the Gas Rarefaction of Long HiPIMS Pulses, C. HUO, KTH Royal Institute of Technology, Sweden, M.A. RAADU, Royal Institute of Technology, D. LUNDIN, Université Paris-Sud 11, France, J.T. GUDMUNDSSON, Shanghai Jiaotong University, China, A. ANDERS, Lawrence Berkeley National Laboratory, US, N. BRENNING, Royal Institute of Technology, Sweden

FP-22

Mass and energy spectrometry of a feedback controlled reactive Ti HIPIMS discharge in Ar/O₂, M. AUDRONIS, Gencoa Ltd, UK, Y. GONZALVO, Hiden Analytical Ltd., UK, V. BELLIDO-GONZALEZ, Gencoa Ltd, UK

Thursday Afternoon Poster Sessions

New Horizons in Coatings and Thin Films Room: Golden Ballroom - Session FP

Symposium F Poster Session 5:00 pm

FP-23

Progress in BIPOLAR sputtering technology – new approach to process control and its applications, **W. GLAZEK**, **A. KLIMCZAK**, **P. OZIMEK**, **P. ROZANSKI**, Huettinger Electronic, Poland

FP-24

Effect of hydrogen addition on the residual stress of cubic boron nitride thin film deposited by UBM sputtering method, **J.-S. KO**, **J.K. PARK**, Korea Institute of Science and Technology, Republic of Korea, **J.-Y. HUH**, Unaffiliated, **Y.J. BAIK**, Korea Institute of Science and Technology, Republic of Korea

FP-25

Behavior of cubic boron nitride thin film formation according to the deposition pressure, **E.S. LEE**, **J.K. PARK**, Korea Institute of Science and Technology, Republic of Korea, **T.Y. SEONG**, Korea University, Republic of Korea, **Y.J. BAIK**, Korea Institute of Science and Technology, Republic of Korea

FP-26

Effect of moisture adsorption inside the chamber on the formation of cubic boron nitride thin film, **E.S. LEE**, **J.K. PARK**, Korea Institute of Science and Technology, Republic of Korea, **T.Y. SEONG**, Unaffiliated, **Y.J. BAIK**, Korea Institute of Science and Technology, Republic of Korea

FP-27

Precise modulation of pore diameter of porous anodic alumina templates by hybrid pulse periods at room temperature, **C.K. CHUNG**, **H.C. CHANG**, **S.L. LI**, **M.W. LIAO**, National Cheng Kung University, Taiwan

FP-28

Transparent Anti-fingerprint Protective Coatings Prepared by Duplex Plasma Polymerization, **S.W. CHANG**, Feng Chia University, Taiwan, **C.M. CHEN**, Feng Chia University, Plastic Industry Development Center, Taiwan, **J.L. HE**, Feng Chia University, Taiwan

Applications, Manufacturing, and Equipment Room: Golden Ballroom - Session GP

Symposium G Poster Session 5:00 pm

GP-1

Effect of Pulse Frequency on Physical Properties of Diamond-Like Carbon Films Synthesized under Atmospheric Pressure, **T. SAKURAI**, **M. NOBORISAKA**, **T. HIRAKO**, **T. SUZUKI**, Keio University, Japan

GP-2

Monte Carlo simulation of energy and particle distributions in the molybdenum disulfide sputtering process, **B. VIERNEUSEL**, **S. TREMMEL**, **S. WARTZACK**, Friedrich-Alexander-University Erlangen-Nuremberg, Germany

GP-3

Temperature-induced abnormal sub-threshold leakage current in amorphous Indium-Gallium-Zinc-Oxide thin film transistors, **J.-C. JHU**, National Sun Yat-Sen University, Taiwan, **G.W. CHANG**, National Chiao Tung University, Taiwan, **Y.E. SYU**, National Sun Yat-Sen University, Taiwan

GP-4

Microestructural analysis of Zn-Sn interface with thin films based of Ta over Cu and Si substrates, **S. MEDRANO**, **G. RAMIREZ**, Instituto de Investigaciones en Materiales, Universidad Nacional Autónoma de México, Circuito Exterior s/n, CU, México D.F. 04510, México, **S.E. RODIL**, Instituto de Investigaciones en Materiales, Universidad Nacional Autónoma de México, México, **S. MUHL**, Universidad Nacional Autónoma de México - Instituto de Investigaciones en Materiales, México, **G. GONZALEZ**, Instituto de Investigaciones en Materiales, Universidad Nacional Autónoma de México, Circuito Exterior s/n, CU, México D.F. 04510, México

GP-5

Characterization of Polysilazane Based Sod Films As Function of Process Temperature and Thin Barrier used, **G. GULLERI**, Micron Semiconductor Italia S.r.l, Italy, **F. FUMAGALLI**, Micron Semiconductor Italia S.r.l., Italy, **C. RICCI**, University of Cagliari, Physics Department, Italy

GP-6

A novel multilayer barrier film encapsulated plastics purely prepared by inductively coupled plasma chemical vapor deposition, **L.W. LAI**, **M.H. KO**, **K.W. LIN**, **J.T. CHEN**, **C.H. CHANG**, Industrial Technology Research Institute, Taiwan

GP-7

Surface modification using silane coupling agent for polypropylene with high gas barrier property, **H. TASHIRO**, **A. HOTTA**, Keio University, Japan

GP-8

Manufacturing of mode-conversion type microwave plasma CVD apparatus and applying for synthesis of carbon materials, **T. KAMESHIMA**, Graduate School, Chiba Institute of Technology, Japan, **H. TANAKA**, Shutech Co., Ltd., Japan, **Y. SAKAMOTO**, Chiba Institute of Technology, Japan

GP-9

A novel technique to suppress self sputtering of radio-frequency electrode in capacitively-coupled glow discharge, **X.B. TIAN**, **Y.H. MA**, **C.Z. GONG**, **S.Q. YANG**, Harbin Institute of Technology, China, **P. CHU**, City University of Hong Kong, Hong Kong Special Administrative Region of China

Thursday Afternoon Poster Sessions

Applications, Manufacturing, and Equipment Room: Golden Ballroom - Session GP

Symposium G Poster Session 5:00 pm

GP-10

An experimental study on a large area multi-electrode discharge in the fabrication of microcrystalline thin film solar cell, H. SEO, S. LEE, Y. CHANG, Korea Advanced Institute of Science and Technology, Republic of Korea

GP-11

Advanced PVD coatings in a combination with a new intermetallic substrate for hobs - A major step forward in productivity, P. IMMICH, U. KRETZSCHMANN, U. SCHUNK, R. FISCHER, LMT Fette Werkzeugtechnik, Germany

GP-12

Adhesive-free gas adsorption joining of cycloolefin polymer film and glass sheet, Y. TAGA, Thin film research Center, Chubu University, Japan

GP-13

Silicon oxide permeation barrier coating of PET in microwave plasmas with arbitrary substrate bias, S. STEVES, Electrical Engineering and Plasma Technology, Ruhr-Universität Bochum, Germany, B. OEZKAYA, Technical and Macromolecular Chemistry, University of Paderborn, Germany, M. RUDOLPH, M. DEILMANN, Electrical Engineering and Plasma Technology, Ruhr-Universität Bochum, Germany, C.N. LIU, Technical and Macromolecular Chemistry, University of Paderborn, Germany, N. BIBINOV, Electrical Engineering and Plasma Technology, Ruhr-Universität Bochum, Germany, O. OZCAN, G. GRUNDMEIER, Technical and Macromolecular Chemistry, University of Paderborn, Germany, P. AWAKOWICZ, Electrical Engineering and Plasma Technology, Ruhr-Universität Bochum, Germany

GP-14

Fluidized Bed Machining (FBM) of thermally sprayed cobalt-chromium and chromium oxide coatings, M. BARLETTA, S. GUARINO, V. TAGLIAFERRI, F. TROVALUSCI, Università degli Studi di Roma Tor Vergata, Italy

Post Deadline Discoveries and Innovations Room: Golden Ballroom - Session PDP

Post Deadline Discoveries and Innovations

Moderators: W. Kalss, OC Oerlikon Balzers AG, Liechtenstein, S. Ulrich, Karlsruhe Institute of Technology, Germany

5:00 pm

PDP-1

Oxidation resistance coatings of Ir-Zr and Ir by double glow plasma, W.P. WU, Z.F. CHEN, X.N. CONG, Nanjing University of Aeronautics and Astronautics, China

PDP-2

A comparative study on hot corrosion resistance of three types of thermal barrier coatings: YSZ, YSZ/normal Al_2O_3 and YSZ/nano Al_2O_3 , M. DAROONPARVAR, M.S. HUSSAIN, Universiti Teknologi, Malaysia

PDP-3

Determination of the local mechanical properties and residual stresses of an a-C:H coating system by nanoindentation and FIB milling, C. SCHMID, V. MAIER, SCHAUFLE, M. GÖKEN, University Erlangen-Nuremberg, Germany, K. DURST, University Erlangen-Nuremberg, Germany

PDP-4

A simple FIB milling technique for residual stress measurements on thermally cycled NiAl bond coats, M. KROTTENTHALER, C. SCHMID, R. WEBLER, J. SCHAUFLE, S. NEUMEIER, University Erlangen-Nuremberg, Germany, K. DURST, University Erlangen-Nuremberg, Germany, M. GÖKEN, University Erlangen-Nuremberg, Germany

PDP-5

In-Situ TEM Observations of Indenting Deformation and Fracture of Bone Nanopillars, S.Y. CHANG, Y.T. WANG, Y.C. HUANG, C.M. CHEN, National Chung Hsing University, Taiwan

PDP-6

In situ deposition and characterization of B-C-N films, H. ALAGOZ, M.F. GENISEL, E. BENGÜ, D. INAN, Bilkent University, Turkey

Thursday Afternoon Poster Sessions

Symposium TS Poster Session

Room: Golden Ballroom - Session TSP

TS Poster Session

5:00 pm

TSP-1

A route to strong p-doping of epitaxial graphene on SiC, U. SCHWINGENSCHLÖGL, Y.C. CHENG, N. SINGH, KAUST, Saudi Arabia

TSP-2

Nitrogen Introduced at Interface to Improve Resistance Switching Characteristics with SiGeO_x RRAM Device, Y.E. SYU, National Sun Yat-Sen University, Taiwan, G.W. CHANG, National Chiao Tung University, Taiwan

TSP-3

Electroluminescence of ZnO nanocrystal in sputtered ZnO-SiO nanocomposite light-emitting devices, J.T. CHEN, National Cheng Kung University, Taiwan, W.C. LAI, J.K. SHEU, Y.Y. YANG, Unaffiliated

TSP-4

Sampling the local structure in γ -Al₂O₃ by XPS analysis of embedded Argon, M. PRENZEL, A. RASTGOO LAHROOD, A. KORTMANN, T. DE LOS ARCOS, A. VON KEUDELL, Ruhr Universität Bochum, Germany

TSP-5

Deposition, Microstructure and Mechanical Properties of Mo-doped CeO₂ Films Prepared by Pulsed Unbalanced Magnetron Sputtering, I.W. PARK, J. MOORE, J. LIN, Colorado School of Mines, US, D. HURLEY, M. KHAFIZOV, Idaho National Laboratory, US, A. EL-AZAB, Florida State University, Florida, US, T. ALLEN, C. YABLINSKY, M. GUPTA, University of Wisconsin, Wisconsin, J. GAN, Idaho National Laboratory, US, M. MANUEL, H. HENDERSON, B. VALDERRAMA, University of Florida, US

TSP-6

Effect of stress on the electrical bistability of poly N-vinylcarbazole films, J.C. WANG, Y.S. LAI, National United University, Taiwan

TSP-7

Thin Film Bond and Mass Density Measurements Using Fourier Transform Infrared Spectroscopy, S. KING, Intel Corporation, US

TSP-8

Ordered thin film materials with ultra-low thermal conductivity, C. MURATORE, Air Force Research Laboratory, Thermal Sciences and Materials Branch, US, V. VARSHNEY, UTC/Air Force Research Laboratory, Thermal Sciences and Materials Branch, US, J.J. GENGLER, Air Force Research Laboratory, Thermal Sciences and Materials Branch, US, J.J. HU, UDRI/Air Force Research Laboratory, Thermal Sciences and Materials Branch, US, T.S. SMITH, Air Force Research Laboratory, Thermal Sciences and Materials Branch, US, J.E. BULTMAN, UDRI/Air Force Research Laboratory, Thermal Sciences and Materials Branch, US, A. VOEVODIN, Air Force Research Laboratory, Thermal Sciences and Materials Branch, US

TSP-9

Texture change and off-axis accommodation through film thickness in fcc structured nitrides, A. KARIMI, A. SHETTY, EPFL, Switzerland

Friday Morning, April 27, 2012

Hard Coatings and Vapor Deposition Technology Room: Royal Palm 4-6 - Session B3-1 Ion-Surface Interactions in Film Growth and Post-Growth Processes Moderators: S. Fairchild, Air Force Research Laboratory, US, K. Sarakinos, Linköping University, Sweden		Coatings for Biomedical and Healthcare Applications Room: Sunset - Session D2-1 Coatings for Biomedical Implants Moderators: R. Hauert, Empa, Switzerland, J. Piascik, RTI International, US	
8:00 am	B3-1-1 Tantalum Based Coatings Deposited by Pulsed DC Magnetron Sputtering and Highly Ionized Pulse Plasma Processes, J. BARRIGA, L. MENDIZABAL, U. RUIZ DE GOPEGUI, R. BAYON, Tekniker, Spain	D2-1-1 Invited Functional plasma polymer films engineered at the nanoscale for biomaterial applications, K. VASILEV, University of South Australia, Australia Invited talk continued.	
8:20 am	B3-1-2 Studies on plasma immersion ion implantation of nitrogen on titanium, K. R. M. RAO, Department of Engineering Chemistry, GITAM Institute of Technology, GITAM University, India, E. RICHTER, Institute of Ion Beam Physics for Materials Research, Helmholtz-Zentrum Dresden-Rossendorf, Germany, S. MUKHERJEE, FCIPT, Institute of Plasma Research, India, I. MANNA, Central Glass and Ceramic Research Institute, India		
8:40 am	B3-1-3 Invited On the role of ions during reactive magnetron sputtering, D. DEPLA, Ghent University, Belgium	D2-1-3 Effect of the surface atom ordering on the protein adsorption, P. SILVA-BERMEDEZ, L. HUERTA, S.E. RODIL, Instituto de Investigaciones en Materiales, Universidad Nacional Autónoma de México, México	
9:00 am	Invited talk continued.	D2-1-4 Nanodiamond/DLC Composite Coating Deposited on Ti6Al4V for Orthopaedic Joint Applications, C. ZHANG, Q. YANG, Y. TANG, Y. LI, University of Saskatchewan, Canada	
9:20 am	B3-1-5 In situ characterization of plasma-surface interactions with a quartz crystal microbalance, C. CORBELLA, O. KREITER, S. GROSSE-KREUL, Ruhr Universität Bochum, Germany, D. MARINOV, Ecole Polytechnique, France, T. DE LOS ARCOS, A. VON KEUDELL, Ruhr Universität Bochum, Germany	D2-1-5 Effects of argon plasma treatment on controlling the drug release rate from biocompatible polymers, K. HAGIWARA, Keio University, Japan, T. HASEBE, Toho University Sakura Medical center, Japan, T. SUZUKI, A. HOTTA, Keio University, Japan	
9:40 am	B3-1-6 Compressive stress generation and atom incorporation during growth of low-mobility materials, G. ABADIAS, A. FILLON, A. MICHEL, C. JAOUEN, Institut P ⁺ - Université de Poitiers, France	D2-1-6 In vitro biological response of plasma electrolytically oxidised and sprayed hydroxyapatite coatings on Ti6Al4V alloy, W. YEUNG, A. YEROKHIN, G. REILLY, A. MATTHEWS, University of Sheffield, UK	
10:00 am	B3-1-7 Variation of substrate biasing and temperature and their influence on the crystal orientation of γ -Al ₂ O ₃ films, M. PRENZEL, A. KORTMANN, A. VON KEUDELL, Ruhr Universität Bochum, Germany	D2-1-7 Biocompatibility and Anti-Microbial Properties of Silver Modified Amorphous Carbon Films, A. ALMAGUER-FLORES, Universidad Nacional Autónoma de México, México, R. OLIVARES-NAVARRETE, Georgia Tech, US, G. RAMIREZ, Universidad Nacional Autónoma de México, México, S.E. RODIL, Universidad Nacional Autónoma de México, México	
10:20 am	B3-1-8 High-Voltage Positive Nanopulse Assisted Hot-Filament CVD Diamond Growth, M. TAKASHIMA, N. OHTAKE, Tokyo Institute of Technology, Japan	D2-1-8 Corrosion Resistance and Biocompatibility of Titanium Coated with Tantalum Pentoxide, Y.S. SUN, H.H. HUANG, National Yang-Ming University, Taiwan	
10:40 am		D2-1-9 Mechanical Properties of Fluorinated DLC and Si Interlayer on a Ti Biomedical Alloy, C.C. CHOU, Y.Y. WU, National Taiwan Ocean University, Taiwan, J.W. LEE, Ming Chi University of Technology, Taiwan, J.C. HUANG, Tungnan University, Taiwan, C.H. YEH, Keelung Chang Gung Memorial Hospital, Taiwan	
11:00 am	2013 Abstract Submission Deadline October 1, 2012	2013 ICMCTF April 29 – May 3, 2013	
11:20 am	Thank You & See You Next Year Party, Trellis Courtyard near pool 12:30 – 1:30 pm	Awards Nominations Deadline October 1, 2012	

Friday Morning, April 27, 2012

Tribology & Mechanical Behavior of Coatings and Engineered Surfaces Room: Tiki Pavilion - Session E2-3 Mechanical Properties and Adhesion Moderators: M.T. Lin, National Chung Hsing University, Taiwan, D. Bahr, Washington State University, US, R. Chromik, McGill University		New Horizons in Coatings and Thin Films Room: Royal Palm 1-3 - Session F3-1 New Boron, Boride and Boron Nitride Based Coatings Moderators: H. Högberg, Linköping University, A. Inspektor, Kennametal Incorporated, US	
8:00 am	E2-3-1 Mechanical properties evaluation of the magnetron sputtered Zr-based metallic glass thin films, C.Y. CHUNG, Ming Chi University of Technology, Taiwan, H.W. CHEN, J.G. DUH, National Tsing Hua University, Taiwan, J.W. LEE, Ming Chi University of Technology, Taiwan	F3-1-1	Invited Quantum-mechanically guided materials design of boron-based hard coatings, J. EMMERLICH, D. MUSIC, Materials Chemistry, RWTH Aachen university, Germany, J. SCHNEIDER, RWTH Aachen University, Germany
8:20 am	E2-3-2 Microstructure and mechanical properties of copper-tin shape memory alloy thin films deposited from an anionic liquid electrolyte, N. MOHARRAMI, S. GHOSH, S. ROY, S.J. BULL, Newcastle University, UK	Invited talk continued.	
8:40 am	E2-3-3 Invited Precipitation and Fatigue in Ni-Ti-Zr Shape Memory Alloy Thin Films by Combinatorial nanoCalorimetry, J. VLASSAK, Harvard University, US	F3-1-3	Hard and lubricious Ti-B-C-N nanocomposite coatings via magnetron sputtering, F.J. LI, S. ZHANG, School of Mechanical and Aerospace Engineering, Nanyang Technological University, Singapore, B. LI, Central Iron and Steel Research Institute, China
9:00 am	Invited talk continued.	F3-1-4	Microstructural of study of cubic boron nitride thin film deposited by UBM method with hydrogen addition, J.-S. KO, J.K. PARK, Korea Institute of Science and Technology, Republic of Korea, J.-Y. HUH, Unaffiliated, Y.J. BAIK, Korea Institute of Science and Technology, Republic of Korea
9:20 am	E2-3-5 Investigation of the elastic-plastic properties of thin films on polyimide substrate under controlled biaxial deformation, S. DJAZIRI, Institut P ⁺ - Université de Poitiers, France, D. FAURIE, LSPM-CNRS, Université Paris13, France, P. RENAULT, E. LE BOURHIS, Institut P ⁺ - Université de Poitiers, France, G. GEANDIER, Institut Jean Lamour, France, C. MOCUTA, D. THIAUDIERE, SOLEIL Synchrotron, France, P. GOUDEAU, Institut P ⁺ - Université de Poitiers, France	F3-1-5	Effect of deposition temperature of cubic boron nitride thin film deposited by UBM method with nanocrystalline diamond buffer layer, E.S. LEE, J.K. PARK, Korea Institute of Science and Technology, Republic of Korea, T.Y. SEONG, Unaffiliated, Y.J. BAIK, Korea Institute of Science and Technology, Republic of Korea
9:40 am	E2-3-6 Heat treating effects on the microstructure and mechanical properties of Ti-Cr-B-N thin films, L.W. HO, J.W. LEE, Ming Chi University of Technology, Taiwan, H.W. CHEN, J.G. DUH, National Tsing Hua University, Taiwan	F3-1-6	Microwave-assisted surface synthesis of amorphous and crystalline boron-carbon-nitrogen foams for thermal physisorption applications, R. PAUL, Birck Nanotechnology Center, Purdue University, US, A. VOEVODIN, Birck Nanotechnology Center, Purdue University; Materials and Manufacturing Directorate, Air Force Research Laboratory, US, A. AMAMA, S. GANGULI, A.K. ROY, Air Force Research Laboratory, Materials and Manufacturing Directorate, US, T.S. FISHER, Birck nanotechnology Center, Purdue University; Air Force Research Laboratory, Materials and Manufacturing Directorate, US, J.J. HU, University of Dayton Research Institute/Air Force Research Laboratory, US
10:00 am	E2-3-7 Innovative nanomechanical testing for coating optimisation in severe applications - experiments and modelling, B. BEAKE, Micro Materials Ltd, UK, N. SCHWARZER, SIO, Germany, M. DAVIES, Micro Materials Ltd, UK, W. HELLE, LOT Oriel, T. LISKIEWICZ, Leeds University, UK	F3-1-7	B ₄ C thin films for neutron detection, C. HÖGLUND, European Spallation Source ESS AB/ Linköping University, Sweden, J. BIRCH, Linköping University, Sweden, K. ANDERSEN, European Spallation Source ESS AB, Sweden, T. BIGAULT, J.-C. BUFFET, J. CORREA, P. VAN ESCH, B. GUERARD, Institute Laue Langevin, France, R. HALL-WILTON, European Spallation Source ESS AB, Sweden, J. JENSEN, Linköping University, Sweden, A. KHAPLANOV, European Spallation Source ESS AB, Sweden; Institute Laue Langevin, France, F. PISCITELLI, Institute Laue Langevin, France, C. VETTIER, European Synchrotron Radiation Facility ESRF, France, W. VOLLENBERG, CERN, Switzerland, L. HULTMAN, Linköping University, Sweden
10:20 am	E2-3-8 A new method to measure mechanical properties of very thin top layers (<100nm), G.G. GUILLONNEAU, J.L. LOUBET, S.B. BEC, G. KERMOUCHE, Ecole Centrale de Lyon, France	2013 Abstract Submission Deadline October 1, 2012	
10:40 am	E2-3-9 Invited Extending Thin-Film Mechanical-Property Measurement Techniques for New Applications, N. BARBOSA, L. LIEW, D. READ, National Institute of Standards and Technology, US	2013 Awards Nominations Deadline October 1, 2012	
11:00 am	Invited talk continued.	Thank You & See You Next Year Party Trellis Courtyard near pool 12:30 – 1:30 pm	
11:20 am	E2-3-11 Atomic Force Microscopy for Nanoscale Mechanical Mapping, B. PITTENGER, C. SU, S. MINNE, Bruker-Nano Inc., AFM Unit, US	2013 ICMCTF April 29 – May 3, 2013	

Friday Morning, April 27, 2012

Applications, Manufacturing, and Equipment

Room: Sunrise - Session G6-1

Advances in Industrial PVD & CVD Deposition Equipment

Moderators: M. Rodmar, Sandvik Tooling, Sweden, K. Bobzin, Surface Engineering Institute - RWTH Aachen University, Germany

8:00 am	G6-1-1 Invited Source Technologies for Amorphous Carbon Hard Coatings, R. P. WELTY, Magplas Technik LLC, US	<p>Elsevier Workshop: Reviewing and Refereeing Manuscripts 8:30 am – 1:00 pm Towne Room in the Meeting House</p> <p>Limited seating is still available for this complimentary workshop! (registration is required) Information about this workshop and how to register is found on the ICMCTF web site http://www2.avs.org/conferences/icmctf on the Focused Topics SessionTab(FTS).</p> <p>Or, for additional information as well as registration for this "Refereeing and Reviewing" workshop, please contact Jan Willem Wijnen publisher of several Elsevier journals : j.wijnen@elsevier.com</p>
8:20 am	Invited talk continued.	
8:40 am	G6-1-3 Broadening the application range of HiPIMS coatings in industrial cutting operations, W. KOELKER, O. LEMMER, C. SCHIFFERS, S. BOLZ, CemeCon AG, Germany	
9:00 am	G6-1-4 Technical challenges and solutions for scaling up of High Power Impulse Magnetron Sputtering (HIPIMS) technologies, J. LANDSBERGEN, F. PAPA, R. TIETEMA, M. EERDEN, T. KRUG, Hauzer Techno Coating, BV, Netherlands	
9:20 am	G6-1-5 S3p™ the HIPIMS approach of Oerlikon Balzers, S. KRASSNITZER, M. LECHTHALER, H. RUDIGIER, OC Oerlikon Balzers AG, Liechtenstein	
9:40 am	G6-1-6 Hybrid - PVD coatings: arc evaporation combined with HIPAC, J. VETTER, J. MUELLER, G. ERKENS, Sulzer Metaplas GmbH, Germany	
10:00 am	G6-1-7 Towards uniform coating on complex geometries by PVD techniques, T. TAKAHASHI, R. CREMER, P. JASCHINSKI, KCS Europe GmbH, Germany, K. YAMAMOTO, S. HIROTA, Kobe Steel Ltd., Japan	
10:20 am	G6-1-8 LPPS hybrid Technologies: New Thermal Spray Processes for new emerging Energy Applications, H.-M. HOEHLE, Sulzer Metco Europe GmbH, Germany, M. GINDRAT, A. BARTH, Sulzer Metco AG (Switzerland), Switzerland	
10:40 am	G6-1-9 Development of metal strip cooling equipment for demands of high-rate vacuum coating, J.-P. HEINB, P. LANG, Fraunhofer FEP, Germany	
11:00 am	G6-1-10 Multiple frequency coupled plasmas for enhanced control of PVD processes, S. BIENHOLZ, E. SEMMLER, P. AWAKOWICZ, Ruhr-Universität Bochum, Germany	
11:20 am	2013 Abstract Submission Deadline October 1, 2012	2013 ICMCTF April 29 – May 3, 2013
11:40 am	Thank You & See You Next Year Party, Trellis Courtyard near pool 12:30 – 1:30 pm	Awards Nominations Deadline October 1, 2012

39th ICMCTF

International Conference on Metallurgical Coatings and Thin Films

April 23-27, 2012
San Diego, CA, USA

Town & Country Convention Center www2.avs.org/conferences/ICMCTF/



VISIT THE EXHIBITS !!

EXHIBIT HALL HOURS:

Tuesday	April 24	11am - 7pm
Wednesday	April 25	10am - 2pm

VISIT THE EXHIBIT HALL

- SEE THE LATEST TECHNOLOGY
- FREE Caricatures
- FREE Massages
- FREE Lunch
- FREE Reception (Tuesday 5:30-7pm)
- RAFFLE DRAWINGS



**Free Caricatures
& Massages!!**



Stop by the sponsoring
exhibitor booths to pick
up your tickets to enter
the daily raffle drawings...
GREAT PRIZES !!!





ICMCTF 2012 EXHIBITORS



COMPANY	BOOTH #	COMPANY	BOOTH #
A&N Corporation	406	MeiVac, Inc.	422
Agilent Technologies	402	MELEC GmbH	404
AJA International, Inc.	202	MEWASA North America, Inc.	209
AVS	220	Miba Coating Group, Teer Coatings Ltd.	416
Balazs NanoAnalysis	221	Michalex	307
Brooks Automation	316	Micro Materials, Ltd.	311
Bruker Corp.	212	Nano-Master, Inc.	420
CEMECON AG	313	NanoScience Instruments, Inc.	405
Compass Instruments, Inc.	308	Oerlikon Leybold Vacuum USA, Inc.	219
CSM Instruments	203	Oxford Instruments, Inc.	305
Elsevier BV	210	PLANSEE	323
Fischer-Cripps Labs. Pty Ltd	213	Plasmaterials, Inc.	302
Geib Refining Corp	211	Process Materials Inc.	217
Genco	319	PVT Plasma und Vakuum Technik	322
Hauzer Techno Coating B.V.	320	RBD Instruments, Inc.	303
Hidden Analytical, Inc.	207	Refining Systems	101
Horiba Scientific	102	Saxonian Inst. of Surface Mechanics	205
Impedans Ltd.	312	Soleras Advanced Coatings	223
IonBond	206	South Bay Technology, Inc.	100
J.A. Woollam Co., Inc.	304	Super Conductor Materials	301
Kaufman & Robinson, Inc.	306	Surface Modification Systems, Inc.	318
KOBELCO Japan	218	TRIBOTECHNIC	103
Kratos Analytical	222	Trillium US, Inc.	204
Kurt J Lesker Company	403	UC Components	216
Maney Publishing	108	VAT	317

Bold listings indicate our generous sponsors

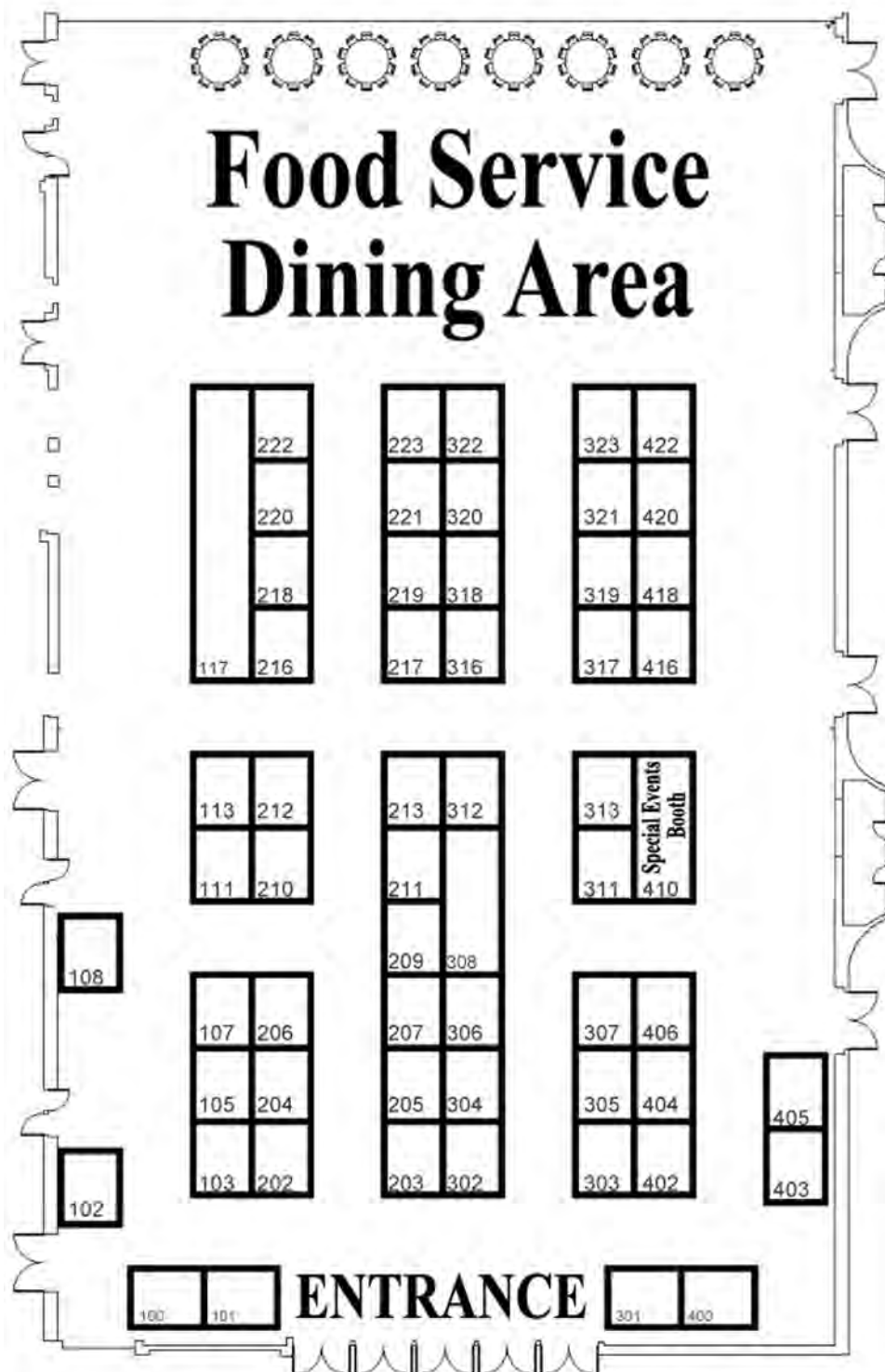
ICMCTF 2012 EXHIBIT HALL

International Conference on Metallurgical Coatings & Thin Films
Towne & Country Resort & Convention Center • San Diego, California

Exhibit Hall Dates & Hours:

Tuesday, April 24, 11:00 am – 7:00 pm

Wednesday, April 25, 10:00 am – 2:00 pm





ICMCTF 2012 SPONSORS



THANK YOU ELSEVIER
for your generous sponsorship of the Cyber Cafe.

Please visit Elsevier at
Booth #210
to show your appreciation!



**THANK YOU
REFINING SYSTEMS**

For your generous
sponsorship of the
ICMCTF 2012
Symposium Notebooks.

Please Visit
Refining Systems at
Booth #101
to show your
appreciation!



**THANK YOU
AJA INTERNATIONAL**

for your generous
sponsorship of the
ICMCTF 2012 Tote Bags

Please visit
AJA International at
Booth #202
to show your appreciation!



**THANK YOU
PLANEE**

for your generous
sponsorship of the
ICMCTF 2012

Exhibit Hall Reception

Please visit
Plansee
at **Booth #323**
to show your appreciation!



**THANK YOU
CemeCon**

for your generous support
of the ICMCTF 2012
Conference & Exhibition

Please visit CemeCon at
Booth #313
to show your appreciation!



**THANK YOU
Oerlikon Balzers**

for your generous
sponsorship of the
ICMCTF 2012

Welcome Mixer

**A VERY SPECIAL THANK YOU TO OUR
MAJOR CONFERENCE SPONSORS**
Please stop by their booths to show your appreciation.



ICMCTF 2012 SPONSORS



 <p>Booth 308</p>	 <p>Booth #320</p>
 <p>Booth 220</p>	 <p>Booth 216</p>  <p>Booth 313</p>
 <p>Booth 301</p>	 <p>Booth 402</p>
 <p>Booth 203</p>	 <p>Booth 212</p>
 <p>Booth 403</p>	 <p>Booth 222</p>
 <p>Booth 302</p>	 <p>Booth 323</p>
 <p>Booth 302</p>	 <p>Booth 323</p>

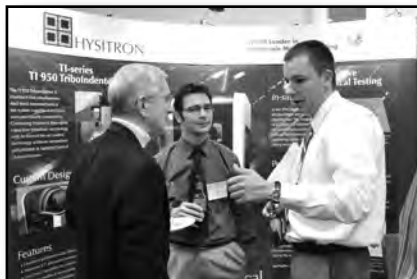
A Special Thank You to all our sponsoring exhibitors for their support of Raffle Prizes, Lunches, Receptions and more!
Please stop by their booths to show your appreciation.



ICMCTF would like to thank all the exhibitors for participating in the 2012 conference by displaying their products and services and taking the time to discuss the needs of the ICMCTF attendees.

Our exhibitors offer a wide range of instrumentation, components and services that apply to the analysis and characterization of metallurgical coatings, thin films and surface modification. Please visit the exhibitors and learn about the latest technology, products and services.

Exhibits are only open Tuesday & Wednesday only - Don't miss it !



VISIT THE EXHIBITS !

EXHIBIT HALL HOURS

Tuesday April 24 11am - 7pm

Wednesday April 25 10am - 2pm



Engineering Solutions

A&N Corporation has the custom fabrication expertise you're looking for.

- Chambers: Cylindrical, Spherical and Box
- Unique Components and Assemblies
- Certified Vacuum Welding Program



Booth# 216

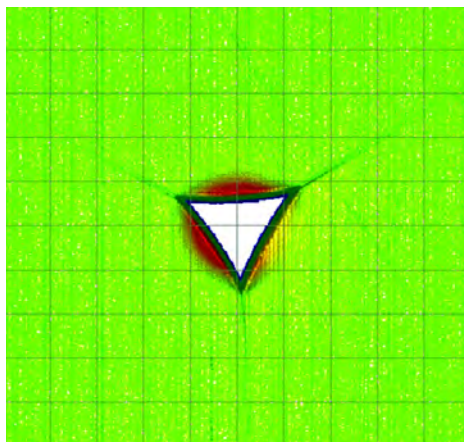
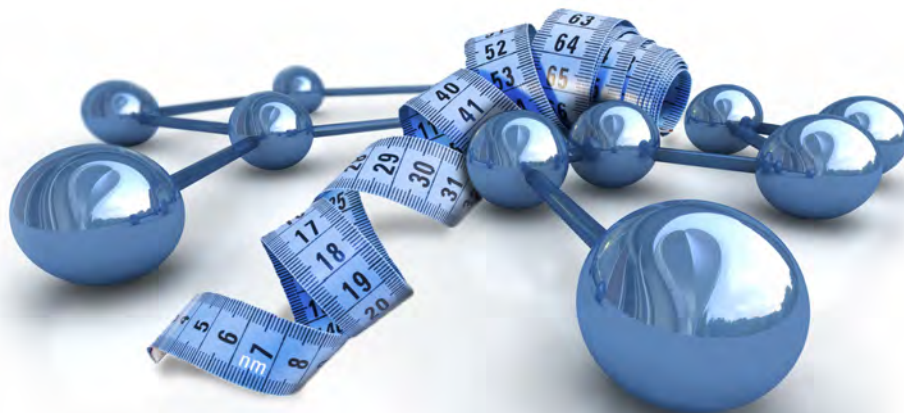
www.ancorp.com

sales@ancorp.com

1-800-352-6431



All in Good Measure



A 24 μm scan of a 1200 nm indent on silica.

Discover More at the Nanoscale

Agilent Technologies offers a comprehensive range of advanced instrumentation that enables you to perform nanoscale research. Agilent develops and manufactures high-precision nanomechanical testing systems and atomic force microscopes to facilitate:

- Materials science
- Polymer science
- Thin film

Expertise in diverse technologies, years of measurement experience, and a thorough knowledge of applications make Agilent a premier scientific solutions provider. Let us help you gain a greater understanding of all things small.

www.agilent.com/find/nano

© Agilent Technologies, Inc. 2009



AJA INTERNATIONAL, INC.

THE #1 CHOICE IN THIN FILM DEPOSITION EQUIPMENT

DUAL CHAMBER SYSTEMS



Metal / Oxide Dual Chamber ATC Sputter System with common cassette load-lock.

ION MILLING SYSTEMS



ATC 1800 Ion Milling System with 6 position load lock cassette

809 Country Way • P.O. Box 246 • N. Scituate, MA 02060 • USA
T: 781-545-7365 • F: 781-545-4105 • topgun@ajaint.com • www.ajaint.com



AVS 59th International Symposium & Exhibition

October 28 - November 2, 2012 • Tampa, Florida

Tampa Convention Center

Call For Abstracts

Deadline:
MAY 2, 2012

Complete details
available online at
www.avs.org



212-248-0200
avsnytc@avs.org



Addressing cutting-edge issues associated with **materials, processing, and interfaces** in both the **research and manufacturing** communities. The weeklong Symposium fosters a multidisciplinary environment that cuts across traditional boundaries between disciplines featuring:

TECHNICAL SESSIONS • SHORT COURSES • EXHIBITS

DIVISION/GROUP PROGRAMS:

- Advanced Surface Engineering
- Applied Surface Science
- Biomaterial Interfaces
- Electronic Materials & Processing
- Magnetic Interfaces & Nanostructures
- Manufacturing Science & Technology
- MEMS & NEMS
- Nanometer-Scale Science & Technology
- Plasma Science & Technology
- Surface Science
- Thin Film
- Vacuum Technology

FOCUS TOPICS:

- Actinides & Rare Earths
- Biofilms & Biofouling: Marine, Medical, Energy
- Biointerphases
- Electron Transport at the Nanoscale
- Energy Frontiers
- Exhibitor Technology Spotlight
- Graphene & Related Materials
- Helium Ion Microscopy
- *In Situ* Microscopy & Spectroscopy
- Nanomanufacturing
- Oxide Heterostructures-Interface Form & Function
- Scanning Probe Microscopy
- Spectroscopic Ellipsometry
- Transparent Conductors & Printable Electronics
- Tribology

.....
Simple to Use
.....

.....
Simple to Justify
.....

.....
Simple to Support
.....

Simplicity Solutions™

from the Granville-Phillips® Portfolio



For state-of-the-art gas analysis instrumentation, keep it simple.

- Full 1-100amu gas compositional analysis < 0.1 seconds
- Calibrate in seconds, using any single gas already in your system
- Measure low mass range gases with no zero blast

Measurement Simplified



Please call us at 1-800-776-6543
or visit us on the web at: www.brooks.com

CC800[®]/9 HIPIMS



Incorporating Coating Technology
into your business

- true integration of HIPIMS into an industrial coating system
- production tested recipes
- all PVD Sputter coatings with one machine

CemeCon AG
Adenauerstraße 20 A4
D-52146 Würselen, Germany
+49 (0) 2405 4470 100
www.cemecon.com, info@cemecon.com



COMPASS

INSTRUMENTS

Fuels, Lubricants and Materials Testing Equipment

We specialize in the sales and service of testing equipment for the evaluation of the physical properties and performance characteristics of fuels, lubricants, and materials.

- Materials
- Lubricants
- Waxes-Bitumen
- Biodiesel
- Fuels



<http://www.compass-instruments.com> • Phone: 630.556.4835 • fax: 630.556.3679

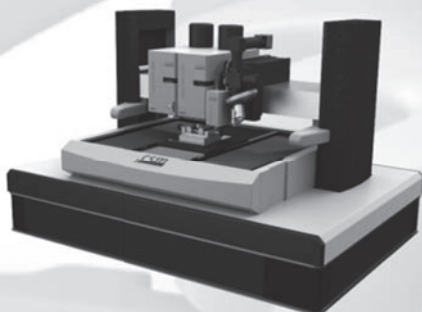
Compass Instruments • 1020 Airpark Drive • Sugar Grove, IL 60554 •
USAcontact : Mr. J. Hepp heppjp@compass-instruments.com

//// CSM INSTRUMENTS

Advanced Mechanical Surface Testing

EXCELLENCE IN NANOINDENTATION, SCRATCH AND TRIBOLOGY

CSM Instruments offers a wide range of instruments and testing services for surface mechanical properties characterization, including indentation (hardness and modulus); scratch testing (coating adhesion, fracture and deformation) and tribometers (friction and wear).

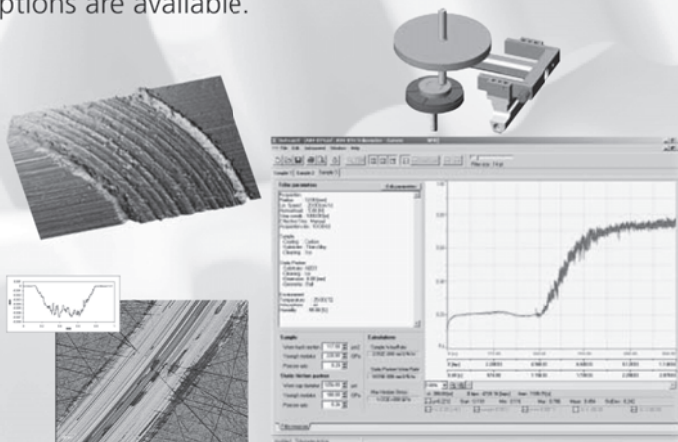


Applications:



> TRIBOMETER Pin-on-disk

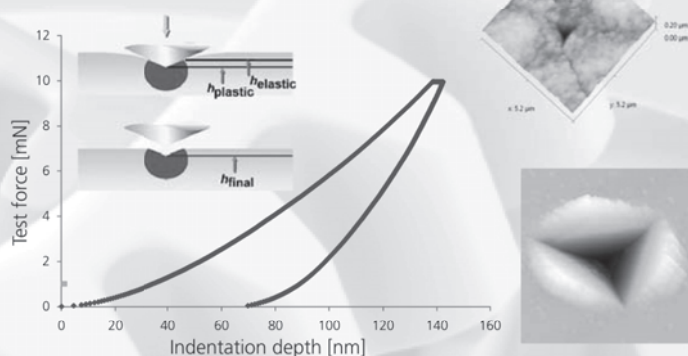
Used to measure the frictional coefficient and wear rate between material pairs, as well as perform lifetime analyses. Based on the pin-on-disc principle, operates both in the Micro and Nano range. High temperature, vacuum or environmental control options are available.



> NANOINDENTATION Tester

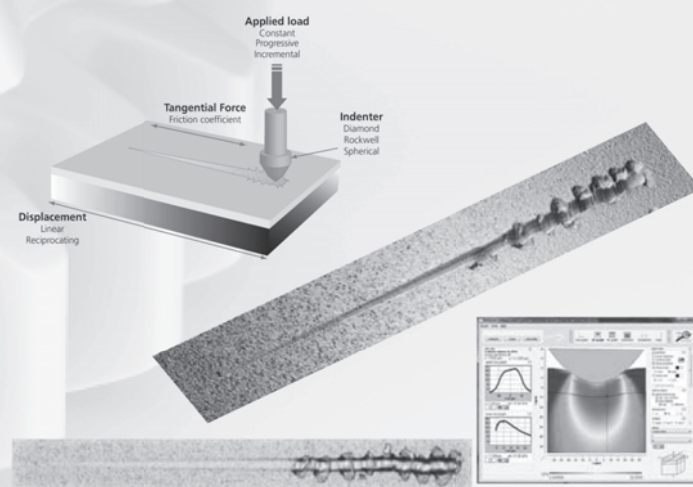
Used to determine the hardness and elastic modulus of coatings and surfaces with extremely high precision at the micro- and nano-scales.

Dynamic testing measurements can be performed to define not only the hardness of the material, but also to evaluate the plastic and elastic deformation, the elastic modulus, creep and more.



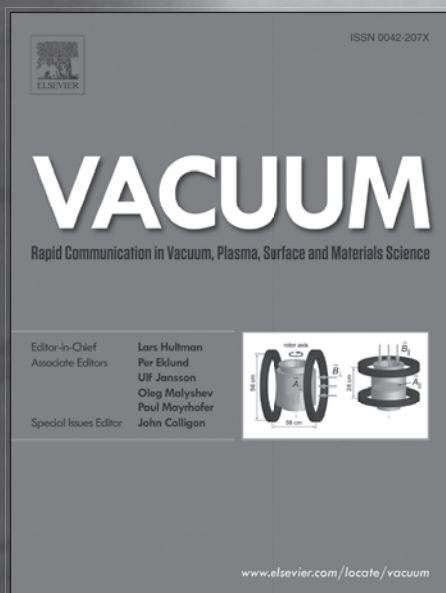
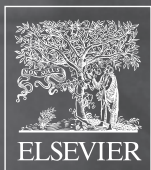
> SCRATCH Tester

Used to measure characteristics such as adhesion of a coating, delamination effects, or cracking in order to optimize coating techniques and determine failure points of the film-substrate system.



www.csm-instruments.com

CSM
Instruments



- **New focus on rapid communications**
- **New editorial team**
- **New aims & scope**

www.journals.elsevier.com/vacuum



Geib Refining Corp.

Dependable Precious Metal Reclamation

Precious metal reclaim from production scrap including:

- ▶ Spent Targets
- ▶ Wafers
- ▶ Chamber Scrapings
- ▶ Boats

Metal recovery can be returned in the form of new source product or through check or wire transfer. We also clean shields to UHV standards. EPA compliant and ITAR registered let Geib professionally handle your precious metal needs Au/Ag/Pt/Pd/Rh/Ir

Geib Refining ♦ 399 Kilvert Street ♦ Warwick, RI 02886
(800)228-4653 ♦ (401)738-8560 ♦ mike@geibrefining.com ♦ www.geibrefining.com

VISIT US AT BOOTH #211 !!

perfect your process

intelligent plasma monitoring and feedback

planar magnetron | rotatable magnetron | speedflo plasma monitor & controller | linear ion source



reactive
sputtering
made easy

speedflo™
genco.com



**Exhibit Hall Reception - Atlas Ballroom
Tuesday Evening 5:30pm - 7:00pm
Free Refreshments & Food
Join Us !**

HORIBA
Scientific

Make us your partner in solid sample analysis

HORIBA Scientific provides a full line of products for solids analysis...from C, S, O, N and H elemental analyzers to Glow Discharge Spectrometers for bulk and surface analysis.

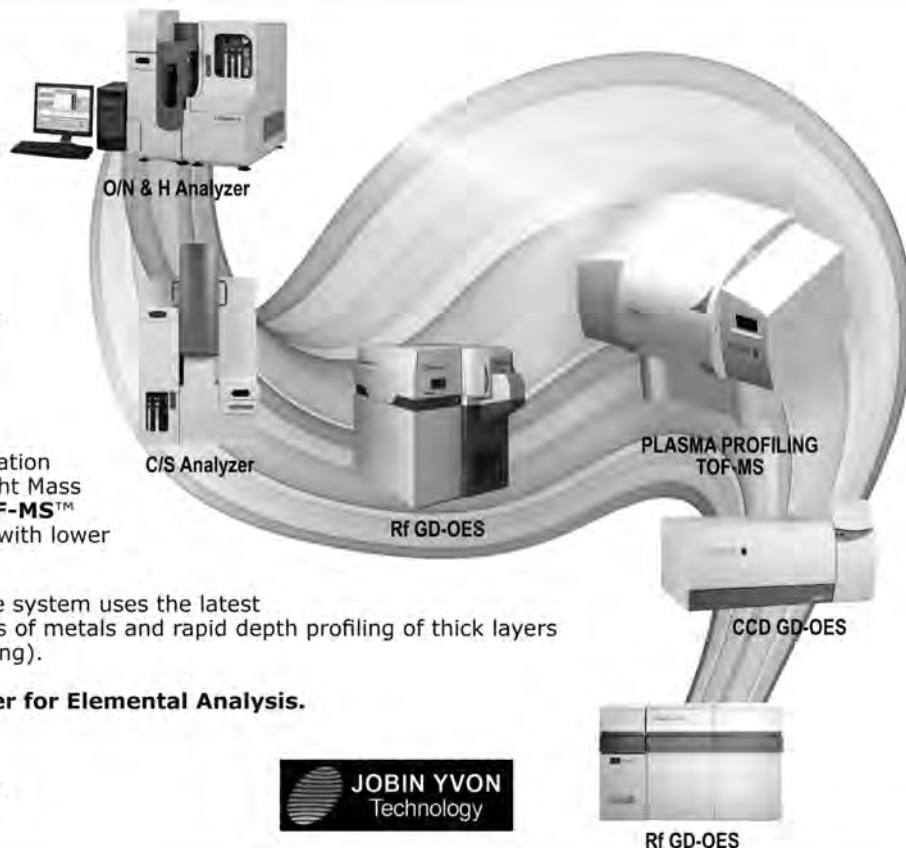
NEW from HORIBA is the exciting combination of GD Plasma Sputtering and Time of Flight Mass Spectrometry. The **Plasma Profiling TOF-MS™** provides advanced depth profile analysis with lower detection limits.

Also the NEW **3D Metal™** Glow Discharge system uses the latest multi-channel technology for bulk analysis of metals and rapid depth profiling of thick layers (heat treatment, Zn coatings, electroplating).

HORIBA Scientific is your solid partner for Elemental Analysis.

www.horiba.com/scientific

email: ad.sci@horiba.com



Explore the future

Automotive Test Systems | Process & Environmental | Medical | Semiconductor | Scientific

HORIBA

HORIBA
Scientific

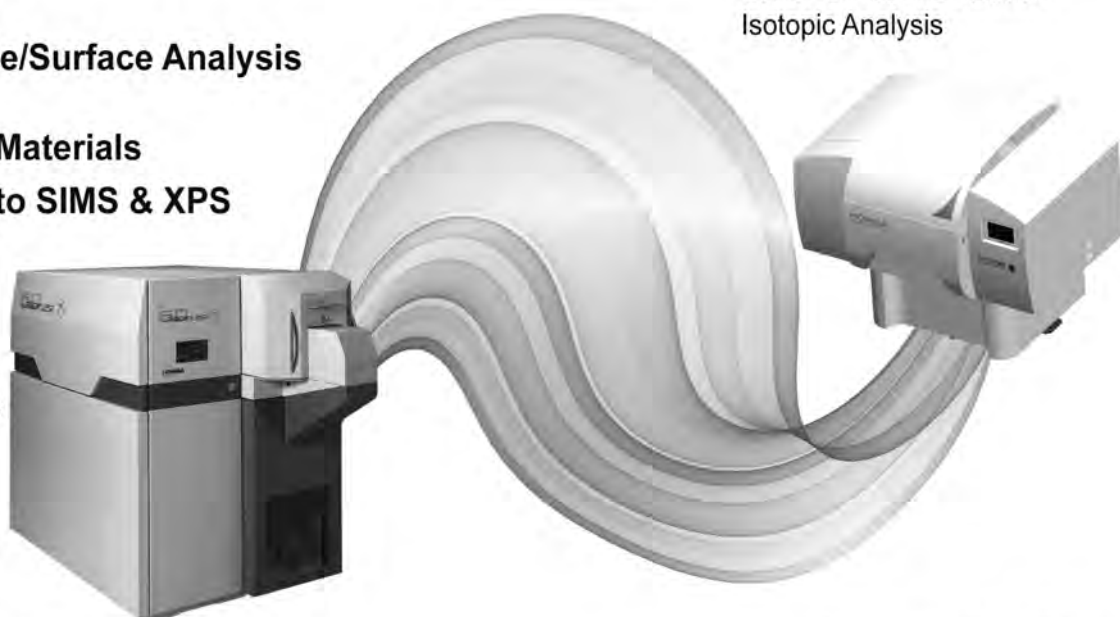
Fast Depth Profile/Surface Analysis

**Conductive &
Non-conductive Materials**

Complementary to SIMS & XPS

**Rf GD-OES
Glow Discharge-OES**

Affordable Elemental
Surface Analysis



Plasma Profile TOF-MS

Lower Limits of Detection
Isotopic Analysis

www.horiba.com/scientific

email: ad.sci@horiba.com



Explore the future

Automotive Test Systems | Process & Environmental | Medical | Semiconductor | Scientific

HORIBA



www.impedans.com

ICMCTF Booth #312

Plasma Diagnostics for
Research and Industry

Applications:

- Plasma Research
- Sputtering
- PECVD
- Ion Beam
- Etch



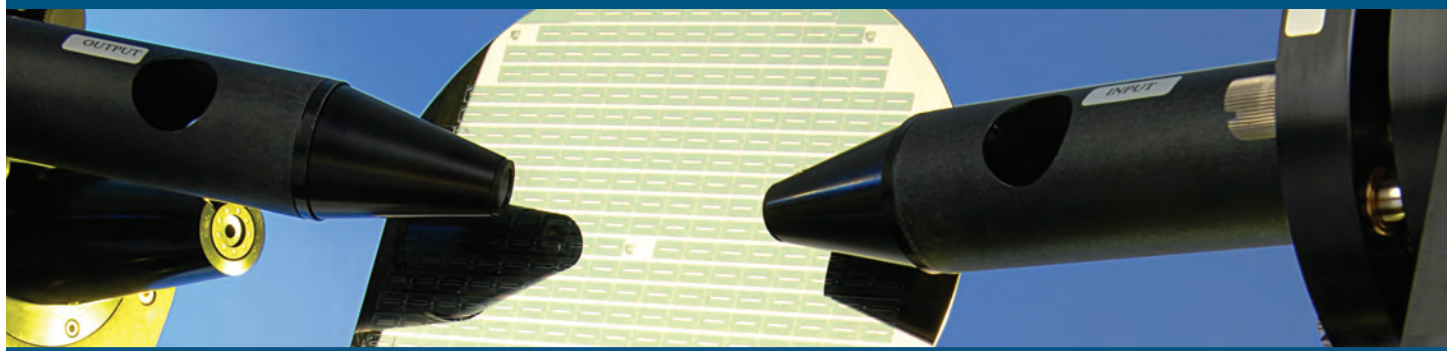
Measure

- Ion energy
- Ion flux
- IEDF
- RF Power
- RF I,V, phase
- Impedance
- Electron Density
- Electron Temperature
- EEDF



J.A. Woollam Co., Inc.

Ellipsometry Solutionssm for your Thin Film Characterization.



J.A. Woollam Co. has the world's widest variety of Spectroscopic Ellipsometers with 8 different models to non-destructively characterize thin film thickness and optical constants. After twenty-four years, over 15,000 samples characterized in our lab, and over 140 patents – we are the Ellipsometry Experts.

www.jawoollam.com • 402.477.7501 • 645 M Street, Lincoln, Nebraska USA

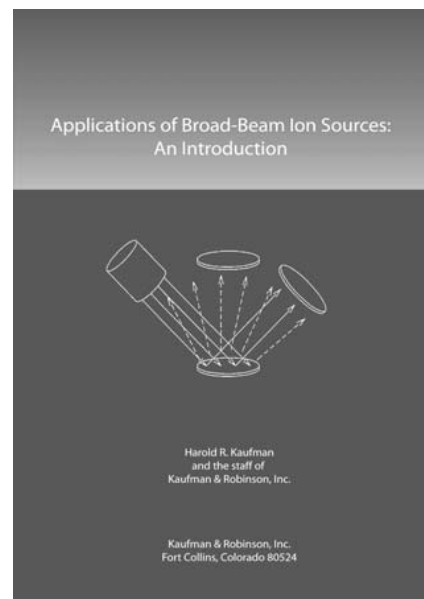


Kaufman & Robinson announces their Newly Released book for applications in ion source processes. Harold R. Kaufman provides a fundamental tool to guide users in the use of broad-beam sources.

"Applications of Broad-Beam Ion Sources"

Understand and improve your process applications, includes:

- Guidance in ion beam deposition and etching
- Selecting the appropriate source configuration
- Optimizing process rates, uniformity and yields
- Understanding material and ion interactions
- Useful tables and figures, including extensive data on etch rates



AVAILABLE FOR PURCHASE

**Benefit from years of experience and insight
in broad-beam processes!**

CONTACT : 970.495.0187





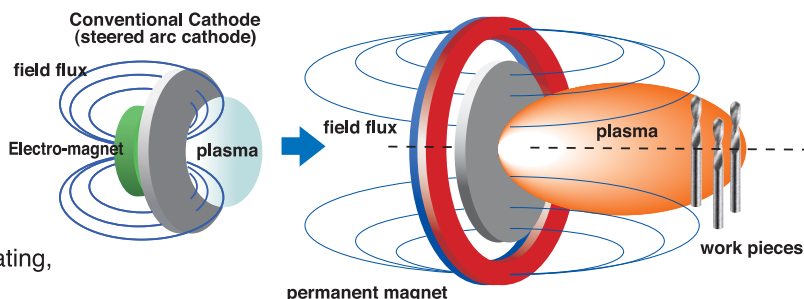
KOBELCO PVD COATING SYSTEM

AIP Cathodic Arc Ion Plating

AIP™ S-series provides innovative technologies from the view point of surface-roughness. Extremely smooth surface is successfully created without jeopardizing deposition rate.

Features of AIP™

- ❶ Droplets, major defect of Cathodic Arc Ion Plating, is successfully minimized by AIP™
- ❷ Thick & dense film with extremely smooth surface
- ❸ High deposition rate by high energy density & high ionization
- ❹ Flexible operation & easy maintenance
- ❺ Applicable of multi layer films & multi process films



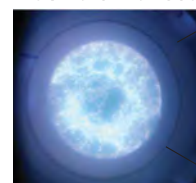
Conventional Cathode



coating

WC-Co

Plasma enhanced cathode



coating

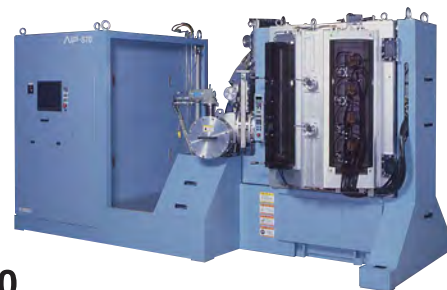
WC-Co

10mm

SEM image of surface morphology of TiAlN

AIP-S series

- Line up of R&D, Mid-Production, and Mass Production models.
- TMP & CT pumping system for wide coating condition
- Wide open doors for easy maintenance
- Easy operation by touch screen



AIP-S70

Coating zone	Evaporating source
φ700×H700 mm	8 sets ~ 16 sets



AIP-S40

Coating zone	Evaporating source
φ450×H500 mm	6 sets ~ 12 sets



AIP-S20

Coating zone	Evaporating source
φ200×H120 mm	1 sets ~ 3 sets

LEADING SURFACE ANALYSIS

AXIS SPECTROMETERS

- XPS with unrivalled energy resolution and sensitivity
- High spatial resolution chemical & elemental imaging
- Flexibility of configuration including optional surface analytical techniques
- Dual mode Ar⁺ / polyatomic ion source capability unique to AXIS spectrometers

Learn more about leading surface analysis by visiting our website

www.kratos.com



T: +1 (845)-426-6700

E: surface@kratos.com

W: www.kratos.com

KRATOS
ANALYTICAL
A SHIMADZU GROUP COMPANY

Kurt J. Lesker Company® is an international manufacturer and distributor of vacuum products. We provide the most complete line of vacuum products in our industry, from simple flanges to turn-key thin film deposition tools. We feature low prices, quick delivery, e-commerce, sales offices around the world, and technical and engineering help for all our customers.

VACUUM MART™ DIVISION

- KJLC® Hardware
- Vacuum Fluids: Fomblin®, KJLC Silicone 704
- KJLC Feedthroughs
- KJLC Gauges
- KJLC Valves
- Vacuum Pumps

PROCESS EQUIPMENT™ DIVISION

- Process Tools for: Sputtering & Evaporation
- Electron Beam & Thermal Evaporation
- OLED, OPV & Organic Electronics
- Atomic Layer Deposition (ALD)
- Engineered Vacuum Solutions

MATERIALS™ DIVISION

- Sputter Targets: Production & R&D
- Evaporation Materials
- Precious Metals
- Thermal Sources
- E-beam Liners
- In-House Bonding Service



Kurt J. Lesker®
Company

www.lesker.com

Kurt J. Lesker Company
United States
412.387.9200
800.245.1656
salesus@lesker.com

Kurt J. Lesker Canada Inc.
Canada
416.588.2610
800.465.2476
salescan@lesker.com

Kurt J. Lesker Company Ltd.
Europe
+44 (0) 1424 458100
saleseu@lesker.com

Kurt Lesker (Shanghai) Trading Company
科特·莱思科(上海)商贸有限公司
Asia
+86 21 62181240
saleschina@lesker.com

Materials Science & Engineering Collection from Maney Publishing

MORE

Maney Online Research E-journals

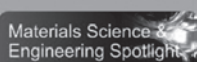
The Materials Science & Engineering Collection is also available as an online package for institutions, providing access to 28 international peer-reviewed journals.

For a free trial, visit
www.maney.co.uk/freetrial

For information on MORE visit:
www.maney.co.uk/more_mse



Titles providing broad coverage of their discipline are complemented by specialist titles focussing on niche areas including materials research, physical metallurgy and surface engineering.



Visit the Materials Science & Engineering Spotlight for more information: www.maney.co.uk/materials

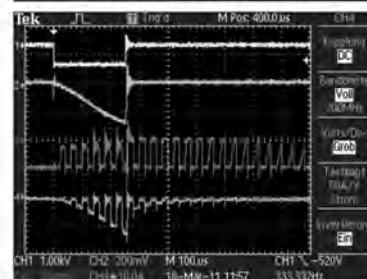


DC Pulse Power Controller for:

- HPPMS / HiPIMS
- Mid Frequency (MF)
- Pulsed Bias (synchronized / non-synchronized)
- DC / Unipolar / Bipolar Pulse Modes
- Superimposed Processes
 - o HiPIMS and DC
 - o HiPIMS and MF
 - o HiPIMS and Pulsed Bias
- Full Synchronization of all power signals are possible
- Full Arc Management

BOOTH# 404

Patents Pending



Innovation in Motion



Miba Coating Group is the specialist in innovative coating solutions. High Tech Coatings GmbH (HTC), Teer Coatings Ltd. (TCL) and Miba Coatings Trading Suzhou build the coatings competence center for the Miba Group as a whole. Miba Coating Group develops individual coating solutions for components. We specialize in polymer coatings like Synthec® or Spacecoat®, electroplated and PVD coatings and the construction of coating equipment.

As an active development partner to our customers, we are heavily geared to progress and innovation, and particularly welcome complex challenges. Customers come to rely on our tailored, innovative solutions and extensive product range.

Company Name: Miba Coating Group, Teer Coatings Ltd.

Company Contact: Zuzana Mellor

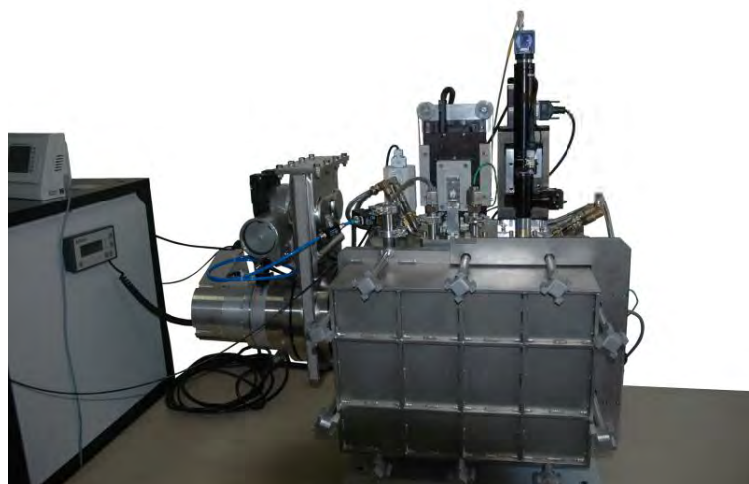
Phone: +44 (1905) 827 550

E-mail: tcl@miba.com

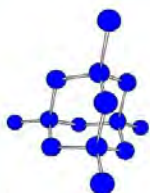
Nanoindenter HTIIS 1000

1000°C !

Unique nanoindenter measuring mechanical properties up to 1000 °C



- Hardness
- Young's modulus
- Creep
- Relaxation
- Fracture toughness
- Thermo Mechanical Fatigue (TMF)
- Strain rate control
- Activation energy calculation
- Unlimited modeling analysis
- AFM imaging

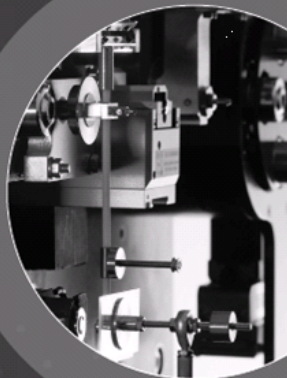
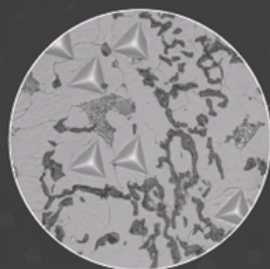


Michalex

NanoTest™

Visit us on
Booth 311

- ▶ Nanoindentation
- ▶ Nanoindentation to 750°C
- ▶ Nano-scratch and wear
- ▶ Nano-impact and fatigue
- ▶ Nanoindentation in liquid



www.micromaterials.co.uk

Thin Film Processing Systems



Ion Beam Etching with Load
Lock and Sputter Option



E-Beam Evaporation
System



PECVD with ICP
for CNT Growth



PECVD with
Liquid Precursors



PECVD/RIE
Dual System



Table Top PA-MOCVD
for InGaN and AlGaIn



Table Top Thermal
Evaporator



Three Gun Sputtering
System w/Touch Screen



Single Wafer/Mask
Cleaner System



Large Substrate Cleaner
for Display Panels



NANO-MASTER, Inc.

3019 Alvin Devane Blvd. Ste. 300, Austin, TX 78741
Ph. 512-385-4552 main@nanomaster.com

Visit us at Booth #420
www.nanomaster.com



Visit Us at Booth 405

Nanoscience Instruments is the leading provider of easy-to-use, robust & affordable surface analysis instrumentation.

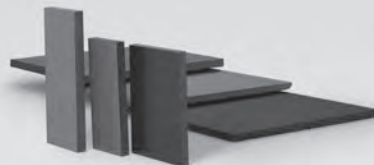
We offer:

AFMs

Desktop SEMs

3D Optical Microscope Profilers

Nanoscience Instruments, Inc.
9831 S. 51st Street
Suite C119
Phoenix, AZ 85044 USA
General: info@nanoscience.com
Sales: sales@nanoscience.com



High performance target materials for PVD coating solutions

PLANSEE is the leading full-range supplier for high purity target material for the hard coating industry. Our portfolio covers a variety of standard compositions as well as new materials.

Our mission is to develop coating solutions that offer real competitive advantages to our customers.

VISIT US!

at our Booth-no. 323

A Step ahead in Technology.



PLANSEE SE, 6600 Reutte, Austria, Tel.: +43 5672 600-0, Fax: +43 5672 600-500, info@plansee.com, www.plansee.com

PLASMATERIALS, Inc.

Our Products

Plasmaterials, Inc. provides high purity Physical Vapor Deposition (PVD) materials in nearly every element, alloy, composition and component available on the periodic chart. Plasmaterials, Inc. provides sputtering targets, backing plates and other segments of the materials market including evaporation material, crucible liners and electron beam starter sources. In addition, Plasmaterials offers backing plates and metallic bonding services for sputtering targets when needed. Our metallic bonding process utilizes a proprietary process for affixing the target directly to the backing plate using low vapor pressure materials. These bonding materials provide the necessary mechanical, thermal and electrical conductivity while allowing differential expansion between the target and backing plate. Backing plates for nearly all commercial available systems are usually in stock for immediate delivery. Custom design backing plates can usually be provided within a short period of time.

*For inquiries and/or quotations, please contact
us at (925) 447-4030 or info@plasmaterials.com
www.plasmaterials.com*



WHAT DO THESE INNOVATIVE PRODUCTS HAVE IN COMMON?

THEY'RE ALL
PRODUCED BY
THE BIGGEST
LITTLE
COMPANY
IN
MATERIALS
SCIENCE

microCMA

COMPACT AUGER ANALYZER



FEATURES

- compact (2.75 in. flange)
- proven design
- USB interface
- affordable

APPLICATIONS

- thin film composition
- depth profiles
- surface film quantization
- IC contamination

IG2

SPUTTER ION SOURCE



FEATURES

- reliable
- long filament life
- 2-year warranty
- affordable

APPLICATIONS

- ion beam etching
- sputter cleaning
- STM tip cleaning

9103

USB GRAPHING PICOAMMETER



FEATURES

- USB control
- data logging/graphing
- target bias options
- auto/manual range

APPLICATIONS

- electron/ion current
- current leakage
- vacuum diode testing
- conductivity

ZCUVE

WATER-VAPOR DESORPTION SYSTEM



FEATURES

- multiple flange sizes
- manual/auto shutter
- sealed UV emitter
- safe for deposition

APPLICATIONS

- O-ring sealed chambers
- deposition chambers
- small load locks



www.rbdinstruments.com

541.330.0723
2437 NE Twin Knolls Dr.
Bend, OR 97701



Refining Systems Inc.



Products Are
Manufactured
According To
Client
Specification



We Offer A
Higher Quality
Product At A
Lower Cost



Fabricators of Precious Metals & Materials For Science & Industry

WWW.REFININGSYSTEMS.COM

702-368-0579

ADAYANI@EARTHLINK.NET



SOUTH BAY TECHNOLOGY, INC.



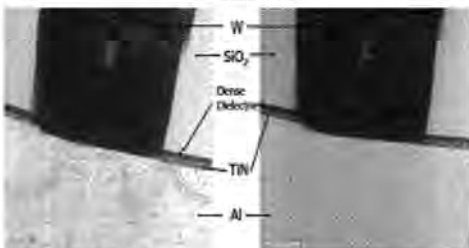
IBSe Ion Beam Deposition and Etch

Large area ion beam polishing and slope cutting is possible with the 1 cm diameter broad beam ion source. The low energy, high current ion source provides rapid EBSD quality ion polishing over areas greater than 1" diameter of difficult, easily smeared materials. Up to four different target materials can be selected under vacuum for multilayer thin film coatings. Table top, turbo pumped dry vacuum system with sample capability up to 4" diameter. Variable speed rotation, rocking, angle and tilt capability.



EBSD Polishing Kit

The EBSD Polishing and Storage Kit utilizes a micrometer controlled lapping fixture with a mounting block to securely hold two pin mount SEM stubs. The kit includes a new pre-tilt EBSD stage piece with three height correction segments for quick repeat analysis. The pre-tilt stage is designed to fit through most load locks and holds a standard pin mount stub at a 70° or 20° angle. With the EBSD kit the sample can be mounted, polished, and transferred directly to an EBSD system or stored in the included SampleSaver™ vessel all without dismounting the sample.



Plasma Trimming/Cleaning

For safe, gentle removal of amorphous damage caused by FIB, high energy ion milling or mechanically thinned samples, the plasma trimming™ process utilizes a controlled argon ion energy to thin a sample from both sides. The system utilizes the exclusive Fortress™ non-destructive sample mount and can be directly transferred from the FIB or SEM direct to the plasma trimming stage without dismounting the sample.

A very thick FIB-prepared device. Thinning occurred including removal of Ga+ damage

South Bay Technology, Inc. • Booth #100

1-800-728-2233 • info@southbaytech.com • www.southbaytech.com



**SUPER CONDUCTOR
MATERIALS, INC.**

845-368-0240

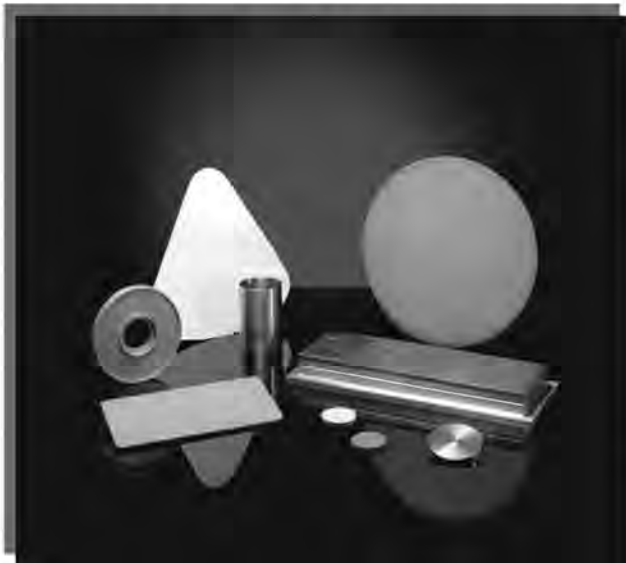
PHONE: (845)368-0240

E-MAIL: SALES@SCM-INC.COM

VISIT US AT: WWW.SCM-INC.COM

THIN FILM MATERIAL & PRODUCTS

SPUTTERING TARGETS • EVAPORATION MATERIALS • CRUCIBLE LINER & E-BEAM PARTS



- **Metals**
- **Oxides**
- **Carbides**
- **Nitrides**
- **Fluorides**
- **Sulfides**
- **Silicides**
- **Tellurides**
- **Selenides**
- **Rare Earth Metals**
- ...and many more!*



SURFACE MODIFICATION SYSTEMS, INC

Specializing in manufacture of rotary targets for thin film deposition

Ag, Al, CdIn, CdSn, Cr, Co Alloys, Cu, CuIn, CuGa, Cu alloys with Sodium donors, CuInGa, In, Mo, Mo with Sodium donors, Nb, NiCr, NiSi, Sn, Sn alloys, SnSi, Ti, TiOx, Zn, Zn Alloys, W and W alloys

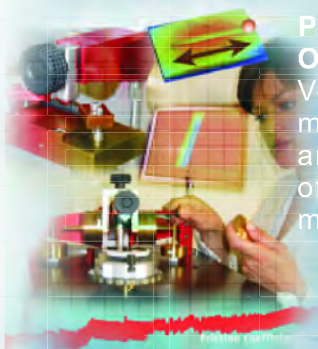
Providing thin film deposition related chamber coatings: Al, Al₂O₃, Y₂O₃ and others specific to customer needs for etch erosion or particulate containment.

SURFACE MODIFICATION SYSTEMS, INC

12917 Park Street, Santa Fe Springs, CA 90670

(562) 946 7472

www.surfacemodificationsystems.com



**Pin-On-Disc
Oscillating TRIBOtester**
Versatile tribometers
measures friction, wear
and tribo corrosion
of coating and bulk
materials

Calotester
New
instrument
fully
equipped
with calculator,
microscope
for measurement
coating thickness



TECHNOLOGICAL LEADER

booth N°103



Scratch Tester Millennium
adherence test characterization
and scratch resistance

**Milli TRIBOtester and
Milli scratch tester**
All in one for
friction, adhesion
and scratch resistance

www.tribotechnic.com

VENTED SCREWS

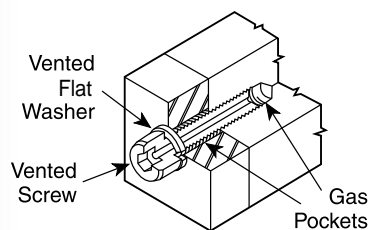
Reduce Pump-Down Times, Eliminate Virtual Leaks, Stop Fastener Galling

Thousands of sizes to choose from

Metric and Inch standards

Cleaned for immediate vacuum service

Coated, Plated, Polished and custom variations available



Now offering Gold Pated Fasteners, Slot-Vented Screws and Vacuum-Baked O-Rings



U-C COMPONENTS, INC.

Phone (408) 782-1929

POB 430 Morgan Hill, CA 95038
sales@uccomponents.com

18700 Adams Ct. Morgan Hill, 95037
www.uccomponents.com



Leader in Vacuum Valves

Visit VAT at Booth #317

- Gate valves, pendulum valves, Vatterfly valves
- Control valves
- Transfer valves and doors for semiconductor production
- Transfer valves and doors for production of flat screens and photovoltaic cells
- Angle valves and diaphragm valves
- Special valves for accelerators and synchrotrons
- Special valves for gases
- Connection components
- Multi-valve modules, Heater, Coatings

Phone: 800-935-1446
Fax: 781-935-3940
us@vatvalve.com
<http://www.vatvalve.com>



Monday Morning, April 23, 2012

Plenary Talk

Room: Golden Ballroom - Session PL

Plenary Talk

8:00am **PL-1 How Interfaces Control the Mechanical Behavior of Biological Materials**, *P. Fratzl*, Director of the Max Planck Institute of Colloids and Interfaces, Germany

INVITED

Biological materials, such as wood, grasses, protein fibres, bone, sea shells or glass sponges are generally composites of different types of polymers as well as mineral. These materials are able to adapt to the mechanical requirements of the environment by growing and assembling structural components in a hierarchical fashion. This implies the existence of various types of interfaces at all levels of hierarchy. From a mechanical viewpoint, interfaces may be considered as defects but, in many natural materials, interface structures emerged which improve rather than deteriorate the overall mechanical properties of the composite. Bone, for example, consists in about equal amounts of a collagen-rich matrix and calcium-phosphate nano-particles. These components are joined in a complex hierarchy of fibres and lamellar structures to a material with exceptional fracture resistance. Similarly, tendon collagen consists of an assembly of fibrils which partly deform by shearing the interface between them. An example for self-healing properties due to molecular-scale interfaces is the byssus fibre used by mussels to attach to rocks. These fibres combine large deformation with stiffness and abrasion resistance. Finally, plant cell walls generate internal stresses and even complex movements upon changes of environmental humidity. This force generation and actuation capabilities are based on water swelling of hemicellulose-rich interfaces between cellulose microfibrils arranged in complex architectures. Unravelling the structural principles of these unexpected material properties may indicate ways towards new types of composite materials with adaptive capabilities.

Monday Morning, April 23, 2012

Hard Coatings and Vapor Deposition Technology Room: Royal Palm 4-6 - Session B1-1

PVD Coatings and Technologies

Moderator: P. Eklund, Linköping University, Sweden, J.H. Huang, National Tsing Hua University, Taiwan, J. Vetter, Sulzer Metaplas GmbH, Germany

10:00am **B1-1-1 Properties of nanocrystalline Al-Cu-O films reactively sputtered by dc pulse dual magnetron.** *J. Blazek, J. Musil (musil@kfy.zcu.cz), P. Stupka, R. Cerstvy, J. Houska, University of West Bohemia, Czech Republic*

The study reports on the effect of the addition of copper in the Al_2O_3 film on its mechanical and optical properties. The Al-Cu-O films were reactively co-sputtered using dc pulse dual magnetron in a mixture of $\text{Ar}+\text{O}_2$. One magnetron was equipped with a pure Al target and the second magnetron with a composed Al/Cu target. The amount of Al and Cu in the Al-Cu-O film was controlled by the length of pulse at Al/Cu target. The Al-Cu-O films with ≤ 16 at.% Cu were investigated in detail. The addition of Cu in Al_2O_3 film strongly influences its structure and mechanical properties. It is shown that (1) the structure of Al-Cu-O film gradually varies with increasing Cu content from $\gamma\text{-Al}_2\text{O}_3$ at 0 at.% Cu through $(\text{Al}_{8-2x}\text{Cu}_{3x})\text{O}_{12}$ nanocrystalline solid solution to CuAl_2O_4 spinel structure, (2) the Al-Cu-O films with ≥ 3 at.% Cu exhibit (i) relatively high hardness H increasing from ~ 15 GPa to ~ 20 GPa, (ii) enhanced elastic recovery W_e increasing from $\sim 67\%$ to $\sim 76\%$ with increasing Cu content from ~ 5 to ~ 16 at.% Cu and (iii) low values of Young's modulus satisfying the ratio $H/E > 0.1$ at ≥ 5 at.% Cu, and (3) highly elastic Al-Cu-O films with $H/E > 0.1$ exhibit enhanced resistance to cracking during indentation test under high load.

10:20am **B1-1-2 Reactive cathodic arc-evaporation of corundum structured crystalline $(\text{Al,Cr})_2\text{O}_3$.** *J. Paulitsch (joerg.paulitsch@unileoben.ac.at), Christian Doppler Laboratory for Application Oriented Coating Development at the Department Of Phys. Metal. And Mater. Testing, Montanuniversität, Austria, J. Ramm, M. Lechthaler, OC Oerlikon Balzers AG, Liechtenstein, P. Polcik, PLANSEE Composite Materials GmbH, Germany, M. Pohler, Christian Doppler Laboratory for Advanced Hard Coatings at the Dep. Of Phys. Metal. And Mater. Testing, Montanuniversität, Austria, D. Holec, P.H. Mayrhofer, Montanuniversität Leoben, Austria*

The arc-evaporation technique is one of the most commonly used deposition technique in industry, as it indicates high growth rates combined with superior coating properties. Nevertheless, reactive cathodic arc-evaporation processes show high influence of the reactive partial pressure used, especially when depositing Al-Cr oxides. Recent investigations pointed out that an increased oxygen partial pressure enhances the formation of crystalline Al-Cr oxides. Such high gas flow rates result in formation of oxide islands on the target surface, increasing the droplet density of the film formed as well as indicates a non-steady-state process. Therefore, investigations were directed to vary the Al to Cr composition in the target to overcome these drawbacks and assure high quality $(\text{Al,Cr})_2\text{O}_3$ films and a controlled process. Here we show first results on arc-evaporated $(\text{Al,Cr})_2\text{O}_3$ using ternary Al-Cr-Si targets and their positive effects on the formation of crystalline corundum structured oxides as well as decreased target poisoning due to oxide formation. Furthermore, theoretical investigations using density function theory are carried out to support the evaluated results.

10:40am **B1-1-3 Wear mechanism of coated cutting tools and improvement of their cutting performance.** *T. Ishikawa (takeshi_ishikawa@hitachi-tool.co.jp), Hitachi Tool Engineering, Ltd., Japan*

INVITED

Hard coatings based on transition metal nitrides have been well established and routinely used for cutting tool applications such as milling, turning and drilling. TiN coatings have been used for milling tools since 1980s for their outstanding properties. Recently, ternary (TiAlN , AlCrN , TiSiN), quaternary (TiAlSiN , AlCrSiN) nitride coatings including their combinations have been used for better efficiency and productivity of industrial dies and molds. In this regard, TiSiN-based coatings attracted particular attention for their superior tool life compared to aluminum-based nitride coatings.

Understanding failure mechanisms of cutting tools and the tool-work interface is necessary for further improvement of tools life. Therefore, in this study, wear and failure mechanisms of coated cutting tools were

studied. TEM cross-sectional analysis was used to observe the cutting edges of tools after being used for machining tests, cutting temperature was evaluated by measuring the thermal electromotive force of tool-material, EPMA was used to analyze the coating surface and to study the effect of Si and Al contents on cutting performance.

The TEM cross-sectional analysis of the cutting edges shown that the coatings deformed plastically toward the axis with formation of micro cracks. The TEM-EDS analysis of the coatings after the cutting test have shown Co-diffusions into the coatings and phase transitions of the coatings in the actual cutting process. According to the measurement of the cutting temperature, the cutting speed found to be an effective factor rather than hardness of work-material.

EPMA analysis of tool-work interface showed that an oxide layer was formed on the coating surface during cutting, which was Mn-Si-O or Al-O. The oxide layer is called "belag". Formation of the Mn-Si-O layer could help increasing the cutting speed compared to formation of an Al-O layer. The belag formation was related to the chemical composition of work materials, chemical composition of the coatings and cutting temperature.

Furthermore, cutting tests using coatings with various chemical composition showed that grain size and crystal structure of coatings has good agreement with the cutting performance. It was concluded that minimizing the grain size of a coating is one of the most important factors for developing cutting tool with higher tool life.

11:20am **B1-1-5 Phase Transformations in Face Centered Cubic $(\text{Al,Cr})_2\text{O}_3$ Thin Films.** *Khatibi (alikh@ifm.liu.se), J. Lu, J. Jensen, P. Eklund, L. Hultman, Linköping University, Sweden*

Face centered cubic $(\text{Al}_{1-x}\text{Cr}_x)_2\text{O}_3$ solid solution films, with x in the range $0.60 < x < 0.70$, have been deposited using dual reactive RF magnetron sputtering from Al and Cr targets in mixed Ar/O_2 discharge at a substrate temperature of 500°C . The films have a strong $\langle 100 \rangle$ preferred orientation. The unit cell parameter is 4.04 \AA determined by x-ray diffraction and high resolution transmission electron microscopy techniques. Nanoindentation shows that the films exhibit hardness values up to 26 GPa and reduced modulus of 220-235 GPa. In the present work, ex-situ annealing studies were performed on as-deposited samples for a series of temperatures up to 1000°C and annealing time of 0-8 h. The fcc structure remains intact up to 700°C . The onset of phase transformation from fcc to corundum is observed in the sample annealed at 900°C for 2 h, where annealing for 2 h at 1000°C results in complete transformation to $\alpha\text{-(Al}_{1-x}\text{Cr}_x)_2\text{O}_3$. There is no indication of any phase separation into $\alpha\text{-Cr}_2\text{O}_3$ and Al_2O_3 prior and after the annealing, confirmed by the in-plane and out-of-plane line scans performed in EDX TEM and long-time small step size $\theta/2\theta$ XRD patterns. The kinetics of phase transformation studied by the Jahnson-Avrami-Mehl model shows the apparent activation energy of the phase transformation process in the range of 380-480 kJ/mol. Ongoing work is focused on theoretical studies of the stability and composition of the structure of the as-deposited fcc- $(\text{Al}_{1-x}\text{Cr}_x)_2\text{O}_3$ solid solution films, which are suggested to have a non-stoichiometric NaCl structure with 33% vacancy occupancy on Al/Cr sites.

11:40am **B1-1-6 Influence of Fe-Impurities in AlCr-Targets on Arc Evaporation Process and Film Properties.** *M. Mühlbacher, R. Franz (robert.franz@unileoben.ac.at), Montanuniversität Leoben, Austria, M. Lechthaler, OC Oerlikon Balzers AG, Liechtenstein, P. Polcik, PLANSEE Composite Materials GmbH, Germany, C. Mitterer, Montanuniversität Leoben, Austria*

Common targets used in physical vapour deposition techniques to synthesise thin films and coatings present a high level of purity in order to avoid the incorporation of impurities into the growing films. The removal or reduction of contaminations during target production, on the other hand, is cost intensive especially if multi-element targets are produced. Only very limited information is available on the effect of impurities in nowadays frequently used target materials regarding the deposition process and coating properties. For the present investigation AlCr targets produced by powder metallurgy were chosen and the influence of Fe contents of up to 2 at.% on structure, mechanical properties and oxidation behaviour of the deposited AlCr(Fe)N coatings was studied. All coatings were synthesised by cathodic arc-evaporation in an industrial-scale Oerlikon Balzers INNOVA deposition system. The analysis by scanning electron microscopy and X-ray diffraction revealed no significant changes in the microstructure and crystal structure. All coatings presented a face-centred cubic structure with grain sizes in the range from 20 to 30 nm. The hardness values measured by nanoindentation were generally ranging from 31 to 33 GPa without a pronounced correlation with the Fe concentration in the coating. The oxidation resistance, on the other hand, reduced with increasing Fe

content. Analyses of the oxidised coatings by X-ray diffraction and Raman spectroscopy revealed the formation of oxides, in the present case Cr_2O_3 , at a temperature of 800°C if Fe was present as compared to 900-1000°C for the reference AlCrN coating.

Fundamentals and Technology of Multifunctional Thin Films: Towards Optoelectronic Device Applications

Room: Pacific Salon 3 - Session C1-1

Recent Advances in Optical Thin Films

Moderator: K. Khajurivala, Janos Technology Incorporated, US, R. Sczupak, Reynard Corporation, US

10:00am **C1-1-1 Manipulation of Photons by Photonic Crystals**, S. Noda (snoda@kuee.kyoto-u.ac.jp), T. Asano, Kyoto University, Japan
INVITED

Photonic crystals are nanostructures for light with periodic refractive index change. They look like periodic air-hole arrays in regular patterns. By manipulating the patterns and developing two- or even three-dimensional structures, various and flexible manipulations of photons become possible. Our research has demonstrated that photonic crystals indeed allow to manipulate photons almost on demand and could contribute to broad applications including communication, information, storage, processing, and even global energy issues.

For example, we have successfully demonstrated that photonic crystals can produce photonic nano-devices with the sizes less than 1/100,000 of conventional on-road devices while achieving excellent optical functions. These devices are very useful to increase the amount of information in optical communications. We have also shown that photonic crystals enable a nanocavity (a cage of light), which can confine light very strongly. The nanocavity can be used for slowing and even stopping light. In the present optical signal processing, light signals are at first converted to electronic signals to store the signals, and then re-converted to light signals. If we could directly store light as it is, the speed of the signal processing could be significantly increased. The nanocavity is also important for quantum information processing and communication, which are considered as the important candidates for the next generation communication and signal processing.

Moreover, we have demonstrated that photonic crystals can produce an unprecedented type of lasers, which cannot be achieved by the conventional technologies. We found that the photonic-crystal lasers can oscillate in a perfect single mode in a broad area and produce on-demand beam patterns with desired characteristics. These results will lead to the realization of various types of novel light sources; for example, a light source with extremely high output powers, a super-resolution light source which can be focused much smaller than the wavelengths, and a light source which can trap and manipulate nontransparent materials such as small pieces of metals. These light sources achieved by the photonic-crystal lasers should be very important for laser processing systems, next generation DVD systems, and versatile optical tweezers systems, etc.

Our works on photonic crystals will also contribute to address global energy issues. Photonic crystals can manage light emission and detection, which has great potentials to produce extremely high-efficient LEDs and solar cells. These are very important to save huge energies for lightings, and also to convert efficiently solar energy to electric one.

References:

(1) Noda, et al, Science 289, 604 (2000)., (2) Noda, et al, Nature 407, 608 (2000)., (3) Noda, et al, Science 293, 1123 (2001)., (4) Song, Noda, et al, Science 300, 1537 (2003)., (5) Akahane, Noda, et al, Nature 425, 944 (2003)., (6) Asano, Noda, Nature 429, doi:10.1038 (2004)., (7) Ogawa, Noda, et al, Science 305, 227 (2004)., (8) Fujita, Noda, et al, Science 308,1296 (2005)., (9) Song, Noda, et al, Nature Materials 4, 207 (2005)., (10) Miyai, Noda, et al, Nature 441, 946 (2006)., (11) Noda, Science 314, 260 (2006)., (12) Noda, et al, Nature Photonics 1, 449 (2007)., (13) Song, Noda, et al, Nature Materials 6, 862 (2007)., (14) Matsubara, Noda, et al, Science 319, 445 (2008)., (15) Noda, Fujita, Nature Photonics 3, 129 (2009)., (16) Ishizaki, Noda, Nature 460, 367 (2009)., (17) Takahashi, Noda, et al, Nature Materials 8, 721 (2009)., (18) Kurosaka, Noda, et al, Nature Photonics, 4, 447 (2010).

10:40am **C1-1-3 Phase transformation, structures and properties of pure and carbon containing titania thin films annealed in air and in hydrogen**, W.C. Lee, M. Wong (mswong@mail.ndhu.edu.tw), National Dong Hwa University, Taiwan

Pure titania (TiO_2) and carbon containing titania(C-TiO₂) thin films were prepared by reactive sputtering titanium metal target and graphite target in argon-oxygen plasma at 100 °C or below. The as-deposited thin films were amorphous and subsequently annealed at various temperatures of 300~800 °C in air and H₂ atmosphere. The effects of annealing on the thin films were systematically studied in terms of phase transformation, activation energy, crystallinity, oxygen vacancies and their optical and photocatalytic properties. The as-deposited TiO_2 transform to anatase at much lower temperature than C-TiO₂. At the same temperature, the H₂-annealed films achieve better crystallinity than the air-annealed. The activation energies of phase transformation for amorphous to anatase were obtained and the values are 126 and 47 KJ/mole for air- and H₂-annealed pure TiO_2 , respectively. The result shows that C-TiO₂ need more energy for phase transformation than pure-TiO₂, and the H₂ atmosphere was able to lower the activation energy. Photocatalytic properties of these films were characterized by degradation of methylene blue under irradiation of visible light, and the C-TiO₂ film annealed at 800°C in H₂ possesses the best performance.

11:00am **C1-1-4 Effect of Laser Power on the Microstructure and Photoluminescence of Silicon-rich Nitride Thin Films by Magnetron Sputtering**, C.K. Chung (ckchung@mail.ncku.edu.tw), C.H. Li, T.S. Chen, Y.T. Lin, National Cheng Kung University, Taiwan

The silicon nanocrystals embedded in dielectric matrix has been extensively studied due to quantum confinement effect and luminescence center for a dramatic improvement of the light generation efficiency in Si nanostructure for potential applications in Si-based optoelectronic integration circuit . Beside, in order to form the Si nanocrystals, conventional furnace annealing at high temperature (over 1000 °C) and sufficiently long time on the entire sample leads to undesirable effects for device production in the post process . In the article, the CO₂ laser annealing method through local heating on selected area was applied to produce Si nanocrystals from silicon-rich nitride (SRN) thin films prepared by RF magnetron sputtering via the SRN target. The various power of CO₂ laser irradiation was used for studying the evolution of micro structure and photoluminescence (PL) of SRN films. Grazing Incidence X-ray Diffraction, Fourier transform infrared transmittance spectra, energy dispersive spectroscopy, Transmission electron microscopy, Raman and photoluminescence spectrum were utilized to characterize the microstructure and PL behavior of films. The Si nanocrystals in SRN films are obtained by focusing on sample at a laser power of 6 W . A broad PL spectrum is observed and suggested the origins from electro-hole pair recombination in Si nanocrystals or luminescence center in the band tail. The relationship between the laser power, microstructure and PL behavior of SRN films is discussed and established.

11:20am **C1-1-5 ZnO light-emitting diodes and laser diodes**, X.W. Sun (exwsun@ntu.edu.sg), Nanyang Technological University, Singapore
INVITED

In this paper, we present our recent works on ZnO light-emitting devices including homojunction nanorod light-emitting diodes, optically pumped whispering-gallery-mode (WGM) lasing and electrically driven WGM heterojunction laser diodes.

Firstly, by applying plasma immersion ion implantation to modify the surface of ZnO nanorods grown from pure Zn and oxygen without catalyst, we found that the electronic defects only reside on the surface. This makes them easy to be doped to p-type. Then by ion implantation of As and P, we realized efficient pure UV emitting LEDs. For optically pumped WGM lasing, we clearly observed the evolution from spontaneous to stimulated emission from ZnO disks. The lasing process has pronounced excitonic signature, that is, inelastic exciton-exciton scattering. The observed lasing modes match well with the theoretical values derived from WGM lasing. The proof-of-concept sensing application based on ZnO WGM lasing is also demonstrated. Lastly, we fabricated the ZnO microrod/GaN heterojunction laser diode, the EL emission mechanism for this diode was discussed. At the current 12 mA, the WGM lasing with distinct multiple-mode structure was realized. This study indicates that the hexagonal ZnO microstructure is of potential in microlaser diodes.

12:00pm **C1-1-7 The deposition of metal oxide coatings for electro-catalytic and photo-active applications by closed field unbalanced magnetron sputter ion plating.** *X. Zhang (xiaoling.zhang@miba.com), K. Cooke, Teer Coatings Limited, Miba Coating Group, UK, G. Eitzinger, High Tech Coatings GmbH, Miba Coating Group, Austria, J. Hampshire, Z. Zhang, Teer Coatings Limited, Miba Coating Group, UK*

Metallic oxides coatings, for example, TiO_2 , are of increasing technological importance in a wide range of industrially relevant functional surfaces on components for the renewable energy sector, including the hydrogen economy. Reactive closed field unbalanced magnetron sputter ion plating (CFUBMSIP) provides an effective, industrially-compatible processing route for the deposition of metallic oxides, with controlled composition, structure, and mechanical, electronic and optical properties.

The current development of TiO_2 -based CFUBMSIP coatings for applications is described, including the electrolytic production of hydrogen (water-splitting - from both direct UV and visible light photo-activity, and via conventional electrolysis), photo-voltaics (PV) with long-life and low cost, and photo-catalytic surfaces with anti-microbial properties.

The optical band gaps of the anatase and rutile TiO_2 phases result in excellent optical transmittance in the visible and near infra-red regions. Stoichiometric TiO_2 is also a good dielectric has a high refractive index. Ultraviolet (UV) light has an energy higher than the band gap (E_g) of TiO_2 , resulting in electron-hole pair generation. If such excited electrons or holes can diffuse to the TiO_2 surface they can induce the formation of different kinds of radicals or ions (and, for example promote the splitting of water molecules, generating hydrogen and oxygen, or degrading or destroying biological matter, creating an antimicrobial surface), or the separated charge carriers can sustain an electrical current (as in a PV device). The intensity of visible light in the solar spectrum is around 9x that of the UV light responsible for the photo-activity of TiO_2 . An efficient process of doping, e.g. the introduction of nitrogen, carbon or iron etc. into TiO_2 can narrow the band gap and thus shift the coatings optical response from UV to visible light.

Well crystallised anatase or rutile-phase TiO_2 structures will be critical for the PV cell application. Deliberately increasing the surface area of the thin film coatings can enhance efficiency in the PV application by increasing the absorption of optical radiation, and in electrolytic applications by increasing the density of active sites within a given area.

The production of well crystallised TiO_2 thin films by the reactive CFUBMSIP process is described. Process parameters, including Ar/O_2 ratio, heating, and elemental doping have been investigated systematically. The effects of various dopants, including N, Fe and Mn on the band gap of TiO_2 and the functional properties of the thin films are discussed, as is the potential for further optimization industrial scale-up.

Fundamentals and Technology of Multifunctional Thin Films: Towards Optoelectronic Device Applications

Room: Tiki Pavilion - Session C2-1/F4-1

Thin Films for Photovoltaics and Active Devices: Synthesis and Characterization

Moderator: T. Terasako, Graduate School of Science and Engineering, Ehime University, Japan, M. Cremona, Pontificia Universidade Católica do Rio de Janeiro

10:00am **C2-1/F4-1-1 The Degradation of $\text{Ti}_x\text{N}_{1-x}/\text{HfO}_2$ p-channel MOSFETs under Hot Carrier Stress.** *J.Y. Tsai (abc_7736@hotmail.com), National Sun Yat-Sen University, Taiwan*

This work investigates the hot carrier (HC) effect in $\text{HfO}_2/\text{Ti}_x\text{N}_{1-x}$ p-channel metal oxide semiconductor field-effect transistors (p-MOSFETs). Generally, the sub-threshold swing (S.S) should increase during HC stress, since the interface states near drain will be generated under high electric field due to drain voltage (V_D). However, the experimental data exhibits the S.S decreases under HC stress and the degradation level is dependent on the concentration of nitrogen in stack gate ($\text{Ti}_x\text{N}_{1-x}$). Besides, the reduction of threshold voltage (V_{th}) illustrates the electrons trap in HfO_2 layer under HC stress. This behavior could be attributed to increase in the entire capacitance due to electron trapping in HfO_2 bulk, improving S.S. Furthermore, the C-V measurement with high and low frequency could detect the defects which approach HfO_2 layer, evidencing the trapping pheromone in this work.

10:20am **C2-1/F4-1-2 Investigation of Random Telegraph Signal with High-K/Metal Gate MOSFETs.** *C.E. Chen (alien_2366@hotmail.com), National Chiao Tung University, Taiwan*

A novel method, called random telegraphy signal (RTS), was constructed to characterize the gate oxide quality and reliability of metal-oxide-semiconductor field-effect-transistors (MOSFETs). With the aggressive scaling of device size, drain current RTS (I_d RTS) become a critical role in carrier transport of MOSFETs. Besides, RTS in gate leakage current (I_g RTS) was denoted as the other new method to understand property of gate oxide. Recently, the study of RTS has also been made in MOSFETs with high dielectric constant and metal gate (high-k/metal gate). However, the RTS in high-k/metal gate MOSFETs, which is related to hot carrier stress (HCS), has not previously been studied yet. This paper investigates the mechanism of HCS in high-k/metal gate MOSFETs and provides a fundamental physical model.

10:40am **C2-1/F4-1-3 Enhancement of Resistive Switching Characteristics in SiO_2 -based RRAM by High Temperature Forming Process.** *Y.T. Chen (d983090005@student.nsysu.edu.tw), National Sun Yat-Sen University, Taiwan*

Forming process with current compliance (soft break-down) is necessary to activate the resistive switching behavior for most of the resistance random access memory (ReRAM). Due to the rich oxygen ions among SiO_2 film, the amount of mobile oxygen ions induced from forming process would exceed the reserving ability of TiN oxygen reservoir as the thickness of SiO_2 films are too thick. The exceeding mobile oxygen ions will recombine with the oxygen vacancies in the SiO_2 film near the TiN/SiO_2 interface and result in forming fail. Through executing high temperature forming process (HTF), it improves the forming process by enhancing the amount of mobile oxygen ions being drove into TiN electrode. Furthermore, the increased mobile oxygen ions can extra repair the conductive filament and reach lower off-current during the reset process that has undergone HTF for activation.

11:00am **C2-1/F4-1-4 The Impact of Strain on Gate-Induced Floating Body Effect for PD SOI p-MOSFETs.** *W.H. Lo, T.C. Chang (tcchang@mail.phys.nsysu.edu.tw), C.H. Dai, NSYSU, Taiwan*

This work studies the influence of gate induced-floating body effect (GIFBE) on negative bias temperature instability (NBTI) in strained partial depleted silicon-on-insulator p-type metal-oxide-semiconductor field effect transistors (PD SOI p-MOSFETs). The experimental results indicate GIFBE causes a reduction in the electrical oxide field, leading to a better NBTI reliability under FB operation. The electron accumulation in the FB can be partially attributed to the electrons tunneling from the process-induced partial n+ poly gate. However, based on different operation conditions, we found the dominant origin of electrons was strongly dependent on holes in the inversion layer under source/drain grounding. This suggests that the mechanism of GIFBE at higher voltages is dominated by our proposed anode electron injection (AEI) model. Moreover, based on this new model, the mechanical compressive strained operation was further introduced to the SOI p-MOSFET. It was found that the strained device under FB operation exhibits a much less NBTI degradation. This behavior can be attributed to the fact that more electrons accumulation induced by strain effect reduces the electric oxide field during NBTI stress.

11:20am **C2-1/F4-1-5 Plasma deposited ZnO layers for thin film photovoltaics: synthesis, characterization and growth mechanism.** *M. Creatore (m.creatore@tue.nl), Eindhoven University of Technology, Netherlands*

INVITED
Due to their wide band gap, transparent conductive oxides (TCOs) exhibit a high transparency in the solar spectral range. Therefore, they are used as transparent electrodes in many applications, e.g. in flat panel displays, architectural and automotive glazing, solar thermal applications and thin film solar cells, either (amorphous/micro-crystalline and poly-crystalline) silicon- or non-silicon based (e.g. CIGS).

In this contribution, the investigation on low pressure plasma-enhanced chemical vapor deposition (PE-CVD) of poly-crystalline (Al-doped) zinc oxide layers serving as TCOs in thin film solar cells, is addressed. An argon-fed expanding thermal plasma where the deposition precursors (diethylzinc, trimethylaluminum and oxygen) are fed in the downstream region is used for the deposition of Al-doped ZnO. The presented studies will highlight the impact of specific plasma and process parameters on the ZnO:Al nucleation phase, grain development (in terms of crystallographic orientation and size) and morphological and electrical properties, coupled to specific demands in thin film solar cell technology, i.e. in terms of band gap, conductivity and morphology/texturing.

In particular, selected insights will be presented in research areas, where a multi-diagnostic approach is adopted in order to investigate:

- The control on the gradient in resistivity of the ZnO:Al layer as function of its thickness, as supported by the correlation between texturing, grain size development and carrier mobility;
- The impact of the surface energy of a thin intrinsic ZnO layer on the development of the morphological and electrical properties of the ZnO:Al layer;
- The influence of the annealing procedure (i.e. solid phase crystallization) on ZnO:Al/amorphous silicon (a-Si:H) stacks on the TCO conductivity and on the crystallization kinetics towards poly-crystalline silicon formation, for thin film poly-Si solar cells.

Coatings for Biomedical and Healthcare Applications

Room: Sunset - Session D1-1

Bioactive and Biocompatible Coatings and Surface Functionalization of Biomaterials

Moderator: D.V. Shtansky, National University of Science and Technology "MISIS", Russian Federation, S. Rodil Posada, Universidad Nacional Autonoma de Mexico, Mexico

10:00am **D1-1-1 The effect of the surface treatment of Ti alloy on the nanomechanical response of bone grown on Ti6Al4V in vitro, J. Chen** (Jinju.chen82@gmail.com), MA. Birch, S.J. Bull, S. Roy, Newcastle University, UK

The long term clinical success of an orthopaedic implant is strongly related to bone formation at the biomaterial–tissue interface. Surface parameters that include topography and roughness influence this process of osseointegration. Electropolishing is a cost effective approach for surface treatment of metallic implant materials such as titanium alloys.

In this study, it is found that the electropolished surface enhances levels of bone formation. However, the mechanical property of the neo–bone remains unknown. In this study, we use nanoindentation with in–situ AFM imaging to identify and characterize the small features (such as calcospherulite) of the neo–bone. The measured Young's modulus and hardness of the neo–bone formed on the electropolished surface is higher, which may indicate the formation of more mature bone. The length scale of the current tests (100nm) is commensurate with the dimensions at which individual cells interact with the extracellular environment. Therefore, understanding the mechanical properties of bone at this scale can reveal the likely role that substrate conformity plays in the control of cell behaviour.

10:20am **D1-1-2 A comparative study on bactericidal efficiency of nano structured pure TiO₂ thin films and Al–TiO₂ composite thin films, A.B. Panda** (atalabit@gmail.com), Mesra, INDIA, SK. Mahapatra, P.K. Barhai, I. Banerjee, Birla Institute of Technology, India

A pure TiO₂ and three Al–TiO₂ composite nano thin films were prepared on glass, quartz and silicon substrates at Ar:O₂ gas ratio of 70:30 in scdm by reactive magnetron sputtering method. For pure TiO₂, titanium target was mounted on the magnetron connected to 200W DC power supply while for Al–TiO₂ composite film an additional aluminium target was connected to RF power supply of 15W, 30W and 45W in a dual magnetron co–sputtering unit. The crystallinity and phase of the films were determined by Grazing Incidence X–ray Diffraction where as the surface chemical composition was obtained by X–ray Photoelectron Spectroscopy. It was found that aluminium was in the form of Al₂Ti_xO_{2–x} and so in the films and in surface it was weakly bonded with oxygen to form its oxides. The band gap was observed to increase as we increase the Al content in the films as compared to pure TiO₂ thin films as calculated from UV– Visible transmission spectra. The Scanning Electron Microscopic image revealed that Al–TiO₂ composite nano thin films displayed rough and flake–like morphology having less porosity with the increase in the Al content. Photoinduced hydrophilicity was examined with the help of OCA. The qualitative and quantitative bactericidal efficiency was observed through SEM image of the treated E.coli cells and optical density (OD) measurement respectively under UV irradiation. The better bactericidal efficiency was observed in the film with 30W of RF power to Al magnetron. The crystallinity, surface chemical composition, band gap in context of Al present in the films was discussed and correlated to bactericidal efficiency.

10:40am **D1-1-3 Surface Engineering and Modification of Biomaterials, P. Chu** (paul.chu@cityu.edu.hk), City University of Hong Kong, Hong Kong Special Administrative Region of China **INVITED**
Development of new artificial biomaterials is typically quite time consuming and demanding due to the stringent requirements by the

government, industry, and consumers. Therefore, it is sometimes faster to improve existing biomedical devices to meet these increasing demands. Surface engineering and modification can be quite useful and selected biomedical and related surface properties can be enhanced while the favorable properties of the bulk materials such as strength can usually be preserved. In particular, plasma immersion ion implantation and deposition which combines energetic ion implantation and low-energy plasma deposition is very useful. In this invited talk, recent research activities pertaining to plasma surface modification and engineering of biomaterials conducted in the Plasma Laboratory of City University of Hong Kong are described. Examples include bone fixation devices, total hip replacements, automatic scoliosis correction devices, biodegradable metallic and polymeric materials, and other biomedical applications.

11:20am **D1-1-6 Surface modification of zirconia nanofiber coatings for biomedical applications, J. Piascik** (jpiascik@rti.org), B. Stoner, RTI International, US, D. Surman, Kratos Analytical Inc., UK, A. Charoenpanich, E. Lobo, North Carolina State University, US

A variety of materials have been investigated for bone reconstructive and regenerative applications; however, delivering clinically viable synthetic alternatives have presented significant challenges. Specific material properties play a critical role in developing alternatives for bone replacement grafts, surface modifications for enhance cell growth, and novel scaffolding for immediate loading. Earlier research presented data of a promising surface modification, whereby, zirconia surfaces are converted to a more reactive surface using a gas-phase fluorination process. This investigation focuses on the modification of biomedical-grade zirconia plates and zirconia electronspun nanofibers by sulfur hexafluoride plasma treatment, characterization of near-surface chemistry products by x-ray photoelectron spectroscopy (XPS), and qualitative analysis of osteoblast viability. Deconvolution of the Zr 3d core level spectra revealed formation of both Zr(OH)_xF_y and ZrF₄ phases. Depth profiling determined the overlayer to be ~4.0 – 5.0 nm in thickness and angle resolved XPS showed no angle dependence on component percentages likely due to fluorination extending into the grain boundaries of the polycrystalline substrates. Importantly, the conversion layer did not induce any apparent change in zirconia crystallinity by inspection of Zr–O 3d_{5/2,3/2} peak positions and full-width-at-half-maximum values, important for retaining its desirable mechanical properties. However, increase in exposure time led to the proposed structures of Zr(SO₄)₂ and Zr(SO₄)_xF_y. It is thus hypothesized that these sulfate surface phases will lead to enhanced osseointegration between natural bone and modified zirconia surfaces. Cell proliferation and differentiation assays determining degrees of osteoblast adhesion will be presented. It is believed that this surface treatment has broad reaching impact when using high strength ceramics in a multitude of bio-applications; such as, nanofiber coated implants or modified surfaces for bone attachment. This research was supported through RTI International research and development fund.

11:40am **D1-1-7 Immobilization of pamidronates on the nanotube surface of titanium discs and their interaction with bone cells, Z.C. Xing, T.H. Koo**, Kyungpook National University, Republic of Korea, S. Moon, Y. Jeong, Korea Institute of Materials Science, Republic of Korea, I.K. Kang (ikkang@knu.ac.kr), Kyungpook National University, Republic of Korea

Bisphosphonates (BPs) are analogues of pyrophosphate, which are widely used for the treatment of different pathologies associated with imbalances in bone turnover. Titanium materials are extensively used for biomedical purposes, especially in medical implants and prostheses, because of their good biocompatibility, biological responses, osseointegration, excellent mechanical properties, corrosion resistance and relatively low cost. The purpose of this study is to immobilize pamidronate (PAM) on the nanotube surface of titanium discs (TiN) and to evaluate their interaction with MC3T3–E1 osteoblasts. PAM-immobilized TiN was prepared by the coupling of aminopropyltriethoxysilane on to TiN, followed by reaction first with L-glutamic acid and then pamidronate. These surface-modified TiN were characterized by electron spectroscopy for chemical analysis (ESCA). The potentiality of PAM-immobilized titanium discs for use as bone substitutes were assessed by culturing osteoblasts and osteoclasts on the surface-modified discs.

Tribology & Mechanical Behavior of Coatings and Engineered Surfaces

Room: Pacific Salon 1-2 - Session E1-1

Friction Wear Lubrication Effects & Modeling

Moderator: Lopez, CSIS-University Sevilla, S. Aouadi, Southern Illinois University, US, V. Fridrici, Ecole Centrale de Lyon, O.L. Eryilmaz, Argonne National Laboratory, US

10:00am **E1-1-1 Assessment of factors influencing the behaviour of MoS₂ coatings by means of factorial design**, *J. Yang (jiao.yang@ec-lyon.fr)*, V. Fridrici, Ph. Kapsa, Ecole Centrale de Lyon, France

Solid lubricants could be used in dry bearings, gears, seals, sliding electrical contacts and retainers in rolling element bearings and many kinds of sliding contacts [1] to reduce wear and to increase durability of the contacts, where the liquid lubricant is undesirable. Molybdenum disulphide (MoS₂) is one of the most widely used solid lubricants to reduce friction and mitigate wear in tribological applications mainly because it is easy to shear in the direction of motion, resulting in a low friction. At present, many efforts have been made to predict its durability under different working conditions such as normal force, displacement amplitude and contact configuration, while there is a lack of a quantitative evaluation of the effect of each factor [2-5].

In this paper, fretting experiments have been carried out under various values of contact pressure, displacement amplitude and two contact configurations (ball-on-flat and cylinder-on-flat). In addition, the method of factorial design has been used to evaluate the effect of each factor and the interaction between each factor.

According to the experimental results, it could be found that the coating presents a longer lifetime in mixed slip regime than that of gross slip regime in both contact configurations, because the central stick-slip will enclose the third layer at the contact center which aims to prolong the coating lifetime. In addition, its durability under ball-on-flat configuration is better than that of cylinder-on-flat.

By the results of factorial design, the contact configuration and displacement amplitude are the controlling factors for the coating lifetime, while the normal force is the controlling factor for the initial friction coefficient. The two factors "interaction" have also strong effect on the coating lifetime especially the interaction between the displacement amplitude and normal force and the interaction between the displacement amplitude and contact configuration. Selection of coatings should consider the contact configuration firstly, the displacement amplitude secondly. Based on the two parameters, the contact force should be then considered.

References

- [1] E. Richard Booser. Handbook of Lubrication (Theory and Practice of Tribology), Vol. II, ed., CRC Press, 1989.
- [2] J.-F. Carton, A.-B. Vannes, L. Vincent. Wear 195 (1996) 7.
- [3] V. Fridrici, S. Fouvry, P. Kapsa, P. Perruchaut. Wear 255 (2003) 875.
- [4] D. B. Luo, V. Fridrici, Ph. Kapsa, T. Murakami. Lubrication Science 21(2009) 193.
- [5] D.B. Luo, V. Fridrici, Ph. Kapsa. Wear 268 (2010) 816.

10:20am **E1-1-2 Application of the friction energy density approach to quantify the fretting wear endurance of DLC hard coatings: influence of temperature and frequency**, *S. Fouvry (siegfried.fouvry@ec-lyon.fr)*, G. Blondy, Ecole Centrale de Lyon, France

The selection of low friction coatings is of great interest to industrial applications. Nevertheless, regarding the lifetime of DLC coatings, the selection criteria often depend on the experimental apparatus and contact configuration and then cannot be directly applied to real cases. In this study, we use a model based on the local dissipated energy due to friction under gross slip conditions in fretting wear. Indeed, the maximum value of the local dissipated energy is a unique parameter that takes into account the two major variables in fretting wear experiments: the normal force and the sliding amplitude. Hence by plotting the "lifetime" versus the "local energy density" a single master curve defining the intrinsic endurance of the coating can be defined. To identify the intrinsic "energy density capacity" variable, characterising the coating fretting wear endurance (i.e. used to model the endurance master curve), a flat on flat contact configuration, allowing constant pressure conditions, is applied. This approach is considered to investigate various DLC systems used in aeronautical applications to protect titanium surfaces in contact. The effects of contact pressure, displacement amplitude, frequency and temperature are investigated. The results show that, the local energy wear approach is suitable to characterize the coating endurance for variable mechanical loading conditions (i.e. sliding amplitude and pressure). By contrast, elevate

sliding frequencies and temperatures, by activating severe tribo oxidation processes, sharply modify the wear processes so that the endurance values, which are significantly reduced, can not be transposed on the fretting wear master curve. Using this friction energy concept, a first quantitative description is nevertheless provided to formalise the lubricant endurance of DLC coatings subjected to severe thermal exposure.

10:40am **E1-1-3 Atomic-Scale Friction of Surfaces and Coatings**, *A. Martini (amartini@ucmerced.edu)*, University of California, Merced, US
INVITED

A promising means of fundamentally understanding tribological behavior is investigation of atomic-scale friction. Atomic-scale friction is relevant on all length scales because any contact can be resolved into the sum of its component asperities, where the smallest such measurable asperities are at the atomic scale. It is also critical for design of materials and devices whose structure and function are controlled at small scales. The focus of this talk will be on recent progress made towards understanding atomic-scale friction using accelerated molecular dynamics simulation. Emphasis will be on determining how to capture the physical properties critical to frictional behavior within the constraints of a fully atomistic model. For example, friction is well known to be affected by real contact area; how can we accurately describe the size, shape, and crystallographic orientation of this contact if in practice it is buried in the interface? Also, particularly at the atomic scale, sliding speed plays a major role in determining frictional behavior; how can realistic speeds be implemented in a model that is typically limited to nanosecond time scales? The discussion will also include analysis of simulation results in the context of the Prandtl-Tomlinson model as a means of interpreting the effects of operating conditions and material properties. This approach enables the atomistic simulation to be partially validated and its limitations to be defined. Once validated it becomes a powerful tool for providing insight into how the chemical and structural evolution of a given material impacts its tribological function. This is also the first step towards enabling design of novel coating materials with properties that are tunable at the atomic-scale.

11:20am **E1-1-5 Imaging Dynamic of Polishing Technology for Digital Surfacing Of Ophthalmic Plastics**, *S. Mezghani, M. El Mansori (mohamed.elmansori@ensam.eu)*, Arts et Métiers ParisTech, France

Optical, mechanical and thermal properties are among the most important properties that govern ophthalmic lens functionality. The functional "Mirror" surface of ophthalmic plastics lenses is actually produced by multi-processes, turning and polishing. The polishing stage has the important role to remove tool marks and to hold the required level of transparency.

This paper examines the effects of polishing cycle at the nanoscale on the surface modifications of ophthalmic plastic. AFM is used to explore topographical and thermal nanoscale imaging as function of polishing time. Simultaneously a multiscale decomposition, based on ridgelets transform, is introduced to explore the produced surface texture from nano to micro scale. This enables a complete description of surface aspect including scratches density, spacing, orientation and distribution. Also, the process map that characterizes the evolution of polished surface features was derived. This mapping plays a tangible role in visualizing processes of abrasive fluid – plastic surface interaction which could previously only be studied indirectly.

Keywords: AFM imaging, ophthalmic plastic, Polishing, Surfacing, Multiscale surface topography

11:40am **E1-1-6 A study on friction coefficient and wear coefficient of coated systems submitted to micro-scale abrasion tests**, *R. Cozza (rcamara@fei.edu.br)*, Centro Universitário da FEI – Fundação Educacional Inaciana "Padre Sabóia de Medeiros", Brazil

Several works on the friction coefficient during abrasive wear tests are available in the literature, but only a few were dedicated to the friction coefficient in micro-abrasive wear tests conducted with rotating ball. This work aims to study the influence of titanium nitride (TiN) and titanium carbide (TiC) coatings hardness on the friction coefficient and wear coefficient in ball-cratering micro-abrasive wear tests. A ball of AISI 52100 steel and two specimens of AISI D2 tool steel, one coated with TiN and another coated with TiC, were used in the experiments. The abrasive slurry was prepared with black silicon carbide (SiC) particles (average particle size of 3 µm) and distilled water. Two normal forces and six sliding distances were defined, and both normal and tangential forces were monitored constantly during all tests. The movement of the specimen in the direction parallel to the applied force was also constantly monitored with the help of a Linear Ruler. This procedure allowed the calculation of crater geometry, and thus the wear coefficient for the different sliding distances without the need to stop the test. The friction coefficient was determined by the ratio between the tangential and the normal forces, and for both TiN and TiC coatings, the values remained, approximately, in the same range (from

$\mu = 0.4$ to $\mu = 0.9$). On the other hand, the wear coefficient decreased with the increase in coating hardness.

New Horizons in Coatings and Thin Films

Room: Royal Palm 1-3 - Session F6-1

Coatings for Compliant Substrates

Moderator: B. Beake, Micro Materials Ltd, UK, R.M.

Souza, Mechanical Engineering Department, Universidade de São Paulo

10:00am **F6-1-1 Deformation and Delamination in Polymer Metal Thin Film Structures**, *N.R. Moody* (*nrmoody@sandia.gov*), *E.D. Reedy*, *E. Corona*, *D. Adams*, Sandia National Laboratories, US, *M. Kennedy*, Clemson University, US, *M. Cordill*, Montanuniversität Leoben, Austria, *J. Yeager*, Los Alamos National Laboratory, US, *D. Bahr*, Washington State University, US

INVITED

Interfaces are the critical feature governing performance of compliant substrate and multilayer polymer-metal thin film structures where differing properties between adjacent films can induce strong interlaminar normal and shear stresses and catastrophic failure. However, it is experimentally difficult to measure properties in these systems at small scales and theoretically difficult to isolate contributions from the films, interfaces, and substrates. Analysis is further complicated with the onset of substrate yielding. As a result our understanding of deformation and fracture behavior in these systems is limited. This has motivated a study of buckle driven delamination of compliant substrate and polymer-metal thin film systems that combined experiments and cohesive zone simulations. One set of experiments employed compressively stressed tungsten films that varied in thickness on commercial and high purity PMMA substrates. A second set of experiments employed spin coating PMMA films with thicknesses ranging from 10nm to 650nm onto copper coated silicon substrates followed with a sputter deposited overlayer of highly stressed tungsten. In both sets of experiments, the high film stresses triggered spontaneous delamination and buckling along the PMMA-tungsten interface accompanied by intense deformation in the PMMA substrates and PMMA layers. Of particular interest, the intensity of deformation varied markedly between each system studied and from model elastic behavior. Cohesive zone simulations that included substrate compliance showed a marked increase in fracture energies over rigid elastic solutions for thick films and compliant substrates. The fracture energies did approach rigid elastic solutions for the thinnest films tested. In this presentation we will use tests and simulations to show that film compliance provides a lower bound to behavior for all but the thinnest samples while constrained yielding accounts for the pronounced differences in behavior between samples. This work was supported by Sandia National Laboratories under USDOE Contract DE-AC04 94AL85000.

10:40am **F6-1-3 Extracting mechanical properties of coatings on compliant substrates using nanoindentation**, *S.J. Bull* (*steve.bull@ncl.ac.uk*), Newcastle University, UK

The move towards functional devices on flexible substrates puts severe demands on the mechanical properties of the coatings from which they are constructed. For instance the use of brittle transparent conducting oxide electrodes in displays and organic light emitting diodes results in failure due to fracture when a flexible substrate is bent to a small enough radius of curvature. In many cases, the materials used in such devices are not available in the bulk form and the only practical technique to measure mechanical data is nanoindentation. Whereas it is possible to make good measurements of coating properties on stiff substrates such as silicon using nanoindentation there are serious issues with the reliability of data obtained from coatings on compliant substrates such as the PET used for plastic electronics. This presentation will highlight the effect of coating architecture and thickness on the indentation response of thin films used in microelectronic devices, displays and OLEDs on stiff and compliant substrates. A simple model to assess the contribution of the coating layers and substrate to the measured contact modulus will be introduced and the results illustrated for single and multilayer coatings on silicon, glass and PET.

11:00am **F6-1-4 Organic ultrathin film adhesion on compliant substrate using scratch test technique**, *X. Boddaert* (*boddaert@emse.fr*), Ecole Nationale Supérieure des Mines de Saint Etienne, France, *G. Covarel*, Laboratoire de Physique et Mécanique Textiles, Université de Haute Alsace, France, *B. Bensaid*, *M. Mattei*, *P. Benaben*, *J. Bois*, Ecole Nationale Supérieure des Mines de Saint Etienne, France

The mechanical properties of interfaces and more precisely the adhesion are of great importance to understand the reliability of Organic Thin Film Transistor (OTFT) on compliant substrate. Since these devices are flexible and intended for different fields of application like sensors and displays, they will undergo a lot of mechanical stress during their useful life. Many adhesion test techniques have been developed to measure adhesion energy of thin films but they are hard to implement in the case of submicronic organic thin film deposited on flexible substrate. Recently, the feasibility and repeatability of the scratch test technique as a tool for testing the adhesion and the damage behaviour of ultra-thin film on polymeric substrate have been demonstrated [1]. However, direct comparison of critical load between samples was not straightforward since different failure mechanisms were induced. In the present work, we have investigated the way to obtain more quantitative data. We have also performed mechanical ageing tests on specimens and proved that the scratch test technique is sensitive enough to monitor the degradation of the interface properties.

[1] G. Covarel, B. Bensaid, X. Boddaert, S. Giljean, P. Benaben, P. Louis, *Surf. and Coat. Technol.*, 2011 in press.

11:20am **F6-1-5 Flexibility and electrical stability of ITO-coated polyethylene terephthalate (PET) and polyethylene naphthalate (PEN) under monotonic and cyclic bending**, *G. Potoczny*, *S. Abell*, University of Birmingham, UK, *K. Sierros*, *D. Cairns*, West Virginia University, US, *S. Kukureka* (*s.n.kukureka@bham.ac.uk*), University of Birmingham, UK

The flexibility and electrical stability of highly conductive and transparent amorphous indium tin oxide (a-ITO), coated on polyethylene terephthalate (PET) and polyethylene naphthalate (PEN) substrates were investigated by bending tests with *in situ* monitoring of resistance changes. Monotonic and fatigue tests of the ITO/polymer systems were conducted. The results show that monotonic bending in tension is more critical for electro-mechanical stability of ITO films than in compression (an increase of resistance was observed at a critical radius of curvature, of ~3 and ~1 mm, respectively for both samples investigated). In contrast, cyclic bending tests showed that compressive stress is more critical than tensile due to fatigue and buckling-driven delamination of the ITO film. In general, better electro-mechanical stability is observed for ITO-coated PEN in comparison with ITO-coated PET. This is important for the selection of polymer substrates and life-time predictions for flexible plastic electronics.

11:40am **F6-1-6 Compliant metallic electrodes for Electroactive Polymer Actuators**, *F. Habrard*, *G. Kovacs*, *J. Patscheider* (*joerg.patscheider@empa.ch*), Empa, Switzerland

Electroactive polymer (EAP) actuators are very promising candidates for the ambitious aim of developing soft actuator systems for artificial muscles, haptic devices and vibration-less actuators. Dielectric elastomer transducers benefit of important advantages compared to other electro-mechanical actuators such as high energy density and large and noise-free deformation capability. Today's EAP devices usually work at high voltage (> 1000 V), which preclude their use in or close to the human body, as such high voltages cause obvious safety problems. The electrode material also presents a challenge, since clean and fast processes suited to miniaturize EAP devices are still missing. To solve these drawbacks, we developed a new fabrication process aiming at reducing the dielectric layer thickness down to <20 μm and to increase the efficiency using highly conductive electrode materials deposited by magnetron sputtering. In this work we show that thin metallic films deposited by magnetron sputtering can be prepared in such a way that they are able to maintain high electrical conductivity at more than 10% stretching. These highly compliant films are characterized by X-Ray Diffraction, electrical conductivity measurements and Atomic Force Microscopy. The film properties and their implications for new EAPs will be discussed.

Advanced Characterization of Coatings and Thin Films Room: Sunrise - Session TS2-1

Advanced Characterization of Coatings and Thin Films

Moderator: P. Schaaf, TU Ilmenau, Germany, F. Giuliani, Imperial College London - South Kensington Campus, UK, S. Korte, University of Erlangen-Nürnberg, Germany

10:00am **TS2-1-1 3D Microstructure Analysis of Thin Films and Coatings in the Micro, Nano and Atomic Scale, F. Mücklich** (muecke@matsci.uni-sb.de), Saarland University and Materials Engineering Center, Germany **INVITED**

The quantitative investigation of the correlation between processing, (spatial) microstructure and properties of coatings and thin films is one of the essential goals of their characterization strategies. The traditional 2D planar section sampling combined with estimations for the spatial situation is powerful but it supplies insufficient information for essential 3D characteristics such as particle volume density and arrangement or connectivity in cases of complex shaped microstructures. Advanced thin films therefore call for an adequate imaging and quantification of the 3D microstructure. Electron tomography is well established but may suffer from a lack of field of view size. Such representative field of view size can be achieved by the help of microstructure tomography based on FIB serial sectioning. This method combines the excellent target preparation possibilities of a focused ion beam (FIB) with all types of SEM contrast including EDX and EBSD. Therefore it enables the exploration of a representative sample volume and the imaging of chemical and structural phenomena with a resolution of a few nanometers. This can be combined locally with a tomography even at the atomic scale using Atom Probe Tomography.

Once the 3D data set is available, their exploitation in 3D image analysis provide detailed quantitative insights into the relation between processing, structure and properties.

So far, the complex formation of multiphase 3D microstructures, the related interface as well as seeding phenomena and also local degradation effects were investigated. The talk will provide an overview of microstructure tomography supported by examples of some technical relevance of coatings, thin films, and surface effects.

10:40am **TS2-1-3 Atom probe tomography of self-organized nanostructuring in Zr-Al-N thin films, L. Johnson** (larsj@ifm.liu.se), N. Ghafoor, Linköping University, Sweden, M. Thuvander, K. Stiller, Chalmers University of Technology, Sweden, M. Odén, L. Hultman, Linköping University, Sweden

The ZrAlN system has recently come under investigation [1] as a system that has an even larger miscibility gap than TiAlN, as well as a large lattice mismatch between ZrN and AlN. Atom probe tomography was performed on magnetron sputtered epitaxial $\text{Zr}_{0.64}\text{Al}_{0.36}\text{N}$ thin films grown on MgO(001) substrates kept at 800 °C. A self-organized nanostructure was resolved, consisting of lamellae of Zr(Al)N and Al(Zr)N with a characteristic length scale of ~4 nm in the film plane and extending in the growth direction. In addition, Al was found to segregate to the film/substrate interface, forming a 1 nm thick layer. This was followed by growth of a 4 nm thick Al-depleted zone, self-organization of the Zr(Al)N and Al(Zr)N lamellas during 5 nm film growth, and finally steady-state growth of the lamellar structure.

[1] L. Rogström, L.J.S. Johnson, M.P. Johansson, M. Ahlgren, L. Hultman, and M. Odén

Scripta Materialia 62 (2010) 739-741

11:00am **TS2-1-4 3D FIB/SEM imaging and 3D EBSD analysis of compressed MgO micropillars, M. Ritter** (ritter@tu-harburg.de), Hamburg University of Technology, Germany, S. Korte, W.J. Clegg, P.A. Midgley, University of Cambridge, UK

The application of FIB/SEM (focused ion beam/scanning electron microscope) instruments is rapidly expanding. This is in part due to the fact that there is a pressing need to understand the structure, composition and physico-chemical properties of modern materials in three dimensions. FIB instruments can unveil sub-surface structural information by creating cross-sections that can easily be imaged or analysed [1]; and serial cross-sectioning expands the instrument's capabilities to the third dimension.

In the process of serial sectioning, small and thin slices of material are removed in bulk samples by means of FIB milling, creating a series of cross-sections in one direction of the sample. State of the art FIB/SEM instruments provide a focused ion beam with small spot sizes so that slices that are only a few nanometres thick can be removed from the bulk material.

Each cross-section can then be imaged and the crystal orientations retrieved by Electron Backscatter Diffraction (EBSD) [2]. The information can then be reconstructed and combined to provide a comprehensive dataset for 3D orientation analysis.

One of the manifold applications is the possibility of characterising plastic deformation in brittle materials due the suppression of cracking in very small bodies. We used 3D EBSD as a way of characterising the three-dimensional (3-D) deformation at high spatial resolution of MgO micropillars compressed ex situ along two crystal directions [3]. We show that for a successful 3D reconstruction of the indexed crystal orientations it is necessary to use the SEM images as reference to correct for offsets. It is also shown that for the reconstruction of compressed and then successively sliced and indexed MgO micropillars, this 3D technique yields information complementary to μ -Laue diffraction or electron microscopy, allowing a correlation of experimental artefacts and the distribution of plasticity.

References

- [1] L. A. Gianuzzi et al., *Introduction to Focused Ion Beams*. Springer, New York, 2005.
- [2] S. Zaeferrer et al., *Mater. Sci. Forum* 495-497 (2005) 3.
- [3] S. Korte et al., *Acta Mater.* 59 (2011) 7241.

11:20am **TS2-1-5 Recent Advances in XPS for the Characterization of Thin Films, D. Surman** (dsurman@kratos.com), Kratos Analytical Inc., UK, C. Blomfield, A. Roberts, S. Hutton, S. Page, Kratos Analytical Ltd., UK

X-ray photoelectron spectroscopy is the most widely applied of a range of surface analysis techniques. Small area analysis from an area of a few microns and imaging XPS with spatial resolution of a few microns is now common place.¹ The advent of small analysis area XPS heralded an era for XPS depth profiling where a sputter crater is formed by an ion beam (typically Ar) and then XPS analysis formed in the crater. In such a way thin films of up to 1-2 microns in thickness can be analysed. XPS depth profiles can therefore elucidate the chemical composition of a thin film with a depth resolution of a few nanometers. XPS can analyse films and substrate materials which are either insulating or conductive. An important factor in the characterization of thin films is the understanding of the chemistry of the various layers as well as the interfacial chemistry. In order to get a better understanding of this, non-destructive methods (chemically rather than necessarily materially) have been refined such as Angle Resolved XPS and the application of advanced mathematical modelling such as MEMS algorithms have enhanced the information that can be extracted. This technique has become especially powerful for very thin films.

Other recent developments have focussed on improved ion gun design, by lowering the Ar ion energy improved interface resolution is possible. To date, XPS depth profiling has been principally applied to inorganic materials but the recent development of polyatomic ion guns using large carbon based molecules such as Fullerene or Coronene has expanded XPS depth profiling into organic materials².

Examples will be given here which describe the state of the art in XPS depth profiling utilizing both ARXPS and MEMS as well as chemically non-destructive profiling with Polyatomic ion species on both organic and inorganic materials. Examples of nanometer depth resolution and quantitative chemical composition of films of several hundred nanometers in thickness from a range of applications will be given.

1. C.J. Blomfield, *Journal of Electron Spectroscopy and Related Phenomena* 143 (2005) 41-249
2. G.X. Biddulph, A. M. Piwowar, J.S. Fletcher, N.P. Lockyer, J. C. Vickerman, *Anal. Chem.* 79, (2007), 7259-7266.

Hard Coatings and Vapor Deposition Technology Room: Royal Palm 4-6 - Session B1-2

PVD Coatings and Technologies

Moderator: P. Eklund, Linköping University, Sweden, J.H. Huang, National Tsing Hua University, Taiwan, J. Vetter, Sulzer Metaplas GmbH, Germany

1:30pm **B1-2-1 Effect of vacuum arc plasma state on the property of nitride coatings deposited by conventional and new arc cathode.**, S. Tanifuji (tanifuji.shinichi@kobelco.com), K. Yamamoto, H. Fujii, Y. Kurokawa, Kobe Steel Ltd., Japan

Due to high deposition rate and ability to form hard and dense coating, arc ion plating (AIP) has been applied in many industrial applications. Meanwhile, emission of macro-particles (MPs) and delamination of the coating due to large compressive residual stress are considered as drawbacks of AIP process. Emission of MPs can be reduced by controlling the movement of arc spot during the discharge which can be manipulated by application of external magnetic field. The new arc cathode was developed through the magnetic field design of the cathode surface. The relationship between the vacuum arc plasma state and the property of the deposited various nitride coatings were investigated for conventional and the newly developed arc cathode. There were three advantages as vacuum arc cathode for new arc cathode. First, the number of MPs on the coating deposited by new cathode can be reduced resulting much improved surface morphology. Yamamoto et al. reported that the improvement of the surface morphology of the coating deposited by new cathode was correlated with the velocity of cathode spot on the surface of the target [1]. Second, Although deposition varies depending on the cathode material, we have observed general increase in deposition rate in case of the new cathode. Third, the residual compressive stress of the TiAl(50/50)N coating deposited by new cathode can be halved compared to conventional cathode, so it is possible to deposit the thick coating on the sharp edge of the cutting tool by the new cathode. To investigate mechanism for these improvements by the new cathode, optical emission analysis of vacuum arc plasma with conventional and new cathode was conducted.

[1] K. Yamamoto et al., presented at ICMCTF 2010 at San Diego G6-7

1:50pm **B1-2-2 Industrial-scale sputter deposition of $\text{Cr}_{1-x}\text{Al}_x\text{N}$ coatings with various compositions from segmented Cr and Al targets.** T. Weirather (thomas.weirather@unileoben.ac.at), C. Sabitzer, S. Grasser, Montanuniversität Leoben, Austria, C. Czettl, Ceratizit Austria GmbH, Austria, P. Polcik, PLANSEE Composite Materials GmbH, Germany, M. Kathrein, Ceratizit Austria GmbH, Austria, C. Mitterer, Montanuniversität Leoben, Austria

Over the last 20-25 years, extensive research has been conducted on ternary MeAlN coatings like TiAlN and CrAlN and their outstanding properties for wear protection, e.g. in cutting applications. While CrAlN in particular exhibits high oxidation resistance, TiAlN has the advantage of higher hardness and a more pronounced age-hardening behaviour. These benefits are enhanced with increasing AlN content in the solid solution, which is, on the other hand, limited by a threshold value at which a transition from the face-centered cubic to the undesired hexagonal wurtzite phase occurs. To study the structure-property evolution in industrial-scale sputtering systems over wide compositional ranges requires numerous deposition runs with several sputter targets if conventional targets with a fixed composition are applied. To reduce this effort, the use of segmented sputter targets is a promising concept to cover a broad compositional range at a high resolution in one single deposition run. In the present study, pairs of triangle-like Cr and Al targets were developed for an industrial-scale magnetron sputtering system to produce 1.4 μm thick $\text{Cr}_{1-x}\text{Al}_x\text{N}$ hard coatings with various compositions. They were deposited on 2.1 μm thick TiAlN base layers to provide constant adhesion to the cemented carbide substrates. The TiAlN layers were grown from homogeneous TiAl targets with an Al content of 60 at.%; all used targets were produced by powder metallurgical methods. Energy-dispersive X-ray emission spectroscopy measurements on the $\text{Cr}_{1-x}\text{Al}_x\text{N}$ layers showed AlN contents in the range of $0.21 < x < 0.46$. Consequently, a single-phase cubic coating structure was observed. Nanoindentation revealed a hardness increase from 22 GPa to 30 GPa with increasing AlN content. Tribological investigations performed at room temperature showed excellent performance of the coatings with friction coefficients in the range of 0.4-0.5 and wear coefficients of $1.8\text{-}3.2 \cdot 10^{-16}$

m^3/Nm , where the low friction is related to the smooth coating surface obtained.

2:10pm **B1-2-3 Preparation of Superhard Tetrahedral Amorphous Carbon, Nano-crystalline Diamond and Cubic Boron Nitride Films with Low Internal Stress by Means of Excimer Laser Ablation and Annealing.** S. Weissmantel (steffen.weissmantel@hs-mittweida.de), G. Reisse, K. Guenther, R. Bertram, H. Gruettner, M. Nieher, University of Applied Sciences Mittweida, Germany, D. Rost, Roth & Rau MicroSystems GmbH, Germany **INVITED**

A review will be given on the preparation of carbon and boron nitride based super-hard coatings by excimer laser deposition. In particular, the conditions under which tetrahedral amorphous carbon (ta-C), nano-crystalline diamond (n-D) and cubic boron nitride (c-BN) films form will be presented. The growth rates, microstructure and mechanical properties of those films will be discussed and compared to other deposition methods and the special advantages of the pulsed laser deposition method will be emphasized.

It will be shown that ta-C, n-D and c-BN films with high hardness in the range of 45 – 65 GPa can be deposited at high growth rates. As the films show high internal stresses due to the high energy of the film forming particles, which results in poor adherence, the preparation of micrometer thick films of those materials requires a suitable method of stress reduction during the deposition process. We developed a special pulsed laser annealing technique, which is applied alternating to the deposition process of thin sub-layers. It will be shown that stress-free ta-C films with 80 to 85 % sp^3 bonds, 60 – 65 GPa hardness and thicknesses in the μm -range can be prepared by using a KrF-excimer laser of 248 nm wavelength for annealing. In the case of c-BN films, a F_2 -laser of 157 nm wavelength has to be used for annealing, where the stresses could be reduced by some 50 %, so far.

The great advantage of the method in comparison to conventional thermal annealing is the short time it requires to completely remove stress (the process itself requires only a few μs) and that it is possible to go over directly from deposition to annealing and vice versa. The latter is of particular significance for the deposition of ta-C films as the substrate temperature during actual film growth must not exceed 90 °C.

In the second part of the talk, the hardness, adhesion, friction coefficient and wear rates of ta-C, n-D and c-BN films prepared by our method on WC-hard metal inserts and various types of steel in dependence of the deposition parameters will be presented and discussed.

Finally, some examples of coated components and tools will be shown and the industrial potentialities of the method will be discussed taking into account the commercially available lasers as well as the costs.

2:50pm **B1-2-5 Ion-assisted epitaxial sputter-deposition and properties of metastable $\text{Zr}_{1-x}\text{Al}_x\text{N}(001)$ ($0.05 < x < 0.25$) alloys.** A. Mei, B.M. Howe (brandonhowe@gmail.com), University of Illinois at Urbana-Champaign, US, N. Ghafoor, M. Oden, H. Fager, E. Broitman, Linköping University, Sweden, M. Sardela, University of Illinois at Urbana-Champaign, US, L. Hultman, Linköping University, Sweden, A. Rockett, J.E. Greene, I. Petrov, University of Illinois at Urbana-Champaign, US

Single-phase epitaxial metastable $\text{Zr}_{1-x}\text{Al}_x\text{N}/\text{MgO}(001)$ ($0.05 < x < 0.25$) thin films were deposited by ultra-high vacuum magnetically-unbalanced reactive magnetron sputtering from a single $\text{Zr}_{0.75}\text{Al}_{0.25}$ target at a substrate temperature of 650°C. We control the AlN content, x , in the films by varying the ion energy ($5 < E_i < 55$ eV) incident at the film growth surface with a constant ion to metal flux ratio of 8. The net atomic flux was decreased from 3.16 to 2.45×10^{15} atoms $\text{cm}^{-2}\text{s}^{-1}$, due to efficient resputtering of deposited Al atoms (27 amu) by Ar^+ ions (40 amu) neutralized and backscattered from heavy Zr atoms (91.2 amu). Consequentially, films varied in thickness from 390 nm to 275 nm during 20 min depositions. HfN buffer layers were deposited on the $\text{MgO}(001)$ substrates to reduce the lattice mismatch from ~ 8 to $\sim 0.5\%$. High resolution x-ray diffraction ω -2 θ scans and reciprocal lattice mapping revealed single-phase NaCl structure with a cube-on-cube orientation relative to the substrate, $(001)_{\text{Zr}_{1-x}\text{Al}_x\text{N}} \parallel (001)_{\text{MgO}}$, and relaxed lattice parameters varying from 4.546 with $x = 0.25$ to 4.598 Å with $x = 0.05$. Film nanoindentation measurements showed that hardness decreases from 28.6 to 23.3 GPa and Young's modulus increases from 263 GPa to 296.8 GPa as x is varied from 0.25 to 0.05. For the same range in x , electronic transport measurements established the films to have electron mobilities increasing from 2.67 to 462 $\text{cm}^2\text{V}^{-1}\text{s}^{-1}$, resistivities decreasing from 249.84 to 14.7 $\mu\Omega\text{-cm}$, and positive temperature coefficients of resistivity spanning from 0.3164 to 1.307 $\Omega\text{-cm K}^{-1}$. Films deposited with incident ion energy above 35 eV ($x < 0.08$) exhibited superconductivity with T_c of 8.26 K.

3:10pm **B1-2-6 The influence of deposited surface structures on mechanical properties.** *M.C. Fuchs* (*marcus.fuchs@s2003.tu-chemnitz.de*), *N. Schwarzer*, Saxonian Institute of Surface Mechanics, Germany

It is well known and logical that certain deposition parameters have a great effect on surface structures like surface roughness, interface roughness, porosity, intergrain interaction, homogeneity or grain size. However, it is almost impossible to find deposition parameters or even ranges of them for processing of specific surface structures which are generally valid for all deposition techniques as there is a broad variety of them. Even with the same deposition technique only slight changes in the geometry of the deposition configuration can cause big differences. But such surface structures can influence the apparent mechanical properties of surface materials due to the method which is usually applied for determining them. Preferably one uses contact experiments like load-displacement sensing indentation measurements with subsequent classic Oliver & Pharr analysis, scratch or highly sophisticated (physicalized [1]) tribological tests. Consequently, deposition parameters can effect the resulting mechanical material properties like yield strength Y , hardness H and elastic modulus E . Such effects should be taken into account during the parameter identification analyses of mechanical material properties. Because they are not only important for quantification of the mechanical behavior of coatings, but also important indicators (e.g. H in relation to E) for the tribological performance (e.g. wear, friction) of tribological coatings. Nevertheless, it is not possible to derive such effects on the mechanical material properties solely from the deposition parameters as a result of the dynamic nature of any deposition process. Hence, it is very important to know the resulting coating structure of a deposition process. It should be measured after processing when the surface is in a static state. Such effects and their partially dramatic influence on the resulting mechanical properties will be demonstrated on the examples of ta-C and nano-composite coatings. For example it will be shown how simple roughness can lead to false apparent ultra-hardness results. In the same context it is demonstrated how inadequate or incomplete analyzes features and theoretical approaches can directly lead to severely flawed conclusion about the actual coatings stability and reliability. Last but not least, of course, it will be shown how it is been done correctly.

[1] Schwarzer et al.: "Optimization of the Scratch Test for Specific Coating Designs". SCT, accepted 2011.

3:30pm **B1-2-7 High Rate Magnetron Sputtering of Chromium Coatings for Tribological Applications.** *K. Nygren* (*kristian.nygren@mkem.uu.se*), Uppsala University, Angstrom Laboratory, Sweden, *M. Samuelsson*, Linköping University, Sweden, *Å. Kassman-Rudolphi*, Uppsala University, Angstrom Laboratory, Sweden, *U. Helmersson*, Linköping University, Sweden, *U. Jansson*, Uppsala University, Angstrom Laboratory, Sweden

Increasing demands on tribological performance drive the development of innovative coating materials and deposition methods. Recent studies of reactively sputtered chromium carbide films show promising results with regards to coefficients of friction [1], and these coatings may be suitable for commercial purposes. However, transfer of a process to industrial conditions poses challenges, such as growing the films at significantly higher deposition rates. While this is known to influence the microstructure and phase content, which in turn determine the tribological performance, the implications for the Cr-C system are not fully understood.

The objective of the present study is to investigate chromium carbide films deposited by direct current magnetron sputtering (DCMS) and high power impulse magnetron sputtering (HiPIMS) in an industrial deposition system, at growth rates up to 500 nm/min. While DCMS offers a higher deposition rate, HiPIMS is known to result in well-adherent, dense, and smooth coatings. Microstructural changes are expected as well as modified tribological and mechanical properties owing to the high deposition rate.

Cr-C coatings were synthesized by sputtering of a Cr target in an Ar/C₂H₂ atmosphere. XRD shows an X-ray amorphous Cr-C phase, in contrast to the nanocrystalline structure usually reported [2-3]. For DC sputtered coatings, XPS reveals a C-C phase which increases according to the phase diagram for Cr-C. The coatings produced by HiPIMS feature a meta-stable, supersaturated Cr-C phase, with a higher C content than predicted for the thermodynamically stable phase Cr₃C₂. Coefficients of friction were obtained from dry-sliding experiments (typically 0.35 – 0.50 for 34 – 0 % C-C), and the values confirm a dependence on phase fractions of C-C and C-Cr. Regarding the mechanical properties, coatings deposited by DCMS have a hardness of 14±1 to 18±1 GPa (51 to 17 at.% C), while coatings deposited by HiPIMS have a hardness of 7±3 GPa to 14±4 GPa (59 to 26 at.% C). Unexpectedly, the coatings deposited by HiPIMS are softer than the ones deposited by DCMS, and this difference may be due to a different grain size or phase content. SEM cross-sections indicate deep Cr implantation in the substrate, which is known to improve adhesion. Further

results will be presented for a wide compositional range, and compared to literature.

References

- [1] Mitterer et al, Proc IME J J Eng Tribol, 223 (2009) 751-757
- [2] Gassner et al, Tribol Lett, 27 (2007) 97-104
- [3] Agarwal et al, Thin Solid Films, 169 (1989) 281-288

3:50pm **B1-2-8 Behavior of DLC Coated Low-Alloy Steel under Tribo-Corrosion: Effect of Top Layer and Interlayer Variation.** *K. Bobzin, N. Bagcivan, S. Theiss, R. Weiß* (*weiss@iot.rwth-aachen.de*), Surface Engineering Institute - RWTH Aachen University, Germany, *U. Depner, T. Troßmann, J. Ellermeier, M. Oechsner*, Institute for Materials Technology - TU Darmstadt, Germany

In many industrial applications components are subjected to mechanical load, while being exposed to corrosive environments. In order to cope with the resulting tribo-corrosion, both corrosion and wear resistant steels are often resorted to. Since those materials are expensive and often difficult to machine, the development of protective thin films deposited on less expensive and easily machinable materials, is of high interest. Due to their chemical stability and high tightness, diamond-like carbon (DLC) coatings deposited via physical vapor deposition (PVD) seem to be appropriate to offer corrosion protection in addition to their well-established wear resistance. This paper deals with the development of DLC multilayer coatings consisting of alternating a-C and chromium based layers and an a-C:H top layer. The coatings were deposited on low-alloy steel (AISI 4140) using reactive magnetron sputter ion plating (MSIP) technology to investigate the possibility of improving the properties concerning tribo-corrosion. The mechanical and tribological properties of the top layer were analyzed depending on the ethine gas flow. Furthermore, the influence of different transitions from the a-C to the chromium based layers on the fatigue strength was investigated. The applicability of the DLC coatings in corrosive environments was proved using potentiodynamic polarization tests in artificial seawater: While the open circuit potential increases significantly from -400 mV_H (AISI 4140) to about 300 mV_H, current density remains below 0,001 mAcm⁻² up to the maximum load of 1200 mV_H (AISI 4140: 100 mAcm⁻²). The tribological analyses regarding continuous sliding abrasion using a pin-on-disk tribometer show that the developed DLC coatings lead to very low wear rates in aqueous environment and in contact with an Al₂O₃ counterpart, nearly independent of the ethine gas flow. Moreover, investigations in an impact tribometer with maximum initial Hertzian stress of about 10 GPa show that pure metallic chromium layers with a soft transition to the a-C layers improve the fatigue strength of the compound. Thus, even after 10⁶ impacts the coatings were proved to be still impenetrable for an electrolyte that could lead to corrosion of the substrate.

4:10pm **B1-2-9 Integration of the Larco®-technology for ta-C-coatings in an industrial hard material batch system.** *M. Holzherr* (*katrin.wagner@vtd.de*), *M. Falz, T. Schmidt*, VTD Vakuumtechnik Dresden GmbH, Germany, *H.-J. Scheibe, M. Leonhardt, C.-F. Meyer*, Fraunhofer-Institut für Werkstoff- und Strahltechnik, IWS, Germany

DLC (diamond like carbon) thin film depositions are carried out in a wide range of CVD- and PVD technologies. Main applications are: tribologically stressed machine components as well as wear protection of tools. As a matter of fact, it could be verified that the hydrogen free DLC-coatings result in advanced thin film properties such as higher hardness which is caused by a higher sp³-bonding content. Therefore evaporation of solid graphite by PVD-technologies has been of considerable advantages.

Especially the vacuum arc evaporation technique stands out for a very high degree of single and multiple ionised carbon atoms with increased energy necessary for condensation in the dense tetragonal amorphous diamond-like carbon film structure (ta-C). Beside low friction also super hard coatings can be deposited by means of that technology.

A commercial hard material coating system has been equipped with a laser arc module (LAM) for the deposition of hydrogen-free ta-C-films. For industrial applications it was necessary to increase deposition rates. Therefore arc pulse current and pulse frequency were varied from 800 A to 1.600 A and 150 Hz to 300 Hz, respectively.

The carbon plasma during deposition process were examined by optical emission spectroscopy (OES) and Langmuir probe and effect on plasma parameters of the thin film properties will be shown.

The influence of the deposition rate on thin film properties is caused by thermal effects. One limitation is a maximal deposition temperature of about 150 °C in order to avoid the graphite film structure which results in reduction of hardness finally.

The thin film depositions were carried out on samples of circular blanks and carbide drills. Hardness, adhesion and elastic force module are the first criteria for evaluating the quality of the deposited ta-C- films. As real

application tests the ta-C coated drills were used to machine an abrasive AlSi-alloy with high Si-content.

4:30pm B1-2-10 Ion-assisted PVD growth of carbon-transition metal nanocomposite thin films, G. Abrasonis (*g.abrasonis@hzdr.de*), Helmholtz-Zentrum Dresden-Rossendorf, Germany **INVITED**

Nanostructures dramatically influence materials properties due to size, shape and interface effects. Thus the control over the structure at the nanoscale is a key issue in nanomaterials science. The interaction range of hyperthermal ions with solid surface is confined to some nanometers. Therefore hyperthermal ion assistance during deposition is of primary relevance in the context of the morphology control of the nanocomposite films.

This contribution will summarize our recent activities in the field of ion-assisted physical vapor deposition (PVD) of carbon-transition metal films with the focus on the growth-structure relationship. This class of materials is relevant in the context of tribology, sensing, fusion, electrochemistry, information storage, spintronics or solar-thermal energy conversion. We have employed ionized physical vapor deposition in the form of a pulsed filtered cathodic vacuum arc (PFCVA) and ion beam assisted deposition (IBAD). The two methods differ in the way the ion energy is transferred into the near surface layers: for IBAD the bombarding Ar⁺ ions transfer the energy via collisions to the near-surface layers of nanocomposite films while for PFCVA the energetic species are themselves the film forming material. The dependences of the film structure on the metal type, metal-to-carbon ratio, ion energy and ion incidence angle will be reported.

The results show that ions have a dramatic effect on the film morphology resulting in a large variety of morphologies such as encapsulated nanoparticles, high aspect ratio nanocolumns or self-organized layered 3D nanoparticle arrays. The latter occurs only due to the presence of energetic ions, and the periodicity is determined by the ion energy. In addition, the ion induced atomic mobility is not isotropic, as it would be in the case of thermally excited migration, but conserves to a large extent the initial direction of the incoming ions. Independently of the growth regime, it results in the morphology tilt: metal nanopatterns no longer align with the advancing surface but with the incoming ions. Such effects allow 3D sculpting of nanocomposites which is due to ion irradiation effects and does not require any glancing incidence conditions.

As the observed effects are of physical origin (ion-solid interactions), we believe that the presented results are applicable to other immiscible or partially miscible systems as well. This presents a possible path towards a material design approach based on material system independent tools to sculpt the morphology at the nanoscale in order to match the requirements of a wide range of applications.

5:10pm B1-2-12 The effect of hydrogen addition on the residual stress of cubic boron nitride film prepared by R.F. magnetron sputtering of B₄C target, J.K. Park (*jokepark@kist.re.kr*), J.-S. Ko, W.-S. Lee, Y.J. Baik, Korea Institute of Science and Technology, Republic of Korea

cBN (cubic boron nitride) shows outstanding mechanical properties such as hardness and wear resistance. In contrast to diamond, cBN is compatible with ferrous materials, which makes it possible to be used as coating materials for machining of ferrous materials at high temperatures. However, amorphous BN and hBN layers inevitably formed before nucleation of cBN weaken the interface stability between cBN film and substrate. Furthermore high stress developed during deposition of cBN film deteriorates adhesive strength of cBN film. Recently, the adoption of compositionally gradient B-C-N buffer layer [1] and the addition of oxygen [2] or hydrogen [3] have been suggested as useful technique to improve interface (hBN) stability and reduce residual stress of cBN film, respectively. By further reduction of residual stress of cBN film with stable interface of hBN layer, the application of cBN as protective coating material is believed to be realized. In this study, therefore, we have investigated the effect of hydrogen addition on the residual stress of cBN film prepared with compositionally gradient B-C-N layer deposited by magnetron sputtering of B₄C target. The deposition was performed on Si (100) substrate under the chamber pressure of 0.27 Pa with substrate bias of -250V. After the deposition of B₄C layer, up to 5 sccm hydrogen was added to a gas mixture of argon and nitrogen flowing 25 sccm and 5 sccm, respectively during sample preparation. The compressive stress of cBN film was observed to be decreased from 9.2 GPa to 4.3 GPa, with increasing hydrogen flow up to 5 sccm. The cBN fraction in these films, however, remained to be about 65%, irrespective of the amount of hydrogen added. The stress reduction observed in cBN film deposited with the addition of hydrogen was discussed in terms of the relation between the penetration probabilities of hydrogen and argon ions into the film, which was main origin of compressive residual stress of the compositionally gradient B-C-N layer with hBN structure.

[1] K. Yamamoto, M. Keuneeck and K. Bewilogua, Thin Solid Films 377-378 (2000) 331-339

[2] M. Lattemann, S. Ulrich and J. Ye, Thin Solid Films 515 (2006) 1058-1062

[3] H.-S. Kim, J.-K. Park, W.-S. Lee and Y.-J. Baik, Thin Solid Films 519 (2011) 7871-7874

This research was supported by a grant from the Fundamental R&D Program for Core Technology of Materials funded by the Ministry of Knowledge Economy, Republic of Korea

Fundamentals and Technology of Multifunctional Thin Films: Towards Optoelectronic Device Applications **Room: Tiki Pavilion - Session C2-2/F4-2**

Thin Films for Photovoltaics and Active Devices: Synthesis and Characterization

Moderator: T. Terasako, Graduate School of Science and Engineering, Ehime University, Japan, M. Cremona, Pontificia Universidade Católica do Rio de Janeiro, Brazil

1:30pm C2-2/F4-2-1 Reactive Deposition of Aluminum-doped Zinc Oxide films using Asymmetric Linked Dual Rotatable Magnetron, M. Audronis (*martynas.audronis@genco.com*), V. Bellido-Gonzalez, Gencoa Ltd, UK

Transparent conductive oxide (TCO) films are a widely used group of functional materials that can be found in a large variety of applications such as consumer electronics (e.g. flat panel displays and touch-screens), solar cells and smart glass/windows. Indium Tin Oxide (ITO) – the most widely applied TCO, exhibits excellent electrical and optical properties and good corrosion resistance. The drawback of ITO is that it is too expensive for the majority of low cost applications and, due to the rarity of In, has a potential to become even more expensive in the near future. Aluminum-doped Zinc Oxide (AZO) is considered to be one of the most viable alternatives to ITO in many application areas.

Deposition of AZO by sputtering can be done non-reactively from ceramic targets or reactively from metal Al doped Zn targets. Reactive deposition mode, as compared to sputtering ceramic targets, offers significant cost savings on the target material and an increase in production rates. Operation in reactive mode however requires a stable and well controlled process. This concerns both, the reactive gas delivery (i.e. partial pressure) and plasma substrate interaction.

In this paper we describe a reactive AZO deposition process using the recently developed asymmetric linked dual rotatable magnetron (ALDRM) sputtering technology. ALDRM lowers the impedance of plasma (hence increases the deposition rate at the same target voltage) and allows control of the plasma-substrate interaction degree. A fast feedback process control system is used in conjunction providing accurate reactive deposition process control and ensuring the required stability. The combination of the above mentioned methods yield AZO films of good electrical and optical properties at high deposition rates.

1:50pm C2-2/F4-2-2 Influence of the Kind and Content of Doped Impurities on Impurity-Doped ZnO Transparent Electrode Applications in Thin-Film Solar Cells, J. Nomoto, T. Hirano, T. Miyata (*miyata@neptune.kanazawa-it.ac.jp*), T. Minami, Kanazawa Institute of Technology, Japan

Impurity-doped ZnO thin films that would be suitable for transparent electrode applications in Si-based thin-film solar cells must necessarily attain not only a decrease of plasma resonance frequency by lowering the carrier concentration while retaining a low resistivity, but also a significant scattering of the incident visible and near-infrared light by surface texturing the film. This paper describes the influence of the kind and content of dopant on the electrical properties and their stability as well as on the light management obtainable by surface texturing in impurity-doped ZnO thin films. Al-, Ga- and B-doped ZnO (AZO, GZO and BZO) thin films were prepared on OA-10 glass substrates at a temperature of room temperature (RT) or 200°C using a pulsed laser deposition (PLD) and magnetron sputtering deposition (MSD). AZO, GZO and BZO thin films were prepared by PLD using an ArF excimer laser. AZO and GZO thin films were also prepared by direct current MSD with superimposed radio frequency power. The electrical properties were evaluated for impurity-doped ZnO thin films prepared with a thickness in the range from 0.5 to 2 µm, because the obtainable electrical properties were considerably dependent on the film thickness. In addition, for impurity-doped ZnO thin films prepared on substrates at 200°C, the following characteristics were found to be considerably dependent on the content of impurity doped into the thin films, irrespective of the deposition methods used: the obtainable

carrier concentration, Hall mobility and their stability in long-term moisture-resistance tests as well as the surface texture structure formed by wet-chemically etching and its resulting haze properties. It should be noted that differences in the obtainable Hall mobility among AZO, GZO and BZO thin films prepared with a low resistivity on the order of $10^{-4} \Omega\text{cm}$ by the different deposition methods were attributed to the content rather than the kind of impurity doped into the thin films. In addition, the influence of rapid thermal annealing (RTA) on surface texture formation as well as on light management was investigated in the impurity-doped ZnO thin films. The RTA treatment significantly improved the obtainable light management in thin-films prepared on substrates at 200°C over that found in thin-films prepared at RT. Comparing AZO, GZO and BZO, the AZO thin films prepared with an appropriate Al content on substrates at 200°C were found to be the most suitable for transparent electrode applications in Si-based thin-film solar cells.

2:10pm C2-2/F4-2-3 Comparative physical properties of Ga-, In-, Zr- and Sn-doped ZnO semiconductor thin films fabricated via sol-gel method. C.Y. Tsay (cytsay@fcu.edu.tw), W.C. Lee, S.S. Lo, C.J. Chang, C.K. Lin, Feng Chia University, Taiwan

Transparent ZnO semiconductor thin films doped with In, Ga, Sn, and Zr were deposited on glass substrate via sol-gel method. The doping concentration defined as $M/(Zn+M)$ atomic ratio where M is the dopant, is 2 at.% for all doped ZnO thin film samples. In this study, authors reported the influence of dopants on the structures, optical, and electrical properties of ZnO thin films. Moreover, composition, chemical bonds, and photoluminescence spectra of undoped and doped ZnO thin film samples were examined. These ZnO-based sol-gel films were preheated at 300 °C for 10 min, and then annealed in ambient air at 500 °C for 2 hr. XRD results show that the doped ZnO thin film exhibited broaden diffraction peaks, and the broadening features were significant in the cases of In, Zr, and Sn doping. All doped ZnO thin films exhibited higher optical transmittances in the visible range than the undoped ZnO thin film. Electrical properties of each ZnO-based thin film were characterized by Hall measurements using the van der Pauw configuration.

2:30pm C2-2/F4-2-4 Temperature Dependence of Electrical Properties of Ga-Doped ZnO Films Deposited by Ion-Plating with DC Arc Discharge. T. Terasako (terasako.tomoaki.mz@ehime-u.ac.jp), Graduate School of Science and Engineering, Ehime University, Japan, H.-P. Song, H. Makino, Kochi University of Technology, Japan, S. Shirakata, Graduate School of Science and Engineering, Ehime University, Japan, T. Yamamoto, Kochi University of Technology, Japan

Ga-doped ZnO (GZO) is one of the promising materials for transparent electrodes in flat panel displays and solar cells. Highly transparent GZO polycrystalline films with low resistivity can be deposited at low temperatures below 473 K. Very little work is currently available in the published literature on temperature dependence of electrical properties; resistivity, r , carrier concentration, n , and Hall mobility, m , of GZO films. In this paper, we have investigated the subject to discuss carrier transport through grain boundaries in the films.

GZO films with a thickness of 200 nm were deposited by ion-plating with DC-arc discharge. Sintered ZnO tablets with different Ga_2O_3 contents ranging from 0.003 to 4 wt.% were used as resources. During the growth process, an oxygen gas was introduced into the deposition chamber to compensate oxygen deficiencies. Hall measurements were carried out using the van der Pauw method at 83-343 K under the magnetic field of 0.47 T.

Analysis of data obtained by the Hall measurements shows that the characteristics of μ - T curve gradients, $\Delta\mu/\Delta T$, plotted as a function of n can be divided into three regions: (1) Region I; n values below $n=1 \times 10^{20} \text{ cm}^{-3}$, the $\Delta\mu/\Delta T > 0$ (grain-barrier-limited transport) and the values decreased with increasing n , (2) Region II; n values ranging from 1×10^{20} to $5 \times 10^{20} \text{ cm}^{-3}$, $\Delta\mu/\Delta T=0$: μ values were independent of T and (3) Region III; $n > 1 \times 10^{21} \text{ cm}^{-3}$, the $\Delta\mu/\Delta T < 0$ (metal-like behavior). This tendency is probably due to the change in dominant scattering mechanism from grain boundary scattering to phonon scattering with increasing n .

In the case of Region I described above, based on the model that carrier mobility is mainly determined by the potential barrier, V_B , at the grain boundary, we applied a charge trapping model to understand the nature of grain boundary scattering on carrier transport for polycrystalline GZO films. As a result, we find the values of the V_B of less than 0.02 eV for all samples in Region I. Considering that even GZO films in the Region I have the V_B values smaller than kT at room temperature, tunneling current can make a major contribution to the carrier transport through grain boundaries for all GZO films under investigation.

2:50pm C4-2/F4-2-6 Doped Cadmium Oxide as a High Performance Transparent Conductive Oxide. R. Mendelsberg, K.M. Yu, Y. Zhu, D. Speaks, S. Lim, Lawrence Berkeley National Laboratory, US, S. Zhao, University of California, Berkeley, US, J. Reichertz, S. Mao, W. Walukiewicz, A. Anders (aanders@lbl.gov), Lawrence Berkeley National Laboratory, US

Cadmium oxide has a high intrinsic electron mobility compared to all other conventional transparent conductive oxides (TCOs) such as ZnO:Al and indium-tin-oxide. Unintentionally doped CdO films can have Hall mobilities greater than $150 \text{ cm}^2/\text{Vs}$ and carrier concentrations in the high 10^{19} cm^{-3} resulting in resistivities in the $10^{-4} \Omega \text{ cm}$ range. However, the small band gap (2.2 eV) severely restricts the visible transmission of undoped CdO, thus limiting its application as a TCO. However, the optical absorption edge can be considerably widened by increasing the electron concentration due to the Burstein-Moss shift which occurs when the Fermi level shifts to higher energy and more conduction band states are filled with electrons from the donor dopants. In this work we report on high quality films of CdO, undoped and doped with indium, deposited by filtered cathodic arc deposition (FCAD) and by pulsed laser deposition (PLD). The properties of films synthesized by both methods will be compared. Using these highly non-equilibrium synthesis methods, we have achieved extremely low resistivities (less than $5 \times 10^{-5} \Omega\text{-cm}$) for In-doped CdO films with an electron concentration greater than $1 \times 10^{21} \text{ cm}^{-3}$ and mobilities as high as $200 \text{ cm}^2/\text{Vs}$. Moreover, due to the high electron concentration, these films have a band gap $> 3.2 \text{ eV}$. The high optical transmittance ($> 85\%$) of this material in the spectral range extending from the visible to 1300 nm in the infrared makes it an ideal TCO for thin film photovoltaics, especially in multijunction solar cells where high infrared transmittance is essential.

3:10pm C2-2/F4-2-7 Current Status and Future Prospects of the CIGS PV Technology. S. Niki (shigeru-niki@aist.go.jp), S. Ishizuka, H. Komaki, S. Furue, K. Matsubara, H. Shibata, A. Yamada, Research Center for Photovoltaic Technologies, AIST, Japan, N. Terada, Kagoshima University, Japan, T. Sakurai, K. Akimoto, Tsukuba University, Japan

INVITED

Overview of the research activities in the CIGS PV technology will be presented. In addition, the current status and future prospects of the CIGS technology will be discussed based upon our research results.

High-efficiency CIGS solar cells and submodules have been developed in our research group. In order to fill the efficiency gap between small-area cells and commercial modules, the multi-stage evaporation technique has been applied to fabricate the monolithically integrated CIGS submodules. The conversion efficiencies of integrated submodules on $10 \times 10 \text{ cm}^2$ sodalime glass and flexible ceramics substrates have been improved up to $\eta=16.6\%$ and $\eta=15.9\%$, respectively. These results indicate that the CIGS technologies are competitive with the current Si and CdTe technologies in terms of both cost as well as performance.

3:50pm C2-2/F4-2-9 Reactive magnetron sputtering of precursors for CZTS solar cells. T. Kubart (Tomas.Kubart@angstrom.uu.se), T. Ericson, J.J. Scragg, C. Platzer-Björkman, The Angstrom Laboratory, Uppsala University, Sweden

At the moment, CIGS (CuInGaSe_2) solar cells show the highest efficiency among industrial scale produced thin film solar cells. Given the present strong increase in production, however, the availability and price of indium will become an issue because of its low abundance in Earth's crust. Therefore, there is strong interest in alternative indium free absorber materials. Kesterites CZTS ($\text{Cu}_2\text{ZnSn(S}_x\text{Se}_{1-x})_4$) attracted most attention owing to the fact that relatively high efficiencies have already been demonstrated and also due to the similarity to CIGS.

In this contribution we report on reactive sputtering for deposition of CZTS precursors. In order to avoid Sn loss at elevated temperatures a two stage process, synthesis of precursor films at relatively low substrate temperature followed by annealing, is used. Depositions are performed by pulsed DC magnetron sputtering from two targets, a CuSn alloy and Zn, in a mixture of Ar and H_2S . The film structure is evaluated by X-ray diffraction and Raman spectroscopy while the composition is analysed by RBS, XRF, EDS and EPMA. Internal stress is measured by deflection of thin substrates. Characteristics of the deposition process are discussed with respect to the discharge power, total pressure, substrate temperature and H_2S flow on the film structure and composition.

Sulphur incorporation can be readily controlled by H_2S flow with the structure changing from amorphous to columnar with increasing S content. The main issue encountered in the depositions is related to the film composition as the ratio between Cu and Sn does not correspond to the target composition. This effect is discussed in detail with respect to the sputtering and transport through the gas phase. Finally, material properties after annealing are briefly summarized.

4:10pm **C2-2/F4-2-10 Investigation of resistive switching characteristic and mechanism on InGaO_x film, J.B. Yang** (hripap@hotmail.com), National Sun Yat-Sen University, Taiwan

In this study, the resistance random access memory (ReRAM) of Pt/IGO/TiN device was fabricated, and the InGaO_x (IGO) film was deposited by co-sputtering the Ga₂O₃ and In₂O₃ targets. Beside the Pt/IGO/TiN device, the control sample of Pt/GaO_x/TiN was fabricated, and the insulation layer of GaO_x film exhibit the bipolar resistance switching characteristic. Compared with the GaO_x film, the resistance switching features of Pt/IGO/TiN included both bipolar and unipolar characteristics. The unipolar resistance ratio can be enhanced to 3 orders, and retention exhibit excellent. From XPS analyzing, we can analysis the composition of IGO film. In order to study the switching mechanisms between bipolar and unipolar in the device of Pt/IGO/TiN, we measure the resistance various temperatures. From the results, the bipolar switching characteristic was demonstrated by the formation and ruptures of oxygen vacancies, which has the semiconductor-like behavior. On the other hand, the device exist the switching characteristic of unipolar due to the metal-like filament.

4:30pm **C2-2/F4-2-11 Influence of forming process on resistance switching characteristics of In₂O₃/SiO₂ bi-layer, J.J. Huang** (happylizard@gmail.com), National Sun Yat-Sen University, Taiwan

In this study, we fabricated and analyzed the resistance switching characteristic for the resistance random access memory (RRAM) in Pt/In₂O₃/SiO₂/TiN structure. By applying oppositely directed electric field to soft break down the insulator constructed of In₂O₃/SiO₂ bi-layer, the RRAM device exhibited different switching behaviors. As positive forming voltage was applied to TiN electrode, the In₂O₃/SiO₂ bi-layer was soft broken down, and the resistance switching behavior was dominated by the bipolar mode. However, both bipolar and unipolar switching characteristics are exhibited in In₂O₃/SiO₂ bi-layer while the negative voltage was employed to forming process. In order to analyze the composition of conduction path and resistance switching mechanism, we extracted the trends of resistance value with temperature. From the analysis, the conduction paths of bipolar and unipolar modes are respectively dominated by oxygen vacancies and metal-like filament. Hence, we considered that the metal-like filament was formed by the migration of indium ions because the unipolar characteristic was exhibited under particular forming condition.

4:50pm **C2-2/F4-2-12 Investigating the multiple high resistance states after ac and dc reset methods for resistance switching memory application, H.C. Tseng** (d982030010@student.nsysu.edu.tw), National Sun Yat-Sen University, Taiwan

This paper studies the reset behaviors of resistive random access memory devices with the Pt/SiO₂/Gd/TiN structure. The ReRAM device has treated a same stopping voltage with ac and dc modes respectively for reset process. Different reset method can influence the oxidation rate of the filament and the oxygen anions escaping rate from the oxygen reservoir, causing different high resistive states. When increasing stopping voltage, more triggered oxygen anions can produce to oxidize with the filament. Furthermore, the device also exist the unipolar switching phenomenon with an atypical reset behavior, and this reset behavior is dissimilar to the typical unipolar reset phenomenon undergoing the dc sweeping method. Utilizing the fast IV measurement simulating the AC operation mode analyzes the reset behavior of bipolar and unipolar. Undergoing the increase ramp speed condition respectively to reset the device on bipolar switching mode, a raising-time dependent relation affects the reset behavior such as reset voltage and stopping current. A mechanism is proposed to explain the bipolar unipolar reset characteristics.

Fundamentals and Technology of Multifunctional Thin Films: Towards Optoelectronic Device Applications

Room: Pacific Salon 3 - Session C3-1

Optical Characterization of Thin Films, Surfaces and Devices

Moderator: J. Krueger, BAM Berlin, Germany, E. Schubert, University of Nebraska-Lincoln, US

1:30pm **C3-1-1 Terahertz Ellipsometry Materials Characterization, T. Hofmann** (thofmann@engr.unl.edu), University of Nebraska-Lincoln, US
INVITED

Ellipsometry is the preeminent technique for the accurate, quantitative determination of complex-valued optical material constants including anisotropy in a spectral range covering VUV to the far-infrared. In the THz frequency domain, however, ellipsometry is still in its infancy. The precise

and accurate determination of optical properties at THz frequencies is essential for the development of increasingly advanced THz optical systems and a prerequisite for the design and manufacturing of optical elements such as windows, focusing optics, optical antireflection coatings, etc. Furthermore, the accurate knowledge of THz dielectric functions will provide new insights into the fascinating excitation mechanisms such as spin-transitions, collective modes of biological molecules, local free-charge carrier oscillations, etc. and may further allow exploration of novel physical phenomena as observed in artificially structured meta-materials [1].

In this talk, recent developments and applications of classical, rotating optical element THz ellipsometry using different electron beam based, quasi-optical light sources will be reviewed [2]. I will demonstrate the potential of high-brilliance THz synchrotron radiation sources, Smith-Purcell-effect type sources, and high power backward-wave oscillator type sources for the use in time-domain spectroscopic THz ellipsometers. Exemplarily, I will report on the determination of complex optical constants of moderately doped silicon, sapphire, and different infrared optical coating materials [3,4]. The application of THz ellipsometry for the contact-free optical determination of free-charge carrier properties for very small doping concentrations and doping profiles in iso- and anisotype silicon homojunctions will be discussed.

Furthermore, recent results on THz optical Hall-effect (generalized ellipsometry in magnetic fields) investigations of the free-charge carrier properties in AlGaIn/GaN high electron mobility transistors structures and epitaxial graphene samples will be presented.

References:

- [1] C. Hou-Tong, *et al.*, *Nat. Photon.* **2**, 295 (2008).
- [2] T. Hofmann, *et al.*, *Rev. Sci. Instrum.* **77**, 063902 (2006); **81**, 023101 (2010).
- [3] T. Hofmann, *et al.*, *Appl. Phys. Lett.* **95**, 032102 (2009).
- [4] T. Hofmann, *et al.*, *Mat. Res. Soc. Symp. Proc.* **1163E**, 1163-K08-04 (2009).

2:10pm **C3-1-3 Modeling the optical properties of 2D colloidal crystals, S. Portal-Marco** (sabineportal@hotmail.com), E. Cabrera, University of Barcelona, Spain, J. Ferre-Borrull, Rovira i Virgili University, Spain, O. Arteaga, New York University, E. Pascual, E. Bertran, University of Barcelona, Spain

Colloidal crystals are materials of the future at the crossroads of different technological areas and with application in photonics, in bioengineering and photovoltaic cells. In this work, large-area 2D colloidal crystals were prepared in one deposition step using a Langmuir-Blodgett system equipped with a large trough. The colloidal crystals were constituted of spherical particles of silica prepared by sol-gel method from hydrolysis of tetraethoxysilane precursor in ethanol. Monolayers of the synthesized particles (from 50 nm to 1 micron diameter with dispersion smaller than 10%) were self-assembled by increasing the surface pressure in the trough and they were deposited on 25 to 100 cm² substrates of silicon and glass with the Langmuir-Blodgett dipper process. Particle size distribution, crystalline structure, domain size and crystal orientation were determined by Atomic Force Microscopy (AFM), Scanning Electron Microscopy (SEM) and interferometric microscopy. Transmittance spectra and ellipsometric measurements provided information about the optical, photonic and anisotropic properties of the colloidal films. Colloidal crystals can be represented as multilayer dielectric structures with in-plane periodic patterning. The ellipsometric data in reflexion were interpreted by calculation of the electromagnetic properties of the colloidal crystals from a scattering matrix treatment, where the internal electromagnetic modes are coupled to external fields. The angle of incidence of the light, the particle size, the crystal structure and the refractive index constituted the simulation parameters for our model, and the calculated tanY and cosD were compared with the measured values. The successful implementation of the model gives the opportunity of tailoring the properties of colloidal crystals.

2:30pm **C3-1-4 Confocal 2D Photoluminescence Mapping of Porous Silicon, A. Abusoglu, T. Karacali, H. Efeoglu** (hefeoglu@atauni.edu.tr), Ataturk University, Turkey

Two dimensional optical activity of semiconductors or devices such as led or lasers is one of the key factor for the assessment of material selection and fabrication techniques. Confocal arrangement with exceptional high resolution is widely used for 3D imaging of biological systems. The advances of laser sources and signal detection hardware provided much better signal/noise ratio during the last decade. Nowadays super resolution down to nanometer scale has been reported by using 4pi-STD, RESOLFT, SIM, GSD, PALM, STORM techniques (Lothar Schermelleh, Rainer Heintzmann, and Heinrich Leonhardt, A guide to super-resolution fluorescence microscopy, The Journal of Cell Biology, July 19, 2010, Mike Heilemann, Fluorescence microscopy beyond the diffraction limit, Journal

of Biotechnology, (149) 2010). In this study a confocal system was adapted to liquid nitrogen cryostat and its application to wavelength resolved surface mapping of porous silicon was provided. Local sampling of surface within micron scale provide us to resolve spectrum of porous silicon, where some of the peaks in the spectrum are merged into one in the traditional PL technique.

2:50pm C3-1-5 Structure, electronic properties and electron energy loss spectra of transition metal nitride films, L. Koutsokeras, M. Matenoglou, P. Patsalas (ppats@cc.uoi.gr), University of Ioannina, Greece
The combination of electrical conductivity, chemical and metallurgical stability, refractory character and lattice constants close to those of III-nitrides and III-phosphides make transition metal nitrides (TMN) promising candidates for electronics and device applications; thus, the study of their electronic properties, such as the conduction electron density and the work function is of major importance [1].

In this work we present a thorough and critical study of the electronic properties of the mononitrides of the group IV-V-VI metals (TiN, ZrN, HfN, NbN, TaN, MoN, WN) grown by Pulsed Laser Deposition (PLD). The microstructure and density of the films have been studied by X-Ray Diffraction (XRD) and Reflectivity (XRR), while their optical properties were investigated by spectral reflectivity at vertical incidence and *in-situ* reflection electron energy loss spectroscopy (R-EELS). The electron density, the plasma energy (equivalent to the conduction electron density) and the conduction electron relaxation time are rationally grouped according to the electron configuration (i.e. of the respective quantum numbers) of the constituent metal; the variation of the conduction electron density in ternary TMN compounds reveals also details on the TM-N bonding.

Last but not least, we report the R-EELS spectra for all the binary TMN and we identify their features (TM-d plasmon and TM-d+N-p plasmon) based on previous [2] *ab-initio* band structure calculations. The assigned and reported R-EELS spectra can be used as a reference database for the colloquial *in-situ* surface analysis performed in most laboratories.

[1] G.M. Matenoglou, L.E. Koutsokeras, and P. Patsalas, Appl. Phys. Lett. 94, 152108 (2009).

[2] G.M. Matenoglou, L.E. Koutsokeras, Ch.E. Lekka, G. Abadias, S. Camelio, G.A. Evangelakis, C. Kosmidis, and P. Patsalas, J. Appl. Phys. 104, 124907 (2008).

3:10pm C3-1-6 Fabrication and characterization of a $V_2O_5/V/V_2O_5$ multilayer thin films for uncooled microbolometers, D. Kaur (dkaurfph@iitr.ernet.in), V. Goyal, Indian Institute of Technology Roorkee, India

$V_2O_5/V/V_2O_5$ multilayer thin films were deposited on glass and silicon substrates using sputtering technique. The crystalline structure, surface morphology, optical and electrical properties of the films were systematically studied by using X-Ray Diffraction, Scanning Electron Microscopy, UV Visible Spectrometer and four probe resistivity method, respectively. XRD analysis revealed the formation of highly oriented films with low values of surface roughness. The transmittance and refractive index was found to be highly influenced by the formation of multilayer structure. $V_2O_5/V/V_2O_5$ multilayer films with good crystalline structure, optical and electrical properties may find potential applications in uncooled microbolometers.

Keywords: Sputtering; Thin films; X-Ray Diffraction; Optical Properties.

3:30pm C3-1-7 Gaschromic Properties of IrO_2 Thin Films Grown by Pulsed Laser Deposition Technique, C.H. Hsu, C.C. Chang (ccchang1978@phys.sinica.edu.tw), Institute of Physics, Academia Sinica, Nankang, Taiwan, M.H. Wen, Institute of Physics, Academia Sinica, Nankang, Taiwan, Y.R. Wu, Y.T. Hsieh, W.H. Chao, Institute of Physics, Academia Sinica, Nankang, Taiwan, C.K. Lin, Feng Chia University, Taipei, Taiwan, M.J. Wang, M.K. Wu, Institute of Physics, Academia Sinica, Nankang, Taiwan

IrO_2 thin films were successfully fabricated by KrF ($\lambda = 248$ nm) pulsed laser deposition (PLD) on transparent substrates. The effects of deposition parameters, such as oxygen ambient pressure and substrate temperature, on the structure/morphology, resistivity and gasochromic effect on IrO_2 thin film were discussed. A layer of platinum (Pt) was evaporated onto the surface of IrO_2 thin films. The oxygen gas sensing performance of platinum (Pt) catalyst activated IrO_2 thin films were then investigated by UV-VIS spectra and Fourier Transform Infrared (FTIR) spectra. Sensor properties of the thin films were reported at room temperature in O_2 - N_2 mixtures containing 0-50 mole% of O_2 and the transmittance change (ΔT) of the IrO_2 oxygen sensor was reported.

Keywords: Gaschromic properties, IrO_2 , sol gel, PLD.

3:50pm C3-1-8 Formation of nanoscale pyramids on polycrystalline silicon by self-mask etching to improve the solar cell efficiency, H.H. Lin, W.H. Chen, F.C.N. Hong (hong@mail.ncku.edu.tw), C.J. Wang, National Cheng Kung University, Taiwan

In order to increase the solar-electricity conversion efficiency, the future silicon wafer solar cells will require the creation of nanostructures on the surface to reduce solar reflection and increase solar absorption. Among all the methods for creating nanostructures, reactive ion etching (RIE) has proven itself as a most efficient and reliable process to reduce light reflection from silicon surface by effectively texturing nanoscale structures on silicon surface.

In this study, reactive gases comprising chlorine (Cl_2), sulfur hexafluoride (SF_6), and oxygen (O_2) were activated by radio frequency plasma in RIE system at a typical pressure of 85~130 mtorr to fabricate the nano-scale pyramids. Poly-Si substrates were etched for 6~10 min to modify surface nanostructure by varying the compositions of SF_6 , Cl_2 , and O_2 gas mixtures in the etching process. However, the dry etching process brought damages to silicon surface, which affected the electrical properties of the surface layer. Therefore, after dry etching process, acid ($KOH:H_2O=1:1$) treatment for 1min was employed to remove the damage layer (100nm). The reflectivity after acid treatment could be significantly reduced to <10% for the wavelengths between 500nm to 900nm. The effects of RIE and surface treatments on the surface nanostructures, optical performance and the efficiencies of solar cells will be discussed and presented.

4:10pm C3-1-9 Production and Characterization of Copper Indium Disulfide Thin Film, Y.R. Wu, C.C. Chang, M.H. Wen, C.H. Hsu, Y.T. Hsieh, W.H. Chao, J.Y. Luo, M.K. Wu, Institute of Physics, Academia Sinica, Nankang, Taiwan, H.S. Koo (frankkoo@must.edu.tw), Ming-Hsin University of Science and Technology, Taiwan

In this paper, the pulsed laser deposition (PLD) was used to deposit $CuInS_2$ thin film and investigated the optical and electrical properties, and demonstrated the relationship between micro-structural and physical properties on different substrates, containing optical band-gap, absorption coefficient and grain. The thin films were characterized by XRD, SEM, UV-Vis-NIR spectrophotometer.

The XRD resultant $CuInS_2$ thin films exhibit the preferred (112) orientation on the substrate temperature high than 530°C, and the films are of high absorption coefficient of $10^4 \sim 10^5$ cm^{-1} . The calculated band gap values of 1.3~1.4 eV, according with the theoretical band gap of $CuInS_2$.

4:30pm C3-1-10 Studying matter with laser driven x-ray sources, J. Spielmann (christian.spielmann@uni-jena.de), Institute of Optics and Quantumelectronics, Friedrich Schiller University Jena, Germany INVITED

In the first hundred years since their discovery x-rays have played an important role in helping us understanding the structures of materials. Nowadays physicists, chemists, biologists and material scientists rely on x-ray static structural analysis on a routine basis. In addition to the static structural information, transient structural information is required for a deeper understanding. Such dynamic processes include the breaking and formation of chemical bonds, protein motions, charge transfer, phase transitions and so on. Many of these problems have already been tackled by means of conventional optical pump/probe spectroscopy. Unfortunately, such optical measurements cannot be directly inverted to give the desired position of the atoms as a function of the times expect in very favorable cases. Unlike optical spectroscopy, x-ray diffraction and x-ray absorption do in principle provide direct ways to reconstruct the motion of atoms during dynamic processes. Thus, time-resolved x-ray diffraction and x-ray absorption may serve as a more direct way to observe ultrafast processes in solid-state materials and surfaces. In this talk we will review methods to generate short x-ray pulses by the nonlinear frequency conversion of laser light. The major advantage of this approach is beside table top size of the x-ray source, the possibility of perfectly synchronized intense laser pulses to excite a dynamical change. The laser induced structural modification will be probed by the temporally delayed x-ray pulse. This approach ensures atomic resolution in time and space. Applications in material science range from functional imaging of nanostructures with x-rays, to time resolved x-ray microscopy, to follow structural changes of laser heated samples with time-resolved x-ray absorption spectroscopy or x-ray diffraction.

5:10pm C3-1-12 Synthesizes of Mesoporous Tantalum Oxide Films by Sol-Gel Process for the Applications in All-Solid-State Electrochromic Devices, Z.Z. Tsai, C.L. Wu, C.K. Wang, Department of Materials Science and Engineering, National Cheng Kung University, Taiwan, S.C. Wang, Department of Mechanical Engineering, Southern Taiwan University, Taiwan, J.L. Huang (jlh888@mail.ncku.edu.tw), Department of Materials Science and Engineering, National Cheng Kung University, Taiwan
 Ta_2O_5 are suitable for ion conducting layer in electrochromic (EC) devices. In our research, mesoporous Ta_2O_5 was synthesized through a sol-gel

process with surfactant on WO₃/ITO substrate to improve the electrochromic properties. The deposition parameters considered were the volume ratio of precursor Ta(OC₂H₅)₅: C₂H₅OH: surfactant and the calcined temperature. The porous tantalum oxide specimens were characterized by XRD, XPS, and FESEM. The optical properties and transmittance change were characterized by UV-visible spectrophotometer. And the electrochromic properties were also examined by potentiostat. Comparing with the dense films, a relationship between ion conduction and porosity was investigations.

5:30pm **C3-1-13 Fabrication and characterization of ZnO/NiTi/ZnO multilayers for optoelectronic applications**, *D. Kaur* (dkaurfph@iitr.ernet.in), *N. Choudhary*, Indian Institute of Technology Roorkee, India

Fabrication and characterization of ZnO/NiTi/ZnO multilayers for optoelectronic applications

Nitin Choudhary, Davinder Kaur*

Functional Nanomaterials Research Lab, Department of Physics and Centre of Nanotechnology, Indian Institute of Technology Roorkee, Roorkee-247667, Uttarakhand, India

*Corresponding author: [mailto:dkaurfph@iitr.ernet.in]

ABSTRACT

Multilayer ZnO/NiTi/ZnO coatings were deposited using dc/rf magnetron sputtering. The structural and surface morphology of the films were investigated using X-ray diffraction, field emission scanning electron microscopy (FESEM) and atomic force microscope (AFM). The electrical and optical properties of the coatings were studied in order to evaluate the effect of NiTi interlayer on the properties of ZnO films. The transmittance, band gap, refractive index and resistivity of ZnO thin films were found to be significantly change due to the presence of NiTi interlayers. The successful formation of ZnO films with NiTi could possibly use the phase transformation kinetics of shape memory NiTi to adjust the electro-optical properties ZnO films and may find potential applications in optoelectronic devices.

Keywords: Multilayers; Sputtering; Electrical properties; Optical properties

Coatings for Biomedical and Healthcare Applications Room: Sunset - Session D3-1

Coatings for Mitigating Bio-Corrosion, Tribo-Corrosion and Bio-Fouling

Moderator: Stack, University of Strathclyde, UK, M.T. Mathew, Rush University Medical Center, US

1:30pm **D3-1-1 Significance of Tribocorrosion and Bio-Tribocorrosion in the Oral Environment: The Case of Dental Implants**, *L.A. Rocha* (lrocha@dem.uminho.pt), Universidade do Minho, Departamento de Engenharia Mecânica, Campus de Azurém, Portugal

INVITED

Tribocorrosion covers the material degradation process resulting from the combined interaction of wear and corrosion phenomena on surfaces subjected to a relative contact movement. Bio-tribocorrosion is the designation used to describe the tribocorrosion behavior of materials in contact with biological environments, as it happens in dental implants.

In fact, dental implants are under a complex congregation of mechanical solicitations and chemical aggressive substances, which can change considerably in magnitude or nature over the day and between individuals. Moreover, dental implants have a strong interaction with cells (soft and hard tissue cells and/or microorganisms) resulting in the local modification of the surrounding environment, both from the chemical and mechanical points of view. For instance, while the adhesion of bone cells to the material is desirable to provide osseointegration, colonization by microbes and the consequent formation of biofilms should be avoided. Surface modification routes are being investigated in order to provide multifunctional properties to the surface of dental implants.

In this work, an overview of the current knowledge of the bio-tribocorrosion mechanisms of Ti alloys used in dental implants will be presented. The effects of biofilms or cultured osteoblastic cells on the bio-tribocorrosion response will be addressed. Special focus will be given to surface modifications techniques which presently appears as promising to provide a good combination of biological and bio-tribocorrosion responses.

2:10pm **D3-1-3 Surface modification using PVD to apply silver-copper-mixed layers**, *G. Gotzmann* (gaby.gotzmann@fep.fraunhofer.de), *C. Wetzel*, Fraunhofer Institut für Elektronenstrahl- und Plasmatechnik, Medizinische Applikationen, Germany, *L. Achenbach*, *N. Özküçür*, *R.H. Funk*, Medizinische Fakultät, Institut für Anatomie, TU Dresden, Germany, *C. Werner*, Leibniz-Institut für Polymerforschung Dresden e.V., Research Division Biofunctional Polymer Materials, Germany

At any time, over 1.4 million people worldwide suffer from infectious complications acquired in hospital –so called nosocomial infections. The most frequent nosocomial infections are infections of surgical wounds, urinary tract infections and lower respiratory tract infections /i/. The resulting health care costs just concerning America rise up to almost 2 billion dollar per year /ii/. With the emergence and increase of microbial organisms resistant to multiple antibiotics, and the continuing emphasis on health-care costs, medical research focuses on the development of new, effective antimicrobial reagents for treatment and prevention of infections. This led to the resurgence in the use of silver based antiseptics. The use of silver as an antimicrobial material is known since antiquity. The combination of silver with other antimicrobial active elements –e.g. copper-might even increase the effectiveness. Complementing silver with copper announces decreased probabilities concerning cytotoxic side effects and improved economic application of the used elements. Physical vapor deposition technology was used for surface modification of polyurethane which constitutes a representative for one of the most used materials in medical devices besides stainless steel. Several layer combinations of silver and/or copper were applied with a final layer thickness of 50 nm. Amounts of silver and copper in the layer composition were determined using SEM/EDX. Energetic surface characteristics and wetting behavior were examined via contact angle measurement. Furthermore also antimicrobial effectiveness was tested using recognized microbiological methods and the model organism *Escherichia coli* K12. The investigations focused on the inhibiting influence of the obtained layers on microbial growth kinetics and possible synergistic effects. In addition cell biological experiments were accomplished to determine cell reaction under direct and indirect contact with the silver-copper layers. The results of this work are the basis to use PVD technology in order to apply antimicrobial coatings – here silver and copper mixtures – for medical-technical applications. Parameters can be adapted specific for every customer and application respectively in order to help you to extend and secure your lead in the market. i World Health Organization, Department of Communicable Disease, Surveillance and Response: Prevention of hospital-acquired infections, A practical guide, 2nd edition; WHO/CDS/CSR/EPH/2002.12 ii 2011 Health Grades Inc: Statistics about Nosocomial infection, http://www.rightdiagnosis.com/n/nosocomial_infections/stats.htm , Last Update: 23 August, 2011 (5:16

2:30pm **D3-1-4 Studies on Corrosion and Tribocorrosion Behaviour of Electrodeposited CoW-WC Nanocomposites**, *S.K. Ghosh* (sghosh@barc.gov.in), BARC, India, *J.P. Celis*, KUL, Belgium

Research for alternatives to electroplated hard chromium coatings is continued because of their tremendous environmental and health hazard concern. Among the various possibilities, recently, electroplated Co-W alloys show promising results like abrasive wear and corrosion resistance close to and even better than electroplated hard chromium. In the present study, the Co-W alloy matrix is further strengthened by incorporating nano-size WC particle via electrochemical codeposition technique. The matrix cobalt helps in binding the WC particles and in return particles strengthen the matrix along with host tungsten as alloy element. In order to understand corrosion resistance of these alloys, potentiodynamic polarization was carried out in 0.5M NaCl solution at room temperature and compared with similar composition CoW alloys. Indeed, it was found that nano-size WC particle helps in improving the corrosion resistance of the composites. The differences in corrosion behaviour were understood by analyzing the corroded surface morphology and composition analysis.

Further importance has been given on corrosion behaviour under mechanical loading conditions (known as **tribocorrosion**) in the same solution to extend the possibility of industrial applications of these coatings. Under mechanical loading and unloading conditions, open-circuit potential (OCP) of a few coatings was measured in order to estimate the material loss under mechano-chemical environment. In this presentation, details of tribocorrosion of these coatings will be discussed correlating with corroded wear scar morphology.

2:50pm **D3-1-5 An Electrochemical Investigation of TMJ Implant Metal Alloys in a Synovial Fluid-Like Environment: The influence of pH variation**, *D. Royhman* (droyhman@gmail.com), University of Illinois at Chicago, College of Dentistry, US, *R. Radhakrishnan*, *M.T. Mathew*, *M. Wimmer*, Rush University Medical Center, US, *C. Sukotjo*, University of Illinois at Chicago, College of Dentistry, US

Temporomandibular Joint (TMJ) disorder affects 30 million Americans, with approximately 1 million new patients diagnosed each year. These pathologic conditions may require reconstruction with total joint prosthesis (TMJ implant) for better treatment prognosis. A total TMJ implant is a metal-on-metal joint, usually made of titanium, cobalt-chromium, or combination of both. In the body environment, the TMJ implant is exposed to variable corrosive conditions from the electrolytic environment, as well as the galvanic effect between the different metals. The primary reason for implant rejection is breakdown and corrosion. Corrosion can severely limit the strength and lifespan of the implant, leading to implant fracture and adverse physiological effects. The objective of this study was to examine the effect of different levels of pH of BCS under simulated physiological conditions on the corrosion behavior of commonly used TMJ implant metals. Corrosion behavior was evaluated using standard electrochemical corrosion techniques and galvanic corrosion techniques. Standard electrochemical corrosion tests were run using a 3-electrode cell as a function of metal type (CoCrMo and Ti6Al4V) and pH (3.0, 4.5, 6.0, and 7.6). Evaluation parameters included: Open Circuit Potential, EIS parameters (R_p and C_p), and Cyclic Polarization parameters (E_{corr} , I_{corr} , and I_{pass}). Galvanic corrosion tests were run using a 3-electrode cell with Ti6Al4V as the working electrode, CoCrMo as a counter electrode, and a saturated calomel electrode (SCE) as the reference electrode ($n=3$). Data was evaluated using Two-way ANOVA, Tukey's post hoc analysis, and two-sample independent t-test ($p=0.05$). The metal surfaces were characterized using white-light-interferometry microscopy and scanning electron microscopy (SEM). The cyclic polarization scan showed that Ti6Al4V had an enhanced, stable, passive layer growth and a better corrosion resistance than CoCrMo. EIS measurements indicated that R_p was inversely related to increased pH. Initial galvanic corrosion measurements exhibit the noble electrochemical behavior of Ti6Al4V. SEM and white-light-interferometry images demonstrate a higher increase in surface roughness (R_a) after corrosion in CoCrMo. We concluded that acidity in BCS accelerated the ion exchange between the Metal-electrolyte interface in both metal types and that Ti6Al4V shows better corrosion behavior than CoCrMo. Additionally, corrosion kinetics are influenced by the potential corrosion inhibition properties of the protein content of the surrounding fluid. Further studies are in progress to generate a better understanding of the transitions in the corrosion kinetics due to these proteins.

3:10pm **D3-1-7 Fretting corrosion with proteins: the role of organic coating about the synergistic mechanisms**, *J. Geringer* (geringer@emse.fr), *J. Pellier*, *B. Forest*, ENSM-SE, France, *D. Macdonald*, CEST-PSU, US **INVITED**

Fretting corrosion is one of the most deleterious mechanisms for the degradation of metallic biomaterials, especially in the orthopedic field. Around 1.5 million of hip prostheses are implanted worldwide. This work is dedicated to study the synergistic effect of proteins and ions concentration on the wear of stainless steel, 316L, against a polymer sample under fretting-corrosion conditions.

A specific device allows reproducing fretting corrosion, i.e. relative displacements of microns between materials in contact. In order to compare with previous investigations, the amplitude was equal to $\pm 40 \mu\text{m}$ with sinusoid dal amplitude. The duration of each test was 14400 s, 4 hours.

The 316L sample size was the same for all samples. 3D roughness of 316L, R_a (3D), was $10 \pm 2 \text{ nm}$. PMMA (PolyMethyl Methacrylate) is cylindrical with a roughness of $35 \pm 5 \text{ nm}$. 4 solutions of NaCl were selected in order to study the effect of the ionic strength: $10^{-3} \text{ mol.L}^{-1}$, $10^{-2} \text{ mol.L}^{-1}$, $10^{-1} \text{ mol.L}^{-1}$ and 1 mol.L^{-1} . Additionally on each solution described previously, concentrations of proteins (pure albumin) were: 0, 1 and 20 g.L^{-1} . Experiments were investigated at temperature of $22 \pm 1^\circ\text{C}$. The potential was equal to -400 mV/SCE and the current density was measured with a particular attention to the device insulation.

The synergistic formalism is:

$W = W_c + W_m + (DW_{cm} + DW_{mc})$; W : total wear volume; W_c : wear volume due to corrosion; W_m : wear volume due to mechanics; DW_{cm} : synergistic wear volume, corrosion enhances wear due to mechanic; DW_{mc} : synergistic wear volume, mechanic enhances wear due to corrosion.

As expected, the main wear volume of stainless steel is due the synergistic terms for a salts concentration close to the one of human physiological liquid. $10^{-1} \text{ mol.L}^{-1}$ is the threshold concentration for increasing wear and the part of the synergy effect. At $10^{-3} \text{ mol.L}^{-1}$ of NaCl, the content of albumin has no significant impact on the wear volume. For fixed salts

concentration higher than the threshold, albumin does not promote the wear of stainless steel surface, it decreases (divided by 3 from 0 g.L^{-1} to 20 g.L^{-1}). The mechanical wear, calculated at applied potential of -800 mV/SCE , does not change according to the albumin concentration.

The most interesting point is the albumin changes the mode of synergy. At 0 g.L^{-1} of albumin, the main synergistic term is the influence of mechanics on corrosion, DW_{mc} . On the contrary, at 20 g.L^{-1} , the main synergistic term is the influence of corrosion on mechanics, DW_{cm} . One might suggest albumin promotes the corrosion after mechanical damage of the passive film. However albumin prevents from mechanical degradation.

3:50pm **D3-1-9 Optimisation of Pulsed Bipolar Plasma Electrolytic Oxidation of Magnesium Alloy for Biological Applications**, *Y. Gao*, *A. Yerokhin* (A.Yerokhin@sheffield.ac.uk), *A. Matthews*, University of Sheffield, UK

Magnesium alloys have been considered as promising biomaterials, although their application in biological area is limited by poor corrosion resistance. Plasma electrolytic oxidation (PEO) has been investigated to solve this problem. Alternating current regimes, for example a pulsed bipolar current (PBC) mode, offer a better control over the PEO process and correspondingly the coatings exhibit higher corrosion resistance compared with those produced in DC mode. Intrinsic problems of the PEO process are associated with low energy efficiency, since significant fraction of current is consumed on collateral electrode processes, such as gas evolution and anodic dissolution of metal substrate. Evaluation of the collateral processes is essential to both understand the coating formation mechanism and optimise the coating process in terms of energy efficiency. In the present study, current efficiency of PBC PEO process is investigated and the corrosion performance of the coatings is also studied. For this purpose, PBC current mode with variable frequency and duty cycle is employed to treat a magnesium alloy in an alkaline electrolyte solution. Gas evolution rate and its composition are determined, together with the amount of substrate material lost to the electrolyte. An online gas flow meter and a residual gas analyser (RGA) equipped with a quadrupole mass spectrometer are utilised. This set-up provides a safe and reliable way to evaluate partial electrode processes during PBC PEO treatment. The corrosion performance of the PEO coated magnesium alloy is tested in a simulated body fluid (SBF) at 37°C using an electrochemical workstation. Based on the experimental results, current efficiency and bio-corrosion performance of PEO coatings are optimised.

4:10pm **D3-1-10 Micro-textured CoCrMo Alloy for MoM joints: An Electrochemical Investigation**, *C. Nagelli* (christopher_nagelli@rush.edu), *M.T. Mathew*, Rush University Medical Center, US, *RP. Pourzal*, *F. Liedtke*, *A. Fischer*, University of Duisburg-Essen, Germany, *M. Wimmer*, Rush University Medical Center, US

In orthopedics, the use of metal-based alloys is a reoccurring practice because of their biocompatibility, low-wear rates and post-operative stability. However, metal-on-metal (MoM) hip joint bearings endure a constant load during articulation while immersed in synovial fluid. This environment has shown to be detrimental because of leaching metal ions and particulate debris in the neighboring tissue that has lead to implant failure and revision surgery. Currently, MoM joints are facing serious challenges with market usage declining from 35% to less than 10%. Tribochemical reactions potentially generate a type of tribolayer on the surface, which has shown a better electrochemical and tribological behavior. However, this layer is very unstable, nonhomogeneous and patchy in appearance. A defined micro-topography of the surface could be a solution facilitating strong film growth. To address these concerns, the aim of the current work is to investigate electrochemical properties of 5 types of topographies on a CoCrMo alloy surface.

Five different topographies were prepared using electrochemical etching. The topographies were adjusted by applying a different current during the etching process. The textured samples were then compared to a control sample that was polished using a conventional polishing process. Corrosion tests were conducted in an electrochemical cell with bovine calf serum (30 g/L protein) as the electrolyte. A standard corrosion test protocol was used that included monitoring of the open circuit potential for 1 hr and an electrochemical impedance spectroscopy test with a frequency range of 100K Hz to 0.005 Hz. Samples were then polarized during the cyclic polarization test from -0.8 V to -0.8 V with a peak voltage of 1.8 V . The surfaces were then characterized using a white light interferometer and scanning electron microscope.

The surfaces with a micro-topography demonstrated an improved corrosion behavior when compared to the control sample. Texturing the surface results in an even distribution of surface depressions. It appears that this topography enhances the adherence of protein resulting in a decelerated corrosion rate. Thus, a micro-topography of the surface is ideal for creating a heterogeneous proteinaceous layer that is analogous to a tribolayer, which

is already reported. To further comprehend the properties of a micro-topography it is essential to expose a tribocorrosive environment, combining the influence of mechanical wear and corrosion. It can be assumed that such topography may reduce the influence of abrasion by particle entrapment and enhances the influence of tribolayer formation resulting in lower wear.

Tribology & Mechanical Behavior of Coatings and Engineered Surfaces

Room: Pacific Salon 1-2 - Session E3-1/G2-1

Development, Characterization, and Tribology of Coatings for Automotive and Aerospace Applications

Moderator: R. Evans, Timken Company, S. Dixit, Plasma Technology Inc., US, H. Rudigier, OC Oerlikon Balzers AG, Liechtenstein

1:30pm **E3-1/G2-1-1 The effective Indenter concept, its uses in measurement analysis and its extension into the time domain, N. Schwarzer, N. Bierwisch** (n.bierwisch@siomec.de), SIO, Germany

The concept of the effectively shaped indenter was introduced by Bolshakov et al in 1995 [1]. It was shown, that this concept is the basis for the so called Oliver and Pharr method [2]. Since then many papers have appeared demonstrating its uses in analyzing not only nanoindentation curves but also much more complex mechanical contact experiments. Among those are also tests on layered materials for normal and multi-axial loading conditions [3, 4].

Within this work the concept will be applied to rough surfaces and time dependent material behavior. It will be shown how the concept of the effectively shaped indenter consistently follows from complex time dependent constitutive material models and how this can be used within new analysis techniques for nanoindentation and physical scratch tests.

[1] A. Bolshakov, W.C. Oliver, and G.M. Pharr, MRS Symp. Proc 356, p 675 (1995)

[2] W. C. Oliver, G. M. Pharr, J. Mat. Res. 7 (1992) 1564-1583.

[3] N. Schwarzer, Phil. Mag. 86(33-35) 21 Nov - 11 Dec 2006 5153 – 5767

[4] N. Schwarzer, J. Mater. Res., Vol. 24, No. 3, March 2009, 1032 - 1036

1:50pm **E3-1/G2-1-2 Effect of BIAS and hydrogen on arc activated high ionization N₂-Ar plasma nitrided maraging steel grade 300, E. Almandoz, J. Fernandez** (jfernandez@ain.es), J.A. Garcia, G.G. Fuentes, R.J. Rodriguez, Asociacion de la Industria Navarra, Spain

Maraging alloys are a group of ultra-high strength steels susceptible to be treated by means of thermochemical processes to improve its mechanical properties. In this paper, a series of arc-activated plasma nitriding processes have been applied on maraging steels (grade 300-aged) in order to investigate the modification of their wear resistance and superficial hardness.

The study focuses on how the BIAS potential applied to the substrates and the effect of hydrogen in N₂-Ar plasma during the nitriding process modify the properties of the treated alloys. The samples have been characterized by roughness measurements, wear resistance tests at room temperature and 450 °C, chemical in-depth profiling, impact tests and Knoop micro-hardness profile tests. The microstructural characterization was realized by optical microscopy, XRD analyses and scanning electron microscopy.

The case layer thickness observed ranged between 20 and 60 microns for BIAS voltages of -200 V and -600 V respectively, thus signaling the effect of the ion energy bombardment. It is shown that the nitriding process increases substantially the hardness on the surface of the substrate and then the wear resistance at room temperature and at 450°C. On the other hand, the presence of hydrogen in the plasma presents a different effect depending on the applied BIAS voltage. The compatibility of the present plasma nitriding treatments and the aging process characteristics of these alloys are also discussed.

Keywords: maraging steel, nitriding, BIAS, hydrogen, wear resistance, hardness

2:10pm **E3-1/G2-1-3 Requirements for Broad Acceptance of DLC Coatings for Tribological Applications in the Commercial Aerospace Market, L. Pingree** (liam.s.pingree@boeing.com), The Boeing Company, US

INVITED

Diamond-like carbon (DLC) coatings have numerous advantages over their plated counterparts for tribological applications. They have higher wear

resistance for a given film thickness, the deposition process does not create an environment where embrittlement is a concern, and they can readily be applied to titanium components. Yet their adoption into the aerospace industry has been quite slow over the past decade.

In early 2000, Boeing specified the use of a DLC coating onto a weapon bay door's safety-lock pin for one of their platforms. To enable this introduction many important processing parameters had to be met, such as low-temperature deposition (to avoid relaxation of cold-worked components). In addition, adequate QC and QA metrics had to be established and specific processing parameters had to be determined to meet the demands of a "stable and repeatable process;" a key to meeting certification requirements.

Even with these challenging constraints met, there remain two key items which have contributed to this slow incorporation: 1) there has been limited in-service data generated with these coatings, and 2) due to their typically thin profile, they are often not suitable as a drop-in replacement for even the thinnest tribological coatings, such as thin-dense chrome.

In this talk, methods to overcome these barriers will be introduced, key aspects to process control and quality issues will be discussed, and critical coating characteristics will be highlighted.

2:50pm **E3-1/G2-1-5 Influence of HVOF spraying parameters on the wear resistance of Al-SiC composites coatings deposited on ZE41 magnesium alloy, A. Lopez** (antoniojulio.lopez@urjc.es), J. Rams, B. Torres, P. Rodrigo, M. Campo, Rey Juan Carlos University, Spain

Magnesium alloys are attracting high attention due to their low density, high specific values of stiffness and strength, great facility of processing and reasonable cost. These properties make these alloys suitable for application in many sectors and especially in the transportation one. Nevertheless, the use of magnesium alloys is limited because their low resistance to wear.

In this work, as an alternative to improve the wear development of a Mg-Zn alloy (ZE41), Al and Al-SiCp composites coatings were prepared by High Velocity Oxygen Fuel (HVOF) spraying on the magnesium alloy substrates.

The influence of coating parameters- such as reinforcement rate (from 0% to 50% vol. SiCp) size of SiCp and number of layers, as well as HVOF spraying parameters (spraying distance, transversal gun displacement)- in the microstructure and wear resistance of the final coatings was evaluated.

The microstructure of the coatings, the wear tracks, the worn surfaces in the transversal section and the debris formed during the wear tests were characterized by scanning electron microscopy (SEM) and light microscopy. Adhesion pull-off strength tests (ASTM D4541-02) of the different coatings were performed. Wear tests were carried out under dry sliding conditions using a pin-on-disc tribometer on the ZE41 substrate and on the different sprayed coatings.

The magnesium alloy suffered minor degradation of its microstructure or mechanical properties after the deposition of the coatings with thickness from 100 to 200 µm. The obtained composite layers were almost free of porosity, with high adhesion to the substrate and after optimization of the sprayed conditions a substantial decrease in the specific wear rates were obtained.

3:10pm **E3-1/G2-1-6 Influence of deposition process parameters on durability and residual stresses in highly oriented MoS₂ films, B. Vieneusel** (Vienneusel@mfk.uni-erlangen.de), S. Tremmel, S. Wartack, Friedrich-Alexander-University Erlangen-Nuremberg, Germany

Unlike earlier types of MoS₂ coatings, innovative MoS₂ films do not show columnar crystal growth but a dense structure without porosity and a basal orientation of the lattice with the gliding plane parallel to the substrate surface. This paper describes the development of this new type of lubricant film by means of design of experiments (DoE) according to Box-Behnken. For the first time, this methodological approach enables a determination of mutual interactions between deposition process parameters on tribological and mechanical MoS₂ film properties.

Furthermore, the experiments show that the tribological properties of dense coatings without columnar structure are sensitive to residual stress. It turned out that compressive residual stress which can be controlled by the process parameters is crucial for film durability due to its influence on adhesion and hardness. The results indicate that the optimum is depending on the loading conditions. Therefore, low wear rates in ball-on-disc tests combined with high durability of the coating-substrate bond were achieved at moderate amounts of internal stress. Deposition induced residual stress of each sample was analyzed by the substrate curvature method. Interactions of residual stress and process parameters are discussed in terms of the kinetic energy of sputtered particles.

The XRD analysis was used to validate the highly basal oriented lattice. A shift in the spectra of the (002) reflex to slightly lower angles was observed.

This shift is already known in literature, but has not yet been entirely clarified. In pursuing annealing experiments a minor effect of residual stress on this shift was observed. Film adhesion was evaluated by a modified scratch test. Film growth, surface topography and failure mechanisms were analyzed by SEM imaging.

Additionally this paper gives advice to select and apply methods suitable for deposition processes from a broad range of methods in the statistical design of experiments (DoE).

3:30pm E3-1/G2-1-8 Numerical analysis of the influence of film thickness and properties on the stress state of thin film-coated piston rings under contact loads., L.G.D.B.S. Lima (luiz.lima@esss.com.br), L.C.S. Nunes, Universidade Federal Fluminense, Brazil, R.M. Souza, N.K. Fukumasu, Universidade de São Paulo, Brazil, A. Ferrarese, Mahle Metal Leve S/A, Brazil

In this work, a series of finite element analyses were conducted to analyze the stresses in thin film-coated piston rings under contact loads. The actual normal and tangential pressure observed during a complete four-stroke gasoline engine cycle (720°) was used as input to load an axisymmetric film/substrate mesh. Four values of coating thickness were analyzed (from 20 to 100 µm) and, for each one, five values of Young's modulus (from 144 to 578 Gpa) were considered. The systems were compared based on the stress distribution, particularly in terms of the intensity and position of the peak stresses in the film and at the film/substrate interface. Results show that the stiffer (or thicker) the film, the higher the stresses at the interface immediately under the film-sleeve contact, and the higher the compressive stresses around this region. The range of thickness and Young's modulus values considered in this work did not provide significant changes in terms of substrate stresses.

3:50pm E3-1/G2-1-9 Numerical analysis of wear and failure zones of coated piston skirt and piston rings under scuffing conditions, N.K. Fukumasu (newton.fukumasu@gmail.com), University of São Paulo, Brazil, L.G.D.B.S. Lima, Universidade Federal Fluminense, Brazil, A. Ferrarese, Mahle Metal Leve S/A, Brazil, R.M. Souza, University of São Paulo, Brazil

In this work, 3D finite element analyses (FEA) were conducted to improve the understanding of wear and failure of coated piston skirt and piston rings under scuffing in fire operating conditions. The model was based on a four-stroke port fuel engine and considered the interaction between the piston, piston rings and the cylinder liner. Piston pin, connecting rod, crankshaft and cylinder wall were modeled as rigid components, allowing the reproduction of the piston dynamics. The influence of the lubricant was considered in the simulations through a time dependent friction coefficient at the contact points. Full combustion cycles (720 degree rotation of the crankshaft) were simulated for velocities between 2000 and 6000rpm. Coatings were considered in piston rings and piston skirt regions in contact with the cylinder liner. The mechanical properties were derived from either carbon-based or nitride-based thin films. Stress results on film surfaces and film/substrate interfaces were analyzed to identify regions more prone to wear due to adhesive/cohesive failure of the films. The numerical prediction presented good correlation with literature results in terms of failure regions and the wear zones in engine components.

4:10pm E3-1/G2-1-10 Effect of chromium on the wear mechanisms of self-adaptive WSC-Cr sputtered coatings, T. Polcar (t.polcar@soton.ac.uk), University of Southampton, UK, F. Gustavsson, Uppsala University, Angstrom Laboratory, Sweden, M. Danek, Czech Technical University in Prague, Czech Republic, A. Cavaleiro, University of Coimbra, Portugal

Transition metal dichalcogenides (TMD) belong to one of the most developed class of materials for solid lubrication. However, one of the main drawbacks of most of the self-lubricating coatings is their low load-bearing capacity, particularly in terrestrial atmospheres. In previous works, alloying TMD thin films based on tungsten disulfide with non-metallic interstitial elements, such as carbon or nitrogen, has been studied in order to improve tribological performance in different environments. Excellent results were reached having the deposited coatings hardness, in some cases, more than one order of magnitude higher than single W-S films.

In this work, W-S-C films were alloyed with Cr by co sputtering chromium and composite WS₂-C targets. Cr-contents in the range [0-25 at.%] were selected for sliding tests (pin-on-disc, 100Cr6 steel ball as a counterpart) under different conditions (dry or humid air, increasing load, etc.) Besides the usual physical, chemical and mechanical characterization, including the evaluation of the chemical composition, the structure, the morphology, the hardness and the cohesion/adhesion, special attention was paid to the friction and wear analyses. The surfaces in the contact were analysed by X-ray photoelectron spectroscopy (bonding), Auger emission spectroscopy (surface chemical composition), and scanning electron microscopy (SEM).

Selected ball wear scars and wear tracks were investigated by transmission electron microscopy (TEM); the samples for them were prepared by focus ion beam (FIB).

Surface and sub-surface structural modification of the coating and composition of the transferred tribolayer are discussed in detail. The main aim of this study is to shed light on following issues: i) the role of Cr in microstructural transformation, ii) the role of Cr in sliding process, iii) the formation of low-friction tribolayer based on tungsten disulfide.

4:30pm E3-1/G2-1-11 Performance impact of honing dynamics on surface finish of precoated cylinder bores, M. El Mansori (mohamed.elmansori@ensam.eu), Arts et Métiers ParisTech, France, B. Goedel, L. Sabri, Renault sas, France

Minimization of the friction losses is a major concern for Internal Combustion Engine designers. The strategy often followed, to reduce losses, is to modify the topography of the rubbing surfaces of the cylinder bores and the piston rings. This strategy aims to reduce metallic friction and to allow less oil consumption and high operational reliability. The surface modification of cylinder bore with improved sliding properties is often produced at industrial level by honing process. Abrasive stones are hence loaded against the bore and simultaneously rotated and oscillated. To guarantee a robust surface production of cylinder bore of specific shape with acceptable dimensional accuracy and surface quality, the stone dynamic effects in continuous balanced contact with the workpiece are of primary importance. This paper addresses these effects on honed surface structure of cylinder bores. The stone dynamic behavior while bore honing was studied at conventional regime ranged from 0,5g to 1,5g as often used in mass bore production. Under these dynamic conditions of bore processing, the dimensional accuracy holds by opposition to the surface appearance. However, the highly accelerated regime in honing up to 2,5g promotes simultaneously the form quality (especially straightness) and reduces the cycle time. The reported results are the first demonstration that the bore surface finish can be dynamically controlled when honing. This technology is enabled by a microscale regeneration mechanism of abrasive stones.

4:50pm E3-1/G2-1-12 Macroscopic simulation of the liner honing process, B. Goedel (benoit.goedel@gmail.com), Renault SAS, France, M. El Mansori, Arts et Métiers ParisTech, France, L. Sabri, Renault SAS, France

The honing process produces surface liners with specific functional properties. Engine performances and life expectancy are directly impacted by the quality of honed surface. The form quality, the roughness and the surface appearance produce by honing determine the friction of the piston in the liner. The process is however mechanically complex and the selection of the process parameters is currently based on empirical methods. The aim of this paper is thus to develop a macroscopic simulation environment which will help end-users during this setting-up stage. The development of this virtual tool is based on a space-time discretization and a macroscopic cutting model taking into account local contacts between the workpiece and the abrasives tool. The space-time discretization allows representing the machine environment with the tool, the workpiece and the machine kinematic. The cutting model allows converting kinematics and abrasive contacts in dynamic data and material removal rate by calculation. Initially the cutting model was adjusted on simple experiments. After, we have extrapolated the stock removal equation to the whole range of stone cutting condition. This approximation allows simulating the real process. The simulation of a whole honing cycle is possible and results were validated by comparison with industrial context experiments. The simulation of the whole honing cycle allow to predict the form quality, one of the roughness criteria and the surface appearance. Simulation results are represented in mapping which allow seeing quality criteria for each point of the surface.

5:10pm E3-1/G2-1-13 Fiction and adhesion of Si and F incorporating diamond-like carbon (DLC) coatings sliding against aluminum, F.G. Sen (senf@uwindsor.ca), X. Meng-Burany, University of Windsor, Canada, M.J. Lukitsch, Y. Qi, General Motors Research and Development Center, US, A.T. Alpas, University of Windsor, Canada

Diamond-like carbon (DLC) coatings exhibit low coefficient of friction (COF) and good adhesion mitigating properties when placed in sliding contact against aluminum but their tribological properties are very sensitive to the environmental conditions. This study examines tribological properties of 20 at % Si and 12 at % F containing DLC coatings (with 14 at % O and 18 at % H) tested against 1100 aluminum under a vacuum atmosphere (0.01 Pa) and an ambient air (39% relative humidity) condition. Pin-on-disk type sliding test showed a COF of 0.08 under both conditions. The changes in contact surface tribo-chemistry and material transfer processes were studied. Carbonaceous transfer layers that incorporated F, Si and O compounds formed on aluminum contact surface under both testing

conditions. The details of the composition and microstructure of the transferred layers were investigated using cross-sectional focused ion beam (FIB), transmission electron microscopy (TEM) and X-ray photoelectron spectroscopy (XPS) methods. The F concentration was the highest at the aluminum/transfer layer interface and formation of an AlF_3 compound was observed. The top surfaces of the transfer layer in contact with DLC were richer in Si and O. Partial pressure variations of residual gases monitored during the vacuum test indicated desorption of H_2O molecules. The observation of low COF values and atmosphere independent tribological properties observed in this coating were interpreted in terms of hydration/de-hydration and passivation mechanisms that operate on contact surfaces.

New Horizons in Coatings and Thin Films Room: Royal Palm 1-3 - Session F1-1

Nanomaterials, Nanofabrication, and Diagnostics

Moderator: Y. Gonzalvo, Hiden Analytical Ltd., S. Kodambaka, University of California, Los Angeles, US

1:30pm **F1-1-1 Diagnostics in Low Pressure Plasmas and Characterisation of Films Properties in HIPIMS Technology, A.P. Ehasarian** (*a.ehasarian@shu.ac.uk*), Sheffield Hallam University, UK
INVITED

Plasma diagnostic studies have been instrumental in revealing and understanding the physics behind the high power impulse magnetron sputtering (HIPIMS) discharge and informing the mechanisms of film growth in its environment.

The plasma inside the confinement region has been studied by several methods which are typically not quantitative due to the lack of theory and limited direct access to optical information. Nevertheless, recent fast camera studies showed the existence of drift waves in the sub-MHz region which regulate particle transport. Multi-pin Langmuir probes were used to detect lower hybrid frequency oscillations that promote anomalous transport out of the magnetic confinement. Time-resolved optical emission spectroscopy has been used to study the development of discharge chemistry from gas- to metal- dominated.

The plasma expanding towards the substrate is more accessible. Emissive probes showed high electric fields near the target, which relax as the voltage pulse is switched off resulting in strong confinement and subsequent release of plasma, including metal ions. Energy-resolved mass spectroscopy has shown the effect of gas rarefaction, especially with high sputter yield materials, which extends the region of metal-rich plasma. Plasma chemistry quantified by optical absorption spectroscopy is rich in metal ions, which can comprise the majority of total particle flux. Plasma composition is influenced by the peak discharge current and can be tuned precisely. In reactive plasmas, oxygen and nitrogen are dissociated to a very high degree, and affect texture in films.

Ion energy studies by E-MS show negative oxygen ions with energy of several hundred eV – corresponding to the potential on the target. Retarding field analysers show fast evolution of ion energy, reaching high values during the pulse.

The energy of metals is enhanced and conserved at high powers due to gas rarefaction. The energy of gas ions is similarly enhanced and leads to rarefaction.

Film growth is strongly influenced by the chemistry and ion energy in the HIPIMS discharge. High fluxes of dissociated nitrogen to the surface bind arriving Ti adatoms thus effectively lowering their diffusion rate and reducing outdiffusion from 200 surfaces.

Highly ionised metal flux improves coverage of high aspect ratio vias, reduces waviness in interfaces between nanolayers and affects nanocomposite grain size and misorientation.

A number of challenges to remain, mainly connected with the transient stages of the discharge, namely, diagnosing the non-plasma breakdown phase, and obtaining fast quantitative data on plasma chemistry, ion energy and electron temperatures.

2:10pm **F1-1-3 Design of new coating materials for neutron detector applications, the example $\text{TM}_{1-x}\text{Gd}_x\text{N}$, B. Alling** (*bjoal@ifm.liu.se*), Linköping University, Sweden, C. Höglund, R. Hall-Wilton, ESS, Sweden, L. Hultman, Linköping University, Sweden

The shortage crisis of ^3He has created an urgent need for alternative neutron detectors based on other elements. Solid state based neutron detectors typically demand the applicability of the neutron reactive element in the form of thin films in order to optimise efficiency and usability. ^{10}B and

^{157}Gd are among the most promising isotopes for usage in solid state neutron detectors as well as in purely absorbing, isolating layers due to their high cross section for neutron reactions. The application of these elements implies the need for new coating materials and the optimisation of a series of materials properties for each particular objective. The requirements for either metallic or semiconducting conductivity, corrosion resistance, and mechanical and thermal stability may be met by producing ceramic compounds based on the neutron detecting element, as was made for B_4C [1]. In this work we show how theoretical first-principles calculations can be used to guide this materials development with the example of an electrically conductive, oxidation resistant, neutron absorbing coating material based on $\text{TM}_{1-x}\text{Gd}_x\text{N}$ ($\text{TM}=\text{Ti}, \text{Zr}, \text{Hf}$) [2]. Results show that GdN , prone for oxidation in its pure form, readily mixes with the chemically more inert nitrides ZrN and HfN , possibly as an ordered compound. On the other hand mixing of GdN with TiN is highly unfavourable due to volume mismatch.

[1] B_4C thin films for neutron detection, C. Höglund, J. Birch, K. Andersen, T. Bigault, J.-C. Buffet, J. Correa, P. van Esch, B. Guerard, R. Hall-Wilton, J. Jensen, A. Khaplanov, F. Piscitelli, C. Vettier, W. Vollenberg, and L. Hultman, Submitted for publication.

[2] Mixing thermodynamics of $\text{TM}_{1-x}\text{Gd}_x\text{N}$ ($\text{TM}=\text{Ti}, \text{Zr}, \text{Hf}$) from first principles,

B. Alling, C. Höglund, R. Hall-Wilton, and L. Hultman, Applied Physics Letters, **98**, 241911 (2011)

2:30pm **F1-1-4 Hierarchical ZnO Nanorod array Films with Enhanced Photocatalytic Performance, C.J. Chang** (*changcj@fcu.edu.tw*), M.H. Hsu, C.Y. Tsay, C.K. Lin, Feng Chia University, Taiwan

Hierarchical thin-film photocatalysts exhibiting surface roughness at two length scales were prepared by the consecutive formation of ZnO microstrips and ZnO nanorod-array. At first, polymeric barrier ribs were formed on the substrate by ink-jet printing and UV-curing reaction. ZnO was deposited in the interstice of polymeric ribs by electrochemical deposition. ZnO stripes with microscale roughness were fabricated after removing the ribs. Then, nanoscale roughness was achieved by the growth of ZnO nanorods on the surface. The surface morphology, structural and optical properties were characterized by FESEM, X-ray diffraction, Electron spectroscopy for chemical analysis, UV-vis, and photoluminescence spectroscopy. The final surface comprising hierarchical microstructures and nanostructures not only increases the surface area of the photocatalyst but also helps the diffusion of organic dye during the photodegradation test. The effects of surface texture and surface modification on the photocatalytic properties were investigated. The photodegradation efficiency of the hierarchical thin-film photocatalyst was improved compared with its flat analog. Photocatalytic performance was further enhanced when Ag nanoparticles were deposited on the hierarchical photocatalyst.

2:50pm **F1-1-5 ZnO Nanostructures Synthesized by CO_2 Supercritical Fluid at Low-Temperature Treatment, K.C. Chang, T.M. Tsai, T.C. Chang** (*tcchang@mail.phys.nsysu.edu.tw*), Y.E. Syu, H.C. Huang, D.S. Gan, T.F. Young, National Sun Yat-Sen University, Taiwan

This study applies a novel synthesis method of nanostructure, supercritical CO_2 (SCCO $_2$) fluid technology, for ZnO nanotubes growth by oxidation from metal Zn thin film on glass substrate at 60°C. A sputtering Zn film was oxidized by post-treatment of SCCO $_2$ fluid in which 0.3 vol % pure water or aqueous ethanol was added. The images of scanning electron microscopy and transmission electron microscopic indicate that high density nanotubes were formed on the glass substrate. Based on material analyses in this study, ZnO nanotubes with a small diameter (10–50 nm) was formed from metal Zn thin film on a glass substrate by SCCO $_2$ fluid technology.

3:10pm **F1-1-6 One-step hybrid pulse anodization for nanoporous anodic aluminum oxide synthesis of aluminum thin films sputtered on Si(100) substrate, C.K. Chung** (*ckchung@mail.ncku.edu.tw*), M.W. Liao, O.K. Khor, H.C. Chang, National Cheng Kung University, Taiwan

Nanoporous anodic aluminum oxide (AAO) fabricated by one-step hybrid pulse anodization from the Al thin films sputtered on Si(100) substrates at various substrate temperatures and deposition times have been investigated. Compared to Al bulk foils, AAO grown on the Si substrates is convenient to further deposit other nanostructured materials. Al thin films with rough surface cause the non-uniform electrical field during anodization process together with poor-ordered nanopore. Also, the limited thickness Al thin film is disadvantageous for proceeding electrochemical polish. Therefore, it is still a challenge for fabricating well-ordered AAO from Al thin film. In this article, Al thin films were deposited at various substrate temperature of 25–400 °C and deposition time of 40–80 min in order to improve the surface fluctuation. All thickness of the Al thin films were less than 1 μm .

The effect of substrate temperature and deposition time on quality of Al thin films was first studied and correlated to AAO performance. The morphology and microstructure of Al films were characterized by atomic force microscope and X-ray diffraction. Anodizing of sputtering Al films was performed in 0.3M oxalic acid at 40 V potential difference by one-step hybrid pulse anodization which differs from conventional direct-current anodization. The pore size distribution of AAO films was examined by scanning electron microscope (SEM) and quantitatively analyzed by image processing of SEM image. The relationship between sputtering parameter, structure, and quality of AAO was discussed and established.

3:30pm F1-1-7 Nanostructured mesoporous surfaces produced by phase separation in Al-Si thin films, P. Martin (*phil.martin@csiro.au*), A. Bendavid, K-H. Muller, L. Randeniya, CSIRO Materials Science and Engineering, Australia

Phase separated Al-Si films were deposited by concurrent deposition of Al using filtered vacuum cathodic arc and Si produced by dc magnetron sputtering deposition. The resulting phase separated films were etched chemically to remove the nanocolumns of Al to produce a SiO_x mesoporous structure. The resulting layer had a pore size that was dependent upon the arrival ratio of the Al:Si atoms at the substrate, substrate temperature and negative substrate bias voltage during film growth. Scanning electron microscope images of the etched AlSi films showed that the average diameter of pores could be varied from 2 nm to 11 nm with a well defined size distribution. The results are interpreted using a model to describe the pore size as a function of substrate temperature and particle impingement energy.

3:50pm F1-1-8 Fabrication and Characterization of Carbon Nanotubes (CNT) and Metal Composite Electrodes for Solar Cell, H. Wang (*huwang@mines.edu*), J. Moore, J. Lin, Colorado School of Mines, US

Carbon nanotubes (CNTs) are molecular-scale 1D wires exhibiting excellent electrical and mechanical properties, in particular the ballistic transport of metallic carbon nanotubes leads to almost zero resistivity. In order to use the excellent properties of CNTs, composite film electrodes for solar cell were synthesized to combine metal and CNTs. A thin transparent FeNi or Fe catalytic layer (several nanometers) was deposited on substrate by pulsed-unbalanced magnetron sputtering (P-UBMS). Vertical CNTs were grown on the deposited metal catalyst nano-layer using PECVD. Then a metal were deposited between or on CNTs by P-UBMS and modulated pulse power (MPP) magnetron sputtering deposition for the formation of the composite film. Different metals were tested for forming an ohm contact between the CNTs and metal in the composite film. CNTs and the composite films were characterized by SEM and TEM. The different between P-UBMS and MPP, and their effects on the composite films were discussed.

4:10pm F1-1-9 Structural and Electronic Properties of Epitaxial Silicene, Y. Yamada-Takamura (*yukikoyt@jaist.ac.jp*), JAIST, Japan
INVITED

Silicene is an atom-thick, honeycomb sheet of silicon: Si-version of graphene. Silicene is increasingly attracting interests owing to the success of graphene. One of the major differences between these two materials is that silicene is predicted to be more stable in slightly-buckled form with neighboring Si atoms displaced out of plane while graphene is perfectly planar. Silicene may therefore form with a variety of lattice constants related to a different degree of buckling. So far, silicene only exists in the form of epitaxial layer on single-crystalline, metallic substrates, such as silver single crystals and ZrB₂ thin films. The relationship between the electronic structure and the atomistic structure of epitaxial silicenes will be discussed in detail.

4:50pm F1-1-11 Carbon-Nanotube-Templated Metallic Microstructures for MEMS: Preparation and Characterization, R. Hansen (*rs.hansen.byu@gmail.com*), Brigham Young University, US, R. Badger, Utah Valley University, US, D. McKenna, B. Jensen, R. Vanfleet, R. Davis, D. Allred, Brigham Young University, US

We discuss a materials breakthrough for MEMS. In contrast with conventional electromechanical devices, whose constituents are chosen from a vast range materials and alloys to optimize fabrication, performance and cost, MEMS have traditionally been made using the same materials and methods as those used in the silicon-based microelectronics industry. In order to make MEMS out of a much richer suite of materials, including metals, semiconductors and ceramics, we have developed a process termed carbon-nanotube-templated microfabrication (CNT-M). In CNT-M we employ patterned, vertically aligned carbon nanotube forests as a three-dimensional microfabrication scaffold to create precise, high-aspect-ratio (~100:1) microstructures. The "as grown," low density (0.009 g/cc) CNT

structures are not useful as mechanical materials because they are extremely fragile, consisting mostly of air. However, when we replace the air spaces between tubes in the forest with a filler material by atomistic deposition, the infiltrated CNT framework becomes a robust microstructure consisting mostly of the filler material. Thus, by patterning the CNT microstructure and limiting the deposition of the filler material, CNT-M allows control over structural features on both the nano and microscales (nanoscale porosity and microscale structure). In the past, we deposited semiconductors (Si and a-C) or dielectrics (SiO₂ and SiN_x) within the CNT framework by chemical vapor infiltration. But many existing MEMS applications would be benefited, and many contemplated applications such as remotely read (via RF), high-temperature accelerometers would be enabled, by the right metals. We now report on the use of chemical vapor infiltration and electrodeposition to create metallic microstructures composed of tungsten, molybdenum or nickel by CNT-M. These materials are desirable in MEMS applications because of their high conductivity, high melting temperatures, resistance to corrosion, low thermal expansion, and their high Young's moduli, hardness and yield strength. We will present electrical, mechanical and structural properties of the metal microstructures and discuss deviations from bulk properties.

5:10pm F1-1-12 Nanocomposite-based wear sensor materials for in-situ process control in cutting applications, S. Ulrich (*sven.ulrich@kit.edu*), C. Klever, H. Leiste, K. Seemann, M. Stueber, Karlsruhe Institute of Technology, Germany

Nano- and microsystem-technologies are doubtlessly the key technologies for future developments of cemented carbides (nanopowder technology), wear-resistant coatings and multifunctional coatings (nanoscale coating design, nanoscale structure, nanoscale interface engineering). An example has been illustrated concerning the design and fabrication of wear-resistant coatings with integrated high-frequency magnetic characteristics. The magnetron sputtered, 1 µm thick TiN/FeCo-multilayer films with 2.6 nm bilayer period and volumetric ratio of 3:1 (TiN:FeCo) are harder than TiN-monolayer films and show a frequency-dependent permeability (about 100) up to 1 GHz. Moreover, enhancement of coating toughness of the multilayer in comparison to the single layers is reasonably anticipated on account of the high FeCo-content (about 25 vol.%), the high interface portion in the 390-layer coatings favoring crack deflection and crack-energy dissipation, and the compressive stress for hindering crack propagation.

Advanced Characterization of Coatings and Thin Films Room: Sunrise - Session TS2-2

Advanced Characterization of Coatings and Thin Films

Moderator: F. Giuliani, Imperial College London - South Kensington Campus, UK, S. Korte, University of Erlangen-Nürnberg, Germany, P. Schaaf, TU Ilmenau, Germany

1:30pm TS2-2-1 Testing of mechanical thin film properties by vibrating Micro-Electromechanical Systems (MEMS), P. Schaaf (*peter.schaaf@tu-ilmenau.de*), R. Griesler, J. Klaus, M. Stubenrauch, K. Tonisch, J. Pezoldt, S. Michael, TU Ilmenau, Germany

Mechanical properties of thin films for micro- and nanoelectromechanical systems can be significantly different from those of the material they are produced of. Double-clamped beams were fabricated in order to determine the elastic modulus and the residual stress of AlGaN heterostructures and hexagonal AlN thin films by a laser Doppler vibrometer. For this, FEM simulations were performed showing the beam's behavior depending on the stimulation at different Eigenmodes and also depending on the torsion modes. Furthermore, the residual stress in the deposited films before structuring was determined by high-resolution X-ray diffraction. The Young's modulus of the heterostructures was determined by nanoindentation of the as deposited thin film. Additionally, FTIR-ellipsometry was applied in order to determine the residual stress of the thin films for micro- and nanoelectromechanical systems. A good agreement of the results can be stated, which will be presented.

1:50pm TS2-2-2 A New FIB-DIC Material Removal Method for Poisson's Ratio and Residual Stress Measurement in thin films, M. Sebastiani (*marco.sebastiani@stm.uniroma3.it*), University of Rome "Roma Tre", Italy, E. Bemporad, F. Carassiti, University of Rome "Roma Tre", Italy

In this work, a new methodology for the simultaneous evaluation of the residual stress and of the Poisson's ratio in thin coatings is presented.

The key idea is to remove material with a focused ion beam (FIB) in order to induce controlled relaxation strains that can be correlated to the in-plane

residual stress and to the Poisson's ratio of the coating. This is done by adopting a unique novel geometry for the milled trench and by means of digital image correlation (DIC) techniques and ad hoc constitutive models.

The method consists of two sequential steps: (1) FIB milling of two parallel slots and analysis of the consequent relaxation strain that might occur in the central area (along the X-direction which is the direction perpendicular to the slots); (2) milling of two additional slots along a direction perpendicular to the previous one, so to induce a full biaxial stress relief of the central square island. The analysis of the relaxation strain after the second milling step is then performed along the same X-direction. The depth of all trenches and the distance between them are kept equal to the coating's thickness. The relaxation strain analysis is performed by means of high-resolution in-situ SEM-FEG imaging of the relaxing surface and a full field strain analysis by digital image correlation (DIC).

A FE modeling approach was also used to demonstrate that, for a wide range of isotropic materials, the ratio between the two acquired X-strains is a unique simple function of the Poisson's ratio of the coatings, independently of the elastic modulus. Furthermore, the analysis of the X and Y relaxation strains at each milling step allows the direct evaluation of the residual stress depth profile in the coating.

The model was experimentally validated on a 3.0 μm CAE-PVD Chromium Nitride (CrN) coating.

An equal-biaxial average stress of -5.04 ± 0.75 GPa was detected and found to be in good agreement with that obtained by XRD (adopting the same elastic constants). Moreover, a Poisson's ratio of 0.23 ± 0.02 was estimated, which is in the range reported in the literature for similar coatings.

The two situations of non-equal biaxial stress and non-isotropic in-plane elastic behavior are analyzed and correcting equations are proposed. Finally, the influence of coating's texture and microstructure on the reliability of the method is discussed.

2:10pm TS2-2-3 Low temperature deformation in complex crystals, V. Schnabel, University of Cambridge, UK, S. Korte, Gordon Laboratory, Department of Materials Science and Metallurgy, University of Cambridge, UK, C. Walter, R. Stearn, W. Clegg (wjc1000@cam.ac.uk), University of Cambridge, UK

The development of new materials for coatings has generally focussed on a limited number of materials with relatively simple crystal structures in which deformation occurs predominantly by the movement of dislocations. However there are crystals with unit cells that are sufficiently large that conventional dislocations are energetically unfavourable. Despite this, such materials are known to be plastic above a ductile-brittle temperature, typically 0.5 – 0.75 of the melting point.

In this paper the low temperature deformation behaviour of single crystals of an orthorhombic Al_3Co_4 and a cubic Mg_2Al_3 has been studied at temperatures using micropillar compression. This allows cracking to be suppressed by making the sample sufficiently small, in this case a few microns in diameter. The materials studied had grains of a sufficient size that micropillars could be milled within individual grains, allowing the single crystal flow behaviour in grains of different orientations to be studied. It is shown that there is a very pronounced yield drop in these materials, and that the yield stress appears to be almost independent of temperature, similar to what has been observed in a metallic glasses. In some orientations, the orientations of the slip traces with respect to the pillar orientation were consistent with what would be expected from the slip systems at higher temperatures. However, this was not observed in many cases, suggesting that the glide bands form on or close to planes of maximum shear stress.

2:30pm TS2-2-4 Carbon-Based Coating for Flexible Fabric Heater Prepared by Arc Ion Plating, C.C. Hsu, C.M. Chen, J.L. He (jlhe@fcu.edu.tw), Feng Chia University, Taiwan

Electric heating textiles have widely been used in many applications, including clothes, furnishings and medical equipments, as well as in recent year, the car or construction interior materials. The traditional metal wire and carbon fiber are currently the two major types of heating element for electric heating textiles. The former suffers non-uniform heating, easy corrosion, uncomfortable to the user and without far infrared emission, while the carbon fabric presents area heating, flexible and particular far infrared emission. However, the carbonization process to prepare carbon fiber is expensive, energy consuming and emitting environmental unfriendly VOCs. Carbon-based coatings such as diamond-like carbon (DLC) film presents high chemical stability and effective far infrared emission. Therefore, in this study, an arc ion plating (AIP) technique, capable of low temperature deposition, is used to prepare carbon-based film on glass fiber fabric, and thus a flexible fabric heater with low processing cost and far infrared emission capability is expected. By adjusting the acetylene flow rate during deposition, the film composition and phase

structure are investigated to reveal how they affect the electrical properties and far infrared emissivity. Experimental results show that the AIP carbon-based film presents a lower electrical resistivity as well as thermal-electrical conversion efficiency when obtained at low acetylene flow rate, but an ultimate far infrared emissivity when obtained at high acetylene flow rate. Such a newly developed flexible fabric heater has been a great potential for usage in the electric heating products.

2:50pm TS2-2-5 Kinetics of Thin Film Growth and Gas-Solid Reactions using in situ High-Temperature Scanning Tunneling Microscopy, S. Kodambaka (kodambaka@ucla.edu), Y. Murata, University of California, Los Angeles, US, V. Petrova, I. Petrov, University of Illinois at Urbana-Champaign, US

INVITED

In situ microscopy is a powerful method that enables *direct* visualization of surface morphological, structural, compositional evolution, and often reveals surprising and previously unknown aspects. Since the observations are carried out at the processing conditions (for example, during growth or annealing in vacuum or in a reactive ambient), the phenomena can be quantitatively described with minimal uncertainties in kinetic rate measurements. In this talk, I will showcase the capabilities of *in situ* variable-temperature scanning tunneling microscopy (VT-STM) using two examples: 1) growth of graphene thin films on SiC(0001) and 2) gas-solid reactions on $\text{TiO}_2(110)$.

In order to follow graphene growth on SiC surfaces, we used high-temperature (~ 1400 K) STM and observed for changes occurring on the SiC(0001) during annealing in ultra-high vacuum. From the time-lapsed STM images, we identify three distinct modes of bilayer graphene growth. We used VT-STM at temperatures between 700 K and 1000 K and studied the influence of ethylene (C_2H_4) on the surface dynamics of rutile-structured $\text{TiO}_2(110)$. STM images were acquired as a function of time, oxygen and ethylene partial pressure, and temperature. From the STM images, we determined the role of gas chemistry on the oxide surface composition.

3:30pm TS2-2-7 In-situ AFM studies of crack initiation in ultra-thin SiO_x films on polymer substrates, B. Ozkaya (oezkaya@tc.uni-paderborn.de), University of Paderborn, Germany, S. Steves, Ruhr Universität Bochum, Germany, C.N. Liu, O. Ozcan, University of Paderborn, Germany, P. Awakowicz, Ruhr Universität Bochum, Germany, G. Grundmeier, University of Paderborn, Germany

Barrier properties of thin films with respect to the diffusion of oxygen and water are of crucial importance in assessing their protection performance. Thin SiO_x plasma polymer films have been intensively researched for their possible application as barrier coatings on engineering metals. Their high formability makes them suitable for applications involving forming processes; whereas their superior barrier properties prevent corrosive electrolytes from reaching the film-metal interface. The key step in the development of these films is the simultaneous optimisation of the mechanical and barrier properties to achieve coatings which can hinder the ingress of electrolyte to the interface and at the same time sustain a high resistance to crack formation during forming processes.

This paper focuses on crack initiation of SiO_x plasma polymer films. Various films are deposited in a low pressure microwave plasma to study the effect of process parameters (plasma gas composition, substrate bias and adhesion promoting pre-treatments) on film properties. For the investigation of deformation at various strain values, plasma polymer films were applied on PET-foils and the crack formation was studied in-situ by means of atomic force microscopy (AFM). A custom build AFM-stage was used to apply the desired strain in a perfectly controlled manner. Moreover, the evaluation of water up-take in barrier films was performed on films deposited on gold electrodes by means of discrete polarisation modulation Fourier transform infrared reflection-absorption spectroscopy (FT-IRRAS) and by collection of cyclic voltammetry data, in atmospheres with controlled humidity and in corrosive electrolytes, respectively. Presented results will demonstrate the correlation between the deposition parameters and crack formation mechanisms. The understanding of the interplay between the plasma parameters and the observed barrier properties will enable the design of high performance thin film coatings.

The authors gratefully acknowledge the support provided by the Deutsche Forschungsgemeinschaft (DFG) within the framework of the SFB-TR 87.

3:50pm TS2-2-8 High Frequency Characterization of Screen-printed Silver Circuits with an Environmental Reliability Test, K.S. Kim, W.R. Myung, S.B. Jung (sbjung@skku.ac.kr), Sungkyunkwan University, Republic of Korea

Printed electronics is a developing alternative to conventional photolithography as "green technology". Direct printing techniques such as inkjet, screen, and gravure printing are adopted to deposit thin films. They are based on an additive manufacturing, which conductive nanoinks or nanopastes are printed on the designated positions, thereby are an

innovative and low-cost metallization method. Despite this advantage of the direct printing, there is still limited usage in microwave and millimeter-wave applications. In order to expand the application fields of the printed electronic devices, the sufficient information for the high frequency performance of the directly printed circuits should be investigated. Also, high reliability of the printed electronic devices must be guaranteed for commercialization of feasible radio frequency (RF) applications. The properties of the printed thin film are determined by heat treatment and user environment. Therefore, RF properties of screen-printed silver (Ag) films were characterized with an environmental reliability test. A Ag nanopaste was screen-printed onto a silicon (Si) substrate passivated with SiO₂. The printed films were sintered at 250 °C for 30 min, and then were placed in a chamber with 85°C/85%RH for various durations (100, 300, 500, 1000 hrs). The microstructural evolution and thickness profiles of the sintered conductive tracks were investigated with a field emission scanning electron microscope and 3D nano-scan view, respectively. Oxide layers on the Ag thin films were analyzed with the Auger electron spectroscopy. A network analyzer and Cascade's probe system in the frequency range of 10 MHz to 20 GHz were employed to measure the S-parameters of the Ag thin films. From the experimental results, the insertion losses at high frequencies increased with increasing the exposure durations to the 85 °C/85% RH due to the thicker oxide layers. The RF properties of the printed Ag films were affected by the microstructural evolution and the oxide layers, which will be deeply discussed in the conference site and full manuscript.

endurance characteristics are exhibited in the Sn-doped SiO₂ resistance switching memory.

4:10pm **TS2-2-10 The Bipolar Resistance Switching Behavior with a Pt/CoSiO_x/TiN Structure of Nonvolatile Memory Device**, *Y.E. Syu* (*syuyongen@gmail.com*), National Sun Yat-Sen University, Taiwan, *G.W. Chang*, National Chiao Tung University, Taiwan

This paper investigates characteristics and physical mechanism of the resistance random access memory (RRAM) device with TiN/CoSiO_x/Pt structure. The device exhibits excellent characteristic with good endurance of more than 10⁵ times, long retention time of 10⁴ s in 125 °C and more stable in resistance switching state. In general, the mechanism is regarded as a redox reaction in the dielectric interface between the TiN electrode and the conductive filament. In this study, both high resistance state (HRS) and low resistance state (LRS) seem to be independent of cell size, so that the formation/rupture of localized conduction filament is preferred as the driving mechanism of the resistance switching in the Pt/CoSiO_x/TiN system. Furthermore, the switching mechanism is investigated by current-voltage (IV) curve fitting to confirmation the filament. Also, the asymmetric phenomenon of the carrier conductor behavior is found at the HRS in high electric field. The switching behavior in the TiN/WSiO_x/Pt device is regarded as tip electric field by localizing filament between the interface of top electrode and insulator. In addition, the resistance state is relating with the thickness of switching layer between the TiN electrode and the conductive filament.

4:30pm **TS2-2-11 A low-temperature method to improve the performance of Ni: SiO₂ -based nonvolatile memory by supercritical CO₂ fluid**, *S.L. Chuang* (*gizvvs@hotmail.com*), National Sun Yat-Sen University, Taiwan

In this study, the highly reliable and uniform bipolar resistance switching behavior was achieved in Pt/ Ni: SiO₂ /TiN resistive random access memory (RRAM) device. This device has above 3 orders (R_{OFF}/R_{ON}) of magnitude memory window, good 10⁶-cycle endurance, and the excellent retention reliability during 10000 sec at 85 °C. Based on the analytic results, the low-temperature supercritical CO₂ (SCCO₂) fluid technology was employed to treat the Ni: SiO₂ resistance-switching layer of device at 150 °C. After SCCO₂ fluid treatment, the current at the high-resistance state (HRS) of device was reduced significantly. Furthermore, the carrier conduction mechanism at HRS transformed from Frenkel-Poole emission to Schottky emission in the high-voltage region. SCCO₂ fluid can deliver the oxidants into Ni: SiO₂ thin film. Based on the XPS and the FTIR material analyses results, a model is presented which describes the traps within Ni: SiO₂ thin film was passivated by SCCO₂ fluid.

4:50pm **TS2-2-12 Resistive switching characteristics induced by doping of Sn in SiO₂-based nonvolatile memory**, *T.M. Tsai, K.C. Chang, T.C. Chang* (*tcchang@mail.phys.nsysu.edu.tw*), *Y.E. Syu, D.S. Gan*, National Sun Yat-Sen University, Taiwan

In this study, we applied doping Sn into the SiO₂ insulator to induce the resistive switching characteristics by the technique of SiO₂ and Sn co-sputtering at room temperature. The fitting results of current-voltage curve indicated that the carrier conduction mechanism at a high resistive state is complied with the Poole-Frenkel emission while the carrier transfer mechanism at a low resistive state is dominated by the Ohmic's conduction. This phenomenon is consistent with the filament theory. The effect of Sn doping in SiO₂ are discussed by fourier transform infrared spectroscopy and X-ray photoelectron spectroscopy. Additionally, good retention and

Tuesday Morning, April 24, 2012

Coatings for Use at High Temperature Room: Sunrise - Session A2-1

Thermal and Environmental Barrier Coatings

Moderator: R. Wellman, Cranfield University, UK, D. Litton, Pratt & Whitney, US, R. Trice, Purdue University, US

8:00am **A2-1-1 Progress in Measuring and Understanding the Delamination Toughness of Zirconia Coatings**, *E. Donohue* (*erin_donohue@engineering.ucsb.edu*), *N. Philips*, *M. Begley*, *C.G. Levi*, University of California, Santa Barbara, US

Failure mechanisms in thermal barrier coatings (TBCs) often involve the propagation of delamination cracks through the ceramic layer. Mode I toughness measurements on air plasma-sprayed, dense, vertically cracked (DVC) 8YSZ TBCs using a double cantilever beam (DCB) test revealed R-curve behavior and steady state toughness values of $\Gamma_{IC} \sim 320 \pm 30 \text{ J/m}^2$. This unexpectedly high value has motivated an analysis of the test itself and the possible mechanisms responsible for the toughness elevation. Examination of local displacement data along the entire length of the cantilevers, including at the load point, reveals the location of the crack front. In analyzing the experiment, the compliant foundation of the cantilever (due to the presence of the TBC) and shear effects at the crack tip must be incorporated. Finite element analysis of the DCB specimen includes a layer with reduced stiffness between the beams that simulates the behavior of the compliant foundation. The model produces results that are consistent with those from experiment; thus it is possible to calculate an energy release rate solely with measured parameters, known material properties, and the displacement data. Additional experiments on a variety of air plasma-sprayed coatings show the evolution of the toughness and the possible contributions of multiple toughening mechanisms, including ferroelastic domain switching, crack bridging and pull-out.

8:20am **A2-1-2 Monitoring Delamination of Thermal Barrier Coatings by Combined Photoluminescence Piezospectroscopy Imaging and Upconversion Luminescence Imaging Techniques**, *J.I. Eldridge* (*jeffrey.i.eldridge@nasa.gov*), NASA Glenn Research Center, US, *B. Heeg*, Lumium, Netherlands

Previous work has demonstrated that delamination progression of thermal barrier coatings (TBC) composed of yttria-stabilized zirconia (YSZ) can be monitored by photoluminescence piezospectroscopy (PLPS) and more recently by upconversion luminescence imaging of TBCs composed of YSZ incorporating a thin base layer co-doped with erbium and ytterbium (YSZ:Er,Yb). The recent development of imaging mode PLPS using a tunable filter now allows the comparison of both techniques by direct imaging of the same specimens. In this study, both PLPS imaging and upconversion luminescence imaging were performed to monitor the delamination progression of electron-beam physical vapor deposited (EB-PVD) TBCs at different stages of interrupted furnace cycling to 1163 °C. In addition, the extent of mechanically induced delamination produced by Rockwell indentation at selected stages of TBC cyclic life was evaluated by both techniques. The TBC damage associated with the imaging results was verified by post-imaging SEM inspection of the specimen cross-sections. While each technique has its own strengths and weaknesses, it is shown that the information provided by both techniques is complementary and provides a better identification of the location/depth at which delamination cracks occur than by either technique alone. The complementary nature of these techniques can be attributed to their very different mechanisms for achieving the contrast between different stages of delamination. In particular, the delamination contrast for PLPS imaging relies on the reduction in stress in the thermally grown oxide (TGO), while upconversion luminescence imaging relies on the total internal reflection that occurs at cracks within or below the YSZ:Er,Yb layer. Therefore, PLPS imaging is more sensitive to damage to the TGO or to the TGO/bond coat interface, whereas upconversion luminescence imaging is more sensitive to damage at the TGO/TBC interface or above.

8:40am **A2-1-3 The influence of transient thermal gradients and substrate constraint on the delamination of thermal barrier coatings**, *Hutchinson* (*jhutchin@fas.harvard.edu*), School of Engineering and Applied Sciences, Harvard University, US **INVITED**

The influence of steep thermal gradients combined with rapid hot surface cooling on delamination of thermal barrier coatings is investigated. Transient thermal gradients induce stress gradients through the coating and substrate which, in turn, produce overall bending if the substrate is not very

thick and if it is not constrained. Substrate thickness and constraint are important aspects of the mechanics of delamination due to transient thermal loading of coating-substrate systems. These aspects must be considered when laboratory tests are designed, and they must be considered for lifetime assessment under in-service conditions.

9:20am **A2-1-5 Raman Spectroscopy and Neutron scattering of Ferroelastic Switching in Ceria Stabilized Zirconia**, *A. Bolon*, *M. Gentleman* (*mgentleman@tamu.edu*), Texas A&M University, US

Ferroelastic switching has been identified as a method for increasing the toughness of thermal barrier materials. Here we present the results of observations of ferroelastic switching by Raman spectroscopy and neutron scatter as a function of time and temperature to understand the effectiveness of the ferroelastic process in toughening ceria stabilized zirconia. Results will demonstrate the effect of temperature on domain motion as well as the resulting bulk surfaces of a highly switched material.

--

9:40am **A2-1-6 Thermo-mechanical properties of lanthanide added zirconia film deposited by EB PVD**, *Y.S. Oh* (*ysoh30@kicet.re.kr*), *K.H. Kwak*, *H.T. Kim*, *S.W. Kim*, *S.M. Lee*, Korea Institute of Ceramic Engineering and Technology, Republic of Korea, *B.K. Jang*, National Institute for Materials Science, Japan

For its excellent thermo-mechanical stability in high temperature, Electron Beam (EB) PVD method has been developed to replace the conventional plasma spray method to fabricate the thermal barrier coating of gas turbine. However, industrial application is limited for its low cost efficiency and higher thermal conductivity compared to plasma sprayed film despite the excellent mechanical properties.

To lower the thermal conductivity, we have used the mixture of lanthanide and zirconia as a film source. The pore distribution and column structures were developed to sustain mechanical properties in high temperature condition. Deposition rate was increased up to $\sim 3 \mu\text{m/min}$ by control the EB scanning condition of ingot during the evaporation. Thermal conductivity of thick film, over $300 \mu\text{m}$, was measured by laser flash method. Hardness and adhesion of film was measured by Vickers hardness tester and tensile test. The phase of lanthanide doped composite film was revealed as pyrochlore from X-ray diffraction and also the thermal conductivity was calculated as under $1.5 \text{ W/m}\cdot\text{K}$. Adhesion force of composite film was found to 3 times higher than YSZ film by conventional plasma spray coating.

10:00am **A2-1-7 Effect of post heat treatment on thermal durability of thermal barrier coatings in thermal fatigue tests**, *S. Myoung*, *H. Kim*, *M. Kim*, *S. Lee*, *Y. Jung* (*jungyg@changwon.ac.kr*), Changwon National University, Republic of Korea, *S. Jung*, *T. Woo*, Sung Il Co., Ltd. (SIM), Republic of Korea

The hot-section stationary components of gas turbine are protected by thermal barrier coatings (TBCs), normally deposited by the air plasma spray (APS) and electron beam physical vapor deposition (EB-PVD) processes. The APS is more commercial method, because of less expense and lower thermal conductivity than the EB-PVD, even though there are lots of defects such as pores, microcracks, and unmelted powders. However, the TBC prepared by the APS shows a less thermal stability due to the low strain tolerance. Therefore, in this study, the effects of post heat treatment and its sequence on the microstructural evolution and oxidation behavior at the interface between the bond and top coats have been investigated in a specially designed apparatus—one side of the sample is exposed by flame and the other side air cooled. The TBC system with the thicknesses of 2000 and 200 μm in the top and bond coats, respectively, were prepared with the APS system using 9MB gun using $\text{ZrO}_2\text{-}8\text{wt}\% \text{ Y}_2\text{O}_3$ (METCO 204 C-NS) for the top coat and Ni-based metallic powder (AMDRY 962) for the bond coat. The post heating was performed in two ways — one is after the bond coat deposition and the other after the top coat deposition. The flame thermal fatigue tests were performed at a surface temperature of 1100 °C with a temperature difference of 800 °C between the surface and bottom of sample, with a dwell time of 10 min. for 860 cycles (18000 EOH; Equivalent Operating Hour). The TBC after the post heat treatment is more efficient in improving thermal durability than that without the treatment, and the post heat treatment on the TBC after the top coat deposition show a higher adhesive strength and a better thermal durability than that after the bond coat deposition. Results indicate that the post heat treatment is to propose the efficient process in improving lifetime performance of TBC at high temperature environments. The influences of thermal fatigue condition on the microstructural evolution and thermal durability of TBC are discussed.

10:20am **A2-1-8 New Perspectives on the Phase Stability Challenge in Zirconia-based TBCs**, **J. Krogstad** (*jkoschmeder@engineering.ucsb.edu*), S. Krämer, University of California, Santa Barbara, US, R. Leckie, Los Alamos National Laboratory, US, M. Lepple, Karlsruhe Institute of Technology, Germany, Y. Gao, D. Lipkin, GE Global Research, US, C.G. Levi, University of California, Santa Barbara, US

Zirconia-based ceramics have long been used to provide thermal protection to the structural components of modern gas turbine engines. Economic and environmental considerations have motivated higher engine operating temperatures, potentially leading to more rapid degradation of thermal barrier coating (TBC) systems dependent on a metastable phase, namely t' -8YSZ ($\text{ZrO}_2+7\text{-}8\text{wt}\%\text{YO}_{1.5}$) TBCs. The t' -phase was originally thought to decay slowly into the equilibrium Y-lean tetragonal phase and Y-rich cubic phase, the former of which may undergo further transformation to the monoclinic phase. However, it has recently been shown that the t' -phase destabilizes at a small fraction of the time necessary to form the deleterious monoclinic phase. The rapid decay of t' -YSZ into a modulated microstructure of coherent domains offers additional insight on the importance of microstructural control in the phase evolution of YSZ TBCs. Traditional phase stability characterization techniques have been reevaluated in order to provide a more complete description of this process. In particular, x-ray diffraction (XRD) techniques, both at room temperature and elevated temperatures, have been used to quantify the changing phase fractions and composition of each phase, with additional implications for the equilibrium phase diagram. XRD is more powerful when used in conjunction with microstructural observations. As such, three different starting morphologies will be compared on the basis of phase stability. Stemming from this comparison, potential pathways for further delaying the onset of the monoclinic transformation will be explored. While the effectiveness of these measures is expected to be modest, lessons can be learned from the t' -8YSZ system. In particular, maintaining a high degree of tetragonality over the entire range of relevant temperatures may be key to supporting or improving the in service toughness and durability. A novel TBC system will be introduced in which a relatively large single phase tetragonal field with exceptional tetragonality has been stabilized and has demonstrated comparable or improved toughness, making it a promising alternative for next generation TBCs.

This work was partially supported with funding from the US DoE via Cooperative Agreement DE-FC26-05NT42643 and the NSF via FRG-GOALI Contract NSF/DMR0605700. Any opinions, findings, conclusions or other recommendations expressed are those of the authors and do not necessarily reflect the views of the US Department of Energy or the National Science Foundation.

10:40am **A2-1-9 Influence of the mechanical behaviour of the under layer in coating spallation**, **V. Maurel** (*vincent.maurel@mat.enscm.fr*), A. Koster, Mines-ParisTech, UMR CNRS 7633, France, L. Rémy, Mines-ParisTech, UMR CNRS 7633, France **INVITED**

Coatings designed for high temperature protection, Aluminium rich intermetallic coating as well as thermal barrier coatings (TBC), are prone to damage when exposed to stages of high temperature and cooling. Coupling thermal and mechanical loading tests provide an accurate simulation of in-service loadings and the generation of subsequent realistic damage. Thus, the aim of this study is to clarify the way the mechanical behaviour of the under-layer interacts with surface damage. This point will be examined for room temperature mechanical tests performed up to oxide or TBC spallation. The specimens were initially subjected to high temperature thermal loading for both isothermal and thermal cycling.

When single crystals coated with TBC are subjected to mechanical compression, the strain localisation arising in the single crystal has been already shown to drive the ceramic coating to spallation. In the same manner, when the oxide is growing on a free surface, the oxide spallation due to mechanical compression is dependent of the local behaviour of the coating. Indeed, for a typical CVD-NiAl coating, strain localisation is related to the coating microstructure. Moreover, the oxide morphology will also contribute to localisation of strain and hence oxide spallation. The chosen experimental methodology will be explained since it offers a complement to thermo-gravimetric analysis. It particularly includes the intensive use of full-field analysis by surface strain field measurement. This technique enables a quantitative characterisation of surface damage and can be used to define intrinsic rupture material parameter. Complementary finite element analysis of both test configuration and principal microstructural features are performed. It allows a close view of the mechanical state leading to rupture to be obtained. Finally, assessment of thermo-mechanical coupling will be discussed for complex loading paths.

11:20am **A2-1-11 Inhibiting High Temperature Densification Through Multi-Phase TBCs**, **J.S. Van Sluytman**

(*jason.vans@engineering.ucsb.edu*), C.G. Levi, University of California, Santa Barbara, US, V.K. Tolpygo, Honeywell Aerospace, Phoenix, AZ, US Thermal barrier coatings (TBCs) are essential for the effective operation of turbine blades in high temperature gas environments. The drive for next generation TBCs, however, poses new demands that the current TBC, 7.6 mol% $\text{YO}_{1.5}$ stabilized zirconia (7YSZ) is unlikely to satisfy. At issue is the phase stability of the coating and its resistance to sintering, both of which are explored in the $\text{YO}_{1.5}$ - $\text{TaO}_{2.5}$ - ZrO_2 (Y-Ta-Zr) system. This research addresses the issue of high temperature densification and its mitigation using multi-phase compositions within this ternary system. In addition to the baseline 7YSZ, four compositions were selected for investigation representing four different phase constitutions: 16Y-16Ta-Zr (stable tetragonal, t); 20Y-20Ta-Zr (two-phase tetragonal zirconia solid solution, t , and monoclinic yttrium tantalate, m - YTaO_4); 22Y-13Ta-Zr (two-phase *non transformable tetragonal*, t , and fluorite, c); and finally 18Y-28Ta-Zr (three-phase mixture of t , m - YTaO_4 , and orthorhombic Zr_3TaO_8 phases). Densification studies were performed at 1250 °C with dwell times of 1, 4, 9, and 300 h. Pore size distributions have been quantified at each sintering time using BET analysis. Remarkably, the 18Y-28Ta-Zr composition increased only to 55% of its theoretical density from a green body density of 49% after 300 h. Pore size analysis indicates that the pores are relatively stable from 1 to 300 h at 1250°C. This compares with 22Y-13Ta-Zr and 7.6YSZ, which reached 70% and 85% of their theoretical densities, respectively, after the same exposure. The 22Y-13Ta-Zr, along with 18Y-28Ta-Zr, which are also phase stable and offer lower thermal conductivity than 7YSZ, suggests alternate regions within the Y-Ta-Zr system offering promise for future development.

Hard Coatings and Vapor Deposition Technology

Room: Royal Palm 4-6 - Session B1-3

PVD Coatings and Technologies

Moderator: P. Eklund, Linköping University, Sweden, J.H.

Huang, National Tsing Hua University, Taiwan, J. Vetter, Sulzer Metaplas GmbH, Germany

8:00am **B1-3-1 Preparation and characterization of anti-wear and anti-bacteria TaN-Cu, TaN-Ag, TaN(Ag,Cu) nanocomposite thin films**, **J.H. Hsieh** (*jhsieh@mail.mcut.edu.tw*), Ming Chi University of Technology, Taiwan **INVITED**

The processes and functions of MeN-(soft metal) nanocomposite films were first reviewed. Following that, the processing, structure, and multifunctional properties of TaN-Cu, TaN-Ag, and TaN-(Cu,Ag) nanocomposite films were discussed and compared. The TaN-(soft metal) films were prepared by a hybrid process that combines co-sputtering deposition and rapid thermal annealing. After the surface morphologies as well as the microstructures were analyzed and compared, the samples were examined for their tribological properties. It is found that the tribological properties could be improved when the soft metals were smeared out and functioned as solid lubricants. All TaN-(soft metal) nanocomposite thin films showed similar behaviors. However, it is found further that Cu-incorporated films could behave better under low load or low contact temperature while Ag-incorporated films could do better under high load or high temperature. For TaN-(Cu,Ag), the films might behave more like Ag-incorporated films. The samples were also tested for their anti-bacterial behaviors against Gram-negative (*E. coli*) and Gram-positive (*S. Aureus*) bacteria. It is found that the antibacteria efficiency against either *E.coli* or *S. aureus* can be much improved for TaN-(Cu,Ag), comparing with TaN-Ag or TaN-Cu films. The annealing temperature for TaN-(Cu,Ag) can be as low as 200 °C. Being annealed at this temperature, the film still shows good antibacterial behaviors against either bacterium. The synergistic effect due to the co-existence of Ag and Cu would be discussed.

8:40am **B1-3-3 Effects of sputtering gas for the preparation of CNx films by RF reactive sputtering**, **T.S. Shiroya** (*s0721171KH@it-chiba.ac.jp*), Graduate School, Chiba Institute of Technology, Japan, Y. Sakamoto, Chiba Institute of Technology, Japan

CNx is nitrogen contained Diamond-Like Carbon (DLC) and it has excellent mechanical properties such as high hardness and low friction coefficient especially in nitrogen gas atmosphere. These properties may be controlled by controlling of nitrogen content. In addition, CNx is capable of preparation by using thin film deposition techniques both Physical Vapor Deposition (PVD) and Chemical Vapor Deposition (CVD) and expected to apply for mechanical parts. On the other hand, reactive sputtering is one of method prepared oxide and nitride easily by chemical reaction with the

reactive gases with the target material. So, investigation was carried out the effects of sputtering gases for the preparation of CN_x films by RF reactive sputtering. CN_x films were prepared using RF magnetron sputtering apparatus. Graphite was used as a target and Si was used as the substrate. The substrate was pretreated to immerse on BHF for 5 minutes. RF power and pressure were fixed to 200W and 0.4Pa, respectively. Ar and N₂ were used as sputtering gases and their ratio was Ar/N₂=1/0, 1/1, 1/3, and 1/5. The sputtering time was 60 minutes. The CN_x films were prepared after pre-sputtering using same condition for 10 minutes. The deposits were estimated by using of SEM, XPS and Raman spectroscopy. From the cross-sectional SEM images, deposition rate was increased by adding of N₂ to Ar sputtering gas and floating substrate holder potential. As a result of Raman spectroscopy, the DLC broad peak center around 1550cm⁻¹, D-band peak center around 1350cm⁻¹, G-band peak center around 1580cm⁻¹ and S-band peak center around 1200cm⁻¹ were observed in spectra of each samples. As a result of XPS, the peaks of C-C and -C=O bond were observed in C1s spectra of the deposit prepared using Ar. The peaks of C-C, C=O, N=O-, C-N, =C=N-C- and -C≡N bond were observed in C1s and N1s spectra used mixture of Ar and N₂ as sputtering gases. As mention above, the deposit contain nitrogen was obtained using the mixture of Ar-N₂ gases. As a result of preparation of CN_x films by RF reactive sputtering, DLC was obtained using Ar as the sputtering gases. On the other hand, it was possible to prepare CN_x using the mixture of Ar and N₂ gases as a sputtering gas.

9:00am **B1-3-4 Zirconium carbonitrides: study of tribological properties with deposition parameters, J. Barriga** (*jbarriga@tekniker.es*), L. Mendizabal, U. Ruiz de Gopegui, Tekniker, Spain

In the last years a great effort has been done in the development of carbon based coatings for tribological applications. As a consequence, the slip-rolling resistance of DLC thin films was improved considerably. On the other side, zirconium has been used widely in the decorative industry because of its corrosion resistance and wide range of affordable metallic colors. But the use of Zr in tribological thin films is not very broad. However, recent developments show that zirconium based coatings could perform better than DLC thin films in tribological contacts under severe contact conditions [1].

In the present work, zirconium carbonitride thin films have been developed on M2 steel by cathodic arc evaporation under a wide range of deposition parameters. BIAS voltage has been varied from 30 to 400 V. Temperature during the process has also been controlled from 500°C to 300°C, in order to study the possibility of doing the deposition at low temperatures opening the range of substrate steels. Finally, the flux of acetylene gas has also been varied to study the influence of carbon content in the properties of the film.

A wide characterization procedure has been taken with the resulting ZrCN coatings: Calotest, SEM, X-Ray analysis, adhesion tests and, finally, a battery of sliding tribological tests. With this we have analyzed the influence of deposition parameters on the films and looking for the proper applications of the best performing films.

[1] Charles-Alix Manier, Holger Ziegele, Javier Barriga, Josu Goikoetxea, Mathias Woydt, Zirconium-based coatings in highly stressed rolling contacts as alternative solution to DLC and ta-C coatings, *Wear* 269 (2010) 770–781.

9:20am **B1-3-5 Comparison of sputter deposited WC coatings from alternative sources, H. Alagoz** (*alagoz@bilkent.edu.tr*), E. Uzun, M. Ugras, N. Uddin, E. Bengu, Bilkent University, Turkey

Transition metal nitride and carbide coatings attracted a lot of attention in the last decades due to their good wear, erosion, corrosion and high temperature oxidation resistance. In this study, an alternative synthesis approach was used for the synthesis of carbide coatings in the W-C system. New W₂C_y coatings were synthesized by reactive magnetron sputtering technique with various target combinations and gas compositions on Si(100) and steel (100Cr6) substrates. Instead of the frequently used carbon sources such as WC(1:1) or graphite target, and CH₄ or C₂H₂ gases, a B₄C target was used as an alternative for C source and N₂ gas was fed through the chamber during deposition. For comparison, another set of coatings were synthesized using an additional graphite target together with allowing C₂H₂ gas feed instead of N₂ flow in order to see the effect of increasing C content in the coatings. We investigated the change in the phase composition, chemical bonding, hardness, room-temperature and high-temperature wear rates of these two sets of coatings. Scanning electron microscopy (SEM) was used to understand the effect of process parameters on surface roughness and microstructure of the films. The hardness values of the films were measured using the nano-indentation technique and, we used a high-temperature tribometer (up to 800°C) to investigate the wear-rates of the coatings. X-ray photo-electron spectroscopy (XPS) has been employed to understand the bonding states of tungsten and carbon as well as boron, nitrogen and oxygen on the as-deposited surfaces. Our results

showed that the coatings are mostly combinations of W+WC, W+W₂C and BN in the case of N₂ flow. Coatings containing BN species are showing considerably good hardness (up to 31.5 GPa) and wear performances (up to 2.0x10⁻⁷ mm³/Nm at room-temperature and 2.0x10⁻⁶ mm³/Nm at 500°C). Increasing the C content of the films in the second set of experiments did not cause a significant change on the wear rates but gave a gradual decrease to the hardness and friction coefficient of the films.

9:40am **B1-3-6 The influence of the magnetic field strength on the poisoning behavior of Tantalum, R. Hollerweger** (*robert.hollerweger@unileoben.ac.at*), Montanuniversität Leoben, Austria, M. Lechthaler, OC Oerlikon Balzers AG, Liechtenstein, P. Polcik, PLANSEE Composite Materials GmbH, Germany, J. Paulitsch, P.H. Mayrhofer, Montanuniversität Leoben, Austria

Reactive magnetron sputtering requires precise knowledge of the chemical and physical processes in the plasma itself as well as at the target surface. Therefore, a lot of investigations are focusing on the poisoning behavior in dependency of parameters like power density, reactive gas partial pressure, total pressure or magnetic field configuration. Especially the change of the magnetic field strength due to progressing target erosion has a pronounced influence on the target poisoning as well as plasma conditions and hence, on the plasma and film properties. To investigate this effect, voltage hysteresis curves were recorded while sputtering a Ta target in Ar-O₂ atmosphere. The magnetic field strengths and DC current densities were subsequently varied from 45 to 90 mT and from 13 to 26 mA/cm², respectively. Due to these variations, a shift of the different sputtering regimes within the hysteresis can be detected. Selected points, referring to oxygen gas contents of 42, 70 and 100 % of the total gas flow, were used for the deposition and characterization of Ta₂O₅ thin films, which indicate hardness values in the range of 15 GPa, crystalline structure and high thermal stability. This comprehensive study of the sputtering behavior helped to gain well-founded knowledge of possible influences on the poisoning behavior of Tantalum as well as on the film formation processes of the resulting pentoxide.

10:00am **B1-3-8 Cavitation and abrasion resistance of Ti-Al-Y-N coatings prepared by the PIII&D technique from filtered vacuum-arc plasma, V. Belous, V. Vasyliov, A. Luchaninov, V. Marinin, E. Reshetnyak, V. Strel'niiskij**, National Science Center "Kharkov Institute of Physics and Technology", Ukraine, S. Goltvyanytsya, V. Goltvyanytsya (*vladmt@gmail.com*), Real Ltd., Ukraine

Ti-Al-Y-N coatings with small Y percentage have demonstrated high hardness and excellent oxidation resistance which provides their application for protection the machine parts which operate under extreme environmental conditions. In our recent work [1] we investigated structure and properties of such coatings prepared by the plasma immersion ion implantation and deposition (PIII&D) using filtered vacuum-arc plasma source.

Deposition from the filtered vacuum arc plasma is the widely used effective method of manufacturing high quality protective wear resistant coatings. A high-voltage pulsed bias applied to the substrate permits the deposition of thicker coatings with good adhesion and low residual stresses. In the present work we examined the cavitation and abrasion resistance of PIII&D deposited Ti-Al-Y-N coatings doped with yttrium (≤ 1 at.%) and analyzed correlation between their properties and structure.

Ti-Al-Y-N coatings with thickness of 5-6 micron were deposited on the 302 stainless steel substrates from filtered vacuum-arc plasma at nitrogen pressure of 0.1 Pa. Ti_{0.5-x}Al_{0.5}Y_x alloys (x = 0, 0.002, 0.004 and 0.01) produced by vacuum-arc remelting in argon atmosphere (by Real Ltd., Zaporozhye, Ukraine) were used as cathodes in the vacuum-arc plasma source. The substrate potential was either DC (-150 V) or negative pulsed, the amplitude A₀ varied in the range of 0-2.5 kV.

The erosion resistance of the coatings was evaluated on the measured mass loss during cavitation treatment in distilled water. The tests were continued until visually watched open-ended pores in the coating were formed. Abrasion wear was determined in the scheme substrate plane – rotating abrasion disk.

The substrate potential during deposition process and Y content in the coatings were found to be important factors influencing the rate and character of their cavitation damage. The coating deposited at A₀=0 was subjected to pitting erosion. Long cracks prevailed on the surface of the cavitation treated coating deposited at DC (-150 V) potential. High voltage pulsed substrate potential contributed to decrease by 3-5 times in the rate of the mass loss under cavitation, quantity of the erosion defects on the treated surface diminishes sharply. Increase of Y content resulted in improvement of wear durability. Mean rates of cavitation and abrasion wear of (Ti,Al)N+1at.%Y were a factor of 3 to 5 times lower than that of (Ti,Al)N and tenfold lower than that of TiN.

Suppression of the columnar growth, formation the nanocrystalline structure and decrease in the internal stress level seem to be the reason of such dependencies.

[1] V.A. Belous et al. *Surface and Coatings Technology*, in press.

10:20am **B1-3-9 Synthesis and Tribological Properties of W_xN_y Coatings**, H. Alagoz, M. Ugras, E. Uzun, M.F. Genisel, E. Bengu (bengu@fen.bilkent.edu.tr), Bilkent University, Turkey

Transition metal nitrides are frequently used in industry for their protective properties such as their good wear, erosion and corrosion resistance and high thermal stability. In the following work, W-N system was investigated in order to synthesize protective coatings which have good wear resistance at room temperature (RT) and high temperature (HT, 500°C) as well. For this purpose, coatings were synthesized in a reactive magnetron sputtering system at various N_2 flow, W target power, bias voltage settings and number of bilayers (W/WN) for multilayer coatings on Si(100) and steel (100Cr6) substrates. We investigated the change in the crystal structure, hardness, RT and HT wear properties and surface roughness of these coatings. Scanning electron microscopy (SEM) was used to understand the effect of process parameters on surface roughness and microstructure of the films. The hardness values of the films were measured using the nano-indentation technique and, we used a HT tribometer (up to 800°C) to investigate the RT and HT wear-rates of the coatings. X-ray photo-electron spectroscopy (XPS) has been employed to understand the bonding states of tungsten to nitrogen and oxygen on the as-deposited surfaces. Our findings revealed that with increasing N_2 flow, the hardness values for the films increased (from 24.2 to 28 GPa) together with a decreasing wear rate (from 4.0×10^{-6} to 5.0×10^{-7} mm³/Nm) and friction coefficient at room temperature. However, HT wear rates indicated an almost opposite trend (2.0×10^{-6} to 6.0×10^{-6} mm³/Nm) and friction coefficients were doubled of the RT ones. Increasing the bias voltage have led to a considerable improvement in the wear performance (8.3×10^{-7} at RT, 7.4×10^{-6} at HT), while multilayer coatings did not indicate a performance increase ($\sim 10^{-6}$ mm³/Nm levels for RT and $\sim 10^{-5}$ mm³/Nm levels for HT).

10:40am **B1-3-10 Excellent thermal stability of Cu films containing insoluble Ru, RuN_x and ReN_x for advanced barrierless Cu metallization**, W. Diyatmika, J. Chu (jpcchu@mail.ntust.edu.tw), National Taiwan University of Science and Technology, Taiwan, C. Lin, Asia-Pacific Institute of Creativity, Taiwan

For the Cu metallization in Si-based microelectronics technology, a layer of diffusion barrier is required to prevent detrimental reactions between Cu and Si. To cope with the miniaturization, however, manufacturing of reliable and extrathin barrier layer is even difficult. As a prospective solution, a barrierless interconnect with the concept of enhanced thermal stability Cu alloy films has been proposed. In this study, we report the excellent thermal stability of Cu(Ru), Cu(RuN_x) and Cu(ReN_x) films.

Cu alloy films added with dilute amounts of Ru, denoted as Cu(Ru), were deposited onto barrierless (100) Si substrates by magnetron co-sputtering. Cu alloy films with dilute Ru or Re deposited in Ar/ N_2 ambient, are denoted as Cu(RuN_x) and Cu(ReN_x), respectively. Post-annealing was carried out under a vacuum condition in isothermal and cyclic modes up to 730°C. The films were characterized by EPMA and SIMS, XRD, FIB, and TEM to investigate the composition, crystallography and microstructure. The electrical resistivity of the film was measured by the four-point probe technique. The leakage currents were determined by measuring the current-voltage (I-V) curves of metal-oxide-semiconductors (MOSs) multilayer structures.

Cu(ReN_x) films exhibit a better thermal stability film which can stable up to 730°C for 1 hour without detectable copper silicide in XRD patterns. Adding such insoluble substances into Cu film can prevent the diffusion reaction between Cu and Si by inhibiting recrystallization and grain growth after annealing at high temperatures, as well as their nitrides. More detailed analytical results will be presented and discussed.

Keywords

Cu metallization, barrierless, thermal stability, insoluble substance, annealing

11:00am **B1-3-11 Microstructural features and thermal stability of AlN:Ag and Al-Si-N:Ag nanostructured films**, A. Siozios, D. Anagnostopoulos, P. Patsalas (ppats@cc.uoi.gr), University of Ioannina, Greece

Aluminum nitride (AlN) is a well known, wide bandgap semiconductor which exhibits absorption in the far UV spectral range, while being totally transparent in the visible spectral region. In addition, it has excellent mechanical properties and substantial chemical and metallurgical stability making it suitable for various applications in coatings' industry, especially if blended with Si [1]. As a covalent ceramic AlN is intrinsically brittle and

the incorporation of a ductile metal (e.g. Er [2] or Ag [3]) is used to control its ductility and adhesion.

In this work we deal with the growth of AlN and Al-Si-N nanostructured films with Ag inclusions (AlN:Ag and Al-Si-N:Ag). The Ag into the AlN is distributed either as individual atoms (atomic dispersion) or as nanospheres or nanosheets (<2 nm). The atomically dispersed AlN:Ag and Al-Si-N:Ag films and the laminated structures were grown by Multi-Cathode Confocal Reactive Magnetron Sputtering (MCRMS) in (a) co-deposition of Ag and AlN or Al-Si-N using two magnetron sources, or (b) sequential growth of AlN or Al-Si-N and ultra-thin Ag layers (as thin as to approach the island coalescence threshold), respectively. On the other hand, the films with embedded Ag nanospheres were grown by Pulsed laser deposition (PLD) [4].

We investigate the effect of target power on the microstructure of the pure AlN films; AlN films can be either amorphous (a-AlN) or crystalline having the wurtzite crystal structure (w-AlN). In addition, we investigate the phases of Al-Si-N vs. the Si content and we study how the structures and the bonding of AlN and Al-Si-N change after the incorporation of Ag. For this purpose we used X-ray Diffraction (XRD), X-Ray Reflectivity (XRR) and Wavelength-Dispersive X-Ray Fluorescence (WD-XRF), using Bruker's D8 and S4 instruments, in order to determine the film's crystal structure, density and chemical state, respectively.

Finally, in order to determine the thermal stability of the films and the diffusion of Ag in a-AlN, w-AlN and Al-Si-N, we thermally annealed the produced films at various temperatures. We find that annealing at more than 600 °C results in outdiffusion of Ag on the surface.

[1] A. Pelisson-Schecker, H.J. Hug, J. Patscheider, J. Appl. Phys. 108, art. no. 023508 (2010).

[2] J.C. Oliveira, A. Cavaleiro, M.T. Vieira, Surf. Coat. Technol. 132, 99 (2000).

[3] Ch.E. Lekka, P. Patsalas, Ph. Komninou, G.A. Evangelakis, J. Appl. Phys. 109, art. no. 054310 (2011).

[4] A. Lotsari, G.P. Dimitrakopoulos, Th. Kehagias, P. Kavouras, H. Zoubos, L.E. Koutsokeras, P. Patsalas, Ph. Komninou, Surf. Coat. Technol. 204, 1937 (2010).

11:20am **B1-3-12 Hard yet Tough Ceramic Coatings via Magnetron Sputtered Multilayers in Nanocomposite and Polycrystalline Architecture**, Y. Wang, S. Zhang (msyzhang@ntu.edu.sg), Nanyang Technological University, Singapore, J.W. Lee, Ming Chi University of Technology, Taiwan, W. Lew, Nanyang Technological University, Singapore

For industrial applications, hard yet tough coatings are much desired but difficult to come by. In this study, toughening of CrAlSiN nanocomposite was realized by alternative stacking of nanocrystalline CrAlN and nanocomposite nc-CrAlN/a-SiNx (nc-: nanocrystalline a-: amorphous) in Ar/ N_2 mixture via magnetron sputtering. Multilayers with bilayer thickness of 10, 20, 40, 60 nm in constant thickness ratio of 1:1 were fabricated on Si wafer and stainless steel discs (SUS420), and the CrAlN and CrAlSiN monolayer were deposited as the counterparts. Glancing Angle X-ray Diffractometry (GAXRD) and Transmission Electronic Microscopy (TEM) were employed to investigate the microstructure. The results of High-resolution TEM suggested the interruption of columnar CrAlN grain growth as a result of the insertion of the CrAlSiN nanocomposite layer. Nanoindentation test demonstrated the enhanced hardness of multilayers (maximum at ~ 33 GPa). In the meanwhile, the toughness determined through the micro-scratch test indicated the improved resistance to the crack initiation and propagation in the multilayers as compared to the monolayer nanocomposite nc-CrAlN/a-SiNx. Thus, the study shows that the achievable hard yet tough feature via the stacking of nanocrystalline layers and nanocomposite layers was successful.

Computational Design and Experimental Development of Functional Thin Films

Moderator: B. Alling, Linköping University, Sweden, A. Amassian, KAUST, P. Patsalas, University of Ioannina, Greece, D. Holec, Montanuniversität Leoben, Austria

8:00am **B7-1-1 Time domain effect on growth kinetics of thin silver films**, *D. Magnfält*, Linköping University, IFM-Material Physics, Plasma and Coatings Physics Division, Sweden, *G. Abadias*, Université de Poitiers-CNRS-ENSMA, France, *U. Helmersson*, *K. Sarakinos* (*kostas@ifm.liu.se*), Linköping University, Sweden

In this study we employ an ultra-fast plasma based film deposition process termed High Power Impulse Magnetron Sputtering (HiPIMS) to control the kinetics during growth of thin silver (Ag) films. In HiPIMS, power is applied to a conventional magnetron sputtering source in short unipolar pulses of several tens to several hundreds of μs with energies ranging from several tens to several hundreds of mJ at frequencies smaller than 2 kHz. We use the time-dependent character of the HiPIMS process to modulate the flux of the film forming species seeking to control the adatom diffusion times and the nucleation process. In practice this is achieved by applying power to a Ag sputtering cathode in three different ways:

- (i) In pulses of constant energy and width at various frequencies ranging from 50 Hz to 1000 Hz.
- (ii) In pulses of constant width, at a certain pulsing frequency varying the pulse energy from 20 mJ to 400 mJ.
- (iii) In pulses of constant energy and at a constant pulsing frequency by varying the pulse width from 50 to 500 μs .

Time- and energy-resolved mass spectrometry is employed to study the effect of the process parameters on the temporal profile of the deposition flux. Films are deposited on Si (100) substrates covered by ~ 2 nm native SiO_2 layer. In-situ measurements of the evolution of the residual stresses in the films using a multiple-beam optical stress sensor are combined with ex-situ imaging techniques, such as Atomic Force Microscopy, to study the nucleation characteristics and determine the film thickness at which a continuous film is formed (percolation thickness). It is shown that by increasing the pulsing frequency from 50 Hz to 1000 Hz the percolation thickness decreases from 206 Å to 146 Å. Depositions are also performed using the continuous DC Magnetron Sputtering (DCMS) process at same range of growth rates (0.1 to 10 Å/s) as those used in HiPIMS. Analysis of the DCMS grown films shows that the percolation thickness of ~ 160 Å does not undergo significant changes. The latter indicates that control over the nucleation and growth is a unique feature of the time domain of the pulsed process.

8:20am **B7-1-2 Analysis of the particle velocity range for deposition and the optimum velocity of cold sprayed particles using smoothed particle hydrodynamics method**, *A.M. Manap* (*abchan3324@yahoo.com*), *T. Okabe*, *K. Ogawa*, Tohoku University, Japan

In this study the critical, maximum and optimum velocity of a single cold sprayed (CS) particle is estimated using the smoothed particle hydrodynamics method (SPH) by evaluating the impact shape, the coefficient of restitution and the rebound and deposit energy ratio. The contact surfaces of the particle and substrate is modeled as intersurface forces using the Dugdale-Barenblatt cohesive zone model. The application of the SPH method permits simulation of the CS process without the use of mesh and thus avoids the disadvantages of traditional numerical method in handling large deformations and tracing moving interfaces. The impact of cold sprayed particles is simulated using various metals and powder particle sizes. The materials are classified into four impact cases (soft/soft, hard/hard, soft/hard, and hard/soft), according to their physical and mechanical properties. The influence of powder and substrate material and particle size on the particle velocity range for deposition and the optimum velocity is discussed. Furthermore the numerically estimated critical, maximum and optimum velocity of the soft/soft impact case agreed well with previously obtained experimental values.

8:40am **B7-1-3 Molecular Dynamics Studies of Grain Boundaries in Mazed-bicrystal Thin Films**, *M. Asta* (*mdasta@berkeley.edu*), University of California, Berkeley; Lawrence Berkeley National Laboratory, US, *D. Ohmsted*, University of California, Berkeley, US, *C. Ophus*, Lawrence Berkeley National Laboratory, US, *T. Radetic*, Lawrence Berkeley National Laboratory, US; University of Belgrade, Serbia, *U. Dahmen*, University of Belgrade, Serbia **INVITED**

In this talk we will describe the results of molecular-dynamics simulations examining processes related to the shrinking of island grains in Authin films. The island grains investigated in this work are bounded by $\langle 110 \rangle$ tilt grain boundaries with 90 degree misorientations, but varying grain-boundary inclinations. Our interest in this system is motivated by parallel experimental investigations of the dynamics of the same type of island grains in mazed-bicrystal thin films, using in-situ electron-microscopy. We focus in this talk on analyses of the simulation results designed to probe the magnitudes of the grain-boundary stiffnesses and mobilities underlying the rate of grain shrinkage derived in the simulations. In addition, we analyze the variations in these properties with grain-boundary inclination, and discuss the relationship between these anisotropies and the dynamic shape of the island grains. Comparison with experimental observations obtained by in-situ microscopy will also be presented.

9:20am **B7-1-5 A non-equilibrium thermodynamic model for the formation of a Cu-Sn intermetallics film on a Cu substrate**, *F.D. Fischer* (*mechanik@unileoben.ac.at*), Montanuniversität Leoben, Austria, *J. Svoboda*, Academy of Sciences, Czech Republic

When a solid Cu substrate gets in contact with liquid Sn at 250°C for 5 seconds, two intermetallic layers with the sequence Cu_3Sn (phase) and Cu_6Sn_5 (phase) are formed at the substrate covered by a remaining thin layer of Sn. The typical thickness of these layers are 80 nm (phase) and 1000 nm (phase), building an intermetallics film on the Cu-substrate. The thermodynamic extremal principle [1] (in Ziegler's formulation) is used for the treatment of the evolution of the Cu-Sn system with the assumption of no sources and sinks for vacancies in the bulk, see e.g. [3], or non-ideal sources and sinks for vacancies in the bulk, see [4]. The interfaces between the individual phases are assumed either as ideal sources and sinks or no sources and sinks for vacancies. If these models are used for the simulation of the kinetics, no quantitative agreement is obtained for the current diffusion couple (the simulated kinetics is more than one order of magnitude slower).

The microscopic observations indicate that the newly formed intermetallic layers have a sub-micron grain structure and, thus, grain boundary diffusion can significantly contribute to the system kinetics. That is why the recent thermodynamic concept is extended so that it incorporates also the grain boundary and interface diffusion in both intermetallic phases and, thus, each intermetallic layer may develop by an interaction of bulk and interface/grain boundary diffusion. This occurs in a pronounced way in the phase, which forms a scalloped morphology, see e.g. [4]. Finally a thin film with a strongly varying microstructure develops, which is captured by the current model. An effective tracer diffusion coefficient for each component in each phase can be derived by means of the thermodynamic extremal principle [1]. Also the branching (polyfucation) of the initial contact (Kirkendall) plane, i.e. the original solid Cu, liquid Sn contact plane, is shown, which may be exploited for the determination of the effective tracer diffusion coefficients of Cu and Sn in the and phase. A comparison of the modelling results with a series of experimental results is provided.

- [1] J. Svoboda, J., I. Turek, I., F.D. Fischer, Phil. Mag., 85, 3699-3707, 2005
- [2] J. Svoboda, E. Gamsjäger, F.D. Fischer, E. Kozeschnik, J. Phase Equilibria Diff., 27, 622-628, 2006
- [3] J. Svoboda, F.D. Fischer, R. Abart, Acta mater., 58, 2905-2911, 2010
- [4] M.S. Park, R. Arróyave, Acta mater., 58, 4900-4910, 2010

9:40am **B7-1-6 Epitaxially Grown $\text{V}_x\text{Mo}_{1-x}\text{N}/\text{MgO}(001)$ Thin Films by Reactive Magnetron Sputtering**, *H. Kindlund* (*hanki@ifm.liu.se*), *J. Lu*, *E. Broitman*, *J. Birch*, Linköping University, Sweden, *I. Petrov*, *J.E. Greene*, University of Illinois at Urbana-Champaign, US, *L. Hultman*, Linköping University, Sweden

Pseudobinary transition metal nitride alloys, such as V-W-N and V-Mo-N, exhibit an electronic structure consisting of alternating high and low electron density regions, according to DFT calculations [1], leading to a simultaneous enhancement in hardness and ductility. Thus, such alloy systems are promising candidates as coatings with enhanced toughness. Recently, we demonstrated the growth of epitaxial $\text{V}_x\text{W}_{1-x}\text{N}$ thin films on $\text{MgO}(001)$ by reactive magnetron sputtering [2]. Here, we explore the effect of growth variables on the mechanical properties of $\text{V}_x\text{Mo}_{1-x}\text{N}$ on $\text{MgO}(001)$.

$V_x\text{Mo}_{1-x}\text{N}$ thin films with $0.3 \leq x \leq 1$, as determined by EDX and RBS, were deposited on $\text{MgO}(001)$ substrates by dual reactive magnetron sputter epitaxy (MSE) in a 5 mTorr $\text{Ar}+\text{N}_2$ gas mixture. The substrate temperature was varied from 100 to 700 °C. For the entire composition range, at $T_s = 700$ °C, we obtain single-phase cubic-B1-structure $V_x\text{Mo}_{1-x}\text{N}$ as determined by XRD. Cross-sectional HR-TEM and SAED confirms the cubic $V_x\text{Mo}_{1-x}\text{N}$ solid solution viewed along both $\langle 100 \rangle$ and $\langle 110 \rangle$ zone axes. The lattice parameter varies from $a = 4.149$ Å for $x = 0.8$ to $a = 4.167$ Å for $x = 0.4$, increasing with increasing Mo content. High-resolution XRD reciprocal space mapping of a $V_{0.4}\text{Mo}_{0.6}\text{N}$ film grown at 700 °C shows that the film is relaxed with $a = c = 4.167$ Å. At temperatures between 500 and 300 °C, with $x = 0.5$, we obtained single phase B1 $V_x\text{Mo}_{1-x}\text{N}(001)$ films.

The nanoindentation hardness H and elastic modulus E of the $V_x\text{Mo}_{1-x}\text{N}$ alloy films are $H = 14.3$ GPa and $E = 286$ GPa for $x = 0.6$, and $H = 12.3$ GPa and $E = 243$ GPa for $x = 0.4$.

[1] D.G. Sangiovanni, L. Hultman, V. Chirita, *Acta Mater* **59** (2011) 2121-2134

[2] H. Kindlund *et al.*, ICMCTF 2011, Abstract #266

10:00am **B7-1-7 Atomistic study of crack formation in strained thin films**, A. Oila (*Adrian.Oila@ncl.ac.uk*), S.J. Bull, Newcastle University, UK

We present the results of Kinetic Monte Carlo (KMC) studies on dislocation and crack formation in strained nanometre thick coatings. The Kinetic Monte Carlo (KMC) computer program developed (NUKIMOCs) enables atomistic simulation of the mechanical processes which occur at the nanoscale in thin films. The code performs off-lattice KMC calculations to determine the strain in a material at the atomic scale and how this changes with time. Off lattice KMC allows atoms to occupy any position in space as in a real atomic lattice with interaction between atoms defined by interatomic potentials. Therefore, both the elastic and kinetic properties of an off-lattice KMC model are entirely defined by the interatomic potential. The underlying physics of strain-induced microstructural evolution can therefore be presented accurately and on meaningful time and length scales.

The parameters of the interatomic potentials have been determined by fitting the energy surface obtained from first principles calculations, the elastic constants and the coefficient of thermal expansion to the unit cell. Different initial and boundary conditions were applied in order to study the behaviour of defects such as vacancies and dislocations. The local relaxation process was performed after every 10 simulation steps within a radius of three interatomic distances from the location of the event. The energy barrier between two states - the activation energy - was calculated by the 'frozen crystal approximation'. For energy minimisation we employed a limited-memory BFGS method.

Our KMC modelling shows that an atomically smooth surface under tensile strain will spontaneously develop a surface roughness to minimise the energy of the system and crack nuclei can develop from the roughness profile generated. The most important relaxation processes are dislocation generation and propagation.

10:20am **B7-1-8 Classical Molecular Dynamics Studies of Initial Nucleation Kinetics during TiN Thin Films Growth**, D. Sangiovanni, D. Edström, V. Chirita (*vio@ifm.liu.se*), L. Hultman, Linköping University, Sweden, I. Petrov, J.E. Greene, University of Illinois at Urbana-Champaign, US

Advancements in Modified Embedded Atom Method (MEAM) formalism present the opportunity to perform, previously not possible, realistic large scale classical Molecular Dynamics (MD) simulations of important model material systems such as TiN. As a preliminary step in achieving this goal, we report the first MD study of typical processes occurring during the initial nucleation stages of TiN thin film growth. We use an improved TiN MEAM parameterization, which reproduces the experimentally observed trends in the diffusion of single species (Ti, N), Ti-N dimers and TiN_2 complexes, and correctly accounts for the all-important Ehrlich-Schwöbel (ES) step-edge barriers on most representative, (100) and (111), steps/surfaces for TiN growth. Simulations totaling hundreds of nanoseconds are carried out at 1000 K, in statistically independent runs of between 2 and 10 ns, and concentrate on the diffusion of Ti and N single adatoms, as well as Ti-N complexes, on the (001) surface and islands. Results show significant differences in terms of total migration distance and the diffusion mechanisms between different species. As it will be shown, on the (001) surface, Ti and N adatoms migrate via single and/or multiple jumps along different diffusion channels, with Ti recorded as the leading diffusion species. Diffusion mechanisms are observed to become considerably more complex for Ti-N dimers and TiN_2 complexes. On islands, for single adatoms, the primary mechanism to overcome the ES step-edge barrier is that of push-out exchange with island edge-atoms. However, this situation changes for TiN_2 , case in which results point to hopping-over the island edge as the preferred pathway for descent on the terrace. We quantify the

events observed in terms of total migration distance and residence times on islands for each species studied, and discuss the potential effects of our findings on initial nucleation kinetics, which clearly affect TiN thin film growth modes.

10:40am **B7-1-9 Do nitride alloys exhibit Vegard's-like linear behaviour?**, D. Holec (*david.holec@unileoben.ac.at*), P.H. Mayrhofer, Montanuniversität Leoben, Austria

Early transition metal nitrides (TMN) and their alloys with Al are widely used in various protective coatings due to their outstanding mechanical and thermal stability. The increasing demand on coating performance from the application-side often requires sophisticated designs of the protective thin films. The major routes in a knowledge-based materials selection and design are by architecture (e.g. use of multilayer or patterning) by alloying, and by the combination of these two.

In the present paper we use Density Functional Theory (DFT) calculations to address a topic related mostly to alloying, i.e. to assess the extend of Vegard's-like linear behaviour of ternary TM-Al-N and TM-TM-N, and quaternary TM-TM-Al-N (TM=Sc, Ti, Zr, Nb, Ta, Hf) alloys. In particular, we will discuss the compositional dependence of lattice parameters, energies of formation, bulk moduli and elastic properties.

As an example we will show that although some systems for various properties exhibit reasonably linear dependence on composition (e.g. lattice parameter of cubic $\text{Ti}_{1-x}\text{Al}_x\text{N}$), in general it is dangerous to blindly use the so-called „Vegard's rule“. A consequence of the non-linear dependence of the lattice constants on e.g., the driving force for decomposing the metastable c-TM-Al-N phases will be discussed. On another front, detailed calculations of single crystal elastic constants of ZrN-AlN system reveal that the elastic response of the cubic ternary system is very similar to ZrN up to AlN mole fraction ~40%, only after which the elastic properties change drastically towards the AlN elastic behaviour.

11:00am **B7-1-10 Toughness Enhancement in Transition Metal Nitride Thin Films by Alloying and Valence Electron Concentration Tuning**, D. Sangiovanni, V. Chirita (*vio@ifm.liu.se*), L. Hultman, Linköping University, Sweden

Enhanced toughness in hard and superhard thin films is a primary requirement for present day ceramic hard coatings, known to be prone to brittle failure during *in-use* conditions, in modern applications. Based on the successful approach and results obtained for TiN- and VN-based ternary thin films [1,2], we expand our Density Functional Theory (DFT) investigations to TiAlN-based quaternary thin films. $(\text{TiAl})_{1-x}\text{M}_x\text{N}$ thin films in the B1 structure, with $0.06 < x < 0.75$, are obtained by alloying with $\text{M} = \text{V}, \text{Nb}, \text{Ta}, \text{Mo}$ and W , and results show significant ductility enhancements, hence increased toughness, in these compounds. Importantly, these thin films are also predicted to be hard/superhard, with similar and/or increased hardness values, compared to TiAlN. For $(\text{TiAl})_{1-x}\text{W}_x\text{N}$ these results have experimentally been confirmed recently [3]. The general, electronic mechanism responsible for the ductility increase is rooted in the enhanced occupancy of $d\text{-}t_{2g}$ metallic states, induced by the valence electrons of substitutional elements (V, Nb, Ta, Mo, W). This effect is more pronounced with increasing valence electron concentration (VEC), and, upon shearing, leads to the formation of a layered electronic structure, consisting of alternating layers of high and low charge density in the metallic sublattice. This unique electronic structure allows a selective response to tetragonal and trigonal deformation: if compressive/tensile stresses are applied, the structure responds in a "hard" manner by resisting deformation, while upon the application of shear stresses, the layered electronic arrangement is formed, bonding is changed accordingly, and the structure responds in a "ductile/tough" manner as dislocation glide along the $\{110\}\langle 1\text{-}10 \rangle$ slip system becomes energetically favored [2]. The findings presented herein open new avenues for the synthesis of hard, yet tough, ceramic coatings, by tuning the VEC of alloying elements to optimize the hardness/toughness ratio in relevant applications.

[1] D. G. Sangiovanni *et al.* *Al. Phys. Rev. B* **81** (2010) 104107.

[2] D. G. Sangiovanni *et al.* *Al. Acta Mater.* **59** (2011) 2121.

[3] T. Reeswinkel *et al.* *Al. Surf. Coat. Technol.* **205** (2011) 4821.

11:20am **B7-1-11 Bridging atomic structure with properties in III-Nitride heterostructures**, Komninou (*komnhnroy@auth.gr*), Aristoteles University of Thessaloniki, Greece

INVITED

New III-Nitride technology involves 1 -, 2- and 3-dimensional (nanowires, quantum wells, quantum dots) nanostructures as the building blocks of emerging novel photonic and electronic device applications. This technology, although one of the most "environment-friendly" available in the market is still far from being mature and hence devices are far from their intrinsic limits. Much more research efforts are needed to address materials related issues which are the bottleneck against the rapid advances of these

emerging fields. State-of-the-art transmission electron microscopy (TEM) along with the associated spectroscopies comprise the key techniques for the structural characterisation of these heterostructured materials systems down to the atomic scale and it should be interactively combined with computational design and modeling of structures, defects and properties.

Materials issues encountered by TEM involve: a) An atomic-scale investigation of interfacial and defect structures, b) Understanding of defect introduction mechanisms and related phenomena. c) Local strain field and chemistry d) Electronic structure of defects and interfaces.

In this presentation, examples will be presented in which an hierarchical integrated multiscale framework is employed comprising high resolution TEM (HRTEM), quantitative HRTEM (qHRTEM), analytical methods provided in the scanning TEM (STEM) such as energy dispersive X-ray spectroscopy (EDX) and high-angle-annular-dark-field (HAADF) or Z-contrast imaging combined with computational modeling. Results of empirical interatomic potential simulations and density functional theory (DFT) calculations will illustrate modeling of the energetically favorable defect/interface structures and electronic properties. Image simulations using the resulting models for correlation with the corresponding experimental HRTEM images will be also shown.

Acknowledgment: Support under the FP7 Project DOTSSENSE (Grant No. STREP 224212) is gratefully acknowledged.

Fundamentals and Technology of Multifunctional Thin Films: Towards Optoelectronic Device Applications

Room: Tiki Pavilion - Session C2-3/F4-3

Thin Films for Photovoltaics and Active Devices: Synthesis and Characterization

Moderator: T. Terasako, Graduate School of Science and Engineering, Ehime University, Japan, M. Cremona, Pontificia Universidade Católica do Rio de Janeiro, Brazil

8:00am **C2-3/F4-3-1 The I-V transfer characteristics of a-IGZO TFTs deteriorated owing to the copper diffusion in the process of the source/drain metal**, *H.L. Chiu, Y.H. Tai (yhtai@mail.nctu.edu.tw), L.S. Chou, C.M. Li*, National Chiao Tung University, Taiwan

Abstract—

In this work, the influence of copper on amorphous type Indium-Gallium-Zinc-Oxide (a-IGZO) thin-film transistor's (TFTs) transfer curve is studied. The source/drain of a-IGZO TFTs are made in the structures of Cu / Ti and Ti/Al/Ti. The I_D - V_G curves of those TFTs are compared and the results show that the copper deteriorates the performance of the TFTs. It is attributed to the presence of the copper in the channel region of the device, which is verified by SIMS analysis. A Cu-dipping experiment is conducted by dipping devices into the solution of CuSO_4 and the deteriorated I_D - V_G curves are also observed. The simulation of IV curve's degradation is realized through ATLAS device simulator produced by Silvaco, Inc which helps us understand that what kind of trap Cu ions formed in IGZO during the conventional BCE process used in a-Si TFT.

8:20am **C2-3/F4-3-2 Light-accelerated instability mechanism depending on bias and environment in amorphous Indium-Gallium-Zinc-Oxide Thin Film Transistors**, *Y.C. Chen (oa_ccc@hotmail.com)*, National Sun Yat-Sen University, Taiwan

The bias and environment dependence on the light-accelerated instability of amorphous indium-gallium-zinc-oxide thin film transistors is examined in this study. The experiment result shows the electrical characteristic degradation of devices is not monotonously relying on the charge trapping mechanism for different negative gate bias under illumination. It is also implicated the adsorbent gas species upon surrounding environment (atmosphere, oxygen, moisture and vacuum). During negative gate bias under illumination in oxygen or atmosphere ambient, the negative shift in electrical characteristic is suppressed comparing to the result in vacuum. Thus, a physical model is proposed for transiting dominant mechanisms from photon-created carrier trapping mechanism to adsorbed/desorbed gases phenomenon.

8:40am **C2-3/F4-3-3 Suppressed Temperature-dependent Sub-threshold Leakage Current of amorphous Indium-Gallium-Zinc-Oxide Thin Film Transistors by Nitrous Oxide Plasma Treatment**, *G.W. Chang (b922030049@gmail.com)*, National Chiao Tung University, Taiwan, *Y.E. Syu*, National Sun Yat-Sen University, Taiwan

N_2O plasma treatment suppressed the temperature-dependent sub-threshold leakage current of amorphous indium-gallium-zinc-oxide thin film transistors (a-IGZO TFTs). The transfer curve exhibits abnormal sub-threshold leakage current at high temperature. The abnormal electrical properties are explained by the energy band diagrams at both forward and reverse sweep. Above 400K, the hole could be generated from trap-assisted transition and drift to the source side that induced the source barrier lowering. The source side barrier lowering enhances electrons injection from the source to channel and causes an apparent sub-threshold leakage current. This phenomenon only appears in the device without N_2O plasma treatment, but not in the device with N_2O plasma treatment, which is experimentally verified. The results suggested that the density of states for a-IGZO with N_2O plasma treatment is much lower than that for without plasma treatment. The N_2O plasma treatment repairs the defect to suppressed temperature-dependent sub-threshold leakage current.

9:00am **C2-3/F4-3-4 Investigating of Negative Bias Stress Induced Temperature-Dependence Degradation for InGaZnO TFTs under Dark and Light Illumination**, *M.C. Chen (iro926@gmail.com)*, *T.C. Chang, S.Y. Huang, M.H. Wu*, National Sun Yat-Sen University, Taiwan, *K.H. Yang*, University of Toronto, Canada, *M.C. Yang, T.C. Chen, F.Y. Jian*, National Sun Yat-Sen University, Taiwan

The Negative Bias Stress (NBS) with varying temperature induce instability under dark and illumination environment was investigated in this study. The experiment result indicates that the tendency of negative threshold voltage (V_T) shift increase gradually as the temperature increasing during negative bias temperature stress (NBTS) under dark. This phenomenon of electrical property imputes that the thermal disturbance induces the carriers released from weak bond between metal and oxygen in the IGZO film during the NBTS. In addition, the negative bias temperature stress under light illumination (NBTIS) exhibits unusual stretch-out of the subthreshold swing and obvious negative V_T shift, which dependence of the temperature during NBTIS. The recovery characteristics exhibits the V_T can be recovery to initial, but the unusual stretch-out of the subthreshold swing (S.S) still exists. The stretch-out of the S.S is induced by the defect generated in the interface between gate insulator and active layer near the S/D region. On the other hand, the obvious negative V_T shift is attributed to the hole trapping in the interface between gate insulator and active layer during NBTIS. Hence, the V_T can be recovered to the initial state by the hole de-trapping. Moreover, this work also employs the capacitance-voltage measurement in variation frequency further clarify the mechanism of degradation behaviors.

9:20am **C2-3/F4-3-5 Optimising OLED devices for solid state lighting applications using optical spectroscopy**, *P. Monkman (a.p.monkman@durham.ac.uk)*, Durham University, UK **INVITED**

To fully understand the complex electrical and optical properties of an organic light emitting device, it has been critical to develop new tools to probe working devices, in this way we can capture the photophysics of excitons generated by charge recombination and their subsequent decay. Most important is the role of the 'non-emissive' triplet excitons which are the dominant exciton thus created. In my talk I will describe the various time resolved laser spectroscopies and electro-optic techniques we use and the key insights into the photophysics of OLEDs that we have discovered which have changed the way we understand these devices and point to new materials and device architectures for ever higher efficiencies. I shall focus on the role of triplet fusion, the process of light generation from two annihilating triplet excitons and how the triplet exciton population can generate between 15 to 37 % of the total electroluminescence output of a device without the use of phosphorescent dopants. This has very important ramifications for device lifetime as blue phosphorescent dopants place severe limitations of achievable lifetime and device performance.

10:00am **C2-3/F4-3-7 New rare-earth quinolate complexes for organic light-emitting devices**, *H. Camargo, M. Cremona (cremona@fis.puc-rio.br)*, Pontificia Universidade Católica do Rio de Janeiro, Brazil, *T. Paolini, H. Brito*, Universidade de São Paulo, Brazil

The tris(8-hydroxyquinoline) aluminum Alq_3 is one of the most famous and widely used organic material because of its thermal and morphological stability and its optical and electrical properties. Alq_3 is used as an electron transporting layer, as well as emitting layer in organic light-emitting devices (OLEDs). The study of potential substitutes for this coordination compound plays an important role in organic electronics. In this work, the investigation on new rare-earth tetrakis quinolate complexes presenting similar properties to that of Alq_3 compound was performed. The 8-hydroxyquinoline is commonly used as ligand because of its excellent

complexing properties with a large number of transition metal ions, including the rare-earth ions. However, the complexes formed in this case are tris complexes and are not very stable. On the other hand, the inclusion of one more quinoline group stabilizes the compound. Here, $\text{Li}[\text{RE}(\text{q})_3]$ complexes ($\text{RE}^{3+} = \text{La}^{3+}, \text{Lu}^{3+}$ and Y^{3+}) were synthesized in our laboratories and then used as electron transporting and emitting layer in OLEDs. The organic thin films were deposited in high vacuum environment by thermal evaporation onto quartz and silicon substrates, at a base pressure of 2.0×10^{-3} Pa and with a 0.1 nm/s deposition rate. The optical characterization of the RE-complexes showed emission in the range 510–525 nm, the same observed in the Alq_3 spectra, while the absorption was observed in different wavelengths: 382 nm for Y/La-complexes and 388 nm for Lu-complex. The OLEDs were fabricated with indium tin oxide layer (ITO) as anode, NPB as hole transporting layer (25 nm), $\text{Li}[\text{RE}(\text{q})_3]$ as both electron transporting and emitting layer (40 nm), and aluminum as cathode (120 nm). The electroluminescence (EL) spectra presented a broad band from 520 to 540 nm and exhibited green color emission related to the 8-hydroxyquinoline ligand without intramolecular energy transfer from quinoline to RE^{3+} ions. Moreover, in the EL spectra was also observed an interesting dependency between the maximum energy peak position and the half-width of emission band with the atomic radius of the RE ion used. For the fabricated OLED, the best luminance result was achieved to $\text{Li}[\text{Y}(\text{q})_3]$ complex, with a maximum luminance of 30 cd/m^2 taken at 11 V and with a current of 2 mA. The results obtained for our devices are comparable with similar devices based on Alq_3 , presenting similar optical and electrical properties.

10:20am **C2-3/F4-3-8 Effect of the deposition process and substrate temperature on the microstructure defects and electrical conductivity of thin Mo films**, *H. Köstenbauer* (*harald.koestenbauer@plansee.com*), Plansee SE, Austria, *D. Rafaja*, *U. Mühle*, *G. Schreiber*, TU Bergakademie Freiberg, Germany, *M. Kathrein*, *J. Winkler*, Plansee SE, Austria

Thin molybdenum films are commonly used as back electrodes in $\text{Cu}(\text{In,Ga})\text{Se}_2$ thin film solar cells and as contact material for thin film transistors/liquid crystal displays. For these applications, high electrical conductivity of the films is essential. As it follows from the classical Drude theory of the electrical conductivity in metals, all microstructure defects are in principle acting as scattering centres for electrons. Consequently, the microstructure defects increase always the electrical resistance of the material, but their “scattering cross sections” for electrons are supposed to differ strongly. In our study, we quantified the effect of point defects, dislocations and grain boundaries on the electrical resistivity of molybdenum films having a constant thickness of 500 nm.

The kind and density of the microstructure defects in the Mo films were modified by applying different physical vapour deposition methods (DC magnetron sputtering, pulsed DC magnetron sputtering and RF magnetron sputtering) and by depositing the thin films at different deposition temperatures (room temperature, 150°C, 250°C and 350°C). As expected, the electrical resistivity of the Mo films, which was measured using a 4-point probe, decreased with increasing substrate temperature. Furthermore, the highest resistivity was observed in RF magnetron sputtered samples, where also the effect of the substrate temperature was most pronounced.

The microstructure of the thin films was characterised by using a combination of glancing angle X-ray diffraction (GAXRD), X-ray reflectivity (XRR), XRD pole figure measurement, scanning electron microscopy with electron back scattered diffraction (SEM/EBSD) and transmission electron microscopy (TEM). GAXRD revealed residual stresses, stress-free lattice parameters, crystallite size and microstrain in the molybdenum films. XRR together with SEM and TEM gave information about the morphology of the films; this information was complemented by texture measurements performed using XRD and EBSD. The stress-free lattice parameters were used as a measure of the density of point defects, the microstrain as a measure of the dislocation density and the crystallite and grain size as a measure of the distance between the grain boundaries. The kind of the grain boundaries was deduced from the mutual orientation of crystallites. It was concluded that the point defects have the highest impact on the electrical conductivity of physical vapour deposited molybdenum thin films, followed by dislocations, and grain and crystallite boundaries.

10:40am **C2-3/F4-3-9 Study of the electrical performance of rf magnetron sputtered TiO_2 source and CuO drain split gate transistor**, *S. Gopikishan*, *P. Laha*, *A.B. Panda*, *P.K. Barhai*, Birla Institute of Technology, India, *A.K. Das*, *Bhabha Atomic Research Center*, India, *I. Banerjee*, *S.K. Mahapatra* (*skmahapatra@bimtesra.ac.in*), Birla Institute of Technology, India

We have fabricated split-gate field effect transistor based on $\text{Si}/\text{Al}_2\text{O}_3$ substrate. TiO_2 thin film (n-type) used as source, CuO thin film (p-type) as drain and platinum thin film as gate of the transistor. The separation between the two platinum gates was $\sim 0.1 \mu\text{m}$ and confirmed by Scanning Electron Microscope (SEM). The crystallinity of the Al_2O_3 , TiO_2 and CuO

films was confirmed by the GIXRD. Resistance (R_s), conductance (G), and I-V measurement of the split-gate field effect transistor were performed by Impedance analyzer and source meter respectively. The field effect on the transistor current was studied by applying different bias voltage between the splitting gate thin films of platinum. It was found that the conductance and current were varied in a quantized step of $2e^2/h$ with varying gate voltage. The Shubnikov-de Haas effect in channel resistance (R_c) vs B at different reverse bias of the transistor was also studied.

11:00am **C2-3/F4-3-10 Characteristics and photocatalytic reactivity of TiO_2 beads synthesized using a microwave-assisted hydrothermal method**, *W. Wu* (*wanyu@mdu.edu.tw*), *Y. Tsou*, *S. Huang*, MingDao University, Taiwan

In this study, a two-step process involving sol-gel and microwave hydrothermal techniques are used to synthesis a novel TiO_2 structure, so called as TiO_2 beads. It exhibits the required characteristics for photocatalysis such as large surface area and well anatase crystallinity. Various synthesis parameters were investigated to evaluate the proper processing window of TiO_2 beads such as the complex amount in the sol-gel process, temperature and heating time in the microwave hydrothermal process. It was found that microwave hydrothermal techniques can much reduce the process time and the size of TiO_2 nanocrystalline. The texture and morphology of obtained nanoporous TiO_2 beads were examined using scanning electron microscopy (SEM) and transmission electron microscopy (TEM). The crystalline phase was analyzed using x-ray diffractometer (XRD) and Raman spectroscopy. The surface chemical bonding state was examined using x-ray photoelectron spectroscopy (XPS). The specific surface, pore diameter and pore volume of beaded TiO_2 was examined using BET. UV-visible diffuse reflectance spectra were achieved using a UV-visible spectrophotometer. The photocatalytic reactivity was obtained by degradation the Methylene blue.

11:20am **C2-3/F4-3-11 Effect of growth parameters and annealing on some properties of sputtered ZnO thin films**, *R. Chander* (*rcohri@yahoo.com*), GPC Bhikhiwind, India

ZnO thin films were deposited by RF magnetron sputtering technique onto silicon (001) and fused quartz substrates. The X-ray diffraction studies revealed (002) plane oriented growth of ZnO nano-grains. Grain size and surface roughness analysis performed onto AFM scans showed that av. grain size of film ~ 75 nm and r.m.s. roughness of film ~ 7 nm. The effect of oxygen partial pressure during deposition was studied. Optical studies revealed $\sim 12\%$ increase in transmittance in the visible range for thin films grown in oxygen partial pressure than films grown without oxygen during deposition. Films exhibited direct optical band gap ~ 3.2 to 3.37 eV for films grown at different oxygen partial pressure as obtained from transmittance data. The observed change in optical band gap is corroborated with compositional analysis that showed deficiency of oxygen in ZnO matrix, which decreases for films grown at higher oxygen partial pressure. Refractive index and extinction coefficient was calculated by fitting the spectroscopic ellipsometry data obtained for 0.5 oxygen partial pressure film. Post deposition annealing of thin films in ambient environment led to surface reconstruction and change in the morphology of grains along with their growth during annealing at higher temperature.

Fundamentals and Technology of Multifunctional Thin Films: Towards Optoelectronic Device Applications

Room: Pacific Salon 3 - Session C4-1

Transparent Conductive Films: Inorganic Oxides, Organic Materials, Metals

Moderator: P. Kelly, Manchester Metropolitan University, UK, S. Lim, Lawrence Berkeley National Laboratory, US

8:00am **C4-1-1 ZnO films deposited from a filtered cathodic vacuum arc: characterization and device applications**, *J.G. Partridge* (*jim.partridge@rmit.edu.au*), *E.H. Mayes*, *M.R. Field*, *D.G. McCulloch*, RMIT University, Australia, *H-S Kim*, *R. Heinhold*, *S. Elzwawi*, *G.C. Turner*, *R.J. Reeves*, *M.W. Allen*, University of Canterbury, New Zealand

Existing applications for zinc oxide thin films include transparent electronic devices, transparent conducting electrodes and ultraviolet photonics. Deposition methods such as molecular beam epitaxy and pulsed laser deposition are normally required to achieve films with sufficient quality for electronic device applications. Unfortunately, these methods typically incur high cost and provide limited scalability. The filtered cathodic vacuum arc (FCVA) deposition technique offering both low cost and high throughput is routinely employed to produce aluminium doped ZnO for degenerate

transparent conducting layers. However, the potential for this technique to produce large area, low-defect ZnO films for electronic devices has largely been overlooked.

We report on the structural, optical and electrical characteristics of ZnO films deposited on a-plane sapphire substrates by FCVA. These films exhibit desirable properties including high transparency, moderate intrinsic carrier concentrations ($10^{17} - 10^{18} \text{ cm}^{-3}$), Hall mobility up to $10 \text{ cm}^2/\text{Vs}$ and low surface roughness (with RMS values typically $<5\%$ of the film thickness). These properties can be further improved after annealing the deposited films in oxygen at elevated temperatures. Schottky diodes featuring AgO_x and IrO_x anodes formed on annealed FCVA grown ZnO films exhibit low ideality factors (<1.20) and high rectification ($\sim 10^6$). Subsequent production of ZnO MESFET (metal semiconductor field effect transistor) devices with excellent characteristics and yield confirm the potential of these films for electronic device applications.

Since the interface regions within the Schottky diodes and MESFETs are crucial to their performance, cross-sectional transmission electron microscopy (TEM) and electron energy loss spectroscopy (EELS) have been used to study the microstructure and composition of IrO_x/ZnO Schottky barriers. These barriers were formed by reactively pulsed-laser-depositing IrO_x onto single crystal ZnO wafers. EELS showed that Zn could be found within the IrO_x anode in a region extending up to 10 nm from the interface. This strongly suggests that zinc diffuses across the device interface during the deposition of the anode, leading to the creation of Zn vacancies (acceptors) in the ZnO sub-interface region. Evidence also existed for oxygen passivation near the interface, probably resulting from the presence of active oxygen during the pulsed-laser-deposition process.

8:20am C4-1-2 Filtered cathodic arc deposited ZnO:Al assisted by a high-flux low-energy constricted gas plasma source, S. Lim (sunnielim@lbl.gov), R. Mendelsberg, Lawrence Berkeley National Laboratory, US, N. Friederichsen, RWTH Aachen University, Germany, Y.K. Zhu, Harbin Institute of Technology, China, K.M. Yu, A. Anders, Lawrence Berkeley National Laboratory, US

Metal oxides are a class of materials playing an increasingly important role in opto-electronic devices, solar cells, low emissivity windows and many other applications. Aluminum doped zinc oxide (AZO) has been identified as an especially promising material due to its great abundance and the low cost of its constituting elements. In previous work we have shown that cathodic arc deposition of AZO resulted in high quality material with resistivities in the mid to low $10^{-4} \Omega \text{ cm}$ and mobilities as high as $60 \text{ cm}^2 \text{ V}^{-1} \text{ s}^{-1}$ [1], comparable to the more expensive indium tin oxide (ITO). To further assist the deposition process by ionization of the gas, we have incorporated a constricted plasma source which is a special kind of glow discharge plasma generator characterized by its simple design and a low kinetic energy of the downstream ions [2]. Preliminary results indicate that increasing the current (or equivalently power) of the constricted plasma source resulted in an increase of the electron mobility of AZO thin films even when grown at relatively low temperatures, a highly desirable feature critical to promote the broad application of AZO.

[1] R.J. Mendelsberg, S.H.N. Lim, Y.K. Zhu, J. Wallig, D.J. Milliron, A. Anders, J. Phys. D-Appl. Phys. 44/23 (2011).

[2] A. Anders, M. Kuhn, Rev. Sci. Instrum. 69/3 (1998) 1340.

8:40am C4-1-3 The material challenges in oxide electronics: Recent progress in oxide films for electronic applications, B. Szyzka (bernd.szyzka@ist.fraunhofer.de), Fraunhofer IST, Germany, C. Elsaesser, FhG-IWM, Germany, B. Malic, JSI, Slovenia, G. Kiriakidis, FORTH, Crete, L. Pereira, R. Martins, UNINOVA, Portugal, K. Gehrke, Osram, Germany, N. Young, Phillips Research, UK, V. Lambertini, Fiat CRF, Italy, U. Weimar, EKUT, Germany

INVITED

The backbones of the current microelectronics industry are components based on Si semiconductors. Modern data processing and telecommunications almost exclusively relies on the use of these single crystalline materials while amorphous or polycrystalline films are used in large scale for TFT devices, for example in flat panel displays. Large sectors of global industry are engaged in their production, further processing and application. However, the perspectives for further developments are limited since the constraints of the material such as non-availability for flexible devices; optical opacity and need for high temperature processing are obvious. The emerging class of oxide semiconductors is able to overcome many of those restrictions, especially because some of them can be prepared as thin (transparent) films under comparatively moderate conditions.

Within this paper, we give an overview on the status of our current research in the framework of the large-scale integrated European research project "Orama" on metal oxides for electronic applications. We utilize a holistic approach starting with first principle materials modelling and ending with certified materials for the main applications indium free oxide TFTs, oxide

based "CMOS" devices, advanced chemical sensors and advanced LEDs. A detailed overview on the current state of the research will be presented.

9:20am C4-1-5 Enhanced stability performance for Ga-doped ZnO films by indium co-doping, H.-P. Song (song.huaping@kochi-tech.ac.jp), H. Makino, N. Yamamoto, T. Yamamoto, Research Institute, Kochi University of Technology, Japan

Ga-doped ZnO (GZO) is a promising electrode for use in flat display panels and thin film solar cells. Electrical and optical properties of GZO films are comparable to Sn-doped In_2O_3 (ITO) films. The environmental stability of GZO is an interesting and crucial research topic for practical applications. For a 150-nm-thick or thicker GZO film deposited on glass substrates, it is easy for the variation in electrical resistivity before and after reliability test for 500 h under the condition of 60°C and 95% relative humidity (RH) to be less than 10%. To date, achieving this stability level has proven to be quite difficult for a 100-nm-thick GZO film. Herein, we report a successful materials design: indium co-doping (GZO:In target: 3 wt% Ga_2O_3 and 0.25 wt% In_2O_3) gives a solution to the crucial issue. The 100-nm-thick GZO:In films were deposited on glass substrates at 200°C by ion plating with direct current arc-discharge under various oxygen gas flow rates (from 0 to 25 sccm). All the samples have an average optical transmittance over 83% in the visible and infra-red regions ranging from 450 to 1200 nm. The reliability test results show that the stability performance is enhanced for GZO:In films. With the oxygen flow rate of 15 sccm, the 100-nm-thick GZO:In film has a resistivity of $4.24 \times 10^{-4} \Omega \text{ cm}$, carrier concentration of $6.37 \times 10^{20} \text{ cm}^{-3}$ and Hall mobility of $23.1 \text{ cm}^2 \text{ V}^{-1} \text{ s}^{-1}$. The variation in resistivity before and after the reliability test is 7.8%, which is much better than the case without indium co-doping. Room temperature Hall measurement results show that, as oxygen flow rate increased, the carrier concentration in GZO:In film was monotonic decreased, while the Hall mobility had a maximum and resistivity had a minimum in the oxygen flow rate range from 10 to 15 sccm. The role of indium co-doped in GZO film on film stability should be further investigated.

This work was supported by New Energy and Industrial Technology Development Organization (NEDO) under the National Project of Rare Metal Indium In Substitute Materials Development.

9:40am C4-1-6 Temperature dependence of electrical properties in polycrystalline Ga-doped ZnO films deposited on oxide nanosheet seed layer, H. Makino (makino.hisao@kochi-tech.ac.jp), Kochi University of Technology, Japan, T. Shibata, National Institute for Materials Science, Japan, H.-P. Song, N. Yamamoto, Kochi University of Technology, Japan, T. Sasaki, National Institute for Materials Science, Japan, T. Yamamoto, Kochi University of Technology, Japan

Ga-doped ZnO (GZO) is one of promising candidates as transparent electrodes in optoelectronic devices. It is well known that resistivity of GZO strongly depend on their film thickness. However, key parameters, which dominate the thickness dependence, has not been understood yet [1]. Recently, nanosheet seed layers were proposed to control crystal orientation of polycrystalline films on amorphous substrates [2]. By using nanosheets with two dimensional hexagonal lattices, we can control c-axis orientation and lateral crystalline size of GZO films. In this paper, we report temperature dependence of Hall effects in polycrystalline GZO films deposited on glass substrates with and without the nanosheet seed layer.

The GZO films with thickness between 30 and 350 nm were deposited by ion-plating with direct current arc discharge. The Hall effect measurements were performed in temperature range from 11 to 300 K. The resistivity of GZO films at room temperature rapidly decreased with the increase of thickness up to 100 nm. With further increasing the thickness, the resistivity gradually decreased. These observations were common for both of GZO films deposited with and without the nanosheet. In the temperature dependence, the GZO films thicker than 100 nm showed metallic behavior, that is, the resistivity increased with increasing the temperature. While, the GZO films with thickness of 40 nm showed minimum resistivity at around 80 K. The resistivity decreased with increasing the temperature up to 80 K, then turned to increase with further increasing the temperature. This anomaly was caused by increase of carrier concentration with the increase of temperature. The increase in carrier concentration can be attributed to thermal delocalization from some localized states possibly exist in such thin films. For the GZO films with thickness of 100 nm, the carrier concentration was nearly independent on the temperature as expected in degenerate semiconductors. On the other hand, the Hall mobility decreased with increasing the temperature for all the samples. The observation suggests that phonon scattering dominate the temperature dependence of the Hall mobility. The Hall mobility at the lowest temperature should be dominated by static scattering centers such as ionized impurities and some defects. The Hall mobility at the lowest temperature monotonously increased with increasing the film thickness over the range studied here. The variation of the Hall mobility showed strong correlation with the degree of c-axis orientation.

[1] T. Yamada et al., Appl. Phys. Lett. 91, 051915 (2007); J. Appl. Phys. 107, 123534 (2010).

[2] T. Shibata et al., Adv. Mater. 20, 231 (2008).

10:00am **C4-1-7 Optical and Electrical Characterization of Ga-doped ZnO Thin Films Grown by Atmospheric Spray Pyrolysis**, *K. Yoshino* (*t0b114u@cc.miyazaki-u.ac.jp*), *N. Kamiya*, *M. Oshima*, University of Miyazaki, Japan

ZnO attracts attention as a substitute of indium tin oxide because ZnO is a low cost and abundant material. ZnO has shown promise for many applications including gas sensors, transport electrodes, piezoelectric devices, varistors and surface acoustic wave devices. Its direct optical bandgap of 3.4 eV at room temperature is wide enough to transmit most of the useful solar radiation in ZnO/CuInSe₂ based solar cells. Furthermore, ZnO is a good candidate to substitute for ITO (In-doped In₂O₃) and FTO (F-doped SnO₂) in transparent conductive electrodes. Many techniques have been employed to produce the ZnO thin films including molecular beam epitaxy, metal organic chemical vapor deposition, radio frequency magnetron sputtering, spray pyrolysis and sol-gel methods. Furthermore, low temperature growth of ZnO is important for compatibility with photovoltaic device fabrication processes. In our previous work [1], undoped ZnO films on glass substrates were grown by a spray pyrolysis method at room temperature (RT, ~ 300 °C). Polycrystalline ZnO thin films were successfully grown at RT under an air atmosphere. Diethylzinc (DEZ) was used as the Zn source material. The DEZ solution was diluted by some solvent in order to use safely under an air atmosphere. X-ray diffraction indicates that (10-10) and (10-11) peaks are dominant. The lattice constants of the *a* and *c* axes are larger than that of ICDD data. The samples develop a *c* axis (0002) orientation with increasing substrate temperature. Furthermore, the lattice constants of the *a* and *c* axes become closer to those of ICDD data with increasing substrate temperatures. In this work, growth of Ga-doped ZnO/PET film using DEZ solution was carried out by spray pyrolysis at 150°C. The average transmittance of undoped and Ga-doped ZnO films showed 80%. The sheet resistivity of Ga-doped ZnO decreased to 50 W/sq. by UV irradiation for 120min.[1] *K. Yoshino*, *Y. Takemoto*, *M. Oshima*, *K. Toyota*, *K. Inaba*, *K. Haga*, *K. Tokudome*, Jpn. J. Appl. Phys. **50** (2011) 040207.

10:20am **C4-1-8 Investigation of different techniques for achieving optimal p-type doping in transparent conductive zinc oxide by a metal-nitride codoping approach**, *A. Poppleton*

(*alice.poppleton@sydney.edu.au*), *M. Bilek*, *D. McKenzie*, University of Sydney, Australia, *S. Lim*, Lawrence Berkeley National Laboratory, US, *B. Abendroth*, TU Bergakademie Freiberg, Germany

Transparent conducting oxides (TCOs) are a crucial component of many modern technologies. The demand for transparent conductors is high and rapidly growing. The most common TCO used in these technologies is ITO. Unfortunately indium is rare, expensive, toxic and particularly difficult and environmentally damaging to extract. Additionally, TCOs based on the indium-tin system are unavoidably n-type, limiting their usefulness as only transparent metal-imitators.

An extremely promising alternative TCO is ZnO, which is more abundant in several regards. Zinc is a cheap, abundant, environmentally friendly and benign element, making processing and disposal much easier and safer. Unlike ITO, ZnO can theoretically be an ambipolar semiconductor, leading to potential applications in transparent electronics, photocatalysis and, owing to its ~2.4 eV band gap, UV LEDs. However, it is notoriously difficult to achieve p-type doping in ZnO.

In this paper we will discuss a range of techniques for the deposition of intrinsic ZnO thin films and the subsequent chemical modification of a highly transparent ZnO film to achieve p-type doping. This will serve as a foundation for a highly transparent p-type material. We will compare magnetron sputtering with cathodic arc plasma deposition. In addition, we will discuss a novel deposition technique which uses a high-frequency plasma in a magnetron sputtering system.

We also investigate codoping as a way to achieve p-type doping. Due to its similarity to oxygen, low toxicity, and abundance, N is a popular candidate for p-type doping in ZnO. It is widely recognised that doping with N alone is ineffective, due to poor solubility of the dopant and depth of the acceptor level within the band. To overcome both of these problems, a metal-nitride codoping approach has been suggested, improve nitrogen solubility and build up the valence band edge, solving the acceptor depth problem. Recently, Duan et al. (PRB 83, 2011) have performed first-principles DFT calculations which indicate that TiN may surpass the popular AlN and GaN as a codoping material, due to the exceptional stability of the TiN₄ complex in ZnO. It may also be more efficient, as each TiN₄ cluster should act as a double acceptor.

To date, achieving an excess of available nitrogen relative to metal dopant has been a significant experimental stumbling block for all codoping approaches. We examine methods to enhance available nitrogen in the deposition plasma. In particular, we report on the degree of N incorporation

from regular DC magnetron sputtering plasma, compared with injection of gas at the target in HiPIMS and DC arc depositions, as well as the effect of ICRF plasma ionisation of the gas upon injection near the substrate.

10:40am **C4-1-9 Electrical Transport in ZnO and ZnMgO Films: A Comparison**, *K. Ellmer* (*ellmer@helmholtz-berlin.de*), *A. Bikowski*, *T. Welzel*, Helmholtz-Zentrum Berlin für Materialien und Energie, Germany

INVITED

Zinc oxide belongs to the material class of transparent conductive oxides (TCO) which is both of scientific as well as technical interest, due to the fact that TCO layers are used on a large scale for transparent electrodes in many technical fields: flat panel displays, low emissivity glass coatings [1], organic light emitting diodes (OLEDs) or thin film solar cells [2]. TCOs are degenerately doped ($N \gg 10^{19} \text{ cm}^{-3}$) n-type compound semiconductors with wide bandgaps ($E_g > 3 \text{ eV}$) and low resistivities in the range of 10^{-4} to $10^{-3} \Omega \text{ cm}$ [3]. For its application as transparent electrodes they have to be highly conductive and transparent at least in the visible spectral range. The electron density N in ZnO is limited to about $1.5 \cdot 10^{21} \text{ cm}^{-3}$. Higher dopant (electron) concentrations are not possible due to the formation of secondary phases of the dopant and the host atoms. One goal is therefore to achieve a low resistivity $\rho = (eN\mu)^{-1}$ by maximizing the mobility μ of the electrons. The carrier transport in single-crystalline TCO semiconductors at such high carrier concentrations is limited by ionized impurity scattering [4]. For the application as transparent electrodes, however, polycrystalline TCO films have to be used, which exhibit additional scattering processes: grain boundary scattering and scattering at other crystallographic defects, further reducing the electron mobility. ZnO alloys, like $\text{Zn}_{1-x}\text{Mg}_x\text{O}$, are of scientific interest, since the addition of other elements changes the band gap. With respect to electrical transport, the so-called alloy scattering has to be taken into account. In this paper the electrical transport in epitaxial and polycrystalline ZnO and ZnMgO films is compared. For the film deposition, magnetron sputtering as a well-known large-area deposition method is used. Since in magnetron sputtering high-energetic negative ions (for instance O⁻) occur, which can introduce crystallographic defects or interstitial oxygen atoms, special emphasis is given to the radial variation of the electrical properties and its correlation to the bombardment of the films by negative ions. For this purpose, radially resolved ion distribution functions of negative oxygen ions and other species at a growing film were measured, both for new and eroded targets.

[1] J. Szczyrbowski, G. Bräuer, M. Ruske, H. Schilling, A. Zmely, Thin Solid Films 351 (1999) 254.

[2] K. Ellmer, A. Klein, B. Rech (Eds.), Transparent Conductive Zinc Oxide: Basics and Applications in Thin Film Solar Cells, Springer, Berlin, 2008.

[3] T. Minami, MRS Bull. 25/8 (2000) 38.

[4] K. Ellmer, R. Mientus, Thin Solid Films 516/30 May (2008) 4620.

11:20am **C4-1-11 Study of reactively Co-sputtered Sb-Sn oxide**, *G. Ding* (*gding@intermolecular.com*), *M. Le*, *F. Hassan*, *Z. Sun*, *M. Ngugen*, Intermolecular Inc, US

Sb-Sn oxide (ATO) thin film was generated by reactively co-sputtered PVD process on a flat glass. The film was characterized as the Sb contents and annealing temperature, by transmission, reflection, absorption, resistivity, film thickness, refractive index *n* and *k*, XRD, carrier density/mobility and their gradience. The mechanism of those gradience are discussed

An ellipsometry method was developed to determine the ATO film carrier density and gradience. There are some reports on the resistivity evaluation based on the Drude model through ellipsometer measurements. However, the uniqueness of the model fitting is poor in many conditions, (many values could fit the model, so that no unique value could be precisely determined). In theory: Tauc-Lorentz and Drude could give good description of the band-gap and free carrier physics of the ellipsometry spectra. The reason of poor uniqueness value in model fitting lies in that the measurement data content is not enough to uniquely determine physical parameters; thus the simulation will face uniqueness issue for the solution.

How to increase the measurement data content is a key to improve the uniqueness of the simulation. Multiple angles did not help much on this data content issue. The transmission and reflection spectra measurements were helpful at some cases. However, the uniqueness is still poor in many other cases in our ATO film study. Here we presented a new method that combined resistivity measurement into modeling, instead of simulating resistivity ρ . Thus, this method increases measurement data content, so it significantly improved the uniqueness of the solution in the modeling; thus, through Drude model relationship, the carrier density and mobility of the ATO film could be uniquely determined.

The gradience profile simulation is widely used for ellipsometry simulation, combined with the above method, the gradience of carrier density and mobility can be estimated. In comparison of Hall probe measurements, two

methods provide similar carrier density and mobility, but the former here could provide gradience information.

In this study we will present the absorption, n , k , resistivity, carrier density, scattering time, mobility trend with Sb content varied in Sb-Sn oxide, and we give interpretations of those observations. The trend for annealing temperature effects was presented and discussed.

The gradience of the carrier density and mobility in ATO film will be presented, and this gradience will be discussed through the oxygen vacancy model.

11:40am **C4-1-12 Investigation of p-type conducting Cu-Al-O mixtures**, C. Schulz (christina.schulz@ist.fraunhofer.de), C. Balmer, B. Szyszka, Fraunhofer IST, Germany

P-type conductive TCOs like delafossite type CuAlO_2 films can open the way to transparent electronics when combining them with well-established n-type TCOs. So, it is necessary to investigate into this relatively young field of materials to get an understanding of the basics of the preparation route.

The authors report on experiments on Cu-Al-O-mixtures with compositions slightly deviating from the delafossite stoichiometry CuAlO_2 .

Thin films of $\text{Cu}_x\text{Al}_y\text{O}_z$ are prepared by RF-magnetron-cosputtering at room temperature. The stoichiometry is influenced by different sputtering parameters and controlled via lambda-probe setup. After preparation, the films are annealed in inert gas atmosphere at different temperatures. Depending on the film stoichiometry, the annealed films show different TCO properties: They are either transparent or opaque in the visible spectrum. They are either p-type, n-type or non-conducting. And they are crystallized in different phases. So, the preparation way for p-type CuAlO_x is narrow but can be controlled very well.

A matrix will be shown that sums up the experiments and results. Different (narrow) pathways to gain p-type conductive Cu-Al-O-thin films are suggested and implemented into that preparation-route matrix.

Tribology & Mechanical Behavior of Coatings and Engineered Surfaces

Room: Pacific Salon 1-2 - Session E1-2

Friction Wear Lubrication Effects & Modeling

Moderator: Lopez, CSIS-University Sevilla, S. Aouadi, Southern Illinois University, US, V. Fridrici, Ecole Centrale de Lyon, France, O.L. Eryilmaz, Argonne National Laboratory, US

8:00am **E1-2-1 Friction induced evolution of mechanical properties of engineered surfaces**, T. Liskiewicz (t.liskiewicz@leeds.ac.uk), J. Kubiak, Leeds University, UK

Metallic materials subjected to alternating sliding tend to generate a specific transformed layer on the top surface. This layer, called a Tribologically Transformed Structure (TTS), has a particular nanocrystalline structure corresponding to the chemical composition of the primary material. Under successive sliding cycles TTS is fragmented and a wear scar becomes saturated with debris. Wear debris is then subjected to the progressive oxidation process and, as a result, sliding surfaces are separated by a film of fully oxidized particles. In this paper, evolution of mechanical properties of metallic substrates and coated systems induced by fretting wear is investigated. Friction process is related to the dynamics of TTS formation and successive surface damage. Nanoindentation measurements of damaged surfaces allows to correlate evolution of mechanical properties of materials with tribological degradation process. Hardness and elastic modulus are mapped within the contact area showing distinctive behavior of tested materials. Evolution of fretting wear volume is compared with changes in mechanical properties of tested materials. The obtained results are discussed in relation to coated systems design process.

8:20am **E1-2-2 Frictional Behavior of Silver Nano-pattern Fabricated by Thermal Dewetting**, H.-J. Kim, D.E. Kim (kimde@yonsei.ac.kr), Yonsei University, Republic of Korea

Thermal dewetting of metallic thin films is a relatively simple and effective method to create uniform nano-scale patterns on solid surfaces. Nano-patterns formed by this method have been utilized for various applications such as catalysts to grow carbon nanotubes, etch masks for fabrication of nano/micro patterns and friction reduction films. Generally, it has been known that reduction of real contact area is advantages to decrease adhesion

and frictional force. In this regard, fabrication of nano-pattern is one of the ways to make the real contact area smaller than a flat and smooth film.

In this study, Ag thin film of about 20 nm in thickness was deposited on Si wafer by RF sputtering. Then, annealing was conducted in a vacuum chamber for 1 hour. Different annealing temperatures from 250 to 550°C were applied to assess the effects of temperature on the film morphology. As a result, circular shaped Ag nano-patterns were formed on the Si wafer by thermal dewetting mechanism. As expected, the morphology of the Ag nano-pattern varied with respect to the annealing temperature.

Experiments were carried out to assess the frictional behavior using the Ag nano-patterned specimens. Friction tests were performed using an atomic force microscope (AFM) with a modified cantilever. A micro-sized sphere was attached to the cantilever to increase the contact region compared with the normal sharp probe tip to investigate the effect of contact area between the nano-pattern and the counter surface. Both initial and steady state frictional forces were measured. It was found that the frictional force of nano-patterned specimens was significantly lower than the smooth Ag thin film. Moreover, there was an optimum annealing temperature that resulted in the lowest frictional force. The effect of contact area on the frictional force was also assessed based on the experimental results and contact analysis.

ACKNOWLEDGEMENT

This work was supported by the National Research Foundation of Korea (NRF) grant funded by the Korean government (MEST) (No. 2011-0000409).

8:40am **E1-2-3 Scaling effects between micro- and macro-tribology for a Ti-MoS₂ coating**, P. Stoyanov, R. Chromik

(richard.chromik@mcgill.ca), H. Strauss, McGill University, Canada

Molybdenum disulfide coatings, doped with metals such as Au or Ti, exhibit good tribological properties over a wide range of environmental conditions and contact pressures. For macroscopic contact sizes (order of 10 – 100 microns), solid lubrication, friction reduction and wear resistance are accomplished by the formation of thin, stable transfer films (order of 10 – 100 nm in thickness). Recent studies in the literature have proposed the use of MoS₂ coatings for micro-electromechanical systems (MEMS), such as gears and switches, and therefore increased the demand for investigating microscale contacts (order of 0.1 - 10 microns) on these coatings. The goal of this work was to provide a direct comparison between the tribological performance of a Ti-MoS₂ coating at the two length scales. A 'real time' study of the transfer film behavior and velocity accommodation modes (VAMs) at the macro-scale was conducted with an *in situ* tribometer, while on the micro-scale, transfer films were analyzed *ex situ* on the counterface by means of atomic force microscopy. Higher friction was observed with microtribology compared to macrotribology and was attributed to, in some cases, different velocity accommodation modes as compared to macroscopic scales. For dry sliding, the behavior of microscopic contacts on Ti-MoS₂ deviates only slightly from macroscopic results, showing higher limiting friction and microplowing. For humid sliding, microscopic contacts deviate significantly from macroscopic behaviour, showing plowing behaviour and absence of transfer films.

9:00am **E1-2-4 Mechanisms responsible for compositional variations of films sputtered from a WS₂ target**, E. Sarhammar

(erik.sarhammar@angstrom.uu.se), J. Sundberg, H. Nyberg, Uppsala University, Angstrom Laboratory, Sweden, T. Kubart, The Angstrom Laboratory, Uppsala University, Sweden, S. Jacobson, U. Jansson, T. Nyberg, Uppsala University, Angstrom Laboratory, Sweden

Transition metal dichalcogenides (TMDs) such as WS₂ are well-known for their layered structure and solid lubricant properties. However, beside low friction, a solid lubricant coating must also have a long wear life in order to perform well in a tribological situation. Thus, by adding carbon to the material the mechanical properties can be improved. However, when using a magnetron sputtering process, the resulting thin films are found to be sub-stoichiometric with respect to sulphur. This is due to a number of different effects; take-off angle, scattering, different sticking coefficients and energetic particle bombardment of the substrate.

In this work we have used a non-reactive magnetron sputtering process to see how these effects affect the resulting film stoichiometry, and hence the tribological properties. This was done by changing the process pressure, DC-RF power, the location of the substrate (in and off axes) and by adding carbon to the material. Also, a newly developed Monte Carlo computer model is presented which makes it possible to simulate and predict how these changes will affect the resulting film stoichiometry.

Simulations and experiments alike show that by reducing the energetic particle bombardment of the substrate, the S/W ratio increases. Tribological evaluation of the films concludes that an increasing S/W ratio is beneficial as it decreases the coefficient of friction of the films.

9:20am **E1-2-5 Tribological characteristics of carbon nitride synthesized using MW-PCVD.** *I. Tanaka* (s0721210PM@it-chiba.ac.jp), Graduate School, Chiba Institute of Technology, Japan, *Y. Sakamoto*, Chiba Institute of Technology, Japan

Carbon nitride has fascinating properties such as high hardness and high current density of field emission and so on. In addition, if α -C₃N₄ or β -C₃N₄ structure can be synthesized, it is possible to obtain high hardness exceeding that of diamond. Authors tried to obtain crystalline carbon nitride, crystalline deposits were obtained from a CH₄-N₂ reaction gas system using microwave plasma CVD. On the other hand, it has been reported that the friction coefficient of amorphous carbon nitride (CN_x) was lower than 0.01 in N₂ atmosphere. However, tribological characteristics of crystalline carbon nitride were not cleared. So, investigation was carried out on the tribological characteristics of crystalline carbon nitride synthesized using MW-PCVD.

Carbon nitride was synthesized using microwave plasma CVD. The mixture of CH₄-N₂ gas was used as a reaction gas. CH₄ flow rate was varied from 1 to 3 SCCM, and N₂ flow rate was fixed to 100 SCCM. Synthesis pressure was fixed to 4.0 kPa, and microwave power was fixed to 200 W. Reaction time was fixed to 3h. Si was used as the substrate. Surfaces of the deposits were observed using SEM. The deposits were estimated by Raman spectroscopy, AES, and XPS. Tribological properties of the deposits were estimated by using a ball-on-disk friction tester. Measurements are conducted by using of load 0.1N, speed of sliding 6.2mm/s and counterpart materials SUJ2 or Si₃N₄ 4.7mm in diameter, respectively. Wear properties of the deposits were estimated by using of a surface roughness tester.

As a result of SEM observation, crystalline deposits similar to the rods of hexagonal were observed for all conditions. The particle size was increased with increasing of CH₄ flow rate. From AES estimation, the peaks of C, N, O, and Si were observed in AES spectra of each sample. N₂ content was increased with increasing of CH₄ flow rate. From XPS measurement, C-N bond and Si₃N₄ were observed in XPS spectra of each sample. The lowest coefficient about 0.51 against SUJ2 was obtained for deposits synthesized in CH₄ flow rate 3 SCCM in the estimation of tribological properties. And the lowest coefficient is about 0.41 against Si₃N₄ for deposits synthesized in CH₄ flow rate 1 SCCM. As a result of estimation of wear depth, wear depth was decreased with increasing of CH₄ flow rate.

As a conclusion, tribological characteristics of crystalline carbon nitride synthesized using MW-PCVD were depended on N₂ content of the deposits.

9:40am **E1-2-6 The Role of Planar Defects in Achieving Low Friction and Wear in Lubricious Oxide Coatings.** *V. Ageh, H. Mohseni, T. Scharf* (scharf@unt.edu), The University of North Texas, US

This presentation will discuss how defect structure in atomic layer deposited ceramic coatings (transition metal oxides and in situ formed carbides) determines the thermal/oxidative and friction/wear properties in cellular solids, such as carbon-based composites and foams. Specifically, we will discuss (a) how interstitial carbide and oxide phases, such as ZrC and ZrO₂, provide thermal and oxidation resistance to carbon, and (b) how lubricious, nanocrystalline layered ceramics, such as high basal stacking fault density ZnO, and low crystallographic shear, oxygen deficient Magnéli phases, such as TiO_{2-x}, mitigate friction and wear. Two important questions will be addressed: (1) Can the coating systems be processed with thermodynamically and kinetically stable oxide and carbide phases and interfaces? (2) How will the defect structure (planar stacking faults and vacancies/interstitials) of these phases be able to accommodate interfacial shear while providing sufficient hardness and elastic modulus?

10:00am **E1-2-7 Structure and properties of nanocomposite DLC coatings on hard and soft substrates.** *J.T. DeHosson* (j.t.m.de.hosson@rug.nl), University of Groningen, Netherlands **INVITED** Combined HR-XTEM and nanoindentation investigations were carried out to study the deformation behavior and toughening mechanism of DLC films deposited by pulsed DC magnetron sputtering on hard substrates (steel) and soft substrates (rubber). In case of nc-TiC/a-C(:H) nanocomposite films the nanocomposite structure evolves from a multilayer structure with a wavelength of about 10 nm to uniform nanograins with increasing Ti contents. Depth sensitive nanoindentations revealed excellent toughness with significantly suppressed cracking tendency while maintaining high hardness. These results will be compared with DLC coatings on viscoelastic substrates like rubber and focusing on the nature of the coefficient of friction (CoF). The relative importance of the various contributions, e.g. viscoelastic and adhesive contributions to the overall friction will be discussed.

10:40am **E1-2-9 Synthesis and Tribological Behavior of MoS₂-Au Nanocomposite Films.** *R. Goeke* (rsgoeke@sandia.gov), Sandia National Laboratories, US, *T. Scharf*, The University of North Texas, US, *P. Kotula, S. Prasad*, Sandia National Laboratories, US

Robust solid lubricant coatings are needed to survive humid oxidizing environments in many applications. The addition of dopants to MoS₂ films has been previously shown to enhance the lubricant durability [Acta Mater., 58 Scharf et al.]. This study focuses on the synthesis of Au doped MoS₂ nano-composite thin films created by co-sputter deposition as a function of temperature. The ratio of the deposition flux was adjusted to control the composition to about 10% Au by weight. (Scanning) transmission electron microscopy (S)TEM revealed that the room temperature deposited nanocomposite consisted of 2-4 nm size Au particles in a matrix of semi-crystalline MoS₂. With increasing growth temperatures, the nano-composite exhibited dramatic structural changes: the Au nanoparticles coarsened by diffusion-driven Ostwald ripening to 5-10 nm size and the MoS₂ basal planes encapsulated the Au nanoparticles thereby forming a novel solid Au core MoS₂ nano-onion like structures. In comparison, a room temperature deposited film was heated, post deposition, to 600°C inside a TEM. *In situ* TEM heating revealed that Au nanoparticles also coarsened, but unlike heating during film growth, the highly ordered basal planes with reactive edge sites did not encapsulate the Au. This suggests that MoS₂ surface diffusivity and energy during film growth is different than MoS₂ bulk diffusion where the thermal activation energy for diffusion is likely smaller in the latter. Friction and wear measurements were made using a ball-on-disk tribometer in air with 50% RH. The role of these novel structures on the tribological behavior of the films in humid environments will be discussed.

Sandia National Laboratories is a multi-program laboratory managed and operated by Sandia Corporation, a wholly owned subsidiary of Lockheed Martin Corporation, for the U.S. Department of Energy's National Nuclear Security Administration under contract DE-AC04-94AL85000

11:00am **E1-2-10 Electrodeposited of gold-multiwalled carbon nanotube to improve lubrication of composite films.** *P.-A. Gay* (pierre-antoine.gay@he-arc.ch), Haute Ecole ARC Ingenierie, Switzerland

Gold-multiwalled carbon nanotube (MWCNT) composite films were elaborated by electrodeposition and co-deposition of CVD process. Tribological properties were investigated by a pin-on-disk type friction testing using an electronic system to measure in same time the electrical conductivity of the composite coatings.

Friction coefficient of gold-MWCNT composite films decreased with increasing MWCNT content. Implantation of MWCNT on the surface, plating parameters, MWCNT concentration and the stirring rate of the bath were systematically investigated in order to find a relationship between incorporation rate *V* and friction coefficient and electrical conductivity. The Au-0.5 mass% MWCNT composite film showed the minimum friction coefficient value of 0.15. In this case, wear resistance of Au-MWCNT is three times better.

11:20am **E1-2-11 A systematic study of superlubricity potential of ta-C coatings.** *V. Weihnacht* (volker.weihnacht@iws.fraunhofer.de), *S. Makowski, G. Englberger, A. Leson*, Fraunhofer IWS, Germany

Hydrogen-free tetrahedral amorphous carbon (ta-C) films are known to display super-low friction behaviour under mixed lubrication conditions in combination with specific polyalcohols. There is a huge interest to use this effect for technical application in order to reduce friction loss e.g. on engine components or gears and using environmentally friendly lubricants at the same time. Although there are some tribological investigation and first approaches to explain the phenomenon there is still a lack of comprehensive data and understanding of superlubricity behaviour of ta-C.

In this contribution, ta-C coatings with different sp³-contents deposited by laser-arc evaporation were investigated by oscillating ball-on-disk tribometry at different temperatures. For lubrication, glycerine, glycerolmonooleate, glycol, and other OH-containing lubricants were tested in order to find out the chemical origin of the superlubricity effect. By systematic variation of testing conditions a critical temperature and a kick-in behaviour for superlow-friction effect was observed depending on sp³-content and lubricant type. A significant influence of lubricant type on wear behaviour was found which does not correlate with friction behaviour. Besides experimental friction and wear data, analytical investigation of friction surfaces helped to understand some experimental findings.

11:40am **E1-2-12 The wear resistance of boride layers in the four-ball lubricant test.** *E. Garcia-Bustos, M.A. Figueroa-Guadarrama, G.A. Rodriguez-Castro, E. Gallardo-Hernandez, I. Campos-Silva* (icampos@ipn.mx), Instituto Politecnico Nacional, Mexico

This study evaluated the wear resistance of FeB/Fe₂B layers applying the four-ball lubricant test. First, the boride layers were obtained at the surface

of AISI 52100 steels by developing the powder-pack boriding method. The treatment was carried out at a temperature of 1223 K with 1 h of exposure. The boriding of AISI 52100 steels results in the formation of a superficial flat front growth of FeB/Fe₂B layers with a total layer thickness of 72 microns. In addition, the hardness at the surface of borided steels was 1900 HV.

The four-ball lubricant tests were performed in the borided samples (with a surface roughness of 0.043 microns) and unborided steels with a surface roughness of 0.025 microns considering dry and lubricant conditions. The wear resistance of borided and unborided steels in the dry condition was estimated by three different loads of 49, 98 and 147 N with a constant speed and time test of 1200 rpm and 150 s, respectively. For the case of the lubricated condition, the borided and non-borided steels were exposed to applied loads of 147 and 392 N according to the ASTM D4172 standard using commercial SAE 15W40 engine oil. For all cases, the friction coefficients of borided and unborided steels were monitoring by a full bridge load cell, and the temperature was sensed through a thermocouple in real time during the four-ball lubricant test. The wear scar diameter and the wear scar surfaces of the AISI 52100 borided and non-borided steels in both experimental conditions were measured using an optical microscope and scanning electron microscopy (SEM) to understand the wear mechanisms involved.

Considering the dry condition, the results of the friction coefficient showed that the presence of boride layers at the surface of AISI 52100 steels denote solid lubricating features, where this characteristic is increased in lubricant conditions as a function of the different applied loads.

New Horizons in Coatings and Thin Films

Room: Sunset - Session F2-1

High Power Impulse Magnetron Sputtering

Moderator: D. Lundin, Université Paris-Sud 11, France, J. Sapieha, Ecole Polytechnique de Montreal, Canada, R. Bandorf, Fraunhofer Institute for Surface Engineering and Thin Films IST, Germany

8:00am **F2-1-1 Energetic aspects of thin film growth in HiPIMS and in other pulsed plasmas.** *L. Martinu* (lmartinu@polymtl.ca), *J. Capek*, *M. Hala*, *O. Zabeida*, *J.E. Klemberg-Sapieha*, École Polytechnique de Montréal, Canada

INVITED

The microstructure and the resulting properties of coatings and thin films strongly depend on the growth mechanism which in turn is closely related to the energetic aspects of surface reactions during the material's synthesis. It has been accepted that the microstructural evolution of films grown in ionized and plasma environments can be well described in terms of the ion energy and ion flux, or specifically, in terms of the "universal parameter: the energy per deposited atom".

Film growth, while under ion bombardment, leads to growth-related effects such as interfacial atom mixing, high surface mobility (diffusion) of deposited species, resputtering of loosely bound species, and deep penetration of ions below the surface, leading to the displacement of atoms (forward sputtering or knock-in effects). The energy and flux of ions can generally be controlled, to different levels of selectivity, by the use of ion beams, by surface biasing, and by the control of plasma density. Compared to more traditional PECVD and PVD techniques (including DC, pulsed DC, and medium-, radio- and microwave frequency discharges), there has been a lot of progress in generating very dense plasmas in pulsed discharges, more recently in High Power Impulse Magnetron Sputtering (HiPIMS). The latter technique offers a unique possibility to obtain films from a high flux of highly ionized materials.

In this presentation, we will critically evaluate the energetic aspects of the film growth in HiPIMS plasmas, and compare the resulting film characteristics with those obtained by other techniques. Examples will include hard protective coatings (conductive or partially conductive), as well as optical (generally non-conductive) coatings. We will review different strategies for the control of the deposition process, and discuss various effects related to the pulse management, to the suppressions of hysteresis, and to the magnetic field configuration at the target surface.

8:40am **F2-1-3 Unique Property of Our Brand New Technology Based On High Power Pulse Sputtering.** *S. Hirota*

(hirota.satoshi@kobelco.com), *K. Yamamoto*, Kobe Steel Ltd., Japan, *R. Cremer*, KCS Europe GmbH, Germany

We introduce a brand new technology based on High Power Pulse Sputtering at industrial scale. The New Technology is a magnetron

discharge process like conventional sputtering, however, momentarily input power is approximately ten times higher in magnitude. Conventional magnetron sputtering is a low current - high voltage discharge and the ionization rate of the target material is quite low, usually in the order of a few percent and the plasma is mainly consisting of gas ions. On the other hand the New Technology realized stable operation with high current - high voltage discharge with high ionization rate of the target material and high deposition rate compared to conventional sputtering. This unique property is characterized by controlling pulse shape of input power, this means the film property generated by the New Technology can be modified with great flexibility.

In this study, we analyzed film property by changing coating condition and compared with another coating process. For example, different types of nitride coatings including standard TiAlN were deposited by industrial arc ion plating (AIP), unbalanced magnetron sputtering (UBMS) and New Technology. TiAlN coatings deposited by the New Technology process show strong preferred (111) orientation and a relatively high hardness up to 35 GPa. Whereas AIP TiAlN coatings are characterized by a moderate hardness up to 30 GPa and (200) or nearly random orientation at an equivalent substrate bias condition. High magnification image of cross sectional TEM observations of both coatings revealed that many lattice defects can be observed for the New Technology coating and is hardened by many atomic defects, possibly highly stressed as a consequence.

In the presentation, a comparison between AIP, UBMS and the New Technology coating by different power supply, arc source and deposition conditions will be shown, not only from property of the coating but also from industrial perspective such as productivity.

9:00am **F2-1-4 Influence of pulse shape and peak current on the resulting properties of Ti-Si-C composite films deposited by HIPIMS.** *R. Bandorf* (ralf.bandorf@ist.fraunhofer.de), *M. Scholtalbers*, *G. Bräuer*, Fraunhofer IST, Germany

In recent years the interest in ternary systems, especially so called M_{n+1}AX_n phases has grown. This interest is motivated by the exceptional structural, electrical, and mechanical properties of these materials. Besides several investigations of DC sputtered Ti₃SiC₂ Alami et al. reported on HIPIMS deposition. The film structure was reported being columnar, both in dc and HIPIMS. While the HIPIMS films obtained a dense structure, the dc films were rough and porous. This paper shows that with HIPIMS deposition even a featureless glassy structure can be realized, depending on the deposition parameters. XRR measurements showed that by using HIPIMS with target current density of approx. 0.5 A/cm² a film density of 4.5 g/cm³, correlating with the bulk value was reached. Furthermore, the resulting structure and properties (electrical and mechanical) depending on the used pulse shape during deposition are discussed.

9:20am **F2-1-5 Highly ionized carbon plasmas for the growth of diamond-like carbon thin films with magnetron sputtering.** *A. Aijaz*, *K. Sarakinos*, *D. Lundin*, *U. Helmersson* (ulfhe@ifm.liu.se), Linköping University, Sweden

The physical vapor deposition methods, characterized by highly ionized deposition fluxes of the film forming species, provide added means for the synthesis of tailor-made materials. Cathodic arc and pulsed laser deposition are examples of such discharges where electron densities in the order of 10²¹ m⁻³ can be obtained. These techniques, while providing a very high degree of ionization of the deposition flux, often exhibit several drawbacks, such as macroparticle ejection from the target, lack of lateral film uniformity, and difficulty to scale up. Magnetron sputtering based techniques are technologically interesting, owing to their inherent advantages of conceptual simplicity, scalability, and film uniformity. However, electron densities in magnetron discharges are significantly smaller, in the range of 10¹⁴-10¹⁶ m⁻³ and therefore generation of a highly ionized deposition flux is often difficult. This difficulty is overcome by high power impulse magnetron sputtering (HiPIMS), where plasma densities on the order of 10¹⁹ m⁻³ are achieved. HiPIMS has been successful in enhancing the ionization for most common metals (Cu, Al, Ta, Ti), but it is challenged by C. Previous investigations have shown that C⁺/C ratio in HiPIMS does not exceed 5% [1]. In the present study we address the low degree of C ionization by increasing the electron temperature of the plasma. This is achieved in the HiPIMS discharge by using Ne as sputtering gas instead of Ar. It resulted in an energetic C⁺ ion population with a three-fold increase in the total number of C⁺ ions as compared to a conventional HiPIMS process. The enhanced ionized fraction of carbon facilitates the growth of carbon films with mass densities as high as approx. 2.8 g/cm³ as determined by high resolution x-ray reflectivity measurements.

[1] B.M. DeKoven, P.R. Ward, and R.E. Weiss, D.J. Christie, R.A. Scholl, W.D. Sproul, F. Tomasel, and A. Anders, Proceedings of the 46th Annual Technical Conference Proceedings of the Society of Vacuum Coaters, May 3-8, 2003, San Francisco, CA, USA, vol., p.158

9:40am **F2-1-6 Characterization of hard coatings deposited by HIPIMS system and their cutting performance.** *T. Sasaki* (*tomoya_sasaki@hitachi-tool.co.jp*), Hitachi Tool Engineering, Ltd., Japan
High Power Impulse Magnetron Sputtering (HIPIMS) has been of interest over the past decade owing to its ability to ionize sputtering materials at higher ionization energy. It is possible to modify coating properties in ways which are not easily possible with DC sputtering due to the higher ionization of HIPIMS. Therefore, HIPIMS technology is expectedly applicable in the field of hard coatings for cutting tools. The aim of this work is to study the effect of deposition parameters of coatings applied by HIPIMS and to study its applicability in the field of cutting tools.

In this study, bias voltage during coating was investigated in details. In the same regard, chemical composition, morphology and crystal structure of coatings were analyzed using Electron Probe Micro Analyzer (EPMA), Scanning electron microscope (SEM) and X-Ray Diffraction (XRD) under different deposition parameters. Furthermore, cutting tests were made with different deposition parameters. The coatings made by HIPIMS system showed better cutting performance than the coatings made by DC sputtering showing good possibility of application in the field of cutting tools.

10:00am **F2-1-7 Properties of $Ti_{1-x}Al_xN$ films grown by HIPIMS and in hybrid HIPIMS-DCMS configuration: a comparative study.** *G. Greczynski* (*grzgr@ifm.liu.se*), *J. Lu*, *J. Jensen*, Linköping University, Sweden, *M. Johansson*, Seco Tools AB, Linköping University, Sweden, *I. Petrov*, *J.E. Greene*, University of Illinois at Urbana-Champaign, US, *W. Kölker*, *O. Lemmer*, CemeCon AG, Germany, *L. Hultman*, Linköping University, Sweden

Metastable cubic structure $Ti_{1-x}Al_xN$ alloy thin films are grown in an industrial scale coating unit by high-power pulsed magnetron sputtering (HIPIMS or HPPMS) using segmented Ti-Al targets. The properties of resulting films are analyzed and compared to layers grown from elemental Al and Ti targets using a hybrid approach in which HIPIMS was combined with dc magnetron sputtering (DCMS). All films are analyzed by x-ray diffraction, scanning electron microscopy, transmission electron microscopy, elastic recoil detection analysis, and nanoindentation. Ion fluxes at the substrate position are determined using in-situ mass spectroscopy. Hardness of $Ti_{1-x}Al_xN$ films grown from segmented targets peaks at 31 GPa for AlN concentrations well below $x = 0.6$, above which it stays low around 20 GPa. Residual stresses determined by $\sin^2\psi$ analyses are compressive and high, reaching -4 GPa at $x = 0.50$ for a Si substrate. Relaxed cubic lattice parameters $a_c(x)$, obtained from θ - 2θ scans acquired at the strain-free tilt angle ψ^* , decreases monotonically with increasing AlN concentration up to $x = 0.58$, corresponding to a kinetic solubility limit of AlN in TiN. Comparison to $Ti_{1-x}Al_xN$ alloys grown in a hybrid configuration with either Al or Ti target operated in HIPIMS mode (Al-HIPIMS/Ti-DCMS or Ti-HIPIMS/Al-DCMS, respectively) reveals that properties of purely HIPIMS films obtained from segmented targets are better than in the case of Ti-HIPIMS/Al-DCMS films and worse than for Al-HIPIMS/Ti-DCMS films. These results fully support our recent assessment [1] concerning the detrimental role of Ti^{2+} ions, created in large concentrations during HIPIMS operation of the Ti target, which upon application of a mild substrate bias lead to creation of residual defects, high compressive stresses, and precipitation of hexagonal AlN phase

[1] *Selection of Metal Ion Irradiation for Controlling $Ti_{1-x}Al_xN$ Alloy Growth via Hybrid HIPIMS/Magnetron Co-sputtering*, G. Greczynski, J. Lu, M. P. Johansson, J. Jensen, I. Petrov, J.E. Greene, and L. Hultman, Vacuum 2012, in press.

10:20am **F2-1-8 ($Cr_{1-x}Al_x$)N: A Comparison of Direct Current, Middle Frequency Pulsed and High Power Pulsed Magnetron Sputtering for Injection Molding Components.** *K. Bobzin*, *N. Bagcivan*, *S. Theiss* (*theiss@iot.rwth-aachen.de*), Surface Engineering Institute - RWTH Aachen University, Germany

In 2006 nearly 245,000 kt of plastics products were produced by means of extrusion and injection molding. Due to rapidly increasing demands on individualized products, higher process stability and lower amounts of rejects new material concepts have to be developed. For this reason coatings for extruder components and injection molding tools deposited by physical vapor deposition (PVD) have come under scrutiny. Cr-Al-N based coating systems have shown good properties regarding corrosion as well as wear resistance especially against adhesion of plastics melt. Another challenge is the complex geometry of injection molding tools. High power pulse magnetron sputtering (HPPMS) offers new possibilities to adapt the thickness uniformity as well as the mechanical and chemical properties of the coatings. This paper deals with the development of Cr-Al-N based coatings by using three different PVD technologies. On the one hand conventional direct current (DC) magnetron sputtering ion plating (MSIP) is used. On the other hand middle frequency pulsed (MF) MSIP and HPPMS are used. The aluminum content of the $(Cr_{1-x}Al_x)N$ coatings was varied in

the range of 5 at-% and 77 at-%. Morphology, mechanical properties and phase composition were analyzed. It can be shown that the sputter rate of aluminum is increased by using HPPMS compared to DC and MF. This leads to an increase of the deposition rate from 1.32 $\mu m/h$ at 13 at-% Al to 1.67 $\mu m/h$ at 76 at-% while the deposition rates of the DC and MF variants show a drop from about 2.45 $\mu m/h$ to 1.3 $\mu m/h$. Nevertheless, mechanical analyses show an advantage of HPPMS for aluminum contents below 30 at-% and an advantage of MF and DC for higher aluminum contents. For all variants the formation of hex-AlN can be seen at an Al content of about 60 at-%. Due to a higher degree of ionization phase analyses show a preferred 200 orientation by using HPPMS compared to isotropic phase formation by using DC and MF. In addition the surface free energy of the coatings and the adhesion energy to some common plastics by means of contact angle measurements as well as the thickness uniformity on complex parts were quantified.

10:40am **F2-1-9 Structure evolution in $TiAlCN/VCN$ nanoscale multilayer coatings deposited by reactive High Power Impulse Magnetron Sputtering technology.** *P. Hovsepian* (*p.hovsepian@shu.ac.uk*), *A. Ehiastian*, *G. Kamath*, Sheffield Hallam University, UK, *I. Petrov*, University of Illinois at Urbana-Champaign, US

2.5 micron thick $TiAlCN/VCN$ coatings were deposited by reactive HIPIMS process. XTEM showed gradual evolution of the coating structure with thickness. The initial structure is nanoscale multilayer with sharp interfaces. This transforms into nanocomposite of $TiAlCN$ and VCN nanocrystalline grains surrounded by C-rich tissue phase and finally changes to an amorphous carbon rich Me-C phase. In contrast deposition in similar conditions using standard magnetron sputtering produces a well defined nanoscale multilayer structure. Compositional depth profiling by AES showed that the carbon content in the HIPIMS coating gradually increased from 27% at the coating substrate interface to 35% at the top thus supporting the TEM observation. Energy- resolved mass spectrometry revealed that HIPIMS plasma is a factor of 10 richer in Carbon ions and therefore more reactive as compared to the plasma generated by standard magnetron discharge at similar conditions. The peculiar structure evolution in HIPIMS is discussed in relation to target poisoning effect and carbon outward diffusion during coating growth.

11:00am **F2-1-10 Structure and properties of thick CrN/AlN multilayer coatings deposited by the hybrid modulated pulsed power and pulsed dc magnetron sputtering.** *J. Lin* (*jlin@mines.edu*), Colorado School of Mines, US, *W. Sproul*, Reactive Sputtering, Inc., US, *Z. Wu*, *M. Lei*, Dalian University of Technology, China, *J. Moore*, Colorado School of Mines, US

Modulated pulsed power (MPP) magnetron sputtering and middle frequency pulsed dc magnetron sputtering (PMS) techniques have been used to synthesize thick CrN/AlN multilayer coatings (up to 10 μm). The Cr target was powered by the MPP technique while the Al target was powered by the PMS technique simultaneously in an Ar/N_2 mixture. The bilayer period of the coatings was varied in a range of 10 nm to 2.5 nm by varying the ratio of the N_2 flow rate to the total gas flow rate. The microstructure and properties of the CrN/AlN coatings were characterized using electron probe microanalysis, X-ray diffraction, scanning electron microscopy, transmission electron microscopy, scratch test, nanoindentation, and ball-on-disk wear test. The thick CrN/AlN coatings have been annealed in the ambient air at 900 °C and 1000 °C for 2 hours and at 850 °C for 200 hours. The MPP+PMS CrN/AlN coatings showed good adhesion. Superhardness values of 40-45 GPa and low wear rates in the low $10^{-8} mm^3 N^{-1} m^{-1}$ range have been achieved in the coatings with the bilayer period in a small range of 2.5 to 3.2 nm. No oxides were identified in the coatings and the coating maintained cubic structure after annealing at 1000 °C for 2 hours and at 850 °C for 200 hours.

11:20am **F2-1-11 The uniformity in thickness and microstructure of CrN films fabricated using plasma ion implantation-deposition based on high power pulsed magnetron sputtering.** *X.B. Tian* (*Xiubotian@163.com*), *Z.Z. Wu*, *C.Z. Gong*, Harbin Institute of Technology, China, *P. Chu*, City University of Hong Kong, Hong Kong Special Administrative Region of China

The uniformity in thickness and microstructure of CrN films fabricated using plasma ion implantation-deposition based on high power pulsed magnetron sputtering

Xiubo Tian¹, Zhongzhen Wu¹, Chunzhi Gong¹, Paul. K. Chu²

¹State Key lab of Advanced Welding & Joining, Harbin Institute of Technology, Harbin, China

²Department of Physics & Materials Science, City University of Hong Kong

The high power pulsed magnetron sputtering (HPPMS) has gained more interest due to higher ionization rate. A novel plasma ion implantation

deposition based on high power pulsed magnetron discharge has been proposed in our group (RSI vol. 82, vol. 3, pp. 033511-1 – 033511-5 (2011)). A higher adhesion between the substrate and deposited film is easily achieved. More important multiple combination of high-voltage pulses applied to samples and HMMPS pulses leads to flexible processes including pure ion implantation, deposition assisted by ion implantation and pure deposition. This paper focuses on the uniformity of the thickness of CrN films achieved by plasma based ion implantation using high power pulsed magnetron discharge. The sample bias varied from 10kV to 30kV in addition to a lower bias ($\sim 100V$) test. In comparison, the CrN films were also fabricated using the conventional DC magnetrons sputtering mode in the same facility. The thickness and microstructure at different sites on the exposed surfaces were analyzed. The experimental results demonstrated that the non-uniformity of films by HPPMS was greatly decreased compared to that from the conventional DC mode.

11:40am **F2-1-12 Characterization of chromium and chromium nitride obtained by DC and HiPIMS sputtering techniques**, *A. Ferrec* (axel.ferrec@cnsr-imm.fr), IMN - Nantes, France, *A. Tricoteaux*, *C. Nivot*, LMCPA-Maubuge, France, *F. Schuster*, Laboratoire Commun MATPERF CEA-Mecachrome, France, *M. Ganciu*, National Institute for Laser, Plasma and Radiation Physics, Romania, *P-Y. Jouan*, *A. Djouadi*, IMN - Nantes, France

CrN is an excellent wear and corrosion resistant material. There is much interest in the research community to develop CrN thin films for coating tools for metal and wood machining operations [1,2]. Chromium nitride was widely studied and developed by classical magnetron sputtering [3] and more recently for further improvements by HiPIMS [2,3].

In the frame of this work Cr and CrN thin films have been deposited using both DC and HiPIMS techniques. Two different HiPIMS discharges were used, one is conventional HiPIMS technology [6] and the other one is a new process based on a pre-ionisation system [7]. It allows working with pulses of few microseconds, while remaining in very stable conditions and avoiding the arc formation. The range of the pulse width was varied between 10 and 200 μ s and we have operated with a frequency between 80 and 1000 Hz. Physico-chemical (XPS, AFM, XRD, SEM+EDS) were performed. Structure and properties (especially residual stress) of the films, and aspects of film growth processes and their effects on film properties are discussed. The mechanical properties such as hardness have been characterised by microindentation tests. The Jönsson and Hogmark model [8] was applied to separate the contributions of the substrate and the films in order to determine their true hardness. These hardness results were analyzed and discussed according to the film microstructure.

Keywords

HiPIMS, DC sputtering, Chromium nitride

References

- 1 M.A. Djouadi et al. / Surface and Coatings Technology 116–119 (1999) 508–516
- 2 C. Labidi et al. / Surface & Coatings Technology 200 (2005) 118– 122
- 3 Z.G. Zhang et al. / Vacuum 82 (2008) 501–509
- 4 A.P. Ehasarian et al. / Surface and Coatings Technology 163 –164 (2003) 267–272
- 5 G. Greczynski et al. / Surface & Coatings Technology 205 (2010) 118–130
- 6 V. Kouznetsov et al. / Surf. Coat. Technol., 122 (1999), 290
- 7 M.Ganciu et al, European Patent Appl., No. 4447072.2 / 22.03.2004 (CNRS and Materia Nova)
- 8 B. Jönsson et al. / Thin Solid Films, 1984, 114, 257–269

Tuesday Morning, April 24, 2012

Exhibition

Room: Golden Ballroom - Session EX

Exhibition Keynote

9:40am **EX-1 Rotatable Magnetrons, Today and Tomorrow, R. De Gryse**, Ghent University, Belgium **INVITED**

The continuously increasing demand for a higher quality of life requires the fabrication of products with improved functionality at ever decreasing prices. Moreover, environmental awareness requires that these products are manufactured with so-called “clean“, technologies. These demands have led to a rapid technological progress within the thin film industry. Physical Vapor Deposition (PVD) has been proven able to cope with these requirements, and within the PVD family, magnetron sputtering in all its varieties is probably the best known and most widely spread deposition technology. This success is mainly due to the thin film quality, reproducibility, and flexibility, as well as the scalability of the sputtering process. The concept of magnetron sputtering has been used under many different forms. Probably the best known implementation of magnetically assisted sputtering is to be found in the “classics“ such as in the planar magnetrons, either circular or rectangular. However, magnetically assisted sputtering is also used in many other forms such as inverted magnetrons, cylindrical-post magnetrons, cylindrical hollow cathode magnetrons, facing target magnetrons and rotatable cathode magnetrons. This last variety, the rotatable magnetron, is maybe the least known to the general public but most intensively used in large area coating applications like in web coating and glass coating. In this instance, we will focus on rotatable magnetrons, and their benefits and drawbacks, in addition to their peculiarities. For example, it turns out that in reactive sputtering their behavior is quite different in comparison to a rectangular magnetron of similar dimensions. Also, new trends in rotatable magnetron sputtering will be discussed from a technological point of view, as well as from the viewpoint of market demands.

Tuesday Afternoon, April 24, 2012

Coatings for Use at High Temperature Room: Sunrise - Session A2-2

Thermal and Environmental Barrier Coatings

Moderator: R. Wellman, Cranfield University, UK, D. Litton, Pratt & Whitney, US, R. Trice, Purdue University, US

1:50pm **A2-2-1 Process and Equipment for Advanced Thermal Barrier Coating Systems**, **A. Feuerstein** (albert_feuerstein@praxair.com), C. Petorak, L. Li, T.A. Taylor, Praxair Surface Technologies, Inc., US
INVITED

Hot section components in aero and power generation engines utilize advanced thermal barrier coating systems for life extension and better efficiency. Thermally-sprayed ceramic / bondcoat systems are extensively used for combustors and power generation blades and vanes whereas EBPVD TBC on Pt modified diffusion aluminide coating is the coating of choice for highly stressed airfoils in aero engines. New technologies such as the suspension plasma spray process (SPS) are finding more and more interest for applying TBC's. In addition, challenges such as the trend to low thermal conductivity and CMAS resistant coatings require new compositions, and respective processing technology. The process and coating characteristics of 7wt% YSZ based APS low density and dense vertically cracked (DVC) ZircotTM TBC as well as EBPVD coatings are described, highlighting recent advances with ultra pure Zirconia for improved sintering resistance. New coating compositions for low thermal conductivity TBC's and CMAS resistant TBC's are also addressed. Lastly, the properties of new coating processes such as SPS are compared with conventional coating processes.

2:30pm **A2-2-3 Calcium-Magnesium-Alumino-Silicate (CMAS) degradation of EB-PVD thermal barrier coatings: solubility of different oxides from ZrO₂-Y₂O₃ and ZrO₂-Nd₂O₃ systems in the molten model CMAS**, **N. Chellah**, M.H. Vidal-Sétif (Marie-Helene.Vidal-Setif@onera.fr), Thermal and Environmental Barrier Coatings, France
Thermal barrier coatings (TBCs) are used to protect blades and vanes in the hot sections of gas turbines. They consist of a series of layers: the Ni-based superalloy substrate is coated with an alumina forming metallic bond coat onto which a porous ceramic top coat of yttria partially stabilized zirconia (YPSZ) is deposited. The TBC system allows higher gas temperatures, resulting in enhanced engine efficiency and performance. However, in service, engines ingest dust, sand and ash particles which melt on the hot TBC surface at these high operating temperatures and form calcium-magnesium-aluminosilicate (CMAS) glass deposits. Previous investigations on blades removed from service showed that the molten CMAS penetrates into the open porosity of the top coat. Firstly, upon cooling, the molten CMAS solidifies and the infiltrated TBC becomes rigid. Thus, delamination cracks can develop in the coating leading to progressive TBC spallation during in-service thermal cycling. Secondly, a chemical interaction can take place between the molten CMAS and the TBC leading to the dissolution of the YPSZ TBC in the molten CMAS.

This paper investigates the chemical degradation of an electron beam physical vapor deposited YPSZ TBC by a synthetic model CMAS. The chosen CMAS was the tridymite-pseudowollastonite-anorthite eutectic composition in the ternary (CaO-Al₂O₃-SiO₂) system, melting at 1170°C. The model system has given very good replication of the CMAS corrosion observed on ex-service blades in terms of thermochemical interaction: TBC infiltration, TBC dissolution in the CMAS melt and formation of new crystalline phases.

In order to understand the mechanisms of degradation by dissolution of the YPSZ TBC in the molten CMAS, a method was used which was designed initially to measure the solubility of oxides in a glass. First the solubility of different compositions of the ZrO₂-Y₂O₃ system in the glassy model CMAS was studied at several temperatures, in order to access the dissolution kinetics. The solubility limits and thermodynamic equilibrium constants were determined and possible new crystalline phases were identified. The results enabled to improve the understanding of the mechanisms of the chemical degradation of the YPSZ TBC by the CMAS. In a second part, solubility tests of different compositions of the ZrO₂-Nd₂O₃ system in the same model glass were performed. These allowed selecting a new composition to substitute YPSZ for mitigating CMAS attack. The selected new oxide was tested as a dense ceramic and actually it showed restricted chemical degradation by the model CMAS.

2:50pm **A2-2-4 Bond Coat Cavitation under CMAS-Infiltrated TBCs**, **K. Wessels** (kwessels@engineering.ucsb.edu), University of California, Santa Barbara, US, D. Konitzer, GE Aviation, US, C.G. Levi, University of California, Santa Barbara, US

Turbine airfoils in advanced aircraft turbine engines are protected from the aggressive environment by thermal barrier coating systems (TBCs) comprising an insulating oxide and a metallic bond coat. Environmental contaminants ingested with the intake air form deposits generically known as CMAS (calcium-magnesium aluminosilicates) on the protective coatings. As the deposits melt during the engine cycle a silicate glass forms that infiltrates the porous coating and crystallizes under the imposed thermal gradient, stiffening the TBC and compromising its strain tolerance. Delamination failures have been documented in the past. A new failure mechanism that involves the formation of cavities within the bond coat under regions of the TBC penetrated by CMAS has been identified recently. Examination suggests that cavity formation occurs in regions subject to lateral thermal gradients; channel cracking and scalloping of the TBC are also observed above the bond coat cavities. Once the voids grow large enough to compromise the bond coat, the TBC delaminates and eventually spalls, leaving behind a thermally unprotected airfoil with a residual bond coat. This presentation will discuss the characteristics of this failure mode, and the possible underlying mechanisms.

3:10pm **A2-2-5 Assessing the Delamination Behavior of CMAS Infiltrated TBCs under a Thermal Gradient**, **R.W. Jackson** (rwesleyjackson@engineering.ucsb.edu), E. Zaleski, C.G. Levi, University of California, Santa Barbara, US

With rising operating temperature, the prevalence of calcium magnesium aluminosilicate (CMAS) deposits melting on the surface of thermal barrier coatings (TBCs) used in gas turbines has increased. These molten CMAS deposits infiltrate and crystallize within the pores of the structure, stiffening the penetrated layer and leading to a loss of strain tolerance. The loss of compliance promotes coating delamination when the strain energy generated from the thermal expansion mismatch during thermal cycling reaches a critical level. A laser thermal gradient test (LGT), in which the thermal gradient and cooling rate can be controlled, was used to assess the TBC durability by imposing a range of thermal stresses. Both 7YSZ and gadolinium zirconate (GZO) TBCs, with and without CMAS deposits, were subjected to the LGT. In the absence of CMAS, no microstructural degradation was observed for either composition. When loaded with CMAS, TBC degradation was found to increase with increased cooling rate, and was generally higher for GZO than for 7YSZ, both materials processed by EB-PVD. The CMAS penetration, phase evolution and crack morphology of the thermally cycled TBCs have been characterized as a function of the thermal history and will be analyzed in the context of current delamination models.

This investigation was sponsored by the Office of Naval Research under grant N00014-08-1-0522, monitored by Dr. David Shifler

3:30pm **A2-2-6 CMAS infiltration of YSZ thermal barrier coatings and potential protection measures**, **V. Kuchenreuther** (veronica.kuchenreuther@ict.fraunhofer.de), V. Kolarik, M. Juez Lorenzo, Fraunhofer ICT, Germany, W. Stamm, Siemens Power Generation, Germany, H. Fietzek, Fraunhofer ICT, Germany

Yttria stabilized zirconia (YSZ) thermal barrier coatings (TBC) are widely used to protect the components in the hot area of power generation turbines. One identified cause of TBC failure is the degradation by molten deposits, mostly calcium-magnesium-alumina-silicates (CMAS), which enter the turbine from the environment. It infiltrates the pores and cracks, reacts with the YSZ and leads to its destabilization. The main purpose of the current research is to investigate to which extent the attack by molten CMAS can be reduced by coating the TBC with alumina.

A model CMAS, composed of 38 mol% CaO, 6 mol% MgO, 5 mol% Al₂O₃, 50 mol% SiO₂ and 1 mol% Fe₂O₃, ultra-milled, molten two times for 4 h at 1400°C and milled again, was deposited on the surface of a free standing sample from a commercial APS TBC. The samples were exposed to 1100°C and 1240°C for 50, 100 and 200 hours in air and were analyzed by X-ray diffraction with micro-focus (μ-XRD) and by field emission SEM. Surface scans by μ-XRD stepwise from the unaffected area to the CMAS infiltrated surface area show at 1100°C considerable portions of the monoclinic phase from the first exposure time of 50h. The micrographs however reveal only superficial infiltration. At 1240°C again the phase decomposition is detected already after 50 h and a deep infiltration is observed in the micrographs, almost across the whole TBC.

Depositing an alumina coating on top of the TBC by a novel cost efficient approach a notable reduction of the CMAS infiltration and TBC destabilization was achieved at both 1100°C and 1240°C. The XRD analysis reveals the formation of anorthite, which has a higher melting temperature and leads to a reduction of molten CMAS phases.

3:50pm **A2-2-7 Overview of Environmental Barrier Coatings for Ceramic Matrix Composites**, **K. Lee** (*Kang.N.Lee@rolls-royce.com*), Rolls Royce, US **INVITED**

Silicon carbide (SiC) fiber-reinforced ceramic matrix composites (SiC/SiC CMCs) are the leading candidate for next generation gas turbine engines due to their high temperature capabilities and light weight. High temperature capabilities lead to reduced need for cooling air and therefore higher engine efficiency and reduced fuel consumption. High liner temperature in the combustor is beneficial for reduced emissions. The light weight of CMC components compared to metallic components results in increased engine power density. Unprotected SiC/SiC CMCs, however, have a critical environmental durability issue: they are eroded severely by water vapor in combustion due to water vapor-silica reaction and the resulting volatilization of protective silica scale. Currently the most promising solution to preventing this attack is an external environmental barrier coating (EBC). An EBC physically shields a CMC from water vapor and, thus, is an enabling technology for CMCs. Key components of current EBCs include mullite, barium strontium aluminum silicate (BSAS), and rare earth silicates. This paper will discuss the evolution of EBC from its birth in the early 1990s and the current understanding on key issues for EBC durability and lifing.

4:30pm **A2-2-9 Progress In Depositing Solution Precursor Plasma Spray Thermal Barrier Coatings**, **M. Gell** (*mgell@mail.ims.uconn.edu*), E. Jordan, J. Roth, University of Connecticut, US

The Solution Precursor Plasma Spray (SPPS) process has the potential of providing more durable and low thermal conductivity thermal barrier coatings (TBCs). The increased durability derives from a highly strain-tolerant microstructure consisting of fine, through-coating-thickness cracks and an increased inter-splat crack resistance associated with ultra-fine splats (<2 microns). Low thermal conductivity SPPS TBCs are associated with unique planar arrays of nano- and micro-porosity that are referred to as inter-pass boundaries (IPBs).

Previous University of Connecticut SPPS work has shown inconsistent spallation lives during thermal cycle testing of yttria stabilized zirconia (YSZ) TBCs. For a variety of bond coats, the spallation life of SPPS YSZ TBCs varied from 1.0 to 2.5X air plasma spray YSZ. The key appears to be the initial bond coat oxide formed and whether spallation occurs within the ceramic or at the bond coat to ceramic interface. The longer lives are associated with ceramic (white) failure.

This presentation will discuss the progress made in producing SPPS YSZ TBCs with improved durability. It will also describe SPPS process optimization trials to produce low thermal conductivity YSZ microstructures using IPBs. Success in this effort will extend the use of YSZ TBCs and minimize the use of rare-earth elements required in most alternate low thermal conductivity TBCs.

4:50pm **A2-2-10 Thermoelastic characteristics in thermal barrier coatings with graded layer between the top and bond coats**, **Go, S. Myoung, J. Lee, Y. Jung** (*jungyg@changwon.ac.kr*), S. Kim, Changwon National University, Republic of Korea, U. Paik, Hanyang University, Republic of Korea

Deposition process for thermal barrier coatings (TBCs) exerts a critical influence on the determination of its thermomechanical properties such as elastic modulus, thermal conductivity, and coefficient of thermal expansions. Moreover, failure phenomena usually occur at the interface between the top and bond coats due to the mismatch of mechanical and thermal properties, as TBC system applies to a high operating temperature and cools down to the ambient. In order to reduce the risk of failure a graded layer was created at the interface between the top and bond coats, and thermoelastic behaviors were investigated through mathematical approach. The microstructure of top coat in TBC specimens prepared with TriplexProTM-200 system was controlled by changing the feedstock and using a multiple hopper system, showing the dense/intermediate/porous microstructures from surface to interface or the reverse microstructure. Thermoelastic theory was applied to derive a couple of governing partial differential equations. Since the governing equations are too involved to solve analytically, a finite volume method was developed to obtain approximations. The thermoelastic characteristics of the TBC with graded layer obtained through mathematical approaches coincided with experimental results, and the various analyses may be useful to discover technologies for enhancing the thermomechanical properties of TBCs.

5:10pm **A2-2-11 Stability of Silicates for Environmental Barrier Coatings**, **E. Opila** (*opila@virginia.edu*), University of Virginia, US, N. Jacobson, NASA Glenn Research Center, US **INVITED**

Environmental Barrier Coatings (EBCs) are required for use of SiC-based composites in combustion environments. EBCs prevent volatilization of thermally grown silica scales which occurs via the reaction $\text{SiO}_2 + 2\text{H}_2\text{O(g)} = \text{Si(OH)}_4\text{(g)}$ at high temperatures and high gas velocities. EBCs must be chemically compatible with the SiC/SiO₂ system, must have a good thermal expansion match to SiC, and must be stable in high temperature water vapor to enable long term use of SiC in combustion environments. Binary silicates are promising EBC candidates since they are chemically compatible with the thermally grown silica and often have reasonable thermal expansion matches with the SiC substrate. Thus, an understanding of the stability of binary silicates in high temperature water vapor is key to EBC selection. In this paper, the stability of binary silicates of the form $x(\text{MeO})y(\text{SiO}_2)$ are systematically reviewed for their potential as EBCs. Criteria for identifying potential EBCs include high melting point, formation of compound binary silicate phases, stability of the metal oxide (MeO) towards volatilization, and reduced silica activities in the binary silicate relative to ideal mixture phases. In particular, the thermochemical data for predicting silica activity in the binary silicates is often unavailable and estimates from phase diagrams have been made assuming a regular solution model. Available data for all binary silicates are reviewed and recommendations for promising EBC compositions are made.

Hard Coatings and Vapor Deposition Technology Room: Royal Palm 4-6 - Session B4-1

Properties and Characterization of Hard Coatings and Surfaces

Moderator: J. Lin, Colorado School of Mines, US, C.

Mulligan, U.S. Army ARDEC, Benet Laboratories, US, B.
Zhao, Exxon Mobile, US

1:50pm **B4-1-1 Epitaxial growth of sputtered TiO₂ films on $\alpha\text{-Al}_2\text{O}_3$** , **C. Mitterer** (*christian.mitterer@unileoben.ac.at*), Montanuniversität Leoben, Austria, M. Mühlbacher, Materials Center Leoben Forschung GmbH, Austria, C. Walter, J. Keckes, Montanuniversität Leoben, Austria, M. Popov, J. Spitaler, Materials Center Leoben Forschung GmbH, Austria, C. Ambrosch-Draxl, Montanuniversität Leoben, Austria

Seed layers are often used to control nucleation, phase formation and texture of top layers. Within this work we studied the growth of sputtered rutile TiO₂ layers on $\alpha\text{-Al}_2\text{O}_3$ single crystals with (00.1) orientation, with the goal to illuminate the epitaxial relations between both materials and to determine stable interface structures by ab-initio modeling. Reactive magnetron sputtering from Ti targets in an Ar+N₂ atmosphere has been used; the substrate temperature was set to 770°C and a moderate bias voltage of -50 V has been applied. Films showing the rutile TiO₂ structure with a thickness of 450 nm have been grown. Transmission electron microscopy and pole figure measurements indicated a sharp TiO₂ preferred orientation, with TiO₂ (100) oriented parallel to the interface. Three different variants of TiO₂ (100) on (00.1) $\alpha\text{-Al}_2\text{O}_3$ representing TiO₂ domains with three different but crystallographically equivalent orientations have been found. Their epitaxial relationship corresponds to $[010]\text{TiO}_2 // [10.0]\text{Al}_2\text{O}_3$ and $[001]\text{TiO}_2 // [21.0]\text{Al}_2\text{O}_3$. Ab-initio calculations indicate that this interface can be assumed to be oxygen-rich, with a stacking sequence of O – Al – Al – O – O – Ti, which is characterized by a high work of separation and Young's modulus, compared to an oxygen-poor interface of type O – Al – Al – Ti – O – O.

2:10pm **B4-1-2 Cu-dependent thermal transformations in hard Al-Cu-O coatings**, **P. Zeman** (*zemanp@kfy.zcu.cz*), S. Proksova, R. Cerstvy, J. Musil, University of West Bohemia, Czech Republic

Oxide ceramics are well known to be hard materials with high chemical stability and long durability. A drawback of these materials is, however, their brittleness after passing threshold energy during deformation. A general way, how to improve toughness of oxides, is an addition of ductile metal. In such a case, it is, however, necessary to determine thermal stability of such material system.

Recently, Al-Cu-O coatings prepared in our laboratories by co-sputtering of aluminum and copper in argon-oxygen gas mixture have showed an enhanced hardness and resistance to cracking [1]. The present paper brings data on maximum thermal stability and transformation processes occurring in these coatings during their heating up to 1300°C. The coatings were deposited with various copper contents (up to 10 at.%) by dual pulsed dc magnetron sputtering on silicon wafers and aluminum foils. Powdered

coatings removed from the aluminum substrates were investigated by means of differential scanning calorimetry and the structure of all the coatings was characterized by X-ray diffraction. It was found that all the as-deposited coatings are nanocrystalline one-phase materials with a cubic lattice structure independently of the Cu content. The lattice parameter varies from $\gamma\text{-Al}_2\text{O}_3$ to CuAl_2O_4 with increasing Cu content. At lower Cu contents (1.5 and 5 at.%) the as-deposited cubic structure decomposes to $\alpha\text{-Al}_2\text{O}_3$ and CuAl_2O_4 at about 950°C during exothermic reaction. The highest thermal stability of the as-deposited cubic structure is achieved for the Al-Cu-O coating with the Cu content about 10 at.% and reaches 1100°C. An endothermic reaction detected above 1100°C will be discussed as well.

[1] J.Blazek, J.Musil, P.Stupka, R.Čerstvý, J.Houška: Properties of nanocrystalline Al-Cu-O films reactively sputtered by dc pulse dual magnetron, Appl. Surf. Sci. (2011), in print.

2:30pm **B4-1-3 Multicomponent nanostructured coatings with high thermal stability, corrosion-, oxidation resistance, and improved lubrication**, D.V. Shtansky (shtansky@shs.misis.ru), K.A. Kuptsov, National University of Science and Technology "MISIS", Russian Federation, Ph.V. Kiryukhantsev-Korneev, A.N. Sheveiko, National University of Science and Technology "MISIS", Russian Federation, E.A. Levashov, National University of Science and Technology "MISIS", Russian Federation

INVITED

Multicomponent nanostructured coatings based on refractory transition metal carbides and nitrides remain the material of choice for a wide variety of high-temperature tribological applications, such as high-speed and dry cutting tools, press-forming tools, mechanical components of automobile, aircraft, and space industry. High hardness, thermal stability, corrosion-, and oxidation resistance, as well as improved solid lubrication are important properties which are required for such applications. A proper choice of element and phase compositions allows meeting these requirements. Our previous work has demonstrated that multicomponent nanostructured coatings with enhanced multifunctional properties can be deposited by sputtering of composite targets produced by self-propagating high-temperature synthesis.

Here we present experimental studies of various multicomponent nanostructured coatings with emphasis on the high-temperature tribological applications. The concept of the "comb" like nanocomposite structure, which shows a very high thermal stability in the temperature range of 25-1300°C with hardness well above 37 GPa is presented. The influence of Al and Cr on the high-temperature oxidation resistance and tribological performance, fatigue failure under dynamic impact tests both in air and NaCl solution, as well as electrochemical behavior of TiCN and TiSiCN coatings is described. An approach to decrease the friction coefficient without influence on the hardness and wear resistance by the incorporation of solid lubricant phase into hard coatings is demonstrated. The results of cutting tool tests are also reported.

3:10pm **B4-1-5 Influence of residual stresses on the spinodal decomposition of metastable $\text{Ti}_{1-x}\text{Al}_x\text{N}$ coatings**, N. Schalk (nina.schalk@mcl.at), Materials Center Leoben Forschung GmbH, Austria, C. Mitterer, Montanuniversität Leoben, Austria, C. Michotte, M. Penoy, Ceratizit Luxembourg S.à.r.l., Luxembourg

At elevated temperatures, the metastable $\text{Ti}_{1-x}\text{Al}_x\text{N}$ solid solution decomposes in cubic AlN and cubic TiN. Besides the chemical driving force, the residual stresses can be assumed to control whether the decomposition starts with more volume consuming TiN or smaller cubic AlN domains. Thus, within this work the effect of residual stresses on the decomposition of sputtered $\text{Ti}_{1-x}\text{Al}_x\text{N}$ coatings was investigated. Using different bias voltages, a series of $\text{Ti}_{1-x}\text{Al}_x\text{N}$ coatings ($x=0.63$) with stresses ranging from +670 to -550 MPa was synthesized on silicon (100) substrates. Vacuum annealing treatments and subsequent X-ray diffraction measurements showed that those coatings having compressive stresses start with the precipitation of AlN at temperatures of about 950 °C, while tensile stresses lead to the formation of TiN domains at slightly lower temperatures. These findings have been corroborated by high-temperature X-ray diffraction and differential scanning calorimetry investigations.

3:30pm **B4-1-6 In-situ small angle X-ray scattering and phase field study on the microstructural evolution at isothermal annealing of TiAlN thin films**, A. Knutsson (knutsson@ifm.liu.se), J. Ullbrand, L. Rogström, Linköping University, Sweden, J. Almer, Advanced Photon Source, US, B. Jansson, Seco Tools AB, Linköping University, Sweden, M. Odén, Linköping University, Sweden

The cubic phase $\text{Ti}_{1-x}\text{Al}_x\text{N}$ has been used to coat cutting tools since the late 1980's. Extensive research has shown that the excellent tool performance is closely related to age hardening at elevated temperature where c- $\text{Ti}_{1-x}\text{Al}_x\text{N}$ decomposes to domains of c-TiN and c-AlN. However, the number of in-situ studies is limited and especially isothermal annealing experiments of

the transformation are lacking in the literature. Here, we use a combination of *in-situ* x-ray scattering experiments during isothermal annealing and phase-field simulations to study the evolution and coarsening of the domains. Further we investigate how the composition and annealing temperature affect the decomposition.

Coatings of two compositions, $\text{Ti}_{0.34}\text{Al}_{0.66}\text{N}$ and $\text{Ti}_{0.50}\text{Al}_{0.50}\text{N}$, were grown by reactive arc evaporation using $\text{Ti}_{34}\text{-Al}_{66}$ and $\text{Ti}_{50}\text{-Al}_{50}$ compound cathodes in a N_2 atmosphere. *In-situ* high energy small-angle x-ray scattering (SAXS) were used to follow the decomposition at two isothermals, 850 and 900 °C, which were reached with a heating rate of >130 °C/min. Simultaneous wide angle scattering (WAXS) measurements allowed for determining of the strains in the coatings during the annealing. The x-ray scattering experiments were performed at the synchrotron x-ray at the Advanced Photon Source, Illinois, USA, beamline 1-ID.

The maximum entropy method was used to fit and extract a domain size from the SAXS patterns. At both 850 and 900 °C the growth rate of the domain size is slightly faster for the coating with higher Al content, which is consistent with its predicted higher driving force for decomposition. The results further show a significantly faster growth rate of the domain at 900 °C compared to 850 °C for both compositions, which is also predicted by phase field simulations. A peak shift in the SAXS pattern over time suggests that the growth of the domains is due to coarsening i.e. the spinodal decomposition is in its latter stage. STEM imaging and EDX mapping of the post annealed coatings reveal that the $\text{Ti}_{1-x}\text{Al}_x\text{N}$ has decomposed and coarsened to domains rich of Al and Ti with a size coinciding with the size extracted from the SAXS fitting. With this work we show the difference in microstructure evolution at different compositions and temperatures. The results are discussed in terms of enthalpy of mixing and metal diffusivities in this alloy system.

3:50pm **B4-1-7 Towards an Improved Stylus Geometry for the Scratch Test and Superficial Rockwell Hardness**, G. Favaro, CSM Instruments SA, Switzerland, N.M. Jennett (nigel.jennett@npl.co.uk), National Physical Laboratory, UK

Diamond scratch styli are defined by the Rockwell geometry specification in ISO6508 part 2. However, it is well known that the main uncertainty responsible for poor scratch test reproducibility is variability in Rockwell diamond stylus geometry (EC (S,M&T) contract No.MAT1-CT 940045 'FASTE' & EC contract No.SMT4-CT98-2238 'REMAST') and a certified reference material (BCR-692) exists to identify poor stylus performance. Part of the problem is an inadequate definition of Rockwell stylus geometry and measurement in ISO6508. Improvements are being actively considered, both at ISO, and by the defining metrology committee for hardness CCM-WGH. The main problem appears to be variability in radius over the spherical cap of the stylus. A VAMAS intercomparison (VAMAS TWA22 project 6) has been set up to develop improved measurement specifications to define better this key parameter and the results are presented here.

The geometry of 30 Rockwell diamonds (nominal radius 200 µm) from various manufacturers have been measured, using different metrological methods, to determine tip radius as a function of distance from the tip. Radius values were obtained from fits to 2D profiles of each tip using different width fitting windows (40 µm, 80 µm, 120 µm and 160 µm) centred on the stylus central axis. Styli, even those compliant with the ISO 6508:2 tolerances of 200 ± 15 µm when averaged over a wide fit window, frequently were very significantly outside tolerance over the smaller windows; results ranging from 140 µm < R < 320 µm for a fit window of 40 µm. This is a serious problem when Scratch testing hard coatings. Scratch tests on an a-CH DLC showed that the contact diameter at the first critical load was 40 µm. In these contact conditions, the strong variation in geometry are directly correlated to poor reproducibility of the Scratch Test.

It is becoming clear that the demands placed upon a Rockwell stylus by scratch testing are more stringent than those required for Rockwell hardness testing in which only the "superficial" scales (A, N & T) have test depths within the spherical cap region. To evaluate the effect of the observed radius variability on the Rockwell test, Rockwell HRN tests were performed on a Rockwell N scale hardness reference block. A significant effect of tip geometry on the Rockwell HRN test result was found.

The full results from 30 styli show clearly the importance of using a scratch test reference material (or regular direct inspection and measurement) to exert adequate quality control over a scratch test stylus. Proposals will be presented for an improved Rockwell stylus geometry definition.

4:10pm **B4-1-8 Surface Characterization of Optimized TiSiN Coating Deposited Via A Combination of DC and RF Magnetron Sputtering.** *A.R. Bushroa, Abdul Razak (bushroa@um.edu.my)*, University of Malaya, Malaysia, *T. Ariga*, Tokai University, Japan, *S. Singh, M. Haji Hasan*, University of Malaya, Malaysia, *M.R. Muhammad*, Multimedia University, Malaysia

TiSiN coatings were deposited on high speed steel substrates in a PVD technique using a combination of DC and RF magnetron sputtering by varying DC power. The optimized sample was coated at 500 W, and controlled samples were deposited at 300 and 400 W. Surface morphology showing that rectangular shaped grains of the optimized sample were observed in stack. Trend of surface roughness was correlated with the observed surface morphology. Cross sectional coatings were compared with structural zone model. There was no evidence of columnar growth that associated with the impurity of Si content in the coating for above 3.0 at.%. Nevertheless, columnar growth was observed for lower Si content of 1.0 at.%. Approximated method was utilized to calculate crystallite size and micro strain via XRD line broadening. The approximated crystallite size was varied but could be associated with the DC power, thickness and surface morphology of the coatings. The XRD showed all samples were oriented at (111), (200) and (220). A plane of (111) was dominant in the optimized sample that was corresponded to low micro strain and compressive stress. Orientations at (200) and (220) were preferred in the other samples since these were the less dense planes when the Si content was above 4.5 at.%. There was evidence of nanocrystalline TiN and an amorphous phase of Si N indicating that all samples were successfully deposited with TiSiN coating.

4:30pm **B4-1-9 Surface Analysis of TiAlON and CrAlN Coatings Deposited by Means of HPPMS.** *C. Kunze (kunze@tc.uni-paderborn.de)*, *C. Gnoth*, University of Paderborn, Germany, *M. to Baben, S. Theiss, N. Bagcivan, K. Bobzin, J. Schneider*, RWTH Aachen University, Germany, *G. Grundmeier*, University of Paderborn, Germany

Plasma deposited coatings of TiAlON and CrAlN are a promising approach to decrease wear and friction of tools within plastics processing such as extrusion and injection molding. Up to now the exact mechanisms of interactions between the coating and the polymer melt are not well understood yet.

An experimental approach is presented that analyzes the surface chemistry of TiAlON and CrAlN coatings as a function of chemical composition and deposition parameters by means of X-ray photoelectron spectroscopy (XPS) and infrared spectroscopy (FTIR). Surface energies of CrAlN and TiAlON coatings were measured by static and dynamic contact angle experiments. The coatings were synthesized via High Power Pulse Magnetron Sputtering (HPPMS) in case of TiAlON and direct current (DC), pulsed middle frequency (MF) sputtering or HPPMS in case of CrAlN, respectively.

It could be shown that the surface composition of CrAlN coating significantly differs from the bulk composition. Although the CrAlN phase is supposed to be inert under a wide range of environmental conditions the surface is oxidized to a CrAlON phase upon contact with air. These effects have to be taken into account considering adhesion phenomena and the interaction with the polymer melt.

Additionally, a contamination layer of low-weight (hydro-)carbon species being omnipresent in the environmental atmosphere is formed on the surface of the coatings, which was followed from contact angle experiments and XPS analysis. The observed surface energy values measured by dynamic and static contact angle experiments were in the range of 35 ± 10 mJ/m² which is much smaller than the expected high surface energy values in the range of hundreds of mJ/m² for TiAlON derived from DFT calculations.

The properties of the contamination layer and the oxidized CrAlON surface were investigated in detail via angle resolved XPS and depth profiling experiments with respect to their influences on the surface chemistry of the subjacent coating. To remove the organic contamination layer for advanced surface analysis under UHV conditions a cleaning process via a He plasma was evolved. It could be shown by means of in-situ photomodulated infrared spectroscopy (PM-IRRAS) that this process of He plasma cleaning is applicable to remove organic contaminations from the film surface without changing its surface chemistry.

4:50pm **B4-1-10 Nanoprobe measurements of anisotropy in thin-film nanocrystalline coatings.** *A. Jankowski (alan.jankowski@ttu.edu)*, *H. Ahmed*, Texas Tech University, US

The mechanical properties of thin film coatings are routinely investigated at the nanoscale using nanoindenter probes. Properties measured normal to the coating surface with nanoindentation require specific analytic assumptions for interpretation. Additional measurements are now obtained using the tapping mode where Hertzian point contact occurs between the indenter tip and the coating surface. Nanostructured crystalline coatings with elastic

anisotropy are investigated as produced by magnetron sputter deposition. These coatings have a random in-plane crystalline texture but a single texture normal to the coating surface. Materials examined include single element coatings and laminated structures composed of face-center-cubic metals as well as body-center-cubic metals. Comparison is made between results using these different nanoprobe methods. It is found that anisotropic mechanical properties can be identified as texture dependent. This work was supported by the J.W. Wright Endowment for Mechanical Engineering at Texas Tech University.

5:10pm **B4-1-11 TaSiN Thin Films: Si Influence on the Optical and Electrical Properties.** *G. Ramírez*, Universidad Nacional Autónoma de México - Instituto de Investigaciones en Materiales, Mexico, *S.E. Rodil*, Instituto de Investigaciones en Materiales, Universidad Nacional Autónoma de México, México, *S. Muhl*, Universidad Nacional Autónoma de México - Instituto de Investigaciones en Materiales, Mexico, *M. Rivera*, Instituto de Física - Universidad Nacional Autónoma de México, México, *D. Oezer, R. Sanjines (rosendo.sanjines@epfl.ch)*, EPFL, Switzerland

The optical and electrical properties of Tantalum Silicon Nitride (TaSiN) thin films have been investigated as a function of the Si content. Films of 1.2 m thickness were deposited using two independent magnetron sputtering systems. The silicon content of the samples was varied from 2 to 12 at% by controlling the RF power applied to the Si (99.999% purity) target from 60 to 340 W. Meanwhile, the DC power applied to the Ta (99.95% purity) target remained fixed at 400 W, as well as the Ar/N₂ flow ratio (6/14). The dielectric properties of the films were investigated using ellipsometry spectroscopy from 1.5 to 5.0 eV. The ellipsometric spectra were modeled to consider the existence of a rough surface layer using a Drude-Lorentz dispersion model for the film and a Bruggeman effective medium (50% voids + 50% film) for the rough layer. From the Drude terms, i.e. the plasma frequency and damping factor, the optical resistivity of the films was estimated. The optical resistivity increases gradually from about 100 to 610 $\mu\Omega\text{cm}$ as the Si content increases from 2 at% to 10.35 at%, then, it increases sharply up to 3250 $\mu\Omega\text{cm}$ for Si at% of 11.7. The last sample exhibits an amorphous like structure, while the others show the fcc phase of TaN. The dc electrical resistivity was measured by the van der Pauw method at RT and as a function of the temperature. Typical dc resistivity values are in the range of 200-300 $\mu\Omega\text{cm}$ in agreement with those deduced from optical measurements. In addition, the surface electrical properties and surface morphology of the films was investigated by scanning tunneling microscopy (STM). Both the optical and electrical properties of TaSiN films are correlated with changes in chemical composition and film structure due to the addition of Si.

Hard Coatings and Vapor Deposition Technology Room: Royal Palm 1-3 - Session B7-2

Computational Design and Experimental Development of Functional Thin Films

Moderator: B. Alling, Linköping University, Sweden, A. Amassian, KAUST, D. Holec, Montanuniversität Leoben, Austria, P. Patsalas, University of Ioannina, Greece

1:50pm **B7-2-1 The effect of nitrogen content on stability and elastic properties of TiAlN studied by ab initio calculations and combinatorial reactive magnetron sputtering.** *M. to Baben (to_baben@mch.rwth-aachen.de)*, *J. Emmerlich, L. Raumann, J. Schneider*, Materials Chemistry, RWTH Aachen university, Germany

Ti_{1-x}Al_xN_y, as one of the most studied hard coatings, is widely applied on cutting tools. The influence of the Ti to Al ratio on mechanical properties, phase stability and oxidation resistance has been investigated for stoichiometric TiAlN. As sub- and super-stoichiometric Ti_{1-x}Al_xN_y have been observed experimentally [1,2] the effect of the nitrogen concentration on the aforementioned properties has to be explored. Alling et al have studied the decomposition pattern for Ti_{1-x}Al_xN_y theoretically [3]. However, the effect of nitrogen concentration on unit cell volume and elastic properties of sub- and super-stoichiometric Ti_{1-x}Al_xN_y are yet to be determined.

Here, we study the material system Ti_{1-x}Al_xN_y both by ab initio calculations and experiments. We show, based on ab initio data, that metal vacancies are responsible for super-stoichiometric ($y > 1$) Ti_{1-x}Al_xN_y, rather than nitrogen interstitials. Furthermore, we report lattice parameters and bulk and Young's modulus of Ti_{1-x}Al_xN_y. As experimental data are rare, a method of combinatorial reactive magnetron sputtering was developed that allows depositing Ti_{0.5}Al_{0.5}N_y films with a lateral nitrogen gradient in a single deposition run. The nitrogen content measured by energy dispersive X-ray

spectroscopy varies from 25 at% to 50 at% and thus enables studying $\text{Ti}_{1-x}\text{Al}_x\text{N}_y$ films over a broad composition range. In combination with experimental details on the combinatorial synthesis route, structural results from X-ray diffraction and elastic properties measured by nanoindentation will be presented and compared to *ab initio* calculations.

- 1: J. Bujak et al., Surf. Coat. Tech. 180-181 (2004), 150.
- 2: T. Zhou et al., Vacuum 83 (2009), 1057.
- 3: B. Alling et al., Appl. Phys. Lett. 92 (2008), 071903.

2:10pm B7-2-2 First principle molecular dynamics simulations of high temperature properties in transition metal nitrides, P. Steneteg (*petst@ifm.liu.se*), I. Abrikosov, B. Alling, Linköping University, Sweden
Equation of state for chromium nitride has been debated in the literature in connection with a proposed collapse of its bulk modulus at the pressure induced transition from the paramagnetic cubic phase to the antiferromagnetic orthorhombic phase [F. Rivadulla et al., Nat Mater 8, 974 (2009); B. Alling et al., Nat Mater 9, 283 (2010)]. Experimentally the measurements are complicated due to the low transition pressure, while theoretically the simulation of magnetic disorder represent a major challenge. Here a first-principles method is suggested for the calculation of thermodynamic properties of magnetic materials in their high temperature paramagnetic phase. It is based on *ab-initio* molecular dynamics and simultaneous redistributions of the disordered but finite local magnetic moments. We apply this disordered local moment molecular dynamics method to the case of CrN and simulate its equation of state both at high and low temperature. In particular the debated bulk modulus is calculated in the paramagnetic cubic phase and is shown to be very similar to that of the antiferromagnetic orthorhombic CrN phase.

2:30pm B7-2-3 Simulating the slow structural evolution of materials using Accelerated Molecular Dynamics, D. Perez (*danny_perez@lanl.gov*), Los Alamos National Laboratory, US **INVITED**
A significant problem in the atomistic simulation of materials is that molecular dynamics simulations are limited to microseconds, while important reactions and diffusive events often occur on much longer time scales. Although rate constants for infrequent events can be computed directly, this requires first knowing the transition state. Often, however, we cannot even guess what events will occur. In this talk, I will discuss the accelerated molecular dynamics approach, which we have been developing over the last decade, for treating these complex infrequent-event systems. The idea is to directly accelerate the dynamics to achieve longer times without prior knowledge of the available reaction paths. In some cases, we can achieve time scales with these methods that are many orders of magnitude beyond what is accessible to molecular dynamics. I will briefly introduce the methods and discuss some examples of applications to surface diffusion and thin film growth.

3:10pm B7-2-5 Stabilization of cubic AlN in TiN/AlN and CrN/AlN bi-layer systems by combined FEM and *ab initio* analysis, V. Chawla, D. Holec, P.H. Mayrhofer (*paul.mayrhofer@unileoben.ac.at*), Montanuniversität Leoben, Austria

Epitaxial stabilization of various crystal structures by the template effect is the topic of many research activities (e.g. superlattice studies) due to the outlook to control the properties of coatings by engineering the structures at the nanoscale. Multilayers that consist of two nanoscale layered materials with the same crystal structure and a small lattice mismatch may grow hetero-epitaxially. In this study we aim at understanding the fundamental aspects of the phase stability due to the fully or partially coherent interfaces combined with the effect of crystallographic and mechanical properties of a substrate. As a model system we investigated two bi-layer configurations: TiN/AlN and CrN/AlN. AlN has two crystal structures, a stable wurtzite structure (w) with hexagonal symmetry and a metastable NaCl structure with cubic (c) symmetry. The elastic energy stored in TiN/AlN and CrN/AlN bi-layer systems with different substrates were investigated by finite element method (ABAQUS) in addition to *ab initio* calculations. A three dimensional model was simulated with 500 nm thick substrate and bi-layer film thicknesses varied in the nanometer range for the FEM studies. 8-node linear bricks with elastic and anisotropic behavior for different crystallographic orientations were employed. The results showed that for fully epitaxial TiN/AlN bi-layer system, initially the c-AlN phase is preferred as it allows for a lesser internal energy (chemical energy and strain energy) in the range of 0.17 (Si) to 0.32 nm (Sapphire) AlN thickness when grown on c-TiN with different substrates. For thicker AlN layer thicknesses the wurtzite structure possesses smaller energy. The c-AlN is predicted to vary between 0.6 (Si) to 1.0 nm (Sapphire) for the CrN/AlN bi-layer system, while w-AlN is energetically favorable for thicker films. In addition, the effect of not fully coherent interface between c-TiN and w-AlN (i.e. an interface containing misfit dislocations) will be addressed. In conclusion, we demonstrate using a combined FEM and *ab initio* modeling

and rationalize the trends in substrate-induced mechanisms of stabilizing c-AlN when grown on c-TiN or c-CrN, as well as the effect of the quality of the interface, which can be further used for a targeted coating design.

3:30pm B7-2-6 Structural and elastic properties of polycrystalline $\text{Al}_{1-x}\text{Cr}_x\text{N}$ alloys : multiscale computations versus experiments, T. Pham, Institut P' - Université de Poitiers, France, K. Bouamama, Ferhat Abbas University, Algeria, P. Djemia (*djemia@univ-paris13.fr*), University Paris 13, France, L. Belliard, UPMC, France, D. Faurie, University Paris 13, France, E. Le Bourhis, P. Goudeau, Institut P' - Université de Poitiers, France

First-principles pseudopotential calculations of the lattice constants and of the single-crystal elastic constants for $\text{Al}_{1-x}\text{Cr}_x\text{N}$ ($0 \leq x \leq 1$) alloys considering the cubic B1-rocksalt structure were first carried out. These calculations were performed using density functional perturbation theory (DFPT) and the supercell method (SC) for the ordered alloys. For the exchange-correlation potential we used the generalized gradient methods (GGA). The calculated equilibrium lattice parameters exhibit a positive deviation from Vegard's rule corresponding to a positive bowing parameter while the calculated single-crystal stiffness, namely C_{11} and C_{44} , gradually increases or decreases, respectively from AlN to CrN phases. In a second stage, we have estimated by homogenization methods in the frame of anisotropic elasticity, the averaged stiffnesses $\langle C_{ij} \rangle$, direction dependent Young's moduli and Poisson's ratios of polycrystalline $\text{Al}_{1-x}\text{Cr}_x\text{N}$ ($0 \leq x \leq 1$) alloys considering a {002}-fiber texture. Finally, comparisons are made for $0.4 \leq x \leq 1$ with the shear elastic modulus $G_{yz}=G_{xz}$ and the out-of-plane longitudinal elastic constant C_{33} measured by Brillouin light scattering and picosecond ultrasonics, respectively.

Keywords

Ab initio, VCA, DFPT, supercell, nitride materials, elasticity, Brillouin light scattering, picoseconds ultrasonics.

3:50pm B7-2-7 Theoretical spectroscopy investigation of hard TiN/SiN_x interfaces, W. Olovsson (*weine.olvesson@gmail.com*), B. Alling, L. Hultman, I. Abrikosov, Linköping University, Sweden

The knowledge of the structure and geometry of the SiN_x tissue phase in TiN/SiN_x nanocomposites is crucial for understanding their favorable mechanical properties. Perhaps the most promising experimental techniques for obtaining information about bonding in the tissue phase and between the tissue phase and the TiN grains, are x-ray photoelectron spectroscopy (XPS), x-ray absorption near-edge structure (XANES) and related spectroscopies. Unfortunately, the results of these experiments are difficult to interpret on their own for these complex interface structures, governed and created through non-equilibrium processes.

In this work we present first-principles theoretical calculations of spectroscopical properties of different complex TiN/SiN_x/TiN interface structures, proposed, but yet not proven to be of relevance for this material system. By comparing the computed spectra from known structures with the measured spectra of the real films, it is possible to gain insights not accessible with either theory or experiments alone.

4:10pm B7-2-8 Elasticity in TiAlN alloys: the significant elastic anisotropy and the dependence on the SQS model, F. Tasnádi (*tasnadi@ifm.liu.se*), M. Odén, I. Abrikosov, Linköping University, Sweden
Substitutional $\text{Al}_x\text{B}_{1-x}\text{C}$ alloys are extensively used in numerous applications from soft piezoelectric devices [1], such as cell phones, satellites etc. to protecting hard coating of cutting or machining tools [2]. Prediction of anisotropic tensorial materials properties of substitutional alloys from first principles is still a challenging and highly required issue in computational materials science [3] Here we present a joint theoretical and experimental study on the elasticity in TiAlN alloys. We discuss the observed significant anisotropy [4] with implications on the spinodal decomposition (microstructure evolution) in TiAlN. We also present a supplementary theoretical approach to justify the applicability and analyze the performance of the special quasirandom structure (SQS) model in predicting non-scalar, anisotropic materials constants of alloys with certain symmetry. The approach is general enough to apply it for elastic tensors of alloys with other symmetry.

[1] F. Tasnádi, B. Alling, C. Höglund, G. Wingqvist, J. Birch, L. Hultman, and I. A. Abrikosov, Phys. Rev. Lett. **104**, 137601 (2010).

[2] A. Hörling, L. Hultman, M. Odén, J. Sjölen and L. Karlsson, Surf. Coat. Technol. **191**, 384 (2005). I. A. Abrikosov, A. Knutsson, B. Alling, F. Tasnádi, H. Lind, L. Hultman and M. Odén, Materials **4**, 1599 (2011).

[3] A. van de Walle, Nature Mater. **7**, 455 (2008).

[4] F. Tasnádi, I. A. Abrikosov, L. Rogström, J. Almer, M. P. Johansson and M. Odén, Appl. Phys. Lett. **97**, 231902 (2010).

4:30pm **B7-2-9 Improving thermal stability of hard coating films via a concept of multicomponent alloying.**, *H. Lind* (halin@ifm.liu.se), *R. Forsén, B. Alling, N. Ghafoor, F. Tasnádi, M. Johansson, I. Abrikosov, M. Odén*, Linköping University, Sweden

We propose a design route for the next generation of nitride alloys via a concept of multicomponent alloying based on self-organization on the nanoscale via a formation of metastable intermediate products during the spinodal decomposition. We predict theoretically and demonstrate experimentally that quasi-ternary (TiCrAl)N alloys decompose spinodally into (TiCr)N and (CrAl)N-rich nanometer sized regions. The spinodal decomposition results in age hardening, while the presence of Cr within the AlN phase delays the formation of a detrimental wurtzite phase leading to a substantial improvement of thermal stability compared to the quasi-binary (TiAl)N or (CrAl)N alloys.

4:50pm **B7-2-10 Packing structure and optical properties of functionalized pentacene.**, *U. Schwingenschlogl* (udo.schwingenschlogl@kaust.edu.sa), *N. Singh, Y. Saeed*, KAUST, Saudi Arabia

By their enormous variability and potential low-cost fabrication, organic electronics attract significant commercial and scientific interest in recent years. In particular, pentacene was studied quite extensively as organic molecular semiconductor in various thin film applications. Although pentacene is currently among the organic materials with the highest charge carrier mobility, it is believed that there is still much room for improvement if the p-p interaction can be enhanced. To this aim, functional substitution can induce modified packing structures and electronic properties. For example, pristine pentacene shows a slipped 1D packing, while (6,13)-bis(triisopropyl-silyl-ethynyl)-pentacene (TIPS pentacene) realizes a brickwork 2D packing. By introducing a trifluoromethyl group on the TIPS pentacene backbone (TIPS-CF₃ pentacene), the system becomes soluble in common organic solvents. Moreover, the bulky side groups interrupt the herringbone pattern and induce a regular columnar stacking of the acene planes.

We study the effect of functional substitution and of the induced packing on the electronic and optical properties of pentacene, TIPS pentacene and TIPS-CF₃ pentacene in comparison to each other in order to evaluate the influence of the functional group. The results are also compared to experimental data. Our calculations are based on density functional theory, using the full potential linearized augmented plane wave method. Exchange and correlation effects are treated within the local density approximation.

An enhanced difference between the band gaps of the molecule and the crystal is found for TIPS pentacene. The frequency dependent dielectric functions and absorption spectra are calculated and analyzed in terms of the transitions between the highest occupied (HOMO) and lowest unoccupied (LUMO) molecular orbitals. It turns out that C and Si states from atoms in the chain which connects the side group to the pentacene account for the main contribution to the optical transitions. The calculated dielectric functions agree well with experimental data. Moreover, the experimentally observed red shift from the molecule to the crystal is confirmed.

Tribology & Mechanical Behavior of Coatings and Engineered Surfaces

Room: Pacific Salon 1-2 - Session E3-2/G2-2

Development, Characterization, and Tribology of Coatings for Automotive and Aerospace Applications

Moderator: R. Evans, Timken Company, US, H. Rudigier, OC Oerlikon Balzers AG, Liechtenstein, S. Dixit, Plasma Technology Inc., US

1:50pm **E3-2/G2-2-1 In situ tribology of cold spray-deposited pure aluminum and Al-Al₂O₃ composite coatings.** *J.M. Shockley, R. Chromik* (richard.chromik@mcgill.ca), *H. Strauss*, McGill University, Canada, *E. Irissou, J.-G. Legoux*, National Research Council, Canada

Cold sprayed aluminum coatings are valued for their good corrosion resistance, but their poor tribological performance limits their use in automotive and aerospace applications where wear resistance is also required. Hard phases such as Al₂O₃ may be co-sprayed along with aluminum powders to create Al-Al₂O₃ composite coatings with improved tribological performance. Traditional ball-on-flat tribometry prevents direct observation of the sliding interface during wear, meaning only *ex situ* analysis of wear surfaces and debris is possible. In the present study, an *in situ* tribometer with a transparent sapphire counterface was used for ball-on-flat testing of cold sprayed aluminum coatings deposited with up to 20

vol.% Al₂O₃ particles. Similar to the use of in situ tribometry for solid lubricants, the technique revealed details of metallic transfer film formation and detachment. It was found that in the Al-Al₂O₃ cold spray coatings, the transfer film was more stable as hard phase content increased, which was also correlated to increase in friction stability and decreased wear.

2:10pm **E3-2/G2-2-2 Thermal Spray Lubricious Oxide Coatings.** *S. Dixit* (sdixit@ptise.com), Plasma Technology Inc., US, *O.L. Eryilmaz, A. Erdemir*, Argonne National Laboratory, US

During the extreme conditions experienced in automobiles and aerospace applications, oil-based lubricants break down at high temperatures. Under such conditions, conventional fluid lubricants either fail early or never are considered as an option. As a result, components of engines that are run at high temperatures to improve their fuel efficiency tend to wear rapidly and require replacement. One solution to extend bearing life is with the implementation of a low friction, high temperature stable, and low wear coatings to the component surface that can perform under extreme conditions. Solid lubricant coatings offer a solution for diverse applications exhibiting extreme and difficult running conditions. Although the most common dry-solid lubricants are graphite, MoS₂, WS₂, TaS₂, and PTFE, they are limited in terms of their high temperature capabilities as well as their wear characteristics. Hence in this paper we propose novel thermal spray lubricious oxide coatings based on a crystal chemical approach. Different combinations of the oxide materials are chosen based on their ionic potential differences and plasma sprayed to a thickness of 150 to 200 microns. Their composition, microstructure and high temperature wear characteristics are reported in this paper.

2:30pm **E3-2/G2-2-3 Tribological properties of plasma sprayed AlSi coatings reinforced by nano-diamond particles.** *M.D. Bao*, Ningbo University of Technology, China, *C. Zhang, D. Lahiri, A. Argarwal* (agarwala@fiu.edu), Florida International University, US

Al-Si coatings reinforced with nano-diamond particles with different volume percentage were prepared by plasma spraying. The composite coatings show a two-phase microstructure of Al-Si matrix with homogeneously dispersed nano-diamond particles. The hardness and elastic modulus of Al-Si coatings reinforced by nano-diamond particles of various concentrations were investigated in comparison with pure Al-Si coatings. The tribological behavior including friction coefficient and specific wear rate of these different coatings were also studied. The mechanism of wear resistance and anti-friction behavior of coatings is discussed in this study.

2:50pm **E3-2/G2-2-4 High temperature abrasive systems.** *J. Davenport* (jrd49@cam.ac.uk), *R. Stearn*, University of Cambridge, UK, *M. Hancock*, Rolls Royce, US, *W. Clegg*, University of Cambridge, UK

Increasing the efficiency of a gas turbine engine requires that any leakage of gas from the working gas path is minimized, of particular importance is leakage around the tips of high pressure (HP) turbine blades. This can be approached by using an abradable sealing system, where abrasive particles embedded in an anchor phase are fixed to the end of the turbine blade tip, and an abradable coating. The turbine blades cut a track through the abradable coating on the shroud, the abrasive particles protect the turbine blade from wearing away against the abradable.

However lifetimes of the current sealing system are unacceptably short, with oxidation of the abrasive and creep of the anchor phase being two major factors.

The abrasion behavior of various abrasives against a magnesium aluminate spinel abradable has been studied using a pin-on-disc abrasion rig at temperatures up to 1300 °C. It has been shown, even at the velocities of just a few metres per second, that abrasion causes fracture of the particles and frictional heating approximately consistent with predictions in the literature. At elevated temperatures and at these velocities it is shown that correcting for the difference in velocity predicts temperature changes about the melting point of the MCrAlY, and even close to that of the abrasive.

3:10pm **E3-2/G2-2-5 Customized Surface Technology for Innovative Automotive and Industrial Products.** *T. Hosenfeldt* (Tim.Hosenfeldt@schaeffler.com), *Y. Musayev*, Schaeffler Technologies GmbH & Co. KG, Germany

INVITED

Modern components and systems for automotive and industrial applications have to meet various requirements in multiple technical fields. Apart from properties that affect the part itself – like geometry, stiffness, weight or rigidity – the surface properties must be adjusted to the growing environmental requirements. This includes measures for corrosion and wear protection, for optimum electrical or thermal conductivity and for optical purposes. Beyond those, coatings are increasingly used to reduce the friction losses of car components, improve fuel efficiency and reduce CO₂-emissions.

This article describes how to use surface technology as a modern design element for components and systems to enable the increasing requirements on market leading automotive and industrial products.

Therefore Schaeffler has developed and established a coating tool box for customized surfaces to apply the right solutions for all that needs and requests with the corresponding coating system made by PVD-/ PACVD-, spraying or electrochemical technology. For innovative products it is extremely important that coatings are considered as design elements and integrated in the product development process at a very early stage.

In this article tribological coatings are viewed within a holistic and design-oriented context. The latest developments of amorphous carbon coatings, its characteristics as well as the technical and economical effects of its use in combustion engines and industrial bearing applications are described.

The presented Triondur® amorphous carbon based coating systems (a-C:H; a-C:H:Me; a-C:H:X and ta-C) are excellent examples for customized tribological systems like bucket tappets, linear guidances and roller bearings.

Triondur® carbon coatings offer the following advantages:

- Super low friction with highest wear resistance.
- Customized surface energy.
- Optimized wettability and interaction with formulated engine oils.
- Low adhesion to the counterpart.

Close collaboration between designers and surface engineers is required in the future. Schaeffler delivers around 70 million high-quality PVD- and (PA)CVD-coated components (Triondur®) every year that enable outstanding applications, preserve resources and meet increasing customer requirements.

3:50pm E3-2/G2-2-7 Ultra-fast Synthesis of Superhard Borides: A Paradigm Shift in Surface Engineering for Tooling and Automotive Applications, A. Erdemir (erdemir@anl.gov), O.L. Eryilmaz, Argonne National Laboratory, US, S. Timur, Istanbul Technical University, Turkey, O. Kahevcioglu, Argonne National Laboratory, US, G. Kartal, Istanbul Technical University, Turkey, V. Sista, Argonne National Laboratory, US

During the last two decades, there has been considerable interest in the development and diverse utilization of novel coatings and surface treatments that can enhance efficiency, durability, and environmental compatibility of a variety of automotive and machine tool components. Among others, the development of DLC and other low-friction coatings has attracted the most attention mainly because of their unique abilities to provide much superior performance under severe tribological conditions. Tribological properties of mechanical components can also be improved by a variety of well-established surface treatments like nitriding, carburizing, and boriding. All of these methods are used extensively by today's automotive industry despite being very time and energy consuming. In this talk, a novel super-fast surface treatment method called ultra-fast boriding will be introduced as a highly robust and low-cost alternative to current surface treatment and coating methods. New boriding process is capable of producing more than 90 micrometer thick boride layers in 30 minutes on a variety of steels and in the case of certain non-ferrous alloys, it is capable of producing ultra-thick and hard boride layers providing more than 45 GPa hardness. The primary focus of this talk will be on the chemical, structural, and mechanical design of such boride layers for severe operating conditions of various engine and tooling applications. Initial test results from a variety of bench-top tribotest machines will also be presented to demonstrate the much superior tribological properties for such boride layers over a broad range of test conditions.

4:10pm E3-2/G2-2-8 A study on tribological behavior of arc-coated Ti-Al-N films on AISI 4340 alloy steel for automotive application, C. Hsu, Tatung University, Taiwan, C. Lin (cklin@fcu.edu.tw), Feng Chia University, Taiwan, D.W. Lai, Tatung University, Taiwan, K. Ou, Taipei Medical University, Taiwan

This study utilized cathodic arc evaporation method to coat Ti-Al-N films on AISI 4340 steel for evaluating the feasibility of prolonging the use-life in the application of landing gears and truck parts. SEM, XRD, and TEM were used to confirm the morphology and structure of the coatings, and some coatings properties, such as adhesion, hardness, Young's modulus, residual stress, and friction coefficient were all analyzed. The results showed that TiAlN film was indeed a single phase of FCC structure. The TiN/TiAlN multi-layered films had a good adhesion (HF1), high hardness (36.5 GPa), Young's modulus (461 GPa), and appropriate residual stress (-5.68 GPa). Moreover, the optimum coatings achieved a remarkable reduction in the steel friction coefficient from 0.81 to 0.45.

4:30pm E3-2/G2-2-9 Predicting lifetime of silver and gold coating depending on their thickness, stress and environmental conditions, O.P. Perrinet (olivier.perrinet@ec-lyon.fr), LTDS, France

The fretting wear phenomenon in electrical contacts is a plague in many applications, especially in the automotive industry, but also in other machines exposed to vibration. It induces severe electrical distortions, high electrical contact resistance and micro cuts.

This has led to the development of numerous coating systems consisting of pure metallic materials, noble and non-noble, doped as well as soft coatings.

Five coating systems were studied: a bronze-nickel-with different types of doped silver coating system and a bronze-nickel-with different types of doped gold coating system.

Using this apparatus, most of the physical conditions, such as relative humidity, temperature, frequency, relative displacement and normal force, can be precisely controlled and monitored.

We have observed and understood the kinetics of wear in connection, disconnection and reconnection simulation of electrical connector. This approach is applied to analyze hard coating wear mechanisms focusing on abrasion and oxidation phenomena.

4:50pm E3-2/G2-2-10 Understanding durability of lubricant/DLC coating interface, L. Austin, T. Liskiewicz (t.liskiewicz@leeds.ac.uk), A. Neville, Leeds University, UK, R. Tietema, Hauzer Techno Coating, BV, Switzerland

DLC coatings are recognised as a promising way to reduce friction and increase wear performance of automotive parts and are currently being introduced for some engine and transmission components. DLC coatings, especially hydrogenated and doped with W or Si DLC coatings, provide new possibilities in improving tribological performance of automotive components, beyond what normally can be achieved with lubricant design only. However, currently used lubricants have been originally designed for metallic surfaces and there is a lack of knowledge on tribological behaviour of DLC coatings when lubricated with these oils, which limits their use in practical applications.

In this project, a W doped DLC coating is tested in lubricated contact simulating the engine tap/follower interface. The role of lubricant/surface interactions is investigated experimentally against a steel counterface. The tribofilm formation process is characterized chemically and mechanically using EDX mapping, XPS and nanoindentation. A link between the tribofilm structure/composition and tribological performance is studied. Hardness and elastic modulus are mapped within the contact area showing the evolution of the tribofilm mechanical properties. The friction process is related to the dynamics of tribofilm formation and tribofilm time dependence is investigated. The emphasis of the paper is on how the coating structure and composition can be adapted for optimal interaction with fully formulated lubricant to enhance the tribological "system" performance.

5:10pm E3-2/G2-2-11 From DLC to Si-DLC based layer systems with optimized properties for tribological applications, D. Hofmann (dieter.hofmann@amg-ct.de), S. Kunkel, AMG Coating Technologies GmbH, Germany, K. Bewilogua, R. Wittorf, Fraunhofer IST, Germany

Diamond-like carbon (DLC) coatings are used in many industrial applications like valvetrain-, fuel injection- and piston-systems etc.. For DLC (a-C:H) coatings, prepared by a magnetron based technique using graphite targets, high indentation hardness values of more than 40GPa were achieved. The wear resistance, the microhardness and the coefficient of friction are shown as a function of the hydrogen concentration in the coatings. In order to reduce the coefficient of friction even more and to increase the operation temperature of the coatings from about 350°C for DLC to near 500°C, a new Si-DLC based layer system was developed using a special magnetron sputter target configuration. This Si-DLC based layer system combines the benefits of a reduced coefficient of friction with a high wear resistance. The DC magnetron based production method allows the deposition of Si-DLC coatings in a wide range of compositions with 5 to 25 at.% Si at low hydrogen contents down to 5 at.%. The new Si-DLC based coatings show favorable conditions for present and future industrial applications.

High Power Impulse Magnetron Sputtering

Moderator: R. Bandorf, Fraunhofer Institute for Surface Engineering and Thin Films IST, Germany, J. Sapieha, Ecole Polytechnique de Montreal, Canada, D. Lundin, Université Paris-Sud 11, France

1:50pm **F2-2-1 HIPIMS Discharge Dynamics: Evolution and Origin of Plasma Instabilities**, A. Hecimovic (ante.hecimovic@rub.de), Institut für Experimental Physics II, Research Department Plasma, Ruhr-Universität Bochum, Germany, T. de los Arcos, Ruhr Universität Bochum, Germany, V. Schulz-von der Gathen, M. Böke, J. Winter, Institut für Experimental Physics II, Research Department Plasma, Ruhr-Universität Bochum, Germany

High power impulse magnetron sputtering (HIPIMS) combines impulse glow discharges at power levels up to the MW range with conventional magnetron cathodes to achieve a highly ionised sputtered flux. If observed with a low time resolution, the optical emission from the HIPIMS discharge may appear to be homogeneous during the pulse. However, we have shown recently that the HIPIMS plasma may develop drift wave type instabilities [1]. They are characterized by well defined regions of high and low plasma emissivity along the racetrack of the magnetron and cause periodic shifts in floating potential. The structures rotate in ExB direction at velocities of $\sim 10 \text{ km s}^{-1}$ and frequencies up to 200 kHz. It has already been shown in literature that the magnetron configuration may exhibit two-stream instabilities due to the difference in confinement of electron and ions and the associated differences in particle fluxes [2]. However the characteristic frequency of these instabilities is of the order of a few MHz, well above drift wave type instabilities we have observed.

In this paper a detailed analysis of the temporal evolution of the saturated instabilities using four consequently triggered fast ICCD cameras is presented. The influence of mass of the target material and working gas on the instability properties was investigated using titanium (Ti) and aluminium (Al) targets in either Ar or Kr gases. Furthermore working gas pressure and discharge current variation showed that the shape and the speed of the instability strongly depend on the working gas and target material combination. In order to better understand the mechanism of the instability, different optical interference band pass filters (of metal and gas atom, and ion lines) were used to observe the spatial distribution of each species within the instability. It was found that the optical emission from the instabilities comprises ion emission (both target material and gas ion lines) with strong depletion of the emission lines of the target material atom lines, concluding that instabilities are of generalised ion drift wave type.

[1] A. Ehasarian, A. Hecimovic, T. de los Arcos, J. Winter, R. New, V. Schulz-von der Gathen, M. Böke, Appl. Phys. Lett. submitted

[2] D. Lundin, P. Larsson, E. Wallin, M. Lattemann, N. Brenning and U. Helmersson, Plasma Sources Science and Technology, 2008, (17), 035021

Acknowledgement: This work was funded within Subproject A5 of SFB-TR 87. We gratefully acknowledge valuable discussions with Prof. A. Ehasarian and the kindness of Prof. H. Soltwisch and Dr. P. Kempkes on borrowing us the four cameras setup.

2:10pm **F2-2-2 Modes of operation in HiPIMS: Understand and optimize the discharge pulse**, D. Lundin (daniel.lundin@liu.se), C. Vitelaru, Université Paris-Sud 11, France, N. Brenning, Royal Institute of Technology, U. Helmersson, Linköping University, Sweden, T. Minea, Université Paris-Sud 11, France

High power impulse magnetron sputtering (HiPIMS) is one of the most promising sputtering-based ionized physical vapor deposition (IPVD) techniques and is already making its way to industrial applications. The major difference between HiPIMS and conventional magnetron sputtering processes is the mode of operation. In HiPIMS the power is applied to the magnetron (target) in unipolar pulses at a low duty factor ($< 10\%$) and low frequency ($< 10 \text{ kHz}$) leading to peak target power densities of the order of kW cm^{-2} . These conditions result in the generation of a highly dense plasma discharge, where a large fraction of the sputtered material is ionized and thereby providing new and added means for the synthesis of tailor-made thin films. In this work we dissect the HiPIMS discharge and thereby expose several important physical mechanisms operating during different stages of the discharge pulse. Recent experimental results on the evolution of the process gas (neutral Ar and Ar^{2+}) and in-situ measurements of the transport of charged particles have been combined with HiPIMS plasma modeling of the dense plasma region in front of the target to establish a more coherent picture of the HiPIMS discharge, which includes time- and

space-resolved characteristics on mechanisms such as process gas depletion, gas and metal sputtering, degree of ionization, as well as current distribution. Special attention is paid to how these internal pulse features can be influenced by the choice of discharge pulse configuration.

2:30pm **F2-2-3 High-rate reactive deposition of multifunctional Ta-O-N films using high power impulse magnetron sputtering**, J. Vlcek (vlcek@kfy.zcu.cz), J. Rezek, J. Houska, R. Cerstvy, University of West Bohemia, Czech Republic

High power impulse magnetron sputtering of a planar tantalum target (diameter of 100 mm) in various argon-oxygen-nitrogen gas mixtures was investigated at a fixed average target power density of 50 W cm^{-2} in a period. A strongly unbalanced magnetron was driven by a pulsed dc power supply (HMP 2/1, Huettinger Elektronik) operating at the repetition frequency of 500 Hz and the average target power density of up to 2.4 kW cm^{-2} in a pulse with a fixed $50 \mu\text{s}$ duration. The nitrogen fractions in the reactive gas flow were in the range from 0 to 100% at the argon partial pressure of 1.5 Pa and the total pressure of the argon-oxygen-nitrogen gas mixture around 2 Pa. The Si (100) and glass substrates were at a floating potential, and the substrate temperature was less than 250°C . The target-to-substrate distance was 100 mm. An effective reactive gas flow control made it possible to produce high-quality Ta-O-N films of various elemental compositions with high deposition rates (97 to 190 nm/min). Their compositions (in at. %) were varied from $\text{Ta}_{27}\text{O}_{72}$ with a low content (less than 1%) of hydrogen to $\text{Ta}_{38}\text{O}_4\text{N}_{55}$ with 3% of hydrogen. The former films were nanocrystalline with high optical transparency (extinction coefficient less than 10^{-4} at 550 nm), refractive index of 2.12, band gap of 4.0 eV, very low electrical conductivity (resistivity of $7.7 \times 10^9 \Omega\text{cm}$) and hardness of 7 GPa. The latter films exhibited a more pronounced crystallinity, they were opaque with relatively high electrical conductivity (resistivity of $4.2 \times 10^{-2} \Omega\text{cm}$) and hardness of 19 GPa. The $\text{Ta}_{27}\text{O}_{46}\text{N}_{31}$ films with 2% content of hydrogen, produced at the 50% nitrogen fraction in the reactive gas flow with the highest deposition rate of 190 nm/min achieved, were nanocrystalline with the band gap of 2.4 eV, electrical resistivity of $5.5 \times 10^6 \Omega\text{cm}$ and hardness of 8 GPa. Such films seem to be suitable candidates for visible-light responsive photocatalysts. Details of the deposition process and measured properties of the films will be presented.

2:50pm **F2-2-4 Variation of high power pulsed / modulated pulsed power magnetron sputtering based on oscillatory voltage wave forms for the deposition of carbon and aluminum oxide coatings**, W. Sproul (reactivesputtering@cox.net), Reactive Sputtering, Inc., US, J. Lin, Colorado School of Mines, US, B. Abraham, Zond, Inc. / Zpulser, LLC, US, J. Moore, Colorado School of Mines, US, R. Chistyakov, Zond, Inc. / Zpulser, LLC, US

A new plasma generator with its roots in the HiPIMS/MPP sputtering technology that now produces oscillatory waveforms was used for the deposition of carbon and aluminum nitride coatings. The amplitude and the frequency of the voltage oscillations control the discharge current and the plasma ionization: $I_d = f(U_d, f_w)$. At constant discharge voltage achieved by adjusting the frequency of the voltage oscillations, the discharge current could be increased by a factor of up to 7 times. With this new plasma generator, DLC coatings that are hydrogen free could be deposited with hardnesses that approach superhard values. The hardness of the DLC films is a function of the substrate bias voltage, substrate temperature, frequency of the voltage oscillations, and the field strength of the magnetron design. The new plasma generator has also been used for the reactive deposition of such films as AlN. A very interesting side effect of this new plasma generator is that at constant discharge voltage it is possible to generate a near arc free discharge for reactive sputtering processes while still producing a stream of ions from the sputtered material. An arc free process removes one of the disadvantages of HiPIMS sputtering as originally practiced. More will be presented about reactive sputtering using this new plasma source at the meeting.

3:10pm **F2-2-5 The development and the application of a high power impulse inverted cylindrical magnetron sputtering system for the elaboration of nanomaterials on wires or fibers**, A. Choquet (choquet@lippmann.lu), D. Duda, A. Lejars, O. Vozniy, T. Wirtz, CRP Gabriel Lippmann, Luxembourg

The elaboration of new nanomaterials on wires and on fibers is of great interest for industry. One possibility to manufacture these innovative products is to deposit thin films in a continuous way on wires or fibers. This solution offers possibility to synthesize new materials with a large flexibility for the process utilization.

An instrumental prototype designed as a continuous air-to-air in-line wire-coating has been set-up with the capability to run with speed lines between 5 to 30 m/min . A new Inverted Cylindrical Magnetron (ICM) plasma deposition reactor operated in the HiPIMS mode has been developed. It has

been demonstrated both theoretically and experimentally that this configuration allows a high ionization degree of sputtered target material while reaching the same high deposition rate as for planar magnetrons operated in the DC mode. It has been shown that this ICM configuration, which is moreover ideally adapted for a homogeneous wire coating due to its cylindrical symmetry, promotes a better self-assistance with target ions and allow for a repeated use of ionized species to maintain a high ionization degree in metal plasma. Also, the magnetron was intentionally designed with an unbalanced system of magnets to ensure the diffusion of the plasma electrons along the force lines of the magnetic field to the central part of the discharge volume. This magnetic field can permit to form a channel from the target surface to the wire, where the plasma volume can be extended down to the substrate area with minimal losses. It has also been shown that a non-stationary magnetic field allows to a better stabilization of the discharge voltage even at a high degree of the target erosion.

The outstanding performance of the ICM prototype, which is characterized by a much higher deposition rate than in conventional planar systems, was validated in direct measurements. The values of the deposition rate for the ICM were compared with a reactor equipped with 4 planar magnetrons surrounding the wire for the same power input per the cm² of the target surface. It was concluded that a 10 times higher deposition rate can be achieved with this ICM designed system. Also, in order to demonstrate the performance of the wire coated prototype instrument, elaborations of ZnO and AlTiSiN films on wires have been achieved. The structural and chemical properties of the ceramic films has been established and correlated with end-used performances.

3:30pm F2-2-6 Low pressure High Power Impulse Magnetron Sputtering systems for deposition of biomedical functional thin films, V. Stranak (*stranv00@centrum.cz*), University of Greifswald, Germany, *M. Cada, Z. Hubicka*, Academy of Sciences, Czech Republic, *S. Drache, A.P. Herrendorf, H. Wulff, R. Hippler*, University of Greifswald, Germany
INVITED

The high ionization of sputtered metal particles is a main advantage of High Power Impulse Magnetron Sputtering (HiPIMS) discharges. Large quantity of ionized sputtered material leads to the growth of smooth and dense films, allows control of the crystallography phase, mechanical and optical properties etc. Because of these positive effects there is reason to develop sputtering sources with high level of metal ionization. It is already known that namely energy of ions and incoming particles to growing film is a key parameter which influences film property. In our contribution we report two novel HiPIMS-based techniques which allow energy control in wide range.

The first system is a unipolar hybrid-dual HiPIMS based on a combination of dual-HiPIMS (the system where two magnetically and electrically confined magnetrons are alternately operated in HiPIMS mode, $f = 100$ Hz, duty cycle 1 %) with mid-frequency (MF) discharge operated at $f = 94$ kHz and duty cycle 30 %. The second system is based on sputtering of HiPIMS driven electrode inserted in RF discharge with an additionally superimposed magnetic field (ECWR). The most important feature of these hybrid methods is the pre-ionization effect which causes/allows: (i) significant reduction of working pressure by nearly two orders of magnitude, (ii) intensive ionization of metal atoms with substantial amount of double ionized species, (iii) increase of HiPIMS power density and other discharge parameters, (iv) faster ignition and development of HiPIMS pulses.

Enhanced time-resolved diagnostic of developed plasma sources has been done. From time-resolved Langmuir probe measurements was estimated mean electron energy, electron density and electron energy probability function (EPPF). The plasma density reached values about 5.10^{18} m^{-3} during HiPIMS pulses at low pressure (0.04 Pa). The time-resolved measurements of Ion Velocity Distribution Functions (IVDFs) and Ion Energy Distribution Functions (IEDFs) were performed. It was found that ion energies during HiPIMS pulses are strongly enhanced (about 20-30 eV) while in background (MF or RF) discharge were measured much lower values. Parameters from Langmuir probe diagnostic serve also as input for calculation of influx contributions of particular species, e.g. neutral particles. The study of plasma transport effects was done by fast optical emission imaging and spectroscopy.

This work was supported by Deutsche Forschungsgemeinschaft through SFB/TR 24 and by the German Federal Ministry of Education and Research (BMBF) through Campus PlasmaMed. Further projects KAN301370701 of ASCR, IM06002 of MSMT and project 202/09/P159 of GACR are acknowledged.

4:10pm F2-2-8 Material properties of Aluminum Metal (Titanium/Chromium) Nitride coatings deposited by High Power Impulse Magnetron Sputtering (HIPIMS⁺) technology., F. Papa (*fpapa@hauzer.nl*), *A. Campiche, R. Tietema, T. Krug*, Hauzer Techno Coating, BV, Netherlands, *T. Sasaki, T. Ishikawa*, Hitachi Tool Engineering, Ltd., Japan

Aluminum Metal (Titanium/Chromium) Nitride coatings have been deposited from targets consisting of tiles from 4 different aluminum metal compositions using HIPIMS⁺ technology. In such a configuration, the changes in material properties such as hardness and crystal orientation can be analyzed for many coating compositions while keeping the plasma conditions constant. The peak cathode current has been used as the control variable as this has a strong influence on the metal ion content within the plasma and the plasma density. As the peak cathode current is increased, the crystal size and structure change significantly. The effect of varying the plasma density on the proportion of the cubic/hexagonal phase for such materials as Al(Ti/Cr)N is of great interest for hard coatings for cutting tool applications.

4:30pm F2-2-10 On the Influence of superimposed MF and HPPMS/HiPIMS pulsed packages on the deposition rate and properties of TiN, J. Alami (*Jones.Alami@inicoatings.de*), *Z. Maric*, INI Coatings Ltd., Germany, *M. Malzer, M. Fenker*, FEM Forschungsinstitut Edelmetalle & Metallchemie, Germany, *M. Mark, J. Löffler, E. Parra Maza, G. Mark*, MELEC GmbH, Germany

High Power Pulse Magnetron Sputtering, HPPMS (also known as HiPIMS), is a promising pulsed plasma technology for deposition of high quality thin films. HPPMS has been shown to exhibit very high electron density and ionization of the sputtered material. The plasma charged particles are easily affected by magnetic and electric fields and present therefore conditions for the thin film developer to control the energy bombardment and subsequently the properties of the deposited thin films. Even if HPPMS has a great potential for bringing new and interesting solutions to the PVD market, it is still inconsistent and not standardized as is always the case for new technologies or techniques. It has been established that in order for HPPMS to function in an optimal fashion, it is of importance to understand not only the plasma condition of the process but also how the different parts of a coating system interact with each other in order to give the right process conditions needed for the deposition.

A number of works have characterized and attempted to correlate the effect of pulsing on the HPPMS process, especially on the deposition rate. These have used different power supplies as well as different power supply combinations in order to achieve the different modes of operation. They found that the pulsing configuration and frequency affect to a large extent the coating process as well as the resulting thin film properties.

Recent approaches supply power to the magnetron source by superimposing a medium frequency (MF) and a HPPMS power unit. The main advantage of such an approach is to provide means to even better architect the plasma conditions that best enable a suitable compromise between deposition rate and ionization. Moreover, the combination of MF and HPPMS allows better tuning of the process parameters and therewith the resulting thin film's properties. This new approach for using the HPPMS technique is appropriate for single and dual magnetron sputtering and synchronized pulsed bias. It is therefore possible to perform stable reactive depositions in continuous operating systems such as inline glass coaters.

The present work investigates the influence of the pulsed power controllers and the mechanisms for producing the very high peak currents needed for the HPPMS process. The influence of MF and HPPMS superimposed pulse packages on the deposition rate during reactive sputtering of titanium in an Ar/N₂ atmosphere will be presented. Additionally the resulting TiN film microstructure and phase/texture composition will be discussed with respect to the corresponding plasma conditions.

4:50pm F2-2-11 Angle-resolved energy flux measurements of a HIPIMS-powered rotating cylindrical magnetron in reactive and non-reactive atmosphere., S. Konstantinidis (*stephanos.konstantinidis@umons.ac.be*), University of Mons, Belgium, *W. Leroy*, Ghent University, Belgium, *R. Snyders*, University of Mons, Belgium, *D. Depla*, Ghent University, Belgium

Energy flux measurements were carried out using a passive thermal probe during sputtering of titanium in a reactive Ar/O₂ atmosphere with a rotating cylindrical magnetron. The data were collected 90° around the cylindrical magnetron cathode. The rectangular voltage pulses had a duration of either 5 or 20 μs and target voltage was set to 600V in order to reach a time-averaged power density over the racetrack of 30 W/cm². As a reference, the energy flux was also measured during DC magnetron under the same working conditions. The energy flux per adparticle was calculated by measuring the deposition rate for all sputter modes and regimes. The lowest deposition rate was measured during reactive HiPIMS, with 20μs-long

pulses. However the highest energy per adparticle was measured for that particular case. This result can be understood based on the increased ion and electron fluxes on the probe surface during the HiPIMS experiments. A possible contribution to the energy flux could also originate from the presence of fast oxygen ions (O^+) emitted from the target surface and accelerated in the cathode sheath. A difference in the angular distribution of the energy deposited per arriving adparticle is noticed when comparing the dc and the HiPIMS discharges. The dc mode has a maximum arriving energy per adparticle at around 50° , while the maximum is located at 60° for the HiPIMS mode.

Applications, Manufacturing, and Equipment

Room: Tiki Pavilion - Session G5-1

Coatings, Pre-Treatment, Post-Treatment and Duplex Technology

Moderator: N. Bagcivan, RWTH Aachen University, Germany, S. Brahmandam, Kennametal Incorporated, US

1:50pm **G5-1-1 Ion treatment and duplex coatings by arc plasma immersion surface engineering processes.**, V. Gorokhovskiy (vgorokhovskiy@vaportech.com), Vapor Technologies, Inc., US **INVITED**

The gaseous plasma of low pressure arc discharge has been used extensively for various surface treatment applications including heat treatment, ionitriding, ion implantation, PECVD and duplex processes. A highly ionized low pressure arc plasma with electron density up to $\sim 10^{12} \text{ cm}^{-3}$ can be generated by a shielded vacuum arc cathode, a hollow cathode or by a thermionic cathode. In this paper, the plasma properties are characterized by electrostatic probes and optical emission spectroscopy. A range of different species can be produced in low pressure arc plasma immersion processes via decomposition of precursor molecules by electron collisions. Surface treatment of different steels and metal alloys in such a dense plasma environment can substantially affect the surface profile. The ionitriding of different types of steel in low pressure arc plasma environment is investigated. The rate of ionitriding as a function of plasma parameters, such as ion current density, pressure and gas composition are established for several types of steel and reach up to 0.5 $\mu\text{m}/\text{min}$ for HSS in a pure nitrogen arc plasma with electron densities ranging from 10^{10} to 10^{12} cm^{-3} . The ionitriding layers can be produced in arc plasma immersion processes at substrate bias as low as 30 volts and substrate temperature as low as 200 deg C, depending on type of steel. Alternatively, ion implantation of nitrogen can be produced at bias voltage exceeding 500 volts at substrate temperatures less than 100 deg C. The distribution of plasma density and uniformity of ionitriding layers in industrial scale vacuum processing chambers are investigated. The duplex coatings were also produced by ionitriding in an arc plasma immersion environment followed by TiN coatings. The ionitriding and duplex coating layers are characterized by structure, thickness, microhardness depth profile, surface roughness and coating adhesion. Surface treatment in conventional glow discharge compared to low pressure arc plasma immersion processes is presented. The results of processing complex shape components are discussed.

2:30pm **G5-1-3 Growth kinetics of electrochemical boriding of titanium**, G. Kartal (kartalgu@itu.edu.tr), S. Timur, Istanbul Technical University, Turkey

Among all the engineering compounds, titanium has been becoming distinct and cost-competitive in many applications by reason of its exceptional strength-to-weight ratio, high toughness, and excellent biocompatibility. However, titanium and its alloys are having many difficulties in tribological functions in consequence of their poor friction and wear resistance. Boriding seems to be a perfect candidate surface hardening process considering the positive contributions on the working efficiency and improvements in service life. In this study, the electrochemical boriding was applied to titanium in a systematic manner and the effects of boriding process parameters on the morphological and chemical state of boride layers were explored. Moreover, kinetic approach was conducted for the boriding of titanium in order to have growth equation of TiB_2 layer and to determine a practical diagram for potential applications. The presence of both TiB and TiB_2 phases were confirmed by the X-ray diffraction method. The cross-sectional examination of borided titanium verified the boride layers consisted of a homogeneously TiB_2 phase on the top and TiB whiskers toward the substrate. The morphology of TiB phase was found to have a strong dependence on boriding temperature and it varied with process temperatures in following order: whiskers structure at around the beta transus temperature ($\approx 1173 \text{ K}$), dendritic branches at the temperature ranging from 1273 K to 1373 K, lateral islands at the temperature of 1473 K

and above. Methodical studies over a wide range of boriding time ($5 \text{ min} \leq t \leq 120 \text{ min}$) and temperature ($1173 \text{ K} \leq T \leq 1373 \text{ K}$) confirmed that the rate of the TiB_2 layer formation has a parabolic character. The activation energy (Q) and the pre-exponential factor (K_0) of TiB_2 layer were determined as 189.9 kJ/mol and $4.66 \times 10^{-7} \text{ m}^2 \text{ s}^{-1}$, respectively. The specific empirical equations that can be used to estimate the thickness of the TiB_2 layers (d_{TiB_2}) was obtained:

$$d_{\text{TiB}_2} = 682.67 \sqrt{(\exp(-22833/T))} \quad 1173 \text{ K} \leq T \leq 1373 \text{ K}; 200 \text{ mA}/\text{cm}^2$$

2:50pm **G5-1-4 Improvement of Electrical Properties of Silicon Oxide Film with Ultraviolet and Organic Gas Assisted Annealings**, T. Ito (ta10004@student.miyazaki-u.ac.jp), T. Matumoto, K. Nishioka, University of Miyazaki, Japan

TFTs (Thin film transistor) are important for electronic devices such as display and other electronic items. The TFT performance strongly depends on the interface properties and the impurities of gate insulator films. Low temperature and inexpensive technology is required for the formation of gate insulator using silicon oxide films.

The generated O from ozone gas attacks the chains of silicone oil and precursor is formed by displacing Si-CH₃ bond into Si-OH bond. Then the silicon oxide film is formed by the dehydration reaction of Si-OH bond. However, remaining Si-OH bond and impurities in the film is observed in the samples formed at low temperature.

In our previous work, we have reported an original method to reduce Si-OH bond from the silicon oxide films by dipping in ethanol before the post annealing in methanol gas. As a result, the dielectric property was improved by removal of Si-OH bond.

In this study, to modify the quality of silicon oxide formed at low temperature, UV light was irradiated to the sample before the organic gas assisted annealing.

Dimethyl-silicone-oil ($[\text{SiO}(\text{CH}_3)_2]_n[\text{Si}(\text{CH}_3)_3]_2$), was coated on p-type Si (100) substrates by a spin coater. This sample was set on the hot plate at 250°C and 8% ozone gas was introduced on the sample at 15 min. The film thickness was 150 nm.

In order to modify the quality of silicon oxide thin film, the sample was irradiated UV (254 nm, 60W) for 2 hr (UV annealing) and was dipped in ethanol at room temperature for 15 min before annealed on the hot plate in methanol gas at 250 °C for 15 min (organic gas assisted annealing).

The molecular structure of the silicon oxide was measured by Fourier transform infrared spectroscopy (FT-IR). The metal-oxide-semiconductor (MOS) structures were fabricated depositing Aluminum. Then, the current density-electric field ($J-E$) characteristics were measured.

The sample with UV and organic gas assisted annealings was evaluated by FT-IR. A peak of Si-O cage structure was decrease with the annealings. The Si-O cage structure (incomplete structure) was changed to the Si-O stretch structure by irradiating UV and annealing in organic gas. The decrease of the incomplete structure is good for the improvement of electrical properties.

The dielectric property of organic gas assisted annealing sample was poor, and the leakage current was more than $10^{-4} \text{ A}/\text{cm}^2$ even at 5 MV / cm. On the other hand, the leakage current of the UV and organic gas assisted annealings sample was $10^{-6} \text{ A} / \text{cm}^2$ at 5 MV / cm. The dielectric property was improved by reduction of Si-O cage structure. The $J-E$ characteristic was considerably improved by the UV annealing before organic gas assisted annealing.

3:10pm **G5-1-5 Enhancement of gas barrier properties of polypropylene by surface treatment before DLC coating**, H. Tashiro, A. Hotta (hotta@mech.keio.ac.jp), Keio University, Japan

Polypropylene (PP) materials are widely used as food packaging due to their lightness, low cost, and optical transparency. However, most of the polymer materials have low gas barrier property which may cause a great damage on the quality of food products. Thus the improvement of the low gas barrier property is widely desired.

Recently, thin solid coatings by diamond-like carbon (DLC) and silicon oxide (SiO_x) using plasma have become prominent methods. Several researches have been reported on the gas barrier properties of polymers coated with DLC, eventually improving the gas barrier properties of certain types of polymers such as polyethylene terephthalate (PET) used for bottles. However, DLC-coated PP could hardly show high gas barrier property. In order to solve this problem, surface modification prior to the DLC deposition was introduced.

For the surface modification, silane coupling treatment was investigated. A silane coupling agent is a common adhesion promoter which is widely used in polymeric composites with glass or silicate substrates. In addition, the silane coupling agent possesses high optical transparency, and it can easily spread over polymer films while coating since it is in a liquid state.

Furthermore, the silane coupling agent can solidify itself through hydrolysis and condensation processes which can be an easy and fast way to modify the surface of PP.

According to the results of the gas permeation test, it was found that the polymers modified with a variety of silane coupling agents prior to DLC coating showed high gas barrier properties. Especially the silane coupling agents with an amino group showed very low oxygen transmission rate, which was comparable to that of DLC-coated PET with extremely high gas barrier property. The barrier improved factor (BIF) became approximately 300 times higher than that of the untreated PP. This method can be applicable to several types of polymers including polyethylene (PE).

It is concluded that the surface modification using silane coupling agent is expected to be a great method to produce high barrier DLC on several polymers, which would expand the industrial application of the DLC-coated polymers.

3:30pm **G5-1-6 Cathodic Arc Plasma Treatment for Surface Alloying and Modification.** *M. Urgan* (*urgen@itu.edu.tr*), Istanbul Technical University, Turkey **INVITED**

In this talk, the motivation and principles behind "Cathodic Arc Plasma Treatment" (CAPT), a method involving application of high and low bias voltages to the substrate in a cyclic-pulsing manner during cathodic arc evaporation process will be introduced. This method differs from other relevant techniques since it does not aim to modify coating structure or surfaces with ion bombardment or ion implantation. It aims to benefit from the diffusion enhancing atomic - bulk heating effects induced through substrate - ion collisions during high bias voltage applications for alloying the substrate material with the condensing cathode material. The role of substrate temperature, magnitude, duration and type of high bias voltage and cathode current on surface alloying and intermetallic formation will be discussed based on studies conducted on binary Al-Cu¹ Cu-Al^{2,3}, and Co-Cr⁴ and Al-Fe-Cu¹ ternary systems.

References:

Corlu, B., Urgan, M. (2009). *Surf. Coat. Tech.*, 204(6-7), 872-877

Corlu, B., Urgan, M. (2010) *Surf. Coat. Tech.* 205(2), 540-544.

Arpat E., Urgan M., *Intermetallics* 19 (2011) 1817-1822

Akkaya, S.S, Sireli, E., Alkan B., Urgan M., *Surf. Coat. Tech.*, doi:10.1016/j.surfcoat.2011.09.046

4:10pm **G5-1-8 Microstructure and tribological properties of laser textured PVD coatings on tool materials.** *M. Adamiak* (*marcin.adamiak@polsl.pl*), Silesian University of Technology, Poland

Optimisation of manufacturing processes in mechanical engineering which involve high surface loads, machining speed or high working temperatures is today under intensive investigation worldwide. Recent advances in laser technology open new roads for modification of surface tribological properties, by generation of the solid lubricant reservoirs in hard coatings. The application of TiN, TiAlN and Ti(C,N) PVD coatings deposition and their laser surface texturing to permit storage of solid lubricants using the dimple reservoir concept on several tool steels was studied as possibly technology to improve the work life of tools made from them. Simulation of selected tribo-systems, microstructure and mechanical properties examination were carried out. The results show that significant increase of wear life (cost saving) can be achieved. It was discovered that the laser texturing of PVD coatings with optimum area for dimple reservoirs when combined with a low cost solid lubricant application, is a useful and cost effective tool for wear and friction control.

4:30pm **G5-1-11 Evaluation of Electrochemical Boriding of Inconel alloys.** *V. Sista* (*vsista@anl.gov*), Argonne National Laboratory, US, *O. Kahvecioglu*, Istanbul Technical University, Turkey, *G. Kartal*, Technical University of Istanbul, Turkey, *Q.Z. Zeng*, Xian Jiaotong University, China, *O.L. Eryilmaz*, *A. Erdemir*, Argonne National Laboratory, US, *S. Timur*, Istanbul Technical University, Turkey

Inconel alloys are very common nickel based super-alloys which are used extensively for a variety of high-temperature and aggressive environment applications such as metal seat ball valves, high temperature fasteners, nuclear reactors etc. They are extremely resistant to high temperature corrosion and boriding them would further enhance their corrosion resistance and improve their tribological properties. In this study, we performed electrochemical molten salt boriding which was carried out in a borax bath at 950°C for just 15 minutes to produce a very homogeneous, boride layer of 81µm in thickness. Different boride phases were identified by X-ray diffraction and the morphology of the borided surfaces was characterized by both optical and scanning electron microscopy (SEM). Microhardness measurements for different layers of nickel borides were measured and found to be in the range of 1500-1900 HV. Pin on disk wear

tests were performed under dry and lubricated conditions and much superior wear performance of borided surfaces with a wear depth of 1-1.5 µm was confirmed compared to the base Inconel alloys with a wear depth of 13-15 µm. The aim of this study is to show that electrochemical boriding is applicable to Inconel alloys and this method can be considered as an alternative way of producing hard boride layers on Inconel and hence make them more resistant to mechanical and environmental degradations.

4:50pm **G5-1-12 Electrochemical Boriding of Molybdenum.** *O. Kahvecioglu* (*kahveciog3@itu.edu.tr*), Istanbul Technical University, Turkey, *V. Sista*, *O.L. Eryilmaz*, *A. Erdemir*, Argonne National Laboratory, US, *S. Timur*, Istanbul Technical University, Turkey

In this study, we explored the possibility of electrochemical boriding of molybdenum (99.5% purity) plates in a molten borax electrolyte. Electrochemical boriding was performed at 950-1000 °C for 2-3 h and at a current density of 0.5 A/cm². The boride layers formed on the test samples were 40 to 48 µm thick depending on process temperature and duration. It was found that two distinct boride phases (namely Mo₂B₃ and MoB) could be obtained on molybdenum substrate. The mechanical, structural, and chemical characterization of the boride layers was carried out using a Vickers micro-hardness test machine, optical and scanning electron microscopes, and a thin film x-ray diffractometer. The hardness of boride layer was in the range from 1800–2700 ± 50 HV depending on the load and the region from which the hardness measurements were taken. Cross-sectional micro-hardness tests showed that the boride layers were well adhered within each other whereas Rockwell C adhesion test applied on top of surface showed delamination. Structurally, the boride layers were very homogenous and uniformly thick across the borided surface area.

5:10pm **G5-1-13 Mechanical and Microstructural Characterization of Nitrided AISI 4140 steel with Electroless NiP Coating.** *R. Torres* (*ricardo.torres@pucpr.br*), *P. Soares*, Universidade Católica do Paraná, Brazil, *M. Soares*, IFSC, *R.M. Souza*, Mechanical Engineering Department, Universidade de São Paulo, Brazil, *P. Souza*, Universidade Católica do Paraná, Brazil, *C. Lepiesnski*, UFPR, Brazil

Electroless nickel (NiP) is widely applied in the off shore industry, due to its superior corrosion behavior in environments rich in H₂S and CO₂. The Electroless nickel is deposited onto steel substrates by a self-catalytic process, which involves temperatures and time to create a layer with thickness around 75 µm. The major drawback of electroless nickel is the post treatment process, which results in softening of the steel substrate due to exposition to high temperatures for long periods of time. This post treatment process creates a diffusion layer between the steel and NiP. The aim of this ongoing research is to investigate the effect of introducing a nitrided layer prior to deposition of NiP layer, as an attempt to avoid the softening of the steel substrate in areas close to the NiP coating. To this end, NiP coatings were obtained over nitrided and non-nitrided steel substrates. The nitriding process was conducted in plasma environment using 75% nitrogen and 25% of hydrogen. The nitriding temperature and time were 480oC and 6 hours, respectively. The NiP deposition temperature was 90oC, the deposition times were 2 or 4 hours, to produce two different coating thicknesses. The post treatment process temperature and time were 610oC and 12 hours, respectively. Specimens were analyzed in terms of coating thickness, structure and hardness. It has been found that the nitrided layer reduces the NiP deposition rate, even though the diffusion layer thickness and spatial distribution of P and Ni remains practically unchanged in comparison with the non-nitrided specimens. During the post treatment procedure, the nitrided layer avoided the softening of the substrate area in contact with NiP.

Wednesday Morning, April 25, 2012

Coatings for Use at High Temperature Room: Sunrise - Session A1-1

Coatings to Resist High Temperature Oxidation, Corrosion and Fouling

Moderator: D. Naumenko, Forschungszentrum Jülich GmbH, Germany, L-G. Johansson, Chalmers University of Technology, Sweden, B. Hazel, Pratt and Whitney, US, J. Pérez, Universidad Complutense de Madrid, Spain

8:00am **A1-1-1 Hot corrosion of NiAl diffusion coatings by gaseous Na_2SO_4 .** *K. Stiller* (*stiller@chalmers.se*), *H. Lai*, *P. Knutsson*, L-G. Johansson, Chalmers University of Technology, Sweden **INVITED**

The results from a novel method for hot corrosion testing by gaseous Na_2SO_4 attacks will be presented. In this hot corrosion test, sodium sulphate vapour is continuously supplied to the surface of the exposed samples through salt evaporation from a crucible placed inside the furnace. The temperature of the furnace and the position of the test coupons are chosen so that there is no condensation of the salt on the specimen's surfaces during the exposures. In this work NiAl diffusion coatings with and without Pt were exposed at 900° C up to 1000 h and investigated using different high-resolution techniques. It will be shown that already after 100 hours of testing there is an observable corrosion attack, characterized by a penetrated protective oxide and the formation of sulfides at the oxide/metal interface. The possible scenario of reactions taking place during the testing is presented and the obtained results are compared with those from testing using a well-established ex-situ salt hot corrosion method.

8:40am **A1-1-3 Early Stages during Exposure of Uncoated and Coated HK40 Steel to Carburizing Atmospheres.** *D. Melo-Máximo*, TRAMES, S.A de C.V, Mexico, *O. Salas* (*osalas@itesm.mx*), *J. Oseguera*, Instituto Tecnológico y de Estudios Superiores de Monterrey-CEM, Mexico, *R. Reichelt*, Institut fuer Medizinische Physik und Biophysik Westfaelische Wilhelms-Universitaet, Germany

Coated and uncoated samples of HK40 steel were exposed to a carburizing atmosphere at high temperature for short periods of time in order to get more insight into the role of coatings in protecting this material in carburizing environments. The coated samples were produced by applying a surface thin film of $\text{Cr/Cr}_2\text{O}_3$ by reactive magnetron sputtering. Both, coated and uncoated, samples were subjected to a carburizing atmosphere of CH_4 decomposition (+ residual oxygen) at 800°C for 10 minutes, 30 minutes, 60 minutes and 5 hours. The resulting structures were characterized by scanning electron microscopy + energy dispersive spectroscopy, high resolution scanning electron microscopy, and x-ray diffraction. The results indicate that the dendritic structure of the HK40 steel and the presence of residual oxygen in the carburizing had a strong influence in the microstructural evolution during carburization.

9:00am **A1-1-4 New results and improvements of the catalytical poisoning concept against metal dusting.** *C. Geers* (*geers@dechema.de*), *M. Galetz*, *M. Schütze*, Dechema e.V., Frankfurt am Main, Germany

Under conditions of carbon activities higher than one and low oxygen partial pressures steels and nickel base alloys can be destroyed by a corrosion mechanism called metal dusting, in the temperature range of 400 to 900°C. A carbon activity higher than one means that the gas phase is beyond equilibrium and a strong driving force exists for the deposition of carbon from the gas phase onto the metal surface. This process is promoted by the catalytically triggered disintegration of hydro carbons or carbon oxides in the gas environment. As a consequence of the carbon deposition on the metal surface, carbon can diffuse into the material and precipitate as graphite at preferred crystallographic orientations in the metal subsurface causing total metal disintegration and the formation of 'metal dust'.

Metals catalytically triggering this type of corrosive attack are iron, nickel and cobalt. In order to inhibit the catalytic promotion of carbon oxide or hydro carbon disintegration and by this the deposition of carbon a catalytic poisoning concept was developed. Tin was shown to occupy the catalytically active centers of nickel on the metal surface via the formation of an intermetallic Ni_3Sn_2 -phase with the latter suppressing any catalytic effect of the surface.

The performance of this phase was studied for 3000 hrs for several conventional alloys. In the work described in this paper the influence of alloy composition on the stability of the intermetallic phase will be discussed.

For technical applications, the performance of the intermetallic phase at the surface under oxidizing conditions is also a point of interest as start up and shut down processes usually occur in air. The influence of oxidation during these periods on the stability of the intermetallic phase was investigated as well and the results will be reported here.

A third part presented in this paper deals with possibilities to further improve the protection concept.

9:20am **A1-1-5 Structural Evolution of Candidate Coatings for Protection against Corrosion at High Temperature.** *L. Melo*, Instituto Politécnico Nacional, Mexico, *O. Salas* (*osalas@itesm.mx*), *J. Oseguera*, Instituto Tecnológico y de Estudios Superiores de Monterrey-CEM, Mexico, *V. Lopez-Hirata*, Instituto Politecnico Nacional, Mexico, *R. Torres*, Pontificia Universidade Católica do Paraná, Brazil, *R.M. Souza*, Universidade Federal de Sao Paulo, Brazil

The effect of several process variables on the structure of $\text{Cr/Cr}_2\text{O}_3$ films deposited on various stainless steel substrates was investigated as a tool to design effectively protective coatings for these materials during exposure to carburizing atmospheres at high temperatures. The coatings were produced by unbalanced magnetron sputtering varying: the type of substrate (304, 316 and HK40 steels), the rate of oxygen feeding, the partial pressure of oxygen, the application of bias voltage, and adding a nitriding treatment on the substrates. The structure of the films produced was analyzed by scanning electron microscopy + energy dispersive spectroscopy. The results indicate that the type of substrate material seems to affect the growth mode of the films, and the residual stresses developed. A higher flow of oxygen or the application of a negative bias voltage leads to the formation of denser film structures and a change in the residual stresses. The presence of a nitrided surface affected the surface roughness of the coatings and the evolution of the residual stresses. The effect of the rate of oxygen feeding was not significant in the ranges studied.

9:40am **A1-1-6 Fundamental Approaches to Optimizing the Hot-Corrosion Resistance of Coatings.** *B. Gleeson* (*bgleeson@pitt.edu*), University of Pittsburgh, US, *Z. Tang*, Iowa State University, US **INVITED**

The composition and related microstructure of alloys and coatings can greatly influence their resistance to a highly accelerated form of sulfate-deposit induced degradation termed "hot corrosion". This presentation examines the effects of metallurgical factors such as phase constitution, composition and volume fraction on the hot-corrosion resistance (Type I-900°C and Type II-700°C) of Ni-based alloys and coatings. Both types of hot corrosion conditions were simulated by depositing Na_2SO_4 on the test samples and then exposing those samples to a catalyzed $\text{O}_2\text{:SO}_2$ atmosphere. It will be shown that duration of protection against hot corrosion (*i.e.*, the incubation period) is very much linked to the oxidation behavior of the alloy or coating and, in particular, its ability to heal its thermally grown oxide scale. It will also be shown that sulfur from either the combustion gas or the sulfate deposit can accelerate establishment of the stable $\alpha\text{-Al}_2\text{O}_3$ scale during exposure at 900°C. Finally, the results from a recent study that systematically explored the effects of Ni:Co ratio and Cr content on the phase equilibria and high-temperature oxidation and hot corrosion behavior of CoNiCrAlY systems will be presented. The fundamental results derived are directly relevant to the development of optimum MCrAlY coating compositions.

10:20am **A1-1-8 High temperature oxidation studies of Detonation-Gun sprayed $\text{NiCrAlY}+0.4\text{wt}\%\text{CeO}_2$ coating on Fe and Ni -Based Superalloys in air under cyclic condition at 900 °C.** *S. Kamal* (*s_d_kamal@rediffmail.com*), Sharda University, India, *D. Mudgal*, *R. Jayaganthan*, *S. Prakash*, I.I.T-Roorkee, India

An addition of rare earth oxides to superalloy coatings could enhance the high temperature properties of the coatings in the actual service condition due to the purification of its microstructures. High temperature oxidation studies of D-Gun sprayed MCrAlY coatings (Where M = Ni or Fe) with minor addition of CeO_2 is scarce in the literature. Therefore, the present work was focused to study the effect of rare earth oxide (CeO_2) on the high temperature oxidation behavior of D-Gun sprayed NiCrAlY coatings on Ni- and Fe- based superalloys. Cyclic oxidation tests were carried out for 100 cycles at 900 °C to study the oxidation kinetics of un-coated and coated superalloys. The corroded products obtained during cyclic oxidation of coatings were subjected to XRD, FE-SEM/EDAX and X-ray mapping analysis to elucidate the high temperature oxidation mechanisms.

Keywords: Detonation-Gun process; Superalloys; Coatings; Oxidation; Rare earth, thermal spray coating

10:40am **A1-1-9 High temperature oxidation studies of D-gun sprayed Cr₃C₂-25(NiCr) and Cr₃C₂-25(NiCr) + 0.2wt%Zr coatings on Ni and Co based superalloys in air at 900 °C.** *D. Mudgal* (deep1dmt@iitr.ernet.in), Indian Institute of Technology Roorkee, India, *S. Kamal*, Sharda University, India, *S. Singh*, *S. Prakash*, Indian Institute of Technology Roorkee, India

The addition of small amount of rare earth material such as Zirconium in the high temperature coatings has been found to significantly enhance the adherence of the oxide scale. The present study focused on comparison between the high temperature oxidation behaviors of D-gun sprayed Cr₃C₂-25(NiCr) and Cr₃C₂-25(NiCr) + 0.2wt%Zr coatings on Ni and Co based superalloys. Oxidation kinetics of the bare and coated superalloys in air at 900 °C under cyclic condition was investigated using the thermogravimetric techniques. The results analysis has been carried out using FESEM/EDAX, XRD and X-ray mapping.

11:00am **A1-1-10 Oxidation behavior of Hf-modified aluminide coatings on Haynes-188 at 1050°C.** *Y. Wang* (yongqingblessing@yahoo.com), *M. Suneson*, SIFCO Minneapolis, US

Simple β-(Co,Ni)Al coatings, Hafnium (Hf)-modified β-(Co,Ni)Al coatings, Pt-diffused coatings, Pt-modified β-(Co,Ni,Pt)Al + ξ-PtAl₂ coatings, and Hf-Pt-modified β-(Co,Ni,Pt)Al coatings on Haynes-188 substrates were tested at 1050°C in air for up to 4670h. Surface morphology and cross-section microstructure of the tested specimens were inspected and compared by using Scanning Electron Microscope (SEM) equipped with energy dispersive spectroscopy (EDS). Experimental results showed that the Pt-diffused Haynes 188 specimen failed first in 600h; the testing of other four coatings was stopped at 4670h. HfO₂ particles were observed in the oxide scale on Hf-modified or Hf-Pt-modified aluminide coatings. The difference between coatings with or without Hf, as well as the oxidation performance difference between Ni-base superalloy substrate and Co-base superalloy substrate will also be discussed.

Key Words: Hafnium, aluminide coatings, Co-base alloys, oxidation testing

Hard Coatings and Vapor Deposition Technology Room: Royal Palm 4-6 - Session B4-2

Properties and Characterization of Hard Coatings and Surfaces

Moderator: J. Lin, Colorado School of Mines, US, C. Mulligan, U.S. Army ARDEC, Benet Laboratories, US, B. Zhao, Exxon Mobile, US

8:00am **B4-2-1 Design and plasma synthesis of tribological surfaces for titanium.** *A. Leyland* (a.leyland@sheffield.ac.uk), University of Sheffield, UK, *G. Cassar*, University of Sheffield, UK; University of Malta, Malta, *A. Matthews*, University of Sheffield, UK **INVITED**

Although plasma-assisted processing techniques are now widely established for the production of wear-resistant coatings and treatments on machine tools and engineering components manufactured from traditional (mainly ferrous), metallic substrate materials, there remain considerable scientific and technical challenges in applying such techniques effectively to address the increasing demand for tribological functionality on articles made from non-ferrous and composite materials. Although such materials in general tend to offer (amongst many desirable engineering properties) high specific strength - and excellent static and/or bulk-material load-bearing properties - the opposite is often true of their surface wear and corrosion behaviour when subjected to dynamic contact forces. In principle, techniques such as plasma-assisted physical vapour deposition (PVD) are an ideal choice to apply hard, wear-resistant coatings to - for example - light alloys (which the aerospace automotive and biomedical sectors of industry would ideally choose to use more widely); however, in practice the relatively low yield strength and compliant nature of many such materials is not conducive to optimising the performance of stiff ceramic thin films.

Taking the example of titanium alloy substrates, one efficient approach that can be adopted to improve the performance and durability of PVD ceramic thin films is to diffusion pre-treat the substrate material prior to coating. In this regard, nitrogen and oxygen diffusion treatments are promising candidates - particularly if they can be performed by plasma-assisted techniques which may be i) more rapid, flexible and controllable than other available methods and ii) possible to integrate seamlessly and cost-effectively within the PVD coating process cycle. Despite the fact that such 'duplex' plasma diffusion/coating techniques have been commonly investigated (and reported in the literature) over the last 15-20 years, their commercial exploitation remains somewhat lower than might be expected.

One widely known issue in the duplex treatment/coating of ferrous materials (where nitriding is frequently the substrate pretreatment of choice) is that of surface nitride compound layer control and/or elimination - although the means to achieve this are now quite well understood.

For titanium alloys however, the situation is considerably more complex and less well resolved; the response of different alloy materials to diffusion treatment by either nitrogen or oxygen is critically dependent on both alloy composition and microstructure (the latter also being, in some cases, very sensitive to treatment temperature). Furthermore, the nature and thickness of the surface compound layers produced during such treatments can also strongly influence the growth characteristics of the underlying diffusion zone - which (on the one hand) needs to be sufficiently deep to provide the necessary load support to a PVD coating subsequently applied, but (on the other) also needs to be produced as rapidly as possible, to make the duplex process cost-effective (whilst at the same time not compromising significantly the substrate bulk properties in terms of mechanical strength and/or fatigue resistance).

Here we present details of a hot-filament enhanced (triode) plasma processing technique, which can be used both to triode-plasma diffusion treat and (by electron-beam evaporative PVD) to duplex treat/coat selected titanium alloys. The diffusion treatments comprise triode plasma nitriding (TPN), triode plasma oxidation (TPO) and a sequential 'oxy-nitriding' (TPON) approach, each of which can be optimised to suit different substrate materials and applications. Structural, mechanical and tribological properties provided by such treatments are discussed in the context of two Ti-alloys; the (ubiquitous) α/β alloy Ti-6Al-4V and a metastable β alloy, Ti-15Mo - each of which illuminate particular (and different) treatment design and processing considerations, both for the diffusion treatment efficiency/performance and for their receptiveness to subsequent duplex PVD coating.

8:40am **B4-2-3 Study of the environment effect on the tribological behavior of TiN, TiAlN and CrN coatings deposited by Reactive Magnetron Sputtering.** *J.S. Restrepo* (johansrestrepo@hotmail.com), *S. Muhl*, Universidad Nacional Autónoma de México - Instituto de Investigaciones en Materiales, Mexico, *M.F. Cano*, *F. Sequeda*, *J.M. Gonzalez*, Universidad Del Valle, Colombia

We have been deposited CrN, TiAlN and TiN films by reactive magnetron sputtering to evaluate the tribological properties in different environment conditions (vacuum, room and nitrogen) using the pin on disc test. The aim of the study was to investigate the effect of the presence of oxide wear particles on the friction and wear coefficient. The formation of such wear debris is known to be important but the details of the effect on the tribological behavior of coatings are not completely clear. Our results show that under room conditions the CrN films has an initial stable friction coefficient, due to the formation of roll-shaped wear particles that can easily support the load. Meanwhile, the TiN film showed the formation of a higher and unstable friction coefficient due to generation of angular particles that causes surface ploughing because of its greater hardness than the coating; this is what directly produces the higher wear coefficient. The TiAlN coating shows a similar wear mechanism to the TiN but the friction coefficient is more stable because the material has a higher plastic deformation and oxidation resistance allowing for distortion of the wear particles.

9:00am **B4-2-4 Wear behaviour of plasma sprayed Cu-Ni coatings on Al7075.** *M.J. Ghazali* (mariyam@eng.ukm.my), Universiti Kebangsaan, Malaysia, *E. Mat Kamal*, Universiti Teknikal Malaysia, *S. Abdullah*, *J. Sheng*, Universiti Kebangsaan, Malaysia

Despite of its poor tribological properties (low hardness and low resistance to friction wear and abrasion) and a poor seizure resistance, aluminium has become a potential material in the automotive lightweight engineering. To overcome these weaknesses and increase the engine lifetime, a surface treatment can be one of the best options. In this work, Cu-Ni alloy that has such excellent properties such as; ductility, corrosion and wear resistance, good electrical and thermal conductivity as well as it can be easily joined or fabricated into useful shapes was chosen. The work aims to study the wear behaviour of Cu-Ni coatings deposited on Al7075 substrates using an atmospheric plasma spray (APS) with different plasma powers. Lubricated wear test were carried out on a pin-on-disc tester under an applied load of 100 N with fixed sliding speed of 0.851 ms⁻¹ at room temperature (23 °C). It was found that a decrease in plasma power from 40 to 30 kW promoted finer microstructures and higher hardness of the coatings, up to 39%. At 30 kW plasma power, the formed splats presented a high degree of flattening and solidification without many splashes. At greater power of 40 kW, the velocity and temperature of the droplets were increased, resulting rough coating structures that most likely caused by overlapping splats. This, however, weakened the bonding between splats. In general, an increase in the wear resistance of Cu-Ni coatings on Al7075 was found from ~ 6 x 10⁻⁵

mm³/Nm to $\sim 18 \times 10^{-5}$ mm³/Nm, indicating a mild wear regime, as expected, was attributed to the increase of the coating hardness.

9:20am **B4-2-6 Abrasive wear properties of AlCrN, AlTiN and CrN coatings.** J.L.M. Mo, M.H. Zhu, Southwest Jiaotong University, China, A. Leyland, A. Matthews (A.Matthews@sheffield.ac.uk), University of Sheffield, UK

Abrasive wear properties of AlCrN, AlTiN and CrN coatings deposited by a multiple arc vapor deposition technique on cemented carbide substrates were evaluated on a micro-scale abrasion tester under different normal loads ($F_n=0.2, 1$ N) and different numbers of ball revolutions ($N=10, 20, 50, 100, 200$ rev). A micro-blasted 25 mm diameter hardened steel sphere was used as counterface ball and a suspension of SiC particles (mean size of 4-5 μ m) as the abrasive slurry. After the wear tests, the wear craters were studied by stylus profilometer and Scanning Electron Microscopy (SEM) and the wear behaviors were investigated. It was shown that the AlCrN coating had much better anti-abrasive wear properties than the AlTiN coating, though the latter had a lower $H_{\text{abrasive particles}}/H_{\text{surface}}$ ratio. The CrN coating exhibited much worse abrasive wear resistance as compared to the two ternary nitride coatings. A three-body rolling wear mechanism was found to be dominant under the relative lower normal load of 0.2 N. However, the three coatings showed different abrasive wear degradation behaviors: the AlCrN coating showed the best resistance to the impact deformation and thus a great potential in rolling wear resistance, the AlTiN coating showed relative higher wear rate with the worn surface being characterized by a heavier deformation, the CrN coating showed the worst abrasive wear resistance by heavier plastic deformation and a dominant wear mechanism of cracking and micro-spalling. The difference between the AlCrN and AlTiN coatings were further studied under higher normal load of 1 N, in that case two-body grooving wear was the relatively dominant mechanism, the AlTiN coating exhibited much heavier grooving wear than the AlCrN coating.

9:40am **B4-2-7 Annealing-induced structural and mechanical property changes of CVD-(Si)-B-C coatings.** C. Pallier, G. Chollon (chollon@lcts.u-bordeaux1.fr), P. Weisbecker, F. Teyssandier, LCTS-CNRS, France

Amorphous B-C and Si-B-C ceramics were deposited by CVD from BCl₃-CH₄-H₂ and BCl₃-CH₃SiCl₃-H₂ mixtures, respectively, at temperatures around 1000 °C and reduced pressure. All the as-deposited (Si)-B-C ceramic coatings are nearly amorphous and consist of a common very disordered boron carbide phase (B₂C) and, in the Si-B-C coatings, sub-nanometric SiC crystals. The proportions of the B₂C and the SiC phases vary with the deposition conditions. A SiC grain growth is observed after heat treatment beyond 1200 °C, while the amorphous B-C-rich phase is gradually transformed into free aromatic carbon and B₂C nanocrystals, in agreement with the thermodynamic equilibrium. This particular crystallization process is expected to lead to a significant time/temperature-dependent change of the density and the mechanical properties. It has to be considered to better understand and predict the behavior of the ceramic matrix composite parts in future aeronautic engines.

The crystallization behavior in inert atmosphere of the (Si)-B-C ceramics is investigated in situ, by differential scanning calorimetry analyses and X-ray diffraction. Ex-situ analyses are also conducted by heat-treating the specimens under high vacuum at different temperatures/durations, and by characterizing the resulting microstructures at short and long range, by solid MAS-NMR, Raman microspectroscopy, neutron diffraction, X-ray absorption, X-ray diffraction and transmission electron microscopy.

Indentation tests are achieved at room temperature on the pristine and annealed coatings, to evaluate their stiffness, hardness and toughness. High temperature tensile tests are also performed on model 1D composites consisting of (Si)-B-C coatings deposited on soft carbon monofilaments. These micro tensile tests allow the evaluation of the changes of (i) the volume (or density), (ii) the Young's modulus, (iii) the creep rate and (iv) the thermal expansion of the coatings. We expect the mechanical behavior and the structural ordering of the (Si)-B-C ceramics to be strongly interrelated. The results obtained on the various specimens will be discussed on the basis of their elemental composition, initial structure and processing conditions.

10:00am **B4-2-8 Thermal evolution of thermal, electrical and optical properties of Ti-Al-N coatings.** R. Rachbauer (richard.rachbauer@oerlikon.com) OC Oerlikon Balzers AG, Liechtenstein, J.J. Gengler, Air Force Research Laboratory, Thermal Sciences and Materials Branch, US, A. Voevodin, Air Force Research Laboratory, US, K. Resch, Materials Science and Testing of Plastics, Montanuniversität Leoben, Austria, P.H. Mayrhofer, Montanuniversität Leoben, Austria
Physically vapor deposited Ti_{1-x}Al_xN thin films are well acknowledged in various industrial applications due to their beneficial effect on lifetime and performance of e.g. cutting or milling tools. The excellent thermal stability

of Ti_{1-x}Al_xN is determined by the incorporation of Al on Ti lattice sites in a cubic (c) supersaturated metastable solid solution of Ti_{1-x}Al_xN after deposition. Thermally activated diffusion processes lead however to a series of decomposition phenomena, involving first recovery of deposition induced defects and then the spinodal decomposition process which accounts for a hardness increase with increasing isostructural decomposition state into c-TiN- and c-AlN-enriched domains [1, 2]. The subsequent recrystallisation and development of a dual phase structure composed of cubic TiN and hexagonal AlN initiates deteriorating mechanical properties. Earlier investigations [3] have proven the big potential of the *age hardening* phenomenon for high temperature applications in cutting applications, however the development of thermal, electrical and optical properties has not yet been investigated as a function of temperature. Hence, the present study focuses on the thermal evolution of heat conductivity, electrical resistivity and optical reflectance from room temperature up to 1400 °C and relates to decomposition induced structural and chemical changes of Ti_{1-x}Al_xN. This contribution aims for a deeper understanding of Ti_{1-x}Al_xN thin films under thermal load, which is necessary for the development of e.g. state-of-the-art protective coatings for cutting tools or thermal barrier coatings for electronic devices.

References:

- [1] P. H. Mayrhofer, A. Hörling, L. Karlsson, J. Sjölen, T. Larsson, C. Mitterer, L. Hultman, *Self-organized nanostructures in the Ti-Al-N system*, Appl. Phys. Lett. 83 (2003) 2049-2051
- [2] R. Rachbauer, S. Massl, E. Stergar, D. Holec, D. Kiener, J. Keckes, J. Patscheider, M. Stiefel, H. Leitner, P. H. Mayrhofer, *Decomposition pathways in age hardening of Ti-Al-N thin films*, J. Appl. Phys. 110 (2011) 023515
- [3] A. Hörling, L. Hultman, M. Odén, J. Sjölen, L. Karlsson, *Mechanical properties and machining performance of Ti_{1-x}Al_xN-coated cutting tools*, Surf. Coat. Technol. 191 (2005) 384-392

10:20am **B4-2-9 Pressure and Temperature Effects on the Decomposition of Arc Evaporated Ti_{1-x}Al_xN Coatings During Metal Machining.** N. Norrby (nikno@ifm.liu.se), M. Johansson, Linköping University, Sweden, R. M'Saoubi, Seco Tools AB., Sweden, M. Odén, Linköping University, Sweden

This study focuses on the coherent and isostructural decomposition of cubic c-(Ti,Al)N thin films during metal machining, i.e. under the influence of large normal stress and elevated temperature typical for the selected cutting application. It is well known that c-(Ti,Al)N decomposes in two steps at elevated temperatures. In the first step, c-(Ti,Al)N decomposes spinodally into coherent isostructural cubic TiN- and AlN-enriched domains and in the second step a transformation from c-AlN to the stable wurtzite AlN occurs. Associated with the first step is an increase in hardness due to a coherency strain between the domains whereas the second step introduces large incoherent precipitates, thus rapidly lowering the hardness. However, the insight on the decomposition process during the application of variable stresses and heat, as in the case of metal cutting is scarce.

Here we have deposited thin films of Ti_{0.6}Al_{0.4}N by cathodic arc evaporation onto tungsten carbide (WC-Co) cutting tool inserts and studied the phase and microstructure evolution after a continuous turning operation for 10 minutes in carbon steel (C45E). For comparison, reference samples have been heat treated with a heating rate of 20 Kmin⁻¹ followed by an isothermal step of 10 minutes at 900 °C and 1000 °C respectively.

During turning at variable cutting speeds, v_c , between 100 m/min and 400 m/min, the peak temperature at the cutting edge was between 750 °C and 950 °C as measured by an IR-CCD camera. The peak normal stress, evaluated from measured contact forces during cutting, was about 2 GPa and independent of the range of cutting speeds investigated. The deduced stress distribution also shows that the normal stress along the rake face is decreasing with an increasing distance from the cutting edge towards the end of the tool-chip contact. Transmission electron microscopy (TEM), including analytical scanning TEM (STEM) has been used for detailed characterizations of the tool-chip interface along the cutting edge. The progression of the spinodal decomposition is determined by the domain size of the TiN and AlN enriched domains and is measured from STEM micrographs. After heat treatments, the results show an increased domain size from 2.8 to 5.0 nm with increasing annealing temperature from 900 to 1000 °C which is expected. After cutting tests however, an increase in domain size from 3.2 to 5.6 nm is seen with the increasing normal stress along the cutting edge. This implies that even relatively small pressures promote coherent isostructural decomposition, which is in line with theoretical studies but has previously not been shown experimentally.

10:40am **B4-2-10 Understanding the deformation kinetics of $Ti_{1-x}Al_xN$ ceramics at moderately elevated temperatures.** C. Ciurea (ccc109@imperial.ac.uk), V. Bhakhri, N. Ni, Imperial College London - South Kensington Campus, UK, P.H. Mayrhofer, Montanuniversität Leoben, Austria, F. Giuliani, Imperial College London - South Kensington Campus, UK

This work presents a comparative study of the influence of temperature on the mechanical behaviour of bulk single crystal (001) TiN (SC-TiN), magnetron sputtered single crystal TiN and magnetron sputtered $Ti_{1-x}Al_xN$ films ($x=0.34, 0.52$) deposited on (001) MgO substrates. High temperature nanoindentation (room temperature to 350 °C) was used to extract fundamental deformation rate-controlling parameters such as activation volume, activation energy and Peierls stress, demonstrating the usefulness of the indentation as an effective experimental technique for investigating kinetics of plastic deformation in ceramics at moderately elevated temperatures.

This analysis showed that the hardness of bulk single crystal TiN dropped from 21 ± 0.5 GPa at 22°C to 10.7 ± 0.45 GPa at 350°C. Interestingly, the hardness of sputtered single crystal TiN and $Ti_{1-x}Al_xN$ with low aluminium concentration ($x=0.34$) also dropped by a similar magnitude although from a higher starting values. However, the $x=0.52$ film exhibited a remarkable hardness stability with the temperature, showing a slight drop in values from 30 ± 1.3 GPa at 22°C to 26 ± 2.6 GPa at 300°C. This suggests that increase in Al addition improved not only the room temperature hardness but also lead to an increase in the activation energy for slip from 0.75 eV for SC-TiN to 1.26 eV for $x=0.52$ film. A heat treatment of this film at 600°C for 24 hours resulted in a slightly lower hardness and a reduction of the activation energy of slip to similar values seen in pure TiN.

It is proposed that this hardening increase is linked to the local distribution of Al within the TiN matrix and this will be supported by high resolution TEM.

11:00am **B4-2-11 The Influence of Bias Voltage on Residual Stresses and Tribological Behavior of Ti/TiAlN and Cr/CrAlN Multilayer Systems.** W. Tillmann (wolfgang.tillmann@tu-dortmund.de), T. Sprute, F. Hoffmann, Technische Universität Dortmund, Germany

The increase of the life span and thus a more efficient use of tools are important goals related to industrial applications. Owing to this purpose, friction as well as wear should be reduced significantly. PVD (Physical Vapour Deposition) coatings such as Ti / TiAlN or Cr / CrAlN meet these requirements and possess a high wear resistance. Due to the high heat resistance of titanium aluminum nitride, these coatings have a great potential for the use in forming tools employed at elevated temperatures. However, the different thermoelastic properties of the multilayer system and substrate can lead to delamination and spallation of the layers after the deposition process due to critical residual stress states. Therefore, the influences of the bias voltage on the residual stresses, as well as the tribological properties, were investigated within the scope of this work in order to understand the operational behavior of multilayer systems. The production parameter should be varied to favorably adjust the residual stress states selectively and to produce a sound coating system. By means of a magnetron sputtering device both multilayer systems were deposited on hot work steel substrates AISI H11. In addition to the metallurgical phase analysis, residual stress measurements were performed using X - ray diffractometry. The structure and the morphology investigations of the coatings were determined by scanning electron microscopy and energy dispersive X-ray spectroscopy. Furthermore, a nanoindenter and a ball-on-disk device were employed in order to characterize the mechanical and tribological properties and to clarify the effect of the process parameter on the service behavior of the PVD coating.

11:20am **B4-2-12 The effect of Yttrium addition on TiAlN coating.** L. Zhu (lh Zhu@mail.shu.edu.cn), M. Hu, Shanghai University, China, W. Ni, Y. Liu, Kennametal Incorporated, US

TiAlYN coating was deposited by cathodic arc evaporation method. The effect of yttrium addition on the microstructure and properties of TiAlN coating was studied. Lattice parameter of TiAlN increases with addition of yttrium. Also, it helps to improve the columnar structure and decrease the grain size. TiAlYN coating exhibits higher hardness and higher residual compress stress than TiAlN coating. The oxidation resistance of TiAlYN coating at 900 °C is superior to TiAlN coating. The anti-oxidation mechanism of TiAlYN coating is also discussed in this paper.

Hard Coatings and Vapor Deposition Technology Room: Royal Palm 1-3 - Session B5-1

Hard and Multifunctional Nano-Structured Coatings

Moderator: J. Paulitsch, Christian Doppler Laboratory for Application Oriented Coating Development at the Department of Physical Metallurgy and Materials Testing, Montanuniversität Leoben, Austria, R. Sanjines, Ecole Polytechnique Fédérale de Lausanne, Switzerland, P. Zeman, University of West Bohemia, Czech Republic

8:00am **B5-1-1 A study of microstructures and mechanical properties of cathodic arc deposited CrCN/ZrCN multilayer coatings.** C.Y. Tong, J.W. Lee (jefflee@mail.mcut.edu.tw), Ming Chi University of Technology, Taiwan, S.H. Huang, National Chiao Tung University, Taiwan, Y.B. Lin, C.C. Kuo, Ming Chi University of Technology, Taiwan, T.E. Hsieh, Gigastorage Corporation, Taiwan, Y.C. Chan, H.W. Chen, J.G. Duh, National Tsing Hua University, Taiwan

The nanostructured CrCN/ZrCN multilayer coatings were deposited periodically by the cathodic arc deposition system. The bilayer period of CrCN/ZrCN multilayer coating was kept at 16 nm. The C_2H_2 gas flow rate was adjusted to fabricate the CrCN/ZrCN multilayer coatings with different carbon contents. The crystalline structure of multilayer coatings was determined by a glancing angle X-ray diffractometer. Microstructures of thin films were examined by a scanning electron microscopy (SEM) and transmission electron microscopy (TEM), respectively. A nanoindenter, scratch tester and pin-on-disk wear tests were used to evaluate the hardness, adhesion and tribological properties of thin films, respectively. It was found that the hardness and tribological properties were strongly influenced by the carbon contents of the CrCN/ZrCN multilayer coatings. Optimal carbon content was proposed in this work.

8:20am **B5-1-2 Effect of Zr content on structural, mechanical and phase transformation properties of magnetron sputtered TiNiZr shape memory alloy thin films.** D. Kaur (dkaurfph@iitr.ernet.in), N. Kaur, Indian Institute of Technology Roorkee, India

The present study explored the in-situ deposition of TiNiZr shape memory thin films on Si substrate using co-sputtering of NiTi and Zr targets. The influence of Zr concentration on phase formation, microstructure, mechanical and phase transformation behavior of TiNiZr was systematically investigated. The crystalline structure, orientation, average crystallite size and phases present in TiNiZr films were determined by X-ray diffractometer. The microstructure of the films was determined by field emission scanning electron microstructure (FESEM) and atomic force microscopy (AFM). The film thickness was determined by using surface profilometer and cross-sectional FESEM. Nanoindentation tests were conducted at room temperature. TiNiZr thin films were found to exhibit high hardness, increased reduced modulus and better wear resistance by increasing the Zr content. Electrical properties were studied by using four probe method demonstrate a very interesting phase transformation behavior leading to two way shape memory effect and transformation temperature was increased by increasing Zr content leading to enhanced response speed of TiNiZr shape memory alloys due to large thermal gradient with environment. The enhanced properties of TiNiZr shape memory alloy films makes them technologically important material for variety of high temperature MEMS applications including micro grippers, Microvalves, Micropumps and micro mirrors.

Keywords: NiTiZr; Magnetron Sputtering; Shape memory; Nanoindentation

8:40am **B5-1-3 Self-Organized nano-Labyrinth Structure in Magnetron Sputtered $Zr_{0.6}Al_{0.4}N(001)$ Thin Films on $MgO(001)$.** N. Ghafoor (naugh@ifm.liu.se), L. Johnson, Linköping University, Sweden, D. Klenov, FEI Company, B. Alling, Linköping University, Sweden, I. Petrov, J.E. Greene, University of Illinois at Urbana-Champaign, US, L. Hultman, M. Odén, Linköping University, Sweden

Self-Organized nano-Labyrinth Structure in Magnetron Sputtered $Zr_{0.6}Al_{0.4}N(001)$ Thin Films on $MgO(001)$

N. Ghafoor¹, L. J. S. Johnson¹, D. O. Klenov², B. Alling¹, I. Petrov^{1,3}, J. E. Greene^{1,3},

L. Hultman¹, M. Odén¹

¹Department of Physics, Chemistry, and Biology (IFM), Linköping University, SE-581 83 Linköping, Sweden

²FEI Company, Building AAE, Achtseweg Noord 5, Eindhoven, The Netherlands

³ [http://www.mrl.uiuc.edu/], [http://www.uiuc.edu/], 104 S. Goodwin Avenue, [http://www.city.urbana.il.us/Urbana/], IL 61801, USA

A unique self-organized nanostructure is reported for (Zr_{0.64}Al_{0.36})N thin films that forms during reactive magnetron sputter deposition from elemental targets on MgO(001) substrates. HRTEM and EDX/STEM imaging shows that it consists of a nanolabyrinth of alternating ZrN-rich and AlN-rich lamellae along the MgO<110> in plane directions, with typical width of a 4 nm and that extends throughout the film thickness. According to *ab-initio* calculations, a significantly higher solid solution mixing enthalpy of c-Zr_{0.6}Al_{0.4}N ($\Delta H=0.392$ eV/f.u.), compared to c-Ti_{0.6}Al_{0.4}N (ΔH 0.178 eV/f.u) results in a comparatively higher driving force for isostructural decomposition in ZrAlN during secondary phase transformation on post annealing. Growth kinetics and pseudomorphic epitaxial forces also effects the segregation to occur during growth.

The phase segregation is studied in 1.5 μ m thick (Zr_{0.64}Al_{0.36})N films grown at different temperatures between 500-900 °C. It is shown that a maximum hardness of ~38 GPa is associated with a nano-labyrinthine nanostructure that forms at higher temperatures. The ZrN/AlN phase separation is complete at 900°C. The ZrN rich platelets retain the original B1 NaCl structure with cube on cube epitaxy with the MgO substrate, whereas the AlN-rich regions transform to wurtzite. The geometrical arrangement and the mutual relationships of the two phases on decomposition will be presented with respect to the growth temperature

9:00am **B5-1-4 Wear/erosion behavior of TiN-based nanocomposite coatings on SS304 and a synchrotron radiation assisted coating failure investigation.** *Y. Li* (yul088@mail.usask.ca), *Q. Yang, A. Hirose*, University of Saskatchewan, Canada, *R. Wei*, Southwest Research Institute, US

Thick TiN and a series of TiN-based nanocomposite coatings have been deposited on SS304 substrates using a plasma enhanced magnetron sputtering technique. The morphology, microstructures were characterized by SEM, AFM and XRD. The mechanical properties are measured by indentation testings (Rc, micro- and nanoindentations). The tribological performances were evaluated by solid particle erosion testing and pin-on-disk wear testing. The results reveal that the hard coatings imposed have significantly improved the tribological properties of the bare steel substrates. A preliminary synchrotron radiation-based analysis was further performed to track the microstructure and composition changes and stress state distribution in the damaged coatings after tribological testing. The coating failure mechanism was discussed.

9:20am **B5-1-5 Erosion Mechanisms of Hard Nanocomposite Coatings.** *E. Bousser* (etienne.bousser@polymtl.ca), *L. Martinu, J.E. Klemberg-Sapieha*, École Polytechnique de Montréal, Canada **INVITED**

Economic and technological progress as well as environmental concerns requires that modern equipment be designed with ever more stringent performance criteria, frequently pushing components to the very limits of their capabilities. Consequently, tribological deficiencies, such as lubrication breakdown, excessive wear and tribo-corrosion, are amplified leading to unnecessary operational costs, decreased efficiency and premature failure. Therefore, appropriate material's selection for a given application must be guided by an accurate understanding of the intervening tribological processes.

Solid Particle Erosion (SPE) occurs in situations where hard solid particles present in the environment are entrained in a fluid stream, and impact component surfaces. It is well known that ductile materials erode predominantly by plastic cutting or ploughing of the surface, while brittle materials do so by dissipating the particle kinetic energy through crack nucleation and propagation. Although the most widely accepted brittle erosion models were developed more than 30 years ago, little has been published on how the material removal process differs for hard brittle coatings when compared to bulk materials. In this presentation, we outline the work performed at École Polytechnique on understanding the material loss mechanisms occurring during the SPE of hard coatings.

In the first part, we will discuss the validity of existing brittle SPE models when applied to the erosion of hard coatings. We examine the mechanisms by which surfaces dissipate the kinetic energy of impacting particles, and compare the erosive response of brittle bulk materials to that of hard coatings. Also, we investigate the means by which surface engineering can enhance erosion resistance, and correlate surface mechanical properties to the erosion behaviour of brittle bulk materials and coatings. We will show that the experimental results are also well supported by the finite element modelling of single particle impacts of coated surfaces.

The second part of the talk will focus more closely on TiN-based hard nanocomposite coatings and on the role microstructure has on the surface mechanical properties and on the enhanced erosion performance. Finally, erosion tests being notoriously inaccurate, we discuss the methodology of

coating erosion testing, and present a novel in-situ erosion characterization technique used for time-resolved erosion testing.

10:00am **B5-1-7 Effects of structure and phase transformation on fracture toughness and mechanical properties of CrN/AlN multilayers.** *M. Schlögl* (manfred.schloegl@unileoben.ac.at), *J. Paulitsch, J. Keckes, C. Kirchlechner, P.H. Mayrhofer*, Montanuniversität Leoben, Austria

Transition metal nitrides, such as CrN are highly attractive materials for a wide range of applications due to their outstanding properties like high hardness, excellent corrosion and oxidation resistance. Consequently, many research activities deal with their synthesis-structure-properties-relations. However, also because the fracture toughness of thin films is a difficult-to-obtain material property, only limited information is available on this topic. Therefore, this work is devoted to the study of the fracture mechanisms of CrN based thin films with the aid of in-situ scanning electron microscopy microbending, microcompression and microtension tests. The small test-specimens are prepared by focused ion beam milling of individual free-standing thin films. As generally monolithic coatings with their columnar structure provide low resistance against crack formation and propagation we perform our studies for CrN thin films and CrN/AlN multilayers. The latter offer additional interfaces perpendicular to the major crack-propagation-direction having different elastic constants and shear modulus and binding characteristics. Adjusting the AlN layer-thicknesses to ~3 and ~10 nm allows studying the impact of a cubic stabilized AlN layer and an AlN layer composed of cubic, amorphous and hexagonal fractions being extremely sensitive to stress fields.

The microtests clearly demonstrate that the monolithic CrN as well as the CrN/AlN multilayer coating with the ~10 nm thin AlN layers (and hence a mixture of cubic, amorphous and hexagonal AlN phases) fail as soon as small cracks are initiated. Contrary, the CrN/AlN multilayer coatings composed of ~3 nm thin c-AlN layers are able to provide resistance against crack propagation. Hence, they allow for significantly higher loads during the tests. Detailed structural investigations, in-situ and after the tests, suggest that the cubic AlN layers, which are stabilized by coherency strains in the CrN/AlN multilayer coatings, phase transform when experiencing additional strain fields and thereby hinder crack propagation.

10:20am **B5-1-8 Nanoindentation and fatigue properties of magnetron sputtered AlN/NiTi multilayer thin films.** *D. Kaur* (dkaurfph@iitr.ernet.in), *N. Choudhary*, Indian Institute of Technology Roorkee, India

The present study explored the in-situ deposition of high damping AlN/NiTi multilayer heterostructures with different bilayer periods (Λ) and bilayer numbers (n) by using dc/rf magnetron sputtering. The heterostructures were characterized in terms of structural, morphological, mechanical and damping properties by XRD, FESEM and Nanoindentation, respectively. XRD analysis revealed the formation of highly oriented AlN and NiTi films. The higher hardness and elastic modulus of multilayer coatings could be attributed to different mechanisms for layer formation with nanometric thickness and better adhesion of AlN layer with NiTi. The enhanced damping and fatigue properties of AlN/NiTi multilayers was due to the combined effect of piezoelectric AlN and NiTi shape memory alloy layers. The obtained results suggest that AlN/NiTi multilayers exhibit higher damping capacity as compared to PZT/NiTi heterostructures.

Keywords: Sputtering; Heterostructures; Nanoindentation; Damping

10:40am **B5-1-9 Hardness of CrAlSiN nanocomposite coatings at elevated temperatures.** *S. Liu* (sl559@cam.ac.uk), *S. Korte*, Gordon Laboratory, Department of Materials Science and Metallurgy, University of Cambridge, UK, *X.Z. Ding, X.T. Zeng*, Singapore Institute of Manufacturing Technology, Singapore, *W. Clegg*, Gordon Laboratory, Department of Materials Science and Metallurgy, University of Cambridge, UK

Cr-based nanocomposite coatings are attracting increasing attention for use as protective coatings in dry machining and aerospace applications where the components are consistently exposed to high temperatures. In this report, CrAlSiN nanocomposite coatings have been deposited with different silicon contents and at different substrate bias voltages using a lateral rotating cathode arc technique. Their composition, microstructure and mechanical properties were characterized using EDS, XRD and nanoindentation respectively and compared with CrN and CrAlN coatings deposited under the same conditions. The flow behaviour around the indent has been studied using AFM and TEM. The mechanical behaviour of the coatings has been determined both from room temperature tests after annealing at elevated temperatures and hot stage nanoindentation, allowing the hardness to be measured at temperatures up to 600 °C. The evolution of the structure and internal stress has been measured in both cases allowing the two approaches to be compared.

11:00am **B5-1-10 Hard nanocrystalline Zr-B-C(N) films prepared by pulsed magnetron sputtering.** *J. Kohout* (jkohout4@kfy.zcu.cz), *P. Steidl, J. Vlcek, R. Cerstvy*, University of West Bohemia, Czech Republic

Hard Zr-B-C(N) films were deposited on Si(100) substrates by pulsed magnetron co-sputtering of a single B₄C-Zr target (127 x 254 mm²) in various nitrogen-argon gas mixtures. The target was formed by a B₄C plate overlapped by Zr stripes which covered 15 or 45 % of the target erosion area. The N₂ fractions in the gas mixture were in the range from 0 to 50 % at the total pressure of the gas mixture of 0.5 Pa. The planar rectangular unbalanced magnetron was driven by a pulsed DC power supply (Rübig 120 MP) operating at the repetition frequency of 10 kHz and the average target power of 500 W in a period with a fixed 85% duty cycle. The substrates were at a floating potential and were heated to 450°C. The target-to-substrate distance was 100 mm. The elemental composition of the films was determined by Rutherford backscattering spectrometry. X-ray diffraction measurements of as-deposited samples were carried out using a PANalytical X'Pert PRO diffractometer. Hardness, reduced Young's modulus and elastic recovery were determined by a Fischerscope H-100B ultramicroindenter. Electrical resistivity was measured by four-point method. Hard (37 GPa) nanocrystalline Zr-B-C films with very low compressive stress (0.4 GPa) and high electrical conductivity (resistivity of $2.3 \times 10^{-6} \Omega \text{m}$) were deposited in argon discharge at the 15 % Zr fraction in the target erosion area. Hard (37 GPa) nanocomposite Zr-B-C-N films with low compressive stress (0.6 GPa) and even higher electrical conductivity (resistivity of $1.7 \times 10^{-6} \Omega \text{m}$) were deposited at the 45 % Zr fraction in the target erosion area and 5 % N₂ fraction in the gas mixture.

11:20am **B5-1-11 Magnetron co-sputtered hard and ductile TiB₂/Ni coatings.** *H. Wang*, Anhui University of Technology, China, *F. Ge*, Ningbo Institute of Materials Technology and Engineering, China, *P. Zhu, S. Li*, Anhui University of Technology, China, *F. Huang* (huangfeng@nimte.ac.cn), Ningbo Institute of Materials Technology and Engineering, China

Titanium diboride (TiB₂) coatings were alloyed with nickel (Ni) in order to improve their ductility. The coatings were co-sputtered from two magnetron sources, with a constant mid-frequency dc and a variable dc powers applied to the TiB₂ and Ni targets, respectively. The microstructure, mechanical properties, as well as tribological tests were obtained. While the effect of Ni addition on the grain size is mixed, more Ni alloying clearly improves the ductility. When the amount of Ni addition is more than 20%, the coating shows clearly ductile behavior in tribological tests, and a high hardness >30 GPa.

11:40am **B5-1-12 Comparative investigation of boride and boronitride hard coatings produced by magnetron sputtering of MeB_x (Me: Mo, Cr, Ti) SHS-targets.** *P. Kiryukhantsev-Korneev* (kiruhancev-korneev@yandex.ru), *A. Shevko*, National University of Science and Technology "MISIS", Russian Federation, *B. Mavrin*, Institute of Spectroscopy of RAS, Russian Federation, *E.A. Levashov, D.V. Shtansky*, National University of Science and Technology "MISIS", Russian Federation

Many engineering materials require a combination of properties: wear-, corrosion-, and oxidation-resistance, thermal stability, high fatigue strength, and low friction coefficient. These properties can be achieved in hard coatings based on borides or boronitrides of transition metals. In the present work, Mo-B(N), Cr-B(N), and Ti-B(N) coatings were deposited by magnetron sputtering of MoB, CrB₂, and TiB_x (x=1 and 2) targets in an Ar atmosphere or reactively in a gaseous mixture of Ar+15%N₂. To evaluate oxidation resistance, the coatings were annealed in the range of 800-1200°C in air. The structure of coatings was studied by means of X-ray diffraction, transmission and scanning electron microscopy, Raman and X-ray photoelectron spectroscopy, and glow discharge optical emission spectroscopy. The mechanical properties of the coatings were measured using nanoindentation and scratch-testing. The tribological properties were evaluated in air using both conventional and high-temperature ball-on-disc tribometer. The electrochemical tests were performed in 5N H₂SO₄ medium. The milling, drilling, and turning tests of the coated WC-Co and HSS tools were also performed.

The results obtained show that the coatings with optimal structure and elemental composition had hardness up to 55 GPa, elastic recovery up to 70%, friction coefficient against WC-Co ball below 0.5 and wear rate <10⁻⁵ mm³N⁻¹m⁻¹. The tribological properties of coatings were shown to be stable in the temperature range of 20-500°C. The reactively deposited coatings showed the better corrosion and oxidation resistance than that of the nitrogen-free coatings. The lifetime of cutting tools coated with Ti-B(N) and Cr-B(N) coatings was increased by 1.5-2.5 times compared with the TiN coating.

Tribology & Mechanical Behavior of Coatings and Engineered Surfaces

Room: Pacific Salon 1-2 - Session E1-3

Friction Wear Lubrication Effects & Modeling

Moderator: Lopez, CSIS-University Sevilla, V. Fridrici, Ecole Centrale de Lyon, O.L. Eryilmaz, Argonne National Laboratory, US, S. Aouadi, Southern Illinois University, US

8:00am **E1-3-1 Solid Lubrication Processes of Diamond-Like Carbon Coatings.** *J. Fontaine* (julien.fontaine@ec-lyon.fr), Ecole Centrale de Lyon, France

INVITED

Thanks to their unique tribological properties, Diamond-Like Carbon coatings are increasingly used in industrial applications. They indeed combine low friction with good wear resistance, while most tribological coatings are either hard wear resistant materials but exhibiting relatively high friction, or soft with easy shear and thus low friction but exhibiting higher wear rates. How to account then for the paradoxical combination of hard DLC coatings exhibiting low wear together with low friction?

Thanks to high hardness, high strain tolerance and smoothness achieved with most DLC deposition techniques, plastic flow is not likely to occur in the contact area, neither as abrasive phenomena nor as shearing of contacting asperities. Nevertheless, adhesive interactions with DLC surfaces can vary significantly depending on counterface nature and environment, from strong covalent bonding to weak Van-der-Waals interactions between passivated surfaces, especially with hydrogen. Solid lubrication processes of DLC films are thus mostly governed by adhesion, which in turn affects the velocity accommodation modes.

From various experimental results obtained with different DLC coatings in several environments, the key-role of adhesive phenomena will be highlighted. These results will point out that formation, behavior and release of adhesive junctions are critical for contact evolution. The strength of adhesive junctions is affected not only by tribochemical reactions with counterface and/or environment, but also by their size and hence by surface topography. The release of these junctions will finally depend on mechanical properties of the contacting surfaces.

8:40am **E1-3-3 Tribological behaviour at high temperature of hard CrAlN coatings doped with Y or Zr.** *J.C. Sánchez-López* (jcslopez@icmse.csic.es), *A. Contreras*, Instituto de Ciencia de Materiales de Sevilla, Spain, *A. García-Luis, M. Brizuela*, Tecnalia, Spain

The tribological properties of CrAlN, CrAlYN and CrAlZrN coatings deposited by d.c. reactive magnetron sputtering are studied during pin-on-disk experiments at room temperature and under heating at 250, 500 and 650 °C using alumina balls as counterparts. The influence of the metallic composition (Al, Y and Zr) in terms of friction and wear properties and oxidation resistance is studied by means of cross-sectional scanning electron microscopy (X-SEM), energy dispersive X-ray analysis (EDAX) and Raman analysis of the contact region after friction tests. The wear mechanism is characterized by the formation of an overcoat rich in chromium and aluminium oxides whose composition is determined by the initial chemical characteristics of the coating and the testing temperature. The increase in temperature above 500°C produces a change in wear mechanism from abrasive to adhesive concomitantly with the formation of surface layer rich in chromium oxides. Thus, the addition of Y, and particularly Zr, favours the preferential formation of Cr₂O₃ versus CrO₂ leading to a reduction of friction and wear of the counterpart. Conversely, the tribological behaviour of pure CrAlN coatings is characterized by higher friction but lower film wear rates as a result of higher hardnesses and major presence of aluminium oxides on the coating surface.

9:00am **E1-3-4 High Temperature Tribometer Investigations of Oxide Coatings Synthesized by Cathodic Arc Evaporation.** *G. Favaro* (gregory.favaro@csm-instruments.com), CSM Instruments SA, Switzerland, *N. Bierwisch*, Saxonian Institute of Surface Mechanics, Germany, *N.X. Randall*, CSM Instruments SA, Switzerland, *J. Ramm*, OC Oerlikon Balzers AG, Liechtenstein, *N. Schwarzer*, Saxonian Institute of Surface Mechanics, Germany, *B. Widrig*, OC Oerlikon Balzers AG, Liechtenstein

Thin film coatings are indispensable in all current design for cutting tool applications. True mechanical properties like hardness, elastic modulus, adhesion and wear resistance are essential parameters which need to be understood in the development of tool design. The general interest of mechanical characterization at small scales is to evaluate the properties of the hard coating as it becomes thinner and to optimize it to be able to fit the increasing and challenging demands of industry.

The objective of this study is to find a test procedure which supports the optimization of coatings for cutting tools by the measurement of the mechanical properties by nanoindentation of the substrate and the coating. An extended Hertzian approach is utilized to derive the specific Young moduli and yield strengths of substrate and coating based on the data obtained from nanoindentation. These mechanical constants are utilized to simulate the stress profiles in the coating-substrate system and to dimension the scratch test as well as the pin-on-disk test at elevated temperatures.

Scratch testing will give information about the critical failure loads and adhesion of the coating, whilst high temperature tribology testing can explain the evolution of the friction force and wear rate versus the working temperature.

This pin-on-disk study up to 1000°C may support an optimization of coatings for specific cutting applications, especially for applications for which the thermal load of the cutting tool is the critical parameter. In addition, the test can also be utilized to understand the wear in tribological systems like in engines.

9:20am E1-3-5 Adaptive Nitride Coatings With Lubricious Behavior From 25 to 1000 °C, S. Aouadi (saouadi@physics.siu.edu), S. Stone, A. Harbin, Southern Illinois University, US, C. Muratore, A. Voevodin, Air Force Research Laboratory, Thermal Sciences and Materials Branch, US

Nitride-based nanocomposite coatings that consist of inclusions of silver, bismuth in vanadium, molybdenum, or tungsten nitride matrices were investigated as potential adaptive coatings to reduce friction in the temperature range from 25 to 1000 °C. These nanocomposite structures were selected based on the premise that a binary metal oxide layer with low shear strength will form on the surface of the coatings at elevated temperatures. The nitride-based coatings were produced using unbalanced magnetron sputtering and their elemental composition was evaluated using x-ray photoelectron spectroscopy (XPS). The tribological properties of the materials against Si₃N₄ balls were investigated at different temperatures. Reduced friction coefficients in the 0.1 to 0.2 range were recorded at high temperatures (600 °C to 1000 °C range) due to the formation of silver- and bismuth-based binary metal oxides as determined by Raman spectroscopy and x-ray diffraction (XRD) measurements on the surface of these coatings after testing. In addition, real-time Raman spectroscopy and HT-XRD (High Temperature XRD) provided valuable insight into the processes that the coating undergoes as a result of thermal and/or mechanical stresses upon heating at temperatures up to 1000 °C.

9:40am E1-3-7 High temperature tribological properties of CrZrSiN coatings, D.J. Kim, J.Y. Kim, B.S. Kim (yann-minz@daum.net), S.Y. Lee, Korea Aerospace University, Republic of Korea, J.J. Lee, Seoul National University, Republic of Korea

In this work, CrZr-Si-N films with various Si contents were prepared by unbalanced magnetron sputtering with various (Cr-Zr-Si) sputtering targets. Three type segment targets which have different atomic ratios of Cr, Zr and Si (11:1vol%, 5:1vol% and 3:1vol%) were used to investigate the properties of coatings as a function of the Si content. The tribological properties of ball-on-disk type were tested at room temperature and 500°C. After wear test the characteristics such as surface roughness, wear rate and wear debris were investigated by atomic force microscopy (AFM), field emission scanning electron microscope (FE-SEM) and Raman Spectroscopy. Preliminary results showed that tribological properties of CrZr-Si-N films at high temperature were significantly better than those of CrZrN coatings due to an improved thermal stability and low surface roughness at 500°C. However at the room temperature CrZr-Si-N films and CrZrN films are observed similar tribological. Detailed experimental results will be presented.

10:00am E1-3-8 Mechanical and Tribological Properties of Ti-Si-C-N Nanocomposite Coatings Deposited using a Plasma Enhanced Magnetron Sputtering (PEMS) Process, A.M. Abd El-Rahman, Sohag University, Egypt, R. Wei (rwei@swri.org), Southwest Research Institute, US

This study is one part of a series of efforts to optimize the mechanical properties and tribological properties of the Ti-Si-C-N nanocomposite coatings. In this study Ti-Si-C-N coatings were deposited on Ti-6Al-4V and Custom 450, a stainless steel used in turbine industry, by Plasma Enhanced Magnetron Sputtering (PEMS) using Ti targets in an argon-nitrogen-trimethylsilane gaseous mixture. The discharge current generated by thermionic emission from W filaments, the bias voltage, the flow rate of N₂ and the flow rate of TMS were the main parameters varied during the deposition process. Scanning Electron Microscopy (SEM) and X-Ray Diffractometry (XRD) were used to study the microstructure and morphology of these coatings. Erosion resistance were determined using 50 µm alumina at 30° and 90° at a velocity of 14 m/s, while the coefficient of friction and the wear resistance were evaluated using a ball-on-disk tester. It was found that a nanocomposite microstructure with a small crystallite size

(5.5-6.8 nm) and a good morphological quality free from any delamination, columnar structure or any defects was achieved at relatively high ion bombardment. The micro hardness of the coatings increases with the increase of both the nitrogen flow rate and the TMS flow rate, and the highest hardness of 46GPa was reached. These coatings also exhibit excellent erosion and wear resistance.

10:20am E1-3-9 Atomic Scale Origins of Friction in Metallic Contacts, M. Chandross (mechand@sandia.gov), S. Cheng, Sandia National Laboratories, US

INVITED

Gold is a desirable material for use in high performance electrical contacts because it offers low contact resistance, does not corrode or oxidize, and can be easily made into thin sheets. However, gold contacts generally suffer from high adhesion and friction. The tribological issues are mitigated in nanocrystalline gold alloys (with, for example, Ni or Co), which can exhibit both low friction and low contact resistance. The atomic scale mechanisms responsible for the change in frictional response are poorly understood. We will present the results of large scale molecular dynamics (MD) simulations which study the tribological response of nanocrystalline films of pure gold and alloys under a variety of sliding conditions. Our results indicate that in pure metals, cold welding and microstructural reorientation lead to the formation of a commensurate sliding interface and high friction resulting from dislocation controlled plasticity. In alloys, however, differing lattice constants suppress the reorientation of grains at the contact point, which leads to grain boundary sliding and lower friction.

11:00am E1-3-11 Tribological study of PVD and CVD coated tool surfaces sliding on PA-6, PET and PTFE polymer substrates, G.G. Fuentes (gffuentes@ain.es), A. Scano, J. Osés, J. Rodrigo, R.J. Rodríguez, Center of Advanced Surface Engineering - AIN, Spain, C. Harth, Fachhochschule Köln, Germany, Y. Qin, University of Strathclyde, UK, J. Housden, Tecvac, UK

In this work, we have investigated the metal-polymer sliding properties of micro-tube-forming tool surfaces coated with various low adhesive thin films. The selected polymer substrates were Polyamide-6, polyethylene terephthalate and polytetrafluorethylene, and the tested coatings: commercial CrN and Cr₂N as deposited by electron beam techniques and diamond like carbon, as deposited by plasma activated chemical vapor deposition.

Ball-on-disc tests have been chosen to gain information about the film wear, polymer surface degradation and material transfer at the tool/polymer contact zone. The tests have been conducted at RT and at 150°C. It has been shown that the coatings decrease the tool surface wear. In addition, the polymer adhesive wear, i.e. the material transfer from the polymer to the tool surface decrease in overall when low adhesion films are deposited on the tool surface, both at RT and at 150°C. More specifically, Cr-based coatings provide better antiadhesion properties than diamond like carbon. No clear difference between RT and 150°C in terms of amount of sticking (within the limits of the approach).

PA-6 is found to be the polymer with the lowest tendency to sticking, probably because of its superior mechanical properties. PTFE exhibited the largest tendency to sticking due to its low mechanical strength. Finally, it has been observed that the COF of all the tool coating / polymer tribopair depend only on the polymer nature, regardless the film properties deposited.

11:20am E1-3-12 Au-ZnO Nanocomposite Coatings for Wear-Resistant Electrical Contacts, S. Prasad (svprasa@sandia.gov), R. Goekse, P. Kotula, Sandia National Laboratories, US

Gold coatings that are ideally suited for low electrical contact resistance (ECR) applications are mechanically soft and exhibit unacceptable amounts of adhesion and friction. In the current study, we explored novel pathways for balancing these fundamentally opposing phenomena, i.e., friction and ECR, through microstructural control at the nanoscale. Using a Triad e-beam evaporation system with capability for co-depositing three elements or compounds, Au-ZnO nanocomposite thin films with 0.1 to 10 vol.% ZnO were synthesized. The sheet resistivity of the bulk film was characterized using a four point probe technique and correlated to the surface ECR value. The films were post annealed to obtain a range of grain sizes and characterized by nanoindentation and high resolution TEM. ECR-friction measurements were made using a pin-on-disk ECR-tribometer where a hemispherically tipped noble metal alloy pin slid on the Au-ZnO nanocomposite film while current was passed through the sliding contact. Friction force and electrical contact resistance data were acquired simultaneously as a function of applied load. Cross-sections of wear scars suitable for TEM were prepared by focused ion beam microscopy. Changes to the grain structure arising from frictional contact with passage of current were analyzed by TEM analysis on cross-sections of wear scars. The role of nanoscale ceramic inclusions on the stability of grain structures during sliding electrical contacts will be discussed.

* Sandia National Laboratories is a multi-program laboratory managed and operated by Sandia Corporation, a wholly owned subsidiary of Lockheed Martin Corporation, for the U.S. Department of Energy's National Nuclear Security Administration under contract DE-AC04-94AL85000

11:40am **E1-3-13 The Effect of Ag Content on Friction Behavior of MoN-Ag and Mo₂N-Ag Nanocomposite Coatings.** *K. Ezirmik (ezirmik@atauni.edu.tr), Ataturk University, Turkey, O. Eryilmaz, Argonne National Laboratory, US, K. Kazmanlı, Istanbul Technical University, Turkey, A. Erdemir, Argonne National Laboratory, US, M. Ürgen, Istanbul Technical University, Turkey*

Mo₂N-Ag and MoN-Ag nanocomposite films were deposited by using a hybrid deposition system composed of cathodic arc and magnetron sputtering. Molybdenum is evaporated by cathodic arc, and silver is introduced into the structure through magnetron sputtering. Sputtering power is used as a variable for changing the silver content of the films. The crystal structure of the films was evaluated using a glancing angle X-ray diffractometer with a thin film attachment. The cross-sectional film morphology and elemental analyses were conducted using a Field emission scanning electron microscope (FE-SEM) equipped with energy dispersive spectroscopy (EDS) unit. The tribological properties of films were investigated under atmospheric conditions against different counterface materials, namely 440C and Al₂O₃. The morphology of coatings and wear tracks of both side were examined using scanning electron microscopy (SEM), light microscopy, and 3D optical profilometry. Wear debris and the coatings were analyzed by micro-Raman system. The results revealed the positive role of silver addition both on film and counterbody wear. Low friction coefficients (0.28 and 0.31) were observed for MoN+8at.% Ag and Mo₂N+10at.% Ag coatings, respectively. Raman investigation showed that silver-molybdate compounds were formed in the wear tracks. The decrease in the friction coefficients was attributed the formation of silver - molybdate phases at the surface during the friction test. Higher Ag content (>22 at. %) caused deterioration of the mechanical properties and wear resistance of the coatings.

Applications, Manufacturing, and Equipment Room: Tiki Pavilion - Session G1-1

Innovations in Surface Coatings and Treatments

Moderator: R. Cremer, KCS Europe GmbH, Germany, L. Bardos, Uppsala University, Sweden

8:00am **G1-1-1 Mathematical modeling of metal dusting during initial stages.** *F. Castillo-Aranguren (francast@itesm.mx), J. Oseguera-Peña, ITESM-CEM, Mexico*

This work presents a mathematical model which describes the initial stages of a metal dusting process on iron. The model is related to a moving boundary value problem and takes into account theoretical and experimental information of the process. In this frame, the existence of a critical value for the carbon activity and its relationship to cementite decomposition and coke formation on iron are studied.

8:20am **G1-1-2 A Dip soldering process for three dimensional integration.** *M. Rao (mrrao@crimson.ua.edu), J.C. Lusth, S.L. Burkett, The University of Alabama, US*

A novel way of three dimensional (3D) chip stacking has been designed as a way to improve heat dissipation across the layers. Chip stacking using vertical interconnections to form microscale channels for coolant to circulate through the gaps. Solder-based self assembled (SBSA) 3D structures have been designed as posts on simulated through silicon vias (TSVs) to prove the processing concept. The processing of SBSA structures using a low temperature solder alloy via dip soldering method will be described. Two types of soldering, face soldering and edge soldering, were studied to fabricate SBSA structures. Face soldering refers to deposition of solder on the complete metal face whereas edge soldering refers to selective deposition of solder on only the edges of the metal face. Mechanical grinding of the 3D structures shows that face soldered SBSA structures are void free and robust enough to be used as a connection post for chip stacking. Edge soldered SBSA structures collapsed when grinding was performed. This suggests a hollow nature to the fabricated edge soldered 3D structure. Face soldered SBSA structures provide a solder bump that serves as a connection paths in the integration of dissimilar electronic technologies. Conventional copper posts, developed in a previous project, can be an effective approach to integrated circuit (IC) stacking. However, the SBSA post provides more variety in size and shape with the potential to also serve as a reservoir for solder to aid in chip bonding. The solder bumps

are heat resistant and uniform thicknesses are obtained across a large array of SBSA structures.

8:40am **G1-1-3 Coatings for Aerospace Applications.** *C. Leyens (christoph.leyens@tu-dresden.de), Technische Universität Dresden, Germany*

INVITED

In aero engines, coatings are facing severe attack under multiple loading conditions. Sand erosion, e.g., can cause great damage to turbine hardware in the compressor, while hot corrosion and oxidation are of concern in the hotter parts of the engines. Today, coatings are widely applied to protect high pressure turbine airfoils, however, their use in the compressor and the low pressure turbine is scarce yet.

The paper will review recent developments in the field of erosion protection of aerospace alloys such as titanium and nickel alloys indicating that coatings can substantially improve the component lifetimes under erosion attack. Moreover, examples of coatings for intermetallic titanium aluminide alloys will be addressed. These alloys are the latest aerospace materials brought into service by General Electric in their GENx for stage 6 and 7 of the low pressure turbine. Yet unprotected today, future application of titanium aluminides at even hotter temperatures will require oxidation and potentially heat protection. Therefore, considerable research efforts are underway to develop coating systems including thermal barrier coatings which will be highlighted in this paper as well.

9:20am **G1-1-5 Solid particle erosion resistance of thick coating deposited by new AIP (Arc Ion Plating) cathode.** *J. Munemasa (munemasa.jun@kobelco.com), K. Yamamoto, H. Fujii, Kobe Steel Ltd., Japan, Y. Iwai, University of Fukui, Japan*

Recent Iceland Volcanic action (known as Eyjafjallajökull volcano) posed a serious threat to jet engine reliability over European sky. Any solid particles sucked into jet engine system are likely to hit the compressor blade at high velocity with various angles. Erosion of the compressor blade leads to change of blade shape and consequence is loss of aero dynamical integrity and engine efficiency. Erosion resistant coatings such as TiN, TiAlN applied by PVD processes can be used to improve the life time of compressor blade. Kobe Steel is developing a new AIP cathode (SFC) which can reduce the residual stress of the coating substantially, make it possible to deposit a thick coating.

In the present investigation solid particle erosion resistance of several nitride coatings including TiAlN deposited by SFC with different thicknesses has been evaluated by using the sand blast test equipment. The sand blast tests have been done by using comparatively large size solid particles as an erodent. To understand the effect of the film thickness to the large particle erosion resistance, TiAlN films with several 10um thicknesses have been tested by using average diameter 190um-silica sand as the erodent with approximately 100m/s air velocity on the test surface and 90deg impact angle. As a result, doubling the film thickness improved the sand blast erosion resistance of the coating by more than 10 times.

9:40am **G1-1-6 Combination of Hardness and Toughness of CVD HARDIDE Coatings Provides Enhanced Protection against Wear and Erosion.** *N. Zhuk (yzhuk@hardide.com), Hardide Plc, UK*

Hardide is a new family of nano-structured CVD Tungsten Carbide/Tungsten coatings used to increase the life of critical parts and tools operating in abrasive, erosive and chemically aggressive environments.

The Hardide coatings consist of Tungsten Carbide nano-particles dispersed in metal Tungsten matrix. This structure gives a combination of ultra-hardness with excellent toughness, crack and impact resistance. From extensive laboratory and field testing it was found that the combination of sufficient hardness with enhanced toughness achieves the optimum protection against both wear and erosion in most applications. The coating's ultra-hardness inhibits the micro-cutting mechanisms of wear and erosion, while its toughness, ductility, residual compressive stresses and homogeneous micro-structure prevent fatigue micro-cracking/chipping and platelet mechanisms of erosion.

Hardide coatings are typically 50 microns thick – exceptionally thick among hard CVD coatings – tough and ductile to withstand 3000 micro-strain deformations without damage; this deformation will crack or chip most other thick hard coatings.

The company developed a low-temperature CVD technology to deposit the coatings at around 500°C. This enables the coating of a wide range of materials: stainless steel, tool steels stable at 500°C, Ni-, Cu-, and Co-based alloys, Titanium. The coating has a strong metallurgical adhesion to these substrates, with the bond strength typically exceeding 70 MPa.

The gas-phase CVD process enables the uniform coating of external and internal surfaces and complex shapes, such as valves, pump cylinders ID and extrusion dies.

Pore-free CVD coatings resist acids and aggressive media.

Among other hard coatings Hardide fills the gap between thin film PVD and CVD coatings, and much thicker rough and non-uniform thermal spray coatings. Compared to thin PVD/CVD coatings, 50-microns thick Hardide has higher load-bearing capacity and is much more durable in abrasive and erosive applications such as oil drilling tools. Unlike thermal spray coatings, Hardide gas-phase CVD coatings can be uniformly applied to internal surfaces and complex shapes.

Hardide is an attractive replacement for Hard Chrome plating, which is under pressure from the US OSHA and the EU REACH regulations, and is especially suitable for coating complex shapes and internal surfaces.

Proven applications for Hardide coatings include critical parts of oil drilling tools, aircraft components, and pumps and valves operating in abrasive, erosive and corrosive environments, where the coating typically triples part life.

10:00am G1-1-7 Improvement of the adhesion force between DLC and polymers by CVD method with photografting polymerization, J. Takahashi, A. Hotta (hotta@mech.keio.ac.jp), Keio University, Japan

Polymers, such as polyethylene (PE), polypropylene (PP), polystyrene (PS), polyurethane (PU), polymethylmethacrylate (PMMA), polydimethylsiloxane (PDMS), and polyethylene terephthalate (PET) are widely used materials in various industrial fields. The polymers, however, have low gas barrier property, low abrasion property and low adhesion property. In order to solve these problems, diamond like carbon (DLC) deposition with a new way of surface modification was introduced. Surface modification is an important method for polymers because it can develop a new function in the polymers through different types of substrates with no loss in the bulk property, while still possessing simplicity and easiness in the surface treatment. We focused on the DLC deposition by the chemical vapor deposition (CVD) method and the photografting polymerization as the surface modification. DLC can induce various functional properties due to its high gas barrier property, abrasion resistance, biocompatibility, and high chemical stability. It was found that the adhesive strengths of photografted and DLC-deposited polymers were drastically increased as compared with untreated polymers. In fact, the adhesive strengths increased by up to 250 times after the photografting process. The photografted layer effectively worked as an intermediate layer between DLC and polymers. The photografting time only lasted for ~15-30 min. Additionally, the tensile strengths of the bulk photografted polymers were also found remarkably increased as compared with untreated polymers. It was therefore concluded that the adhesion and the mechanical properties of polymers could be substantially enhanced by the CVD method with the photografting polymerization.

10:20am G1-1-8 Electrophoretic deposition of carbon nanotube films on silicon substrates, A. Sarkar, D. Hah (dyhah@lsu.edu), Louisiana State University, US

In recent years, electrophoretic deposition (EPD) process has been envisaged as one of the convenient, low temperature and cost effective solution-based techniques that produce carbon nanotube (CNT) thin films on virtually any substrate. Some of the crucial application fields of electrophoretically deposited carbon nanotube films are micro-electronics and microelectromechanical systems (MEMS) technologies where silicon substrates are used predominantly. However, the research and fabrication trend of EPD of carbon nanotubes has been, so far, focused mostly on conductive/metal substrates such as stainless steel, aluminum, nickel, titanium and ITO (indium tin oxide)-coated glass plates. Published reports on carbon nanotube coatings deposited by EPD on silicon substrates are relatively few and thus it offers an interesting thin film research subject to explore. In this study, EPD has been performed extensively to obtain appreciable deposits of carbon nanotubes on silicon substrates with various surface coatings. The process resulted in CNT film thickness up to ~15 µm on metal-coated silicon samples from aqueous suspensions. In addition, successful attempts in selective deposition and characterization of CNT thin films by the subsequent EPD experiments on patterned metals atop insulating layers like silicon dioxide and silicon nitride show compatibility of this process with conventional silicon processes. Interesting phenomenon of agglomeration of carbon nanotubes and subsequent degradation of the CNT dispersed medium during the EPD process has also been observed. The deposited nanotubes exhibited preferential deposition and adhesion only on the metal surfaces even when the DC voltage was supplied to the silicon substrate which was electrically isolated from the metal layer. The observed deposition and adhesion of CNT films on the conducting surfaces is attributed to both electrophoretic mobility of the charged CNTs in the suspension and the hydrophilic interaction on the target surface. Deposition of the nanotubes was confirmed by scanning electron microscopy and Raman spectroscopy. Thickness of the deposited film showed a trend of linear relationship to the electric field strength and the deposition

duration. The results present great potential of CNT films for micro-electronics and MEMS applications.

10:40am G1-1-9 Implementation of Advanced Inorganic Coatings on Military Aircraft, B.D. Sartwell (bruce.sartwell@osd.mil), Department of Defense, US, G. Kilchenstein, Office of Secretary of Defense, US, V. Champagne, B. Gabriel, Army Research Laboratory, US, M. Duffles, MDS Coating Technologies Corp., Canada

INVITED

Military aircraft must operate in significantly more demanding environments and are often required to continue in service much longer than commercial aircraft. Readiness and life-cycle costs associated with maintenance are critical issues associated with weapons systems. This presentation will provide information on the implementation of three different inorganic coatings technologies that are having a major impact on performance and cost reduction: (1) HVOF thermal spray coatings, (2) Cathodic arc PVD coatings, and (3) Cold spray coatings.

The Department of Defense conducted extensive studies to qualify high-velocity oxygen-fuel (HVOF) WC/Co or WC/CoCr thermal spray coatings as a technologically superior, cost-effective alternative to electrolytic hard chromium (EHC) plating which is widely used in manufacturing and repair of aircraft components. EHC plating uses chemicals containing hexavalent chromium, a known carcinogen. Because of the extensive use of EHC on aircraft, separate efforts were undertaken to qualify HVOF coatings on different categories of components including landing gear and engine components. Results of materials and flight testing to qualify the HVOF coatings will be presented. The Air Force is now implementing HVOF coatings on most of its landing gear and they are designed for the newest aircraft, the Joint Strike Fighter.

During aircraft operation, gas turbine engines are continuously exposed to erosive media, such as sand and dirt suspended in the air, that is extremely damaging to the compressor section of the engine, leading to reduced performance and increased fuel consumption. Cathodic arc PVD coatings consisting of a multi-layer ceramic metal matrix, developed by MDS Coatings Technologies Corp., have been implemented on compressor airfoils in the U.S. Marine Corps H-53 and CH-46 helicopters. These coatings have accrued over 1 million operational hours in desert environments, increasing engine reliability and lowering costs.

Research efforts in cold spray (CS) have shown it to be a promising technology to impart surface protection to Mg and other alloy components on helicopters and fixed-wing aircraft. Applications have been developed by ARL, implemented into production, and have been incorporated into such weapon systems as the B1 bomber and the UH-60 Blackhawk helicopter. For the latter application, CS is in the process of qualification by Sikorsky Aircraft Co. for use on the UH-60 to reclaim Mg components. The CS repair has been shown to have superior performance, can be incorporated into production, and has been modified for field repair, making it a feasible method for recovering components, thereby reducing cost.

11:20am G1-1-11 The Wear behavior of Manganese Phosphate coatings applied to AISI D2 steel subjected to different heat treatments, S. Sivakumaran (ilaiyavel@svce.ac.in), Sri Venkateswara College of Engineering, Pennalur, India, A. Alangaram, Sri Venkateswara College of Engineering, India

This paper aims to investigate the wear behavior of manganese phosphate coatings on AISI D2 steel after various heat treatments. Manganese Phosphate is an industrial coating used to reduce friction and improve lubrication in sliding components. The change of hardness and microstructure of AISI D2 steel at various heat treatments also observed. The surface morphology of manganese phosphate coatings was examined by Scanning Electron Microscope (SEM) and Energy Dispersive X-ray Spectroscopy (EDX). The wear tests were performed in a pin on disk apparatus as per ASTM G-99 Standard. The wear resistance of the coated steel was evaluated through pin on disc test using a sliding velocity of 0.35 m/s under normal load of 10 to 60 N and controlled condition of temperature and humidity. The coefficient of friction and wear loss were evaluated. The temperature rise after 15 min and 30 min were recorded for each load. Wear pattern of coated pins were captured using Scanning Electron Microscope (SEM). Based on the results of the wear test after annealing of the manganese phosphate coating exhibited the lowest average coefficient of friction and the lowest wear loss 60 N load.

11:40am G1-1-12 Deposition of low melting point metals by Cold Dipping - Fluidized Bed Coating (CD - FBC), M. Barletta (barletta@ing.uniroma2.it), Università degli Studi di Roma Tor Vergata, Italy, A. Gisario, S. Venettaci, Università degli Studi di Roma La Sapienza, Italy, S. Vesco, Università degli Studi di Roma Tor Vergata, Italy

In the present paper, the deposition of low melting point metals by Cold Dipping - Fluidized Bed Coating (CD - FBC) is proposed. In particular, medium carbon steel flat substrates were coated by dipping them in a

fluidized bed of tin, zinc and aluminium powders at ambient temperature. Coating process was achieved by first depositing a solventborne organic bond layer on the substrate surface. After drying, the pre-coated substrates were dipped in the fluidized metal powders, which were retained on the surface of the adhesive bond layer. Following this, the powder coated substrates were baked in a convection oven to melt the metal powders, until a continuous film was formed. The interaction between metal powders and the substrates pre-coated with the organic bond layer was studied, identifying the effect of the main process parameters, such as dipping time, fluidization velocity and metal powder mesh size. The role of the baking temperature and time was investigated, as well. The thickness and surface morphology of the resulting coatings was evaluated as a function of the process parameters by Field Emission Gun – Scanning Electron Microscopy (FEG-SEM) and contact gauge profilometry. Their hardness and scratch resistance were evaluated by instrumented scratch and indentation testing. Wear performance of the coated substrates were tested by dry sliding linear reciprocating with stainless steel counterpart. CD – FBC allowed the deposition of high performance coatings, whose morphological, mechanical and tribological response could be directly related to the coating thickness and baking conditions.

Key words: Fluidized Bed; Metal Powders; Cold Dipping; Morphology; Hardness; Scratch; Wear.

Graphene and 2D Nanostructures

Room: Sunset - Session TS4-1

Graphene and 2D Nanostructures

Moderator: M. Chhowalla, Rutgers University, US, C.

Teichert, Montanuniversität Leoben, Austria

8:00am **TS4-1-1 Intercalation compounds and cluster superlattices: graphene based 2D composites**, **T. Michely** (*michely@ph2.uni-koeln.de*), University of Cologne, Germany **INVITED**

Carefully optimizing the growth of graphene on Ir(111) by scanning tunneling microscopy and low energy electron microscopy yields a virtually defect free, weakly bound epitaxial monolayer of macroscopic extension.

Graphene on Ir(111) can be used as a laboratory to construct new types of graphene based compound materials. Specifically, patterned adsorption of atoms and molecules takes place resulting in cluster superlattices with exciting magnetic and catalytic properties. Intercalation underneath the graphene allows one to manipulate the properties of graphene itself, e.g. its ability to adsorb atoms and molecules as well as its magnetism.

8:40am **TS4-1-3 Growth Kinetics of Monolayer and Multilayer Graphene on Pd(111)**, **H.S. Mok**, **Y. Murata**, University of California, Los Angeles, US, **S. Nie**, **N. Bartelt**, **K. McCarty**, Sandia National Laboratories, US, **S. Kodambaka** (*kodambaka@ucla.edu*), University of California, Los Angeles, US

Graphene, a two dimensional crystalline sheet of carbon, has attracted significant attention due to its electronic properties, including a tunable band gap and high electron mobility for use in semiconducting devices and sufficiently high transparency and low sheet resistance for use as a transparent conductor. For any of these applications, it is desirable to obtain single-crystalline graphene layers with uniform thickness. This is an extremely challenging task that requires a fundamental understanding of the mechanisms controlling the nucleation and growth of graphene. Here, using *in situ* low-energy microscopy (LEEM), we investigated the growth of graphene via surface segregation of carbon dissolved in the bulk of the substrate. In this process, surface concentration of carbon depends on the substrate temperature T: at T > 920 °C the Pd surface is free of carbon; upon cooling to 880 °C, we observe monolayer graphene formation on the surface; and, at T = 710 °C, we obtain multi-layer graphene. In order to follow the kinetics of graphene growth, we acquired LEEM images as a function of incident electron energy while cooling the sample from 920 °C to 880 °C. From the LEEM images, electron reflectivity (electron energy dependent variations in image intensities) values, a measure of local surface work function, are extracted. This data is used to follow the changes in surface carbon adatom concentration during nucleation and growth of graphene. For monolayer growth, we find that the electron reflectivity decreases non-linearly with annealing time. This behavior is qualitatively similar to that observed during the growth of graphene on Ru(0001) [1], where the graphene layers grow from carbon adatoms present on the surface. In case of multilayer graphene growth induced by cooling the sample to lower temperatures (< 710 °C), we observed spontaneous formation of graphene mounds consisting of multiple layers. Low-energy electron diffraction patterns acquired from the layers reveal that both in-

plane and out-of-plane stacking in the graphene layers is random with respect to the substrate. Moreover, we find that the spot intensities are weaker in the subsequent layers compared to the first layer, suggestive of growth of subsequent layers from below the surface at the graphene-substrate interface.

1. K. McCarty, P. Feibelman, E. Loginova, N.C. Bartelt, Kinetics and Thermodynamics of Carbon Segregation and Graphene Growth on Ru (0001). Carbon 2009, 47(7):1806-1813.

9:00am **TS4-1-4 Self-assembled monolayer nanodielectrics for low-power graphene electronics**, **T. Anthopoulos** (*thomas.anthopoulos@imperial.ac.uk*), **F. Colleaux**, **C. Mattevi**, Imperial College London - South Kensington Campus, UK, **M. Chhowalla**, Rutgers University, US **INVITED**

Successful development of graphene based nano- and macro-electronics would require not only high quality graphene but also the design of low power devices and integrated systems. Energy consumption has become among the three top challenges of current, as well as future technologies, as stated in the International Technology Roadmap for Semiconductors. To this end, the introduction of high-capacitance gate dielectrics in field-effect transistors has been considered a viable route to decrease the operating voltages and thus the overall power dissipation. In this presentation I will discuss the development of low operating voltage (<1.5 V) chemical vapour deposition (CVD) graphene transistors based on different solution processable organic self-assembled monolayer (SAM) nanodielectrics. Despite the simple fabrication paradigm adopted, SAM based CVD graphene transistors show excellent characteristics that includes; hysteresis-free operation, low leakage currents, weak doping effect and bias-stress free operation. Importantly, the electronic properties of the graphene-dielectric interface can accurately be tuned hence opening the possibility for fine control of the operating characteristics of graphene transistors.

9:40am **TS4-1-6 Characterization of graphene on Cu and SiC surfaces**, **A. Voevodin** (*andrey.voevodin@wpafb.af.mil*), Air Force Research Laboratory, US, **A. Kumar**, **R. Paul**, **D. Zemlyanov**, **D. Zakharov**, Purdue University, US, **J. Remmert**, **I. Altfeder**, Air Force Research Laboratory, US, **T.S. Fisher**, Purdue University, US

A microwave plasma chemical vapor deposition MPCVD growth from hydrogen-methane mixture was recently demonstrated by our group as a fast and low temperature method for graphene growth. This paper presents results of surface characterization of graphene films produced by MPCVD on polycrystalline copper foils, (111) oriented single crystal copper, and single crystal SiC substrates. XPS, HRTEM, Raman, AFM, and STM methods were used to characterize chemistry, bonding, and structure of the produced graphene. The results show that films of 3-6 monolayer graphene can be produced over the large areas with no oxygen contamination, nevertheless of the growth without the use of the substrate heating. Films were found to contain some structural defects, leading to disorder peaks in Raman spectra. These defects may result in decoupling vibration resonance in adjusted monolayers, making them to appear as monolayer graphene in characteristic Raman signatures. To overcome this difficulty, an alternative method with XPS thickness measurements was developed, which is using attenuation of escaped photoelectrons while passing through graphene and is shown to work reliably with graphene on both copper and SiC substrates. HRTEM images, as well as STM and thermal AFM analysis are discussed to highlight the effects of graphene structural defects on film electrical and thermal conductivity properties.

10:00am **TS4-1-9 Rapid synthesis and in-situ nitrogen doping of few-layer graphene using microwave plasma chemical vapor deposition (MPCVD)**, **A. Kumar**, Purdue University, US, **A. Voevodin**, Air Force Research Laboratory, US, **R. Paul**, **D. Zemlyanov**, **D. Zakharov**, Purdue University, US, **J. Remmert**, **I. Altfeder**, Air Force Research Laboratory, US, **T.S. Fisher** (*tsfisher@purdue.edu*), Purdue University, US

We report a unique process for rapid synthesis and in-situ doping of few-layer graphene films on various substrates by microwave plasma chemical vapor deposition (MPCVD). Few-layer graphene film on Cu foil, Cu block, Ni foil and on SiC has been demonstrated. The strong plasma/metal interaction helps to promote growth in a very short time. Particularly on a Cu foil the process can produce films of controllable quality from amorphous to highly crystalline by adjusting plasma conditions during processes of only few minutes and with no supplemental substrate heating. Films have been characterized using Raman spectroscopy, X-ray photoelectron spectroscopy, scanning electron microscopy, scanning tunneling microscopy, transmission electron microscopy and atomic force microscopy. The results elucidate MPCVD deposition of thin carbon films on these substrates using the MPCVD method and also open new pathways for a rapid growth of few-layer graphene films. Further, we also show that

the same system can be used for in-situ nitrogen doping of graphene by introducing nitrogen to the gas-phase precursors.

10:20am **TS4-1-10 Soft Carbon Sheets: Synthesis, Processing and Applications in Organic Photovoltaics**, **J. Huang** (*jiaxing-huang@northwestern.edu*), Northwestern University, US **INVITED**

Graphite oxide sheet, now named as graphene oxide (GO), is the product of chemical exfoliation of graphite that has been known for more than a century. Interest in this old material has resurged with the rapid development of graphene since 2004, as GO is considered to be a promising precursor for bulk production of graphene. However, apart from making graphene, GO itself has many intriguing structural features and properties. For example, it can be viewed as an unconventional type of soft material as it has characteristics of polymers, membranes, colloids, liquid crystals and as highlighted here, amphiphiles. In this talk, some new insights into the processing, characterization and properties of this old material will be presented including (1) a high-throughput, high contrast fluorescence quenching microscopy (FQM) technique that can visualize graphene-based sheets on arbitrary substrates and even in solution; (2) the amphiphilicity of GO and the implications of this “world’s thinnest bar of soap” in thin film processing; (3) Making graphene aggregation-resistant by mechanical deformation; and (4) GO based interfacial layer and active layer in solution processed photovoltaic devices.

11:00am **TS4-1-12 Growth and characterization of dense CNT Forests on oxide-free copper foil surfaces for charge storage application**, **G. Atthipalli**, **K. Strunk**, **J. Sopcisak**, **J. Gray** (*jlg99@pitt.edu*), University of Pittsburgh, US

We have studied the effect of the native oxide layer on the growth and performance of aligned carbon nanotubes (CNT) on copper substrates tested as double layer capacitors using a “Swagelok” type arrangement. A sputtered Inconel thin film and iron, delivered in vapor phase from ferrocene decomposition during chemical vapor deposition growth of the CNTs both act as catalysts for CNT growth on the copper surface. We analyzed the effectiveness in using this Inconel-Iron “co-catalyst” combination for dense, aligned CNT growth for potential access to greater surface area and subsequent charge storage. SEM, TEM and Raman measurements were made to study the structure and quality of the CNTs under various growth conditions. The results of the characterization show an improvement in density of the CNTs when the copper native oxide layer was removed before Inconel deposition. In addition, these samples also show larger values of power density and specific capacitance.

11:20am **TS4-1-13 Growth of organic semiconductor films on graphene**, **G. Hlawacek**, **F. Khokhar**, **R. van Gastel**, **B. Poelsema**, **H. Zandvliet**, University of Twente, Netherlands, **C. Teichert** (*teichert@unileoben.ac.at*), Montanuniversität Leoben, Austria

Organic semiconductors offer the possibility to fabricate of low-cost organic light emitting diodes (OLEDs) and solar cells. The novel material graphene bears the potential to be used as transparent flexible electrode in such devices. Thus, the investigation of the growth of organic molecules on graphene is an up-to-date topic.

Here, Low Energy Electron Microscopy (LEEM) and micro Low Energy Electron Diffraction (μ -LEED) have been employed to study in situ the initial growth of the organic semiconductor para-sexiphenyl (6P) on Ir(111) supported graphene. For low deposition temperatures, indeed layer-by-layer growth of lying molecules is observed as it is desired for OLEDs [1]. After formation of a low density layer, the full first monolayer already shows a bulk like structure. The nucleation of the graphene islands occurs at wrinkles in the metal supported graphene layer. Larger islands composed of flat lying molecules detach from the original nucleation sites and move rapidly as entities across wrinkle free substrate areas [2]. μ LEED reveals the surface unit cells in the different growth stages and at various substrate temperatures.

This work has been supported by the FWF project S9707-N20, STW and FOM project 04PR2318.

[1] G. Hlawacek, F. S. Khokhar, R. van Gastel, B. Poelsema, C. Teichert, *Nano Lett.* **11** (2011) 333.

[2] G. Hlawacek, F. S. Khokhar, R. van Gastel, C. Teichert, B. Poelsema, *IBM J. Res. Devel.* **55** (2011) 15:1.

Wednesday Afternoon, April 25, 2012

Coatings for Use at High Temperature Room: Sunrise - Session A1-2

Coatings to Resist High Temperature Oxidation, Corrosion and Fouling

Moderator: J. Pérez, Universidad Complutense de Madrid, Spain, B. Hazel, Pratt and Whitney, US, L-G. Johansson, Chalmers University of Technology, Sweden, D. Naumenko, Forschungszentrum Jülich GmbH, Germany

1:50pm A1-2-1 Microstructure degradation of simple, Pt- and Pt+Pd-modified aluminide coatings on CMSX-4 superalloy under cyclic oxidation conditions. *R. Swadzba* (*rswadzba@gmail.com*), Silesian University of Technology, Poland

The paper presents results of simple, Pt/Pd- and Pt-modified aluminide coatings cyclic oxidation-induced degradation analysis. The coatings were deposited by Pt and Pt+Pd electroplating, followed by vapor phase aluminizing at 1050°C. Cyclic oxidation tests were performed at 1100°C in 23h cycles. Microstructural and phase analysis conducted using SEM, EDS and EBSD methods revealed that the oxide layers that formed on the coatings were composed of three distinctive types of oxides growing according to a specific pattern which is described. The oxide layer that formed on the simple aluminide coating exhibited low adhesion in comparison to Pt- and Pt,Pd-modified aluminide coatings which managed to maintain an adherent oxide layer that contained higher amount of desirable α -alumina. The Al-depleted β NiAl grains remained much larger in the modified aluminide coatings, even after failure. What is more, stripes characteristic for martensitic transformation were discovered in the β phase grains in all coatings. Based on the results a microstructural degradation scheme of the investigated coatings is presented.

2:10pm A1-2-2 Influence of vacuum parameters during heat treatment on surface composition of MCrAlY coatings. *I. Keller* (*i.keller@fz-juelich.de*), *D. Naumenko*, *L. Singheiser*, *W.J. Quadackers*, Forschungszentrum Jülich GmbH, Germany

MCrAlY type ($M = \text{Ni, Co}$) coatings are commonly used as overlay coatings and bond coats (BC's) for thermal barrier coatings (TBC's) in aero engines and industrial gas turbines. It is known that the life time of thermal barrier coatings is crucially affected by the properties of the thermally grown oxide (TGO), which is formed during high temperature service at the TBC/BC interface. The most relevant properties of the oxide scale are growth rate, adherence to the BC, and composition [1]. Several investigations have shown that the TGO-properties depend strongly on the parameters of vacuum heat treatment commonly applied to the MCrAlY coated components prior to TBC deposition [2-4]. Variation of the heat treatment parameters can result in formation of different types of oxide scales on BC's with nominally the same composition, which leads to different lifetimes of the TBC.

In the present study the influence of vacuum parameters and atmosphere composition on the phase equilibrium at the MCrAlY surfaces during heat treatment are investigated. For this purpose free standing MCrAlY coatings (manufactured via VPS or HVOF) with rough and polished surfaces were exposed at 1100 °C for times between 1 and 5 hours in different atmospheres ($<10^{-5}$ mbar, 10^{-4} mbar, 10^{-3} mbar with Argon gas, and 10^{-3} mbar with synthetic Air). The surface scale composition and morphology were analysed by secondary neutral mass spectrometry (SNMS), Raman spectroscopy, X-Ray diffraction, optical metallography, and SEM equipped with EDX and Cathodoluminescence detectors. It has been found that the composition of the rough as well as the polished surfaces depends on the atmosphere and pressure conditions during heat treatment. It is shown that the phase composition at the MCrAlY coating surface is mainly governed by two competing processes, i.e. Cr evaporation and Y oxidation. The latter reaction has been observed to depend strongly on the Y reservoir in the coating.

References

- [1] T. J. Nijdam, W. G. Sloof, Surf. Coat. Technol. 201 (2006) 3894.
- [2] A. Gil, V. Shemet, R. Vassen, M. Subanovic, J. Toscano, D. Naumenko, L. Singheiser, W. J. Quadackers, Surf. Coat. Technol. 201 (2006) 3824.
- [3] U. Schulz, O. Bernardi, A. Ebach-Stahl, R. Vassen, D. Sebold, Surf. Coat. Technol. 203 (2008) 160.

[4] N. M. Yanar, E. S. Pettit, G. H. Meier, Metallurgical Mat. Transactions 37A (2006) 1563.

2:30pm A1-2-3 Effect of Water Vapor on Thermally Grown Alumina Scales on Bond Coatings. *K. Unocic* (*unocicka@ornl.gov*), *B. Pint*, Oak Ridge National Laboratory, US

The role of water vapor on thermal barrier coating (TBC) performance has been investigated for both Pt diffusion and MCrAlY-type bond coatings. The addition of 10% water vapor reduced the average TBC lifetime on MCrAlY and MCrAlYHfSi bond coatings by ~30% compared to dry O₂, but did not affect the lifetime of Pt diffusion coatings. However, the oxide scale formed on Pt-diffusion coatings had a higher average thickness for the specimens oxidized in wet air compared to dry O₂. In both cases, the scale formed beneath the yttria-stabilized zirconia top coat was thicker than on the uncoated side of the specimen. Additional characterization will be presented on both coating systems at higher water vapor contents. Model MCrAl specimens also will be examined to further understand the role of water vapor on scale growth and microstructure.

Research sponsored by the U. S. Department of Energy, Office of Fossil Energy, Coal and Power R&D.

2:50pm A1-2-4 Effect of Water Vapor on the 1100°C Oxidation Behavior of Plasma-Sprayed TBCs with HVOF NiCoCrAlY Bond Coats. *J. Haynes* (*z15@ornl.gov*), *B. Pint*, Oak Ridge National Laboratory, US

The water vapor content of the exhaust in land-based turbines will increase when coal-derived synthesis gas (syngas) or hydrogen are used to replace natural gas. To investigate the perceived detrimental role of water vapor on thermal barrier coating (TBC) lifetime, coupons of single crystal superalloy X4 were sprayed with NiCoCrAlY and NiCoCrAlYHfSi bond coatings by the high velocity oxy fuel (HVOF) process and yttria-stabilized zirconia (YSZ) top coats by air plasma-spray (APS). Furnace cycling was conducted at 1100°C in order to induce TBC failures in <1000h. The bond coatings with Hf and Si produce at least a 20% higher lifetime in all cases. For both bond coatings in 1h cycles, the average TBC lifetime dropped ~30% in air with 10% water vapor compared to cycling in dry O₂. As a potential strategy to improve TBC performance, two versions of X4 with Y and La additions were similarly coated and cycled in 10% water vapor. However, the average TBC lifetimes were statistically similar to the base X4 superalloy. Initial experiments using 50% water vapor have not shown a decrease in lifetime compared to 10% water vapor. To better simulate base-load turbine duty, TBC lifetime in 100h cycles and 10% water vapor also is being investigated. As expected, the average TBC lifetime was much higher than with 1h cycles at 1100°C. Characterization of the failed TBC coatings will be presented quantifying the effect of water vapor on the thermally grown scale thickness and morphology.

3:10pm A1-2-5 High Temperature Oxidation of Mo(Si,Al)₂ Based Materials. *M. Halvarsson* (*mats.halvarsson@chalmers.se*), *A. Ingemarsson*, *J.-E. Svensson*, *S. Canovic*, *A. Jonsson*, *A. Hellström*, *L-G. Johansson*, Chalmers University of Technology, Sweden **INVITED**

MoSi₂-based composites have a high melting point, relatively low density and excellent oxidation resistance at high temperatures. This makes them useful materials for high temperature applications such as heating elements, burner nozzles and tubes in laboratory and industrial heating furnaces. It is well known that the oxidation resistance of molybdenum disilicides relies on the formation of a protective silica scale, formed at high temperatures due to the selective oxidation of Si. Although MoSi₂ composites show excellent corrosion resistance in oxidizing atmospheres, the SiO₂ scale is decomposed in reducing environments due to the evaporation of SiO(g). One way to avoid this problem is to partially substitute silicon with aluminium yielding a MoAl_xSi_{2-x} material. MoAl_xSi_{2-x} composites form a stable and adherent alumina scale at high temperatures and the material can therefore be used in oxidising, reducing and inert atmospheres up to almost 1600°C. In this study, a detailed investigation of the microstructure of the oxide film formed on a MoAl_xSi_{2-x} based composite (Kanthal Super ER) during oxidation in the temperature range 900 – 1500°C, has been carried out, aiming at understand the material's oxidation behaviour.

The isothermal exposures were carried out in horizontal tube furnaces for up to 1000h. The composite consists of three phases, Mo(Si,Al)₂, Mo₅(Si,Al)₃ and alumina. The samples formed relatively pure α -Al₂O₃ scales during the oxidation in the whole temperature range. The Al supply to the growing alumina scale is mainly provided by the Mo(Si,Al)₂ phase in the bulk material. The outward Al transport is counterbalanced by inward diffusion of Si into Mo(Si,Al)₂. Therefore an Al poor Mo₅(Si,Al)₃ phase

forms directly below the scale. In addition, an Al depletion gradient forms in the composite.

3:50pm A1-2-8 Microstructural damage criterion for Ni based single crystal superalloy coated with NiAlPt. *P. Sallot* (*pierre.sallot@mines-paristech.fr*), *V. Maurel*, *L. Rémy*, Mines-ParisTech, France

Platinum-modified aluminide coatings are widely used in both aero-engines and land-based gas turbine because they are essential to the overall life-time of the TBC system, which is of great interest in the industry as for the last two decades environmental and economic issues have raised over. It prevents the superalloy from detrimental oxidation at high temperature by forming a dense and adherent layer of alumina on its surface, and it improves the adhesion of the Thermal Barrier in TBC systems. Coatings investigated in this study are deposited by platinum electroplating followed by a low activity CVD aluminizing. The coating can be described by two layers: an outer β -NiAlPt single-phase layer approximately 50 μm thick and an interdiffusion zone referred to as IDZ. The coating resistance is usually assessed using standard cyclic oxidation tests with 1 hour at the maximum temperature during which the weight of samples is recorded by thermogravimetric methods. Net Mass Gain curves are then obtained and give an overview of the lifetime of the coating or allow the cross comparison of different coatings.

This paper reports upon results of an on-going investigation on degradation mechanisms of a platinum-modified nickel aluminide coating deposited on a Ni-base single crystal superalloy AM1 used by SNECMA for advanced blades. More particularly, a novel approach of the lifetime of platinum-modified coatings is proposed through the detailed study of IDZ evolution and its correlation with Net Mass Gain curves of coatings. The effect of different thermal transients, hold time duration, maximum temperatures as well as thermomechanical loadings on the IDZ evolution has been studied and a close link with the degradation of the coating has been found. Interrupted tests were performed to assess the kinetics of the IDZ evolution and it was monitored using cross section analyses of specimen combining optical microscopy and electron microprobe analysis.

The interdiffusion zone shrinks while the hold time at high temperature increases and has been modeled by simple diffusion laws. The direct relation between IDZ evolution and the coating degradation make it simple to deduce a promising lifetime model for the studied coating.

4:10pm A1-2-9 Compositional and Microstructural Changes in MCrAlY Coatings due to Interdiffusion with the Base Material. *D. Naumenko* (*d.naumenko@fz-juelich.de*), *V. Shemet*, *A. Chyrkin*, *L. Singheiser*, *W.J. Quadackers*, Forschungszentrum Jülich GmbH, Germany
MCrAlY (M = Ni, Co) overlay coatings are commonly used for oxidation protection of Ni- and Co-based superalloys in stationary gas-turbines as well as jet engines. At high exposure temperatures, i.e. above 1000°C, which is typical for laboratory testing of coated superalloys most of the commercially used MCrAlY-coatings possess a two-phase microstructure consisting of gamma Ni solid solution and intermetallic beta NiAl. The phase composition of MCrAlY-coatings is subjected to changes with changing temperature, due to formation of the thermally grown oxide (TGO) as well as due to interaction with the substrate material.

Using a number of examples in the present paper it is shown how the presence of the base material influences the phase composition and microstructure of the coatings. In particular the effects of carbon and Ti incorporated from the superalloy substrate into the coating are elucidated. Furthermore, it is shown that the porosity formation at the bondcoat/superalloy interface can be in many cases attributed to interdiffusion induced phase transformations rather than to the Kirkendall effect, which is commonly claimed to be responsible for the observed porosity. The analytical studies by SEM are complemented with numerical thermodynamic calculations using the software packages Thermocalc and DICTRA.

4:30pm A1-2-10 Effects of Hf and Zr additions on the properties and oxidation resistance of β -NiAl+Cr overlay coatings. *P. Alfano*, *L. Weaver* (*mweaver@eng.ua.edu*), University of Alabama, US

Nickel-based superalloy components in the hot sections of commercial gas turbine engines are often protected by aluminide coatings due to their ability to function in oxidative and corrosive environments. However, the microstructures of these coated systems are metastable and change in service due to interactions with the environment and interdiffusion with the underlying substrate. The extent of these changes depends critically upon coating microstructure, chemistry, and the environment that the coated component operates in. This presentation highlights the influences of chemical composition, post-deposition annealing, and isothermal oxidation at 1050°C on the microstructures and properties of NiAl-Cr-Hf and NiAl-Cr-Zr overlay bond coatings. In particular, the results indicated that coatings containing Hf exhibit lower oxidation mass gains for oxidation

times of less than 100hrs as compared to the Zr containing samples, but higher mass gains above 100hrs of oxidation. This presentation also highlights the effect of processing parameters, such as the addition of a seed layer, on microstructures and coating properties. The results indicate that the addition of a Ni seed layer can improve the adhesion between the substrate and coating.

4:50pm A1-2-11 The application of nanocrystalline NiCrAlY layer in thermal barrier coatings for industrial gas turbines. *M.S. Hussain*, *M. Daroonparvar* (*re_dr7@yahoo.com*), Universiti Teknologi, Malaysia

Thermal barrier coating systems (TBCs) are used to protect turbine blades against high-temperature corrosion and oxidation. They consist of a metal bond coat (MCrAlY, M = Ni, Co) and a ceramic top layer ($\text{ZrO}_2/\text{Y}_2\text{O}_3$). The life expectancy of TBCs is expected to be improved by the application of nanostructured MCrAlY bond coat. This paper therefore, reviews the main techniques used in the synthesis of nano-crystalline NiCrAlY powders using a planetary ball mill and investigates the oxidation behavior of conventional and nanostructured atmospheric plasma sprayed (APS) NiCrAlY coatings at elevated temperatures. Conventional NiCrAlY powder was mechanically milled and then sprayed on a nickel based superalloy (Inconel 738) to form a nanocrystalline bond coat in TBC. Both conventional and nanostructured NiCrAlY coatings were tested by high temperature oxidation at 1000°C for 24hr and then allowed to form the thermally grown oxide layer onto the bond coat. Microstructural characterization was carried out by using X-ray diffraction (XRD); scanning electron microscopy (SEM); field emission scanning electron microscopy (FESEM) equipped with energy dispersive spectroscopy (EDS). The adhesion strength of the as-sprayed TBCs was tested by bond strength test. The thickness of thermally grown oxide (TGO) at the interface of bond coat/ceramic layer, its constituents and the formed mixed oxides within the NiCrAlY bond coat were examined. Nanostructured coating showed much improved oxidation resistance than the conventional one. The observed improved behavior was due to the formation of a continuous, dense, uniform and thinner Al_2O_3 (TGO) layer over the nanostructured NiCrAlY coating. This layer has been able to protect the coating from further oxidation and had reduced the formation of mixed oxide protrusions present in the conventional coating.

Hard Coatings and Vapor Deposition Technology

Room: Royal Palm 4-6 - Session B4-3

Properties and Characterization of Hard Coatings and Surfaces

Moderator: J. Lin, Colorado School of Mines, US, C.

Mulligan, U.S. Army ARDEC, Benet Laboratories, US, B.

Zhao, Exxon Mobile, US

1:50pm B4-3-1 Structure and composition of TiSiCN coatings synthesized by reactive arc evaporation: implications for cutting tool applications. *E. Göthelid* (*emmanuelle.gothelid@sandvik.com*), *L. Löwenberg*, *A. Genvald*, *B. Ericsson*, *M. Ahlgren*, Sandvik Tooling, Sweden

Developing the ultimate all around tool has become some sort of Holy Grail for machining industries. Such a tool should be tough, with good flank and crater wear resistance, a combination which is not easy to achieve. Insert performance can be dramatically improved with the help of an appropriate coating. We present here a novel route for depositing TiSiCN coating on WC-Co substrates. A reactive mixture of trimethyl-silane ($\text{TMS}-(\text{CH}_3)_3\text{SiH}$) and N_2 is used as Si, C and N source while arcing Ti at different substrate bias. Thanks to this approach, the Si to Ti and C to N ratios may be tuned at will. The samples structure was analyzed by XRD and SEM, their chemical composition by EDS and XPS. Hardness and E modulus were also determined. Interesting samples were then performance tested in a turning application. The results show that the Si content plays a crucial role for the texture of the film and the outcome performances. The best variant at ca 6-10 at % Si exhibited a good combination of flank and crater wear resistance. These results will be discussed in the light of the physical data acquired.

2:10pm B4-3-2 Influence of Process Parameters on the Properties of Low Temperature ($\text{Cr}_{1-x}\text{Al}_x$)N Coatings Deposited via Hybrid PVD DC-MSIP/HPPMS. *K. Bobzin*, *N. Bagcivan*, *M. Ewerling*, *R.H. Brugnara* (*brugnara@iot.rwth-aachen.de*), Surface Engineering Institute - RWTH Aachen University, Germany

Ternary nitrides find widespread application as hard protective coating on cutting tools and as corrosion and wear resistant coatings on mechanical components. Concerning to this, ternary nitride such ($\text{Cr}_{1-x}\text{Al}_x$)N deposited via PVD (Physical Vapour Deposition) show outstanding tribological,

mechanical and chemical properties. The combination of these properties makes $(\text{Cr}_{1-x}\text{Al}_x)\text{N}$ coatings suitable for many applications. For an effective protection of coated parts a uniform layer of coating material is also required. In this regard, the HPPMS (high power pulse magnetron sputtering) technology offers possibilities to improve coating thickness uniformity as well as to enhance mechanical properties. The present work deals with the investigation of the influence of process parameters on the $(\text{Cr}_{1-x}\text{Al}_x)\text{N}$ coating properties deposited at 200 °C via combination of DC-MSIP and HPPMS technology. The aluminum content of the $(\text{Cr}_{1-x}\text{Al}_x)\text{N}$ was varied between 22 at-% and 88 at-%. Further, the deposition pressure was varied in the range of 475 mPa and 525 mPa. Subsequently, the bias voltage was varied from 0 up to -200 V in order to analyze the coating thickness distribution on surfaces parallel and perpendicular to cathode. Mechanical properties, morphology and phase composition were analyzed by means of Nanoindentation, SEM (Scanning Electron Microscopy) and XRD (X-Ray diffraction) measurements. The results show that the coating with 31 at-% Al displays higher hardness (20 GPa) and more favorable Young's modulus (370 GPa) compared to the other coatings. The increase of the deposition pressure from 475 mPa to 525 mPa leads to a decrease of the hardness to 7 GPa. With increasing bias voltage a preferred 200 grain orientation and denser crystalline morphology are identified. Regarding coating thickness uniformity, the coating deposited with -150 V shows the lowest deposition rate difference between the surface parallel and perpendicular to cathode. In addition, optical emission spectroscopy (OES) was used to investigate the effect of bias voltage and deposition pressure on intensity of Cr (357 nm) and Cr+ (283 nm) close to substrate during the coating process. In the studied parameter range, the change of the bias voltage shows a light effect on the Cr and Cr+ signal. The increasing of bias voltage from 0 V up to -150 V leads to decrease especially of non-ionized Cr. This effect can also be observed with increasing deposition pressure.

2:30pm **B4-3-3 Development of a new type micro slurry-jet erosion (MSE) test method for evaluation of surface strength of hard thin coatings**, Y. Iwai (yiwai@u-fukui.ac.jp), University of Fukui, Japan, T. Matsubara, Palmeco Co., Ltd, Japan, K. Yamamoto, Kobe Steel Ltd., Japan
INVITED

Versatile and reliable techniques for evaluation of hard thin coatings are necessary for the development and tribological assessment of new coatings. Several different experimental techniques such as a nano-indentation, scratch and wear tests are normally used. However, most of the tests cannot assess properties of coating, substrate and interface independently.

We have proposed a new type of Micro Slurry-jet Erosion test (MSE), i.e. a solid particle impact erosion test for swift evaluation of coatings. In this study, the potential of our developed MSE test is demonstrated for the evaluation of different kind of vapor deposited coatings including PVD or CVD-TiN, TiC, TiAlN, CrN and DLC. Slurry containing 1.2 µm alumina particles was mixed with compressed air in the nozzle and eventually impacted on test materials at high velocity up to 100 m/s. The cross-section of the nozzle exit was a square of 1 x 1 to 3 x 3 mm². The impingement angle was 90 degrees. Wear progressions in depth profiles of the wear scar were measured. The wear depths vs. the amount of impacting particles or test time curves show the individual behavior depending on the properties of coatings, substrate and interface. Their wear rates show a huge difference in the various coatings. The new MSE test generates highly reproducible results and is very sensitive to the quality of the coatings.

So our conclusion is that MSE tests can evaluate (1) coatings and substrate strength, (2) strength or property distribution in the direction of depth from the surface, (3) coating thickness based on strength or functional aspect, (4) interface layer or zone strength, (5) change of substrate properties according to deposition process. Consequently, the MSE test is highly suitable as a screening test when evaluating single and multi-layered coatings, thin coatings with gradients, coating/substrate interfaces, etc.

3:10pm **B4-3-5 Investigation of structural ,mechanical and tribological properties of TiAlN/CrN multilayer films deposited by CFUBMS technique**, C. Laloglu (claloglu@tunceli.edu.tr), Turkey, Ö. Baran, Erzincan University, Turkey, Y. Totik, İ. Efeoglu, Turkey
TiAlN and CrN are using widely in many industrial applications. In this work, TiAlN/CrN multilayer films deposited onto M2 high-speed steel and were examined by closed field-unbalanced magnetron sputtering (CFUBMS). Process parameters of coatings were determined according to Taguchi L₄ (3²) method. The structural properties of coatings have been analyzed by scanning electron microscopy (SEM), X-ray diffraction (XRD) and energy dispersive spectrometry (EDS). Besides, the mechanical and tribological properties were determined by using microhardness tester and pin-on-disc test, respectively. Experimental results showed that TiAlN/CrN multilayer films improved noticeably tribological properties of cutting tools.

3:30pm **B4-3-6 The Phase Transition and Corrosion Resistance of ZrO₂(N) Thin Films on AISI 304 Stainless Steel Deposited by Ion Plating**, J.H. Huang (jhhuang@mx.nthu.edu.tw), P.H. Huang, G.P. Yu, National Tsing Hua University, Taiwan

ZrO₂(N) thin films were deposited on AISI 304 stainless steel substrate using hollow cathode discharge ion-plating (HCD-IP). Our previous study [1] indicated that the adhesion of ZrO₂ thin film on stainless steel was poor due to low wettability. The objectives of the present study were to understand the phase transition of ZrO₂(N) thin films with increasing nitrogen contents and to provide a feasible approach to manufacture ZrO₂(N) coatings on stainless steel with excellent corrosion resistance and good adhesion. By maintaining oxygen flow rate at 10 sccm and adjusting nitrogen flow rate, ranging from 0 to 12 sccm, the compositions and phase ratios of the ZrO₂(N) thin films can be controlled. With increasing nitrogen flow rate, the XRD patterns showed that the phase content of c-ZrO₂ increased while that of m-ZrO₂ decreased, and then ZrN phase increased. The N solubility limit in ZrO₂ for the formation of ZrN was 8.8 at% for the as-deposited thin film. After annealing in vacuum, different phase transitions were found for the specimens. At higher nitrogen content, phase separation of ZrN from c-ZrO₂ occurred in the specimens. The corrosion resistance of the ZrO₂(N)-coated stainless steel specimens was evaluated by potentiodynamic scan in both 5% NaCl and in 1N H₂SO₄ solutions, and salt spray test was employed to assess the durability of the films. Corrosion resistance was associated with film packing density and major phases. The results showed that the HCD-IP method can effectively overcome the surface wetting problem of ZrO₂ on stainless steel, and hence the ZrO₂(N) coating on stainless steel possesses excellent adhesion and corrosion resistance. ZrO₂(N) thin films containing ZrN ranging from 14.4 % to 28.8 % were found to have better corrosion resistance than pure ZrO₂ thin films.

[1] Jia-Hong Huang, Tzu-Chun Lin, Ge-Ping Yu, Surf. Coat. Technol., 206(2011)107.

3:50pm **B4-3-7 Synthesis and Characterization of Boron/Nitrogen Incorporated Diamond-Like-Carbon Thin Films**, L.L. Zhang (liz286@mail.usask.ca), Y. Li, Y. Tang, Q. Yang, A. Hirose, University of Saskatchewan, Canada

Boron (B) and/or nitrogen (N) incorporated diamond-like-carbon (DLC) composite thin films have been synthesized from a simultaneous ion beam deposition of DLC films and ion beam sputtering of boron carbide (B₄C) and boron nitride (BN) targets, respectively. Raman Spectroscopy, Scanning/Transmission Electron Microscopy, Atomic Force Microscopy, X-ray Photoelectron Spectroscopy and synchrotron-based Near Edge X-ray Absorption Fine Structure were applied to investigate the film microstructure, morphology, electronic structure and bonding state. Nanoscratch tests were conducted using a nanoanalyzer to measure the mechanical properties of the synthesized films including both hardness and elastic modulus, as well as to evaluate the adhesion property. The electronic structure, bonding state and mechanical properties of the B/N incorporated DLC films were compared with those of unincorporated DLC film, and the relationships between the processing conditions, structures and properties were addressed.

4:10pm **B4-3-8 Hardness Percolation in Plasma Enhanced Chemical Vapor Deposited a-SiC:H Thin Films**, S. King (sean.king@intel.com), Intel Corporation, US

Plasma Enhanced Chemically Vapor Deposited a-SiC:H thin films are compelling materials for both semiconductor nano-electronic and MEMS/NEMS technologies due to the extreme chemical inertness of this material and the ability to tune a variety of material properties across an extreme range of values. As one example of the latter, we demonstrate that the hardness of a-SiC:H thin films can be varied from 0.5 to 40 GPa. Utilizing Fourier Infrared-Transform Spectroscopy, we additionally show that this remarkable range in materials properties is achieved primarily via the incorporation of terminal hydrogen groups which lowers the overall connectivity of the Si-C network bonding. We find that once the average network coordination number for Si and C falls below 2.6, the Si-C network becomes under constrained and there is a loss of rigidity percolating through the system. This rigidity limit constrains the range of materials properties that can be achieved in the Si-C system.

4:30pm **B4-3-9 Tungsten-modified hydrogenated amorphous carbon coatings providing tailored friction properties**, H. Hetzner (hetzner@mfk.uni-erlangen.de), S. Tremmel, S. Wartzack, Friedrich-Alexander-University Erlangen-Nuremberg, Germany

In comparison to pure hydrogenated amorphous carbon coatings (a-C:H), the metal-modified variants (a-C:H:Me) are known to have better adhesion to the substrate due to lower residual stresses and more stable friction in dry sliding against steel. For this reason, particularly in higher loaded applications, a-C:H:Me is usually preferred over a-C:H, even though

hardness and hence abrasion protection tends to be lower. Dependent on the deposition parameters, the properties of a-C:H:Me can be varied over wide ranges: From metal-like and carbide-like to amorphous-carbon-like. On the one hand this allows to a certain extent the adaption of the coating's mechanical properties to the load-carrying and overload capability required by the targeted application. On the other hand, this offers the opportunity to use these coatings for the realization of tailored friction properties.

In the present study, tungsten-modified hydrogenated amorphous carbon coatings (a-C:H:W) were deposited on hardened and tempered tool steel using an industrial scale coating machine. The applied coating technique was reactive magnetron sputtering of a tungsten carbide (WC) target in argon-acetylene atmosphere. To improve the adhesion to the substrate, a thin chromium layer and a WC intermediate layer were deposited by arc evaporation and magnetron sputtering, respectively. For the deposition of the a-C:H:W functional layer, four process parameters, namely cathode power, bias voltage, process gas pressure and argon-to-acetylene flow ratio were varied according to a 2⁴ factorial design.

The coated samples were characterized in terms of structural, mechanical and tribological properties: Micro structure and thickness were evaluated by scanning electron microscopy. Surface roughness was measured using a profilometer. Hardness and Young's modulus were determined by instrumented indentation tests. Rockwell C indentation and scratch tests provided information on cracking resistance and adhesion to the substrate. Friction and wear of the coatings were studied in ball-on-disk tests over a sliding distance of 1,000 meters (13,263 rotations). In dry sliding against 100Cr6 balls, coefficients of friction in the range of 0.10 to 0.43 were determined for the respective coatings. Under oil lubrication, the respective friction coefficient was found to be between 0.05 and 0.11. For almost any of the tested coatings, the observed friction behavior was also sufficiently stable. This proves the potential of providing tailored friction properties by proper choice of the deposition parameters of a-C:H:W coatings.

4:50pm B4-3-10 Characterization of Plasma Electrolytic Oxidation (PEO) Coatings on 6082 Aluminium Alloy. *A. Jarvis, A. Yerokhin (A.Yerokhin@sheffield.ac.uk), University of Sheffield, UK, P. Shashkov, Cambridge Nanolytic, Ltd., UK, A. Matthews, University of Sheffield, UK*

This research characterizes two sets of PEO alumina coatings obtained on BS 6082 series aluminium alloy substrates. One was produced using the more common electrolyte containing silicates, and the other was made without silicates. The coatings were characterized using a variety of methods and their relative wear resistance was evaluated with a reciprocating wear tester. The wear resistance of the coating made using the advanced method is significantly higher than the reference coating. The greater wear resistance of this coating appears to be due to the difference in wear modes: mostly transverse fracture cracks that lead to a gradual loss of material. The silicate containing coating suffers a more severe wear mode of both transverse as well as lateral cracks leading to spalling. The difference in wear resistance appears to be due to both higher micro-scale Vickers indentation hardness, as well as its greater indentation toughness that indicates the resistance to the formation of lateral cracks, and thus spalling. The reasons for this difference in toughness were not determined. The greater hardness of the new coating is likely due to lower porosity. Nanoindentation hardness measurements were used to evaluate the hardness and elastic modulus at a nano scale and tend to support the difference in alpha and gamma alumina phase content found using XRD measurements. Several other coating characteristics were investigated and appeared to have no correlation with wear resistance. The residual stresses in the coatings were measured using two methods: XRD and an optical fluorescence method (piezo-spectroscopic) which both showed the same trends. An attempt was made to quantify the amount of amorphous alumina in the coatings using a quantitative Rietveld method, however the results were inconclusive due to the difficulty in determining the exact gamma alumina phase crystal structure, thought to be a defect spinel structure.

5:10pm B4-3-11 The microstructure and mechanical properties of Cr-Si-Ti-Al-N coatings. *Y.C. Kuo, National Taiwan University of Science and Technology, Taiwan, J.W. Lee (jefflee@mail.mcut.edu.tw), C.J. Wang, Ming Chi University of Technology, Taiwan*

The Cr-Si-Ti-Al-N thin films with various silicon contents were fabricated by a co-sputtering process with three targets. The influences of silicon contents on the microstructure, mechanical and tribological properties of Cr-Si-Ti-Al-N films were investigated in this work. The phase structures of the coatings were determined by a glancing angle X-ray diffractometer (GA-XRD). The microstructures of thin films were evaluated by scanning electron microscopy (SEM) and transmission electron microscopy (TEM), respectively. The hardness and elastic modulus were examined by a nanoindentation. The scratch test, Rockwell-C adhesion and pin-on-disk wear tests were used to evaluate the adhesion quality and tribological properties of thin films. It was found that the column structure was transformed to a dense

structure when the silicon contents were higher than 10 at.%. The hardness and tribological properties were also strongly influenced by the silicon concentration of the Cr-Si-Ti-Al-N coatings.

Hard Coatings and Vapor Deposition Technology Room: Royal Palm 1-3 - Session B5-2

Hard and Multifunctional Nano-Structured Coatings

Moderator: J. Paulitsch, Christian Doppler Laboratory for Application Oriented Coating Development at the Department of Physical Metallurgy and Materials Testing, Montanuniversität Leoben, Austria, R. Sanjines, Ecole Polytechnique Fédérale de Lausanne, Switzerland, P. Zeman, University of West Bohemia, Czech Republic

1:50pm B5-2-1 Tribological properties of Cr_{0.65}Al_{0.35}N-Ag self-lubricating hard coatings from room temperature to 550 °C. *C. Mulligan (c.mulligan@us.army.mil), U.S. Army ARDEC, Benet Laboratories, US, P. Papi, Rensselaer Polytechnic Institute, J. Lin, W. Sproul, Colorado School of Mines, US, D. Gall, Rensselaer Polytechnic Institute*

Cr_{0.65}Al_{0.35}N-Ag composite layers, 5-µm-thick and containing 10-15 at.% Ag, were deposited by reactive magnetron co-sputtering from Cr, Al, and Ag targets on Si(001) and 440C stainless steel substrates. The layer composition was controlled by the relative power to sputtering targets. The layers exhibit a nanocomposite structure with segregated Ag grains homogeneously distributed throughout a CrAlN matrix. The tribological properties against alumina counterface were evaluated from testing temperatures, T_t = 25-550 °C in ball-on-disk dry sliding operation. Cr_{0.65}Al_{0.35}N-Ag composite layers demonstrate low friction (<0.25) across a wide temperature range from room temperature to 550 °C. This is in contrast to similarly processed CrN-Ag coatings, which exhibit higher friction coefficient in the range of 0.45-0.55 at room temperature along with higher wear rates when sliding against alumina. For Cr_{0.65}Al_{0.35}N-Ag composite layers the friction of coefficient drops to a minimum of 0.13 at temperatures exceeding the growth temperature, T_g = 400 °C. The difference in testing and growth temperature, ΔT = T_t - T_g, is the key parameter that determines lubricant transport and is therefore used to control the level of solid lubrication at elevated temperature.

2:10pm B5-2-2 Mechanical, tribological and thermal properties of sputtered a-C:H:N:Nb coatings. *M. Fenker (fenker@fem-online.de), H. Kappl, FEM Forschungsinstitut Edelmetalle & Metallchemie, Germany*

INVITED

High hardness combined with a low friction coefficient against a counterpart and high temperature stability (up to several hundreds of degree Celsius) are properties which are of main importance for hard protective thin films. A disadvantage of a lot of developed coating materials, like e.g. diamond-like carbon coatings, is that they fulfill only one or two of the three coating properties.

The present work discusses the properties of niobium-alloyed nitrogen-containing diamond-like carbon coatings. So far, the system a-C:H:Nb has been poorly studied and no published data on a-C:H:Nb could be found. The coatings have been deposited by reactive magnetron sputtering in an Ar/C₂H₂/N₂ atmosphere. The microstructure of the coatings has been investigated by X-ray diffraction, transmission electron microscopy and scanning electron microscopy. Most of the coatings are X-ray amorphous with low amounts of crystalline phases. The mechanical (hardness, adhesion) and tribological (pin-on-disc) behavior of the coatings with respect to the C₂H₂ and N₂ flow is presented. The influence of temperature (up to 500°C in air) on this behavior is discussed. A coatings hardness up to 2800-3000 HV with a friction coefficient in the range of 0.25 – 0.5 has been measured. A fairly good temperature stability was found for a-C:H:Nb coatings.

2:50pm B5-2-4 DLC-MoS₂ Composite Coatings by Hybrid Technique of Ion Beam Deposition and Sputtering. *H. Niakan (hamid.niakan@usask.ca), J.A. Szpunar, Q. Yang, University of Saskatchewan, Canada*

Diamond-like carbon (DLC) exhibits many favorable chemical and mechanical properties, which makes it an attractive candidate as corrosion and wear resistant coating for a variety of applications including aerospace industry. However, stress concentration at the interface between metallic substrates and DLC coatings causes problems in endurance life and adhesion of the coatings exposed to mechanical loadings. Besides, the long

duration for super-low friction seems to be a big issue for its application. DLC based nanocomposite coatings are promising to solve the problems. In this work, pure DLC coatings on Ti-6Al-4V plates and Si wafers were firstly investigated using direct ion beam deposition technique in order to optimize the processing parameters. Then, nanocomposite coating samples of DLC-MoS₂ were deposited on the Ti-based substrate by a hybrid technique of ion beam deposition and target biased ion beam sputtering. The structure of the nanocomposite samples were investigated by Raman Spectroscopy, X-ray photoelectron spectroscopy (XPS) and X-ray diffraction (XRD). Their mechanical and tribological properties were studied using nanoindentation, scratch testing, nanoanalyzer, and pin-on-disc. The results show that the nanocomposite coatings have much improved adhesion to the substrate and comparable hardness and tribological properties with that of pure DLC coatings.

3:10pm B5-2-5 Growth of Amorphous Hf-Al-Si-N Thin Films by DC Magnetron Sputtering. *H. Fager* (*hanfa@ifm.liu.se*), Linköping University, IFM, Thin Film Physics Division, Sweden, *A. Mei*, University of Illinois at Urbana-Champaign, US, *B.M. Howe*, Air Force Research Laboratory, US, *J.E. Greene*, *I. Petrov*, University of Illinois at Urbana-Champaign, US, *L. Hultman*, Linköping University, IFM, Thin Film Physics Division, Sweden

Crystalline and nanocrystalline transition metal nitrides have attracted a lot of interest over the years, and they are well known to have a wide range of outstanding properties that makes them suitable in many different applications. In comparison with crystalline transition metal nitrides, and also compared to corresponding carbides and oxides, very little has been reported on amorphous transition metal nitrides and most of their properties are still unknown. Nevertheless they are potentially attractive, e.g., as wear resistant coatings, due to their homogeneous structure. We propose amorphous multicomponent transition metal nitrides as a new class of refractory materials.

Using kinetically limited growth techniques - including low growth temperatures and high deposition rates - is one of the keys to growing amorphous transition metal nitride films. In this study, we investigate the HfN-AlN-Si₃N₄ system, where the difference in atomic size and bond coordination between the constituent elements, in combination with kinetically limited growth, promotes the formation of an amorphous structure. Hf_{1-x-y}Al_xSi₃N₄ thin films were grown on Si(001) substrates by reactive magnetron sputtering from a single Hf_{0.6}Al_{0.2}Si_{0.2} target. We show that we can control the film morphology, from nanocrystalline to amorphous, by varying the ion flux and growth temperature, and also the film composition by varying the ion energy.

Compositional analysis of the as-deposited films was performed by energy dispersive x-ray spectroscopy (EDS), and the structural information was gained by x-ray diffraction and analytical transmission electron microscopy. We will report on hardness and elastic properties of the films, as well as temperature dependent resistivity.

3:30pm B5-2-6 Nanocomposite coatings in the Al-Ge-N system: synthesis, structure and mechanical and optical properties. *E. Lewin* (*erik.lewin@empa.ch*), *M. Parlinska-Wojtan*, *J. Patscheider*, Empa, Switzerland

Coatings in the Al-Ge-N system have been synthesized using reactive DC magnetron sputtering and characterized with the goal to explore the structure and properties, as well as their potential use as hard optical coatings. The composition was varied from pure AlN to pure GeN_y. Also experiments varying substrate temperature and sample bias were conducted. Coatings were analyzed using X-ray diffraction, X-ray photoelectron spectroscopy (XPS) and scanning and transmission electron microscopy. Besides the binary reference samples, ternary samples with Ge-contents from 5 to 30 at.% were synthesized, and found to be nanocomposites of a nanocrystalline, Ge-containing AlN-phase, nc-(Al_{1-x}Ge_x)N, and an amorphous, N-deficient GeN_y-phase. The grain size of the (Al_{1-x}Ge_x)N phase decreased with increasing Ge-content from about 30 to 15nm. Additionally the (Al_{1-x}Ge_x)N -phase was found to exhibit two different textures depending on the Ge-content: at low Ge content a (001) preferred orientation was observed, while at increased Ge-content the (110) orientation became dominant. The GeN_y phase was found to be highly susceptible to sputter damage during sputter-cleaning prior to XPS analysis.

A nanocomposite-hardening, similar to what has been observed for e.g. the AlN/Si₃N₄ system, was observed: the hardness increased from 19 GPa (for the AlN reference sample) to 25 GPa for the hardest ternary sample. Samples were found to have a high transparency in the visible region, and the index of refraction shows a slight dependence of Ge-content, increasing from about 2.0 to 2.2 as Ge-content increases from 0 to 30 at.%. Thus these coatings have a potential use as protective coatings for optical components operating in the visual or near IR range.

3:50pm B5-2-7 Shape- Recovery of Thin Film Metallic Glasses Upon Annealing. *C. Rullyani*, *C. Li*, *J. Chu* (*jpchu@mail.ntust.edu.tw*), National Taiwan University of Science and Technology, Taiwan

Thin film metallic glasses (TFMGs) possess many excellent and unique properties, including high strength, ductility, annealing-induced amorphization and good adhesion between the substrate and film. Like ordinary metallic glasses, the TFMGs in general undergo the glass transition and crystallization at temperatures of T_g and T_x, respectively, upon annealing. Another exceptional property of TFMGs is the shape-recovery ability during annealing at temperatures between T_g and T_x (or so-called the supercooled liquid region, ΔT) due mainly to the low viscosity flow. Surface defects such as indentation marks on the scales up to a few micrometers tend to shrink in size or even disappear without crystallization in ΔT.

In this study, 200 nm-thick TFMGs with different compositions are deposited on Si substrates. Nanoindentation tests are performed to evaluate the film properties. Surface morphology and microstructure before and after annealing within ΔT are examined and reveal that the size of indentation mark decreases after annealing. As a result, the shape-recovery behavior is confirmed and detailed characterization results of various TFMGs as a function of annealing time will be discussed.

Keyword: thin film metallic glass, annealing, shape recovery

4:10pm B5-2-8 Thin Film Metallic Glasses: Unique Properties and Potential Applications. *J. Chu* (*jpchu@mail.ntust.edu.tw*), National Taiwan University of Science and Technology, Taiwan **INVITED**

A new group of thin film metallic glasses (TFMGs) have been reported to exhibit properties different from conventional crystalline metal films, though their bulk forms are already well-known for the high strength and toughness, large elastic limits, excellent corrosion and wear resistances because of the amorphous structure. In recent decades, bulk metallic glasses (BMGs) have gained a great deal of interest due to the substantial improvements in specimen sizes. On the other hand, much less attention has been devoted to the TFMGs, despite the fact that they have many properties and characteristics which are not readily achievable with other types of metallic or oxide films. Furthermore, these TFMGs have been progressively used for engineering applications and thus deserve to be recognized in the field of thin film coatings.

In addition, while the BMGs are still difficult to use because of their brittle macroscopic nature and difficulty of processing, TFMGs are a possible solution to make use of their great properties of high strength, large plasticity, and excellent wear resistance. In this presentation, many advantages and properties of TFMGs are discussed. These are such as mechanical properties, tribological properties, annealing-induced amorphization and resulting smooth surface, some of which lead to useful applications, for example, for substrate fatigue property enhancements. In addition, potential applications in microelectronics and optoelectronics are mentioned. Ironically, there have been enormous research efforts dedicated to developing metallic glasses with large critical sizes only to reveal that the best use for these materials may, in fact, be in thin film applications. It is thus hoped that this talk serves the purpose of calling attention to the importance of TFMGs such that many more studies and applications may be explored.

4:50pm B5-2-10 Improving the corrosion resistance and hardness of TaN films by silicon addition. *G. Ramirez* (*enggiowa@hotmail.com*), *S.E. Rodil*, *S. Muhl*, *G. Galicia*, Universidad Nacional Autónoma de México - Instituto de Investigaciones en Materiales, Mexico, *E. Camps*, *L. Escobar-Alarcón*, Instituto Nacional de Investigaciones Nucleares de México, México, *D. Solis-Casados*, Universidad Autónoma del Estado de México - Centro de Investigación en Química Sustentable, Mexico

The aim of the present work was to obtain dense thin films that present simultaneously good corrosion resistance and hardness. For this, we propose the deposition of nanocomposite thin films where tantalum nitride (TaN) nanocrystals were embedded in an amorphous silicon nitride (SiN_x) phase. The deposition was done using two magnetrons; one of pure Si and the other of pure Ta and the amount of Si into the samples was varied by changing the RF power (20 - 340 W) applied to the Si target. The N₂/Ar ratio was fixed at the value optimized for the stoichiometric deposition of tantalum nitride films (6/14). The TaN-SiN_x samples were deposited on silicon and their composition, structure and hardness were evaluated by X-ray photoelectron spectroscopy, X-ray diffraction and nanoindentation, respectively. The results indicated that the silicon content increased linearly from 1 to 12 at% as the RF power was increased. Meanwhile, the hardness showed a maximum around 5.4 at% of silicon attaining 40 GPa, representing a 20 % hardness enhancement in comparison to the fcc phase of the TaN film. From the structural analysis, it was observed that the TaN d -fcc phase was stabilized due to the addition of Si. However, for the

largest Si at%, a quasi-amorphous phase and softer film (23 GPa) was obtained.

The TaN-SiNx samples were deposited on AISI 304L stainless steel and the corrosion resistance was evaluated using DC and AC electrochemical techniques. The DC techniques include potentiodynamic polarization and polarization resistance, data that were analyzed using the Tafel method. The electrochemical impedance spectroscopy was used to evaluate the properties of the different interfaces present using electronic equivalent circuits to model the variations of the coatings parameters as a function of the silicon content. The results showed that the polarization resistance (R_p) of the TaN-SiNx film that presents the highest hardness value was double than the R_p of both the AISI304L and the TaN film. Similarly, the corrosion current density (I_{corr}), which is proportional to the corrosion rate of the material, was approximately one order of magnitude lower than the substrate and the TaN films.

Acknowledgements: We wish to acknowledge the financial support from DGAPA-UNAM IN103910. G. Ramírez acknowledges CONACYT for his PhD scholarship.

5:10pm **B5-2-11 Combinatorial studies of co-sputtered chromium-titanium oxide composite films.** *Y. Sun (pameloyusun123@hotmail.com), J. Chang, M. Wong (mswong@mail.ndhu.edu.tw),* National Dong Hwa University, Taiwan

We adopted a combinatorial approach to develop a series of Ti-Cr oxide films with a full composition spread. The films were deposited on silicon and quartz substrates by co-sputtering a metallic titanium target and a chromium target simultaneously onto a stationary long-strip of substrate in a gas mixture of argon and oxygen at 250 °C and without substrate bias. The location of substrates in relation to targets is found to be very crucial for the result. At the two ends of the substrate strip corresponding to Ti and Cr metal targets, crystalline rutile-structured TiO₂ and corundum-structured Cr₂O₃ are formed, respectively, while in the middle region, the films are amorphous. No film of mixed phases is observed. The nanoindentation hardness values of the rutile-structured TiO₂ and the corundum-structured Cr₂O₃ films are 18 and 23 GPa, respectively, while those of the amorphous films vary with the lowest down to 13 GPa. As the dopant content varies from the both ends, the film structure and crystallinity transform from crystalline to amorphous-like phase and its morphologies and microstructures change from rough surface of columnar grains to smooth surface of nanocomposite. Composition mapping of the rutile-structured TiO₂ and the corundum-structured Cr₂O₃ films shows that the dopant element is present along grain boundaries, which indicate the two oxides have low solubility for each other or are even immiscible.

Keywords : Combinatorial approach, chromia, titania, mixed oxide, nanoindentation.

Tribology & Mechanical Behavior of Coatings and Engineered Surfaces

Room: Pacific Salon 1-2 - Session E4-1/G4-1

Coatings for Machining Advanced Materials and for use in Advanced Manufacturing Methods

Moderator: M. Arndt, OC Oerlikon Balzers AG, Liechtenstein, X. Nie, University of Windsor, Canada

1:50pm **E4-1/G4-1-1 Development of Coating Technology Platforms for Wear Component Applications.** *I. Spitsberg, S. Brahmandam (sudhir.brahmandam@kennametal.com), D. Siddle,* Kennametal Incorporated, US **INVITED**

The global economic pressures and escalating energy costs create increasing demands on performance of engineered components used in various wear related applications. Surface engineering is an important tool to reach these objectives, especially because of its potential to significantly improve performance without changing structural properties of the substrate. To enable timely and effective development of new products, it is critical to establish smart approaches for leveraging, re-engineering and enhancing the existing technologies to make them suitable for new applications.

This talk discusses the engineering challenges and systematic methodology for developing new thin coating platforms for wear resistant components starting with the current state of the art in metal cutting coating. The methodology is based on understanding fundamental limitations of currently available coatings with respect to the new application area, and developing approaches for modeling, testing and evaluation.

2:30pm **E4-1/G4-1-3 Oxygen Plasma Etching of Diamond-Like Carbon Coated Mold-Die for Micro-Texturing.** *T. Aizawa (taizawa@sic.shibaura-it.ac.jp),* Shibaura Institute of Technology, Japan, *T. Aizawa,* Mitsue Mold Engineering, Co. Ltd., Japan

Carbon-based materials have sufficient high temperature strength in inert atmosphere; they are attractive as a substrate material of mold-die for mold-stamping the oxide glasses into optical elements. In recent, most of optical lens system equips diffractive optical elements; e.g. Fresnel pattern is a typical micro-pattern on these elements. Here, new technique is needed to imprint the designed micro-pattern or micro-texture onto glassy carbon substrate or amorphous carbon coatings on the metallic alloy substrate.

In the present paper, diamond-like carbon (DLC) coating via PVD/CVD on the SKD11 substrate is employed to make micro-texturing by using oxygen plasma etching. Original pattern by metal-chromium is first line-drawn on the surface of DLC coating; then, it is subjected to oxygen plasma etching. Even without any hazardous etchants such as CF₄, high etching rate is attained only by using oxygen gas; i.e. 2.5 to 3 µm/H. Plasma diagnosis by spectroscopy proves that this etching process is controlled by activated oxygen atom flux of {O, O*}. Direct chemical reaction by C (in DLC) + O* → CO, or, C (in DLC) + O* → C-O, drives this etching. Detection of CO peaks in the wave length range of 200 to 300 nm also proves that this oxygen plasma etching should be advanced by chemical reactions. This etching behavior is insensitive to line width (d) and pitch width (L) for 2 µm < d < 100 µm and 5 µm < L < 100 µm. Scanning electron microscope and laser-profilometer are used to make precise measurement on the etched profiles.

2:50pm **E4-1/G4-1-5 Tensile properties of magnetron sputtered aluminum-scandium and aluminum-zirconium freestanding thin films: a comparative study.** *J. Kovac (kovac@iwt-bremen.de), H-R. Stock, B. Köhler, H. Bomas, H-W. Zoch,* Stiftung Institut fuer Werkstofftechnik Bremen, Germany

Micro cold forming processes require thin sheets of high strength materials often with a thickness below 30 µm. Due to its good resistance, grain refining and anti-recrystallisation properties, aluminum-scandium is a very promising material for such processes, but cannot be rolled down to such a thickness because of its high strength. A suitable alternative to this issue is to produce aluminum-scandium thin sheets in the form of freestanding thin films using magnetron sputtering. However, a major limitation to the mass production of these sheets is the high cost of scandium. Zirconium, on the other hand, has been reported to act in a similar way as scandium in aluminum alloys, providing precipitation strengthening, grain refining and anti-recrystallisation properties to the material, but features the advantage to be much cheaper than scandium. This study aims to investigate the influence of the deposition process and post treatment parameters on both aluminum-scandium and aluminum-zirconium magnetron sputtered freestanding thin films and to compare their properties regarding to the micro forming process.

The sheets were deposited with a d. c. magnetron sputtering unit using two different targets: aluminum with 1.2 at% scandium and aluminum with 1.2 at% zirconium and argon as process gas. An unalloyed steel sheet of 100 µm was used as substrate. After deposition the steel was chemically removed in a concentrated nitric acid solution which results in a freestanding sputtered film. Several sheets were produced, each time with a different combination of target power and substrate temperature. The samples were then heat treated at 300 °C for 1 hour, and the mechanical properties of both as deposited and heat treated samples were measured with a tensile tester designed for thin samples.

Scanning electron microscopy showed a reduced columnar morphology for both aluminum-scandium and aluminum-zirconium films. It could be shown that the substrate temperature and the post heat treatment both influences the tensile strength of the sheets. Aluminum-scandium thin sheets reached more than 400 MPa and aluminum-zirconium thin sheets more than 500 MPa but were apparently less ductile than the previous one. Additionally, coating defects were observed at the cross section of tested samples and suspected to initiate cracks and therefore limiting deformation.

3:10pm **E4-1/G4-1-6 Near frictionless based on W-S-X magnetron sputtering coatings for Micromouldings.** *A. Manaia, M.T. Vieira (teresa.vieira@dem.uc.pt), R. Alves,* Coimbra University, Portugal

The optimization of moulding surfaces for microinjection of thermoplastics is crucial to attain the manufacturing specifications for high quality of microengineering components or devices.

This paper is aimed on the perspective of evaluate the near frictionless character of thin films based on W-S-Cu system with and without C, to be used to optimize machining surfaces for plastic moulding. The friction characteristics will be evaluated in condition close to the conditions during the polymer injection process. W-S-X coatings were deposited by magnetron sputtering doped with X= Cu and/or C (from 0%at. to 30% at. on

stainless steel DIN X42Cr13 surface moulding micromanufactured by laser beam machining (LBM), followed by electron beam machining (EBM) as the finishing process. The selection of the best coatings was based on the conditions for setting to create high density and low roughness of the surface, hardness in the range from 6-8 GPa and an adhesion critical load better than 40N. Low friction characteristics were previously measured when testing against the different surface coated with the polymers (PP, PMMA, PA and POM) balls. These results were compared with those evaluated using a moulding friction equipment (homemade) that is homothetic of the extraction conditions during the injection process.

3:30pm **E4-1/G4-1-7 Tribological contact analysis of a CrN coated surface under inclined impact-sliding wear tests against steel and WC balls**, *J.F. Su, X. Nie* (*xnie@uwindsor.ca*), *H. Hu*, University of Windsor, Canada

An inclined impact-sliding tester has been developed to evaluate the wear and fatigue behaviour of hard coatings for tooling and machining which involve both impact and sliding movements. In this project, finite element analysis (FEM) was used to analyse the stress, material deformations and fracture conditions of a CrN coating on D2 steel substrate under a 200 N/400 N impact-sliding load combination. The studied tribological contacts were steel/WC balls impacting and sliding on the CrN coated sample. The balls were modelled as elastic-plastic; the coating was linearly elastic and the steel substrate was elastic-plastic taking into account strain hardening effects. The stresses and strains generated in the surface along the impact-sliding tracks during impacting and sliding suggested the origin and position of different failure mechanisms such as chipping and peeling. Experimental observations were carried out using scanning electron microscope (SEM) and energy dispersive X-ray spectroscopy (EDX) on cross sections along the impact-sliding tracks. The results of experimental studies were illustrated well with the FEM analysis.

3:50pm **E4-1/G4-1-8 PVD coating development for advanced metal cutting**, *J. Kohlscheen* (*joern.kohlscheen@kennametal.com*), Kennametal, Essen, Germany

To meet the ever increasing demands in metal cutting new PVD coatings are constantly being developed. A trend is clearly detectable to develop high end coatings for niche applications outperforming standard coatings like TiAlN or AlCrN. Development strategies include elemental doping, optimization of layering sequences or plasma intensification (e.g. HiPIMS). We present a variety of cutting results on steel 4140 and ductile cast iron with different coating-substrate combinations. The resulting wear patterns on carbide inserts and associated wear mechanisms will be discussed. It will be shown that advanced PVD coatings can have a beneficial effect but do not always outperform tools with conventional coatings.

Applications, Manufacturing, and Equipment Room: Tiki Pavilion - Session G3-1

Atmospheric and Hybrid Plasma Technologies

Moderator: H. Barankova, Uppsala University, Sweden, R. Gesche, Ferdinand Braun Institut, Germany

1:50pm **G3-1-1 Atmospheric plasma-assisted deposition of antimicrobial coatings on textiles**, *M. Fleischman, V. Rodriguez-Santiago, L. Piehler, D. Pappas* (*daphne.pappas@us.army.mil*), US Army Research Laboratory, US, *J. Leadore*, United States Army Research Laboratory, US

In this work, we applied a dielectric barrier discharge deposition process under atmospheric pressure conditions for the growth of thin coatings with antimicrobial properties on polymer films and textiles. The precursor used was 1,1,3,3-tetramethylguanidine (TMG), and we studied the effect of concentration, deposition time and discharge power on the composition of the deposited coating. X-ray photoelectron spectroscopy, scanning electron and atomic force microscopy were employed to study the impact of plasma parameters on the chemical structure and surface morphology of the deposited coatings. It was observed that for prolonged plasma deposition times, etching and oxidation occurred in the coatings. Both effects adversely affect the desired polymerization process and were reduced through the choice of proper experimental conditions. Also, the wettability of the coating and its stability were investigated. Once the optimal TMG coating was developed, antimicrobial tests were performed on nylon/cotton fabrics coated with the TMG film. Preliminary testing showed that the coated fabrics have high antimicrobial activity against Gram-negative *Escherichia coli* and Gram-positive *Staphylococcus aureus* bacteria, using the AATCC 100 test method. These promising results are an indication that atmospheric plasma processing can provide coatings that can lead to the

development of lightweight, breathable textiles with both self-cleaning and antimicrobial properties.

2:10pm **G3-1-2 Cold Atmospheric Plasma Inside Water**, *H. Baranková* (*Hana.Barankova@angstrom.uu.se*), *L. Bardos*, Uppsala University, Sweden

The Fused Hollow Cathode (FHC) atmospheric plasma source has been adapted for generation of a cold plasma submerged in a liquid. The reactor with a special arrangement has been built and used for testing the plasma without and with an auxiliary gas, argon, neon, nitrogen and air, forming bubbles and transporting the plasma into a wide area. The FHC source has been powered either by a pulsed dc generator or rf generator. The pulsed plasmas can be excited at the average power as low as 2 W. Results of first experiments in water, changes in the plasma geometry and measurements of the optical emission spectra from the plasma at different power and gas flow conditions are introduced. Potential applications of the submerged plasmas are briefly discussed.

2:30pm **G3-1-3 Deposition of DLC Films by Nanopulse plasma CVD at atmospheric pressure**, *N. Ohtake* (*ohtaken@mech.titech.ac.jp*), Tokyo Institute of Technology, Japan

INVITED

1. Introduction

DLC film consists of sp³ carbon bonds coexisting with sp² bonds of carbon atoms, and shows high hardness and self-lubricant properties. Therefore, DLC film is expected to be an excellent material for wear-resistant coatings. DLC films are usually deposited by physical vapor deposition (PVD) and chemical vapor deposition (CVD) processes under low pressure, typically below 10 Pa (1x10⁻⁴ atm.). Preparation of DLC films at atmospheric pressure will promote a variety of new applications of the films, because in-process and in-use coating of DLC films will be realized. However, it has been generally believed that it is difficult to deposit DLC films at atmospheric pressure because carbon and hydrocarbon ions are needed to fabricate hard films. Here we report the development of the nanopulse plasma CVD method using a nanopulse generator and the application of the synthesis method for the deposition of DLC films, and show that DLC film can be prepared at atmospheric pressure.

2. Experimental

We performed the deposition of DLC films at subatmospheric pressure (26.7kPa) using the nanopulse plasma CVD method. A stainless-steel anode of 10 mm in diameter is set 20 mm above the Si(100) substrate. Positive pulse voltage is applied to the stain-less-steel anode. The streamer discharges are generated between the anode and Si substrate. The diameter of the discharge on the substrate is approximately 20 mm. CH₄ and He gases are injected from the gas inlet nozzle. The flow rates of CH₄ and He are 3 L/min and 50 L/min, respectively. The flow rate is set approximately tenfold higher than in the conventional CVD method, in order to prevent the polymerization of the hydrocarbon species in the plasma. The applied pulse voltage is 5.0 kV and the maximum current is 19 A. A uniform film of approximately 20 mm in diameter was fabricated on the Si substrate. The deposition area is in good agreement with the area of the streamer discharges generated.

The thickness of the film is approximately 1.6μm with a smooth surface. The surface roughness of the film is as low as 0.07 nmRa, as determined by atomic force microscope (AFM) analysis. The Raman spectrum of the deposited film shows that the peak consists of the G-band and D-band, indicating a DLC film. The hardness of the DLC film as measured with a nanoindenter is 21.5 GPa and the elastic modulus is 187 GPa. These results suggest that the DLC film has excellent mechanical performance. Consequently, we fabricated DLC films in open air using pipe-electrode.

3:10pm **G3-1-5 A study of the interactive effects of hybrid current modes on the tribological properties of a PEO Plasma Electrolytic Oxidation coated AM60B Mg-alloys**, *R. Hussein, D. Northwood, X. Nie* (*xnie@uwindsor.ca*), University of Windsor, Canada

The automotive industry in its efforts to reduce the weight of vehicles, thereby reducing the consumption of gas, is increasingly looking towards Magnesium alloys. However, the applications of magnesium alloys have been limited by their inferior to corrosion and wear properties. PEO is an electrochemical process that uses a non-hazardous aqueous electrolyte to oxidize the metal surfaces to form ceramic oxide coatings which impart a high corrosion and wear resistance. In this study we investigated the effect of current mode, unipolar, bipolar or hybrid (combination of both) on the properties of PEO coatings formed on an AM60B magnesium alloy (mass fraction: Al 5.6–6.4%, Mn 0.26–0.4%, Zn ≤ 0.2%, balance Mg). Optical Emission Spectroscopy (OES) was employed to study how the plasma species influenced by the current mode. The morphology and microstructure of the coatings were investigated using Scanning Electron Microscopy (SEM). The tribological properties of the PEO-coated materials

were evaluated under the dry sliding conditions show a higher coefficient of friction but a lower wear rate than the uncoated Mg alloy. It was also found that the coatings formed using the hybrid current mode showed different wear behavior of both the coating and counterpart pins due to their modified coating microstructure and surface morphology. The microstructures of the coatings and their relationships to the tribological performance are discussed in detail.

3:30pm **G3-1-6 Insight into Plasma Discharge in PEO: *In-situ* Impedance Spectroscopy Study**, A. Yerokhin (A.Yerokhin@sheffield.ac.uk), C.-J. Liang, University of Sheffield, UK, E. Parfenov, Ufa State Aviation Technical University, Russian Federation, A. Matthews, University of Sheffield, UK

Plasma electrolytic oxidation (PEO) is an advanced anodising technology which operates at voltages that trigger plasma discharge at the metal-electrolyte interface. Due to transient nature and unusual environment such plasma is difficult to investigate by conventional means. Here we report on the results of *in-situ* impedance spectroscopy studies that provide insights into the structure of plasma discharge in PEO. The impedance characteristics of the PEO process on Al were obtained and effects of polarisation voltage and processing time discussed. In the impedance spectra, four time constants ranging from 10^{-5} to 10^{-2} s were resolved, indicating processes taking place at different scales. Discharge appears to be dominated by typical of plasmas inductive response, with negative resistance likely to be associated with sheath behaviour also being prominent. These processes are coupled with a relatively fast capacitive and a rather slow inductive response that may be due to charge transfer through the metal-oxide interface and plasma thermal relaxation respectively.

3:50pm **G3-1-7 Control of ion distribution functions in capacitive sputter sources**, D. Eremin, S. Gallian, D. Szeremley, R.P. Brinkmann, T. Mussenbrock (mussenbrock@gmail.com), Ruhr Universität Bochum, Germany

The ion energy distribution function (IEDF) plays a major role in plasma based surface modification. The control of IEDFs is therefore strongly desirable, particularly in the context of sputter deposition. Due to their unique properties capacitive multi-frequency discharges are promising candidates not only for sputtering dielectric (non-conductive) materials but also for allowing for tailoring IEDFs.

The paper discusses a technique which enables the tailoring of IEDFs. The technique exploits the electrical asymmetry effect (EAE) in geometrically symmetric and asymmetric capacitive discharges which leads to the generation of a DC self-bias voltage. The DC self-bias voltage as the key parameter for IEDFs can be controlled using the phase shift between the two consecutive harmonics of the driving radio-frequency. By means of self-consistent kinetic plasma simulations performed on Graphics Processing Units (GPUs) it is shown that the energy of ions impinging on both the target and the substrate can be controlled almost independently from the ion flux.

4:10pm **G3-1-8 Tandem of DBD and ICP RF Atmospheric Plasma Systems for Yttrium Oxide Nanocoating of Consumable Semiconductor Parts**, Y. Glukhoy (glukhoy1@aol.com), A. Ryaboy, T. Kerzhner, Nanocoating Plasma Systems Inc., US

An ICP atmospheric plasma torch is proven to be an excellent tool for yttrium oxide plasma corrosion protective nanocoating of consumable parts for plasma etching processes. It provides a residence time of nanoparticles in a high temperature area that is enough for a total melting and evaporation. A gaseous focusing of such torch allows the size reduction of the spot in order to deliver Y₂O₃ vapor into the gas distribution holes of the showerheads. Unfortunately, susceptibility of the precursor to agglomeration deteriorates these advantages. RF power is not enough for the thermal decomposition of aggregates on the fly. Contaminated by the clusters, this coating has risk of flaking. We found that an atmospheric dielectric barrier discharge (DBD) can provide decomposition of clusters with a much lower energy. Both, single nanoparticles and nanoparticles in aggregation are charged negatively when they are passing through the plasma bulk. The repulsive electrostatic forces break down of the multi-charged clusters into small pieces suitable for the following evaporation in the ICP torch.

Our linear reactor consists of the 12 mm quartz tube with array of tungsten needles, welded alongside and connected to the 13.56 MHz RF generator. Length is enough to provides the passage of nanoparticles with residence time for separation. The DBD discharge is generated at the 100W RF power and the gas flow of 40 cfm. Therefore, tandem of the DBD and the ICP atmospheric plasma systems can replace a DC plasma spray low adhesion coating can be a solution for the development of the size unlimited chamber-less coating for transition to 450 mm wafers. The first results show the reduction of cluster contamination verified by SEM and ATF.

Surface Engineering for Thermal Transport, Storage and Harvesting

Room: Sunset - Session TS1-1

Surface Engineering for Thermal Transport, Storage and Harvesting

Moderator: B. Cola, Georgia Technical Institute, US, C. Muratore, Air Force Research Laboratory, Thermal Sciences and Materials Branch, US

1:50pm **TS1-1-1 Textured CrN Thin Coatings Enhancing Heat Transfer in Nucleate Boiling Processes**, E.M. Slomski (slomski@mpa-ifw.tu-darmstadt.de), M. Oechsner, S. Fischer, P. Stephan, H. Scheerer, T. Troßmann, Technische Universität Darmstadt, Germany

Subsequent research work aims to investigate the potential of PVD thin coatings for new fields of application. The present study is based on measurements of electrical conductivity, light absorption and thermodynamic nucleate boiling tests of specific textured Cr/CrN-coatings with predominant (1 1 1), (3 1 1) or (2 0 0), (2 2 0) crystal lattice orientations. Those tests reveal promising results concerning thin film applications in the field of heat transfer enhancement during nucleate boiling. High Power Impulse Magnetron Sputtering (HiPIMS) in combination with Direct Current Magnetron Sputtering (DCMS) was applied to deposit CrN coatings of 3-4 µm thickness on different substrate materials. An ultrathin coating of pure Cr was used as adhesive interlayer between substrate and CrN coating. The crystallographic phases and orientations of the coatings were determined by X-ray analyses (XRD) using glancing-incidence and $\theta/2\theta$ mode and texture coefficients were calculated. High resolution scanning electron microscope (SEM) analyses visualize the different shapes, sizes and orientations of the grains. Finally selected Cr/CrN coatings were deposited on heater samples and boiling curves were measured in nucleate boiling experiments in order to determine heat transfer coefficients and critical heatflux (CHF) at dryout of the heater surface. Results show an up to 2.2 times higher CHF of the coated heater, compared to an uncoated pure copper heater.

2:10pm **TS1-1-2 Effects of strain on thermal conductivity in amorphous thin films**, M.T. Alam, M.P. Manoharan, Penn State University, Mechanical & Nuclear Engineering Department, S.V. Shenogin, UES/Air Force Research Laboratory, Materials and Manufacturing Directorate, Thermal Sciences and Materials Branch, US, A. Voevodin, A.K. Roy, C. Muratore (chris.muratore@wpafb.af.mil), Air Force Research Laboratory, Materials and Manufacturing Directorate, Thermal Sciences and Materials Branch, US, M.D. Haque, Penn State University, Mechanical & Nuclear Engineering Department, US

To investigate mechanisms of thermal conductivity in amorphous materials, we developed a technique for microfabricating freestanding ultrathin films with built-in strain actuation and instrumentation for thermal conductivity measurement. Using a combination of infrared thermal micrography, 3-omega analysis, and multi-physics simulations, we measured the thermal conductivity of amorphous silicon nitride and silicon oxide films under a range of tensile strains. The thermal conductivity of the silicon nitride film showed a remarkable decrease with tensile strain, dropping down by an order of magnitude at approximately 2% strain when compared to the unstrained film. Silicon oxide showed no change in thermal conductivity up to 1% tensile strain. The theoretical analysis was performed using classical molecular dynamics and lattice dynamics simulations, showing that amorphous silicon nitride has unusual vibrational properties resembling those of amorphous silicon and other chemically uniform glasses. The unusual relationship between strain and thermal conductivity in amorphous silicon nitride suggests that an additional mechanism such as long-range unharmonic coupling between oscillators plays an important role in heat conduction, as the conductivity agrees with harmonic theory predictions at large values of tensile strain (>2%). This work is supported by AFOSR Low Density Materials Program, Task #2306CR7P.

2:30pm **TS1-1-3 Surface engineering for improved thermal transport at metal/carbon interfaces**, *S.V. Shenogin*, UES/Air Force Research Laboratory, Materials and Manufacturing Directorate, Thermal Sciences and Materials Branch, US, *J.J. Gengler*, Spectral Energies, LLC/Air Force Research Laboratory, Thermal Sciences and Materials Branch, US, *J.J. Hu*, *J.E. Bultman*, UDRI/Air Force Research Laboratory, Thermal Sciences and Materials Branch, US, *A.N. Reed*, *A. Voevodin*, *A.K. Roy*, *C. Muratore* (*chris.muratore@wpafb.af.mil*), Air Force Research Laboratory, Materials and Manufacturing Directorate, Thermal Sciences and Materials Branch, US

Carbon nanotubes are appealing for diverse thermal management applications due to their high thermal conductivity (as high as 3,000 W m⁻¹ K⁻¹) coupled with interesting mechanical properties (super-strong, but also exhibiting foam-like deformation in CNT arrays). Unfortunately, CNT surfaces are generally non-reactive and demonstrate weak bonding to other materials, limiting thermal interfacial conduction. To better understand the nature of interfacial resistance in carbon nanotubes, modeling and experimental studies investigating engineered interfaces on highly oriented pyrolytic graphite (HOPG) substrates were conducted. This substrate was selected as a practical 2-dimensional analog for nanotube sidewalls to facilitate modeling and experimentation, however there are differences between HOPG and CNTs which are addressed in simulations to account for differences in metal-carbon interfaces. Measurements of thermal conductance at these interfaces were made by analysis of the two-color time domain thermoreflectance (TDTR) data from the samples. The TDTR analysis of the different metals on HOPG was made possible by having an optical parametric oscillator on the probe beam which allows for tuning the probe beam wavelength to match absorption bands for each metal studied. Metal films were selected to identify effects of atomic mass, chemical interactions (i.e., interfacial carbide formation) and electron configuration. Measurements of chemically "inert" metals at the carbon interface, including Al, Cu and Au demonstrated a strong dependence on Debye temperature, with conductance values differing by a factor of 3. For metals known to exhibit in situ formation of an interfacial carbide layer when in contact with a carbon substrate, such as titanium and boron, conductance values were roughly a factor of 4 higher than for inert metals. The effects of thermal formation of interfacial carbide layers with varied areal densities on HOPG surfaces on thermal conductance were also examined, in addition to metal interlayers specifically selected for acoustic matching to other materials, as in a composite structure. This work is supported by AFOSR Low Density Materials Program, Task #2306CR7P.

2:50pm **TS1-1-4 Heat flow across heterojunctions: Toward useful nanoscale thermal interface materials**, *T.S. Fisher* (*tsfisher@purdue.edu*), *S.L. Hodson*, *A. Kumar*, Purdue University, US, *A. Voevodin*, Air Force Research Laboratory, US **INVITED**

Improved understanding of thermal energy transport at nanometer scales has enabled a broad range of technological advances in recent years. Today, new materials can be designed at the atomic level and are projected to improve the efficiency of information processing, heat transfer, and energy conversion, among other applications relevant to aerospace vehicles and systems. For the transfer of energy by phonons, approaches based on atomistic Green's functions have been recently developed and offer the possibility of including atomic-scale detail at material interfaces, while mesoscopic scales can be modeled with the particle-based Boltzmann transport equation. This review will summarize a framework for the inclusion of such high-fidelity atomistic modeling within multi-scale modeling tools that are needed to understand complex interfacial transport processes and scaling principles in thermal interface materials enhanced with carbon nanotubes (CNTs). Experimental validation and refinement on model components is essential to this work, and includes highly localized techniques such as transient thermoreflectance techniques, as well as traditional 1D reference bar approaches to assess overall performance. As an example of recent work, we briefly describe critical results related to contact resistance measurements with CNT arrays and other graphene-based structures. The talk will conclude with enumeration of important questions related to heterojunction bonding and materials processing for scaled-up manufacturing.

3:30pm **TS1-1-6 Factorial increases in interfacial thermal conductance using a monolayer**, *P. O'Brien* (*obriep3@rpi.edu*), *S.V. Shenogin*, *J. Liu*, *M. Yamaguchi*, *P. Keblinski*, *G. Ramanath*, Rensselaer Polytechnic Institute, US

Manipulating interfacial thermal transport is a compelling need for a number of technologies including nanoelectronics and biomedical devices, solid-state lighting, energy generation, nanocomposites, and device packaging. Here, we demonstrate that introducing a strongly-bonding organic nanomolecular monolayer (NML) at a metal-dielectric interface leads to a factor of four increase in the interfacial thermal conductance to values as high as 450 MW/m²-K. Molecular dynamics simulation and a

vibrational analysis of NML-tailored interfaces verify that this remarkable interfacial conductance enhancement is due to strong NML-silica and NML-metal bonding. The strong overlap of broadband low-frequency vibrational states at the interface further facilitates efficient heat transfer through the molecules comprising the NML. These results provide a rational means of increasing heterointerfacial thermal conductance through molecular functionalization with adhesion-enhancing functional groups for a wide variety of material systems and applications.

3:50pm **TS1-1-7 Ruthenium organometallic complexes with photo-switchable wettability for boiling heat transfer applications**, *N. Hunter* (*chad.hunter@wpafb.af.mil*), Air Force Research Laboratory, Materials and Manufacturing Directorate, Thermal Sciences and Materials Branch, US, *B. Turner*, Universal Technology Corporation, US, *R. Glavin*, Air Force Research Laboratory, Materials and Manufacturing Directorate, Thermal Sciences and Materials Branch, US, *M. Jespersen*, University of Dayton Research Institute, US, *M. Check*, *S. Putnam*, Universal Technology Corporation, US, *A. Voevodin*, Air Force Research Laboratory, Materials and Manufacturing Directorate, Thermal Sciences and Materials Branch, US

Liquid to vapor phase change technology utilizing latent heat of vaporization, which can have heat transfer rates orders of magnitude higher than single phase liquid cooling, is necessary for advanced aircraft due to the onboard heat generated by high power (electrical and chemical) components. The wettability of engineered surfaces used in these cooling systems, in addition to other parameters such as surface roughness, is strongly correlated to the performance of the heat exchanger systems that use these materials. In addition to optimizing performance using passive means (e.g., surface texturing), it would also be advantageous to control heat transfer rates using applied stimuli (e.g., light or sound waves), which could result in weight savings and/or energy optimization. Oxide photocatalysts have been investigated to influence boiling performance on surfaces¹, but time scales for switching between wettability states are on the order of tens of minutes to hours, much longer than for practical use to control boiling processes. In previous work, synthesis of [Ru(bpy)₂(pox)]Cl₂, an organometallic complex which undergoes reversible photo-isomerization that changes the inherent water affinity of the molecule, was achieved². In the current research, new ruthenium-centered organometallic complexes with functionalized bipyridine (bpy) ligands are synthesized. The functionalization allows the Ru complexes to be covalently tethered to metallic substrates. Surface chemistry is investigated with XPS, indicating a character of the bonding linkage, which is then correlated with contact angle measurements of the surface energy modification with and without UV-VIS light irradiation. Water boiling heat transfer studies during UV-VIS light irradiation are conducted on these samples and correlated with the reversible switching of surface wetting.

¹Takata, et al., International Journal of Chemistry Research, 2003.

²D.B. Turner, et al., Inorganic Chemistry, in preparation.

4:10pm **TS1-1-8 From hard coatings to thermoelectrics: effects of nanostructure on fundamental physical properties of transition metal nitride, oxide, and oxynitride thin film alloys**, *B.M. Howe* (*brandonhowe@gmail.com*), Air Force Research Laboratory, US

Recent advances in aerospace and defense technologies have lead to an increasing need to develop novel materials with exotic physical properties for use in a variety of applications involving extreme, high-temperature, high mechanical stress, and oxidizing environments. Transition metal nitrides (TMN), oxides, and oxynitrides are well known to have remarkable range of unique physical properties including high hardness and mechanical strength, high melting temperatures (>>2000 °C), and tunable optical-electronic properties. One method to further enhance the physical properties of many binary transition metal nitrides is to alloy them with a second thermodynamically immiscible nitride to form metastable compounds with enhanced physical properties. Many of these properties are accompanied by the formation of nanoscale compositional modulations during film growth as well as post annealing experiments, however, very little has been reported on the ability to control this nanostructure, and as a result, the effects of these nanostructures on fundamental physical properties is relatively unknown.

Nanostructuring methods using these kinetically-limited growth techniques involving high-flux low-energy ion bombardment during film growth, lead to a unique independent control of both electric and thermal transport. The right materials system, combined with said growth techniques, would allow for the realization of hard, chemically inert, environmentally-friendly, and refractory thermal-to-electrical energy conversion thin films materials to tackle a variety of demanding defense applications.

I have used Hf_{1-x}Al_xN as a model system to study the nanostructures of interest. I begin by reporting on the effects of nanostructure on the optical, electronic, thermal transport and elastic constant properties of Hf_{1-x}Al_xN

single crystal layers grown on MgO(001) by reactive unbalanced magnetron cosputtering using ellipsometry, temperature dependent hall effect, picosecond probe thermoreflectance and acoustic transport measurements, respectively. I will also present thermal transport studies of nanocrystalline SrTiO₃ (a promising oxide thermoelectric) and SrTiO₃/TiO₂ systems, as a first step towards understanding thermal and electron transport in nanostructured oxide thin films.

4:30pm **TS1-1-9 Modified Lithium Alanate for High-Capacity Thermal Energy Storage**, *A. Amama* (*Placidus.Amama@wpafb.af.mil*), Air Force Research Laboratory, US, *J. Grant*, UDRI/Air Force Research Laboratory, Thermal Sciences and Materials Branch, US, *P. Shamberger*, *A. Voevodin*, Air Force Research Laboratory, US, *T.S. Fisher*, Purdue University, US

The development of novel and efficient thermal energy storage (TES) materials is a major challenge in addressing needs in a variety of applications, from intermittent solar energy harvesting to thermal management of transient, high-flux heat loads. Lithium alanate (LiAlH₄) is a potential TES material that possesses extraordinarily high inherent thermal energy density, and the possibility of a system that is compact and lightweight. However, the high desorption temperature at atmospheric pressure and slow kinetics represent significant challenges to the use of this material for TES. In order to address these challenges, the present work focuses on the modification of LiAlH₄ via high-energy ball milling with Ti-based catalysts, resulting in nanoscale features. The doping of LiAlH₄ with Ti-based catalysts has resulted in improved thermal energy storage properties. Quasi in situ X-ray photoelectron (XPS) study of the dehydrogenation reaction of LiAlH₄ has provided new insights into the role of the catalysts.

5:10pm **TS1-1-11 Heat reduction of concentrator photovoltaic module using high radiation coating**, *K. Nishioka* (*nishioka@cc.miyazaki-u.ac.jp*), *Y. Ota*, University of Miyazaki, Japan, *K. Tamura*, *K. Araki*, Daido Steel Co., Ltd., Japan

Light concentration is important for the development of advanced PV system using high efficiency solar cells. High efficiency multi-junction cells under high concentration operations have been investigated for terrestrial application. Also, low concentration operations with multi-junction cells have been investigated for space satellite. It is considered that the temperature of solar cells considerably rises under light concentrating operations.

It is very important for concentration photovoltaic (CPV) modules to decrease their temperature. A heat release from aluminum chassis of CPV module should be enhanced. In this study, a heat radiation layer was coated on the aluminum chassis of CPV module, and the effect of the layer on cell temperature was evaluated and discussed.

A CPV module consisted of 25 pairs of Fresnel lens (160 mm x 160 mm) and triple-junction solar cell (7 mm x 7mm), and an aluminum chassis was used. A heat radiation layer (PELNOX LTD., PELCOOL(R)) was coated on the aluminum chassis of CPV module. The triple-junction solar cells were arrayed on the aluminum chassis. In order to detect the cell temperature, a Pt100 was embedded just below the triple-junction solar cell. A CPV module was fabricated by connecting 25 lens-cell pairs in series.

The cell temperature of CPV module with heat release coating was about 15K lower than that without coating. The effect of the high radiation layer was remarkable, and the output powers of the CPV module with and without coating were 170.7 W and 162.4 W, respectively.

This study was carried out in Japan. Since the effect of the high radiation layer becomes remarkable, as the temperature of the heat source is higher, it can be expected that the high radiation coating for the CPV module works more effectively in more higher temperature area.

Coatings for Use at High Temperature Room: Sunrise - Session A1-3

Coatings to Resist High Temperature Oxidation, Corrosion and Fouling

Moderator: D. Naumenko, Forschungszentrum Jülich GmbH, Germany, B. Hazel, Pratt and Whitney, US, F. Perez Trujillo, Universidad Complutense de Madrid, Spain, L-G. Johansson, Chalmers University of Technology, Sweden

8:00am **A1-3-1 Development of high-temperature oxidation resistant coatings by electrodeposition**, X. Peng (xpeng@imr.ac.cn), Institute of Metal Research, Chinese Academy of Sciences, China **INVITED**

A novel concept is proposed for designing high-temperature oxidation-resistant coatings using electrodeposition. The electrodeposited coatings have a nanocrystalline Ni matrix with nano length scale dispersion of nanoparticles of Cr or/and Al. The Ni nanostructured coatings are oxidation-resistant based on a model on the easily selective oxidation to form a protective scale of Cr_2O_3 or Al_2O_3 as proposed as follows. Numerous Cr or/and Al nanoparticles on or close to the surface act as the "diffusionless" sites for nucleating the corresponding oxides at the onset of oxidation and those in deeper areas simultaneously supplies sufficient flux of the Cr or/and Al along the abundant grain boundaries in the Ni matrix, toward the surface for a rapid linkage of the oxide nuclei through their lateral growth. The validity of the model is verified by characterization of the scales formed in the initial oxidation stage and comparison of the oxidation of these coatings with that of component-similar materials of two other types, composites electrodeposited using Cr or/and Al microparticles and coarse-grained alloys prepared by arc-melting.

8:40am **A1-3-3 Producing high temperature multifunction coatings on the basis of micro-sized spherical aluminum particles**, R. Roussel, M. Juez, Lorenzo, V. Kuchenreuther, V. Kolarik (vladislav.kolarik@ict.fraunhofer.de), Fraunhofer ICT, Germany

Micro-sized spherical Al particles in the range of 1 to 20 μm deposited as slurry by brushing and spraying on the surface of a Ni- or Fe-based alloy oxidize at high temperatures to a top-coat from sintered hollow alumina spheres while forming an aluminized diffusion zone in the substrate. The top-coat has the potential to effectuate as a thermal barrier coating by gas phase insulation and the diffusion zone forms a protective alumina layer. The adherence of the top-coat and the formation of the diffusion zone depend on the heat treatment and are influenced notably by the particle size of the aluminium.

Samples from Alloy 321 and IN738 were coated with single size spherical aluminium particles with 2-3 μm and a multi-size mixture of 1-20 μm and subjected to a heat treatment. PEG was used as binder. For Alloy 321 the Al particles oxidize rapidly enough for forming sintered hollow alumina spheres with sufficient wall thickness at temperatures around the melting point. Simultaneously diffusion takes place. For the Ni-based IN738 the suitable heat treatment temperatures are higher. At 900°C and 950°C a homogeneous diffusion zone with an adherent top-coat was formed. For both alloys reproducibility was observed keeping the heat treatment parameters constant. The multi-size source particle powder seems to benefit the adherence of the top-coat. The results indicate that the smaller particles contribute more to diffusion while mechanically more stable alumina scales form on larger particles. Exposure experiments to 2000 h confirm the higher stability of the coating when using the multi-size Al particles.

9:00am **A1-3-4 Thermal barrier coatings on γ -TiAl protected by the halogen effect**, S. Friedle, M. Schütze (schuetze@dechema.de), Dechema e.V., Frankfurt am Main, Germany, N. Nießen, R. Braun, DLR - Deutsches Zentrum für Luft- und Raumfahrt, Germany

Nickel-based superalloys protected by thermal barrier coating (TBC) systems of yttria-stabilized zirconia (YSZ) are the existing standard high temperature material in aero-engines. A current research goal is to substitute these alloys to some extent with lightweight γ -TiAl, which have a low specific weight and high specific strength at elevated temperatures. The oxidation resistance of γ -TiAl, which is limited to approximately 750°C, is significantly improved by the halogen effect, affording an oxidation protection up to 1050°C. In this process, treatment of γ -TiAl surfaces with fluorine promotes the selective formation of a slow-growing α -alumina layer. A halogen-affected zone of only 1-3 μm provides a constant supply of halogen to maintain the oxidation resistance even under cyclic conditions in water-vapor and sulfur-containing atmospheres. With this well-established

method, γ -TiAl alloys could potentially replace heavy-weight nickel-based superalloys in some industrial applications in the future. For increased turbine efficiency, application of a TBC is necessary in order to improve the lifetime of turbine blades and vanes. TBCs have therefore previously been tested on γ -TiAl by applying bond coats of aluminide and Ti-Al-Cr based intermetallic coatings as well as nitride coatings. These applications, however, suffered from problems such as the formation of brittle TiAl_3 and TiAl_3 phases, interdiffusion between the bond coat and the substrate, and an inefficient oxidation resistance at long-term exposures above 900°C. Here, we present a novel concept that combines TBCs with the halogen effect on γ -TiAl, eliminating the disadvantages that have been observed using traditional bond coats on these alloys. The halogen treatment is also a very simple and economical process showing great potential for industrial applications, representing an additional noteworthy advantage. For the first time, we demonstrate the successful application of EB-PVD TBCs on γ -TiAl protected by the halogen effect. The γ -TiAl based alloys were treated with fluorine by means of gas and liquid phase treatment and plasma immersion ion implantation. Subsequently, YSZ thermal barrier coatings were deposited using electron-beam physical vapor deposition at substrate temperatures of ~1000°C. The oxidation behavior of the specimens was determined under cyclic oxidation conditions at 900°C in air, revealing excellent adhesion of the TBC on oxide scales existing predominantly of α -alumina.

9:20am **A1-3-5 High Temperature Protection of Ferritic Steels by Nano-Structured Coatings: Supercritical Steam Turbines Applications**, S. Mato, P. Hierro, I. Castañeda, A. Alcalá, I. Lasanta, Universidad Complutense de Madrid, Spain, M. Tejero, Universidad Complutense de Madrid, Spain, J. Sánchez, Instituto de Ciencia de Materiales de Sevilla, Spain, M. Brizuela, Tecnalia, Spain, J. Pérez (fjperez@quim.ucm.es), Universidad Complutense de Madrid, Spain

In many applications at high temperature, micro-structured coatings have been applied in order to protect structural materials against a wide range of different environments: oxidation, metal dusting, sulphidation, molten salts, steam, etc... The resistance achieved by the use of different kind of coatings have been optimum, and with late design such as TBC's and FGM's coatings. Although, the lifetime of them are related with inter-diffusion, and different CET as main degradation mechanisms.

In the case of supercritical steam turbines, many attempts have been made in terms of micro-structural coatings design, mainly based in aluminides, and another diffusion coating systems.

In order to consider another alternatives to minimize those problems, nano-structured coatings, applied by PVD and HIPIMS-PVD based in Cr, Ti and Al design, have been applied onto high temperature structural materials in order to analyze their high temperature oxidation resistance in steam environments.

The gravimetric results obtained have been analysed upto 2.000 hours, jointly with the evaporation behavior analysed by TG-Mass spectrometry. Excellent results have been achieved for the nano-structured coatings tested. Those results are comparables with the results obtained for micro-structured coatings, and in some case better for nano-structured coatings.

According to the results obtained, the nano-structured coatings have a potential application as protective systems in high temperature, for some applications will be proposed.

Coatings for Use at High Temperature Room: Sunrise - Session A3-1/F8-1

Coatings for Fuel Cells & Batteries

Moderator: G. Dadheech, General Motors, US, E. Yu, Newcastle University, UK

10:00am **A3-1/F8-1-7 Oxidation of SOFC Interconnects**, M. Ueda (mueda@mtl.titech.ac.jp), K. Kawamura, T. Maruyama, Tokyo Institute of Technology, Japan **INVITED**

Solid oxide fuel cells (SOFCs) are promising power generating system to achieve high energy efficiency and less CO_2 emission. Operating temperature has been lowered from 1273 K to 1023 K and the candidate materials for interconnects changes from ceramics to ferritic Cr_2O_3 -forming alloys.

This paper focus on high temperature oxidation of metal interconnects and the effects of atmosphere and electric current on oxidation behavior of

metal interconnects are discussed. Moreover, the improvement of electrical performance by the coating of $\text{La}_{0.85}\text{Sr}_{0.15}\text{CoO}_3$ will be also mentioned in this paper.

Interconnects are exposed to both fuel and air sides at operating temperature and electric current passes through interconnect during the operation. The oxidation of Fe-16Cr ferritic alloy was carried out at 1073 K in the single atmosphere.¹⁾ Cr_2O_3 scale formed on the alloy and Mn-Cr spinel was located on the top of the Cr_2O_3 scale. The oxidation in dual atmosphere without electric current exhibited the similar morphology and growth rate to those in the single atmosphere.²⁾ Parabolic rate constants in both sides were almost the same because the n-type defect structure may be predominant in both cases. The oxidation of Fe-25Cr ferritic alloy at 1073 K in dual atmosphere with electric current prevailed that the growth of Cr_2O_3 scale was accelerated at the anode side and suppressed at the cathode side.³⁾ The kinetic equation describing the growth rate of Cr_2O_3 scale was derived in terms of electric current, which enables to estimate both the scale thickness and areal specific resistivity (ASR). The control of oxidation kinetics at the anode side is essential to improve electrical performance of interconnect during the long-term operation.

The coating of $\text{La}_{0.85}\text{Sr}_{0.15}\text{CoO}_3$ onto alloy surface is effective way of improving electrical conductivity of interconnect in oxidizing atmosphere at high temperatures.^{4,5)} Solid state reaction between the coating and Cr_2O_3 scale gives the conductive oxide phases in the Sr-Cr-O ternary system.⁶⁾

- 1) T. Brylewski, M. Nanko, T. Maruyama and K. Przybylski, *Solid State Ionics*, **143**, 131-150(2001).
- 2) H. Kurokawa, K. Kawamura and T. Maruyama, *Solid State Ionics*, **168**, 13-21(2004).
- 3) K. Kawamura, T. Nitobe, H. Kurokawa, M. Ueda and T. Maruyama, unpublished data.
- 4) T. Kadowaki, T. Shiomitsu, E. Matsuda, H. Nakagawa, H. Tsuneizumi and T. Maruyama, *Solid State Ionics*, **67**, 65-69(1993).
- 5) T. Shiomitsu, T. Kadowaki, T. Ogawa and T. Maruyama, *Proceeding of The Electrochemical Society*, **PV 95-1**, 850-857(1995).
- 6) T. Maruyama, T. Inoue and K. Nagata, *Proceeding of The Electrochemical Society*, **PV 95-1**, 889-894(1995).

10:40am **A3-1/F8-1-9 Microstructural Investigation of Co- and RE-nanocoatings on FeCr Steels**, *S. Canovic* (sead.canovic@chalmers.se), *J. Froitzheim, R. Sachitanand, M. Nikumaa, M. Halvarsson, L-G. Johansson, J.-E. Svensson*, Chalmers University of Technology, Sweden

For the solid oxide fuel cell (SOFC) design, both ceramic and metallic materials are considered as construction materials for the interconnectors. Compared to the ceramics, metallic materials are easier to fabricate, and therefore cheaper, they are less brittle, easier to machine and they possess higher electrical and thermal conductivity than most ceramics. Based on the requirements such as oxidation resistance, low thermal expansion coefficient and electrical conductivity of surface oxide scales, high-Cr ferritic steels seem to be promising metallic interconnector materials. However, there are some problems that have to be overcome. The main problem for application of metallic interconnector materials in SOFCs is their reactivity with the anode and cathode side environments at the high operating temperatures. The resulting high temperature corrosion leads to e.g. dimensional changes, deterioration of mechanical properties and formation of oxide scales on the surface that often leads to low electrical conductivity. Another related problem is the chromium evaporation from the steel resulting in poisoning of the electrode surfaces in the fuel cell. One way to overcome these problems is to coat the steel with a thin (in the nm range) coating that improves the relevant properties of the steel. In this work Co- and reactive element (RE)-coatings have been deposited on FeCr steel (Sanergy HT). Furnace exposures are used to evaluate the effect of the coatings. The exposures are made in cathode-like environment (air containing 3% H_2O) during 168 h at 850°C.

The surface morphology and microstructure of the grown oxide scales were characterized using transmission electron microscopy (TEM), scanning electron microscopy (SEM), scanning transmission electron microscopy (STEM) and energy dispersive X-ray analysis (EDX). Cross-section TEM thin foils were prepared using a combined FIB/SEM (focused ion beam/scanning electron microscope) instrument, whereby electron transparency was achieved throughout the coating thickness. The detailed microstructure of the different coatings will be described in this work.

11:00am **A3-1/F8-1-10 Nafion membrane surface coated with self-assembly membrane containing nanometer-sized Pt-Sn particles to mitigate methanol crossover**, *C.H. Lin*, National Chung Hsing University, Taiwan, *C.H. Wan* (chiehhao@mdu.edu.tw), MingDao University, Taiwan, *M.T. Lin, W. Wu*, National Chung Hsing University, Taiwan

This paper uses a self-assembly membrane of PAH/PSS (PAH, poly (allylamine hydrochloride); PSS, polystyrene sulfonic acid sodium salt) containing the $\text{Pt}_{50}\text{-Sn}_{50}$ nanoparticles that adsorbed on Nafion membrane surface using the layer-by-layer technique to suppress the methanol crossover and improve the cell performance. Nanometer-sized $\text{Pt}_{50}\text{-Sn}_{50}$ particles dispersed in the self-assembly PAH/PSS membrane are synthesized by the reduction of Pt and Sn ions which adjacent to the $-\text{SO}_3^-$ groups of PSS in the presence of NaBH_4 . Formation of $\text{Pt}_{50}\text{-Sn}_{50}$ nanoparticles and the growth of self-assembly membrane on Nafion membrane were monitored by the UV-visible spectroscopy. The methanol crossover rate and proton conductivity of Nafion membrane were measured by the CO_2 sensor at the cathode exhaust and impedance analyzer. According to the results, the particle size depends on the molar ratio of PSS to Pt and Sn ions in the solution. Nafion membrane with $\text{Pt}_{50}\text{-Sn}_{50}$ nanoparticles dispersed in PAH/PSS self assembly membrane reduces the methanol crossover up to 15% and improves output power of 20% as compared to the cell with the un-modified Nafion membrane. Furthermore, the thickness of self-assembly layers strongly affected the rate of methanol crossover and the proton conductivity of membrane. The existence of $\text{Pt}_{50}\text{-Sn}_{50}$ nanoparticle in PAH/PSS self assembly membrane is believed to react with the crossed-over methanol. It thus reduces the mixture potential effect at cathode and improves the output power of DMFC.

11:20am **A3-1/F8-1-11 Suppression of methanol crossover with self-assembly membrane containing $\text{Pt}_{35}\text{-Ru}_{65}$ catalyst particles coated on Nafion membrane surface**, *C.H. Wan* (chiehhao@mdu.edu.tw), MingDao University, Taiwan, *M.T. Lin*, National Chung Hsing University, Taiwan, *Y. Jheng*, MingDao University, Taiwan

Methanol crossover is one of the key barriers for the commercialization of Direct Methanol Fuel Cell (DMFC). In this paper, a bilayer of self assembly membrane of poly (allylamine hydrochloride) (PAH)/ polystyrene sulfonic acid sodium salt (PSS) containing $\text{Pt}_{35}\text{-Ru}_{65}$ catalyst particles is coated on the Nafion membrane surface through the layer-by-layer technique to mitigate the methanol crossover and enhance the cell performance. Nanometer-sized $\text{Pt}_{35}\text{-Ru}_{65}$

particles dispersed in the self-assembly membrane are produced using the reduction of Pt and Ru ions in PSS. The content of Pt and Ru ions in the bilayer and the bilayer thickness are monitored by UV-visible spectroscopy. SEM, EDS and XRD are adopted to characterize the surface morphology, chemical composition, phases, crystalline and particle size of the resulted Pt-Ru. Experimental results show that the thickness of 5 bilayer of PAH/PSS self-assembly membrane is 30nm. Nafion membrane surface coated with $\text{Pt}_{35}\text{-Ru}_{65}$ particles dispersed in PAH/PSS self-assembly membrane mitigates the methanol crossover up to 25% and performance improvement of 15% at 80 °C . This is because the $\text{Pt}_{35}\text{-Ru}_{65}$ catalyst particles in self-assembly membrane react with the crossed-over methanol and the low methanol permeability of PAH/PSS self-assembly membrane reduces the rate of methanol crossover. Therefore, self-assembly membrane with $\text{Pt}_{35}\text{-Ru}_{65}$ catalyst particles functions like a reactive methanol filter and methanol barrier. The thickness of self-assembly membrane strongly affects the suppression of methanol crossover and performance improvement.

11:40am **A3-1/F8-1-12 Supercapacitance of Bamboo-Type Anodic Titania Nanotubes Array**, *Z. Endut* (rg253c@yahoo.com), *M.H. Abd Shukor*, Center of Advanced Manufacturing and Material Processing, Malaysia, *W.J. Basirun*, University of Malaya, Malaysia

Oriented titania nanotubes array can be formed by self-organizing anodization of Ti foil in organic electrolytes with fluoride ions. Bamboo-type of titania nanotubes array was introduced to investigate the effect of tube smoothness on pseudocapacitive properties. Field emission scanning electron microscopy (FE-SEM) and transmission electron microscopy (TEM) were used to characterize surface morphological and tube smoothness while cyclic voltammetry, charge-discharge testing and electrochemical impedance spectroscopy is used to investigate suitability of these nanostructures as pseudocapacitor electrodes. Bamboo-type titania nanotubes array showed higher specific surface area and high specific capacitance and energy density with excellent reversibility and long-term stability. This simple and cost saving binder free electrode is considered as a promising candidate for supercapacitor application.

CVD Coatings and Technologies

Moderator: F. Maury, CIRIMAT, France, S. Ruppi, Walter AG, Germany

8:00am B2-1-1 AlTiN-CVD coatings - a new coating family for cast iron cutting with a high productivity. *P. Immich* (*pimmich@lmt-fette.com*), *U. Kretschmann*, *U. Schunk*, *M. Rommel*, LMT Fette Werkzeugtechnik, Germany, *R. Pitonak*, *R. Weißenbacher*, Böhlerit, Austria

The ever increasing demand for higher productivity in manufacturing requires advanced hard coatings. The coatings can be tailored using PVD and CVD processes to exhibit for example higher hardness and / or enhanced oxidation resistance and good adhesion. Nowadays most PVD coatings based on the Ti-Al-N system with addition of silicon, chromium, boron or yttrium and are commercial available. The system Ti-Al-N offers a very good combination of a hardness and ductility. PVD coatings offering compared to CVD coatings compressive stresses without any post treatment and high deposition rates. But the development horizon on the PVD Ti-Al-N system is limited, because starting at around 66at% Aluminium content a phase change from the cubic to the wurzite structure can be seen.

On the other side CVD processes offering a good adhesion and are very stable process behaviour especially at the deposition of oxide coatings. Also they offering compared to the PVD processes even using the new HIPIMS process a nearly homogenous coating distribution around the cutting edge. Depending on the insert geometry a high coating thickness on the cutting face offering high wear resistance. Since the last couple of years no new hard coatings systems were investigated and developed in the CVD sector. The development focus was often - working on the stress behaviour in the coating or the coating architecture.

Today in the field of cast iron cutting PVD-TiAlSiN or even PVD-AlTiN coatings with a high hot hardness compete against well establish CVD TiN/TiCN/alpha-Al₂O₃ or kappa-Al₂O₃ coatings gaining more and more market share in the milling and also in the turning operation.

The logic development way is now the combination of the good things from both worlds: the system Ti-Al-N from PVD and the good adhesion and coating distribution from CVD.

By using a new developed the CVD process it is possible to deposit cubic AlTiN-CVD coatings even above 70% Aluminium with superior coating properties.

In this regard this coating family was analysed using common thin film techniques revealing hardness, Young's modulus and coating adhesion. This new develop coating is tested in milling experiments in cast iron comparing conventional state of the art hard-coatings. The developed coating shows a significant increase of tool life even at higher cutting speeds.

8:20am B2-1-2 C₂H₆ as precursor for low pressure chemical vapour deposition of TiCN hard coatings. *C. Czettel* (*christoph.czettel@ceratizit.com*), Ceratizit Austria GmbH, Austria, *C. Mitterer*, Montanuniversität Leoben, Austria, *M. Penoy*, *C. Michotte*, Ceratizit Luxembourg S.à.r.l., Luxembourg, *M. Kathrein*, Ceratizit Austria GmbH, Austria

Multilayered hard coatings grown by chemical vapor deposition (CVD) are used for wear protection of indexable cemented carbide inserts, applied in turning, milling, parting and grooving operations. A TiCN base layer deposited at low temperatures is a crucial feature for wear resistance and toughness of the tools. Beside the medium-temperature TiCN process using CH₃CN as carbon feed, which is commonly used for hard coatings, C₂H₆ can be applied to deposit TiCN with high carbon content at temperatures around 920 °C. In order to influence the structure and properties of this base layer, three different amounts of BCl₃ were added to the feed gas. The deposition runs were carried out using an industrial-scale low-pressure CVD system. The coatings were grown using a TiCl₄-C₂H₆-H₂-N₂-BCl₃ feed gas system with a total flux of 65.6 l/min. The deposition temperature was 920 °C, the deposition pressure 1.6×10⁴ Pa. The thickness of the coatings was measured by light optical microscopy on polished cross-sections. Phase composition and preferred orientation of crystallites were characterized by X-ray diffraction and transmission electron microscopy. Surface topography and fracture cross-sections were investigated by scanning electron microscopy. Surface roughness was measured using a confocal profilometer. Indentation hardness and indentation modulus of the coatings were determined using nanoindentation with a Berkovich indenter. The chemical composition of the different coatings was analyzed by glow discharge optical emission spectroscopy. The increasing amount of BCl₃ in

the feed gas resulted in higher boron contents of the coating, which in turn yielded higher hardness and modified microstructures. The grain size decreased with increasing boron content, while the morphology changed from equiaxed grains to a fine lamellar structure. Transmission electron microscopy analyses showed that the incorporation of boron led to a homogenous distribution of voids within the TiCN grains and to an increasing density of defects with increasing boron content. In milling and turning tests, an increased lifetime for coatings with low amounts of boron compared to the TiCN coatings without boron was obtained.

8:40am B2-1-3 The Effects of Microstructure and Thermal Stresses on the Hardness of CVD Deposited α-Al₂O₃ and TiC_xN_(1-x) Coatings. *H. Chien*, Carnegie Mellon University, US, *Z. Ban*, *P. Prichard*, *Y. Liu*, Kennametal Incorporated, US, *S. Rohrer* (*rohrer@cmu.edu*), Carnegie Mellon University, US

INVITED

The microstructures of four different CVD Deposited α-Al₂O₃ and TiC_xN_(1-x) coatings were determined by cross sectional electron backscatter diffraction mapping. The hardnesses of the layers were also measured by nanoindentation. Using the microstructural data as input, two-dimensional finite element analysis was used to calculate the residual thermal stresses in these materials. The thermal stresses and stored elastic energy in the α-Al₂O₃ layer are larger than those in the TiC_xN_(1-x) layer. Furthermore, the mean value and distribution of stored elastic energy are influenced by the texture in the alumina layer. Coatings with weaker texture have a broader distribution of thermal stresses. Coatings with alumina oriented so that the [0001] direction is parallel to the film growth direction have less stored elastic energy. This is because the thermal expansion perpendicular to [0001] is less than the thermal expansion parallel to [0001] and, therefore, the thermal expansion mismatch between the alumina coating and the substrate is minimized when grains are oriented with [0001] perpendicular to the substrate. The thermal stresses in hypothetical coatings with synthetic microstructures were also computed. These calculations tested the effects of coating thickness, channel crack spacing, composition of the TiC_xN_(1-x) layer, grain aspect ratio, and cobalt enrichment of the substrate on the thermal stresses. Based on the thermal stresses, it is concluded that the three most significant factors influencing coating hardness, ordered from most significant to least significant, are the composition of the TiC_xN_(1-x) layer, the channel crack spacing, and the cobalt enrichment of the substrate.

9:20am B2-1-5 3D EBSD analysis of CVD ceramics coatings. *M. Igarashi*, *A. Osada* (*aosada@mmc.co.jp*), Mitsubishi Materials Corporation, Japan, *C. Schuh*, Massachusetts Institute of Technology, US

Al₂O₃ and TiCN coatings have been widely used in cutting tools. TiCN has high hardness. Al₂O₃ maintains high hardness and excellent oxidation resistance under such a severe cutting condition. Moreover, it is well known that the orientations of these coatings effect their performance. For instance, specific oriented Al₂O₃ represents higher performance than the other orientations. These coatings are deformed during cutting, and wear out at last. Therefore it is necessary to investigate the deformation mechanism of such ceramics coatings.

In this study, (422) and (220) oriented TiCN coatings and (006) oriented Al₂O₃ coatings with low and high CSL boundaries are prepared. These samples are indented with Micro Vickers . Deformed areas are observed in 3 dimension s with FIB and EBSD system. The effects of orientations and grain boundaries on deformation are discussed in details.

9:40am B2-1-6 TiSiN and TiSiCN hard coatings by CVD. *I. Endler* (*Ingolf.Endler@ikts.fraunhofer.de*), *M. Höhn*, *J. Schmidt*, *S. Scholz*, *M. Herrmann*, Fraunhofer IKTS, Germany, *M. Knaut*, TU Dresden, Germany

TiN and TiC_xN_y are commercial CVD coatings widely used for cutting tool applications. A promising route for improving hardness and oxidation resistance is the addition of silicon. Thermal CVD method was employed using gas mixtures containing TiCl₄ and the silicon chlorides SiCl₄ or Si₂Cl₆. This work is focussed on the investigation of structure, composition and properties of the TiSiN and TiSiCN coatings deposited on hardmetal inserts.

TiSiN layers with a nanocomposite structure were obtained with SiCl₄ as well as Si₂Cl₆ in a temperature range between 800°C and 900°C. In both cases ammonia was used as nitrogen precursor. The crystalline phases TiN, and at 900°C Ti₅Si₃ as well, were analysed by XRD. From the TEM investigation of a layer deposited at 850°C it is evident that the nanocrystalline TiN is embedded in an amorphous phase. The amorphous phase is silicon nitride. The hardness correlates well with the silicon content and the grain size. A maximum hardness about 37 GPa was observed at a silicon content between 6 and 8 at.% if SiCl₄ was applied as silicon precursor. In this silicon concentration range a TiN grain size of 14.5 nm was determined. If Si₂Cl₆ was used the hardness maximum of 38 GPa was already achieved at a lower silicon content of 3.5 at.%. The corresponding TiN grain size is 16.4 nm. The investigation of the oxidation behavior

showed an increase of the oxidation resistance with the silicon content. In the case of layers with silicon contents between 5 and 8 at.% an oxidation resistance up to 700°C was observed. At this temperature a weak TiO₂ formation occurred at the surface.

Furthermore TiSiCN coatings were deposited using the same titanium and silicon precursors. The ratios of the silicon precursors to TiCl₄ were varied. Hardness values up to 40 GPa were measured for optimum ratios. The structure was analysed by SEM, XRD and XPS.

The examination of the adherence of TiSiN and TiSiCN layers showed that a diffusion barrier is necessary for suppressing the cobalt diffusion from cemented carbide substrate into the layers. If interlayers of TiN or TiCN were applied critical loads of 80 N for TiSiN and 50 N for TiSiCN layers were obtained from scratch test measurements.

10:00am **B2-1-7 High temperature chemical vapor deposition of highly crystallized and textured silicon on metals for solar conversion.** *O. Gourmala, R. Benaboud, G. Chichignoud, E. Blanquet, C. Jimenez, B. Doisneau, K. Zaidat, M. Pons (michel.pons@simap.grenoble-inp.fr), Grenoble INP, France*

Highly crystallized silicon layers were grown on metal sheets at high temperature (950°C) by thermal CVD from silane. An intermediate buffer layer (TiN layer) was mandatory to prevent interdiffusion and silicide formation but also to compensate lattice parameters and thermal expansion coefficients mismatches between metal and silicon and ideally transfer some crystalline properties (grain size, texture) from the substrate to the silicon layer. After a thermodynamic study, intermediate titanium nitride diffusion barrier was selected and processed by CVD. Special attention is given to the substrate surface preparation for texture transfer. The structure and the interfaces stabilities of these silicon/nitride/metal stacks were studied by FEED and TEM, X-ray diffraction, Raman and energy dispersive X-ray spectroscopy.

By both optimizing substrate preparation and silicon processing conditions, this multilayered structure could be able to provide an efficient and reliable converter, comparable with classical crystalline silicon wafers in terms of solar conversion yield, while overcoming their majors drawbacks: due to ingot sawing and squaring as well as wafer slicing.

10:20am **B2-1-8 In-line Deposition of Silicon-based Films by Hot-Wire Chemical vapor Deposition.** *L. Schäfer (lothar.schaefer@ist.fraunhofer.de), T. Harig, M. Höfer, A. Laukart, Fraunhofer IST, Germany, D. Berchert, Keipert-Colberg, Fraunhofer ISE, Germany, J. Trube, Leybold Optics GmbH, Germany*

Silicon-based films such as hydrogenated amorphous (a-Si:H), and nanocrystalline silicon (μc-Si:H), and hydrogenated amorphous silicon nitride (a-SiN_x:H) were deposited by hot-wire gas phase activation (HW-CVD). To evaluate the opportunities of the HW-CVD technology for thin film deposition in solar industry an in-line hot-wire CVD system was used to deposit a-Si:H films for passivation of crystalline solar cells as well as for the fabrication of thin film silicon solar cells. The HW-CVD system consists of seven vacuum chambers including three hot-wire systems with maximum deposition areas of 500 mm by 600 mm for each hot-wire activation source. The deposition processes were investigated by applying design of experiment methods to identify the effects and interactions of the process parameters on the deposition characteristics and film properties. The process parameters investigated were silane flow, pressure, substrate temperature, film thickness, as well as temperature, diameter and number of wires, respectively. Growth rates up to 2.5 nm/s were achieved for a-Si:H films. Intrinsic a-Si:H films for passivation of different crystalline solar cell types yielded carrier lifetimes of more than 1.000 μs for film thickness values below 20 nm. Films with thickness values of about 350 nm show microstructure factors of less than 0.1 measured by FTIR and photosensitivity ratios of up to 10⁶. For n-doped a-Si:H films prepared with PH₃ as dopant gas specific electrical resistances are in the range of 10² Ohm x cm. P-doped a-Si:H films prepared with B₂H₆ as dopant gas show electrical resistances of about 10⁵ Ohm x cm. The results of these investigations are not only aiming at the passivation of crystalline solar cells but also at the application of hot-wire CVD processes for the fabrication of heterojunction solar cells as well as thin film silicon solar cells.

10:40am **B2-1-9 Oxidation Resistance of Graphene Coated Metal Films: A Protective Coating.** *PramodaKumar. Nayak, Chan-Jung. Hsu, National Cheng Kung University, Taiwan, S.C. Wang, Southern Taiwan University, Taiwan, JamesC. Sung, KINIK Company, Taiwan, Jow-Lay. Huang (jlh888@mail.ncku.edu.tw), National Cheng Kung University, Taiwan*

The requirement of protective coating to prevent refined metals from reactive environments is very important in industrial as well as in academic applications. Most of the conventional methods used for this purpose introduce several negative effects including increased thickness and changes

in the optical, electrical and thermal properties of the metal. In this paper, we demonstrate the coating of graphene films using methane as carbon source by chemical vapor deposition to protect the surface of Ni substrates from air oxidation. In particular, graphene prevents the formation of oxide on the metal surface and protect it from reactive environment. Two methods are adopted to induce oxidation on the graphene coated Ni surface: i.e. by heating the specimen in air for several hours and then, by immersing into a solution of 31% hydrogen peroxide (H₂O₂). The specimens have been characterized by X-ray diffraction, Optical micrograph, Raman spectroscopy, X-ray photoelectron spectroscopy, and the results indicate that oxidation resistance of graphene coated Ni films is only effective up to a maximum temperature of 500° C in air. It is also observed that graphene provides effective resistance against H₂O₂. The results have been compared with that of graphene coated Cu films in literature. The detailed analysis of graphene as oxidation resistance against air and H₂O₂ has been presented.

11:00am **B2-1-10 Highly chemically reactive AP-CVD coatings: Influence of the deposition parameters and application for thermally reversible interfacial bonding.** *M. Moreno-Couranjou (moreno@lippmann.lu), A. Manakhov, N.D. Boscher, Centre de Recherche Public - Gabriel Lippmann, Luxembourg, J.J. Pireaux, University of Namur (FUNDP), Belgium, A. Choquet, Centre de Recherche Public - Gabriel Lippmann, Luxembourg*

In this work, we present the plasma copolymerization of Maleic Anhydride (MA) and Vinyltrimethoxysilane (VTMOS) performed in an Atmospheric Pressure-Dielectric Barrier Discharge process for the formation of highly reactive anhydride functionalized coatings.

In the first part of the presentation, we will show how the tuning of the electrical parameter led to coatings with different combination of anhydride/carboxylic group surface density, morphology and deposition rate. For that goal, the power (P) delivered by the source was varied from 50 to 150W. Moreover, the discharge electrical mode was operating in a continuous wave or a pulsed wave with a pulse ON-time (t_{on}) fixed at 10ms and a pulse OFF-time (t_{off}) ranging from 10 to 60ms. The different coating chemistries have been studied by XPS for the estimation of the anhydride/carboxylic surface density and by ATR FT-IR to investigate the conservation or the destruction of the cyclic anhydride group related to the incorporation of the MA monomer in the coatings. The average power (P_{av}), defined as P_{av}=P.[t_{on}/(t_{on}+t_{off})], appeared as a key parameter to control the anhydride surface functionalization within a range of 2 to 13 at.%, independently of the coatings morphology or deposition rate.

In the second part, we will present how the coatings reactivity has been exploited for the elaboration of a thermally reversible interfacial bonding property based on a Diels-Alder reaction. For that, MA-VTMOS deposits have been performed on a rigid polished aluminium and on a kapton foil and subsequently, treated through a chemical gas phase reaction for the grafting of the required diene and dienophile groups. The complete chemical path reaction will be exposed with some adhesion results dealing with the Diels-Alder and the retro-Diels-Alder reactions.

11:20am **B2-1-11 Optical properties of the ZnO thin films grown on glass substrates using catalytically generated high-energy H₂O.** *E. Nagatomi, S. Satomoto, M. Tahara, T. Kato, K. Yasui (kyasui@vos.nagaokaut.ac.jp), Nagaoka University of Technology, Japan*

Zinc oxide (ZnO) is useful for many applications such as transparent conductive films in solar cells and flat panel displays, optoelectronic devices operating at short wavelengths. Despite the advantages of MOCVD for industrial applications, ZnO film growth by conventional MOCVD consumes a lot of electric power to react the source gases and raise the substrate temperature. To overcome this, a more efficient means of reacting oxygen and metalorganic source gases is needed. In addition to the low reaction efficiency, conventional CVD methods yield low-quality ZnO films, due to incomplete reaction of metalorganic source gases with oxygen source gases in the gas phase. If thermally excited water is used to hydrolyze the metalorganic source gases, however, reactive ZnO precursors are produced in the gas phase, allowing growth of ZnO films under energy-saving conditions.

In this study, we present a ZnO film growth on glass substrates aiming at the application for transparent conductive thin films, using the reaction between dimethylzinc (DMZn) and high-energy H₂O produced by a Pt-catalyzed H₂-O₂ reaction. CVD apparatus is comprised of a catalytic cell with a fine nozzle, gas lines for H₂, O₂ and DMZn supplies, and a substrate holder. H₂ and O₂ gases were admitted into a catalyst cell containing a Pt-dispersed ZrO₂ catalyst, whose temperature increased rapidly to over 1300 K due to the exothermic reaction of H₂ and O₂ on the catalyst. The resulting high-energy H₂O molecules were ejected from the fine nozzle into the reaction zone and allowed to collide with DMZn ejected from another fine nozzle. ZnO films were grown on glass substrates at 573-873K and the film properties were evaluated.

X-ray diffraction patterns of the ZnO films grown at 673-873K exhibited intense (0002) peak at $2\theta=34.42-34.47^\circ$, which means that small tensile stress exists in the ZnO/glass films grown in our method. Average transmittance in the wavelength between 500 nm and 2000 nm was higher than 85%.

In the photoluminescence (PL) spectra measurement at room temperature, band edge emission of ZnO films appeared at 3.27-3.30eV. The PL spectra at 17.8K showed the strongest emission peaks at 3.357-3.360eV, which are attributed to the neutral-bound excitons D^0_{X} . The FWHM value of the strongest peak of the film grown at 673K was as low as 6.34 meV, which is smaller than that previously reported for ZnO (10meV) obtained by MOCVD grown on sapphire substrates (using $\text{Zn}(\text{C}_2\text{H}_5)_2$ and N_2O as source gases).

11:40am **B2-1-12 Efficiency of indium oxide with doped tin by thermal evaporation and their optoelectronic properties**, *K.Y. Pan*, National Tsing Hua University, Taiwan, *L.D. Lin*, Chinese Culture University, Taiwan, *L.W. Chang*, *H.C. Shih* (*hcsih@mx.nthu.edu.tw*), National Tsing Hua University, Taiwan

Three nano-architectures of indium oxide (In_2O_3) have been successfully synthesized by thermal evaporation, which include nanorods, nanotowers, and tin-doped indium oxide (ITO) nanorods. Judging from the images of transmission electron microscope (TEM) analysis and the x-ray diffraction (XRD) analysis, the slight doping of tin did not affect and change the growth direction and in-situ micro-structure of nano indium oxide. The qualitative analysis of ITO nanorods were analyzed by energy dispersive spectrometer (EDS) and x-ray photoelectron spectroscopy (XPS), which confirmed that slight tin were totally doped into nanorods of indium oxide via thermal evaporation. The optoelectronic properties of In_2O_3 and ITO nanorods were tested by cathodoluminescence (CL) analysis. There are blue shifts in the CL spectrums, which also means tin was definitely added in In_2O_3 nanorods. The results of I-V curve show that the resistance of nanorods, nanotowers and ITO are 1.32 k Ω , 0.65 k Ω and 0.063 k Ω . According to this result, doping slight tin is a good approach to enhance the conductivity of In_2O_3 nanorods.

Hard Coatings and Vapor Deposition Technology Room: Royal Palm 1-3 - Session B6-1

Coating Design and Architectures

Moderator: C. Mitterer, Montanuniversität Leoben, Austria, M. Stüber, Karlsruhe Institute of Technology, Germany

8:00am **B6-1-1 Combinatorial Development of Transition Metal Nitride Thin Films for Wear Protection**, *R. Cremer* (*cremer@kcs-europe.de*), KCS Europe GmbH, Germany **INVITED**

The ever increasing complexity of modern coatings triggers the need of sophisticated technologies for rapid and commercially advantageous development methods. One possibility to significantly increase the speed of materials development is the use of combinatorial approaches.

In this paper, the applicability of such combinatorial methods in developing advanced materials is illustrated presenting various examples for the deposition and characterization of one- and two-dimensionally laterally graded coatings, which were deposited by means of magnetron sputtering, arc ion plating and plasma-enhanced chemical vapor deposition.

To illustrate the advantages of this approach for the development of advanced materials, the multi-component metastable hard coatings (Ti,Al)N, (Ti,Al,Hf)N, (Ti,Al,Cr)N and (Ti,Al,Si)N were investigated with respect to the relations between structure and composition on one hand and physical properties like hardness, erosion resistance, cutting performance and oxidation behavior of these coatings on the other.

8:40am **B6-1-3 Compositional and Structural Evolution of Sputtered Ti-Al-N Thin Films as a Function of the used Target**, *P.H. Mayrhofer* (*paul.mayrhofer@unileoben.ac.at*), *B. Grossmann*, Montanuniversität Leoben, Austria, *R. Rachbauer*, OC Oerlikon Balzers AG, Liechtenstein, *P. Polcik*, PLANSEE Composite Materials GmbH, Germany

The compositional and structural evolution of $\text{Ti}_{1-x}\text{Al}_x\text{N}$ thin films has been studied as a function of the total working gas pressure (p_T), the N_2 -to-total pressure ratio (p_{N_2}/p_T), the substrate position, as well as the energy and ion-to-metal flux ratio of the ion bombardment during reactive sputtering of powder-metallurgically prepared $\text{Ti}_{0.5}\text{Al}_{0.5}$ targets of varying grain size (50, 100, 150, and 200 μm). Based on this variation we propose that the different poisoning state of the Ti and Al particles of the $\text{Ti}_{0.5}\text{Al}_{0.5}$ targets in addition to scattering and angular losses of the sputter flux cause a significant modification in the Al/(Ti+Al) ratio, x , of the synthesized $\text{Ti}_{1-x}\text{Al}_x\text{N}$ thin

films with $0.5 < x < 0.67$. The dependence of the chemical composition on the N_2 -partial pressure shows a strong correlation with the grain size of the powder-metallurgically prepared $\text{Ti}_{0.5}\text{Al}_{0.5}$ target.

Additionally, the compositional variation induces a corresponding structural modification between single-phase cubic, mixed cubic-hexagonal and single-phase hexagonal. Our results show, that in particular, the N_2 -to-total pressure ratio in combination with the sputtering power density of the $\text{Ti}_{0.5}\text{Al}_{0.5}$ compound targets has a pronounced effect on the Al/Ti ratio and the structure development of the coatings prepared. The maximum Al content for single-phase cubic $\text{Ti}_{1-x}\text{Al}_x\text{N}$ strongly depends on the deposition conditions and was obtained with $x = 0.66$ when applying a deposition temperature of 500 $^\circ\text{C}$, $p_T = 0.4$ Pa, and $p_{\text{N}_2}/p_T = 17\%$. Furthermore we show that also the grain size of the Ti-Al targets has a specific influence, especially on the chemical composition (and local element distribution) of the films prepared, but also on the obtained morphology and evolving nanostructure. By modifying the target grain size, while keeping all other deposition conditions unchanged, $\text{Ti}_{1-x}\text{Al}_x\text{N}$ thin films can be developed which already show a pronounced formation of Al-rich and Ti-rich cubic domains in the as-deposited.

The results obtained highlight the need for optimized target materials in order to design specific application tailored thin film structures and architectures.

9:00am **B6-1-4 Deposition of TiAlN based coatings combined with subsequent electron beam surface treatment**, *K. Weigel*, *M. Keunecke*, *K. Bewilogua* (*klaus.bewilogua@ist.fraunhofer.de*), Fraunhofer IST, Germany, *R. Zenker*, TU Bergakademie Freiberg; Zenker Consult, Germany, *S. Schmied*, TU Bergakademie Freiberg, Germany

Hard coatings cannot exploit the full range of their excellent properties (high hardness, good wear resistance) if the used substrate materials, e.g. steels, are too soft. Therefore it can be beneficial to carry out an additional heat treatment before or after the coating process. Especially if the coating deposition requires higher temperatures a case hardening after coating deposition is an effective approach. The investigations presented here were focused on a combination of the deposition of TiAlN coatings and a subsequent electron beam surface hardening. The TiAlN coatings with variable compositions and mechanical properties were deposited by reactive magnetron sputter deposition onto two different steel substrate materials (AISI D2 cold working steel and AISI 6150 tempering steel). The TiAl targets and the substrate were excited both by DC and pulsed DC voltage. The atomic ratio Ti/Al of the coatings varied in the range between 0.57 and 1.90, the hardness values ranged from 1100 to 2900 HV. For electron beam hardening (EBH) a rectangular energy transfer field was used. The energy distribution within the field caused a nearly constant hardening temperature on the material surface during the whole hardening process. Besides composition and structure of the coatings before and after electron beam treatment their hardness and adhesion were studied. Depending on the coating's composition and thickness morphological changes of the coatings could be observed. Coatings of 1 μm thickness showed severe cracks while these were not observed on coatings of 3 μm thickness and more. Especially for coatings with insufficient adhesion on untreated steel the electron beam hardening caused a significant improvement. This could be caused by diffusion processes in the coating-substrate-interface region. The considered combination of coating deposition and subsequent EBH seems to have a high potential for locally highly loaded tools or components.

9:20am **B6-1-5 Influence of the plasma characteristic on the structure, properties and cutting performance of the (Ti,Al)N coatings deposited by cathodic arc evaporation**, *D. Kurapov* (*denis.kurapov@oerlikon.com*), *S. Krassnitzer*, *J. Bachmann*, *J. Hagmann*, *M. Arndt*, *W. Kalss*, *H. Rudigier*, OC Oerlikon Balzers AG, Liechtenstein

In this work the (Ti,Al)N coatings were produced by cathodic arc evaporation using powder metallurgical targets. The magnetic field configuration on the targets surface was varied in order to influence the electron trajectory to the anode surface. The plasma characteristic was studied by optical emission spectroscopy (OES) as well as by Langmuir probe. The chemical composition of the coatings was investigated by means of energy dispersive X-ray spectroscopy (EDX). The evolution of the growth morphology and crystallographic structure as a function of plasma characteristic was studied by scanning electron microscopy (SEM) and X-ray diffraction (XRD), respectively. The elastic modulus of the coatings was measured by nanoindentation method.

The variation of the magnetic field configuration on the cathode surface was found to be crucial for the plasma conditions near the substrate. The coating analysis shows strong dependence of the coating structure and properties on the plasma characteristic. The correlation between coating growth conditions and the cutting performance of the coatings is discussed.

9:40am **B6-1-6 Effect of the interlayer coating architecture on the optimization of diamond deposition.** *A. Poulon-Quintin (a.poulon@icmcb-bordeaux.cnrs.fr), A. Hodroj, C. Faure, L. Teule-Gay, J.-P. Manaud, ICMCB-CNRS, France*

Diamond films grown by Chemical Vapor Deposition (CVD) are widely used as surface overlay coating onto WC-Co cutting tools to improve their tooling performances. However, due to the diffusion of cobalt towards the substrate surface, the adhesion of diamond coatings on WC-Co substrates is insufficient. The Co binder catalytic properties can suppress sp^3 diamond growth because the formation of sp^2 graphitic species is favored. To prevent cobalt diffusion and to enhance the adhesion of diamond, suitable diffusion barrier interlayers have been synthesised onto WC-Co substrates (10wt%Co).

The present work aims to study the effect of the architecture of zirconium nitride and/or tantalum nitride diffusion barrier interlayers as well as their microstructure, on the quality of the interface with the diamond top layer in terms of presence or not of graphite. To improve the nuclei density of diamond during CVD processing, a thin Mo extra layer has been added (<500 nm) whatever the diffusion barrier used.

Bilayer (Ta/N/Mo) and multilayer systems composed of TaN and ZrN thin film (resp. 50 and 30nm) sequences, have been tested to optimize nano crystalline diamond (NCD) deposition grown under negative biased substrates. For all systems, after diamond deposition, XRD analyses show a massive carburization of molybdenum and tantalum nitride whereas zirconium nitride is not modified. TEM cross-section observations are carried out for better understanding of the diffusion phenomena occurring at the interfaces during the diamond deposition.

Architecture of the diffusion layer is an available solution to significantly reduce the diffusion of cobalt at the interface with diamond and as a consequence, reduce the presence of graphite so increase the adhesion on substrate.

10:00am **B6-1-7 Application Oriented Design of PVD-Coatings for Tools and Components.** *K. Bobzin (info@iot.rwth-aachen.de), Surface Engineering Institute - RWTH Aachen University, Germany, N. Bagcivan, RWTH Aachen University, Germany, M. Ewering, Surface Engineering Institute - RWTH Aachen University, Germany* **INVITED**

For the synthesis of new coatings different coating architectures depending on the type of application are considered. This includes the development of nanocomposites, multi- or nanolayers as well as graded coatings. In the present work different types of coating architectures as well materials are presented. In this regard the production process and application of gear components serves as an example.

Gear components like gear shafts can be produced by cold forging. PM (powder-metallurgical) high speed steels are increasingly employed as tool materials for this applications due to their high abrasion resistance and toughness. Nevertheless, the machining of these materials is very challenging due to vanadium and iron carbides which lead to high abrasive wear on the cutting edges as well as the high toughness of these materials which leads to adhesive wear. To meet these challenges nitride nanocomposite coatings seem to be promising. In the present work the development of a (Ti,Cr,Al,Si)N coating is presented. The developed coating was tested in milling of S790PM, 62HRC (1.3345, M3 class 2) in comparison to two different commercial coatings: (Ti,Al)N deposited via MSIP and (Ti,Cr,Al,Si)N deposited via Arc Ion Plating. It was shown that, depending on the cutting parameters, the tool life is increased by 20 - 30% by the new developed coating.

After production of the mould the forging process is examined in a second step. Cold forging of steel leads to high forming loads and high adhesive and abrasive wear caused by friction between tool and workpiece material. To reduce friction the workpiece material is bonderized by a zinc phosphate conversion coating before forming operation. This coating step is very time-consuming, expensive and environmentally harmful. In this regard replacing the tribological function of bonder coating by PVD-coated tools and lubricants is interesting. The development of a (Ti,Zr)N/CrN nanolayer with a friction reducing CrN top layer is presented. In first application tests the production of 500 parts without zinc phosphate conversion coating was possible.

In a third step the application of the produced gear components is considered. Gear components in tribological contact are subjected to high mechanical loads. At the Surface Engineering Institute low-temperature component coatings like the carbon based graded Me-DLC (metal containing diamond like carbon) coating zirconium carbide (ZrC_x) and the hard coating chromium aluminum nitride ((Cr,Al)N) were developed. The coatings exhibit hardness values up to 21 GPa and excellent friction behaviour as proven by tribological tests.

10:40am **B6-1-9 Structural model for the spinodal decomposition of Nb-Si-N nanocomposites based on ellipsometric results.** *G. Ramírez (enggiova@hotmail.com), S.E. Rodil, S. Muhl, Universidad Nacional Autónoma de México - Instituto de Investigaciones en Materiales, Mexico, M. Rivera, Instituto de Física - Universidad Nacional Autónoma de México, México*

In this work, we prepared thin films of Nb-Si-N using two separate magnetrons, where one target was Si and the other Nb. The atmosphere was a variable mixture of argon and nitrogen. The film composition and structure was modified by varying the power of the two magnetrons independently. For the Si target, the rf source was varied between 20-300 W and for the Nb target, the power was fixed at 300 W.

Ellipsometric spectroscopy was used to obtain the optical resistivity of the films as the silicon content was increased. The pseudo-dielectric function changed from metallic-like to semiconductor-like character at certain silicon content. The ellipsometric spectra were modeled using a Drude-Lorentz dispersion function for the film and including a small roughness layer, Bruggeman effective medium approximation (50% voids and 50% film) From the Drude terms it was possible to estimate the optical resistivity, which showed three different regimes as the Si at% increased. The first regime, at very low Si contents (> 5 at%), corresponds mainly to NbN containing silicon within the crystalline structure, either as a substitution or interstitial atomic defect. The second regime corresponds to Silicon contents where the solubility limit has been reached and the silicon is largely segregated into the grain boundaries forming a layer of amorphous silicon nitride which covers the NbN crystal. Finally, at the largest Si content (13 at%), there is a large distortion of the NbN crystalline structure, leading to a quasicrystalline Nb-N-Si phase.

These results were confirmed by scanning tunneling microscopy images and X-ray diffraction that showed a decrement in the NbN grain size as a function of the Si content and variations in the film strain. Moreover, by analyzing the X-ray photoelectron signals from the Si, Nb and N atoms and the ellipsometric results, we proposed a model to determine the silicon nitride coverage of the NbN crystal, obtaining as results that the maximum hardness of the films was obtained when the coverage is about 1 monoatomic layer. The geometric model proposed is a combination between the model of Sandu et al. [1] for Nb-Si-N and Veprék et al. [2] for Ti-Si-N.

[1] C.S. Sandu et al. Surface and Coatings Technology 201 (2006) 2897–2903

[2] S. Veprék et al. Surface and Coatings Technology 133-134(2000)152-159

11:00am **B6-1-10 Characterization of the tribological and abrasive wear behaviour of carbon fibre reinforced epoxy composites in contact with a diamond-like carbon layer.** *H.-J. Scheibe (hans-joachim.scheibe@iws.fraunhofer.de), Fraunhofer IWS, Germany, M. Andrich, W. Hufenbach, K. Kunze, Technische Universität Dresden, Germany, J. Bijwe, Indian Institute of Technology, India, A. Leson, M. Leonhardt, Fraunhofer IWS, Germany*

The design process for components made of carbon fibre reinforced composites (FRP) demands an increased level of interest for tribological questions, especially concerning load application zones. The tribological behaviour of FRP, particularly in contact with steel, is to be estimated as relatively weak. As a promising improvement the application of modern coatings is considered.

In this context the results of frictional and wear investigations of unidirectional carbon fibre reinforced epoxy composites (CF-EP) in contact with a coated and uncoated steel material are introduced. The used coating is based on a graduated build-up and extremely hard Diamor® layer consisting of amorphous, diamond-like carbon which was applied on the steel surface by means of a commercial Laser-Arco® process. It has been proven that this coating is extremely abrasion-resistant. Furthermore, the frictional coefficient of the material combination CF-EP/ coated steel is significantly lower in comparison with the combination CF-EP/ hardened and polished steel without coating. Also a remarkable outcome is the decrease of the specific wear rate over more than two magnitudes for the basic material (CF-EP). Based on these results the opening up of the material combination CF-EP/ coated steel to sliding application fields, so far reserved to specially developed maintenance-free slide bearings or slideways, can be attained. Therefore the achieved results are of great interest to applications with tribologically stressed contact zones between FRP components and metal structures.

11:20am **B6-1-11 Direct current magnetron sputtering of ZrB₂ from a compound target**, **H. Högborg** (hans.hogberg@liu.se), Linköping University, Sweden **INVITED**

Transition metal diborides MeB₂ are ceramics with high hardness, high melting points, and high temperature stability. These characteristics originate from their hexagonal and layered crystal structure, space group 191, where the transition metal atoms constitute the A layers (0,0,0) and the boron atoms occupy the trigonal prism interstitials ($\frac{1}{3}$, $\frac{2}{3}$, $\frac{1}{2}$) and ($\frac{2}{3}$, $\frac{1}{3}$, $\frac{1}{2}$) present in the structure. This arrangement enables both strong Me-B bonds given the electron transfer from the metal atom to the boron atoms and Me-Me overlap to yield metal-like properties as exemplified by a good electrical conductivity seen for the transition metal diborides. Furthermore, the boron atoms will form a covalently bonded honeycombed structured sheet, in which the electron injection from the metal results in graphite-like properties; the sheet sometimes being referred to as "borophene". The above described property envelope suggests many potential applications for transition metal diborides as thin films ranging from hard protective coatings to high temperature resistant conductive layers.

For the transition metal diboride ZrB₂, we have studied growth at different conditions of target effect, substrate temperature, substrate bias, base pressure etc., using sputtering from a compound target in an industrial scale high vacuum system, CemeCon, CC 800[®]/9 ML as well as growth in a laboratory scale ultra high vacuum system.

Our results from x-ray diffraction recorded from films deposited on Si(100) substrates show that 0001 oriented films can be deposited in both type of systems without external heating of the substrate and at growth rates of ~3nm per second. Such films are close to stoichiometric, B to Zr ratio of 2 to 2.1, and total level of contaminants less than 2%. Transmission electron microscopy and scanning electron microscopy images display a columnar growth mode. Nanoindentation performed on the films show that they are hard ~20-25GPa and with an elastic recovery of 96%. Four point probe measurements on films deposited on 1000 Å SiO₂/ Si(100) substrates yield resistivity values in the region of 150 to 180μΩ cm

Increased substrate temperatures affects the preferred 0001 oriented growth mode by allowing the nucleation of grains with other orientations as 10 $\bar{1}$ 1 and 10 $\bar{1}$ 0, and at temperatures above ~500 °C the deposited films are 10 $\bar{1}$ oriented.

Tribology & Mechanical Behavior of Coatings and Engineered Surfaces

Room: Tiki Pavilion - Session E2-1

Mechanical Properties and Adhesion

Moderator: M.T. Lin, National Chung Hsing University, Taiwan, D. Bahr, Washington State University, US, R. Chromik, McGill University, Canada, W. Clegg, University of Cambridge, UK

8:00am **E2-1-1 Strain hardening behavior in multilayer thin films**, **D. Bahr** (dbahr@wsu.edu), **RL. Schoeppner**, **S. Lawrence**, **I. Mastorakos**, **H. Zbib**, Washington State University, US

Thin film multilayers, where the layer thickness is between 5 and 25 nm, have been shown to exhibit significant strength enhancements over the constituent components, appealing for wear resistant coatings. The vast majority of research in this area has been focused on bi-layer systems (e.g. Cu-Ni, Cu-Nb). The particular strengthening mechanisms depend on the interface structure; FCC-FCC interfaces tend to strengthen due to elastic modulus mismatch while FCC-BCC interfaces do not transmit dislocations and additionally can provide the ability to shear to accommodate the presence of dislocations. Additionally, the ability to have locally disordered interfaces provides a sink for defects due to radiation damage. However, these high strength materials often do not have substantial ability to sustain high strains, and their ductility decreases with decreasing layer thickness. Recently we have demonstrated that tri-layer films, Cu-Ni-Nb, exhibit additional strain hardening due to the ability to have dislocations in the FCC layers cross slip because of the presence of the FCC-BCC interface adding strength to the system. This presentation will demonstrate the use of nanoindentation techniques to extract strain hardening behavior from thin films, and compare the results from microtensile behavior of free standing films with those of the films on oxidized silicon substrates. The hardness behavior is tracked as a function of included angle of the indenter to generated different effective strains. The pile up around the indentation is also tracked to correlate to the strain hardening coefficient. These complementary techniques are then compared to tensile testing of free standing, sub-micron thick films using digital image correlation for strain

measurements. A combination of molecular dynamics and dislocation dynamics is used to demonstrate the likely mechanism which causes this additional strain hardening behavior.

8:20am **E2-1-2 Adhesion of tetrahedral amorphous carbon (ta-C) coatings deposited on different substrates: Simulations and experimental verification**, **N. Bierwisch**, Saxonian Institute of Surface Mechanics, Germany, **G. Favaro**, CSM Instruments SA, Switzerland, **J. Ramm**, OC Oerlikon Balzers AG, Liechtenstein, **N. Schwarzer**, Saxonian Institute of Surface Mechanics, Germany, **M. Sobiech** (matthias.sobiech@oerlikon.com), **B. Widrig**, OC Oerlikon Balzers AG, Liechtenstein

The performance of cutting and forming tools can be significantly improved by ta-C coatings. Different applications of such tools implicate coating deposition on different materials. Moreover, the pre-treatment of the tools to be coated becomes complicated due to the necessity to perform the deposition at low temperature. Therefore it follows that a procedure to predict coating adhesion on different substrate materials would be of great benefit in order to design straightforwardly the coating-substrate system.

In this work, the mechanical properties of ta-C coatings deposited on 1.2842 (90MnCrV8) steel and tungsten carbide (6wt.% Co) have been investigated. The specific Young's moduli and yield strengths were derived from nano-indentation measurements, and multi-axial load stress profiles were simulated accordingly to Ref. [1]. The von Mises and normal stress profiles obtained from simulations are utilized to predict the locations within the coating-substrate systems where either the yield strengths or the critical tensile stresses are exceeded. This prediction is confirmed by scratch tests for which the load range and indenter geometry is optimized for the depth of interest by simulation (test dimensioning as elaborated in [1]). On the basis of these results, it was assumed that stress relaxation could be significantly dependent of the substrate material (i.e. steel or tungsten carbide). Therefore, non-destructive X-ray diffraction stress-depth profiling [2] was used to investigate the near-surface regions of both substrate materials. Thus, on this basis a straightforward interface design suitable for particular applications becomes possible.

[1] N. Schwarzer, Q.-H. Duong, N. Bierwisch, G. Favaro, M. Fuchs, P. Kempe, B. Widrig & J. Ramm: *Optimization of the Scratch Test for Specific Coating Designs*, submitted to SCT, accepted August 2011

[2] A. Kumar, U. Welzel & E.J. Mittemeijer: *A method for the non-destructive analysis of gradients of mechanical stresses by X-ray diffraction measurements at fixed penetration/information depths*, J. Appl. Crystal. **39**, 633, 2006

8:40am **E2-1-3 Analysis on the stress transfer and the interfacial strength of carbon coatings on metallic substrate using in-situ tensile and nanobending experiments in SEM and Raman spectroscopy**, **K. Durst** (Karsten.Durst@ww.uni-erlangen.de), University Erlangen-Nuernberg, Germany **INVITED**

The interface between a coating and a substrate is often crucial for the performance of coating systems. During deformation of the substrate, shear stresses are transferred at the interface into the coating, leading there eventually to cracking and delamination. In this work, the properties of carbon coatings on ductile metallic substrates (diamond on Ti and a-C:H on steel) are studied, using new in-situ methods for analyzing the stress transfer as well as the interfacial strength of the coating in dependency of the microstructure and the local chemical composition.

The first part of the talk is concerned with the analysis of the stress transfer from a ductile Ti-substrate to a brittle diamond coating under tensile straining using micro-Raman spectroscopy and analytical modeling. The coating contains initially compressive residual stresses of ~5.4 GPa, which turn into the tensile regime during plastic straining of the substrate. Once the fracture strength of the coating of ~1.5 GPa is reached, normal cracks appear in the coating followed by a reduction in crack spacing and finally delamination. The stress measurements across different cracked coating segments using Raman spectroscopy, indicated tensile stresses at the middle and compression near the edges of the segment under tensile load. Coating fragmentation leads to a relaxation of the stress within the cracked coating segment. Further cracking of the smaller segments requires larger strains. The classical shear lag model is extended to derive the stress distribution in the coating bonded to the substrate, considering both residual stress and cracking using a fracture criterion. The model captures nicely the failure behavior of the coating as well as the stress profiles in cracked coating segments.

In the second part of the talk two a-C:H-coating systems on steel with the same microstructure, but different adhesion layers and qualitative different adhesion behaviour were investigated. The coatings were characterized in terms of their mechanical properties, microstructure and the chemical composition using nanoindentation tests and Auger electron spectroscopy on small angle cross sections of the a-C:H-coatings. There strong gradients

in the mechanical properties indicate bad adhesive properties for one coating. For quantitative measurement of the interfacial fracture strength and fracture toughness, micro-cantilevers with a length of about 1.5 μm and a thickness of about 0.5 μm were prepared by focused ion beam so that the highest bending stress or stress intensity occurs right at the interface. Using a force measurement systems, the micro-cantilevers were loaded inside the SEM and the fracture properties were evaluated. The interfacial fracture strength of the different interfaces is discussed in terms of the microstructure, the local mechanical properties and the chemical gradients in the adhesion layer. It is found that a reduction in the bending strength of the interface of ~40% results on a macroscopic scale in a change from good to bad adhesion properties. Furthermore the results of fracture toughness and bending strength of the interface are compared to the properties of pure a-c:H.

Using these different approaches, a better understanding on the damage behavior of thin brittle coatings on ductile substrates is achieved and the local adhesion strength is correlated to the coating microstructure and chemical composition.

Funding by DFG Cluster of Excellence Engineering of Advanced Materials (EAM)

9:20am **E2-1-5 Study of adhesion and cracking of TiO₂ coatings on a Ti alloy using an impact-sliding testing instrument.** *X. Nie (xn timer@uwindsor.ca), University of Windsor, Canada*

Different thickness and surface porosity of TiO₂ coatings on Ti alloys appear to have a different combination of bioactivity and chemical stability. For bio-implants of dentals, the coating thickness and surface morphology would also influence mechanical integrity. There is a need in further study on fatigue cracks and wear property of the coatings under simulated load conditions of dental surgery operations and implant applications. In this paper, a newly-developed impact-sliding testing instrument is used to simulate those dental applications under a variety of forces where impacts, scratch, fretting, and other relevant wear behaviour occur. The research result showed that the wear behaviour was significantly affected by the coating thickness and surface porosity. The impact-sliding instrument can be used as a tool in study of coating adhesion and cracking for dental implant applications.

9:40am **E2-1-6 Influence of oxide film properties on the adhesion performance of epoxy-coated aluminium.** *Ö. Özkanat (o.ozkanat@tudelft.nl), Delft University of Technology, Netherlands; Materials innovation institute (M2i), Netherlands, J.M.C. Mol, J.H.W. de Wit, Delft University of Technology, Netherlands, H. Terryn, Vrije Universiteit Brussel, Materials innovation institute (M2i), Belgium*

Adhesion of organic coatings and corrosion resistance of polymer/(hydr)oxide/aluminium interfaces plays pivotal role in the engineering of lightweight components. Interfacial bonds at the polymer/metal joints have to withstand high mechanical forces and corrosive attack to protect the functional properties of coated metals. Therefore, it is crucial to understand and to control the delamination of organic coatings and the molecular adhesion forces originating at the interface in order to achieve the long-term stability of these composites. Adhesion strength is both influenced by the functionality of the organic molecules at the interface and the surface properties of thin oxide film e.g. hydroxyl content, oxide thickness and surface morphology. In this work, we present how the surface properties affect the adhesion performance of coated systems. First, different pretreatments (acid, alkaline and immersion in boiling water) were given in order to create variations in the surface properties of aluminium substrate. Then differently pretreated bare surfaces were characterized by means of surface sensitive techniques^[1] in which Scanning Kelvin Probe (SKP), X-Ray Photoelectron Spectroscopy (XPS), Visible Spectroscopic Ellipsometry (VISSE) and Fourier Transform Infrared Spectroscopy (FTIR) were utilized in order to evaluate Volta Potential, hydroxyl fraction, oxide thickness and chemical composition, respectively. Since the oxide properties of aluminium might be extremely sensitive to the small changes in the environmental conditions, effect of ambient humidity (40% RH or 90% RH) and aging (40min vs 240min) on the oxide film properties was also revealed. Results showed^[1] that pseudoboehmite oxide exhibited the highest hydroxyl fraction and oxide thickness; it was also shown that all differently pretreated surfaces along with the reference surface were influenced by both ageing and humidity. This was followed by the molecular bonding of functional groups - representative interfacial adhesive molecules- on differently pretreated surfaces by means of Volta potential shift^[2] (SKP) and affinity (XPS). Finally, the influence of the oxide film properties on macroscopic adhesion of epoxy-coatings was investigated by means of mechanical testing to evaluate the performance of coated systems. It was observed from Shear testing and Bell Peel testing that variations in the thin oxide film properties resulted in different adhesion performance. This research presents a relation

between the adhesion performance and the oxide film properties of the aluminium substrates.

[1] Ö. Özkanat, B. Salgin, M. Rohwerder, J. M. C. Mol, J. H. W. de Wit, H. Terryn, Journal of Physical Chemistry C 2012, 116, 1805.

[2] Ö. Özkanat, B. Salgin, M. Rohwerder, J. H. W. de Wit, J. M. C. Mol, H. Terryn, Surface and Interface Analysis 2012, Accepted.

10:00am **E2-1-7 Adhesion and fatigue properties of TiB₂-MoS₂ composite coatings deposited by closed-field unbalanced magnetron sputtering.** *F.B. Bidev, Ö. Baran (obaran@erzincan.edu.tr), E. Arslan, Y. Totik, İ. Efeoglu, Ataturk University, Turkey*

In this work, TiB₂-MoS₂ composite coatings deposited by closed-field unbalanced magnetron sputtering (CFUBMS) technique using Taguchi L₉(3⁴) experimental method. The structural properties of TiB₂-MoS₂ composite coatings were analyzed SEM and XRD. The hardness of coatings were measured using microhardness tester. Adhesion and fatigue properties of coatings have been scratch tested in two modes. A multi-mode operation was used as sliding-fatigue, like multi-pass scratching in the same track at different fractions of critical load (unidirectional sliding) and a standard mode using progressive load operation. Failure mechanisms were discussed according to SEM examinations of the scratch tracks.

Key Words: TiB₂-MoS₂, Taguchi method, Adhesion, Multi-pass scratch

10:20am **E2-1-8 Coating thickness and interlayer effects on CVD-diamond film adhesion to cobalt-cemented tungsten carbides.** *P. Lu, The University of Alabama, US, H. Gomez, University of South Florida, US, X. Xiao, M.J. Lukitsch, A. Sachdev, General Motors, US, D. Durham, A. Kumar, University of South Florida, US, K. Chou (kchou@eng.ua.edu), The University of Alabama, US*

In this study, diamond coating adhesion on cobalt-cemented tungsten-carbide (WC-Co) substrates was investigated using scratch testing. In particular, the methodology was applied to evaluate the effects of the coating thickness and interlayer on coating delaminations. In the coating thickness effect study, substrate surface preparations, to remove the surface cobalt, prior to diamond depositions was common chemical etching using Murakami solutions. On the other hand, to study the interlayer effect, by halting the catalytic effect of the cobalt binder, two different interlayers, Cr/CrN/Cr and Ti/TiN/Ti, were deposited to WC-Co substrate surfaces (no chemical etching) by using a commercial physical vapor deposition (PVD) system in a thickness architecture of 200nm/1.5 μm /1.5 μm , respectively. Diamond films were synthesized by using a hot-filament chemical vapor deposition (HFCVD) reactor at a gas mixture of 6 sccm of CH₄ and 60 sccm of H₂, with varied deposition times.

Scratch testing was conducted on the fabricated specimens using a commercial machine, at a maximum normal load of 20 N and a speed of 2 mm/min. It is noted that the onset of coating delamination can be clearly identified by high-intensity acoustic emission (AE) signals when such events occur, which can be used to determine the critical load. Scratched track geometry was also characterized by white-light interferometry and scanning electron microscopy.

The results show that the adhesion of the diamond coating increases with the increased coating thickness, with a nearly linear relation, in the range tested. In a previous investigation, finite element (FE) simulations of scratching on a diamond-coated carbide were developed, using a cohesive zone model, to evaluate coating delaminations related to interface characteristics. The FE model was applied in this study to investigate the coating thickness effect on delamination critical loads and the results suggest a linear relation too. For the two types of interlayer materials tested, either of them seems to be effective and the diamond coating with Ti-interlayer shows poorer adhesion comparing to the Cr-interlayer coating.

10:40am **E2-1-9 On the effect of pressure induced change of Young's modulus, hardness and yield strength.** *N. Schwarzer (n.schwarzer@siomec.de), Saxonian Institute of Surface Mechanics, Germany*

It will be shown how relatively simple models simulating the bond interaction in solids applying effective potentials like Lennard-Jones and Morse can be used to investigate the effect of pressure induced changes of Young's modulus and yield strength of these solids. Relatively simple dependencies of the bulk-modulus B on the pressure P being completely free of microscopic material parameters are derived wherever the solid bond interaction can be described or at least partially described by Lennard-Jones potentials. Instead of bond energies and length only specific integral constants like Young's modulus and Poisson's ratio are of need. The influence of the pressure induced Young's modulus change B(P) is discussed especially with respect to mechanical contact experiments. Thereby it is also shown how the extraction of critical decomposition

loading situations could help to obtain somewhat more generic parameters for tribological simulations and life-time predictions.

In a second part of the presentation and based on the results obtained for B(P) a theoretical feasibility study will tackle the question whether or whether not it is possible to obtain hardness values higher than 100GPa (so called "ultra hardness") for nano-composite TiN/a-Si₃N₄ and nano-composite TiN/a-Si₃N₄/TiSi₂ coating materials. For this an effective indenter concept is used which also takes into account the pressure induced increase of the Young's modulus and yield strength during indentation. It will be shown that these hardnesses could IN PRINCIPLE be obtained.

11:00am **E2-1-10 A review of claims for ultra hardness in nanocomposite coatings.** A. Fischer-Cripps (tony.cripps@ibisonline.com.au), Fischer-Cripps Laboratories Pty Ltd, Australia **INVITED**

There has been intense interest over the past 10 years concerning claims of the production and mechanical property measurement of ultra-hard ($H > 100$ GPa) nano composite coatings, particularly in relation to the work of Prof S. Veprék of the Technical University, Munich. In 2006, the present author prepared a critical review of the methods used to characterise these coatings for measurements of elastic modulus and hardness. At that time, various serious errors in procedure were identified in previous works that called into question the validity of the claimed values of elastic modulus and hardness. It was not possible to directly verify the claimed hardness values in excess of 100 GPa for the coatings under review. Since then, Professor Veprék and colleagues have published numerous works which deal with the reasons why such coatings could be made, with the implication and statement that their earlier coatings, whose hardness has now degraded, must have indeed been ultra-hard as claimed. In this presentation, earlier data will be re-examined in the light of new information about the coatings, as well as a critical review of the more recent papers dealing with the supporting theories in relation to these coatings. It is shown that contrary to the claims made, the expected upper limit of hardness achievable with these types of coatings is expected to be about 65 GPa and that the coatings themselves, made many years ago, most likely had a hardness of between 55 and 60 GPa.

Tribology & Mechanical Behavior of Coatings and Engineered Surfaces

Room: Pacific Salon 1-2 - Session E4-2/G4-2

Coatings for Machining Advanced Materials and for use in Advanced Manufacturing Methods

Moderator: M. Arndt, OC Oerlikon Balzers AG, Liechtenstein, X. Nie, University of Windsor, Canada

8:00am **E4-2/G4-2-1 New Coating Systems for Temperature Monitoring in Turning Processes.** M. Kirschner (kirschner@isf.de), K. Pantke, D. Biermann, Institute of Machining Technology, Germany, J. Herper, W. Tillmann, Institute of Materials Engineering, Germany

High temperature loads in cutting processes can cause high tool wear and damages in the subsurface zone of the workpiece. Especially the interaction between the different cutting parameters affects the thermal loads in the cutting zone. Hence, the knowledge of temperatures in cutting processes is an important fact and is under the main focus of current investigations. Therefore, this paper deals with an in-process monitoring system for the resulting temperatures in a turning process. In contrast to the investigations performed hitherto, this research deals with a new tool sensor system for temperature measurement. This sensor system is realized by a PVD coating of a Nickel and a Nickel-Chromium layer on the rake face of cutting inserts. On the junction points of this layer system, three thermocouples are formed. The development of the coating system and the resulting measurement is shown. Additionally, the results are discussed in comparison to thermal imaging system and conventional thermocouples.

8:20am **E4-2/G4-2-2 Hybrid TiSiN, CrCx/a-C:H PVD Coatings Applied to Cutting Tools.** W. Henderer (ted.henderer@kennametal.com), F. Xu, Kennametal Incorporated, US

A very new development in cutting tools has been made for machining aluminum. Hybrid PVD coatings consisting of a superhard TiSiN base layer and a low friction CrCx/a-C:H top layer are used on cutting tools where the combination of low friction and resistance to abrasion is required. For example when machining aluminum silicon, CrCx/a-C:H resists the adhesion and galling of aluminum to the cutting tool by reducing friction and TiSiN strongly resists abrasive wear.

Coatings deposited by sputtering Cr targets in an Ar + CH₄ glow discharge have been previously studied. A nanocomposite microstructure was formed containing CrCx crystallites in a Cr containing amorphous diamond-like C:H matrix [1].

In this research, TiSiN films with a CrCx/C top layer have been produced in a hybrid cathodic arc/sputter physical vapor deposition system. Applied by cathodic arc plasma deposition, X-ray diffraction shows TiN changes from a (111) preferred orientation to (200) texture structure with silicon additions. When CrCx/C is subsequently deposited by sputtering, CrC XRD peaks are not found. The material is amorphous. SEM and TEM reveal the complex microstructure of the hybrid coating.

Measured by nano-indentation hardness tests, Si is shown to increase the hardness of TiSiN. When machining abrasive 390 aluminum, the wear resistance of taps coated with TiSiN base layer and a low friction CrCx/C top layer is likewise improved with silicon additions to TiN. The CrCx/C top layer is shown to have frictional and wear characteristics similar to DLC coatings.

[1] Gassner, G., et al., "Structure of Sputtered Nanocomposite CrCx/a-C:H Thin Films", J. Vac. Soc. Technol. B, Vol. 24, No. 4, July/Aug 2006

8:40am **E4-2/G4-2-3 Effect of the Cutting Edge Entry Impact Duration on the Coated Tool's Wear in Down and Up Milling.** K.-D. Bouzakis (bouzakis@eng.auth.gr), Aristoteles University of Thessaloniki; Fraunhofer Project Center Coating in Manufacturing, Greece, G. Katirtzoglou, E. Bouzakis, S. Makrimalakis, G. Miliaris, Aristoteles University of Thessaloniki; Fraunhofer Project Center Coatings in Manufacturing, Greece

The knowledge of tool wear mechanisms in milling is pivotal for explaining the coating failure and adjusting appropriately the cutting conditions. In the described investigations, coated cemented carbide inserts were applied in up and down milling hardened and stainless steel for monitoring the tool wear at various repetitive cutting loads and durations. The variable stress, strain and strain rate fields developed in the tool during cutting affect the film-substrate deformations and in this way the resulting coating loads and fatigue failure.

For investigating the influence of cyclic impact loads magnitude and duration on the film fatigue failure of coated specimens, an impact tester was employed which facilitates its force signal modulation. By this device, repetitive impact loads with variable duration and time courses were exercised on coated cutting inserts. These loads approximately simulated the developed ones in milling at various kinematics and process parameters. The attained tool life up to the film fatigue failure was associated to a critical force and an entry impact duration. The latter factors converge sufficiently to the tool life in all investigated milling kinematics and material cases.

Keywords: PVD coatings, milling, film fatigue, fatigue critical force, entry impact duration

9:00am **E4-2/G4-2-4 Cutting performance of PVD coatings during dry drilling of sustainable austempered ductile iron (ADI).** A. Meena (anilme05@gmail.com), M. El Mansori, Arts et Métiers ParisTech, France

The present paper investigates the cutting performance of PVD coatings during dry drilling of sustainable ADI material produced by the continuous casting-heat treatment process [1]. The cutting tools used were PVD coated carbide tools. SEM and EDS analyses were performed to investigate the surface characteristics of PVD coatings. Cutting performance of different coatings was evaluated by measuring cutting forces, chip types and under-surface chip morphology. The phenomena and the causes of the tool wear were studied too. The surface alteration at the machined subsurface was confirmed from the hardness variation. It was shown that the major cause of improved cutting performance and wear behavior of PVD coated tool is the enhanced tribological adaptability of multilayer (Ti,Al,Cr)N coating. The adaptability of multilayer (Ti,Al,Cr)N coating can be explained by the formation of oxide layers on the cutting tool's surface, which further increase tool wear resistance and lubrication at cutting zone. These oxide layers reduce the severity of friction at the tool-chip interface by reducing the strength of adhesion bonds at this interface.

9:20am **E4-2/G4-2-5 Process design for the machining of high-strength steels.** F. Felderhoff (fabian.felderhoff@de.bosch.com), Robert Bosch GmbH, Germany **INVITED**

In order to increase the efficiency and to reduce the emissions of internal combustion engines for current and future generations of vehicles the increase of the fuel injection pressure is needed.

In the field of diesel injection, pressures of up to $p = 2500$ bar are currently implemented. As a result, stresses of the materials require special steels with good levels of purity, so that the alloying with lead or sulfur to improve machinability is no longer possible. Those steels are machined with geometrically defined cutting edge in an annealed condition, which

represents a particular challenge in terms of chip breakage. On the other hand, steels are also machined in the heat treatment condition needed for the application to avoid additional heat treatment steps and costs. One example is quenched and tempered steel which is drilled with a material hardness of 40 HRC.

In the area of fuel injection, the injection pressures are not comparable high, but because of the corrosive attack by the fuel stainless steels are used mostly. Due to the high content of alloying elements stainless steels have a specific property profile. Compared to engineering steels the heat capacity is higher and thermal conductivity is lower.

Thus the tool coating is of utmost importance for the process design. Particularly when machining stainless steels and high strength steels, the coating acts as a thermal barrier. A smooth surface is necessary for drilling processes to remove chips out of the hole safely. Reproducible and long tool lives are also important for a trouble-free production. However, the short time of modern production development cycles allows no extensive testing for each machining task to determine the optimal coating. Therefore, the development of hard coatings with a broad application is also important.

The results of this investigation show examples for the design of modern precision machining processes for the high-volume production of components for diesel and gasoline injection technology.

10:00am **E4-2/G4-2-7 A nanostructured cutting edge, J. Rechberger** (johann.rechberger@fraisa.com), J. Maushart, Fraisa SA, Switzerland

Right at the cutting edge of a carbide tool many features of very small dimensions interact to form a complex material. As a result of the grinding process crushed and embedded nanometer size tungsten carbide grains form a thin interface layer between substrate and coating. Most beneficial compressive internal stresses also introduced through the grinding process near the surface increase the bending fatigue strength of the material. Common edge preparation techniques locally remove the highly plastically deformed interface layer and reduce the extend of the compressive zone. The breakage of micro burrs leaves behind a small fracture surface with tiny cracks along the cutting edge. For the subsequently deposited coatings this is only a weak base ground. Shadowing effects of microscale periodic grinding marks on the rake face lead either to favorable coating stress relief sites or to the unwanted exposure of substrate material. All these and other highly relevant micro-features affect the wear behavior, especially in the initial stage. The wear mechanisms change at the slightest variation of any of these edge parameters. Even post coating treatments for the droplet removal cause changes at the cutting edge. For a coated high performance milling tool some of these interesting micro and nano features are analyzed and set in relation to the wear behavior.

10:20am **E4-2/G4-2-9 Application of thick PVD coating deposited by new AIP cathode SFC for machining of automotive component, K. Yamamoto** (yamamoto.kenji1@kobelco.com), S. Tanifuji, Kobe Steel Ltd., Japan, G. Fox-Rabinovich, McMaster University, Canada

CGI (compacted graphite cast iron) has been known for since long as ductile iron from 1940's and recently becomes more popular to be used for blocks of a diesel engine. CGI has almost twice tensile strength than conventional gray cast iron and more heat resistant than aluminum alloys. CGI, on the other hand, is known to be a hard-to-machine material due to its high tensile strength and usually CVD coated thick oxide coating (more than 10 microns) is a choice for machining. Wet turning test of CGI with commercial thin TiAlN indicated that main wear is concentrated on the flank face and once the coating is worn out and WC-Co is exposed, intensive adhesive wear is observed. So our idea is to apply thick PVD coating to the level of more than 10 microns to prevent the worn out of the coating.

Conventional PVD coating process is usually limited thickness less than 10 um due to high residual stress involved. We have developed a new magnetically modified cathodic arc evaporation source thatenables to reduce the intrinsic stress substantially, making it possible to deposit thick PVD nitride coatings more than 10 microns. (Ti1-xAlx)N coatings with different compositions (x=0.25 to 0.6) were deposited by conventional and the new arc cathode. Cutting tests were performed against CGI, using WC-Co cutting inserts. Cutting conditions were 250m/min, DOC=0.25mm, Feed=0.34mm/rev. The effect of Al concentration on the life time of cutting tool is investigated in detail. As the criteria for tool life was set to 300 um of flank wear, TiN failed only cutting length of ca. 2.9km. The tool life was increased as the Al content was increased and reached maximum value of 15.7 and 17.5 km for 10 um (Ti0.5Al0.5)N and (Ti0.4Al0.6)N coatings deposited by the new cathode. Whereas commercially available (Ti0.5Al0.5)N coating failed at 10km. This clearly shows the advantage of thick PVD coating deposited by the new cathode. The effect of coating thickness on the tool life will also be reported.

10:40am **E4-2/G4-2-10 Evaluation of the Abrasive Wear Resistance of Nitride, Oxynitride and Oxide PVD Coatings at High Temperatures, P. Dessarzin, P. Karyankova, M. Morstein** (m.morstein@platit.com), Platit AG, Switzerland, J. Nohava, CSM Instruments SA, Switzerland

While protective PVD tool coatings have, over the past years, become more and more resistant to the extreme environments associated with modern machining processes, a new challenge has occurred, to create measureable and homogeneous wear of such films in tribological lab-scale testing. Common pin-on-disk tribotests at elevated temperatures can often lead to either erratic wear mechanisms, that do not correlate well with cutting tests, or even to no measureable wear at all. In order to establish a valid set of high-temperature wear test conditions, we used a state-of-the-art high-temperature pin-on-disk tester and optimized conditions such as normal load, sliding speed and -distance. For this study, two families of coatings covering a range of physical properties such as hardness, modulus and adhesion strength were deposited using an industrial rotating cathodes arc PVD process.

The first set of coatings comprised a series of nanostructured Al-Cr-based oxynitrides deposited on cemented carbide, where nitrogen was subsequently substituted with up to 100 at.% of oxygen. These coatings are known to withstand extremely high temperatures in dry milling and turning of high-strength materials while still maintaining low mechanical wear, and differentiation of their wear resistance by laboratory tribotest had, in the past, proven difficult.

The second set of coatings investigated were thick nanolayered AlTiCrN PVD coatings deposited on cold-working steel, designed for use in challenging forming processes of high-strength steel. Here, the practical benefits of the coatings are rather related to a good fracture toughness and lubricious properties, while temperature resistance is limited by the substrate base material.

High-temperature pre-tests against alumina balls were run in order to identify the optimum parameters in ambient air at 600°C (AlCrON series) and 400°C (tool steel samples). The key parameter turned out to be the applied normal load, but a long enough total sliding distance was needed, too. The wear under these conditions was found by profilometry to be very low for the best coatings ($\leq 10^{-16} \text{ m}^3\text{N}^{-1}\text{m}^{-1}$) and governed by an abrasive mechanism, where some micro-scale cohesive fracture was also observed, which was confirmed by FIB cuts. A straightforward correlation of the wear coefficient to coating hardness was not found. EDX mapping revealed that oxidation played a limited role for nitride coatings, while oxynitrides remained inert at 600°C thanks to their superior oxidation resistance. Therefore, supplementary experiments were conducted on selected AlCrON samples, using an increased temperature of 800°C, which allowed for a proper wear ranking.

11:00am **E4-2/G4-2-11 Application-oriented coating and post-treatment for high performance broad band drilling operations, T. Michalke** (thordis.michalke@oerlikon.com), Oerlikon Balzers Germany GmbH, Germany, S. Stein, M. Arndt, OC Oerlikon Balzers AG, Liechtenstein

Drilling is a cutting application with very high demands on the wear resistance of PVD-coatings: They have to withstand a high temperature influence at the cutting edges and along the margin, as well as the high friction and squeezing area along the main cutting edge and at the tip.

To solve these demands, a new (Al,Ti)N-based coating was developed. (Al,Ti)N-coatings are applied in a wide range of cutting applications today. An optimized coating architecture and a defined grain size result in a tailored hardness and fracture toughness of the coating, just as high oxidation and thermal shock resistance. With these optimizations the new coating offers a high performance as well as a broad band solution for drilling of different steels and cast iron even with a high variety of cutting parameters.

For the realization of the new coating, the chemical inertness of the surface was as important against chip adhesion as a smooth and polished surface in the flute. Therefore, the post-treatment is an important factor for the wear behaviour and the performance of drills. A detailed investigation of different post-treatment methods gives an overview and shows their influence by drilling test results. To understand the effectiveness and influencing parameters of post-treatment methods, a systematic investigation of selected processes was done. Their impact to the surface roughness and overall quality, the coating thickness as well as the coating stress and the micro hardness will be shown and are combined with the results of cutting tests and torque measurements. This leads to an essential input for the understanding of the correlations between post-treatment and machining results.

Energetic Materials and Micro-Structures for Nanomanufacturing

Room: Sunset - Session TS3-1

Energetic Materials and Micro-Structures for Nanomanufacturing

Moderator: C. Rebholz, University of Cyprus, Cyprus, C. Doumanidis, University of Cyprus, Cyprus, T. Ando, Northeastern University, US

8:00am TS3-1-1 Recent ADvances in Nanolaminate Energetic Materials, C. Rossi (rossi@laas.fr), ICNRS; LAAS, France INVITED

Since more than a decade, nanostructured thermite materials, which classically consist of a mixture of oxidizer and fuel nanoparticles, have drawn considerable interest due to enhanced energy release rates in comparison to their macro-scale counterparts which arises from an increased fuel and oxidizer interfacial contact area. In comparison with other energy sources such as batteries, capacitors, fuel cells, nanothermites energy and power density is orders of magnitude higher, making them ideal candidates to provide high energy density local source of heat or pressure for mechanical and/or electrical power. Since 2005, progress in nanotechnologies paved the way to engineering nanothermites on a chip. Typically, magnetron sputtering method permit to stack alternatively metal and metal oxide nanofoils, typically Al and CuO, each foil being accurately controlled in thickness (from 25nm-100nm with a precision of 5nm) and high purity. This deposition technique places the reactants in intimate contact reducing notably the diffusion distance between reactants compared to the same material prepared by powder mixing.

Al-CuO nanolaminates are magnetron sputter deposited from Al and Cu targets using DC power supplied, on oxidized silicon wafer. Copper Oxide thin films are deposited by dc reactive magnetron sputtering method under argon and oxygen plasma from a Cu target.

We compared the ignition characteristics and combustion rate of Al/CuO nanolaminate for different Fuel (Al) to Oxidizer (CuO) ratio (stoichiometric, fuel rich and fuel poor) and for different Al and CuO individual reactive layer thickness. Results show that Al/CuO nanolaminates provide unparalleled selectivity to tailor their energetic response to satisfy desired application based on material composition, structure and stoichiometry.

Second point discussed in this paper is the formation and role of the intermixing zone at the interface of Al and CuO reactive layers. We find that an interface layer formed during sputter deposition of aluminum on CuO is composed of a mixture of Cu, O and Al through Al penetration into CuO, and constitutes a poor diffusion barrier (low ignition temperature); and in contrast atomic layer deposition (ALD) of Al_2O_3 using trimethylaluminum (TMA) produces a conformal coating that effectively prevents Al diffusion (higher ignition temperature) even for ultra-thin layer thicknesses (~0.5 nm). These findings evidence that interface layers plays a crucial role in the characteristics and performances of energetic nanolaminates. We have combined *in-situ* FTIR and *ex-situ* X-ray, DSC and HRTEM to identify the stable configurations that can occur at the interface.

8:40am TS3-1-3 Comparison of engineered nanocoatings on the combustion of aluminum and copper oxide nanothermites, E. Collins, M. Pantoya (michelle.pantoya@ttu.edu), A. Vijayasai, T. Dallas, Texas Tech University, US

Water-repellent nanocoatings for submerged combustion of nanoenergetic composite materials were developed. Some of the possible applications of submerged combustion are - oceanic power generation, underwater ordnance, propulsion, metal cutting, and torch technologies. Nanocoatings were deposited on thermite pellets by a vapor-phase technique. Two types of deposition techniques, namely chemical vapor deposition (CVD) and atomic layer deposition (ALD) were studied. A total of six types of nanocoatings were applied on the thermite pellets. Various process parameters to produce the coatings were explored. Characterization of the nanocoatings was carried out using FTIR, SEM, AFM and contact angle goniometry. Submerged combustion tests of the nanocoated thermite pellets were performed as a function of submerged time. The pellets were submerged in deionized water for 3, 5 and 10 days. The bubble energy produced was analyzed and compared to other types of nanocoated pellets. Initial results were analyzed using a fluorocarbon (FSAM) based monolayer coating (type 1 - thickness ~1.8nm) and compared with a nanoparticle+FSAM coating (type 2 - thickness ~300nm).

Results suggest that with increasing submerged time, there is a decrease in the ratio of bubble energy to total energy of combustion ($K_c = K_{\text{bubble}}/K_{\text{combustion}}$). The bubble energy of the pellets with type 1 and type

2 coating was 532.6 and 528.6 (KJ/Kg) respectively, with immediate ignition after submersion and 27.6 and 48.2 (KJ/Kg) respectively, after 10 days. The value of K_c for Type 1 coating decreased by a factor of 19.3 whereas the Type 2 coating decreased by a factor of 11.0. The hydrophobic coating is critical for energy generation because without it, the pellets do not ignite, resulting in 100% loss of energy. Other coatings are being explored to improve durability of submerged pellets.

9:00am TS3-1-4 Study of the reactive dynamics of nanometric metallic multilayers using molecular dynamics : the Al-Ni system., O. Politano (politano@u-bourgogne.fr), F. BARAS, Université de Bourgogne - CNRS, France

A molecular dynamics study of a layered Ni-Al-Ni system is developed using an embedded atom method type potential. The specific geometry is designed to model a Ni-Al nanometric metallic multilayer. Based on this microscopic approach, we are able to detect the development of the spontaneous dynamics at nanoscale. A nanometric Al-slice embedded in Ni, is initially thermally stable up to a temperature of 500 K. Both pure metals are stable. However, at a critical temperature, we first observe the interdiffusion of Ni and Al at the interface which is followed by the spontaneous phase formation in the Al layer. The solid-state reaction is accelerated with a rapid system's heating which further enhances the diffusion processes. NiAl phase is organized in small regions separated by grain boundaries. Such crystallites are larger in the direction parallel to the interface than in the perpendicular one. This study confirms the hypothesis of a layer by layer development of the new phase. For longer times, the temperature is notably higher (> 1000 K) and the system may partly lose some its B2 NiAl microstructure in favor of the formation of Ni_3Al in L12 configuration. This work shows the spontaneous development of a real exothermic solid-state reaction in metallic nanosystems mostly constituted by interfaces. It allows to explain the extreme reactivity of such systems and gives the basic mechanisms at its origin.

9:20am TS3-1-5 Exothermic metal-metal multilayers: Pulsed laser ignition thresholds, reaction modes and effects of environment, D. Adams (dpadams@sandia.gov), R. Reeves, P. McDonald, D. Jones, Jr., M. Rodriguez, Sandia National Laboratories, US INVITED

Vapor-deposited, metal-metal multilayers are an ideal class of materials for systematic, detailed investigations of reactive material properties. Created in a pristine vacuum environment by sputter deposition, these high purity materials have well-defined reactant layer thicknesses between 1 and 1000 nm, minimal void density and intimate contact between layers. With this presentation, we describe the ignition characteristics, reaction behaviors and final phase formation of multiple exothermic metal-metal pairs. This includes equiatomic Al/Pt, Co/Al and Ni/Ti. Regarding initiation, we show how pulsed laser ignition thresholds vary with material system. For a given reactive material system, the thresholds for ignition are also shown to depend on (i) pulse duration (evaluated from decisecond to femtosecond time scales) and (ii) nanolaminate periodicity. With regards to steady-state propagation, we show that some nanolaminate systems (Al/Pt) exhibit stable propagation modes characterized by rapid reaction rates and microscopically-smooth reaction front morphologies. Other kinetically-constrained systems (Co/Al, Ni/Ti) exhibit an in-plane spin-like (unstable) propagation mode characterized by transverse propagation bands and colliding wavefronts. Regarding phase formation, we describe how reaction environment can affect final phase.

Sandia is a multi-program laboratory managed and operated by Sandia Corporation, a wholly owned subsidiary of Lockheed Martin Company, for the United States Department of Energy's National Nuclear Security Administration under Contract DE-AC04-94AL85000.

10:00am TS3-1-7 Time-Resolved Emission Spectroscopy Of Electrically Heated Energetic Ni/Al Laminates, C. Morris (christopher.j.morris58.civ@mail.mil), U.S. Army Research Laboratory, US, P. Wilkins, C. May, Lawrence Livermore National Laboratory, US, T. Weihs, Johns Hopkins University, US

The nickel-aluminum (Ni/Al) intermetallic system is useful for a variety of reactive material applications, and reaction characteristics are well studied at the normal self-heating rates of 10^3 – 10^6 K/s. Our experiments at 10^{11} – 10^{12} K/s have measured the kinetic energy of material ejected from the reaction zone relative to input electrical energy, indicating an exothermic effect from Ni and Al laminates despite the extremely high heating rate.

In order to better probe reaction phenomena at these time scales, we reported at the 2010 ICMCTF meeting on emission spectroscopy of electrically heated, patterned Ni/Al bridge wires, time resolved over 350 ns through the use of a streak camera. We conducted these experiments in rough vacuum, but found the emission to be dominated by argon (Ar) and nitrogen (N) lines in addition to the expected emission of Al and Ni. Using spectral information from this Ar, we analyzed expected Boltzmann

distributions for several peaks to yield temperature values of 2.24 to 3.27 eV, and found them to be within reasonable estimates based on the measured electrical energy delivered to each device.

More recently, we acquired streak spectrographs from Ni/Al laminates encapsulated with vacuum-deposited parylene. This process insured that any emission came only from the electrically Ni/Al laminates, and should allow better quantification of temperature without the same level of interference from residual gases. The encapsulation layer caused a much slower 60 ns rise to peak emission intensity, compared to 8 ns for previous, un-encapsulated tests. This rise time likely corresponded to a physical acceleration of a portion of the encapsulation layer away from the substrate, which we will measure and report in the final paper. We will also correlate spectroscopic emission at early times with measured electrical input, and gain insight into phase changes, mixing, and expected exothermic release over these extremely short timescales. These studies are important for future nanomanufacturing techniques, where it may be necessary to control spatial thermal distributions much more precisely by careful control of the timescales over which reactions take place.

10:20am **TS3-1-8 Numerical simulations of self-propagating reactions and analysis of reacted microstructures in Ru/Al multilayers.** *K. Woll* (*k.woll@mx.uni-saarland.de*), Functional Materials, Dept of Materials Science and Engineering, Saarland University, Germany, *I. Gunduz*, *C. Rebholz*, Dept. of Mechanical and Manufacturing Engineering, University of Cyprus, Cyprus, *F. Mücklich*, Functional Materials, Dept of Materials Science and Engineering, Saarland University, Germany

Energetic materials based on equiatomic Ru/Al multilayers have been recently introduced by our group. The unusual combination of high temperature as well as room temperature properties makes the equiatomic Ru/Al system interesting as a new energetic material. So far, self-propagating reactions in Ru/Al multilayers have been studied with a focus on the early stages of reaction. Parameters such as front velocity and reaction temperature as well as the reaction mechanism have been experimentally determined and compared to other systems. These results clearly demonstrate that the Ru/Al system expands the reaction parameter range of previously used systems in terms of velocity and temperature. However, for a more detailed understanding of the reactions, numerical simulation which focuses on the early reaction stages as well as microstructural analysis to reveal the processes during later stages of cooling was performed. Experimental studies were carried out to investigate the effects of the interaction with surrounding air as a function of multilayer period. For this, pyrometric measurements to follow the temperature evolution during the reaction and cross sectional transmission electron microscopy analysis of reacted foils were performed.

10:40am **TS3-1-9 Fabrication, Characterization and Applications of Novel Nanoheater Structures.** *Z. Gu* (*Zhiyong_Gu@uml.edu*), *Q. Cui*, *J. Chen*, *J. Buckley*, University of Massachusetts Lowell, US, *T. Ando*, *D. Erdeniz*, Northeastern University, US, *P. Wong*, Tufts University, US, *C. Rebholz*, *A. Hadjiafxenti*, *I. Gunduz*, *C. Dumanidis*, University of Cyprus, Cyprus

Nanoheaters are reactive nanostructures that can generate localized heat through controlled ignition. Besides the widely used nanofoil structure with multiple alternative aluminum-nickel (Al-Ni) layers, various new nanostructures have been fabricated in the last several years, including consolidated compacts, bimetallic nanoparticles, and ball milled micro/nano powders. In this presentation, we show that (1) Al-Ni compacts can be fabricated by a novel ultrasonic powder consolidation (UPC) method, using Al and Ni nanopowders as source materials; (2) Al-Ni bimetallic nanoparticles have been synthesized by a galvanic replacement reaction method using Al nanoparticle templates; (3) Al-Ni micro/nanopowders can be prepared by a ball milling method using Al and Ni powders. The structure and compositions of the nanoheater structures have been characterized by electron microscopies (SEM and TEM), energy dispersive x-ray spectroscopy (EDS), and x-ray diffraction (XRD). The ignition of these nanoheater structures has been initiated by the electrical (ohmic) method, microplasma (plasma arc discharge) method, etc. The reaction characteristics of the nanoheater structures were investigated using high speed optical and infrared imaging, and the thermal characteristics of the samples were studied using differential scanning calorimetry (DSC). These novel nanoheater structures have great potential to be used in micro-joining, microelectronics assembly, and flexible electronics bonding.

11:00am **TS3-1-10 Effect of Mechanical Activation on SHS and Structure Formation in Nanostructured Geterogenous Reaction Systems.** *N. Shkodich* (*n.f.shkodich@mail.ru*), *Vadchenko*, *Rogachev*, *Sachkova*, Institute of Structural Macrokinetics and Materials Science RAS, Russia, *Neder*, *Magerl*, Institute of Crystallography and Structural Physics, University of Erlangen-Nürnberg, Germany

One of the possibilities to produce nanostructured materials is the combination of two non-equilibrium processing techniques, namely mechanical activation (MA) and self-propagating high-temperature synthesis (SHS). Mechanical activation provides the possibility of both modifying the conditions of the chemical reaction run and changing the thermal parameters of the synthesis (temperature, combustion velocity, heating rate, and others) thus leading to the different structures and properties of the final product.

Our investigation aimed at establishing the influence of MA on SHS. The Ni—Al, Ti—BN and Ti—SiC—C systems were studied. Green mixtures were prepared by dry mixing of the initial components in china crucibles at the stoichiometric ratios corresponding to the following reactions: $\text{Ni} + \text{Al} = \text{NiAl}$, $3\text{Ti} + 2\text{BN} = 2\text{TiN} + \text{TiB}_2$ and $3\text{Ti} + \text{SiC} + \text{C} = \text{Ti}_3\text{SiC}_2$.

Preliminary MA was performed in a water cooled planetary ball mill (AGO-2) type at room temperature under argon. The milling procedure was carried out at the ball/mill ratio of 20: 1. The milling time varied from 0.20 s to 30 min.

The resultant mechanically activated particles were composed of layers of the initial components alternating with each other at the nano level [1, 2].

During mechanical activation of Ni+Al mixtures up to 7 min, specific contact area between reagents Ni and Al increased approximately 15-20 times for each fraction.

Using high-resolution SEM and TEM methods for microstructural investigation of Ni—Al activated samples, nanoscale structural components were observed. Their average atomic weight was intermediate between the Ni and Al. The main influence on the reactivity of heterogeneous systems Ni — Al during milling is formation of nanoscale X-ray amorphous phases and solid solutions.

Ignition temperature was measured for small amounts of activated mixtures in the form of activated particles, pressed pellets, and rolled foil. The dependences of the ignition temperature on the MA duration and the way of the sample preparation were studied. It was found that after MA for 0 – 30 min the ignition temperature lowered by approximately 600°C for Ti—BN and Ti—SiC—C systems; after MA for 0– 7 min it could be diminished by 300–400 °C for N—Al system.

For the determination of the internal microstructure, the particle size and microstrains of mechanically activated powders 3Ti+2BN and 3Ti+SiC+C and of the combustion products were analyzed by X-ray powder diffraction on a Huber Guinier diffractometer at the Institute of Crystallography and Structural Physics, in Erlangen, Germany.

Analysis showed that an increase in the MA duration of the 3Ti+2BN and 3Ti+SiC+C mixtures led to a decrease in the peak intensities and broadening of the Ti peaks. With increasing activation time, the BN reflexes in the 3Ti+2BN reaction mixtures were instantly broadened and in three minutes their intensity became comparable to that of the background. Similar behavior was also observed in case of graphite in the activated 3Ti+SiC+C mixtures. This evidences the destruction of the crystal structure (amorphization) of boron nitride and graphite in the MA process [3].

The effect of milling time on the crystalline size and strain in the powder mixtures and SHS products we determined from line broadening analysis of the XRD peaks. The Rietveld full profile refinements were carried out with the Fullprof Suite. As a result of up to 30 min MA, the average size of the Ti crystallites was found to reduced down to 25 and 50 nm in the Ti + BN and Ti—SiC—C systems, respectively. Mechanical activation was found to affect the size of product crystallites. The value of the micro stains increased with the MA duration.

Formation of nanocomposites at the stage of mechanical activation provides proper conditions for synthesizing nanostructured SHS materials with a complete inheritance of the precursors' structural morphology.

References

- [1] N.F. Shkodich, N.A. Kochetov, A.S. Rogachev, D.Yu. Kovalev, N.V. Sachkova, *Izv. Vyssh. Uchebn. Zaved. Tsvetn. Metall.*, 5, (2006) 44-50.
- [2] M.A. Korchagin, M.R. Sharafutdinov, N.F. Shkodich, B.P. Tolochko, P.A. Tsygankov, I.Yu. Yagubova, *Nuclear Instruments and Methods in Physics Research A*, 575, (2007) 149-151.
- [3] Shkodich N. F., Rogachev A. S., Neder R. B., Magerl A., S.G. Vadchenko, and O. Boyarchenko, *High-Temperature Ceram. Mater. Composites*, 911 (2010) 881-887.

Acknowledgement

The present work was supported by the Russian Foundation for Basic Research (Project no. 10-03-00217-a) and the Council of the RF President Grants for Support of Leading Scientific Schools (Grant no. NSh-6497.2010.3).

Thursday Afternoon, April 26, 2012

Coatings for Use at High Temperature Room: Sunrise - Session A3-2/F8-2

Coatings for Fuel Cells & Batteries

Moderator: E. Yu, Newcastle University, UK, G. Dadheech, General Motors, US

1:30pm **A3-2/F8-2-1 A Study on the high temperature charge-discharge characteristics of Si-xAl thin film anode for Li-ion batteries.** *Y.T. Shih, C.H. Wu, F.Y. Hung (fjhung@mail.ncku.edu.tw), T.S. Lui, L.H. Chen*, National Cheng Kung University, Taiwan

In this study, Al element was added into Si matrix as the buffer (Si-10Al, Si-25Al, Si-45Al) by co-sputtering to prevent the drastic volumetric expansion of pure Si thin film anode during lithiation and delithiation at high temperature (55°C). Increasing Al content, the electrochemical reaction of Si-xAl anodes would transfer from Si-Al co-dominated to Al dominated and decreased the capacity of first cycle. After the first cycle testing, the anode with lower Al content showed the capacity fading result from impedance increased and electrochemical reaction degraded. In addition, the higher diffusion velocity of lithium ions raised the total capacity and decreased the initial reaction voltage and cycle stability. After annealing, Si-25Al anodes had excellent electrochemical performance at high temperature then as-deposited.

1:50pm **A3-2/F8-2-2 Pseudo-capacitive performance of the Manganese oxide/Carbon Nanocapsules (CNC) electrode by Sol-gel technique.** *C. Lin, C.H. Wu, C.W. Wang, C.Y. Chen*, Feng Chia University, Taichung, Taiwan, *Lee (n5891119@ccmail.ncku.edu.tw)*, National Cheng Kung University, Taiwan

Manganese oxide/carbon nanocapsules (CNC) electrode were prepared by sol-gel process. Effects of the carbon nanocapsules addition and post heat treatment on the material characteristic and pseudocapacitive performance were investigated. Surface morphologies and crystal structures of the electrodes were examined using a scanning electron microscope and an X-ray diffractometer, respectively. X-ray photoelectron spectroscopic analyses were also performed to probe the chemical states. Moreover, electrochemical properties of the electrodes were evaluated by cyclic voltammetry (CV). Experimental results showed that the Mn oxide/CNC film was composed of Mn₂O₃ and Mn₃O₄ phase after heat treatment. The CNC addition for the Mn oxide electrode was exhibited the excellent electrochemical performance. The Mn oxide film with 0.025 wt% CNC after heat treating at 350 °C exhibited the optimum capacitance of 314 F/g. Furthermore, Capacitance-retained ratio of the Mn oxide/CNC electrode after 1000 charge-discharge cycles was ~64%, better than its pristine manganese oxide counterpart.

2:10pm **A3-2/F8-2-3 Electrified Vehicles for Personal Transportation and the Critical Role of Surface Coatings for Lithium Ion Batteries.** *M. Verbrugge (mark.w.verbrugge@gm.com), X. Xiao*, General Motors Research and Development Center, US, *R. Deshpande, J. Li, Y.T. Cheng*, University of Kentucky, US **INVITED**

We seek energy sources that are affordable, readily available, clean in terms of environmental concerns, and sustainable. Although automobiles emit far less unwanted emissions than in the past, personal transportation is challenged in that nonrenewable petroleum, which supplies about a third of the World's energy needs, is used almost exclusively for transportation purposes. Great progress has been made in recent years relative to traction battery technology, as exemplified by the Chevy Volt extended range electric vehicle (EREV).

In this talk, we will cover recent advancements in electrified vehicles. In addition, we will look at the critical role surface coatings take on in terms of making current lithium ion batteries function, and we will discuss associated open questions.

2:50pm **A3-2/F8-2-5 Comparison of corrosion behaviors between AISI 304 stainless steel and Ti substrate s coated with TiZrN/TiN thin films as bipolar plate for unitized regenerative fuel cell.** *M.T. Lin*, National Chung Hsing University, Taiwan, *C.H. Wan (chieh hao@mdu.edu.tw)*, MingDao University, Taiwan, *W. Wu*, National Chung Hsing University, Taiwan

Unitized regenerative fuel cell (URFC) works as fuel cell when supplied with hydrogen and oxygen fuel, and as electrolyzer when fuelling with water. Bipolar plate of URFC should have good corrosion resistance to acid and oxygen oxidation. In this work, a composite layer of TiZrN/TiN

deposited on AISI 304 stainless steel and titanium metal substrates is prepared by using the cathodic arc evaporation techniques to improve the corrosion resistance and anti-oxidation capability of the substrates. SEM, EDS and XRD are used to characterize the microstructure, thickness, chemical composition, crystalline and phase states of the deposited thin films. Potentiodynamic polarization measurement is performed in the simulated environment in URFC, i.e. the simulated anode and cathode environment are at -0.1V versus SCE purged with H₂ and 0.6V versus SCE purged with O₂, respectively, tested in 0.5M H₂SO₄ with 3 ppm F⁻ solution at 65 °C. Results demonstrate that the corrosion resistance of stainless steel and titanium substrates with TiZrN/TiN coating is better than that of the AISI 304 stainless steel and titanium metal without coating. This is because the rod-like crystals structure and similar NaCl structure of TiZrN/TiN coating contribute to the corrosion resistance of the substrates. Titanium substrate with TiZrN/TiN coating performs superior corrosion resistance than the AISI 304 stainless steel due to the better interface adhesion between substrate and TiZrN/TiN coating.

3:10pm **A3-2/F8-2-6 Progress towards, thin, cost-effective coatings for PEMFC metallic Bipolar Plates by closed field unbalanced magnetron sputter ion plating.** *H. Sun, K. Cooke (kevin.cooke@miba.com)*, Teer Coatings Limited, Miba Coating Group, UK, *G. Eitzinger*, High Tech Coatings GmbH, Miba Coating Group, Austria, *P. Hamilton, B. Pollet*, University of Birmingham, UK

Compared to graphite and composite plates, metallic bipolar plates (BPPs) for polymer electrolytic membrane fuel cells (PEMFCs) have many advantages due to their high strength, mechanical durability and electrical conductivity, even for the minimum thickness required to achieve weight and space savings essential for transport applications. However a protective, electrically conductive coating is required to inhibit corrosion, ensure continued electrical functionality and adequate longevity in the aggressive electrochemical environment of the fuel cell.

Maximising system efficiency requires the minimisation of electrical impedance, decreasing parasitic losses. Combined with the reduced plate thickness, this supports an overall reduction in stack size. Power density [kW/kg] is enhanced as the mass of the coated plates is minimised, combined with easier thermal management and reduced packaging requirements, both especially attractive for automotive applications of PEM fuel cells. End of life considerations are also addressed by the potential for conventional re-use and ultimate recyclability of coated metallic plates. Coatings also play a role in the management of water within the cell, however the requirements are complex: hydrophilicity of the coated plate may offer advantages at start up, under low RH conditions, whereas when a stack is operating at high power and approaching 100% RH a hydrophobic surface may assist in the clearance of the water from the cells.

Closed field unbalanced magnetron sputter ion plating (CFUBMSIP) produces dense, well adhered coatings, and both transition metal nitrides and graded, nano-composite, non-hydrogenated amorphous carbon, demonstrating the combination of properties required in this application. The quality of the coatings allows coating thickness to be minimised (typically <1micron) while still providing adequate functionality and longevity, and of course this is also critical to the minimisation of production costs. Ultimately this technology is compatible with low-cost manufacturing techniques similar to those already employed for many automotive parts.

We describe the progress towards the industrial production of CFUBMSIP coatings for the metallic BPPs, using high rate reactive magnetron sputtering for transition metal nitrides (including CrN, TiN and ZrN) and carbon-based coatings (from elemental metal and solid graphitic magnetron sputtering targets). The characterisation of the coatings, in terms of their properties, relevant to the PEMFC application is described, and future developments are discussed.

3:30pm **A3-2/F8-2-7 Silica-Based Hydrophilic Bipolar Plate Coatings for PEM Fuel Cells.** *G. Dadheech (gayatri.dadheech@gm.com), Blunk*, General Motors, US

Metal Bipolar plates are getting widely popular due to their fast and easy high volume manufacturing. One of the metals of choice is stainless steel materials which have good corrosion stability due to the naturally occurring native oxide on its surface. However, stainless steel offers a high contact resistance when connected in series, and its surface energy is not conducive in removal of product water from the cell, which has a water contact of 65 (+/-) 5 degrees. Water removal is very important to avoid potential flooding at the electrode and eventual failure of the cells. Bipolar plate hydrophilicity is desired for effective water management and fuel cell stack operational benefits, such as voltage stability at low powers. Results on the durability of

silica-based hydrophilic coatings in PEM fuel cells for enhanced water management would be discussed in this talk.

3:50pm **A3-2/F8-2-8 Surface morphology and catalyst activity of Sn-Pt nanoparticles coated on anodizing aluminum oxide.** *C.C. Chen, C.L. Chen, Y.S. Lai* (*yslai@nzu.edu.tw*), National United University, Taiwan

In this work, we present the characteristics of Sn-Pt nanoparticles on the AAO templates anodized by various electrolytes and pore widening process. The results suggest that the specific surface area increases with the deposition of Sn nanospheres. The growth of Sn nanospheres deposited by sputtering is dependent on the surface roughness and the deposition time. The contact angle between Sn nanospheres and the AAO surface increases with the increase of surface roughness. The thickness of the Pt coating determined by angle-resolved X-ray photoelectron spectroscopy is about 2.7 nm, equivalent to a Pt loading of 5.79 mg/cm². As a result, the Sn-Pt nanospheres on phosphoric anodized AAO show the largest electrochemical activity area (EAA) of 57.6 m² Pt/g Pt. In addition, the Sn/Pt nanospheres on oxalic anodized AAO show the EAA of 38.6 m² Pt/g Pt. Both of the EAA values are larger than that of Sn-Pt nanospheres deposited on Si wafer.

Hard Coatings and Vapor Deposition Technology Room: Royal Palm 4-6 - Session B2-2

CVD Coatings and Technologies

Moderator: S. Ruppi, Walter AG, Germany, F. Maury, CIRIMAT, France

1:30pm **B2-2-1 CVD – Opportunities and Challenges.** *H. Holzschuh* (*helga.holzschuh@sucotec.ch*), SuCoTec AG, Switzerland **INVITED**

Although the Chemical Vapor Deposition (CVD) technique is 160 years old there are still opportunities and challenges. The tool manufacturing industries have generated a growing demand for novel material applicable for large scale production.

Due to advances in CVD technology the transfer of new coating materials from lab scale to production size is made possible. These advances allow us to question results generated in the last decades of CVD. They will give rise for better understanding of the CVD processes and consequently it will give new chances for novel coatings.

Because of its large application potential the main focus of this work will be on hard materials. A review of state of the art coatings and post treatments in tool manufacturing industries will be given. But what will be the next challenges for CVD?

2:10pm **B2-2-3 SiC coatings grown by liquid injection chemical vapor deposition using single source metalorganic precursors.** *G. Boisselier, F. Maury* (*francis.maury@ensiacet.fr*), CIRIMAT, France, *F. Schuster*, CEA, France

Silicon carbide is an attractive material used for instance as protective ceramic coating or as functional layer in electronic devices. As a result, there is a great interest for growth processes aiming low temperatures, high deposition rates, large-scale capacity, and other constraints imposed by the application. To meet such requirements, SiC coatings have been grown in a horizontal hot wall chemical vapor deposition reactor assisted by pulsed direct liquid injection (DLI-CVD) using metalorganic compounds as single sources. Commercial 1,3-disilabutane and polycarbosilane were used as 1:1 Si:C liquid precursors. Amorphous and stoichiometric SiC coatings were deposited on various substrates in the temperature range 650- 750 °C and under a total pressure of 5-50 Torr. Thickness gradients due to the temperature profiles and the precursor depletion were observed in the reactor axis but the thickness uniformity can be improved as a function of the deposition conditions. Growth rates as high as 90 µm/h were obtained using pure precursors. The injection of toluene solutions significantly reduces the deposition rate and allows a better control of the growth rates and of the microstructure of coatings. In that case, they exhibit a smooth surface morphology and a very dense structure. Under the explored conditions (reactor temperature and dwelling time of reactive species) the decomposition rate of toluene was found negligible. As a result, the presence of solvent vapor in the CVD reactor is not a source of carbon contamination for the SiC coatings that keep the 1:1 stoichiometry. The influence of the substrate temperature, the solvent and the nature of precursor used in this DLI-CVD process is discussed and preliminary properties are presented.

2:30pm **B2-2-4 Multilayer Diamond Coatings: Theory, Implementation in Production and Results in different Applications.** *J.C. Bareiss* (*christian.bareiss@cecon.de*), *W. Koelker, C. Schiffers, M. Weigand, O. Lemmer*, CemeCon AG, Germany

Since many years diamond coatings are a well established technique to enhance the lifetime of cemented carbide tools in the machining of extremely abrasive materials like graphite, carbon fibre reinforced plastics (CFRP) and some aluminum alloys. The main advantage of crystalline diamond films in machining applications is their outstanding hardness and durability, but these properties also come along with an enormous brittleness of diamond coatings. So for further improvement of the coating and tool lifetime, we have to understand first the different failure mechanisms, which may lead to damages and delaminations of the diamond coating. Typical damages in diamond coatings during machining are the formation of small cracks in the film, which may expand along the grain boundaries and cause film delamination in large areas according to the brittleness of diamond.

The CemeCon AG developed Multilayer CVD diamond coatings to combine the unique durability of diamond coatings on cemented carbide tools in machining performances with an enhanced tolerance to small cracks and damages in the diamond film without catastrophic failure. These multilayer diamond coatings are alternating layers of tough micro-crystalline and smooth nano-crystalline films. The achieved difference in crystal size between these two types enables a homogeneous dissipation of the initial crack energy by continuous change of the crack growth direction as shown in the figure. The implementation of these multilayer coatings in the machining of the most challenging materials like CFRP led to a further tool performance improvement compared to completely micro- or nano-crystalline diamond films.

CemeCon will present the theory of crack growth in these multilayer coatings and some examples of the diamond film performance in industrial applications.

2:50pm **B2-2-5 Adhesion of the DLC film on iron based materials as a function of gradient interlayer properties.** *D. Baquião, G. Faria, L. Silva Junior*, Institute for Space Research, Brazil, *L. Bonetti*, Clorovale Diamantes S.A., Brazil, *E. Corat, V. Trava-Airoldi* (*vladimir@las.inpe.br*), Institute for Space Research, Brazil

Diamond-like Carbon (DLC) films have attracted considerable interest over due to their high hardness, low friction coefficient, high wear resistance, high thermal conductivity, high elastic modulus, chemical inertness, biocompatibility, and more recently because of the real possibilities of deposition inside of the long iron based tubes for unlimited applications. In this case very adherent DLC films can give to scientific and development areas special opportunities to solve some problems related to transportation of aggressive liquids like petroleum based and other minerals. The major disadvantage of hard DLC film deposition is a relatively low adhesion of these films on iron based substrates. To overcome the low adhesion problems of these films on iron based substrates, different coating concepts have been proposed, normally on high temperature condition, which is not appropriated for iron based material structure. In this work it was proposed an interlayer, obtained at low temperature by using low energy ion implantation, emerging from the bulk of the substrate and overlapping with DLC films. A convenient unique body of substrate-DLC films with mechanical and tribological gradient properties near substrate surface was obtained and related to its higher adhesion, lower stress, and hardness. The interlayer and DLC films at very high growth rate were obtained by using an enhanced asymmetrical bipolar PECVD DC pulsed power supply system. The adhesion and hardness were evaluated by scratching test and nano indentation, respectively. Also, a simulation of the interlayer gradient by using TRIM/SRIM software for low energy ion implantation was obtained with good agreement with experimental data.

3:10pm **B2-2-6 Effect of the carrier gas flow rate on boron-doped diamond synthesis using mode-conversion type microwave plasma CVD.** *H.S. Shimomura* (*zephyros44@gmail.com*), *Y. Sakamoto*, Chiba Institute of Technology, Japan

Although diamond is well known an electrical insulator with a resistivity of the order of 10¹⁶ Ω · cm, it is changed to the semiconductor by inclusion of the dopant such as boron or phosphorus. Generally, diborane (B₂H₆) or trimethyl-boron {B(CH₃)₃} are used as B sources to synthesize boron-doped diamond. However, these dopants are toxic to humans. On the other hand, trimethyl-borate {B(OCH₃)₃} is safety, against to B₂H₆ or B(CH₃)₃. The investigation was carried on the effect of the carrier gas flow rate for the boron-doped diamond synthesis using mode-conversion type microwave plasma CVD.

The boron-doped diamond films were synthesized using mode-conversion type microwave plasma CVD apparatus. The Si substrate was scratched by diamond powder and then cleaned ultrasonically in acetone solution.

Reaction gases were used CH₄ (15 SCCM) and H₂ (100 SCCM). Vapor of B(OCH₃)₃, the boron source, was carried by H₂ carrier gas into the vacuum chamber with its flow rate of 1 to 6 SCCM. Pressure was 20.0 kPa and microwave power was 1.0 kW. Reaction time was fixed to 3 h. The surface and cross sectional morphologies of deposits were observed by SEM. Qualities of the deposits were estimated by Raman spectroscopy. Electrical resistivities were measured by the four-point probe method.

As a result of the SEM observation, the grain sizes of deposits were 1 to 3 μm . The maximum thickness of 6 μm was obtained for carrier gas flow rate ; 3 SCCM. From the Raman spectra of the deposits, the broad peak at about 500, 1230 cm^{-1} and the weak peak at 1333 cm^{-1} were observed for each samples. These peaks due to including high concentration of boron in the films. In addition, the intensities of the peaks at 1333 cm^{-1} were decreased with increasing of the carrier gas flow rate. As a result of the electrical resistivity measurements by the four-point probe method, the electrical resistivities of boron-doped diamond films decreased with increasing of carrier gas flow rate. The minimum electrical resistivity of $2.5 \times 10^{-1} \Omega \cdot \text{cm}$ was obtained for carrier gas flow rate ; 6 SCCM.

As a conclusion, the boron-doped diamond films were fabricated with each carrier gas flow rates. In the Raman spectra of the films, the peaks caused high boron inclusion were observed.

3:30pm B2-2-7 Low temperature chemical vapor deposition of boron-carbon films for use in neutron detectors, H. Pedersen (*henke@ifm.liu.se*), Linköping University, Sweden, **C. Höglund**, European Spallation Source ESS AB/ Linköping University, Sweden, **J. Birch, J. Jensen, A. Henry**, Linköping University, Sweden

A novel design for neutron detectors based on the isotope ¹⁰B instead of ³He has been suggested by the European Spallation Source (ESS), to overcome the very limited availability of ³He. In the detector design, very large area aluminum blades are coated with a thin film containing high amounts of ¹⁰B. ¹⁰B₄C was chosen as the thin film material instead of pure ¹⁰B, since it is easier to handle in a deposition process and due to its high resistance towards oxidation and wear. Here we demonstrate the synthesis of thin, amorphous, boron-carbon films at low temperature (400-600 °C), by thermally activated CVD using the organoborane triethylboron, B(C₂H₅)₃, (TEB) as single precursor. Since the neutron detectors will be based on aluminum, there is an upper temperature limit of approximately 600 °C, which limits a number of possible CVD-processes and also the aluminum substrate prevents the use of BCl₃ as boron precursor. Deposition by TEB is done on both single crystalline Si (100) substrates and aluminum plates; the deposition rate at 600 °C was close to 1 $\mu\text{m/h}$ in argon and 0.35 $\mu\text{m/h}$ in hydrogen. The film density, as measured by X-ray reflectivity (XRR), for films deposited at 600 °C in hydrogen was 2.42 g/cm³ (97 % of bulk B₄C) and 2.14 g/cm³ (86 % of bulk) for films deposited at 600 °C in argon. The atomic content of the deposited films were analyzed by Time of Flight Elastic Recoil Detection Analysis (ToF-ERDA), films with B/C-ratio of 4.6 and 3.6 were deposited at 600 °C in hydrogen and argon respectively, the hydrogen content in the films was 3-4 at%, regardless of deposition ambient. Both the film composition and film density was found to vary significantly with deposition temperature and deposition ambient. Based on our results, a deposition mechanism for boron-carbon films from TEB, where the TEB molecule is decomposed to BH₃ and hydrocarbons, is suggested.

3:50pm B2-2-8 Synthesis of diamond/carbon nanotube composite thin films by chemical vapor deposition, L. Yang, Q. Yang (*qiaoqin.yang@usask.ca*), **Y. Li, Y. Tang, C. Zhang, L.L. Zhang**, University of Saskatchewan, Canada

Diamond/Carbon nanotube (CNT) composite thin films have been successfully synthesized on silicon wafers using both microwave plasma enhanced chemical vapor deposition and hot filament chemical vapor deposition (CVD) technique. Iron was used as catalyst for CNT growth, and a mixture of CH₄ and H₂ gases was used to grow both diamond and CNTs. The synthesized thin films were characterized by Raman spectroscopy, transmission electron microscopy, scanning electron microscopy, X-ray diffraction, nanoanalyzer, and field electron emission measurements. The results show that diamond was deposited with high nucleation density and high purity, and the CNTs synthesized can be either randomly distributed or vertically aligned depending on the deposition conditions. The results has demonstrated that composite films with well aligned CNT arrays and nanocrystalline diamond can be achieved and the films exhibit superior field electron properties including large field enhance factor, excellent current stability and very low turn on field.

4:10pm B2-2-9 Effects of ammonia/acetylene mixtures on the properties of carbon films prepared by thermal chemical vapor deposition, L.H. Lai, S.T. Shiue (*stshiue@dragon.nchu.edu.tw*), National Chung Hsing University, Taiwan

When ammonia is added in acetylene to form carbon films using thermal chemical vapor deposition, effects of different ammonia/acetylene ratios on the deposition rate and microstructures of carbon films are investigated. The deposition temperature, working pressure, and deposition time of the thermal CVD process were set to 1113 K, 8 kPa, and 25 min, respectively. The total mass flow rate of acetylene and ammonia were kept at 40 cm³/min, and five kinds of carbon films were prepared with the ammonia/acetylene ratio of 0, 4/36, 8/32, 12/28, 16/24, and 20/20. Experimental results indicate that the deposition rate of carbon films decreases as the ammonia/acetylene ratio increases. The mean crystallite size and ordered degree of carbon films increase with increasing the ammonia/acetylene ratio. Moreover, when the ammonia/acetylene ratio increases, the carbon films have more sp³ carbon atoms and shift to diamond-like. Few nitrogen and hydrogen atoms are incorporated into carbon films. The deposition rate of carbon films is proportional to the partial pressure of acetylene with a power of about eighth order, and thus, the pyrolysis of acetylene with added ammonia is controlled by the adsorption process of sixteen-carbon species on the substrate. The results of thermal CVD carbon deposition using acetylene and ammonia are compared with those using acetylene and nitrogen.

4:30pm B2-2-10 Hollow-Cathode Deposition of Thin Films Via Metal Hydride Formation and Decomposition, S. Muhl (*muhl@unam.mx*), Universidad Nacional Autónoma de México - Instituto de Investigaciones en Materiales, Mexico, **L. Lopez**, IIM-UNAM, Mexico, **Y. Pena-Rodriguez**, Autonomous University of Madrid, Spain

Approximately 30 to 40 years ago the group of Stan Vepřek of the University of Zurich described that thin films of polycrystalline silicon could be prepared utilizing a reversible chemical reaction. In their paper they described how pieces of silicon were exposed to a low-pressure high-density hydrogen plasma promoting the formation of volatile silicon hydride, this was then transported within the reactor to a hot substrate which caused the decomposition of the hydride and the deposition of the silicon film.

Hydrogen plasmas have also been used for chemical etching of various materials and, for example, in the case of the deposition of diamond films the preferential etching of sp² bonded carbon is considered to be of fundamental importance.

In this paper we describe the etching of a metal (Mo or Ni) by hydrogen which was plasma-activated in a RF hollow cathode where the water-cooled cylindrical cathode was lined with the appropriate metal. The metal hydride vapour generate in the plasma was directed to quartz substrates which were maintained temperatures in excess of 300 °C. The metal hydride was thermal decomposed and a thin film of the metal was deposited. A special substrate heater was constructed such that four quartz substrates could be simultaneously exposed to the metal hydride vapour, but with each substrate at a different temperature; each approximately 20°C less than the neighbouring one. In this way, depositions under identical conditions could be carried out at the same time but at four different temperatures. We report the deposition rate as a function of the substrate temperature and the RF plasma power applied to the hollow cathode.

Hard Coatings and Vapor Deposition Technology Room: Royal Palm 1-3 - Session B6-2

Coating Design and Architectures

Moderator: C. Mitterer, Montanuniversität Leoben, Austria, M. Stüber, Karlsruhe Institute of Technology, Germany

1:30pm B6-2-1 A Knowledge-Based Approach for Optimized Coating Architecture, R. Daniel (*Rostislav.Daniel@unileoben.ac.at*), **J. Keckes, C. Mitterer**, Montanuniversität Leoben, Austria **INVITED**

Physical properties of nanocrystalline thin films are strongly related to their structure. It, in turn, depends on the deposition conditions, which affect atomistic processes acting during film growth. An understanding of the growth-structure-property relations in thin solid films is thus crucial in optimizing their performance. The attempt of this study is to reveal the origin of depth-profile variations in film texture, morphology, stress state and thermal properties based on the evolutionary nature of the film structure due to competitive growth. We will demonstrate how the variation in the stress state and thermal properties is related to the volume fraction of grain boundaries, which typically develops in nanocrystalline films to a different

extent depending on the actual growth stage. The role of weakly bonded atoms of the interfacial area will be discussed with respect to the development of intrinsic and thermal stresses, which are related to the efficiency of defect generation by incident particles from the deposition flux, the incorporation of an excess of weakly bonded surface adatoms in grain boundaries, the degree of interaction between adjacent grains during film growth and thermal expansion. Based on these findings, a guideline how to tailor the stress state and stress gradients in nanocrystalline films by their controlled growth will be given. Moreover, a concept for enhancement of mechanical properties and wear resistance by structural design of single and multilayered coatings based on nanoindentation experiments and analytical modeling will be discussed.

2:10pm B6-2-3 Gradient chemical composition in layered pulsed reactive sputtered coatings for decorative purposes, A. Cavaleiro (albano.cavaleiro@dem.uc.pt), N.M.G. Parreira, University of Coimbra, Portugal, T. Polcar, University of Southampton, UK, T. Kubart, Uppsala University, Angstrom Laboratory, Sweden, M. Vasilevskiy, University of Minho, Portugal

A new design of decorative coatings will be presented. The coatings have a multilayer design consisting of alternating metallic W and W-O layers. The coatings were deposited by magnetron sputtering from a tungsten target and pulsing the oxygen as reactive gas. The controlled injection of the reactive gas can produce a concentration profile gradient from pure tungsten to tungsten trioxide, determining the final apparent colour of the coating. To this gradient layer corresponds a graded refractive index.

A dynamic sputtering model was built to simulate the growth of the coating during the reactive gas pulsing which was validated by direct measurement of the gradient of the oxygen content in the deposited coatings. By depositing monolithic coatings with increasing oxygen coatings it was possible to determine the optical properties for each individual coating and, thus, the gradient of the optical properties in the multilayer film. These results were used for an optical model allowing the optical properties of the deposited tungsten oxide layer to be described, again validated by experimental analysis. This procedure allows the deposition of coatings with the desired colour by using the models to finding the optimal oxygen pulse parameters. In this way, a suitable gradient chemical composition layer will be deposited to which corresponds a specific refractive index gradient which will give rise to a specific colour. This proposed method can be easily applied to almost any metal/metal oxide system.

2:30pm B6-2-4 Investigation of the nucleation behavior of oxides synthesized by reactive arc evaporation from Al, Cr and Al-Cr targets, M. Döbeli, ETH, Zürich, Switzerland, J. Ramm (juergen.ramm@oerlikon.com), H. Rudigier, OC Oerlikon Balzers AG, Liechtenstein, J. Thomas, Leibniz-Institut für Festkörper- und Werkstofforschung, Germany, B. Widrig, OC Oerlikon Balzers AG, Liechtenstein

Binary and ternary oxide coatings can be synthesized by reactive arc evaporation. The nucleation and formation of the oxides proceed under non thermal equilibrium conditions. More detailed investigations are necessary to understand the first steps in oxide synthesis which are especially important for the coating adhesion at high temperatures and most probably also for the formation of a temperature stable crystal structure. Cemented carbide substrates were pre-treated by metal ion etching or deposition, respectively. Targets of aluminum, chromium and composite Al-Cr targets with a composition of Al(70at.)/Cr(30at.%) were utilized to produce pure metallic vapour, i.e. without admixtures of reactive or inert gases. The substrate bias was varied between 50 V and 800 V and the composition and depth profiles of the condensed metal vapour and mixing with the substrate surface atoms were measured by ion beam analysis (RBS, ERDA). TRIDYN simulations are utilized to compare the effect of the surface bombardment with Cr and Al metal ions with the simultaneous Al-Cr ion bombardment obtained from the composite target. Oxide growth was initiated on a metal layer thickness of 20 nm and compared with the oxides synthesized at substrate surfaces for which no layer growth occurs (controlled by the substrate bias). The crystal structure of the layers was investigated by electron beam diffraction in cross sectional TEM. The different behavior in the nucleation process is discussed with respect to target material and oxidation kinetics.

2:50pm B6-2-5 Phase stability of TiAlNO, M. to Baben, J. Schneider (schneider@mch.rwth-aachen.de), Materials Chemistry, RWTH Aachen university, Germany

INVITED

Sarakinos et al. has recently highlighted the importance of defects for the phase formation in high power pulsed sputtered HfNO thin films.[1]

Using ab initio calculations, the role of defects in TiAlN as well as oxygen incorporation in TiAlN were studied. Vacancies, substitutions, interstitials

and combinations thereof in different configurations have been investigated in terms of crystal energies, enthalpies of formation and bulk moduli.

The energy of mixing of TiAlN and hypothetical isostructural TiAlO is negative which may imply the possibility to form TiAlNO in NaCl structure. The influence on enthalpy of formation of metal vacancies is calculated as well as on enthalpy of formation of interstitial oxygen. It is shown that oxygen on the nitrogen sublattice leads to spontaneous incorporation of interstitial oxygen. Possible reasons are discussed.

Thin films of TiAlNO are prepared using high power pulsed magnetron sputtering of a TiAl target in mixed nitrogen and oxygen atmosphere. It is shown that a high oxygen flux leads to the formation of amorphous films. The influence of temperature on structure, and elastic properties is determined. Furthermore, thermal stability and thermogravimetric data are presented.

[1] K. Sarakinos, D. Music, S. Mráz, M. to Baben, K. Jiang, F. Nahif, A. Braun, C. Zilkens, S. Konstantinidis, F. Renaux, D. Cossement, F. Munnik, and J.M. Schneider: On the phase formation of sputtered hafnium oxide and oxynitride films, [<http://jap.aip.org/japiau>] 108 (1) (2010) 014909-1.

3:30pm B6-2-7 On the formation of cubic and corundum structured (Al,Cr)₂O₃ coatings synthesized by cathodic arc evaporation, H. Najafi (hossein.najafi@epfl.ch), A. Karimi, EPFL, Switzerland, P. Dessarzin, M. Morstein, Platit AG, Switzerland

In previous ICMCTFs, we have presented the formation and structure-property relation in Al-Cr-O-N oxynitride system. In this paper we report on the latest results on this system which correspond to the growth of *fcc*-(Al,Cr)₂O₃ at early stage of deposition which gives rise to the corundum structure *a*-(Al,Cr)₂O₃ subsequently. This transition has a significant effect on film properties. Although the formation of *a*-(Al,Cr)₂O₃ is frequently observed under our deposition conditions, the occurrence of *fcc*-(Al,Cr)₂O₃ is rather unexpected. First a cubic interlayer which was used for adhesion of coating was suspected for epitaxial growth of *fcc*-(Al,Cr)₂O₃. To remove this effect an interlayer with hexagonal structure was applied instead of cubic one and same growth behaviour was observed. XPS studies and simulation of XRD diffractions showed that the formation of *fcc*-(Al,Cr)₂O₃ with the (200) preferred orientation can be originated from the presence of a metastable CrO films with a B1 structure. The replacement of Cr²⁺ by Al³⁺ results in the development of vacancies in the Cr positions that leads to the stabilization of *fcc*-(Al,Cr)₂O₃. However, as the thickness of coating increases, the occupation of the antibonding orbitals leads to a loss of structural stability and, thus, the system will transform into the thermodynamically stable *a*-(Al,Cr)₂O₃. In this paper the formation mechanism of the *fcc* and corundum (Al,Cr)₂O₃ will be discussed with respect to structural properties.

3:50pm B6-2-8 Parametric Study on the Effect of Reactive Nitrogen on the Growth, Morphology and Optical Constants of ZrO_xN_y Thin Films, V. Ramana (rvchintalapalle@utep.edu), M. Hernandez, University of Texas at El Paso, US, L. Campbell, Air Force Research Laboratory, US

Zirconium-based oxides and nitrides, which exhibit quite interesting and diverse structures, properties and phenomena, have potential for a wide range of scientific and technological applications. The outstanding chemical stability, electrical and mechanical properties, high dielectric constant, and wide band gap of Zr-oxide makes it suitable for several industrial applications in the field of electronics, magneto-electronics, structural ceramics, and optoelectronics. In this work, ZrO_xN_y thin films were deposited on silicon (100) and quartz substrates employing RF magnetron sputtering technique under variable reactive nitrogen pressure. Parametric and characterization study was performed on the grown carried out on ZrO_xN_y thin films employing X-ray photoelectron spectroscopy (XPS), grazing incidence X-ray diffraction (GIXRD), scanning electron microscopy (SEM), atomic force microscopy (AFM), and ex-situ spectroscopic ellipsometry (SE). The effect of reactive nitrogen during deposition on the structure and optical properties is evaluated. In SE, ZrO_xN_y thin films were modeled as an isotropic and homogeneous layer and the optical constants (refractive index, *n*, and extinction coefficient, *k*) were derived. Thickness values determined from SE analysis were in the range ~5-40 nm. The results indicate that the crystal structure, surface morphology, and the optical constants are sensitive to the reactive nitrogen environment. The entire spectrum of results obtained by the various methods of characterization aforementioned and correlation will be presented and discussed.

4:10pm **B6-2-9 Stage-gate approach for the development of corrosion and erosion resistant PVD multilayer coatings**, **J. Ellermeier** (ellermeier@mpa-ifw.tu-darmstadt.de), **U. Depner**, **T. Troßmann**, **M. Oechsner**, Zentrum für Konstruktionswerkstoffe - TU Darmstadt, Germany, **K. Bobzin**, **N. Bagcivan**, **S. Theiss**, **R. Weiß**, Surface Engineering Institute - RWTH Aachen University, Germany

Many components need a protection against superimposed corrosion and wear (abrasion, erosion) loading, e.g. in off-shore applications. The goal of the research has been to develop PVD multilayer coating by systematically altering the layer architecture in order to protect components against corrosive environments and erosive loadings. The development of the PVD multilayer coatings was staged in four phases. These are investigations of corrosion-, wear-, combined erosion corrosion-resistance and verification of the development, for example by field testing.

This paper deals with first phase of the development, i.e. the investigation of the corrosion resistance of the PVD multilayer coating. Polarisation tests have been identified to be an adequate tool to investigate the different multilayer architectures.

The investigated coatings were applied on a plasma nitrided mild steel and consist of a CrN/CrCN interlayer, different numbers of graded (g) CrCg/aC layers and an a-C:H top layer. The investigations were focused on the necessary number of CrCg/aC layers and the thickness of the a-C:H top layer to achieve excellent corrosion protection. In addition to the influence of the architecture various substrate pre-treatments like substrate nitriding and polishing have been investigated regarding their potential to improve the corrosion resistance as well.

As a result of the PVD multilayer development no corrosion could be detected when immersing in artificial seawater after more than 500 hours.

The results of the polarization tests were assisted by metallographic and SEM investigations and GD-OES analyses.

4:30pm **B6-2-10 Biomimetics in thin film design – Enhanced properties by multilayer coatings and nanostructured surfaces**, **J.M. Lackner** (juergen.lackner@joanneum.at), **W. Waldhauser**, Joanneum Research Forschungsges.m.b.H., Institute of Surface Technologies and Photonics, Functional Surfaces, Austria, **L. Major**, Polish Academy of Sciences, Institute for Metallurgy and Materials Science, Poland, **C. Teichert**, Montanuniversität Leoben, Austria, **P. Hartmann**, Joanneum Research Forschungsges.m.b.H., Institute of Surface Technologies and Photonics, Functional Surfaces, Austria

Biological materials are highly organized from the molecular to the nanoscale, microscale and macroscale in a hierarchical manner. Material and surface properties result from a complex interplay between the surface structure and the morphology, being optimized by evolution for multifunctionality in their natural habitat. Understanding these functions and mimicking them in biologically inspired design using nanotechnology offers a wide variety for smart materials. Elastic instability based wrinkling of thin films on soft polymer substrates as well as hard-soft phase multilayer coatings are two examples for biomimetic design by our PVD techniques, based on plant leave ridges, cell membrane blebs or mollusc shells, respectively. Tribological behaviour is drastically enhanced by the application of Ti, TiN, Cr, CrN, and diamond-like carbon based nanoscaled multilayer structures on soft substrate materials (austenitic steel, fibre reinforced polymers), deposited by magnetron sputtering and pulsed laser deposition techniques. These enhancements are shown to be based on plastic deformation in nanostructures down to a few nanometers thick metal layers improving the compound toughness. Fractal (nano-)wrinkles originating from intrinsic compressive film growth stresses enhance surface wetting and friction behaviour of Ti, TiN and diamond-like carbon coated polyurethane polymer surfaces.

Fundamentals and Technology of Multifunctional Thin Films: Towards Optoelectronic Device Applications

Room: Sunset - Session C5-1/F7-1

Polarisation Phenomena in Thin Films and Devices

Moderator: D. Holec, Montanuniversität Leoben, Austria, S. Moram, University of Cambridge, UK

1:30pm **C5-1/F7-1-1 Recent Advances in the Thin Film Electro-Acoustic Technology**, **I. Katardjiev** (Iliia.Katardjiev@Angstrom.uu.se), **V. Yantchev**, Uppsala University, Angstrom Laboratory, Sweden **INVITED**
The classical Electro-Acoustic (EA) technology is a highly developed technology today with applications ranging from telecom, medical, military, scientific, radio and TV, sensors, pharmaceutical industry, etc. Only the

telecom industry consumes billions of RF filters annually. It is based on the use of single crystalline piezoelectric materials such as quartz and others. The combination of acoustic waves and low losses in these materials allows the fabrication of compact, low cost devices with extreme performance. Typical EA devices are RF filters, resonators, oscillators, delay lines, various sensors (physical, chemical and biochemical), etc. Amongst the major drawbacks of the EA technology are the limited choice of piezoelectric materials (and hence properties) as well as its incompatibility with the IC technology. Further, the explosive development of mobile communications in recent years has necessitated the use of larger bandwidths thus requiring higher frequencies of operation. This is where the classical EA technology becomes expensive due to increased fabrication costs.

In view of the requirements for high bandwidth, miniaturization and low cost, the so called thin film electro-acoustic (TEA) technology has been recently developed for applications in the microwave region. It makes use of thin piezoelectric films that are grown using the planar technology which makes the IC and the TEA technologies fully compatible with each other. The material of choice so far is AlN while others are currently being developed. The deposition methods employed (PVD, CVD, etc) allow tuning various properties of the thin films (composition, crystallographic structure and texture, roughness, density, stress, etc) which in turn allows to tailor these properties in view of the application in mind. Thus, for instance, the design of filters with a large bandwidth requires the synthesis of highly c-textured AlN films, while in view of resonator operation in liquids (biochemical sensors) excitation of shear waves is needed which in turn requires either films with a c-axis tilted under a certain angle relative to the surface normal or even better, highly a-textured films. In a different perspective, certain applications may require high piezoelectric constants while others may require low losses (both acoustic and electrical) or to exhibit high functional stability with temperature variation, etc. In other words, the race is on for the synthesis of thin piezoelectric films with various functional properties in view of the broad range of potential applications.

The talk will focus on recent advances in the area in terms of both film synthesis and application development.

2:10pm **C5-1/F7-1-3 Asymmetric electrical properties for dual-gate InGaZnO TFT under gate bias and light illumination**, **T.C. Chen** (a49136@gmail.com), NSYSU, Taiwan

The electrical properties and degradation behavior of a-IGZO TFT with dual gate structure was investigated in this paper. The increase of the on-current for dual-gate TFT compared with single gate TFT indicates that the dual-gate structure is applicable for the current-driven AMOLED display. With dual gate structure, the IGZO TFT exhibits asymmetric electrical properties under top gate or bottom gate operation. For bottom gate operation, the application of the negative bias by top gate will induce a parallel V_t shift, whereas the positive top gate bias merely increase the on current. For top gate operation, the different electrical properties compared with the bottom gate operation indicate that the gate control area dominates the difference under measurement. Furthermore, the instability of dual-gate IGZO TFT under light illumination was investigated. The asymmetric light sensitivity under bottom gate and top gate operation was caused by the illumination and the gate control area. With the different light sensitivity for top and bottom gate operation, the dual gate IGZO TFT can be used as a light sensor and apply in the touch panel technology without Black Matrix in comparison with the a-Si TFT.

2:30pm **C5-1/F7-1-4 A systematic *ab-initio* study of the piezoelectricity in wurtzite nitride alloys: ScAlN, ScGaN, ScInN, YAlN, YInN**, **C. Tholander** (chtho@ifm.liu.se), **F. Tasnádi**, **I. Abrikosov**, Linköping University, Sweden

New types of piezoelectric materials need to be intelligently designed to further improve the performance of modern wireless telecommunication devices, satellites, sensors or optoelectronic devices together with opening new future commercial applications in biomedical engineering, neuroscience and bio-nanotechnology. Our recent physical explanation on the origin of the enhanced piezoelectric effect in wurtzite ScAlN alloys [1] has introduced a simple, free-energy landscape based phenomena in finding new materials with giant piezoelectric response. Here, we present a systematic *ab-initio* investigation of this strategy on several wurtzite IIIA-IIIB nitride alloys. The special quasirandom structure (SQS) approach provides a successful computational scheme to model substitutional random alloys and predict thermodynamics and, in case of special care, also mechanical and electronic properties. The here presented results will bring a refined understanding of the applicability of the free energy flattening phenomena in the wurtzite IIIA-IIIB nitride alloys and indicate more general rules/strategies in searching for new piezoelectric materials. These new rules and refined strategy will be introduced and discussed by our comparative study.

[1] F. Tasnádi, B. Alling, C. Höglund, G. Wingqvist, J. Birch, L. Hultman, and I. A. Abrikosov, Phys. Rev. Lett. **104**, 137601 (2010).

2:50pm **C5-1/F7-1-5 Investigation of the bias illumination stress for an InGaZnO TFT with and without Al₂O₃ passivation layer**, S.Y. Huang (aramis8888@gmail.com), T.C. Chang, National Sun Yat-Sen University, Taiwan

In this paper, the Al₂O₃ passivation layer enhancing the illumination stable was investigated. The Al₂O₃ passivation layer suppresses the gas adsorption/desorption in the back channel of a-IGZO film. It induces the electrical property shows a more stability ($\Delta V_{th} < 0.5$ V) under illumination for 1000s. In contrast, no passivation device shows a larger negative V_{th} shift ($\Delta V_{th} \sim 5$ V) than the Al₂O₃ passivation device because the holes generated from light inducing electron-hole pairs react with the absorbed O₂⁻ to reduce into O₂ under illumination. In addition, this work presents the light-color-dependent negative bias stress (NBIS) effect on a-IGZO thin film transistors (TFTs) with the Al₂O₃ passivation layer. The colors of incident photon are varied from red to blue, that incident photon energies are all lower than the optical band gap of a-IGZO (3.2 eV). The experiment results show that the Al₂O₃ passivated devices present stable electrical behaviors under different incident lights ($\Delta V_T < 0.1$ V of dark and red, $\Delta V_T < 1$ V of green, and $\Delta V_T < 4$ V of blue), whereas the unpassivation devices exhibit observable negative shifts during NBIS ($\Delta V_T < 1$ V of dark and red, $\Delta V_T > 8$ V of green, and $\Delta V_T > 15$ V of blue). The degradation mechanism of the NBIS is dominated by the photo-excitation model. The subgap photon excitation occurs from the deep-subgap DOS inducing that the hole generates and traps in the insulator or IGZO/insulator interface under NBIS, resulting in the apparent negative V_{th} shift. However, the Al₂O₃ passivation device exhibits a slighter V_{th} negative shift than the no passivation device under NBIS due to the decrease of hole trapping. The hole trap decreases because the Al₂O₃ passivation layer decreases the deep-subgap density that results in the photo-excitation behavior decrease. Hence, Al₂O₃ is an effective passivation layer to suppress gas absorption on InGaZnO back channel and decrease photo-excitation behavior.

3:10pm **C5-1/F7-1-6 Control and Engineering of Spontaneous and Piezoelectric Polarisation in Nitride-based Nanostructures**, E. O'Reilly (eoin.oreilly@tyndall.ie), Tyndall National Institute; University College Cork, Ireland, S. Schulz, Tyndall National Institute, Ireland, M. Caro, Tyndall National Institute; University College Cork, Ireland **INVITED** III-nitride materials (InGaAlN) have direct energy gaps that cover the full spectral range from infra-red to UV, but there are significant challenges to their application, primarily due to the presence of strong built-in spontaneous and piezoelectric polarisation fields arising from the underlying wurtzite structure. As a consequence, III-nitrides are well established as blue laser and LED sources, but their efficiency drops rapidly both at longer (green/yellow) and at shorter (UV) wavelengths, due to these polarisation fields.

We consider several approaches being pursued to control the built-in potential, including growth on non-polar and semipolar substrates, use of polarisation-matched alloys and growth of III-N quantum dots (QDs). The design of any optoelectronic device relies on a good knowledge of material parameters. However, there remains controversy regarding several key III-N parameters, including the sign of the shear piezoelectric coefficient, e_{15} , the magnitude of the valence band deformation potentials (which determine light polarisation characteristics), and the influence of potential fluctuations in alloyed heterostructures. We address these issues, and their consequences for polarisation engineering and control.

We argue that $e_{15} < 0$, based on an analysis of QD structures grown on non-polar substrates, and on a comparison of wurtzite and (111)-oriented zinc-blende heterostructures. We then show that $e_{15} < 0$ allows the built-in potential to be significantly reduced by growth of QD rather than conventional quantum well nanostructures. Using current growth techniques, an InGa_{0.13}N QD in a GaN matrix can reduce the field in a visible emitter by up to 50%, allowing efficient emission to longer wavelengths, of benefit for yellow/green and white light sources.

For UV emitters, we show that careful choice of alloy composition can allow polarisation matching between well and barrier layers. Growth of III-N heterostructures on nonpolar and semipolar substrates can also minimize the potential drop across a quantum well structure over a wide spectral range, with the crystal anisotropy leading to linearly polarized light emission, potentially interesting for applications such as LCD backlight modules. Moreover, using a combination of density functional and valence force field calculations we show that there can be significant local polarisation potential fluctuations within an alloy layer, leading to carrier localization. We discuss the consequences of this localization and of inhomogeneous strain relaxation for recombination both in ideal c-plane and non-polar heterostructures.

3:50pm **C5-1/F7-1-8 Growth and characterization of magnetron sputtered wurtzite Y_xAl_{1-x}N thin films**, A. Zukauskaitė (agne@ifm.liu.se), G. Wingqvist, C. Tholander, F. Tasnádi, J. Birch, L. Hultman, Linköping University, Sweden

There is a recent interest to tailor the properties of group IIIA nitrides by alloying with group IIIB transition metal nitrides, both for optoelectronic and electroacoustic applications. For example, it has been shown for AlN alloyed with ScN that there is an increase in the piezoelectric response d_{33} [1] as well as electromechanical coupling [2]. The increase in d_{33} was theoretically predicted to be an intrinsic alloying effect [3] related to a metastable layered hexagonal phase of ScN. This brings a strong mismatch with the wurtzite group IIIA nitrides, so the challenge is to extend the obtainable composition range of such alloys. The solubility and stability of the alloys has been investigated for w-Sc_xAl_{1-x}N, results show elemental fluctuations on the nanoscale for $x=0.2$ [4]. YN possesses the same metastable phase as ScN [5], but has not yet been explored for alloying with group III nitrides. Preliminary theoretical predictions suggest increased softening of the material with addition of Y, but less pronounced increase in piezoelectric constant e_{33} as compared to ScAlN.

Here, we present experimental and theoretical results from growth and structural, electrical, as well as optical characterization of wurtzite Y_xAl_{1-x}N thin films with $0 \leq x \leq 0.2$. Dual reactive magnetron sputter deposition from elemental Y and Al targets was used to grow thin films onto Al₂O₃(0001) and Si(001) substrates in N₂/Ar discharge in an UHV chamber. ERDA showed that the films are stoichiometric with respect to the metal/N ratio and that they contain less than 2 at.% of impurities. XPS measurements show that the N1s peak is shifting towards lower energies with addition of Y. According to I-V and C-V measurements performed on Y_{0.13}Al_{0.87}N/TiN/Al₂O₃ structures, films show no leakage current, low dielectric dissipation and relative dielectric constant increases up to 11, as compared to 9 in a pure AlN sample. Results from optical measurements showing changes in the bandgap for different Y concentrations will be presented as well. Initial HRTEM studies show that films are polycrystalline and have a columnar microstructure. For films with $x=0.13$ there is no detectable elemental segregation according to STEM. XRD confirms that both lattice parameters c and a are affected when increasing Y concentration. The results follow preliminary theoretical predictions, thus suggesting that compound forming is a solid solution.

[1] M. Akiyama, et al., Adv. Mater. 21, 5 (2009).

[2] G. Wingqvist, et al., Appl. Phys. Lett. 97, 11 (2010).

[3] F. Tasnádi, et al., Phys. Rev. Lett. 104, 13 (2010).

[4] C. Höglund, et al., Physical Review B, 81, 22 (2010).

[5] Y. Cherchab, et al., Physica E, 40, 3 (2008).

4:10pm **C5-1/F7-1-9 Investigating Degradation Behavior of InGaZnO Thin-Film Transistors induced by Charge-Trapping Effect under DC and AC Gate-Bias Stress**, T.Y. Hsieh, T.C. Chang (tcchang@mail.phys.nsysu.edu.tw), T.C. Chen, M.Y. Tsai, Y.T. Chen, National Sun Yat-Sen University, Taiwan, F.Y. Jian, National Chiao Tung University, Taiwan, W.S. Lu, National Sun Yat-Sen University, Taiwan

This paper investigates the degradation mechanism of amorphous InGaZnO thin-film transistors under DC and AC gate bias stress. Comparing the degradation behavior at equal accumulated effective stress time, more pronounced threshold voltage shift under AC positive gate bias stress in comparison with DC stress indicates extra electron-trapping phenomenon occurs during the duration of rising/falling time in pulse. Contrarily, illuminated AC negative gate bias stress exhibits much less threshold voltage shift than DC stress, which suggesting the photo-generated hole does not has sufficient time to drift to the interface of IGZO/gate insulator and causing hole-trapping under AC operation. Since the evolution of threshold voltage well fits the stretched-exponential equation, the different degradation tendencies under DC/AC stress can be attributed to the different electron- and hole-trapping efficiencies, and this is further verified by varying pulse waveform.

4:30pm **C5-1/F7-1-10 Piezoelectric Response During Nanoindentation in Scandium Aluminum Nitride Alloy Thin Films**, E. Broitman (esbro@ifm.liu.se), A. Zukauskaitė, G. Wingqvist, P. Sandström, L. Hultman, Linköping University, Sweden

Recent theoretical calculations have revealed the origin of the anomalous, 400% increase of the piezoelectric coefficient in scandium aluminum nitride alloys [1]. In this work, the piezoelectric response during nanoindentation of Sc_xAl_{1-x}N ($0 \leq x \leq 0.2$) thin films has been investigated. Films of 250-500 nm thick were deposited by reactive magnetron sputtering from elemental Al and Sc targets onto Al₂O₃(0001) substrates with a conductive TiN(111) seed layer, at substrate temperatures in the range 400-800 °C. Microstructure and composition were analyzed by x-ray diffraction and transmission electron microscopy. Structural analysis confirms epitaxial

growth; all films are c-axis oriented and have a columnar structure, but the alloying of AlN with ScN results in a deterioration of the crystalline quality due to phase instabilities.

Nanoindentation with simultaneous measurement of load and electrical voltage was used to characterize the nanoscale electromechanical properties of the piezoelectric films. Testing was done by a TI-950 Hysitron Triboindenter configured to perform electrical measurements with a conductive Berkovich boron-doped diamond tip. For all compositions, the films show a linear relationship of the applied force to the generated voltage. For loads ranging from 0.1 to 11 mN, output maximum voltages from 2 to 60 mV were obtained, depending on applied forces and composition. Consistent values of generated voltages were measured after multiple force cycles with no hysteresis observed in the results. No influence of the nanoindentation loading rate on peak voltage generation was detected. The results were also correlated to data obtained by piezoresponse force microscopy (PFM).

[1] F. Tasnádi, B. Alling, C. Höglund, G. Wingqvist, J. Birch, L. Hultman, and I. A. Abrikosov, *Phys. Rev. Lett.* 104, 137601 (2010).

4:50pm C5-1/F7-1-11 Investigating the degradation behavior under Hot Carrier Stress for InGaZnO TFT with symmetric and asymmetric structure, M.Y. Tsai (baxiatwice@yahoo.com.tw), NSYSU, Taiwan

This letter studies the hot-carrier effect in indium-gallium-zinc oxide (IGZO) thin film transistors with symmetric and asymmetric source/drain structures. The different degradation behaviors after hot carrier stress in symmetric and asymmetric source/drain device indicate that different mechanisms dominate the degradation. Since the C-V measurement is highly sensitive to the trap state compared with the I-V characteristics, thus, the C-V curves are utilized to analyze the hot carrier stress induced trap state generation. Furthermore, the asymmetric C-V measurements (gate-to-drain capacitance, gate-to-source capacitance) are useful to analyze the trap state location. For asymmetric device structure, different source/drain structure under hot carrier stress will induce asymmetric electrical field and cause different degradation behaviors. In this work, the on-current and subthreshold swing (SS) degrade under low electrical field, whereas the apparent V_t shift occurs under large electrical field. The different degradation behavior indicates that the trap state generates under low electrical field and channel-hot-electron (CHE) effect occurs under large electrical field.

Tribology & Mechanical Behavior of Coatings and Engineered Surfaces

Room: Tiki Pavilion - Session E2-2

Mechanical Properties and Adhesion

Moderator: M.T. Lin, National Chung Hsing University, Taiwan, W. Clegg, University of Cambridge, UK, R. Chromik, McGill University, Canada, D. Bahr, Washington State University, US

1:30pm E2-2-1 Micromechanical testing at up to 700 °C and in vacuum, S. Korte (sandra.korte@cantab.net), University of Erlangen-Nürnberg, Germany, L. Shiyu, R. Stearn, W. Clegg, University of Cambridge, UK

Indentation and, more recently, microcompression are often used to characterise the mechanical properties of ceramics and hard coatings. However, although high temperature properties are often of interest, testing is rarely carried out above room temperature. This is due mainly to the technical difficulties encountered at elevated temperatures, in particular thermal drift and oxidation of the sample surface and indenter tip. In this paper, the adaption of a commercial nanoindenter to allow experiments in vacuum is shown. Testing at up to 700 °C has recently been demonstrated and results from nanoindentation and microcompression experiments on range of materials from soft metals to hard coatings will be presented to illustrate the capabilities of the technique and material specific phenomena observed in different testing geometries.

1:50pm E2-2-2 Characterization of a self assembled monolayer using a MEMS tribogauge, A. Vijayasai, T. Dallas (tim.dallas@ttu.edu), G. Sivakumar, C. Anderson, R. Gale, G. Ramachandran, Texas Tech University, US

A MEMS tribogauge was used for on-chip and in-situ characterization of nano-tribological phenomena (stiction, friction, and wear). The measurements were made on the sidewall surfaces on the tribogauge at the fourth structural polysilicon layer in the device. The device consists of two

orthogonally oriented comb-drive mechanisms that are used for both actuation and sensing functions. One actuator applies a normal load (F_n) to a contacting surface, while the other actuator induces a tangential load (F_t). A LabVIEW controlled AD7747 capacitance sensor is used to measure the position of the interacting surfaces. This data is converted into adhesive force information. The spatial resolution of the characterization apparatus is ± 10 nm.

Experiments were conducted with tribogauges with and without a self-assembled monolayer (SAM) coating. The SAM coatings being explored have either a fluorocarbon tail or a hydrocarbon tail group. The tribogauge with no SAM coating is UV/Ozone cleaned to remove organic contaminants, leaving behind -OH bonds on top of the MEMS surface (native oxide, SiO_2). The tribogauge characterization includes: measurement of baseline stiction force, static and dynamic coefficient of friction, and induced stiction force calculated after specific load cycles (F_{induced}). The UV/Ozone treated tribogauge was used to measure the baseline stiction force (F_{plasma}). Additional experiments showed that the induced stiction force increases in proportion to the increase in the number of load cycles, indicating erosion of the SAM coating and topographical changes to the interacting surfaces.

2:10pm E2-2-3 In-situ SEM mechanical testing for adhesion energy mapping of multilayered Cu wiring structures in integrated circuits, S. Kamiya (kamiya.shoji@nitech.ac.jp), N. Shishido, H. Sato, K. Koiba, Nagoya Institute of Technology, JST CREST, Japan, M. Omiya, Keio University, JST CREST, Japan, C. Chen, Nagoya Institute of Technology, Japan, M. Nishida, Nagoya Institute of Technology, JST CREST, Japan, T. Nakamura, T.S. Suzuki, Fujitsu Laboratories Limited, Japan, T. Nokuo, T. Nagasawa, JEOL Limited, JST CREST, Japan

INVITED

The local distribution of interface strength in a large scale integrated circuit (LSI) micro structure, which was not uniform nor the same as the average value obtained with conventional macro scale specimens, was investigated by applying a recently developed evaluation technique with a sub-micron range spatial resolution.

Three dimensionally stacked interconnect structures in LSIs frequently suffer from unexpected fracture, especially at the interfaces, due to stresses arisen in many steps of fabrication process. In spite of intensive efforts to avoid such damages, it still threatens the development process to push up the risk and thus the cost. The most likely reason for this frustrating situation could be that they are designed essentially on the basis of average strength data, obtained only from macro-scale specimens with blanket films of the composing materials by applying conventional techniques such as four point bending tests. For the case of micro-scale structures, there must be expected scatters of local strength, leading to weak spots from which cracks may extend. Therefore establishment of microscopic testing method was necessary to evaluate local strength distribution of interface, i.e., to map the strength of structural components with the same range of resolutions corresponding to the actual structure dimensions in LSI.

A dual beam system with a scanning electron microscope (SEM) and a focused ion beam (FIB) is further equipped with a nano-indenter for mechanical loading. In order to evaluate the interface adhesion energy between Cu damascene lines and cap layers, which is the weakest interface in such LSI interconnect systems, specimens were fabricated by FIB as blocks of the insulation layer with the dimensions down to sub-micron range. Fracture loads obtained by the experiment with the indenter under SEM observation were compared with the elastic-plastic interface crack extension simulations to determine the bonding energy, i.e. the toughness of interface. Furthermore, not only the toughness but also the crystallographic orientations of Cu at the points of experiment, which was expected to be a cause of difference in the strength, was mapped by using an electron beam back scatter (EBSD) analyzer installed in the system. The correlation among the toughness, crystallographic structure and configuration of interconnects was investigated in detail on the basis of those distribution maps with a sub-micron resolution, aiming at establishing a possible design scheme to avoid unexpected fracture during the fabrication process of LSI.

2:50pm E2-2-5 Preparation and Characterization of Super- and Ultrahard Nanocomposites, S. Veprek (stan.veprek@lrz.tum.de), M. Veprek-Heijman, Technical University Munich, Germany, A.S. Argon, Massachusetts Institute of Technology, US

In the first part of our presentation, we shall identify several serious inconsistencies and methodological mistakes in the presentation of Fischer-Cripps as far as we can identify them presently from the press release on his home page and from a manuscript available to us [1]. We shall further show that the hardness of the nc-TiN/a-Si₃N₄/TiSi₂ of about 80 to 100 GPa reported in our earlier papers (see [2] for a review) is supported by our indentation measurements as well as by scanning electron micrographs of the remaining indentations. We shall further briefly outline the issue of the

reproducibility of the preparation of these unique materials. The emphasis of our presentation will be, however, on the future ways which will assure the reproducible preparation of nc-TiN/a-Si₃N₄ and related nanocomposites in dedicated laboratory apparatuses as well as in large-scale industrial coating equipment, which will assure achieving high hardness, high resistance against brittle fracture, high thermal stability and oxidation resistance.

[1a] www.ibisonline.com.au/IBIS_News/PressReleaseAug11.pdf

[1b] A.C. Fischer-Cripps et al., submitted, as quoted in Ref. [1a]

[2] S. Veprek et al., *Thin Solid Films* 476 (2006) 1

3:10pm **E2-2-6 An expression to determine the Vickers indentation fracture toughness of Fe₂B layers obtained by the finite element method.** **A. Meneses-Amador**, Instituto Politécnico Nacional, Mexico, *I. Campos-Silva* (icampos@ipn.mx), SEPI ESIME Zacatenco, Mexico, *J. Martínez-Trinidad*, Instituto Politécnico Nacional, Mexico, *S. Panier*, Ecole des Mines de Douai, France, *G.A. Rodríguez-Castro*, *A. Torres-Hernández*, Instituto Politécnico Nacional, Mexico

A reverse analysis of the Vickers indentation fracture toughness was carried out to derive a numerical expression to estimate the fracture resistance of Fe₂B layers. The boride layers were formed at the surface of AISI 1018 steels by developing the powder-pack boriding process at temperatures of 1193 and 1243 K with 4, 6 and 8 h of exposure for each temperature. From the set of experimental conditions of boriding process, Vickers indentations were performed with applied loads of 0.49, 0.98, 1.96, and 2.9 N at 15 and 30 microns from the surface of borided steels, respectively. The crack lengths created from the corners of the Vickers indentation prints were analyzed in the Palmqvist crack regime with the aid of dimensional analysis and finite element method (ABAQUS software program), considering the residual stress field generated by the indentation loads in the boride layer. The numerical expression of the fracture toughness of the Fe₂B layer was estimated by the superposition technique, where the fracture resistance is a function of the elastoplastic properties of the layer, and with different crack lengths superimposed according to the residual stress field caused by Vickers indentation loads.

The results of the fracture toughness of the Fe₂B layer estimated by the finite element method were compared with the values obtained by traditional Palmqvist crack models proposed in the literature.

3:30pm **E2-2-7 Mechanical properties of FeB and Fe₂B layers estimated by Berkovich nanoindentation on tool borided steels.** **G.A. Rodríguez-Castro**, Instituto Politécnico Nacional, Mexico, *I. Campos-Silva* (icampos@ipn.mx), SEPI ESIME Zacatenco, Mexico, *E. Chávez-Gutiérrez*, *J. Martínez-Trinidad*, *I. Arzate-Vázquez*, *A. Torres-Hernández*, Instituto Politécnico Nacional, Mexico

In this study the mechanical behavior of FeB and Fe₂B layers formed at the surface of AISI D2 steels was estimated by Berkovich nanoindentation technique. The boriding of AISI D2 steels was developed by the powder-pack method at temperatures of 1223, 1273 and 1323 K in the range of exposure times of 3 - 7 h for each temperature. The mechanical characterization was performed related to the set of experimental parameters of boriding process and considering two procedures: first the nanoindentations were performed along the depth of surface layers with a constant load of 250 mN to determine the hardness gradient and the state of thermal residual stresses in the boride layers. In addition, applied loads in the range of 10 to 300 mN were carried out in the "pure" zone of the FeB layer at 10 microns from the surface, and in the "pure" zone of the Fe₂B layer (40 microns), respectively.

The results showed, for a constant load of 250 mN, that the state of thermal residual stresses and hardness of both FeB and Fe₂B layers are a function of the temperature and exposure time of the process, where the hardness decreases due to the presence of grain coarsening in the surface layers at a temperature of 1323 K with more than 5 h of exposure. Moreover, the presence of the indentation size effect (ISE) in the FeB and Fe₂B layers was verified in the range of applied loads, in which the apparent or real hardness was estimated by traditional models according to the boriding experimental parameters. Finally, the fracture resistance and brittleness of the boride layers was evaluated in the range of nanoindentation loads as a function of boriding temperatures and exposure times; the estimated values are in the range of 1.36-2.82 and 1.98-3.80 MPa m^{1/2}, with the presence of compressive stresses in the range of 162 to 1604 MPa for the FeB and Fe₂B layers, respectively.

3:50pm **E2-2-8 Measurement of Fracture Toughness on TiN thin film.** **A.N. Wang**, **G.P. Yu**, **J.H. Huang** (jhhuang@mx.nthu.edu.tw), National Tsing Hua University, Taiwan

This research was in an attempt to develop a new method without applying external stress for measuring fracture toughness of transition metal-nitride

thin films. TiN thin film was selected to be the model material, owing to its well-characterized mechanical properties and appropriate elastic isotropy. At present, there has been no standard methodology or test procedure for assessing the fracture toughness of hard coatings. Previous literatures have proposed various approaches on the measurement of fracture toughness, which can be divided into two categories: stress based or energy based. However, those methods need to design special specimen geometry because of the requirement in producing valid pre-cracks, and thus the substrate effect cannot be eliminated. In addition, special stages are often needed to externally apply stress, which increases the difficulty of the test methods. TiN thin films deposited by PVD methods normally have high residual stress which can be controlled by adjusting deposition parameters and measured nondestructively. Instead of externally applying stress, the residual stress was utilized in the assessment of fracture toughness. From Griffith's criterion, energy stored in the film due to elastic mismatch strain can be released by the formation of cracks. The difference in stress states before and after crack initiated was used to evaluate the average energy release rate, from which fracture toughness can be calculated by fracture mechanics. This method involved residual stress measurement by laser curvature technique and elastic modulus measurement by nanoindentation according to ISO 14577-4:2007.

The Poisson's ratio of single-crystal TiN was used. The results were compared with those obtained from other techniques and the strong and weak points of this method were discussed.

4:10pm **E2-2-9 Bi-phase Ceramic Composite through Interpenetrating Network.** **E.H. Kim**, **J. Lee**, **Y. Jung** (jungyg@changwon.ac.kr), Changwon National University, Republic of Korea

SiO₂ phase has been infiltrated into porous Al₂O₃ matrix to enhance the mechanical properties of matrix through interpenetrating network (IPN) method. In this work, in order to increase the addition effect of SiO₂ phase into the Al₂O₃ matrix two types of SiO₂ precursor were used: tetraethyl orthosilicate (TEOS) of the silicate type; and polydimethyl siloxane (PDMS) of the siloxane type. The porous Al₂O₃ green body was prepared with an uniaxial pressing process. And then, SiO₂ precursor was infiltrated into the porous matrix under a vacuum chamber for the homogeneous infiltration of precursor into the all pores of matrix. The SiO₂ precursor-infiltrated matrix was dried at 80 °C for 1 h, and then heat treated at 1600 °C for 1 h. During the drying process, PDMS does not undergo a sol-gel reaction, whereas the TEOS is converted into glass-phased SiO₂ by a sol-gel reaction. It means that the siloxane type has higher conversion ratio of precursor into SiO₂ than the silicate type. The microstructure and mechanical properties of prepared composites were evaluated using various analytic techniques. Mullite (3Al₂O₃ · 2SiO₂) phase was observed at the grain boundary between Al₂O₃ and SiO₂, inducing the improvement of mechanical properties of matrix. Therefore, the Al₂O₃-SiO₂ composites show higher mechanical properties in flexure strength and hardness than the porous Al₂O₃ matrix. In addition, the mechanical properties of composite prepared using PDMS were higher than those of composite prepared using TEOS, caused by the enhancement of glassification by the increase in conversion ratio of SiO₂ precursor, in the absence of a sol-gel reaction. Consequently, bi-phase composites with reasonable properties have been successfully prepared through the IPN method using SiO₂ precursors.

4:30pm **E2-2-10 Probing the origin and evolution of strength in small volumes with in situ TEM nanomechanical testing.** **A. Minor** (aminor@berkeley.edu), University of California, Berkeley; National Center for Electron Microscopy, Lawrence Berkeley National Laboratory, US

Recent progress in both in situ and ex situ small-scale mechanical testing methods has greatly improved our understanding of mechanical size effects in volumes from a few nanometers to a few microns. Besides the important results related to the effect of size on the strength of small structures, the ability to systematically measure the mechanical properties of small volumes through mechanical probing allows us to test samples that cannot easily be processed in bulk form, such as a thin film, a specific grain boundary or a single crystal. This talk will describe our recent results from in situ compression and tensile testing of metals with different starting defect densities and sizes to illuminate the origin of size-dependent yield strength behavior and fundamental deformation structures in nanoscale samples.

Post Deadline Discoveries and Innovations

Room: Pacific Salon 1-2 - Session PD-1

Post Deadline Discoveries and Innovations

Moderator: W. Kalss, OC Oerlikon Balzers AG,
Liechtenstein, S. Ulrich, Karlsruhe Institute of Technology,
Germany

1:30pm **PD-1-1 The Multi Beam Sputtering: a new thin film deposition approach.** *P. Sortais (sortais@lpsc.in2p3.fr), T. Lamy, J. Médard, Laboratoire de Physique Subatomique et Cosmologie de Grenoble (LPSC), France*

Thanks to the latest development of ultra compact and reliable microwave ion sources^{1,2} it is now possible to build an ion beam sputtering system composed of an arbitrary large number of simple ion sources that can be individually tuned. With this new concept of Multi Beam Sputtering (MBS) device, new possibilities are conceivable for the Ion Beam Sputtering (IBS) technology^{3,4}, especially for thin film deposition on large size substrates with high uniformity. With MBS, the deposition profile is not defined by the shape and the tuning of a unique large beam, but by the sum of the contributions of a great number of small, well controlled in size, sputtering spots. The uniformity is the consequence of the geometric sum of all sputtering lobes obtained by each sputtering spot. The ion sources units can be distributed along a circle or a line and each ion beam delivered by an ion source impinges its own target. An individual source of a typical size 3x3x3 cm uses a few watts of microwave power for producing a beam up to 1 mA with energy in the range of 5 to 15 keV. The first operational device, MBS-20, uses 20 of such ion sources distributed on a circle around a 70 mm diameter multi-target holder allowing thin film deposition on 100 to 300 mm diameter substrates with deposition rates in the range of 0 to 1 µm/h. An important point, since each ion source uses an individual target, is that co-evaporation of several components can be done simultaneously. By the way, the deposition of alloys with a controlled stoichiometry is easier than with any other method and without uniformity loss. We will show preliminary results for Cu, Ta, Ta₂O₅, C, SiO₂, Ti, TiN, TiO₂, TiAlN and Th on 100 or 200 mm glass substrate diameters, Mylar 0.5 µm or Si substrates. All these processes can be done with reactive atmosphere allowing oxide or nitride deposition.

¹P. Sortais, T. Lamy, J. Médard, J. Angot, L. Latrasse, and T. Thuillier, Rev. Sci. Instrum. 81 (2010) 02B31

²P. Sortais, T. Lamy, J. Médard, J. Angot, P. Sudraud et al., Rev. Sci. Instrum. 83, 02B912 (2012)

³Patent pending N° 1150981.

⁴Under Grant Grenoble Alpes Valorisation Innovation Technologies (GRAVIT) 080606, may 2009.

1:50pm **PD-1-2 Molecular dynamics simulation and experimental validation of nanoindentation measurements of silicon carbide coatings.** *A.-P. Prskalo (alen-pilip.prskalo@imwf.uni-stuttgart.de), Universität Stuttgart, Germany, S. Ulrich, Karlsruhe Institute of Technology, Germany, S. Schmauder, J. Lichtenberg, C. Ziebert, Kit, Iam-Awp, Germany*

Molecular dynamics simulation of the nanoindentation was used to investigate mechanical properties of single layer silicon carbide coatings on silicon substrates. Indenter load-penetration depth relation was determined and put into relation to the internal coating structure and the substrate behavior. In order to reach this objective, an indenter tip in the form of a Berkovich indenter was introduced, a discrete indenter motion of 0.2 Å was imposed. For the modeling of the Si-C system, well known bond-order Tersoff potential was used, while the substrate-indenter interaction was modeled by a self-developed short range repulsive pair potential. From the indenter load-penetration depth relation, mechanical values of hardness and Young modulus for the coatings could be obtained. Hardness values determined by molecular dynamics simulations were in the range between 26.4 GPa and 34.4 GPa. These results are in good agreement with experimental measurements using UMIS 2000 system delivering values between 20.1 GPa and 35 GPa in dependence of the micro structure of the coating, the deposition temperature and maximum indentation depth.

2:10pm **PD-1-3 Anatase TiO₂ Beads Having Ultra-fast Electron Diffusion Rates for use in Low Temperature Flexible Dye-sensitized Solar Cells.** *J.-M. Ting (jting@mail.ncku.edu.tw), Ke, National Cheng Kung University, Taiwan*

The first use of mesoporous TiO₂ beads in plastic substrate flexible dye-sensitized solar cell (FDSC) is demonstrated. Pure anatase TiO₂ beads with various sizes (250 to 750 nm) and characteristics are obtained using a

modified and efficient two-step method. The concept of chemical sintering, eliminating the step of additive removal, is used to prepare bead-containing paste for room temperature fabrication of photoanode having good adhesion to the substrate. The obtained photoanodes are examined for their dye loadings and light absorbance properties. Various plastic substrate FDSCs having commercial P25- and bead-containing photoanodes are fabricated and evaluated. The resulting cells are evaluated for the J-V characteristics, electron diffusion time, electron lifetime, charge-collection efficiency, electron-injection efficiency and incident photon-to-electron conversion efficiency. The bead-only cells not only have better efficiencies, as high as ~5%, but also exhibit ultra-fast electron diffusion rates, less than 1 ms. The best efficiency and electron diffusion rates are respectively 15% higher and two-order of magnitude faster than the P25-only cell. The effects of the bead characteristics on the cell performance is presented and discussed.

2:30pm **PD-1-4 MOCVD nano-structured TiO₂ coatings for corrosion protection of stainless steels.** *H. Herrera-Hernández (hhh@correo.azc.uam.mx), M. Palomar-Pardavé, Universidad Autónoma Metropolitana- Azcapotzalco, Mexico, J.A. Galaviz-Pérez, J.R. Vargas-García, Departamento de Ingeniería, Metalúrgica, ESQIE-IPN, Mexico*

TiO₂ nanoparticles were deposited on 316 stainless steel substrates at three different temperatures using a horizontal hot-wall reactor in the presence of a titanium isopropoxide Ti(OC₃H₇)₄ precursor, method known as metal organic chemical vapor deposition (MOCVD). The influence of deposition temperature (T_{dep} 300, 400 and 500 °C) on the structural and protective properties of the TiO₂ nanoparticles was discussed. The morphology and structure of these nanoparticles that form a continuous thin coating over the steel was investigated by X-ray diffraction (XRD), energy dispersive spectroscopy (EDS) and scanning electron microscopy (SEM) techniques. The corrosion resistance of the TiO₂ coatings was evaluated in a strong corrosive solution (0.5M H₂SO₄) by means of electrochemical measurements such as anodic polarization, cyclic voltammetry (CV) and electrochemical impedance spectroscopy (EIS). Anodic polarization results revealed that the pitting corrosion potential (E_{pit}) shifted to a more positive when the deposition temperature increased in comparison to the bare substrate, while CV behaviour showed lower passive current density for TiO₂ coatings. Through the EIS data it was found that TiO₂ nanoparticles deposited at 500 °C for 30 min did not corroded by pits during over exposure for 100 days in such aggressive electrolyte. A higher electrical coating resistance (R_{TiO2} = 59.52 KW-cm²) and lower capacitance (C_{TiO2} = 87.37 mF/cm²) was measured for 500 °C TiO₂ coating in contrast to 300 or 400 °C coatings.

The improve pitting corrosion resistance for TiO₂ nanoparticles deposited at 500 °C is attributed to its morphology features and its uniform & compact anatase structure, which consisted of platelets agglomerates with very small quasi-spherical nano-particles (10-nm) that impedes the free transfer of electrons and mass-transport process across the coating. Therefore, stainless steels surface modification with TiO₂ nanoparticles showed excellent corrosion resistance for long times exposure in sulphuric acid that makes it an attractive material for biomedical applications.

2:50pm **PD-1-5 Improvement on the mechanical and corrosion properties of nanometric HfN/VN superlattices.** *P. Prieto, Excellence Center for Novel Materials, CENM, Cali, Colombia, C.A. Escobar, Universidad del Valle, Colombia, J.C. Caicedo, Universidad del Valle, Colombia, W. Aperador, Universidad Militar Nueva Granada, Colombia, J. Esteve, M.E. Gomez, Universitat de Barcelona, Spain*

The aim of this work is the improvement of the mechanical and electrochemical behavior of 4140 steel substrate using HfN/VN multilayered system as a protective coating. We have grown HfN/VN multilayered via reactive r.f. magnetron sputtering technique in which was varied systematically the bilayer period (Λ), and the bilayer number (n), maintaining constant the total thickness of the coatings (~1.2 µm). The coatings were characterized by X-ray diffraction (XRD), X-ray photo electron spectroscopy (XPS), electron microscopy assisted with selected area electron diffraction. The mechanical properties were analyzed by nanoindentation method. The electrochemical properties were studied by Electrochemical Impedance Spectroscopy and Tafel curves. XRD results showed a preferential growth in the face-centered cubic (111) crystal structure for [HfN/VN]_n multilayered coatings. The best improvement of the mechanical behavior was obtained when the bilayer period (Λ) was 15 nm (n = 80), yielding the highest hardness (37 GPa) and elastic modulus (351 GPa). The values for the hardness and elastic modulus are 1.48 and 1.32 times greater than the coating with n = 1, respectively. The enhancement effects in multilayer coatings could be attributed to different mechanisms for layer formation with nanometric thickness due to the Hall-Petch effect. The maximum corrosion resistance was obtained for coating with (Λ) equal to 15 nm, corresponding to n = 80 bilayered. The polarization resistance and corrosion rate were around 112.19 kOhm cm² and 3.66x10⁻³ mm/year, these values were 98 % and 99 % better than those

showed by the uncoated 4140 steel substrate (0.65 kOhm and 31.13 mm/year), respectively. With this idea, HfN/VN multilayered have been designed and deposited on Si(100) and AISI 4140 steel substrates with bilayer periods (Λ) in a broad range, from nanometers to hundreds of nanometers, in order to study the microstructural evolution with decreasing bilayer thickness and their related mechanical and electrochemical properties in with aim to find novel industrial applications.

Keywords: Multilayer coatings, Magnetron sputtering, Mechanical properties.

PACS: 61.05.c, 62.20.Qp

3:10pm **PD-1-6 Characterization of High Temperature Instrumented Indentation System and Initial Results,** *D. Jardret* (vincent.jardret@michalex.com), Michalex, USA, *M. Fajfrowski*, Michalex, France

Abstract: High temperature instrumented indentation tests results are presented on a silicate glass sample at three temperatures; Room Temperature, 400oC and 600oC using the HTIIS 1000. This data is used to analyzed the thermal stability of the instrument, characterize key parameters such as load frame stiffness and indenter geometry, and finally determine the elastic and plastic properties of the sample at each temperature. The thermal management concept used in the instrument is described in details. A new method is proposed to identify the indenter shape using the shape of the curve \sqrt{P} versus h during the loading segment, and the ratio of $\sqrt{(P_{max})S_{unload}}$. The results show that the thermal management of the instrument provides very good stability during the tests. Tests with two different maximum loads enable a complete characterization of the instrument and the sample at high temperatures. This work will be pursued with the study of other materials and use of different indenter geometries and materials.

Thursday Afternoon Poster Sessions

Coatings for Use at High Temperature Room: Golden Ballroom - Session AP

Symposium A Poster Session

AP-1 Contact Corrosion propriety between Carbon Fiber Reinforced Composite Materials and Typical Metal alloys in an aggressive environment. *Z.J. Peng*, University of Windsor, Canada, *Z.J. Wang*, University of Windsor, Canada, *X. Nie* (*xnie@uwindsor.ca*), University of Windsor, Canada

The demand for the use of carbon-fiber-reinforced materials in automotive and aerospace industry is increasing worldwide. However, a destructive galvanic corrosion is inevitable in the case that carbon fiber contacts with metals. In this research, the galvanic corrosion between carbon fiber and three kinds of commonly used metals, AISI 304 steel, A356 aluminum alloy and Ti6Al4V titanium alloy, were studied. By employing the potentiodynamic polarization corrosion tests and zero resistance Ammeter tests (ZRA), the corrosion potentials and their differences in values were determined. The corrosion behavior of the samples was evaluated in a 3.5% NaCl solution. It was found that all the metals were corroded when they contacted with the carbon fiber. To address the problems, plasma electrolytic oxidation (PEO) technique were employed to synthesize oxide coatings on the stainless steel and aluminum and titanium alloys. The results of the experiments showed that the galvanic corrosion rates could be decreased significantly when the PEO coatings were applied on the metallic surfaces. All the coatings possessed a much better corrosion resistance compared to the uncoated substrates. Key words: Galvanic Corrosion, Carbon Fiber, PEO Coating, Corrosion resistance Corresponding author. E-mail: *xnie@uwindsor.ca*

AP-2 Influence of native oxide scales on the mechanical properties of polycrystalline nickel substrates. *M. Tatat* (*matthieu.tatat@ensma.fr*), *P. Gadaud*, *C. Coupeau*, *X. Milhet*, Institut P², CNRS – ENSMA - Université de Poitiers – UPR 3346, France, *P. Renault*, Institut P² - Université de Poitiers, France, *J. Balmain*, Laboratoire d'Etude des Matériaux en Milieux Agressifs - Université de La Rochelle, France

Severe operating conditions promoting corrosion or oxidation may result to the damage and further ruin of the considered materials. Structural materials that are used in such aggressive environments are consequently usually protected by passive thin films or coatings. In the case of native thermally-grown oxides, only few studies are available in the literature concerning the coupling effect between their ageing and the mechanical behaviour of their associated substrate.

In this context, the influence of thermally-grown oxide films on the mechanical properties of polycrystalline nickel substrates has been investigated using a dynamical resonant method and instrumented indentation tests. Being a major component of superalloys used in the hottest parts of turbojets, nickel appears as a model material for oxidation due to the growth of only one form of oxide (NiO). Oxide scales have been developed at various temperatures and times to study the effect of thicknesses and microstructures on the mechanical behavior.

The dependence of the nickel elastic constants on temperature below the Curie temperature (631 K) is characterized by an anomalous behavior, resulting from its ferromagnetic character. On one hand, it is shown that the NiO layer that represents less than 3% of the total thickness of the specimens affects however significantly the elastic constants of the oxidized material below the Curie temperature, compared to those measured for the substrate in the same temperature range. These experimental results suggest that the internal stresses developed during oxidation play a key role in the competition between the magnetostrictive and elastic expansions. On the other hand, it is believed that these unexplored magnetoelastic coupling of the nickel substrate explains the scattering of the elastic modulus measurements of NiO reported in the literature.

AP-3 Evaluation of galvanic and corrosion behaviour of some commercial aluminium-based coatings deposited by various methods. *O. Fasuba*, *A. Yerokhin*, *A. Matthews*, *A. Leyland* (*a.leyland@sheffield.ac.uk*), University of Sheffield, UK

The galvanic and corrosion behaviour of commercial slurry-coated Al-Cr-Mg-P composite, electrodeposited Al, HVOF-Al and IVD-Al coatings was studied in 3.5 wt. % NaCl electrolyte. The coatings were evaluated by: open circuit potential (OCP), potentiodynamic polarisation, electrochemical noise and electrochemical impedance spectroscopy (EIS) techniques. SEM, EDX, XRD and optical microscopy were used to characterise the coating structure. A comparison of the OCP vs. saturated calomel electrode (SCE)

measurements in 3.5 wt. % NaCl showed that all coatings behave anodically with respect to the steel substrate. During electrochemical noise measurements the galvanic current density and mixed potential of the coatings/bare mild steel couples were measured simultaneously during 12 hours of immersion. In the slurry-coated Al-Cr-Mg-P composite/bare steel and IVD-Al/bare steel couples, bare steel was found to be anodic to the two coatings during the initial stages of the measurement, before a polarity reversal occurred. HVOF-Al and electrodeposited Al coatings showed unstable potential behaviour with a fluctuating variation in current density with increased exposure time. Overall, results of the OCP, polarisation and the electrochemical noise measurements showed that the coatings behaved as the anodic element of the galvanic pairing, with the slurry-coated Al-Cr-Mg-P composite exhibiting the lowest galvanic current density which is a desirable feature for long-term cathodic protection of the steel substrate. The EIS analysis and the results of the structural characterisation of the coatings correlate with that of the OCP, polarisation and electrochemical noise measurements.

AP-4 High Temperature Diffusion Barriers for InSb based IR Detector. *A. Le Priol* (*arnaud.le.priol@univ-poitiers.fr*), *E. Le Bourhis*, *P. Renault*, Institut P² - Université de Poitiers, France, *H. Sik*, *P. Muller*, SAGEM Défense Sécurité, France

InSb based infra-red (IR) detectors are constituted by an Si supported Integrated Circuit (IC) and an InSb matrix which are electrically and mechanically connected thanks to solder balls in pure indium deposited on underbump metallic layers (UBM). This UBM ensures adherence between solder balls on both Si and InSb substrates, acts as diffusion barrier and facilitated the wetting of solder metal. High temperature diffusion occurs during the assembly process with intermetallic compounds (IMC) being formed. This process may short-circuit pixels and hence dramatically affecting the strength of the solder joint at the bonding interface.

To avoid indium diffusion across UBM, different routes have been investigated: (i) variation of residual stresses in W-Ti thin film barrier, and (ii) use of new refractory metal like tantalum and its nitride.

It is well known that refractory metal film deposited under the condition of limited atomic mobility have columnar microstructure. It is unfavorable since indium diffusion occurs along the grain boundaries. Thus, tailoring the columns microstructure from dense under compression stress state to porous under tension stress state has been explored since this should improve the performance of the barrier. We indeed report on the beneficial influence of the working pressure employed during physical deposition (PVD) on barrier performance.

On the other hand, to develop a Ta-based barrier, it is mandatory to obtain the stable phase of Ta (bcc α -Ta), for which deposition conditions have been optimized. Bi-layer TaN / Ta are shown to be a potential diffusion barrier system. TaN underlayer is shown to promote α -Ta growth and improve barrier performance.

AP-5 Improvement on the mechanical and corrosion properties of nanometric HfN/VN superlattices. *P. Prieto*, Excellence Center for Novel Materials, CENM, Colombia, *C. Escobar*, *J. Caicedo* (*jcaicedoangulo@gmail.com*), Thin Film Group, Universidad del Valle, Colombia, *W. Aperador*, Ingeniería Mecatrónica, Universidad Militar Nueva Granada, Colombia, *J. Esteve*, Universitat de Barcelona, Spain, *M. Gómez*, Thin Film Group, Universidad del Valle, Colombia

The aim of this work is the improvement of the mechanical and electrochemical behavior of 4140 steel substrate using HfN/VN multilayered system as a protective coating. We have grown HfN/VN multilayered via reactive r.f. magnetron sputtering technique in which was varied systematically the bilayer period (Λ), and the bilayer number (n), maintaining constant the total thickness of the coatings ($\sim 1.2 \mu\text{m}$). The coatings were characterized by X-ray diffraction (XRD), X-ray photo electron spectroscopy (XPS), electron microscopy assisted with selected area electron diffraction. The mechanical properties were analyzed by nanoindentation method. The electrochemical properties were studied by Electrochemical Impedance Spectroscopy and Tafel curves. XRD results showed a preferential growth in the face-centered cubic (111) crystal structure for [HfN/VN] n multilayered coatings. The best improvement of the mechanical behavior was obtained when the bilayer period (Λ) was 15 nm ($n = 80$), yielding the highest hardness (37 GPa) and elastic modulus (351 GPa). The values for the hardness and elastic modulus are 1.48 and 1.32 times greater than the coating with $n = 1$, respectively. The enhancement effects in multilayer coatings could be attributed to different mechanisms for layer formation with nanometric thickness due to the Hall-Petch effect. The maximum corrosion resistance was obtained for coating with (Λ) equal to 15 nm, corresponding to $n = 80$ bilayered. The

polarization resistance and corrosion rate were around 112.19 kOhm cm² and 3.66x10⁻³ mm/year, these values were 98 % and 99 % better than those showed by the uncoated 4140 steel substrate (0.65 kOhm and 31.13 mm/year), respectively. With this idea, HfN/VN multilayered have been designed and deposited on Si(100) and AISI 4140 steel substrates with bilayer periods (Λ) in a broad range, from nanometers to hundreds of nanometers, in order to study the microstructural evolution with decreasing bilayer thickness and their related mechanical and electrochemical properties in with aim to find novel industrial applications.

Keywords: Multilayer coatings, Magnetron sputtering, Mechanical properties.

PACS: 61.05.c, 62.20.Qp

Acknowledgements

This research was supported by "El patrimonio Autónomo Fondo Nacional de Financiamiento para la Ciencia, la Tecnología y la Innovación Francisco José de Caldas" under contract RC-No. 275-2011. Moreover, the authors acknowledge the Serveis Científic-Tècnics of the Universitat de Barcelona for TEM analysis.

AP-6 Study of the effect of densification on the mechanical properties of porous coatings after nano-indentation, X.J. Lu (xiaojuanlv@hotmail.com), P. Xiao, H. Li, A. Fok, The University of Manchester, UK

Nano-indentation of a porous ceramic coating leads to crushing and densification of the coating under the indenter. During indentation, a densified layer with gradient density was formed beneath the indenter. In this work, finite element (FE) simulation of indentation on the densified layer has been carried out to study the effect of the densified area on measured Young's modulus from nano-indentation. According to the FE simulation, the measured Young's modulus from indentation deviates from the true Young's modulus when the size of densified region is much larger than the indentation region. Based on the simulation results and experimental results from indentation of a porous yttria stabilised zirconia coating produced in this work, the measured Young's modulus should be the true Young's modulus of the coating.

AP-8 Oxygen incorporation in Cr₂AlC, M. to Baben (to_baben@mch.rwth-aachen.de), L. Shang, J. Emmerlich, J. Schneider, Materials Chemistry, RWTH Aachen university, Germany

The MAX phase Cr₂AlC is a promising candidate for high temperature applications because of its oxidation resistance, which is comparable to NiAl [1]. However, neither the early stages of oxidation of Cr₂AlC nor the influence of oxygen impurities in the at % range [1] which are probably introduced due to processing in high vacuum [2] have been studied.

Oxygen incorporation in Cr₂AlC was studied by a combination of ab initio calculations and combinatorial magnetron sputtering. Cr, Al and C targets were sputtered in Ar and Ar+O₂ atmosphere, leading to three different oxygen contents in the thin films. From X-ray stress analysis it was determined how lattice parameters of Cr₂AlC are influenced by the oxygen content.

The energy of formation was calculated for Ti₂AlC_{1-x}O_x, V₂AlC_{1-x}O_x and Cr₂AlC_{1-x}O_x with O occupying interstitial and substitutional sites. For Cr₂AlC_{1-x}O_x the energy difference between interstitial and substitutional incorporation of oxygen is -0.7 eV/oxygen atom, while it is +2.6 and +1.2 eV/oxygen atom for Ti₂AlC_{1-x}O_x and V₂AlC_{1-x}O_x, respectively. This indicates that oxygen does not substitute carbon, as observed for Ti₂AlC_{1-x}O_x [2], but is incorporated interstitially in the Al-layer of Cr₂AlC_{1-x}O_x, even in the presence of carbon vacancies.

Experimentally, an increase of the *a* lattice parameter of +0.18% was observed while the *c* lattice parameter was hardly affected. These experimentally determined volume changes are in good agreement with the predictions from ab initio calculations on interstitial incorporation of oxygen, corroborating the notion of oxygen interstitials in Cr₂AlC. A solubility limit of 3.5 at% of oxygen was observed under the deposition conditions studied within this work. An increase of oxygen content above this limit led to the formation of an x-ray amorphous phase.

[1]: D.E. Hajas et al., Surf. Coat. Technol. (2011), doi:10.1016/j.surfcoat.2011.03.086.

[2]: J. Rosen et al., Appl. Phys. Lett. 92 (2008), 064102.

AP-9 Multicomponent Coatings in Cr-Al-Si-B(N) System Produced by Magnetron Sputtering of Composite SHS-Targets, P. Kiryukhantsev-Korneev (kiruhancev-korneev@yandex.ru), Yu. Pogozhev, D.V. Shtansky, National University of Science and Technology "MISIS", Russian Federation, J. Vlcek, University of West Bohemia, Czech Republic, E.A. Levashov, National University of Science and Technology "MISIS", Russian Federation

The Cr-B-N coatings are promised due to their high hardness, wear- and corrosion resistance. It is well known that introduction of Si and Al to different hard coatings (CrN, TiN, and Ti-B-N) improves the tribological characteristics and oxidation resistance. The aim of present work is to study the structure and properties of Cr-Al-Si-B(N) coatings deposited by magnetron sputtering of composite targets.

Targets were fabricated using the method of self-propagating high-temperature synthesis (SHS) according to the follow combustion reaction $X(\text{Cr}+2\text{B})+(100-X)(4\text{Al}+3\text{C}+\text{Si}_3\text{N}_4)$ ($X=15, 30, \text{ and } 40$). Main advantages of SHS are follow: self-purification of the final product from impurities (adsorbed and dissolved) result in high combustion temperature and combustion rate; achievement of controlled residual porosity of ceramics due to hot pressing of products follow by high-temperature process of combustion; synthesis of metastable supersaturated solid solutions. Targets composition represented by CrB, Cr₃Si₃, and Cr₄Al₁₁ phases.

Magnetron sputtering was performed either in an atmosphere of argon or reactively in a gaseous mixture of argon and nitrogen. During magnetron sputtering, the substrate temperature and bias voltage were kept constant in the range of 300-500°C and -500-0 V, respectively. The silicon and alumina plates, nickel alloy and cemented carbide disks were used as the substrates. The structure, chemical and phase composition of coatings were studied by means of X-ray diffraction, transmission and scanning electron microscopy, Raman spectroscopy, and glow discharge optical emission spectroscopy. The coatings were characterised in terms of their hardness, elastic modulus, elastic recovery, adhesion strength, friction coefficient, wear rate, oxidation resistance, thermal stability, and diffusion barrier properties.

The first experiments demonstrated relatively high hardness till 40 GPa, Young's modulus below 270 GPa, elastic recovery up to 50%, oxidation resistance and good diffusion barrier properties at the temperature high than 1100°C.

AP-10 Performance of Advanced Turbocharger Alloys and Coatings at 850-950°C in Air with Water Vapor, J. Haynes (z15@ornl.gov), B. Armstrong, B. Pint, Oak Ridge National Laboratory, US

Turbocharged gasoline and diesel engines are of significant interest due to their capacity to allow smaller displacement automotive engines with improved fuel economy and lower CO₂ emissions. As exhaust temperatures continue to increase, oxidation resistance and mechanical properties of exhaust manifolds and turbocharger components will become problematic for some alloys of interest. This study compared the 850 and 950°C cyclic oxidation behavior in air plus 10 vol.% water vapor (simulated exhaust gas) of IN713C, HR230, MM247, IN939, CW6MC, and two Ti~48%Al alloys. The room temperature tensile properties of selected alloys were evaluated before and after oxidation at 850° and 950°C by using miniature tensile bars as oxidation specimens. Additionally, selected Ni-based alloys were aluminized via chemical vapor deposition and/or slurry processes, and the resultant coating microstructures and 950°C oxidation behaviors were compared. The TiAl alloys oxidized more rapidly than the Ni-base alloys or aluminide coatings after 100, 1-h cycles and scale spallation was observed at 950°C. However, only minor changes in ductility and tensile strength for TiAl were observed. Larger decreases in ductility were observed for 713C. Longer exposures are in progress.

AP-11 Oxidation Behavior of Ni-Ru Films under Glass Hot Pressing, C.K. Chang, K.Y. Liu, Y.C. Hsiao, F.B. Wu (fbwu@nnu.edu.tw), National United University, Taiwan

Ni-Ru alloy films are fabricated using r.f. magnetron dual gun cosputtering process. The Ru content ranges from 10.4 to 53.5 at.% under an input power control from 10 to 100W, respectively, at a fixed 100W for Ni. The Ni-Ru coatings with lower Ru contents exhibit a granular structure, while a significant columnar feature is observed for the Ni_{46.5}Ru_{53.5} film. The oxidation behavior of the Ni-Ru films against phosphate glasses are demonstrated under hot pressing environment. The heat treatment in air are conducted for comparison. Oxidation reaction penetrates into the Ni-Ru films over 250 nm at a heat treating temperature of 475°C in air. On the other hand, a limited oxidation penetration less than 100 nm is found for the Ni-Ru coatings against phosphate glasses. The granular characteristic and grain boundaries are responsible for oxidation in air annealing. On the contrary, the oxidation reaction is suppressed due to depletion of active oxygen at film/glass contact.

AP-12 Wear characteristics of Zr-Al-Ni based PVD nanocomposite thin films deposited on non-ferrous alloy substrates, J. Lawal, A. Matthews, A. Leyland (a.leyland@sheffield.ac.uk), University of Sheffield, UK

Non-ferrous engineering alloys (eg. titanium and aluminium alloys; nickel alloys and austenitic stainless steels) are increasingly used in the aerospace, automotive, chemical processing, and biomedical industries, owing to combinations of desirable functional properties such as corrosion resistance, high strength-to-weight ratio, biocompatibility, toughness and durability in extreme environments. However, it is well known that such materials exhibit poor tribological properties – especially under conditions of sliding wear and/or abrasion.

Nanocomposite coatings comprising a hard nanocrystalline phase embedded in an amorphous matrix have been found to exhibit improved tribological properties over a range of varying conditions. This study investigates the wear characteristic of Zr-Al-Ni nanocomposite films prepared by reactive magnetron sputtering. The sliding and abrasive wear behaviour of different coating-substrate systems was studied using reciprocating ball-on-plate sliding and slurry microabrasion wear testing, respectively, in different ambient environments. SEM, (with EDX) and XRD evaluations were conducted to determine coating thickness/morphology and chemical/phase composition. Hardness and elastic modulus were also determined by instrumented micro- and nano-indentation measurements.

AP-13 The microstructure, mechanical properties and oxidation resistance of CrAlSiN coatings, Y.C. Kuo, National Taiwan University of Science and Technology, Taiwan, J.W. Lee (jefflee@mail.mcut.edu.tw), C.J. Wang, Ming Chi University of Technology, Taiwan

The CrAlSiN thin films with various Si contents were deposited by a magnetron sputtering system. In this study, effects of silicon contents on the microstructure, mechanical properties and oxidation resistance of CrAlSiN films were investigated. The crystalline structure of thin film was determined by a glancing angle X-ray diffractometer (GA-XRD). The surface and cross-sectional morphologies of thin films were examined by a field emission scanning electron microscopy (FE-SEM). The hardness and Young's modulus of thin film were evaluated by a nanoindenter. The adhesion of coatings was determined by the scratch tester and Rockwell-C hardness tester, respectively. For the oxidation resistance evaluation, the CrAlSiN thin films were annealed at 700, 800, and 1000 °C for 100 hrs in air, respectively. It was found that the microstructure and mechanical properties of CrAlSiN thin films were affected by the silicon content. The oxidation resistance of CrAlSiN coating was enhanced as the silicon content increased. The mechanism for the oxidation resistance improvement of coatings was also proposed in this work.

AP-14 Improvement of interface adhesion and thermal stability in thermal barrier coatings through plasma heat treatment, S. Myoung, J. Jang, K. Lee, Z. Lu, Y. Jung (jungyg@changwon.ac.kr), J. Lee, Changwon National University, Republic of Korea, U. Paik, Hanyang University, Republic of Korea

The thermal durability of thermal barrier coatings (TBCs) is closely related to its adhesive strength and microstructure. Numerous factors have to be considered in practical applications of TBCs, including the thermo-mechanical properties. There is therefore a need to improve the adhesive strength and thermal stability, which are essential to improving the reliability and lifetime performance of the air-plasma sprayed (APS) TBC system. Possible ways for enhancing the thermal durability are to control the surface microstructure of bond coat and to bring a vertical type crack to the top coat. Recently, TriplexPro™-200 system has been launched to offer an advanced TBC performance resulting from higher particle velocity, lower particle oxidation, and higher coating density, compared with the commercial APS system. Therefore, in this study, TBC samples were prepared by the specialized coating system (TriplexPro™-200) and the microstructure of TBC was controlled by reheating the surface of both the bond and top coats without powder feeding in same equipment. The thickness of the bond and top coats was controlled as 200 and 1000 mm, respectively, and Ni-based metallic material (AMDY 962) and ZrO₂-8wt% Y₂O₃ (METCO 204 C-NS) were used as starting powders of the bond and top coats, respectively. In order to investigate the improvement of thermal durability the thermal fatigue tests were performed for the TBC samples with and without surface modification, at a surface temperature of 1100°C with temperature difference of 150°C between the surface and bottom of sample, with a dwell time of 1 h for 850 cycles, in a specially designed apparatus: one side of the sample was exposed and the other side air cooled. The TBC prepared by the surface modification of bond coat is more efficient in improving adhesive strength than that without the surface modification, and the thermal durability is enhanced by introducing the vertical type cracks to the top coat. These evidences allow us to enhance the thermal durability of TBC and to propose the efficient coating in improving lifetime performance of TBC at high temperature environments. The

relationship between the microstructural evolution and thermo-mechanical characteristics of the TBCs with and without the surface modification and vertical cracks is discussed.

AP-15 On Machining of Hardened AISI D2 Steel with Coated Tools, W. Mattes, C. Viana (ceviana@catolicasc.org.br), Brazil
ON MACHINING OF HARDENED AISI D2 STEEL WITH COATED TOOLS

Wilmar Mattes, mattes@catolicasc.org.br; Carlos Eduardo Viana, ceviana@catolicasc.org.br

This paper describes an experimental investigation on machining of a difficult-to cut material, AISI D2 steel of hardness 65 HRC with three tool coatings (AlCr, TiAlN and TiAlN + AlCrN). It was found that the most feasible feeds and speeds fall in the ranges 0.08–0.20 mm/rev and 80–120 m/min, respectively and that most of the tested coatings tools reached the end of life mainly due to flank wear. The highest acceptable values of tool life and volume of material removal were obtained at the lowest speed tested (70 m/min), indicating that this speed is more suitable for machining the selected tool/work material combination. While the highest feed used resulted in the highest volume of material removal, lower feeds resulted in higher tool life values. It was also found that the most appropriate feeds for this type of hardened steel are 0.14 mm/rev for finishing operations and 0.20 mm/rev for roughing operations. The best results were obtained with tools coated with TiAlN + AlCrN for the parameters of lower flank wear, better surface quality and dimensional.

AP-16 Microstructure characterization of diffusion aluminide coatings obtained by gas phase aluminizing on direct solidification Ni base superalloys Rene 142 and Rene 108, B.W. Witala (bartosz.witala@polsl.pl), L.S. Swadzba, Silesian University of Technology, Poland, L.K. Komendera, AVIO Polska Sp. z o.o., Poland, M.H. Hetmanczyk, B.M. Mendala, R. Swadzba, G.M. Moskal, Silesian University of Technology, Poland

Aluminide diffusion coatings plays meaningful role in protection material to high temperature oxidation and corrosion. In this paper result of development and properties of high-temperature coating deposited on superalloys such as direct solidification Ni base superalloys Rene 142 and Rene 108 will be presented. Three different pack cementation and one out of pack process were carried out. There will be shown influence of technological parameters on microstructure, thickness and phase composition of aluminide coatings. Aluminide coatings were investigated by light microscopy (LM), scanning electron microscopy (SEM), electron probe microanalysis (EPMA), glow discharge optical spectroscopy (GDOS) and X-ray diffraction analysis (XRD).

AP-17 Degradation and thickness evaluation of thermal barrier coatings using nondestructive 3D scanning method, G.M. Moskal, R. Swadzba (rswadzba@gmail.com), L.S. Swadzba, M.H. Hetmanczyk, B.M. Mendala, B.W. Witala, Silesian University of Technology, Poland

Thermal barrier coatings applied on turbine blades and vanes provide reduction of temperature on these components, which in turn leads to increasing their lifetimes. Producing TBCs of appropriate thickness and uniform coating material distribution on the surface of a component is of critical importance in meeting their intended performance and durability requirements. This paper presents results of plasma sprayed (APS) thermal barrier coatings investigation using 3D optical white-light scanning method. The purpose of this investigation was non-destructive evaluation of thickness and distribution of TBCs on jet engine turbine vanes, as well as oxidation-induced degradation related to thermally grown oxide (TGO) formation underneath the ceramic top coat. Obtained results provide information concerning coating material distribution on the surface and in cross sections of the turbine vanes. Methodological aspects and final results are discussed and analyzed.

Hard Coatings and Vapor Deposition Technology **Room: Golden Ballroom - Session BP**

Symposium B Poster Session

BP-1 Trends in elasticity of binary and ternary transition metal aluminium nitrides, P. Wagner, Montanuniversität Leoben, Austria, M. Friák, Max-Planck-Institut für Eisenforschung, Germany, P.H. Mayrhofer, D. Holec (david.holec@unileoben.ac.at), Montanuniversität Leoben, Austria

Protective hard coatings make use of the outstanding mechanical and thermal stability of early transition metal nitrides (TMN) and their alloys with Al. Modern applications require sophisticated designs of the protective

thin films in which a multiscale modelling plays an important role. For example, stress management of the thin film is a crucial factor affecting its high temperature stability. This is an ideal task for the finite elements method where elastic properties of the studied materials are the necessary input.

The scatter of published elastic constants for the systems of interest is enormous. For example, for TaN one can find the value of C_{11} ranging from 680 GPa to 880 GPa. This of course raises questions about reliability not only of the first principle calculations but also the subsequent larger-scale modelling using these values as inputs as well as how compatible are the values published in various papers.

In this paper we critically revise the computational methodology of second and third order elastic constants calculations focusing on a large family of binary TMN (TM=Sc, Ti, V, Y, Zr, Nb, La, Hf, Ta) and AlN in their cubic (B1, NaCl prototype) modification. Apart from the single crystal properties, also estimates for polycrystalline samples will be discussed which are more appropriate for modelling of the thin films. In addition, we will present description of the single crystal and polycrystalline elastic behaviour of the ternary $Zr_{1-x}Al_xN$ system.

BP-2 Investigation of the mechanical properties of ternary metal nitrides $TM_xMo_{1-x}N$ and $TM_xW_{1-x}N$ with TM=Ti, Zr, V, Nb, Ta and Cr. K. Bouamama, Ferhat Abbas University, Algeria, P. Djemia (djemia@univ-paris13.fr), D. Faurie, University Paris 13, France, G. Abadias, Institut P' - Universite de Poitiers, France

First-principles pseudopotential calculations of the lattice constants and of the single-crystal elastic constants for ternary metal nitrides $TM_xMo_{1-x}N$ and $TM_xW_{1-x}N$ with TM=Ti, Zr, V, Nb, Ta and Cr ($0 \leq x \leq 1$) alloys considering the cubic B1-rocksalt structure were carried out. These calculations were performed using density functional perturbation theory (DFPT) within the virtual crystal approximation (VCA) for the disordered alloys and the supercell method (SC) for the ordered alloys. For the exchange-correlation potential, we used the generalized gradient methods (GGA). The calculated equilibrium lattice parameters exhibit a deviation from Vegard's rule with a bowing parameter that depends on the transition metal. The calculated single-crystal stiffness, namely C_{44} and C_{12} , gradually increases or decreases, respectively from TMN to (Mo,W)N. In case of Ti and Zr metals, we observe three regions: unstable, ductile and brittle whereas for the other alloys, only the unstable and the ductile behaviours are found. The transition metal concentration x for which occurs the transition from unstable to stable mechanical state depends on the element TM. In a second stage, in the frame of anisotropic elasticity, we have estimated by homogenization methods the averaged stiffnesses $\langle C_{ij} \rangle$, direction dependent Young's moduli and Poisson's ratios of some polycrystalline $TM_x(Mo,W)_{1-x}N$ alloys considering a crystallographic fiber texture for comparisons with experimental results available in literature.

BP-3 Structural and elastic properties of ternary metal nitrides $Ti_xTa_{1-x}N$ alloys: first-principles calculations versus experiments. M. Benhamida, Laboratoire Optoélectronique et Composants, Ferhat Abbas University, Algeria, K. Bouamama, Ferhat Abbas University, Algeria, P. Djemia (djemia@univ-paris13.fr), University Paris 13, France, L. Belliard, UPMC, France, D. Faurie, University Paris 13, France, G. Abadias, Institut P' - Universite de Poitiers, France

First-principles pseudopotential calculations of the lattice constants and of the single-crystal elastic constants for $Ti_xTa_{1-x}N$ ($0 \leq x \leq 1$) alloys with B1-rocksalt structure were first carried out. These calculations were performed using density functional perturbation theory (DFPT) within the virtual crystal approximation (VCA) for the disordered alloys and the supercell method (SC) for the ordered alloys. For the exchange-correlation potential we used the generalized gradient methods (GGA). The calculated equilibrium lattice parameters exhibit a positive deviation from Vegard's rule corresponding to a positive bowing parameter while the calculated single-crystal stiffness C_{12} and C_{44} , gradually increase when C_{11} decreases from TaN to TiN. In a second stage, we have estimated by homogenization methods in the frame of anisotropic elasticity the averaged stiffnesses $\langle C_{ij} \rangle$, direction dependent Young's moduli and Poisson's ratios of polycrystalline $Ti_xTa_{1-x}N$ ($0 \leq x \leq 1$) alloys considering different fiber texture. Finally, comparisons are made with the shear elastic modulus $G_{yz}=G_{xz}$ and the out-of-plane longitudinal elastic constant C_{33} measured by Brillouin light scattering and picosecond ultrasonics on thin films elaborated by magnetron sputtering, respectively.

BP-4 Growth of Zirconium Oxide by Heat Treatment of Zirconium Nitride Film under Controlled Atmosphere and Vacuum. J.W. Shine, G.P. Yu, J.H. Huang (jhuang@mx.nthu.edu.tw), National Tsing Hua University, Taiwan

Previous study (1) indicated poor wettability of ZrO_2 on stainless steel. The purpose of this study was in an attempt to solve this wettability issue by

growing ZrO_2 from heat treatment of ZrN thin films on stainless steel substrate. Thin film specimens of ZrN were annealing at temperatures ranging from 700 °C to 900 °C and over durations ranging from 0 to 4 hours. To prevent severe oxidation, two environments including vacuum (5×10^{-6} Torr) and forming gas ($N_2/H_2=9$) were selected. The behavior of growing zirconium oxide was investigated by analyzing the oxygen penetration depth, phase distribution, microstructure change, and corrosion resistance of the specimens. X-ray diffraction showed that ZrO_2 phase appeared when the specimen was heat treated at 900 °C for 1 hour in vacuum, while ZrO_2 appeared at 700 °C for 1 hour in the forming gas. Furthermore, the morphology of ZrN specimens annealed in vacuum was different from that in the forming gas under the same condition. Since the oxygen content in the forming gas was much lower than that in vacuum, the surface conditions of ZrN thin films may be different in vacuum and the forming gas. During oxidation, cracks and blisters may form on the specimen surface due to large difference in molar volume (about 50%) between ZrO_2 and ZrN. SEM observation revealed that cracks and blisters in ZrO_2 layer on the ZrN specimen appeared in the forming gas environment at temperature 700 °C and above while no blister in ZrO_2 layer was observed in the vacuum environment. The results of residual stress measurement indicated that for the ZrN specimens heat treated in vacuum, the stress induced by volume expansion due to phase transition from ZrN to ZrO_2 was released significantly as ZrO_2 phase showed up. Thus, by selecting a proper environment, a thin layer of ZrO_2 could be grown from ZrN without crack or blister formation, which may provide good corrosion protection.

1. Jia-Hong Huang, Tzu-Chun Lin, Ge-Ping Yu, Surf. Coat. Technol., 206(2011)107.

BP-5 Microstructure and Characterization of Sputtered Ni-based Films Codeposited with Ru and P. K.Y. Liu, Y.C. Hsiao, C.K. Chang, F.B. Wu (fbwu@npu.edu.tw), National United University, Taiwan

The Ni-Ru, Ni-P, and Ni-Ru-P alloy films are manufactured by d.c. sputtering technique. The Ni-Ru films show a granular structure as the Ni-P and Ni-Ru-P coatings exhibit an amorphous feature in the as-deposited state. However, when the Ru content is raised to 52.7 at.%, the Ni-Ru-P transforms to a Ni + Ru + Ru_2P multiphase crystallized microstructure. The granular Ni-Ru coatings possess relatively low corrosion resistivity, while a superior chemical stability is deduced for the P incorporated Ni-based alloy films. The lower corrosion characteristic for the Ni-Ru is attributed to the Ni-based granular structure providing corrosion paths at grain boundaries. The P containing Ni-P and Ni-Ru-P sputtered films show an amorphous phase, in which the fast corrosive paths are eliminated, and thus enhance the corrosion resistance. On the other hand, the chemically stable Ru and Ru_2P phases are beneficial to the superior corrosion resistivity for the multiphase Ni-Ru-P coating with high Ru content.

BP-7 Optimizing the PVD TiN thin film coating's parameters on AL 7075-T6 alloy for higher coating adhesion and better surface quality. E. Zalnezhad (erfan_zalnezhad@yahoo.com), University of Malaya, Malaysia

Abstract
An optimization study on the parameters of Titanium Nitride thin film coating on Al7075-T6 alloy, using magnetron sputtering technique is presented. The effects of the film thickness, temperature, DC bias voltage, rate of nitrogen and DC power on the adhesion and microstructure of the coated samples are investigated. Each sample is coated at two steps. Firstly samples are coated with pure Titanium and secondly they are coated with titanium nitride which this effort is increased the adhesion of TiN to surface profoundly. The coating properties probed in this work included the surface thickness, morphology of deposited coating, adhesion between the coating and substrate, and surface characterization using a field emission scanning electron microscope (FESEM) with energy dispersive X-ray (EDX), X-ray diffraction (XRD). SEM analyses showed that all the films had columnar and dense structure with clearly defined substrate-film interfacial layers. Scratch result showed, the adhesion between substrate and thin film was increased with increasing the DC power from 300W to 500W. The result also showed an increase; in dc bias voltage, the adhesion was increased from 25V to 75V, but with more increasing (100V) the adhesion was decreased.

BP-8 Analysis of damaging phenomena of coated cutting tools using hardened die steels. K. Morishita (kana_morishita@hitachi-tool.co.jp), Hitachi Tool Engineering, Ltd., Japan

Machining of hardened die and mold steels has been increasing due to requirements of manufacturing at short delivery time and reducing manufacturing cost. However, machining of hardened die steels is technically difficult and cause early damage of cuttings tools. It is commonly known that wear of cutting tools can be reduced by formation of an oxide layer "Belag" on cutting edge. In this research, we investigated

damage modes of TiN and TiAlN coated cutting tools and their mechanisms aiming to improve machinability of high-hardness die and mold steels. For this purpose, the wear surface and cross-section after cutting was investigated using FE-EPMA, TEM, and STEM. Particularly, the adhesive materials formed on the cutting edges were analyzed and tools damage was studies.

EPMA analysis of tool-work interface showed that the belag was formed on the coating surface during cutting, which was Mn-Si-O or Al-O. Formation of the Mn-Si-O based belag could help increasing the cutting speed compared to formation of an Al-O based belag, while Al-O based belage was performed as protective layer against wear resistance. The belag formation was related to the chemical composition of work materials, chemical composition of the coatings and cutting temperature.

BP-9 Annealing effects on nanostructure and mechanical properties of laminated Ta-Zr coatings. *Y.I. Chen (yichen@mail.ntou.edu.tw), S.M. Chen*, National Taiwan Ocean University, Taiwan

The as-deposited laminated Ta-Zr coatings exhibited nanocrystalline or amorphous states, depending on the chemical compositions. As annealed in oxygen containing atmospheres, Zr oxidized preferentially. The hardness increased as the oxygen content in the coating increased, due to the formation of ZrO₂. To behave as a protective coating applied in high temperature with an appropriate hardness, such as coatings on glass molding dies, the coating need to endure annealing treatment in an oxygen containing atmosphere at 600 °C. In this study, the periods of laminated coatings were controlled by rotating speeds of the substrate holder. The annealing treatments were conducted at 600 °C under atmospheres of 20 and 50 ppm O₂-N₂, respectively. The variations in crystalline structure, hardness, surface roughness and chemical composition profiles in depth after various annealing times were investigated. The lifetime of a protective Ta-Zr coating was justified by exposed the coating in a 50 ppm O₂-N₂ environment to achieved a high hardness of 10 GPa and then annealed in a 20 ppm O₂-N₂ atmosphere for long times.

BP-10 Influence of thickness on mechanical and corrosion properties of Ti-Si-N coatings on D2 steel by unbalanced magnetron sputtering. *Y.K. Cheng, G.P. Yu, J.H. Huang (jhhuang@mx.nthu.edu.tw)*, National Tsing Hua University, Taiwan

In order to fulfill the requirements in industrial applications, hard coatings possessing both high hardness and good corrosion resistance are demanded. Ti-Si-N is one of the coatings that have been extensively studied in recent years. Most studies on Ti-Si-N coatings were focused on the hardening mechanisms due to structure evolution, composition variation, or impurity effect; however, few studies have been performed on the relation between residual stress and thickness variation. In this study, a series of Ti-Si-N coatings were deposited on AISI D2 tool steel without interlayer using unbalanced magnetron sputtering at different deposition durations. The coating thickness of all specimens was larger than 1 μm. The purpose of this study was to investigate the mechanical properties and corrosion resistance of the Ti-Si-N coatings. X-ray diffraction results showed that the thick Ti-Si-N coatings were composed of nanocrystalline TiN and amorphous Si₃N₄. Coating thickness was obtained from focused ion beam (FIB) measurement. X-ray photoelectron spectroscopy (XPS) was used to characterize the bonding state and compositions of the coatings. The hardness of the coatings was measured by nanoindentation. The residual stress was determined by modified sin²ψ x-ray diffraction and laser curvature methods to explore the residual stress state and stress distribution in the coatings. The adhesion of Ti-Si-N coatings was evaluated by scratch test. The influence of the coating thickness on corrosion resistance was evaluated by potentiodynamic scan and salt spray test. From the corrosion results, the thick Ti-Si-N coatings could effectively prevent the D2 steel from corrosion. The hardness of the coatings was related to the compositions and texture. The coating thickness was correlated to the residual stress, where a critical stress was found for the spallation of the coatings.

BP-11 Effect of Nitrogen Flow Rate on The Structure And Mechanical Properties of TiZrN Thin Films by Unbalanced Magnetron Sputtering. *C.W. Lu, J.H. Huang, G.P. Yu (gpyu@ess.nthu.edu.tw)*, National Tsing Hua University, Taiwan

Nanocrystalline TiZrN films were produced using unbalanced magnetron sputtering. The aim of this study was to investigate the effect of nitrogen flow rate on the microstructure and properties of the TiZrN films with nitrogen flow controlled from 1.3 to 2.5 sccm. Thin films of TiZrN were deposited by magnetron unbalanced sputtering on our previous optimum coating conditions for TiZrN. The results of the variation of nitrogen flow rate did not significantly affect the film thickness. The major effects of the nitrogen flow rate were on the texture coefficient, N/(Ti, Zr) ratio, hardness, and resistivity of the TiZrN films. The texture coefficients could be calculated from the integrated intensity of the corresponding XRD peaks.

The results indicated that (111) plane was the dominant preferred orientation for all TiZrN specimens. Two other peaks (200) and (220) of TiZrN films could be observed for the specimen at higher nitrogen flow rate. The N/(Ti, Zr) ratio of the TiZrN films increased with respect to the nitrogen flow rate, but increased slowly as nitrogen flow rate further increased. Hardness of TiZrN films first increased to its maximum of 33.1 GPa and then decreased as nitrogen flow rate further increased. The result showed that film hardness was not directly dependent on the (111) preferred orientation. The hardness of TiZrN thin films was due to solid solution strengthening and nanograin boundary sliding mechanism. The electrical resistivity and packing density of thin film related to the lattice defects. Similar to hardness, packing density also increased to a maximum at a critical nitrogen flow rate and the lowest resistivity corresponded to the highest packing density.

BP-12 Ternary d-Ti_xTa_{1-x}N: An addition to superhard materials? *L. Koutsokeras*, University of Ioannina, Greece, *A. Skarmoutsou*, National Technical University of Athens, Greece, *G. Abadias*, University of Poitiers, France, *P. Psyllaki*, Technological Education Institute of Piraeus, Greece, *C. Charitidis*, National Technical University of Athens, Greece, *C. Lekka, P. Patsalas (ppats@cc.uoi.gr)*, University of Ioannina, Greece

The quest of ultraperformant, hard protective coatings [1] is of major technological importance due to their applications in cutting tools, automotive and space industry, among others. Within this framework materials that exhibit hardness above 40 GPa are considered as superhard. Superhard materials are usually nanostructured, like the well known nc-TiN/a-Si₃N₄ [1]. Recently it was possible to grow the ternary compound d-Ti_xTa_{1-x}N [2] and its hardness has been measured to be as high as 42 GPa [3]; the later makes it a strong candidate for being a member of the group of superhard materials.

In this work, we investigate the effects of composition and microstructure of d-Ti_xTa_{1-x}N coatings on their mechanical performance. The d-Ti_xTa_{1-x}N coatings have been grown by dual-cathode magnetron sputtering (DCMS) and dual ion beam sputtering (DIBS). The DIBS-grown samples exhibit globular grain morphology and similar grain sizes for all values of x. On the contrary, the DCMS-grown samples exhibit strong variations of their microstructure, from globular to strongly columnar, with varying x, as identified by X-ray Diffraction and Electron Microscopy analyses. Therefore, by comparing their mechanical performance we can discriminate the effects of composition and microstructure. The mechanical testing has been performed in terms of hardness measurements by nanoindentation, tribological testing by lateral force measurements and wear testing by ball on disk measurements. According to *ab-initio* calculations of the elastic moduli, the pure d-TaN was expected to be the hardest member of the d-Ti_xTa_{1-x}N family. However, the experimentally produced d-TaN coatings are defective and underdense [4,5]. Here we prove that alloying TiN with TaN improves the mechanical performance by stabilizing the rocksalt structure for Ta-rich ternary d-Ti_xTa_{1-x}N coatings, which are harder than their constituents (TiN, TaN). Indeed, the Ta-rich d-Ti_xTa_{1-x}N coatings were superior in most aspects of mechanical testing.

[1] S. Veprek, *J. Vac. Sci. Technol.* A17, 2401 (1999).

[2] L.E. Koutsokeras, G. Abadias, Ch.E. Lekka, G.M. Matenoglou, D.F. Anagnostopoulos, G.A. Evangelakis, P. Patsalas, *Appl. Phys. Lett.* 93, 011904 (2008).

[3] G. Abadias, L.E. Koutsokeras, S.N. Dub, G.N. Tolmachova, A. Debelle, T. Sauvage, and P. Villechaise

J. Vac. Sci. Technol. A 28, 541 (2010).

[4] C.-S. Shin, D. Gall, P. Desjardins, A. Vailionis, H. Kim, I. Petrov, J.E. Greene, M. Odén, *Appl. Phys. Lett.* 75, 3808 (1999).

[5] G.M. Matenoglou, L.E. Koutsokeras, Ch.E. Lekka, G. Abadias, S. Camelio, G.A. Evangelakis, C. Kosmidis, and P. Patsalas, *J. Appl. Phys.* 104, 124907 (2008).

BP-13 Paramagnetic centers in hard graphite-like amorphous carbon. *A. Viana, C. Marques (marques@ifi.unicamp.br)*, Universidade Estadual de Campinas, Brazil

In this work we investigate the origin of paramagnetic centers in hard graphite-like amorphous carbon. The films were deposited by 1) plasma enhanced chemical vapor deposition (PECVD) using the decomposition of methane (CH₄) and 2) sputtering, using an argon ion gun to sputter a pure graphite target. High concentration of sp² films was obtained adopting high bias in the PECVD technique. These films have small band gap (0.5-1.0 eV) and hardness of approximately 15 GPa. The films prepared by the sputtering technique have sp² concentration of approximately 90 %, zero energy band gap and hardness of 20-30 GPa. Electron spin resonance (ESR) was performed at the X-band (9.4 GHz) microwave frequency using 100 kHz field modulation. A non-saturating power of 5 mW was adopted. The ESR measurements revealed an unexpected low density of paramagnetic

centers, ascribed to conduction electrons with a g-value of about 2.003. These results are compared with data reported for amorphous carbon films deposited by different techniques and with different sp^2 concentrations.

BP-14 Effects of sputtering gases on the preparation of boron nitride films using RF sputtering. *M. Imamiya* (*s1071006EE@it-chiba.ac.jp*), Graduate School, Chiba Institute of Technology, Japan, *Y. Sakamoto*, Chiba Institute of Technology, Japan

Many researches of thin film preparation and application for nitride films were reported. Nitride films have fascinate properties such as high hardness, wear proof, electrical properties and so on. On the other hand, boron nitride is one of the artificial material which doesn't exist naturally. Cubic boron nitride has high hardness and thermal conductivity next to diamond. Investigation was carried out on the effects of sputtering gases on the preparation of BN films using RF sputtering and preparation of BN films on the CVD diamond substrates.

Boron nitride was prepared using RF reactive sputtering. Si and CVD diamond were used as the substrates. Mixture of Ar-N₂ and Ar-NH₃ were used as reactive sputtering gases. The ratio of Ar:N₂ and Ar:NH₃ were 1:1, 1:3 and 1:5. Sputtering time was fixed to 1 h. CVD diamond substrates were synthesized using microwave plasma CVD. To obtain CVD diamond substrates, CH₄-H₂ was used as a reaction gases for diamond synthesis. CH₄ flow rate was 1 SCCM, H₂ flow rate was 100 SCCM and pressure was 5.3 kPa, microwave power was 400 W, respectively. Reaction time was fixed to 5 h. Surface of deposits was observed using SEM. Deposits were estimated by XPS and Raman spectroscopy.

As a result of SEM observation of the film on the Si substrates, surface morphologies of sputtered films were smooth. From XPS measurement, the B-N bond was observed in XPS spectra of each samples. Hardness of the film was increased and friction coefficient was decreased with increasing of N₂ ratio in Ar-N₂ sputtering gas for the Si substrate. As a result of SEM observation of the film on the CVD diamond substrates, BN film on CVD diamond crystals was recognized in each condition. In addition, diamond peak at 1333cm⁻¹ and the amorphous boron nitride peak at 1550 cm⁻¹ were observed in Raman spectra for Ar-N₂ sputtering gas. From XPS measurement, B-N bond was obtained in XPS spectra of each samples.

As a conclusion, high hardness BN films could be obtained in not so slow deposition rate using Ar-NH₃ sputtering gas. Moreover preparation of the BN film on the CVD diamond substrates could be performed.

BP-15 Influence of Silicon-doping on MSIP Al₂O₃ coatings. *K. Bobzin*, Surface Engineering Institute - RWTH Aachen University, Germany, *N. Bagcivan* (*bagcivan@iot.rwth-aachen.de*), RWTH Aachen University, Germany, *M. Ewering*, Surface Engineering Institute - RWTH Aachen University, Germany

Crystalline alumina PVD-coatings offer high potential for different applications in which high chemical inertness, high hot hardness and high oxidation resistance is important. Especially the metastable γ -phase is topic of many researches because, in comparison to the stable α -phase, it can be deposited by means of MSIP (Magnetron Sputter Ion Plating) at relatively low process temperatures below 650 °C and it is more fine-grained than α -Al₂O₃. At high temperatures γ -Al₂O₃ transforms into α -Al₂O₃, which limits the application temperature. But until now it is not clearly investigated, up to which temperatures γ -Al₂O₃ thin films are stable and which mechanisms influence the stability. In the following paper the influence of doping with Silicon is investigated. DSC (differential scanning calorimetry) as well as XRD (X-Ray diffractometry) measurements show that adding 4 at-% Silicon leads to a high amount of amorphous phase in the as deposited coating and a decreasing in hardness from 18 to 10 GPa. Nevertheless formation of the α -phase is retarded to temperatures above 1200 °C while for the undoped coating the α -phase is formed at temperatures of 1100 °C. For the Si-doped coating a transformation via the θ -phase was detected which is not seen for the undoped coating. In combination with a (Ti,Al)N-interlayer, which is necessary to provide a sufficient adhesion, Silicon improves compound properties after thermal exposure. This was proven by scratchtests and impact testing before and after annealing the samples at 900 °C.

BP-16 3-dimensional DLC coating on microgear by bipolar PBII & D and plasma analysis. *W.S. Park* (*park@sstl.info*), *J.H. Choi*, *T. Kato*, The University of Tokyo, Japan, *W.S. Lee*, Korea Institute of Industrial Technology, Republic of Korea

Diamond-like carbon coatings were deposited on microgears by using a bipolar-type plasma based ion implantation and deposition technique (bipolar PBII&D) and the plasma behavior was analyzed by particle-in-cell Monte Carlo simulation. The gas pressure was 0.4 Pa and negative and positive pulse voltages of -2.0 kV and +1.5 kV, respectively were applied to the target. The particle-in-cell method was used for the analysis of electromagnetic fields and the motion of charged particles and Monte Carlo

collision method was used for the analysis of collisions of ions, electrons and neutrals in the plasma. In this study, we investigated the distributions of potential, electron and ion densities, and ion flux around the microgear immersed in Methane plasma.

BP-17 Mechanical properties and oxidation resistance of TiSiN/CrAlN films synthesized by a cathodic arc deposition process. *Y.Y. Chang* (*yinyu@mail2000.com.tw*), National Formosa University, Taiwan, *Y.Y. Liou*, MingDao University, Taiwan

Transition metal nitrides, such as TiSiN and CrAlN, have been used recently as protective hard coatings due to their excellent tribological properties. In this study, TiSiN, CrAlN and multilayered TiSiN/CrAlN coatings were synthesized by cathodic-arc evaporation with plasma enhanced duct equipment. The deposition of CrN under the TiSiN/CrAlN was used as an interlayer to enhance better adhesion. With different cathode current ratios ($I_{\text{TiSiN}}/I_{\text{CrAlN}}$), the deposited TiSiN/CrAlN coatings possessed different chemical contents and periodic thicknesses. For the high temperature oxidation experiment, the deposited TiSiN, CrAlN and multilayered TiSiN/CrAlN samples were annealed at 800°C in air for 2 hours. The microstructure of the deposited coatings was investigated by a field emission gun high resolution transmission electron microscope (FEG-HRTEM, FEI Tecnai G² 20 S-Twin), equipped with an energy-dispersive x-ray analysis spectrometer (EDS), operated at 200 keV for high-resolution imaging. Glancing angle X-ray diffraction was used to characterize the microstructure and phase identification of the as-deposited and annealed films. The composition, chemical bonding and depth profile were evaluated by X-ray photoelectron spectroscopy. Mechanical properties, such as the hardness and elastic modulus, were measured by means of nanoindentation. To evaluate the impact resistance of the deposited coatings, an impact test was performed using a cyclic loading device. The design of multilayered TiSiN/CrAlN thin films is anticipated to inhibit the grain growth, and leads to grain refinement effect, which expected to increase the hardness and impact resistance of multilayer films. Meanwhile, the multilayered TiSiN/CrAlN, which forms stable and dense diffusion barriers at high temperature, is expected to possess good resistance to high temperature oxidation.

BP-18 Structural, Mechanical and Tribological Properties of TiTaBN CompositeGraded Coatings Deposited by CFUBMS Technique. *Ö. Baran* (*obaran@erzincan.edu.tr*), Erzincan University, Turkey, *İ. Efeoglu*, Ataturk University, Turkey, *B. Prakash*, Lulea Technical University, Sweden

Hard coatings based on transition metal nitrides, carbides or borides gained increasing importance. The properties of these hard coatings have been enhanced by adding with other elements such as Al, Si, Cr, V, Mo, etc. In this study, structural, mechanical and tribological properties of TiTaBN coatings obtained with Ta incorporation into TiBN were investigated. TiTaBN films were deposited on D2 steel and glass substrates using pulsed-dc closed field unbalanced magnetron sputtering (CFUBMS) with Taguchi L₉ (3⁴) experimental method. Morphology and structure of coatings were analyzed by SEM, EDS, XRD, and XPS. The hardness of TiTaBN coatings were determined with microhardness tester. The friction and wear properties of the coatings were analyzed at different test atmospheres (humid air, distilled water, dry nitrogen and synthetic oil) by using pin-on-disc. Consequently, TiTaBN coatings deposited at the R8 coating parameters exhibited dense and a columnar structure. These coatings deposited at the R8 coating parameters contains TiN, TaN, TiB₂ and BN phases and these coatings having ultra hardness (52.55GPa) demonstrated very high wear resistance at the different test atmospheres.

BP-19 Effect of Si⁺ kinetic energy on the physical properties of Ti-Si-N thin films deposited by RCBPLD. *L. Escobar-Alarcon* (*luis.escobar@inin.gob.mx*), *E. Camps*, *V. Medina*, National Institute for Nuclear Research, Mexico, *D. Solis-Casados*, Autonomus University of Mexico State, Mexico, *I. Camps*, Mexican National Autonomus University, Mexico

Metal transition nitrides alloyed with C, Si or Al, have a wide range of applications, mainly in the metal-mechanical field as hard and low friction coatings. It is worth mentioning that the properties of these materials depend strongly on the alloying concentration and therefore a lot of work has been devoted in the last years to investigate deposition techniques capable to form such ternary nitrides with controlled composition. In a previous work, we proposed the so-called Reactive Crossed Beam Pulsed Laser Deposition (RCBPLD) technique as an alternative to produce ternary compounds with controlled composition; particularly, this technique was applied successfully to deposit Ti-C-N thin films controlling the C content. In this work, it is reported the use of the RCBPLD to prepare nanostructured TiSiN thin films. With this experimental configuration, the amount of silicon incorporated in the film is controlled in an easy way varying the mean Si⁺ kinetic energy. The film structure, mechanical

properties, composition and surface morphology were investigated as a function of the Si⁺ kinetic energy. These properties were studied using the following characterization techniques: Raman spectroscopy, X-ray diffraction, nanoindentation, X-ray Photoelectron Spectroscopy and Scanning Electron Microscopy. It was found that the Si content, which was varied from 1.6 to 3.5 at.%, depends, approximately linearly, on the silicon ion kinetic energy. Ti-Si-N films with hardness as high as 34.0 GPa, which is suitable for many mechanical applications, were obtained. The hardness was strongly affected by the silicon ion energy, and there exists an optimal energy value, and consequently a certain value of Si content at which the maximum hardness is reached. These results show that the properties of the deposited material are controlled partially by the Si⁺ kinetic used for thin film growing.

BP-20 The Role of Aluminium for the Nanostructure and Mechanical Properties of Sputtered Ti-B Films. *P. Epaminonda*, University of Cyprus, Cyprus, *K. Polychronopoulou*, Northwestern University, US, *K. Fadenberger*, Robert Bosch GmbH, Germany, *M. Baker*, University of Surrey, UK, *P. Gibson*, Joint Research Centre, Italy, *A. Leyland*, A. Matthews, University of Sheffield, UK, *P.H. Mayrhofer*, Montanuniversität Leoben, Austria, *C. Rebholz* (*claus@ucy.ac.cy*), University of Cyprus, Cyprus

TiB₂ thin films have been studied extensively due to their outstanding properties (e.g. high hardness, high thermochemical stability), making them highly attractive for many applications in erosive, abrasive, corrosive and/or high-temperature environments. Despite their excellent properties, the usability and commercialisation of TiB₂ films has been mainly hindered due to their brittleness and limited film-substrate adhesion, caused by the primarily strong covalent bonding in the hexagonal B network and the high compressive stresses developed in deposited films on various substrates. An effective route for improving adhesion and toughness in hard ceramic films is the introduction of ductile metal additions (e.g. Al) or layers, therefore modifying their bonding type and structure.

In this study, Ti_xAl_yB₂ thin films ($0.88 \leq x \leq 1.04$; $0.12 \leq y \leq 0.31$), with Al contents between 4.1-9.4 at.%, were deposited onto Si (100) and AISI 316 stainless steel substrates by simultaneous co-sputtering from TiAl and TiB₂ targets in an argon discharge at 170°C. The coating stoichiometry, relative phase composition, nanostructure, density and mechanical properties were determined using X-ray photoelectron spectroscopy (XPS), X-ray diffraction (XRD) and Laser Acoustic Surface Waves (LAwave), in combination with nanoindentation measurements. It is shown that Al substitutes for Ti in stoichiometric closed-packed hexagonal nanocrystalline thin films with 4.1 at.% Al, having an average grain size of 2-3 nm. As the Al concentration is increased, the crystallinity, average TiB₂ grain size, density, hardness and elastic modulus decreases from ~2-3 to 1 nm, 4.2 to 3.8 g/cm³, 32.9 to 20.6 GPa and 335 to 250 GPa, respectively, while the film adhesion increases. Density and elastic modulus from *ab initio* calculations are compared to experimental results. The elastic modulus values measured by nanoindentation are lower than the calculated *ab initio* data, attributable to the nanocrystalline nature of the deposited films.

BP-21 Microstructural characteristics of CrZrSiN coatings synthesized by unbalanced magnetron sputtering with CrZrSi segment targets. *Kim, S.Y. Lee* (*sylee@kau.ac.kr*), Korea Aerospace University, Republic of Korea

Segment target have several advantages and theoretically it is possible to deposit almost all materials and to synthesize various multi-component coatings without much difficulties. It does have several advantages, but a high challenge to control the composition and microstructure of the coatings synthesized using segment target. In this study, CrZrSiN films were synthesized by unbalanced magnetron sputtering with CrZrSi segment target. Three types of segment targets with various atomic ratios of Cr+Zr and Si (each ratio of Cr+Zr to Si was 1:1, 2:1, and 3:1) were used in this work. Characterization of the coatings consisted of composition, microstructure, hardness and corrosion properties. The effect of the Si content were investigated by X-ray diffraction (XRD), field emission scanning electron microscope (FE-SEM), transmission electron microscope (TEM), atomic force microscope (AFM), microhardness tester, and glow discharge optical emission spectroscopy (GDOES). The surface images of the coatings were revealed that the coatings have dense and compact microstructure and very smooth surface and the surface roughness decreased as Si content in the coating increased. The microstructure of coatings consisted of mainly Cr(Zr)N crystalline and Si₃N₄ amorphous. The hardness of films approximately 32GPa was maintained up to 10% Si content and further increase in Si contents above 10% in the coatings seemed to decrease the hardness of the coatings below approximately 24GPa. Detailed experimental result will be presented.

BP-22 Synthesis and characterization of CrZrAlN coatings synthesized by unbalanced magnetron sputtering. *J.Y. Kim* (*kimjy@naver.com*), *D.J. Kim*, *B.S. Kim*, *S.Y. Lee*, Korea Aerospace University, Republic of Korea

The Cr-Zr-N films have much improved mechanical properties and very smooth surface roughness. However, even though the outstanding properties, the Cr-Zr-N coatings revealed that the mechanical properties deteriorated severely with increasing Al content above 50 at.%, due to rapid oxidation. Additionally, Al content in the CrZrAlN coatings is expected to improve the high temperature properties of the coatings. In this study, the quaternary Cr-Zr-Al-N coatings with various Al contents were synthesized using CrZrAl segment target by unbalanced magnetron sputtering. The characteristics of films were investigated by X-ray diffraction (XRD), Field Emission-Scanning Electron Microscope (FE-SEM), atomic force microscopy (AFM), glow discharge optical emission spectroscopy (GDOES), and microhardness tester. Preliminary results show that the Cr-Zr-Al-N coatings had outstanding mechanical properties with various Al contents at high temperature especially high temperature thermal stability of the coatings. Detailed experimental results will be presented.

BP-23 Mechanical Performance and Nanoscaled Deformation of Bias-Sputtered (AlCrTaTiZr)NC_y Multi-component Coatings. *S.Y. Lin*, *S.Y. Chang* (*shouyi@dragon.nchu.edu.tw*), *Y.C. Huang*, *F.S. Shieu*, National Chung Hsing University, Taiwan

This work develops (AlCrTaTiZr)NC_y multi-component carbo-nitride films, with the incorporations of quinary metallic elements, nitrogen and carbon, as protective hard coatings by co-sputtering of AlCrTaTiZr alloy and graphite in an Ar/N₂ mixed atmosphere with the application of different substrate biases. All the (AlCrTaTiZr)NC_y films deposited at different conditions exhibited a simple face-centered cubic structure. As the applied substrate bias and graphite-target power increased, the deposited (AlCrTaTiZr)NC_y coatings transformed from a large columnar structure with a (111) preferred orientation to a nanocrystalline or even near-amorphous structure. With increasing substrate bias and graphite-target power, the hardness and H/E ratio of the coatings increased from 18 GPa and 0.07, to much higher values of about 32 GPa and 0.12, respectively, attributed to the densification of the coatings, the introduction of covalent-like carbide bonds, the refinement of grains and the formation of nanocomposite structure. Because of the severe lattice distortions in the multi-component coatings caused by the addition of differently-sized atoms, the dominant deformation mechanism of the coatings was found to be the formation of stacking faults, rather than complete dislocations only.

BP-24 Effects of Substrate Temperature and Bias-Voltage on Mechanical Properties and Oxidation Resistance of TiAlYN Films. *N. Hattori* (*sunmoonstone@live.jp*), Keio University, Japan, *T. Takahashi*, Yungalay Corporation, Japan, *M. Noborisaka*, *T. Mori*, *M. Takahashi*, *T. Suzuki*, Keio University, Japan

It is well known that TiAlN films have been preferred in cutting tools for their mechanical properties and good oxidation resistance. However, many studies have reported that they oxidize over 800 °C. The addition of another element into matrix is one of the techniques to improve the properties. In our previous researches, we reported on the effect of yttrium addition to TiAlN films and investigated the mechanical and thermal properties. It was concluded that the films with the yttrium content 2 at.% showed the highest hardness and excellent oxidation resistance up to 900°C.

In this study, we synthesized Ti₄₉Al₄₉Y₂N films changing substrate temperatures at 100°C, 200°C, 300°C, 400°C and bias-voltages at 50 V, 100 V, 200 V, 300 V and investigated their oxidation resistance and mechanical properties. The films were deposited on Si, WC-Co, and SUS304 substrates by the cathodic arc ion plating (AIP) method. The hardness and adhesion were analyzed by a micro-Vickers hardness tester and Rockwell hardness tester, respectively. For the evaluation of the oxidation resistance, X-ray diffraction (XRD) and glow discharge optical emission spectrometry (GDOES) were performed to identify oxide layers of the films annealing at 900°C for 1 hour in air.

The hardness of all films doped yttrium increased, they were about 33 GPa. The films deposited at a substrate temperature of 200°C showed an excellent substrate adhesion and oxidation resistance. The difference in hardness and oxidation resistance was not observed changing bias-voltage. The results demonstrated that Ti₄₉Al₄₉Y₂N films deposited at bias voltage at 100 V and substrate temperature at 200°C showed high hardness and the oxidation resistance keeping the adhesion strength.

BP-26 Characterization of laser ablation bismuth and iron oxide plasmas used for deposition of bismuth-iron-oxide thin films. *E. Camps (eecamps2@hotmail.com), D. Cardona, L. Escobar-Alarcon, National Institute for Nuclear Research, Mexico, S. E. Rodil, Mexican National Autonomous University, Mexico*

Bismuth-Iron-Oxides (BFO) can be grown in five different phases, which can have very important multiferroic, magneto-optical and optoelectronic properties, making them attractive for different technological applications. The synthesis of these materials in the form of thin films has become quite difficult, being the laser ablation technique one of the most suitable. In the present work, it is proposed the simultaneous ablation of two targets (Bi and Fe_2O_3) in a reactive atmosphere (containing O_2), in order to deposit BFO thin films with different compositions. Prior to deposition, the plasma parameters, such as, mean kinetic ion energy (E_p), plasma density (N_p) and the type of excited species, were studied, in an attempt to correlate these parameters with the properties of the deposited BFO thin films. Deposition of the thin films was carried out at room temperature and the working pressure was varied in the range between 10 and 50 mTorr with an $\text{Ar}/\text{O}_2 = 80/20$ gas mixture. The iron oxide (FO) plasma parameters were kept constant at $E_p(\text{FO}) = 100 \text{ eV}$ and $N_p(\text{FO}) = 2 \times 10^{13} \text{ cm}^{-3}$, whilst the bismuth plasma parameters were varied in the range between 30 and 300 eV for the $E_p(\text{Bi})$ and $8 \times 10^{11} - 9 \times 10^{13} \text{ cm}^{-3}$ for the $N_p(\text{Bi})$. The optical emission spectroscopy (OES) showed that the most abundant excited species present in the plasmas were neutral Fe and neutral, once and three times ionized Bi. The deposited samples were characterized by Raman spectroscopy, X-Ray diffraction, EDS and RBS. The properties of the films are presented as a function of the plasma parameters.

BP-27 A study of W/DLC/WSC composite films fabricated by magnetron sputtering method. *M. Dai (daimingjiang@Tsinghua.org.cn), C. Wei, S. Lin, H. Hou, K. Zhou, Guangdong General Research Institute of Industrial Technology, China*

WS_2 is well known for its solid lubricating behavior in industry applications. However, it is sensitive to environmental atmosphere. In humid ambient air, WS_2 gets easily oxidized, resulting in the deterioration of its tribological properties. Moreover, another problem of the sputtered WS_2 films is their very low adhesion to the substrate, which lead in most cases to poor wear behaviour. In order to improve the properties of WS_2 film in humid air conditions, W/DLC/WSC composite films have been fabricated by magnetron sputtering method. The properties of composite films, as well as the influence of C content in the WSC top layers were researched. The morphology and microstructure of the composite films were characterized by scanning electron microscopy (SEM) and X-ray diffraction (XRD). Vickers microhardness tests were carried out to determine the hardness of composite films. Scratch tests were performed to study the adhesion of the films to the cemented carbide substrate. The tribological behavior was investigated using a ball-on-disk tribometer in humid air. The results show that the composite films exhibit dense and featureless in appearance. None C or WS_2 peaks have been observed in the spectrum of X-ray diffraction (XRD). Thereby, amorphous or nanocrystal structure has been obtained according to the SEM and XRD results. The hardness of composite films can be enhanced obviously and it increases with increasing the C content. Compared to the pure WS_x film, W/DLC/WSC gradational structure can improve the adhesion of films effectively and the maximal critical load of the composite film reaches 62N. Though the friction coefficient of the pure WS_x film (about 0.1) is lower than that of the composite films (0.15–0.25), the wear life of composite films are much longer owing to their higher hardness and better adhesion to the substrate.

BP-28 Comparison of the wear characteristics of TIN Coating with Manganese Phosphate Coating. *S. Sivakumaran (ilaiyavel@svce.ac.in), A. Alangaram, Sri Venkateswara College of Engineering, India*

Manganese Phosphate is an Industrial coating used to reduce friction and improve lubrication in sliding components. In this study, the tribology behavior of TIN (which as produce both PVD and CVD) Manganese Phosphate with Molybdenum disulphide (MoS_2) coated AISID2 steels was investigated. The Surface morphology of manganese phosphate coatings was examined by Scanning Electron Microscope (SEM) and Energy Dispersive X-ray Spectroscopy (EDX). The wear tests were performed in a pin on disk apparatus as per ASTM G-99 Standard. The wear resistances of the coated steel were evaluated through pin on disc test using a sliding velocity of 3.3 m/s under Constant load of 50 N and controlled condition of temperature and humidity. The Coefficient of friction and wear loss were evaluated. The temperature rise after 15 min and 30 min were recorded for each load. Wear pattern of TIN, Manganese Phosphate with Molybdenum disulphide (MoS_2) coated pins were captured using Scanning Electron Microscope (SEM). Based on the results of the wear test the manganese phosphate with Molybdenum disulphide (MoS_2) coating exhibited the lowest coefficient of friction and the lowest wear loss under 50 N load.

BP-29 Exotic mechanical properties of Cu-doped nano-columnar DLC coating. *S. Yukawa (mb11052@shibaura-it.ac.jp), T. Aizawa, Shibaura Institute of Technology, Japan*

Diamond like carbon (DLC) coating has grown up to be a common way to improve the surface properties of dies and punches in dry stamping, by its high wear resistance and low friction coefficient. Aiming at its applications to an oxide-glass stamping mold-dies or a protective coating for MEMS/NEMS, high thermal stability and elasticity are much required. In fact, the stability above the glass-transition temperature of oxide glass and nano-scaled dimensional guaranty are needed in the mold-stamping process of collective lens for solar panel. Nano-columnar DLC coating is suitable for this application because of the high durability and metallic doping is effective to improve the thermal stability at elevated temperature.

Cu-doped DLC coating was prepared on silicon wafer by RF-sputtering with co-doping method. Deposited film was subjected to low energy electron beam (EB) irradiation. Nano-columnar structure with copper, which segregates into the grain boundary, is formed. The size of columns ranges around 20 nm. Raman spectroscopy is utilized to describe the bonding state and structure. Obtained spectrum of Cu-doped EB irradiated film is deconvoluted into two peaks pairs ($D_1:G_1$, $D_2:G_2$). Calculated $I(D_1)/I(G_1)$ and $I(D_2)/I(G_2)$ are 2.11 and 0.30, respectively. D_1 and G_1 correspond to initial amorphous carbon matrix: its in-plane correlation length (L_a) becomes 2 nm. L_a ($D_2:G_2$) is estimated 15 nm and it nearly equals to average of the measured diameter of columns. That is, graphitization takes place in the inter-columnar region and vertically aligned graphitic network is embedded in the disordered amorphous carbon matrix. Compared with undoped sample after EB irradiation, Cu-doped sample is much more graphitized: $I(D_2)/I(G_2)$ for undoped is 0.46. Hardness of the samples, Cu-doped after EB, undoped as-deposited and undoped after EB, obtained by nano-indentation are 1166, 1150 and 1071, respectively. Cu-doped sample shows a great elastic recovery and it is reversible up to 12% of the film thickness. This hardening and elasticity attribute to segregation of copper and graphitization in inter-columnar region.

BP-30 A Fem Supported Method for the Fast Determination of Nanoindenter's Tip Geometrical Deviations. *K.-D. Bouzakis (bouzakis@eng.auth.gr), M. Pappa, G. Malialis, Michailidis, Aristoteles University of Thessaloniki; Fraunhofer Project Center Coatings in Manufacturing (PCCM), Greece*

Nanoindentation is an effective technique for determining mechanical properties of bulk materials and thin films. Prevailing measurement uncertainties in nanoindentations by Vickers or Berkovich diamond pyramids are commonly caused by manufacturing imperfections of the indenter's side angles and tip sharpness. Moreover, the tip geometry changes during the indenter lifetime, due to diamond wear.

The present paper deals with a fast method for estimating diamond indenters' tip nano and micro geometry. On one hand, this method is based on a combination of nanoindentations on Si(100) used as reference material and on the other hand, on FEM supported calculations of Martens hardness. The hardness calculations are conducted using equivalent indenter tip geometry with geometrical characteristics which may vary for a specific set of parameters, describing the real indenter with manufacturing imperfections. These parameters are varied in successive iterations until the calculated hardness converges with that of the reference material.

For a quick determination of these parameters, the software package "TIDE" (Tip Deviations Estimation) has been developed. "TIDE" is based on numerous FEM supported simulation's results of nanoindentations onto the reference material varying the indenter tip geometry. By this software package, a quick prediction of nanoindenters' tip equivalent geometry is facilitated, also for anticipating changes due to wear of the diamond over time.

KEYWORDS: Nanoindentation, tip, imperfections, wear

BP-31 An analysis of the effect of local environments on vacancy formation and diffusion energy barriers in $\text{Ti}_{0.5}\text{Al}_{0.5}\text{N}$ alloy. *F. Tasnadi (tasnadi@ifm.liu.se), M. Odén, I. Abrikosov, Linköping University, Sweden*

Microstructure analysis has attracted high interest in hard coating developments as often the microstructure has a decisive impact on the hardness of materials [1]. For example, the isostructural spinodal decomposition results in hardness enhancement in TiAlN . Modeling microstructure evaluation via diffusion requires not only energetic, mechanical but also kinetic parameters of the materials. Here we present results on vacancy, divacancy formation and migration in $\text{Ti}_{0.5}\text{Al}_{0.5}\text{N}$ alloy using first principles density functional theory calculations. We pay special attention to the analysis of the impact of local environments.

[1] P. H. Mayrhofer, C. Mitterer, L. Hultman and H. Clemens, Prog. Mat. Sci. 51, 1032 (2005).

BP-32 First-principles study of the local environment effects on surface diffusion in multicomponent nitrides. C. Tholander (*chtho@ifm.liu.se*), F. Tasnádi, B. Alling, L. Hultman, Linköping University, Sweden

Growth of multicomponent nitride thin films is typically performed under kinetically limited conditions. Thus, the study of surface diffusion is one key to understanding behavior such as texture development and clustering during crystal growth. An earlier study of diffusion on TiN(001) and (111) surfaces [1] has shown that there is a large difference in diffusivity of adatoms on different surface directions, which greatly influences the preferred growth direction. We present results from first-principle studies using the nudged elastic band technique to calculate the energy barriers on low index crystal surfaces. By introducing different metal atoms and clusters in the surface of TiN and calculating the changes in the surface energy barriers, we show the effects on surface diffusion due to the change in the local environment. For example we show that the introduction of configurational disorder in $\text{Ti}_{0.5}\text{Al}_{0.5}\text{N}$ (001) slow down the Ti adatom diffusion as compared to the pure TiN(001) case.

[1] D. Gall, S. Kodambaka, M. A. Wall, I. Petrov, and J. E. Greene, J. Appl. Phys. 93, 9086 (2003)

BP-33 Effects of electroless Ni and PVD-TiAlZrN duplex coatings on corrosion and erosion behavior of ductile iron. C.H. Hsu (*chhsu@ttu.edu.tw*), K.H. Huang, Y.H. Cheng, Tatung University, Taiwan, C. Lin, Feng Chia University, Taiwan, K. Ou, Taipei Medical University, Taiwan

This study utilized electroless nickel (EN) plating and cathodic arc evaporation (CAE) technologies to deposit the protective coatings onto ductile iron substrates. Polarization corrosion tests were performed in 3.5% sodium chloride. The erosion tests were also carried out using Al_2O_3 particles (~177 μm in size and Mohr 7 scale) of about 5 g, and then surface morphologies of the eroded specimens were observed. To further understand the coating effects on both the corrosive and erosive behaviors of ductile iron, coating structure, morphology, and adhesion were analyzed using XRD, SEM, and Rockwell C indentation, respectively. The results showed that EN coating exhibited an amorphous structure, while TiAlZrN had a multilayered type. With regard to both the corrosion resistance and erosion resistance, the TiAlZrN/EN duplex coated specimens performed better than did the uncoated and monolithic EN or TiAlZrN ones.

BP-34 Microstructure and phase analysis of Cr-Mo-N composite film including different interlayer by hybrid PVD. Y.S. Oh (*ysoh30@kicet.re.kr*), Y.H. Yang, Korea Institute of Ceramic Engineering and Technology, Republic of Korea, I.W. Lyo, Hyundai-Kia Motor Company, Korea, Republic of Korea, S.J. Park, Hyundai Hysco, Korea, Republic of Korea

Chromium nitride film, the representative hard coating together with titanium nitrides, have been developed as protective film of forming tools, anti-corrosive and tribological applications of precision components in various industries. Currently such chromium nitrides film were developed as a form of nanocomposite films which have multi-functions to extend its application fields such as exhaust manifold required high temperature wear resistance and anti-corrosive property.

Mo added chromium nitrides composite films were fabricated by hybrid PVD method with different interlayer in this work. Typical columnar structures were changed to repetitive short pitches and tens of nanometer scale of multi layer was formed inside the matrix of composite film. And the preferred orientation of growth structure was varied according to the different interlayer and bias condition. Microhardness was almost 30GPa for Mo added composite film including metal Mo interlayer from nanoindentation test. Details of microstructures were analyzed by FESEM and STEM.

BP-35 Structure and properties of TiBCN coatings synthesized using unbalanced magnetron sputtering. C.H. Hsieh, C.H. Tsai, W.Y. Ho (*weiyuho@mdu.edu.tw*), Department of Materials Science and Engineering, MingDao University, Taiwan, C.H. Hsu, Department of Materials Science and Engineering, Tatung University, Taiwan, C.A. Lin, Department of Materials Science and Engineering, MingDao University, Taiwan, C.L. Lin, Department of Electro-Optical and Energy Engineering, MingDao University, Taiwan

The development of multifunctional coatings based on nanocomposite and multilayers was design to meet various severe corrosion, oxidation, and wear environmental conditions. Nanocomposite coatings are usually formed from ternary or higher order systems which are supersaturated or metastable solid solutions or comprise at least two immiscible phases. TiBCN coating system was one of the promising nanocomposite coating systems exhibiting super hardness, good tribological properties, and high oxidation and corrosion resistance. TiBCN coating have been successfully synthesized by chemical vapor deposition (CVD), electron beam physical vapor deposition

(EBPVD), and more commonly by dc magnetron sputtering. In the present study, TiBCN nanocomposite coatings were deposited from TiB_2 and Ti dual targets using a unbalanced magnetron sputter system operated with fixed nitrogen flow and different C_2H_2 flows. The effects of the carbon content on the phases, microstructure, mechanical and tribological properties of TiBCN coatings were investigated. It is shown that with the different carbon content in the coatings the microstructures of TiBCN can be tailored to TiBN, TiBCN and TiBCN/Carbon duplex layers. The coated samples were characterised with the following techniques: nano-indentation (hardness), ball-on-disc (wear and friction), scratch test (adhesion), scanning electron microscopy and Raman spectroscopy (microstructure) tests.

BP-36 Low Temperature Plasma Nitriding of F51 Duplex Stainless Steel. A. Tschiptschin (*antschip@usp.br*), L.B. Varela, University of São Paulo, Brazil, C. Pinedo, Heat Tech Technology for Heat Treatment and Surface Engineering Ltd, Brazil

In this work an AISI F51 duplex stainless steel was DC-Plasma nitrided (PN) at 400°C, during 20 hours in a 75% N_2 + 25% H_2 atmosphere. A modulated plasma nitrided layer formed on the specimen's surface: the nitrided layer observed on the ferritic regions was 3 μm thick, while the nitrided layer formed on the austenitic regions of the microstructure was ~2 μm thick. Very fine martensite needles were observed on the ferritic regions, while expanded austenite layer (Y_N) formed on the austenitic regions. The nitrogen content of the nitrided layer was estimated from X-ray diffraction measurements and WDX as being ~3.4 to 4.4 wt % N, leading to colossal supersaturation and strong hardening of the surface, up to 1350 HV. The 400 °C plasma nitrided layer did not impair the corrosion resistance of the duplex stainless steel. These results are discussed based on the hypothesis that, during nitriding, ferrite transforms at first to austenite and then to expanded austenite, due to nitrogen pickup. The expanded austenite formed on ferrite regions transforms to martensite, under stresses developed during the formation of expanded austenite in the neighboring austenite grains.

Keywords: Plasma nitriding, Duplex stainless steel, Expanded austenite, Martensite

BP-37 Residual stress on nanocomposite thin films using $\sin^2\psi$ method. G. Ramírez (*enggiova@hotmail.com*), S.E. Rodil, J.G. González-Reyes, Universidad Nacional Autónoma de México - Instituto de Investigaciones en Materiales, Mexico

Residual stress on thin films can be significantly high, sometimes as large as several gigapascals and they can be either compressive or tensile. For the super-hard coatings, such as metal nitrides or carbides, the hardness and the compressive stress are strongly correlated; in such a way that the high hardness values are usually obtained for highly strained films. This correlation imposes some limitations in both the thickness of the films and their use for high temperature applications. In this work, we have produced nanocomposite thin films of tantalum nitride (TaN) and niobium nitride (NbN) nanocrystals embedded in amorphous silicon nitride (SiN_x) phase. The films were deposited using two magnetrons (pure metal and silicon) and the silicon content on the films was varied by increasing the radio frequency power applied to the Si-target, while the other deposition conditions remained fixed. In both cases, the results showed that the hardness increased as the Si content increased from 0 to 5-6 at%, but further Si incorporation resulted in a decrease in the hardness.

The aim of the present work was to study the possible correlations between the residual stress, the silicon content and the hardness of the films. The residual stress was determined the lattice strain method using X-ray diffraction. The $\sin^2(\psi)$ method was used to determine the stress tensor. The results showed that the films present a triaxial stress state with compressive components in the plane normal to the growth direction and shear components. From this analysis it was demonstrated that even for the nanocomposite films, the maximum hardness films also showed the highest stresses. Stress in the direction x and y are compressive and equivalent in magnitude so that is not a change or stress gradient in the direction perpendicular plane to the film growth. On the other hand, the stress in the z direction (perpendicular to the growth of the film) was tensile.

We concluded that the described method commonly used to study bulk materials can be used to calculate the stress tensor in hard nanocomposite coatings. The results obtained indicated that the hardness was directly related to the stress; larger hardness values were obtained for the samples with the higher stress.

Acknowledgements: We wish to acknowledge the financial support from DGAPA-UNAM IN103910. G. Ramírez acknowledges CONACYT for his PhD scholarship.

BP-38 Stress signature of an amorphous- to- crystalline transition into the β -phase during Ta thin film growth on Si. A. Fillon, J.J. Colin, C. Szala, A. Michel, G. Abadias (gregory.abadias@univ-poitiers.fr), C. Jaouen, Institut P² - Université de Poitiers, France

Tantalum is a refractory metal with low electrical resistivity. Interest in the electrical properties of Ta thin films have been stimulated by its potential applications in electronic devices. Bulk Ta has a *bcc* structure, known as the α -phase. However, during thin film growth, the metastable tetragonal β -phase is commonly formed, especially on Si substrates. β -Ta has a higher resistivity, is also harder and more brittle than α -Ta. Role of impurities, defect concentration and stress state have often been reported. Nonetheless, the preferential formation of the β -phase onto Si substrates is not fully understood.

To address the impact of growth conditions on physical properties of thin sputtered Ta films, we present results obtained by combining highly sensitive *in-situ* stress measurements by the substrate curvature technique and *ex-situ* structural investigations (XRD and HRTEM). Thin films of Ta were grown at room temperature on an amorphous Si layer, or on Si substrates, using magnetron sputter-deposition under Ar atmosphere. A structural change occurring in the nanometric range (~ 3 -4 nm) is clearly identified, from both the real-time stress evolutions and *ex-situ* structural characterizations, which is attributed to a polymorphic crystallization of an amorphous film, initially stabilized by a minimization of the interface energy. The amorphous to β -crystalline transformation is accompanied by the development of an intrinsic growth stress, with a steady-state component ranging from a tensile state to a compressive one as a function of processing parameters (Ar working pressure : 0.1 – 0.8 Pa, substrate bias voltage : 0 – 100V). Finally, these results suggest that the nucleation into the β -phase would be favoured by similar specific volumes of the two metastable amorphous-Ta and β -Ta phases, whereas the β -phase growth at larger thicknesses would be explained by the weak difference between the Gibbs energies of α -Ta and β -Ta.

BP-39 Influence of Bias Voltage on Residual Stresses and Mechanical Properties of Multicomponent TiSiCrAlN Coatings. Y.Y. Chang (yinyu@mail2000.com.tw), National Formosa University, Taiwan, C.Y. Tsai, MingDao University, Taiwan

The extension of the tool life is a considerable goal for cutting and forming tools. Therefore the industry is interested to improve the mechanical performance for such tools. Transition metal nitrides, such as TiSiN and CrAlN, have been used recently as protective hard coatings due to their excellent tribological properties. In this study, TiSiN, CrAlN and multicomponent TiSiCrAlN coatings with different alloy contents were synthesized by cathodic-arc evaporation with plasma enhanced duct equipment. The multicomponent TiSiCrAlN coatings have a high potential as hard and tough coating to improve the tribological behavior of cutting and forming tool surfaces. TiSi and CrAl alloy cathodes were used for the deposition of TiSiCrAlN coatings. During the coating process of multicomponent TiSiCrAlN, TiN was deposited as an interlayer. With different cathode current ratios ($I_{\text{TiSi}}/I_{\text{CrAl}}$), the deposited TiSiCrAlN coatings possessed different chemical contents. Due to the absence of adhesive and cohesive damage processes by the residual stress behavior in the layer near the substrate area, it is critical to measure residual stresses in order to increase tribological resistance. X-ray diffractometry was performed for phase identification using a PANalytical X'pert Pro diffractometer with a high resolution ψ goniometer and Cu radiation in both glancing angle and high-angle configurations. In addition to the phase analysis, the residual stress measurements were also investigated by means of x-ray diffractometry. An experimental method with a grazing-incidence diffraction geometry was used in order to enhance the irradiation volume of thin film samples. The microstructure of the deposited coatings was investigated by a field emission gun high resolution transmission electron microscope (FEG-HRTEM, FEI Tecnai G² 20 S-Twin), equipped with an energy-dispersive x-ray analysis spectrometer (EDS), operated at 200 keV for high-resolution imaging. Mechanical properties, such as the hardness and elastic modulus, were measured by means of nanoindentation. To evaluate the impact resistance of the deposited coatings, an impact test was performed using a cyclic loading device.

BP-40 Effect of degree of ionization on preferred orientation and properties of TiN thin films deposited by high power impulse magnetron sputtering. C.Y. Chen, G.P. Yu, National Tsing Hua University, Taiwan, J.Y. Wu, Institute of Nuclear Energy Research, Taiwan, J.H. Huang (jhuang@mx.nthu.edu.tw), National Tsing Hua University, Taiwan

Due to its high hardness and low electric resistivity, TiN has been widely used as protective coatings on cutting tools and as diffusion barrier in microelectronic devices. The preferred orientation of TiN thin film is one of the major parameters that may affect the film properties. Therefore, many mechanisms have been proposed to explain the evolution of the preferred

orientation of TiN deposited at different conditions. Most TiN specimens in the previous studies were prepared using dc magnetron sputtering. Few studies were performed at highly ionized condition to investigate the effect of ionization on the preferred orientation and the corresponding TiN thin film properties. Recently, high power impulse magnetron sputtering (HIPIMS) has attracted considerable interests in industrial applications. By using power supplies that are able to provide the target with very high pulsing power density within several microseconds while maintain the average target power density similar to dcMS, HIPIMS can generate an ultra-dense plasma (10^{13} - 10^{14} ions/cm³) where the sputtered atoms are highly ionized (70%~100%). As a result, this highly ionized plasma can be used to bombard the substrate, deliver energy to adatoms to facilitate their migration, and even manipulate thin film preferred orientation to tailor the film properties. The purpose of this research was in an attempt to control the preferred orientation of TiN thin film using HIPIMS with different degree of ionization. In this study, by varying pulse shape, or nitrogen flow rate to control the degree of ionization of HIPIMS, TiN thin film was deposited on Si wafer. Subsequently, the microstructure, compositions, and mechanical properties of the TiN thin film were fully characterized. The preferred orientation was characterized by X-ray diffraction. The microstructure and to measure thin film thickness was observed by SEM. The composition of the film was determined by XPS and RBS. Nanoindentation and four-point probe were utilized to measure the film hardness and the electric resistivity, respectively. The residual stress of the TiN film was measured by optical laser curvature method. The results showed that the preferred orientation of thin film varied with the degree of ionization. The mechanical properties and resistivity of the thin film were also sensitive to the degree of ionization. However, since the thin film was extensively bombarded by ion under the deposition conditions, the TiN film possessed very high residual stress. The experimental results indicated that by adjusting the degree of ionization of plasma, the thin film preferred orientation and the accompanying properties can be controlled.

BP-41 Microstructures and mechanical properties of titanium carbide coating obtained by Thermo-reactive deposition process. X.S. Fan (fxs@stu.xjtu.edu.cn), Z.G. Yang, C. Zhang, Tsinghua University, China

Thermo-reactive deposition/diffusion (TRD) process is a method used to prepare hard, wear-resistant coatings of carbides, nitrides, or carbonitrides on steels. In this study, carbide coating was tried to deposit on T10 steels by duplex treatment. The steel substrate was immersed in a molten salt bath consisting of vanadium then in a molten salt bath consisting of titanium at 1000 °C. The obtained coatings were characterized by scanning electron microscopy (SEM), energy dispersive X-ray spectrometry (EDX) and X-ray diffraction (XRD). The results showed that the coating obtained from the duplex treatment was composed of two distinct layers. The outer layer was titanium carbide and the inner layer was vanadium carbide. The substrate /vanadium carbide coating interface and the vanadium carbide coating/ titanium carbide coating interface is distinct and without transition zone. The micro-hardness, scratch and pin-on-disk wear tests were conducted to evaluate the mechanical properties. The results showed the hardness of the duplex coating is higher than the vanadium carbide single layer. And the duplex coating exhibited excellent adhesive strength and outstanding wear resistance.

BP-42 Enhanced Glow Discharge Plasma Immersion Ion Implantation Using an Insulated Tube. Q.Y. Lu, P. Chu (paul.chu@cityu.edu.hk), City University of Hong Kong, Hong Kong Special Administrative Region of China, L. H. Li, City University of Hong Kong; Beijing University of Aeronautics and Astronautics, Beijing, China, R. Fu, City University of Hong Kong, Hong Kong Special Administrative Region of China

Enhanced glow discharge plasma immersion ion implantation (EGD-PIII) conducted using a small pointed hollow anode and large tube cathode has certain advantages over conventional plasma immersion ion implantation (PIII). In EGD-PIII, the plasma is produced by self glow discharge induced by the negative high voltage applied to the sample. The plasma distribution measured by Langmuir probe measurements discloses that the electron density is quite uniform in the vicinity of the negatively biased substrate. Although the impact energy and ion implantation fluence have been demonstrated to be better in EGD-PIII than those in conventional PIII, lateral non-uniformity in the ion fluence is observed during hydrogen implantation into a silicon wafer and the ion focusing effect depends on the plasma density. An insulated tube placed between the chamber and gas inlet is employed to increase the interaction path for electrons and neutrals, and theoretical and experimental studies reveal that the insulated tube can enhance ionization of plasma gases with low ionization efficiency such as hydrogen. However, the implantation current is observed to increase sharply at a certain pressure when the plasma gas consists of diatomic molecules. In this work, we experimentally investigate the implantation current characteristics in EGD-PIII. The plasma potential is measured to investigate

the discharge phenomenon and X-ray photoelectron spectroscopy (XPS) is conducted to corroborate the findings.

BP-43 Electrical transport properties in $\text{ZrN-SiN}_x\text{-ZrN}$ structures investigated by I-V measurements. *D. Oezer, C.S. Sandu, EPFL, Switzerland, R. Sanjines (rosendo.sanjines@epfl.ch), Ecole Polytechnique Fédérale de Lausanne, Switzerland*

Nanocomposite thin films based on polycrystalline transition metal nitride (MeN, Me = Ti, Cr, Zr, ...), in which the metallic MeN crystallites are embedded in an amorphous silicon nitride matrix, are considered as interesting materials due to their rich variety of physical properties, such as high hardness and improved thermal and chemical stability. The mechanical, optical and electrical properties are strongly linked to the architecture of the silicon nitride tissue phase at the grain boundaries. According to our best knowledge the local chemical composition and the thickness of the grain boundaries have never been probed directly so far. However the interpretation of the temperature dependent electrical resistivity data in the frame work of the grain boundary scattering model combined with structural and chemical analyses allows to correlate the evolution of the silicon nitride coverage layer to the electron grain boundary transmission probability. In order to investigate the mechanism of electrical conduction through single grain boundaries, we have investigated the transverse electric transport through well defined $\text{ZrN}_x/\text{SiN}_x/\text{ZrN}_x$ multilayers with varying SiN_x interlayer thicknesses and chemical compositions by means of I-V characteristic curves. At room temperature, depending on the SiN_x thickness linear I-V and symmetric nonlinear I-V characteristics are observed. On the bases of standard models for M-I-M such as the Poole-Frenkel and Tunneling models, we will discuss the applicability of our results to the interpretation of the electric conduction in "real" nanocomposite MeN/ SiN_x systems.

Fundamentals and Technology of Multifunctional Thin Films: Towards Optoelectronic Device Applications

Room: Golden Ballroom - Session CP

Symposium C Poster Session

CP-1 Investigation on Physical Properties of CuInSe_2 Films Prepared by Pulsed Laser Deposition. *M.H. Wen, J.Y. Luo, Y.T. Hsieh, C.C. Chang, C.H. Hsu, Y.R. Wu, W.H. Chao, M.K. Wu, Institute of Physics, Academia Sinica, Nankang, Taiwan, H.S. Koo (frankkoo@must.edu.tw), Ming-Hsin University of Science and Technology, Taiwan*

We report the study on thin films composed of the Cu-rich CuInSe_2 (CISE). The films were deposited on the glass and Mo-coated substrate, respectively, by the pulsed laser deposition (PLD) method at substrate temperatures from 450°C ~ 600°C. Both films revealed an obvious orientation (112) when the substrate temperature above 450 °C. By applying different substrate temperatures, different grain size and crystallinity of CISE films were obtained. The films showed a p-type electrical conductivity with a high absorption coefficient of $10^4 \sim 10^5 \text{ cm}^{-1}$ and optical energy gap of 0.92 ~ 0.97 eV.

CP-2 Electro-optical properties and damp heat stability of Al-doped ZnO thin films prepared by laser induced high current pulsed arc deposition. *J.B. Wu (wujinbao@itri.org.tw), C.Y. Chen, C.C. Shih, J.J. Chang, M.S. Leu, Material and Chemical Research Laboratories, Industrial Technology Research Institute, Taiwan, H.Y. Tseng, Y.C. Lu, BeyondPV Co., Ltd, Taiwan*

Highly transparent conductive Al-doped ZnO (AZO) thin film was deposited at 100 °C by laser induced high current pulsed arc (LIHCPA) from an Al-Zn alloy target (2 and 3 wt.% of Al doping content). The film's properties were highly correlated to the growth conditions, including O_2 partial pressure and Al doping content. The results clearly showed that when the O_2 partial pressure increased from 8×10^{-2} Pa to 3×10^{-1} Pa, the resistivity gradually increased from 4.2×10^{-4} to $1.9 \times 10^{-3} \Omega\text{-cm}$ and 5.2×10^{-4} to $2.3 \times 10^{-3} \Omega\text{-cm}$ for the 3 and 2 wt.% of Al-Zn target. Likewise, the band gap of the AZO films calculated by UV/VIS spectrometer measurement decreased from 3.77 eV to 3.58 eV and 3.56 to 3.44 eV as well. The XRD results showed that the AZO films preferred c-axis orientation along the (002) plane. XPS analysis revealed that the Zn and O chemical state can be assigned to the Zn exists in the oxidized state and O occurs in two chemical state (I) O^{2-} ions on wurtzite structure of hexagonal Zn^{2+} ion array, surrounded by Zn and the (II) chemisorbed oxygen species like O^{2-} , $\text{O}^{\cdot -}$ and $\text{O}_2^{\cdot -}$ at the grain boundaries, respectively. The degradation and performance studies of AZO and its variants have been performed under varied temperature conditions at 85% RH. The results indicated that samples held at 37 °C and 45 °C did not show any degradation of the sheet resistance

upon exposure. However, the final sheet resistance of AZO films held at 85 °C showed 2 times higher than that for as-grown films.

CP-3 Effect of Dopants and Thermal Treatment on Properties of Ga-Al-ZnO Thin Films Fabricated by Hetero Targets Sputtering System. *K.H. Kim (KHKim@kyungwon.ac.kr), Department of Electrical Engineering, Gachon University Republic of Korea, J.S. Hong, N. Matsushita, Materials and Structures Laboratory, Tokyo Institute of Technology, Japan, H.W. Choi, Department of Electrical Engineering, Gachon University, Korea*

For preparation of new material transparent electrode, we prepared the Ga and Al doped ZnO (Ga-Al-ZnO; GAZO) thin film under various conditions by using facing targets sputtering (FTS) system as function of input current and thermal treatment temperature.

The FTS system can prepare the thin film using new materials because it uses two targets. Also, the substrate is located in a plasma-free area apart from the center of plasma so it can suppress high energy particles colliding to the substrate so high quality films can be prepared.

The properties of the as-deposited GAZO thin films were then examined by 4-point probe, atomic force microscope (AFM), X-ray diffractometer (XRD), and field emission scanning electron microscope (FESEM) and UV-VIS spectrometer. As a result, the lowest sheet resistance of the films showed 59.3 ohm/sq and average transmittance about 90% in the visible range. And after thermal treatment, we could observe the more improved properties of GAZO thin film. The lowest sheet resistance (47.3ohm/sq) of the GAZO thin films were shown at thermal treatment temperature of 300°C. It is considered that this is the result of continuous substitutions by dopants and improved crystalline by thermal treatment.

CP-4 Ellipsometry Study of a Reactively Sputtered Transparent Conductive Oxide(TCO). *G. Ding (gding@intermolecular.com), M. Le, F. Hassan, Z. Sun, M. Nugen, Intermolecular Inc, US*

Sb-Sn oxide (ATO), a good TCO, thin film was reactively sputtered on a glass, and characterized as the Sb contents and annealing temperatures, by transmission, reflection, absorption, resistivity, film thickness, refractive index n and k, XRD, Hall probe and ellipsometer (300~1000nm).

An ellipsometry method was developed to determine the ATO film carrier density and gradient. There are some reports on the resistivity evaluation based on the Drude model through ellipsometer measurements. However, the uniqueness of the model fitting is poor in many conditions, (many values could fit the model, so that no unique value could be precisely determined). In theory: Tauc-Lorentz and Drude could give good description of the band-gap and free carrier physics of the ellipsometry spectra. The reason of poor uniqueness value in model fitting lies in that the measurement data content is not enough to uniquely determine physical parameters; thus the simulation will face uniqueness issue for the solution.

How to increase the measurement data content is a key to improve the uniqueness of the simulation. Multiple angles did not help much on this data content issue. The transmission and reflection spectra measurements were helpful at some cases. However, the uniqueness is still poor in many other cases in our ATO film study. Here we present a new method that combined resistivity measurement into modeling, instead of simulating resistivity ρ . Thus, this method increases measurement data content, so it significantly improved the uniqueness of the solution in the modeling; thus, through Drude model relationship, the carrier density and mobility of the ATO film could be uniquely determined.

Drude model: the dielectric constant ϵ is function of resistivity ρ , scattering time τ , and wavelength λ . Then electron density N and mobility μ could be calculated from $\rho = m^*/(Nq^2\tau)$, if assumed m^* is a constant (such as $0.3m_e$)

The gradient profile simulation is widely used for ellipsometry simulation, combined with the above method, the gradient of carrier density and mobility can be estimated, in comparison of Hall probe measurements, two methods provides similar carrier density and mobility, but the former one here could provide gradient information.

In this study, a new method was developed to significantly improve the ellipsometry simulation uniqueness, so that the carrier density and mobility of the ATO film could be uniquely determined. The gradient information could be estimated, and presented.

CP-5 Application-Specific Transparent Conductive Oxide Development using High Productivity Combinatorial Methods. *M.A. Nguyen, M. Le (mle@intermolecular.com), Intermolecular Inc, US*

Transparent conductive oxides (TCO) have become crucial not only as contact layers in photovoltaic applications, but also in electrochromic devices, low emissivity glass for commercial buildings, TFT-LCD displays and touch panels, as well as in flexible PV applications. With new applications come new specifications, and the corresponding need to

simultaneously optimize materials properties for new parameters. Such parameters could include physical properties such as flexibility, or thermal properties such as emissivity.

With increasing numbers of experiments needed to explore expanding process spaces, more efficient technologies and methodologies are needed to be able to develop new materials. Intermolecular Inc.'s (IM) High Productivity Combinatorial (HPC) Physical Vapor Deposition (PVD) platform is capable of screening up to 4 materials at a time. Co-sputtering of multiples sources (two to four) allows for an exponential numbers of site isolated experiments with unique composition to be deposited and characterized simultaneously.

Five different material systems were explored at Intermolecular in less than a month: aluminum zinc oxide (AZO), indium tin oxide (ITO), indium zinc oxide (IZO), indium titanium oxide, and indium silicon oxide. HPC methods allowed for the discovery of a particular IZO composition range (between 5-15% of zinc oxide, 85-95% indium oxide) that shows resistivity comparable or slightly better than the ITO baseline at IM. However, the emissivity was measured to be 10% better while maintaining transparency levels similar to ITO at the same thicknesses. This improvement in emissivity makes IZO a very promising TCO material for low-E and electrochromic applications. IM's baseline for ITO has resistivity of $350\mu\Omega\cdot\text{cm}$ and emissivity of 0.165 (16.5% of standard silver mirror). Unlike the crystallinity of ITO, IZO's amorphous structure provides for a much more robust process window with good repeatability. The amorphous structure also makes IZO a well suited material for flexible PV applications.

Another advantage of using multi source PVD chambers as part of a HPC workflow is the ability to deposit multi-layer TCOs. Stacks of TCO-Metal-TCO films (T-M-T) were explored using only 1 source for the TCO and 1 for the metal. Resistivity, emissivity, and transparency showed a strong correlation to the thickness of the metal layer in the T-M-T stack, as would be expected by theory. Preliminary data already indicated a 75% improvement in resistivity and 33% improvement in emissivity, though with a 23% reduction in transmittance compared to an ITO single layer film.

CP-6 To Properties of Ga-Al doped ZnO films prepared on the polymer substrate, K.H. Kim, H.W. Choi, K.H. Kim (KHKim@kyungwon.ac.kr), Kyungwon University, Republic of Korea

Transparent conductive oxides (TCOs) have been extensively studied because they are one of the most important components for large area electronics devices such as solar cells, organic light-emitting diode (OLED), optical sensors or touch screens. In recent years, there is much interest in the OLED applications like large scale display, flexible display and smart phone and so on. Indium oxide doped with tin ($\text{In}_2\text{O}_3\text{:Sn}$, ITO) is known for a most typical material for a transparent electrode.

However, rare and expensive indium in ITO is also blocking the use of ITO. So it is necessary to find the substitute of ITO and zinc oxide is an excellent candidate. The group 3 elements (Al, Ga B and so on) doped zinc oxide is a promising TCO material for OLED anode because of its high thermal stability and chemical durability.

The facing targets sputtering (FTS) system have been investigated in recently to prepare Ga-Al doped zinc oxide(GAZO) electrode for OLED because of large area uniform, high deposition rate, polymer substrate deposition and plasma damage free sputtering.

The GAZO thin films were prepared on polyethersulfone(PES) substrate by Facing Target Sputtering (FTS) system. We investigated electrical, optical, and structural properties of GAZO thin film with sputtering power 17-86W at working pressure 3mTorr. The optical transmittance of GAZO thin films characters very high transmittance of 90% in the visible range. We obtained the lowest resistivity $14.1\times 10^{-4}[\Omega\cdot\text{cm}]$ at sputtering power 86W from the hall-effect measurement and the strong (002) peak at all deposited thin films from the X-ray Diffractometer (XRD).

Deposition Parameter	Sputtering Condition
	GAZO
Target	AZO 2wt.%, 1EA GZO 3wt.%, 1EA
Tickness	150nm
Base pressure	1.2×10^{-6} Torr(1.3×10^{-4} pa)
Gas flow	Ar : 10sccm
Working pressure	3mTorr(0.39pa)
Function	Input Power : 17-86W (Input Current : 0.05-0.2A)

Table 1. Parameter of GAZO films deposited on PES substrate

CP-7 Charge trapping in indium zinc oxide thin film transistors with active channel fabricated by two-step deposition method, W. Kim, S.H. Lee, H.S. Uhm, J.S. Park (jinsp@hanyang.ac.kr), Hanyang University, Republic of Korea

Recently, many oxide semiconductors as the active channel layer for transparent thin-film transistors (TFTs) and their electronic applications, such as drivers for organic light-emitting diodes and transparent displays have been investigated because of their excellent electrical and optical properties at room temperature. Among those, sputtering-produced amorphous indium-zinc-oxide (a-IZO) thin films exhibit high electron mobility even when they are deposited at room temperature. Also, they can be used both as a channel layer and as source/drain layers of TFTs. Up to recent dates, most of researches have mainly been focused on developing the fabrication method of a-IZO TFTs or improving the device performances, however, the electrical instability including the drain current-gate bias hysteresis should be considered for practical applications. If there is a large hysteresis in TFT devices, non-uniform brightness or flickering phenomenon will occur in driving the liquid crystal display. Generally, the voltage shift (ΔV_{th}) due to hysteresis of TFTs suggests that negative charge carriers are trapped at the channel/gate oxide interface or injected into the dielectric from the oxide channels. It is also known that metal ion vacancies of channel layer in oxide TFTs may act as charge trapping centers to cause the hysteresis. As for a-IZO TFTs, however, there have been scattered data in the literature and the exact mechanism responsible for the hysteresis phenomenon has not been clear yet.

In this study, we have investigated the hysteresis mechanism in a-IZO TFTs with the active channel consisting of two a-IZO thin layers (hereafter, referred to as "two-step a-IZO TFT"). The TFTs were fabricated with a bottom gate structure and the a-IZO channel layers were deposited on thermally oxidized Si substrates (gate) via RF sputtering by following the two-step deposition procedures. The 1st a-IZO layer was deposited at a relatively low oxygen partial pressure (i.e., $\text{O}_2/\text{Ar} < 5\%$) and the 2nd a-IZO deposition was accompanied without stopping the vacuum, only by increasing the oxygen partial pressure (i.e., $\text{O}_2/\text{Ar} > 10\%$). The forward and reverse sweep characteristics of the both of two-step and monolayer a-IZO TFTs were measured in the dark using a semiconductor parameter analyzer at room temperature. Capacitance-voltage characteristic of a-IZO TFTs were measured using an impedance analyzer. In addition, the time dependent electrical properties of a-IZO TFTs were measured. The experimental results showed that the voltage shift due to hysteresis could be significantly suppressed in two-step a-IZO TFTs as compared with conventional single-channel a-IZO TFTs.

CP-8 Fabrication and characterization of transparent thin film transistors with boron-doped silicon zinc oxide channel, H.S. Uhm, S.H. Lee, W. Kim, J.S. Park (jinsp@hanyang.ac.kr), Hanyang University, Republic of Korea

Zinc oxide (ZnO)-based semiconductors as the active channel layer for thin film transistors (TFTs) recently have attracted much attention due to their excellent characteristics such as higher mobility than amorphous silicon, the ability to perform room-temperature deposition, and high transparency. However, most of the successful ZnO-based TFTs incorporate indium and gallium, such as indium zinc oxide (IZO), indium zinc tin oxide (IZTO), and indium gallium zinc oxide (IGZO), which are relatively rare on Earth. This makes those technologies easily subject to a material shortage. Recently, some researchers have reported experimental results which demonstrate new indium and gallium-free oxide semiconductors, such as aluminum zinc tin oxide (AZTO), magnesium zinc oxide (MZO), and titanium oxide (TiO_x), as another alternative channel layer for oxide TFTs.

In this study, we suggest a novel transparent oxide TFT with boron-doped silicon zinc oxide (SZO:B) channel layer. It is believed that group III (such as B, Al, Ga, In) and IV (such as Si, Ge, Ti, Zr, Hf) elements act as effective donors in the ZnO lattice because they may be substitutionally placed on Zn sites and will then enhance the carrier concentration and conductivity. We have investigated a simple method to simultaneously incorporate both boron and silicon elements in the ZnO thin film. The SZO:B TFTs were fabricated with a bottom gate structure. An n-type Si (100) wafer with a low resistance (below $0.002\Omega\text{cm}$) was used as a gate electrode, and a gate insulating layer was formed by thermally oxidizing the Si substrate. Then, the SZO:B channel layer was deposited via RF magnetron sputter at room temperature, using a ZnO target (99.999 % purity, 4 inch diameter) attached by several Si chips (boron-doped p-type Si wafer with a resistivity of $10\Omega\text{cm}$). Because Si chips were located uniformly around the sputtering racetrack, the boron and silicon elements were properly included in the ZnO lattice. As a result, the SZO:B channel layer was successfully deposited on a gate insulating layer. Finally, aluminum (Al) layer was deposited via DC magnetron sputter followed by a lift-off process to form the source-drain electrodes. The electrical, structural, and optical characteristics of SZO:B thin films were evaluated by four-point probe, X-ray diffraction (XRD) and UV/visible

spectrophotometer, respectively. Moreover, to analyze the device characteristics of the SZO:B TFTs, the output and transfer current-voltage characteristics were measured using a semiconductor parameter analyzer (4200-SCS, Keithley).

CP-9 Investigation on High-Performance Aluminum Zinc Tin Oxide Thin Film Transistors. L.F. Teng, P.T. Liu (ptliu@mail.nctu.edu.tw), C.S. Fuh, National Chiao Tung University, Taiwan, Z.Z. Li, Ming-Hsin University of Science and Technology, Taiwan

In recent years, amorphous oxide semiconductors (AOs) are attracted much attention due to high mobility, low temperature deposition, suitable for flexible display, transmission, and good uniformity. The thin film transistors with a-AZTO thin film as the active layer perform higher mobility and better reliability than conventional hydrogenated amorphous silicon TFT (a-Si: H TFT). In addition, the uniformity of a-AZTO TFT is also superior to Low Temperature Polycrystalline Silicon TFT (LTPS TFT). Therefore, the a-AZTO TFTs have the potential to replace a-Si: H TFTs and LTPS TFTs for Active Matrix Organic Light Emitting Display (AMOLED). In this study, we used rf sputter, which is compatible with industry application and integration, deposit a-AZTO active layer and then modulated the different processing oxygen flux, and discussed electrical and optical properties of the device impact.

CP-10 A Magnetization Study of Cobalt Oxide Films Deposited at Different Temperatures by Pulsed Injection MOCVD Using a β -Diketonate Complex of Cobalt as the Precursor. L. Apatiga (apatiga@unam.mx), J. Espindola, N. Mendez, Universidad Nacional Autónoma de México - Centro de Física Aplicada y Tecnología Avanzada, Mexico

The magnetic response of cobalt oxide films was studied using a vibrating sample magnetometer system. A strong magnetic susceptibility, which corresponds to antiferromagnetic spin alignments typical of films with low chemical inhomogeneities was found. The films were deposited by pulsed injection MOCVD using a β -diketonate complex of cobalt mixed in a toluene solution as the precursor, at different temperatures ranging from 650 to 800 °C on silicon substrates (Si (100)). According to the x-ray studies, the Co_3O_4 phase was homogeneously deposited along the entire substrate. In addition, the SEM observations show, together with the FT Raman studies, a high crystallinity, characteristic of the CVD metallic oxide structures.

CP-11 Investigating the Illuminated Hot-Carrier Effect under DC and AC operations for InGaZnO Thin-Film Transistors. T.Y. Hsieh, T.C. Chang (tcchang@mail.phys.nsysu.edu.tw), T.C. Chen, M.Y. Tsai, Y.T. Chen, National Sun Yat-Sen University, Taiwan, F.Y. Jian, National Chiao Tung University, Taiwan

This paper investigates the effect of DC and AC hot-carrier stress under light illumination for amorphous InGaZnO thin-film transistors (TFTs). Drain current-gate voltage (I_D - V_G) as well as capacitance-voltage (C-V) measurements are utilized to analyze the degradation mechanism. Illuminated DC hot-carrier stress leads to not only a negative parallel shift but also a C-V curve distortion at the off-state. This can be attributed to the asymmetric hole-trapping effect induced barrier-lowering near the drain side. To further verify the origin of the degradation behavior, AC bias with identical stress voltage is instead imposed on either gate terminal or drain terminal. It is deduced that hole-trapping phenomenon near the drain is dominated by the voltage across gate and drain, and is responsible for the degradation mechanism under illuminated hot-carrier stress.

CP-12 High Supercapacitive Performance of Sol-Gel ZnO-Added Manganese Oxide Coatings. C.-Y. Chen (chenyci@fcu.edu.tw), C.-Y. Chiang, Feng Chia University, Taiwan, S.-J. Shih, National Taiwan University of Science and Technology, Taiwan, C.Y. Tsay, C.K. Lin, Feng Chia University, Taiwan

In the present study, ZnO-added manganese (Mn) oxide coating were prepared as a function of ZnO addition (≤ 40 at.%) by sol-gel process. After post heat treatment at 300 °C, the influences of ZnO addition on the microstructural characteristics and pseudocapacitive performance of the Mn-oxide films were investigated. The structural analyses identified the sol-gel ZnO-added Mn-oxide powder as a tetragonal Mn_3O_4 phase with a nanocrystalline structure. The formation of spinel $\text{Zn}_x\text{Mn}_{3-x}\text{O}_4$ occurred when ZnO addition was ≥ 20 at.%. The crystallite size of Mn-oxide powder increased when a small amount of ZnO was added, then decreased with increased the ZnO content. The cyclic voltammetry (CV) data showed that the specific capacitance (SC) of the Mn-oxide film in 1 M Na_2SO_4 electrolyte can be increased from 236 F/g to 301 F/g at 25 mV/s by adding with 10 at.% ZnO. The formation of spinel phase tended to inhibit the SC value of the films. After activation of the Mn-oxide film, however, a relatively high cycling efficiency of $> 85\%$ was obtained for all the compositions after 1200 CV cycles.

CP-13 Characterization of dye sensitized solar cells with growth of ZnO passivating layer by Electron-beam evaporation. S.W. Rhee, K.H. Kim, H.W. Choi (chw@kyungwon.ac.kr), Kyungwon University, Republic of Korea

Dye-sensitized solar cells have been studied intensively since the discovery of DSSCs in 1991, has paved the way to cell efficiency as high as 11%, allowing to foresee the possibility of obtaining cost efficient cells.[1] In this study, ZnO thin film have been growth on FTO glass which used for dye sensitized solar cells(DSSC) by electron-beam evaporation. While a great number of various deposition techniques were reported for Zinc Oxide(ZnO) thin films, e.g. R.F and D.C. sputtering, pulsed laser deposition, metal organic chemical vapor deposition, and others. most of the ZnO active layers in TFT have been deposited by physical vapor deposition methods.

Electron was caused in N-719 and get through photoelectron (TiO_2) and TCO. Electron loss occurs at each interface. Specially, TiO_2 electrode on FTO. Fig.1 show the various components of a DSSC. It is also shows the process flow of occurred electron in dye, and electron recombination in TiO_2 to FTO interface. One of the reason deposition ZnO passivating layer can prevent recombination effectively. In addition the interfacial contact properties between the semiconductor metal oxide layer and the transparent conducting oxide (TCO) have been considered to play a significant role in the enhancement of the photovoltaic performance of DSSCs. In theory, ZnO has wide band gap (larger than 3eV) also excellent electron collecting capability and mobility[2]. ZnO passivating layer at room temperature and the chamber pressure was kept below 5×10^{-6} torr at different atmosphere O_2 gas flow. Electron-beam voltage was 8kv. The crystal structure and morphology were observed by X-ray diffraction (XRD) and scanning electron microscopy (SEM). The transmittance of the film was examined using a UV-spectrometer. The conversion efficiency of the DSSC fabricated was measured using I-V solar stimulator.

CP-15 Preparation of $\text{Zn}_x\text{Cd}_{1-x}\text{S}$ thin film by chemical bath deposition and application for dye-sensitized solar cell. C.C. Chang, Institute of Physics, Academia Sinica, Nankang, Taiwan, C.S. Hsu, Feng Chia University, Taiwan, C.H. Hsu, M.K. Wu, Institute of Physics, Academia Sinica, Nankang, Taiwan, C.C. Chan (ccchan@fcu.edu.tw), Feng Chia University, Taiwan

In the present study, $\text{Zn}_x\text{Cd}_{1-x}\text{S}$ thin film was coated on the ITO glass with chemical bath deposition method, using zinc acetate and cadmium acetate as precursors. Dye-sensitized solar cell was prepared from the $\text{Zn}_x\text{Cd}_{1-x}\text{S}$ /ITO glass with Anthocyanin, which was extracted from the grape skin, as a dye. Pt-sputtered ITO glass was used as the counter electrode. The influences of zinc/cadmium ratio and reaction time on the performance of the prepared dye-sensitized solar cell were discussed. FESEM was used to characterize the surface microstructure and sectional thickness of the $\text{Zn}_x\text{Cd}_{1-x}\text{S}$ film. The absorption spectra of the $\text{Zn}_x\text{Cd}_{1-x}\text{S}$ film and Anthocyanin dye were recorded using UV-VIS spectrophotometer. The characteristic of the Anthocyanin dye was also analyzed by FTIR spectrophotometer. Photocurrent-voltage (I-V) measurements were performed using an electrochemical analyzer. According to the UV-VIS results, Anthocyanin dye has a significant absorption band within the wavelength of 400~700nm, which can enhance the visible light absorption of the $\text{Zn}_x\text{Cd}_{1-x}\text{S}$ film. The results that the dye-sensitized solar cell prepared from the $\text{Zn}_{0.3}\text{Cd}_{0.7}\text{S}$ film exhibited the best performance. The open-circuit voltage, short-circuit current, and photo-to-electron power conversion efficiency are 0.695V, 1.408mA, and 4.07%, respectively.

CP-16 Effect of Thermal Treatment on Physical and Electrical Properties of porogen-containing and porogen-free ultralow- k plasma-enhanced chemical vapor deposition dielectrics. W.Y. Chung, National Chi-Nan University, Taiwan, Y.M. Chang, J.I.M. Leu, National Chiao Tung University, Taiwan, T.J. Chiu, Y.L. Cheng (yjcheng@nctu.edu.tw), National Chi-Nan University, Taiwan

The effect of the thermal annealing on the physical and electrical properties of porogen-containing and porogen-free ultralow- k dielectrics prepared by plasma-enhanced chemical vapor deposition (PECVD) was investigated. The porogen-free ultralow- k dielectric is obtained by using UV curing process to remove the organic sacrificial phase and generate open porosity. The results are also compared with the PECVD porogen-containing low- k films without UV curing process and PECVD low- k dielectrics without containing organic sacrificial phase. All low- k films in this study are totally deteriorated after $>800^\circ\text{C}$ thermal annealing. As the annealing temperature below 700°C , low- k dielectrics without containing organic sacrificial phase remain stable. The microstructure of the ultralow- k dielectrics changes with the thermal annealing. However, two kinds of ultralow- k dielectrics after the thermal annealing show the different physical and electrical characteristics. The porogen-containing low- k films without UV curing can produce more pore after the thermal annealing, resulting in the worse electrical performance as compared to the porogen-free ultralow- k dielectrics.

CP-17 Effects of UV Light Treatment for Low-k SiOC(-H) Ultra Thin Films Deposited by Using PEALD. *C.K. Choi* (cckyu@jejunu.ac.kr), *C.Y. Kim, J.W. Ko, J.K. Woo, K.M. Lee*, Jeju National University, Republic of Korea, *W.Y. Jeung*, Korea Institute of Science and Technology, Republic of Korea

Low dielectric constant SiOC(-H) films were deposited on *p*-type Si(100) substrates using PEALD with TMS and oxygen gas as precursors, and the deposited SiOC(-H) films treated at different UV treatment time. As the UV treatment time was increased, more -CH₃ and Si-CH₃ groups were incorporated in the Si-O-Si network. But, Si-CH_n groups of the SiOC(-H) film, after UV treatment time of above 9 min, are replaced with Si-O bond. Because the Si-CH_n bond groups are broken due to UV irradiation. Therefore, the films formed with Si-O bond rich in the Si-O-C(-H) structure. Also, the fixed charge density and the interface state density at the SiOC(-H)/*p*-Si(100) interface decreased as UV treatment time was increased until 6 min. From this results, we can infer that Si-O bonds with the -CH₃ group reduced the fixed charge density. The distribution of the surface state density decreased with the UV treatment, because the fixed positive (Si-CH₃)⁺ and negative (Si-O)⁻ changed the configuration at the SiOC(-H)/*p*-Si(100) interface. From our experimental results, we conclude that a 6 min UV treatment is sufficient to improve the structural properties of SiOC(-H) film.

CP-18 The Impact of Heterojunction Formation Temperature on Obtainable Conversion Efficiency in n-ZnO/*p*-Cu₂O Solar Cells. *Y. Nishi, T. Miyata* (tmiyata@neptune.kanazawa-it.ac.jp), *T. Minami*, Kanazawa Institute of Technology, Japan

Recently, we reported that Cu₂O-based solar cells with conversion efficiencies over 2% were fabricated using Cu₂O sheets prepared by a thermal oxidation of copper sheets. In this paper, the influence of heterojunction formation temperature on the obtainable conversion efficiency was investigated in different types of solar cells with Al-doped ZnO (AZO)/Cu₂O or AZO/non-doped ZnO (ZO)/Cu₂O structures on the front surface of thermally oxidized Cu₂O sheets that function as the active layer as well as the substrate. The Cu₂O sheets, with electrical properties such as resistivity on the order of 10³ Ωcm, hole concentration on the order of 10¹³ cm⁻³ and Hall mobility above 100 cm²/Vs, were prepared by a thermal oxidation of copper sheets under appropriate conditions. The AZO and ZO thin films were prepared by a pulsed laser deposition (PLD) using an ArF excimer laser. The n⁺-AZO/*p*-Cu₂O heterojunction solar cells, consisting of a degenerated semiconductor and *p*-Cu₂O, performed as a Schottky barrier (SB) contact in regard to diode characteristics. A conversion efficiency above 2% was obtained in the AZO/Cu₂O SB solar cells fabricated by depositing an AZO thin film at room temperature (RT), i.e., non-intentionally heated Cu₂O sheets. It was found that the obtainable conversion efficiency in the AZO/Cu₂O SB solar cells decreased markedly as the deposition temperature of the AZO thin film was increased above RT. However, when using Cu₂O sheets with a surface that had been stabilized prior to the AZO thin film deposition, high-efficiency AZO/Cu₂O SB solar cells could be fabricated using an AZO film deposition temperature in the range from RT to approximately 100°C. To improve conversion efficiency, heterojunction solar cells with an n⁺-AZO/*n*-ZO/Cu₂O structure were fabricated. AZO/ZO/Cu₂O solar cells fabricated by forming both the AZO and ZO thin films at RT exhibited a high efficiency of 4%. However, the obtainable conversion efficiency in AZO/ZO/Cu₂O solar cells decreased markedly as the deposition temperature of the ZO thin films was increased above RT. In contrast, if the ZO thin-film deposition, the first stage, was carried out at RT, high efficiencies over 4% could be obtained in AZO/ZO/Cu₂O solar cells fabricated using an AZO film deposition temperature in the range from RT to approximately 100°C. It can be concluded that achieving higher efficiencies in AZO/ZO/Cu₂O heterojunction solar cells requires that the surface of Cu₂O sheets always be stabilized prior to the ZO thin-film depositions and, in addition, the ZO thin-film depositions utilize a low-damage deposition technology at a low-deposition temperature.

CP-19 Effect of Thickness of Atomic Layer Deposition HfO₂ Film on Electrical and Reliability Performance. *Y.L. Cheng* (yjcheng@ncnu.edu.tw), *C.Y. Hsieh, Y.L. Chang*, National Chi-Nan University, Taiwan

The effects of deposition thickness of HfO₂ film prepared by atomic layer deposition on the electrical and reliability properties were reported. Scaling the physical thickness of HfO₂ dielectric did not linearly increase the capacitance due to a thicker interfacial SiO₂ layer through oxidation process in thermal annealing. Additionally, the degree of HfO₂ crystallization is increased after the thermal annealing as the thickness of HfO₂ film is increased, resulting in a higher dielectric constant for bulk HfO₂ film. The breakdown behaviors of HfO₂ gate dielectric film is also not scaled with the thickness, but is improved with the reduction of the thickness. Furthermore, the reliability characteristics of HfO₂ dielectric under unipolar AC stress

were also evaluated. A longer dielectric breakdown lifetime is observed as compared to constant voltage stress. As the thickness of HfO₂ dielectric increases, a larger lifetime enhancement is detected due to the effective charge detrapping for thicker dielectrics under AC stressing.

CP-20 Growth, Structure and Optical Properties of 20%-Ti Doped WO₃ Thin Films. *V. Ramana* (rvchintalapalle@utep.edu), *G. Baghmar*, University of Texas at El Paso, US

The aim of this study is to explore the effect of titanium (Ti) doping on the growth of behavior, microstructure and optical characteristics of tungsten oxide (WO₃), which is an important material with a wide range of technological applications in optical and optoelectronic devices. W_{0.80}Ti_{0.20}O₃ thin films were fabricated using RF magnetron sputtering deposition onto silicon and optical grade quartz substrates in wide range of growth temperatures (25-500 °C). X-ray diffraction (XRD), high-resolution scanning electron microscopy (SEM), optical spectrophotometry and spectroscopic ellipsometry (SE) were performed to study the effect of temperature on the growth behavior, crystal structure, texturing, surface morphology, and optical properties of W_{0.80}Ti_{0.20}O₃ films. The results show that the effect of temperature is significant on the growth, structure and optical properties of W_{0.80}Ti_{0.20}O₃ films. XRD results indicate that the W_{0.80}Ti_{0.20}O₃ films grown up to a temperature of 400°C are amorphous. A temperature of 500 °C is needed to obtain nanocrystalline W-Ti-O films. Annealing at 600°C to 900°C performed on the amorphous films indicate the formation of crystalline W_{0.80}Ti_{0.20}O₃ films. The SEM imaging analysis indicates that the phase transformations are accompanied by a characteristic change in surface morphology. SE analysis indicates the thickness of all the films is ~100 nm, which is in good agreement with the value obtained by other methods. Optical band gap of WO₃ is found to be affected by the Ti-doping. Spectrophotometry and SE analysis indicate that the effect of ultra-microstructure and grain-size was significant on the optical properties of W_{0.80}Ti_{0.20}O₃ films.

CP-21 Gate Bias Dependence on Threshold Voltage Instability in HfO₂/Ti_kN_{1-x} p-MOSFETs. *W.H. Lo*, NSYSU, Taiwan, *T.C. Chang* (tcchang@mail.phys.nsysu.edu.tw), National Sun Yat-Sen University, Taiwan, *C.H. Dai*, NSYSU, Taiwan

This paper investigates the gate bias induced threshold voltage (*V_{th}*) instability for *p*-type metal oxide semiconductor field effect transistors (p-MOSFETs) with HfO₂/Ti_kN_{1-x} gate stack. The experiment results indicate that for different nitride concentration of metal gate, the *V_{th}* shift has a contrary trend under positive and negative gate bias stress, respectively. Applying negative gate bias stress causes an increase in *V_{th}* shift with increasing nitride concentration of metal gate. This phenomenon is associated with amount of interface states caused by nitrogen diffusion from metal gate toward interface of Si/SiO₂. On the other hand, under the positive gate bias stress, the *V_{th}* shift has a gradual decrease while nitride concentration increases in metal gate. This contrary tendency can attribute to the electron trapping effect, which is dependent on amount of existing defects in high-*k* bulk with different nitride concentration of metal gate.

CP-22 Enhanced heating effect of SiO₂-Ag and TiO₂-Ag multi-layered and co-doped thin films. *J.H. Hsieh* (jhhsieh@mail.mcut.edu.tw), *Y.T. Su, J.L. Chang, S.J. Liu*, Ming Chi University of Technology, Taiwan

SiO₂-Ag and TiO₂-Ag multi-layered and co-doped thin films were deposited on glass substrates using reactive sputtering. The mass thickness of Ag was controlled at 3, 5, 7 nm. After deposition, some samples were annealed using a rapid thermal annealing system to understand the plasmonic effect caused by Ag particles. To examine the

films' optical properties, the transmission, reflection, and absorption spectra were measured, and certain plasmonic absorption was identified. The results were then co-related with those obtained from the heating measurement. It was found that the heating enhancement due to the incorporation of Ag particles is significant. The largest temperature increment can reach 45 °C. The increments were dependent on the number of Ag layer, heat treatment conditions, and the oxide matrix. A theory was proposed to explain the enhanced light absorption and, therefore, the enhanced heating effect under light irradiation.

CP-23 The Electrical Properties Correlated with Redistributed Deep States of a-Si:H TFTs on Flexible Substrates with Mechanical Bending. *M.H. Lee* (mhlee@ntnu.edu.tw), National Taiwan Normal University, Taiwan, *B.F. Hsieh*, National Chung Hsing University, Taiwan

Flexible electronics on plastic substrates possess various advantageous characteristics including being lightweight, durable and flexible; and having the capacity to be manufactured in a variety of shapes also leads to great freedom in design. Unlike mobility enhancements in strained-Si FETs or CMOS, which are based on energy band deformation and effective mass reduction, the formation of trapped states by way of mechanical strain

dominates the characteristics of a-Si:H TFTs. The behavior of electrical characteristics with mechanical strain can be explained by trap state redistribution of the bandgap. The disordered bonds may generate a redistribution of trap states, resulting in unstable electrical characteristics such as threshold voltage, subthreshold swing, and mobility of carriers. During mechanical strain the deep states are redistributed in a Gaussian distribution, and are dissimilar to ordinary acceptor-like deep states which manifest with exponential distributions. Electronic states near the Fermi level act as recombination centers for photogenerated carriers, and it may be valuable for illumination of the transistors. We conclude that the gap state density of an a-Si:H layer under mechanical strain is fundamental to the reliability and development of flexible electronics.

CP-25 Effects of RF power on the properties of Si thin films deposited by an ICP CVD system with internal antennas, J.H. Hsieh (*jhsieh@mail.mcut.edu.tw*), **YAN-LIANG. Lai**, Ming Chi University of Technology, Taiwan, **Yuichi. Setsuhara**, Osaka University, Japan

The plasma of an ICP-CVD system attached with four internal antennas was used to deposit doped and un-doped Si thin films. Hydrogenated microcrystalline silicon ($\mu\text{-Si:H}$) films were prepared under various RF power, while the flow ratio of SiH_4/H_2 was fixed at 1/4. During deposition, an OES (optical emission spectrometer) and a plasma probe were used to characterize the conditions of plasma. The crystallinity and opto-electrical properties of the Si:H films were investigated using Raman scattering spectroscopy, XRD, Hall effect measurement system, and UV-Vis photometer. It is found that the crystallinity of $\mu\text{-Si:H}$ film was significantly affected by plasma density which was increased with the increase of the power. This could be caused by the increase of $I_{\text{SiH}}^*/I_{\text{H}}$. It is also found the plasma potential would decrease with the increase of power, while the plasma density would increase with the increase of power. The carrier density, mobility, and photoconductivity were found related to the plasma potential and density which might affect defect density in the films.

CP-27 The different radio-frequency powers on characteristics of boron-doped amorphous carbon films prepared by reactive radio-frequency chemical vapor deposition, T.S. Chen, S.E. Chiou, S.T. Shiue (*stshiue@dragon.nchu.edu.tw*), National Chung Hsing University, Taiwan

Boron-doped amorphous carbon (a-C:B) films were deposited on n-type silicon (n-Si) wafers using reactive radio-frequency (RF) chemical vapor deposition. A boron target was used as the dopant source, and a mixture of pure methane (CH_4) and argon (Ar) gases with flow rates of 2 and 10 sccm, respectively, was selected as the precursor gas. Five kinds of a-C:B films were prepared with RF powers of 100, 200, 300, 400, and 500 W. The substrate temperature and working pressure were set at 298 K and 6 Pa, respectively. The thicknesses of a-C:B films were measured using field emission scanning electron microscopy (FESEM). Alternatively, the characteristics of a-C:B films were analyzed by X-ray photoelectron spectrometer (XPS) and Raman scattering spectra (RSS). After the a-C:B/n-Si junction was sputtered with gold (Au) and aluminum (Al) electrodes, the current-voltage (I-V) and capacitance-voltage (C-V) characteristics of Au/a-C:B/n-Si/Al heterojunction devices were measured.

FESEM results show that all the thicknesses of a-C:B films are about 100 nm. XPS analyzed results reveal that the boron atoms are successfully doped into amorphous carbon films, and the boron content increases from 0.02 to 28.87 at.% as the RF power increases from 100 to 500 W. The RSS data of a-C:B films indicate that the ratio of the integrated intensity of the D band to that of the G band (ID/IG) increases with increasing the RF power from 100 to 300 W, but decreases with increasing the RF power from 300 to 500 W. It implies that the a-C:B film prepared with the RF power of 300 W has a relatively higher graphitization degree. Our analyzed results also show that all the I-V characteristics of Au/a-C:B/n-Si/Al heterojunction devices exhibit the rectifying behavior. When the a-C:B film was prepared with the RF power of 300 W, the Au/a-C:B/n-Si/Al heterojunction device displays the best rectifying I-V characteristics, and its ideality factor is about 1.40. The C-V measurement under the frequency of 1 kHz shows that as the a-C:B film was prepared by the RF power of 300 W, the built-in voltage of the Au/a-C:B/n-Si/Al device is about 0.2 V.

CP-28 InN/GaN Quantum Well Heterostructures: Structural Characteristics and Strain Induced Modifications of the Electronic Properties, -. Kioseoglou, Kalesaki, Aristoteles University of Thessaloniki, Greece, Kominou, Aristoteles University of Thessaloniki, Greece, Karakostas (*karakost@auth.gr*), Aristoteles University of Thessaloniki, Greece

An important step towards optimization of InN/GaN based devices is the identification of the structural characteristics of the corresponding interfaces since the favourable bonding configurations determine the materials polarity and consequently the direction of spontaneous polarization. We have addressed this issue through empirical potential calculations on

InN/GaN interfaces comprising misfit dislocations [1]. An appropriately parameterized Tersoff interatomic potential [2] was implemented and energetic calculations were performed on interfaces of III- and N- polarity, lying at the single- or double bonds and having a wurtzite or zinc blende stacking sequence in accordance with high resolution transmission electron microscopy observations. Based on these results III-polarity interfaces, cutting single bonds are energetically favourable.

In our present study, additional calculations are performed on subcritical thickness InN/GaN QWs, which exhibit lower dislocation densities as well as reduced InN decomposition and are currently implemented in the fabrication of near-UV light emitting diodes [3,4]. *Ab initio* calculations are performed under modified pseudopotentials, accurately reproducing the InN and GaN band gap values, on supercells comprising 1 monolayer (ML) thick InN elastically strained in 5 nm thick GaN barriers having a wurtzite or zinc blende stacking at the interface. The former is found to be energetically favourable. Subsequent calculations on supercells comprising 1 ML thick InN in 8 and 11 nm thick GaN barriers as well as 3 ML InN in 11 nm thick GaN having a wurtzite stacking, depicted a variation in III-N bond lengths. This variation become more significant as the barrier thickness decreases or the QW thickness increases. Hence the strain and consequently piezoelectric polarization are modified. The latter is attested by density of states calculations, which show a vast decrease of the band gap when 5 nm thick barriers are considered, while a significant decrease is also recorded at the 3 ML InN / 11 nm GaN barrier heterostructure in comparison with the 1 ML InN supercell. Our results scrutinize recent experimental observations [3,4] and could prove beneficial for tailoring the optoelectronic properties of InN/GaN QWs.

[1] J. Kioseoglou et al., J. Mater. Sci. **43**, 3982 (2008)

[2] J. Kioseoglou et al., Phys. Stat. Sol. (b) **245**, 1118 (2008)

[3] E. Dimakis et al., Phys. Stat. Sol. (a) **205**, 1070 (2008)

[4] A. Yoshikawa et al., J. Vac. Sci. Technol. B **26**, 1071 (2008)

[5] Work supported by EC under the 7th European Framework Project DOTSENSE (Grant No.

STREP 224212)

CP-29 Optical properties of AlN:Ag and Al-Si-N:Ag nanostructured films and the effect of thermal annealing, A. Stozios, E. Lidorikis, P. Patsalas (*ppats@cc.uoi.gr*), University of Ioannina, Greece

Aluminum Nitride (AlN) is a wide bandgap semiconductor that has been studied extensively because of its remarkable optical, mechanical, physical and chemical properties that make it suitable for a variety of applications such as optoelectronic devices, protective coatings, wave-guides, etc. The incorporation of Ag into an AlN matrix can provide additional functionality through the localized surface plasmon resonance (LSPR): a collective oscillation of conduction electrons, fueled by light illumination at the proper frequency. In this work we investigate under which circumstances LSPR is manifested. In particular, we have grown nanostructured films consisting of an AlN matrix and Ag inclusions in the form of nanospheres, nanosheets and atomic dispersions, by sputtering and pulsed laser deposition (PLD). The refractive index of the matrix was varying by controlling the matrix microstructure and density (amorphous or wurtzite AlN, a-AlN and w-AlN, respectively) and the optical absorption in the visible range was controlled by the incorporation of Si in to the AlN matrix. The refractive index of the films is correlated with the films' density measured by X-Ray Reflectivity (XRR). The optical properties of the films were studied using Optical Reflectivity Spectroscopy (ORS) in vertical incidence in the 1.5-5.25 eV spectral range. The spectroscopic data are critically compared to Finite Difference Time Domain (FDTD) calculations of the optical response. The effect of the thermal annealing to the plasmonic behavior of the AlN:Ag and Al-Si-N:Ag has been studied systematically by repeating the ORS measurement after annealing in inert Ar atmospheres cycles at various temperatures as high as 800 °C.

CP-30 Investigation of photoluminescent characteristics and optical properties of thin film zinc silicate doped with manganese, K.H. Yoon, J.H. Kim (*joohan@cnu.ac.kr*), Chungbuk National University, Republic of Korea

The photoluminescent characteristics and optical properties of manganese-doped zinc silicate ($\text{Zn}_2\text{SiO}_4:\text{Mn}^{2+}$) thin films were investigated. The $\text{Zn}_2\text{SiO}_4:\text{Mn}$ films were deposited by sol-gel spin coating method, followed by thermal annealing in air atmosphere at 600 – 1200 °C. The Zn_2SiO_4 film exhibited a normal optical absorption edge in the near-ultraviolet wavelength region and a high optical transparency in the visible wavelength range. The maximum transmittance reached 0.922 at 597 nm, which was very close to the transmittance of the fused quartz substrate alone. The refractive index of the $\text{Zn}_2\text{SiO}_4:\text{Mn}$ films showed normal dispersion behavior. X-ray diffraction and atomic force microscopy measurements revealed that the as-deposited $\text{Zn}_2\text{SiO}_4:\text{Mn}$ films had an

amorphous structure with a smooth surface morphology. The $\text{Zn}_2\text{SiO}_4\text{:Mn}$ films became crystalline after annealing at 800 °C and the crystallinity of the films was continuously improved up to 1200 °C. The annealed $\text{Zn}_2\text{SiO}_4\text{:Mn}$ films had a polycrystalline rhombohedral structure with no preferred crystallographic orientation of the crystallites. The photoluminescence spectra of the annealed $\text{Zn}_2\text{SiO}_4\text{:Mn}$ films showed broad-band emissions with a peak maximum at around 523 nm in the green range. The PL emission intensity was enhanced as the annealing temperature increased, resulting from the improvement of the crystallinity of the $\text{Zn}_2\text{SiO}_4\text{:Mn}$ films. The excitation band exhibited a peak maximum at 243 nm in the near ultraviolet region, which was considered to be associated with the charge transfer transition of divalent manganese ion in the Zn_2SiO_4 system.

CP-31 Er:Si Silicide Formation and Temperature Dependence of Barrier Inhomogeneity, H. Efeoglu (hefeoglu@atauni.edu.tr), Turkey, Y. Babacan, Erzincan University, Turkey

Stabilized metal silicides with low barrier for ohmic contact or high barrier for rectification has advantages for nanometer scaled device fabrication. The use of silicide instead of impurity doped silicon for drain and source has advantages in terms of processing temperature and much less trap creation during the fabrication. Ultra shallow junction can be formed easily with the metals having low diffusion coefficient in silicon. Low barrier of metal-silicide on source/drain is key point for ultrascaled complementary metal/oxide/semiconductors in future technology. On the other side Schottky barrier as a gate terminal may suffer from barrier inhomogeneity. Because of that, much better performance of SB require careful I-V analysis which gives some of suggestions related to material selection and fabrication parameters. Inhomogeneity of Schottky barrier at room temperature widely studied during the last decade. In this study, the temperature dependence of barrier distribution below room temperature presented for the first time.

With this context, the rectification effect of Er-silicide on p-Si was investigated. Sputter technique is used for deposition and Er-Silicide thermally activated by annealing above 300 °C under the nitrogen atmosphere. I-V-T measurement of multiple diodes was analysed for the barrier inhomogeneity of Er-Silicide/p-Si junctions.

Coatings for Biomedical and Healthcare Applications Room: Golden Ballroom - Session DP

Symposium D Poster Session

DP-1 Characterization and antibacterial performance of biocompatible Ti-Zn-O coatings deposited on titanium implants, M.T. Tsai, Hungkuang University, Taiwan, Y.Y. Chang (yinyu@mail2000.com.tw), National Formosa University, Taiwan, Y.C. Chen, MingDao University, Taiwan, H.L. Huang, J.T. Hsu, China Medical University, Taichung, Taiwan

Titanium(Ti)-based materials have been used for dental/orthopedic implants due to their excellent biological compatibility, superior mechanical strength and high corrosion resistance. A better anti-bacterial performance of Ti implant is beneficial for the osseointegration and for avoiding the infection after implantation surgery. Bacterial colonization may also be prevented or reduced by different surface properties of the material and/or by the use of antiseptic surface coatings. Titanium and zinc oxides have attracted wide interest because of their good photocatalytic activity, high stability, antibacterial property and non-toxicity. In this study, biocompatible Ti-Zn-O coatings with different Zn contents were deposited on a bio-grade pure Ti implant material by using a cathodic-arc evaporation system with plasma enhanced duct equipment. Pure Ti and Zn cathodes were used for the deposition. Characterized by X-ray diffraction (XRD), X-ray photoelectron spectroscopy(XPS) and scanning electron microscopy (SEM), the crystal structure, bonding state and surface morphology of the deposited crystalline Ti-Zn-O were studied. To verify the susceptibility of implant surface to bacterial adhesion, *Actinobacillus actinomycetemcomitans* (A. actinomycetemcomitans) and *Staphylococcus aureus* (S. aureus), found frequently in the implant-associated infections, was chosen for in vitro anti-bacterial analyses by a fluorescence staining method employing Syto9 and bacterial viability agar tests. In addition, the biocompatibility of human gingival fibroblast (HGF) and human primary osteoblasts (hOBs) cells on the coatings was also evaluated. The results suggested that the Ti-Zn-O coatings can improve antibacterial performance with compatible soft-tissue and hard-tissue biological performances.

DP-2 Anti-bacterial Performance of Zirconia Coatings on Titanium Implants, H.L. Huang, China Medical University, Taichung, Taiwan, Y.Y. Chang (yinyu@mail2000.com.tw), National Formosa University, Taiwan, J.C. Weng, Y.C. Chen, MingDao University, Taiwan, C.H. Lai, T.M. Shieh, China Medical University, Taichung, Taiwan

Bacterial adhesion and colonization are considered to play a key role in the pathogenesis of peri-implant disease, an inflammatory process leading to soft and hard tissue destruction around a Ti implant. The osseointegration of titanium implants is related to their composition and surface treatment. Zirconia coatings have been proved to increase their applications in the biomedical fields such as orthopedic devices and dental implants by improving implant osseointegration. In this study, doped ZrO_2 coatings with different Ag and Cu contents were deposited on bio-grade pure Ti implant materials. A twin-gun magnetron sputtering system was used for the deposition of the $\text{ZrO}_2\text{-Ag(Cu)}$ coating. The Ag and Cu contents in the deposited coatings were controlled by the magnetron power and bias voltage. The films were then annealed using rapid thermal annealing (RTA) at 350 °C for 8 min to induce the nucleation and growth of Ag(Cu) particles on the film surface. WDS was used to characterize the composition of the deposited $\text{ZrO}_2\text{-Ag(Cu)}$ coatings. The crystalline structure and bonding states of the coatings were analyzed by XRD and XPS. The antibacterial behavior will vary, depending on the amount and size of the Ag(Cu) particles on the coated Ti sample. In this study, *Actinobacillus actinomycetemcomitans* (A. actinomycetemcomitans) and *Staphylococcus aureus* (S. aureus) found frequently in the implant-associated infections, were chosen for in vitro anti-bacterial analyses by a fluorescence staining method employing Syto9 and bacterial viability agar tests. The antibacterial activity was quantified as the fluorescence detected at 488 nm by an ELISA (enzyme-linked immunosorbent assay). It showed that the nanostructure and Ag and Cu contents of the $\text{ZrO}_2\text{-Ag(Cu)}$ coatings were correlated with the antibacterial performance.

DP-3 Diffusion mechanism and Ag⁺ release kinetics on ZrCN - Ag NPs antimicrobial coatings, S. Calderon V. (secave44@gmail.com), Universidade do Minho, Dept. Física, Portugal, R. Escobar Galindo, Instituto de Ciencia de Materiales de Madrid (ICMM -CSIC), Spain, A. Cavaleiro, University of Coimbra, Portugal, S. Carvalho, Universidade do Minho, Dept. Física, Portugal

Silver nanoparticles (NPs) have been extensively used to provide antibacterial properties to several commercial devices such as sportswear, toys and baby articles, among others. In fact, numerous reports have been published during the last few years regarding silver NPs attaining antimicrobial properties in countless kinds of materials and for a considerably good number of microorganisms. However, the durability of this effect is ignored in most of those reports, precluding their use in long term applications. Thus, this effect gains particular importance when dealing with applications involving the human body: the so-called biomaterials.

In this work ZrCN coatings doped with Ag NPs were produced on SS316L by unbalance magnetron sputtering using two targets, Zr and Zr/Ag in an Ar, C₂H₂, N₂ atmosphere. In order to investigate the evolution of silver dissolution and the corrosion resistance, these ZrCN with Ag NP's were immersed for different periods of time, on three different electrolytes. 0.89% NaCl and phosphate buffer saline (PBS) with and without proteins (1.0 g/l bovine serum albumin) were used to simulate the human body fluids. The former was selected due to its simplicity which permits to avoid the signal from other components in order to determine the kinetic mechanisms of the silver ions release. However, the latter were utilized in order to understand the influence of phosphates and proteins in this process. Inductively coupled plasma optical emission spectrometry (ICP-OES) was used to determine the content of silver ions in the electrolytes, as a function of the immersion time. Electrochemical impedance spectroscopy (EIS) and potentiodynamics curves were used to evaluated the electrochemical response of the samples. A profile evaluation of the films before and after immersion was methodically carried out by means of glow discharge optical emission spectroscopy (GDOES). Structural and morphological characterizations were carried out by X-ray diffraction (XRD) and Scanning electron microscopy (SEM), respectively. Finally, morphological and structural characterization, silver content evolution and electrochemical response have been correlated, and a model containing information about morphology, structure and ions kinetics is performed.

DP-4 Controlling the drug release from biocompatible polymers by changing plasma-treated area, K. Hagiwara, Keio University, Japan, T. Hasebe, Toho University Sakura Medical center, Japan, R. Asakawa, Keio University, Japan, A. Kamijo, Yokohama City University Hospital, Japan, T. Suzuki, A. Hotta (hotta@mech.keio.ac.jp), Keio University, Japan

In this study, plasma surface treatment was introduced as a method for controlling the drug release. Currently, the implantation of DES with surface coating of a drug-containing polymer, is the most powerful way to

treat coronary artery disease. DES contains antithrombotic drugs that suppress the proliferation of smooth muscle cells in the stented segment of the artery. Although DES was remarkably successful in preventing restenosis, DES still has a disadvantage for not preventing restenosis at the implant site due to the relatively vast drug release from the stent surface in the early stage of the release.

To achieve the precise control of the drug release, we focused on plasma treatment which had no risk of damaging the fine surface of the stent. Oxygen and argon were selected as working gas. Several polymers were used as drug-reservoir materials, where it was necessary to achieve the controllable and sustainable drug release from the polymers. Three biocompatible polymer films were selected as base drug-reservoir materials: hydrophilic 2-metacryloyloxyethyl phosphorylcholine (MPC), hydrophobic poly (ethylene-co-vinyl acetate) (EVA), and less hydrophobic polyurethane (PU). These samples were soaked in 2mL of medium of phosphate-buffered saline with 10% ethanol. The drug release rate was measured by a spectrophotometer. By changing plasma treatment area of argon plasma at 0 %, 45%, 65%, and 100%, it was found that the initial burst release of drug, with EVA and PU films, was suppressed. These experimental results show that drug release could be effectively controlled by changing the plasma-treated area, which should be applicable to the next-generation DES system that would eventually prevent restenosis.

DP-5 Ex-situ and in-situ techniques to study protein adsorption: fibrinogen and albumin adsorption on metal oxide thin films, P. Silva-Bermudez (suriel21@yahoo.com), Instituto de Investigaciones en Materiales, Universidad Nacional Autónoma de México, México, M. Rivera, Instituto de Física - Universidad Nacional Autónoma de México, México, S. Muhl, S.E. Rodil, Instituto de Investigaciones en Materiales, Universidad Nacional Autónoma de México, México

Different techniques are used to study protein adsorption on surfaces and each one of them present advantages and limitations. Thus, a combination of techniques allows a better understanding of the adsorption phenomenon.

Spectroscopic (SE) or Dynamic (DE) ellipsometry can be used to study protein adsorption in-situ in real time, i.e. the process kinetics, and the mass adsorbed on the surface at any time during the adsorption process. However, it does not allow chemical identification of the adsorbed material. X-Ray Photoelectron Spectroscopy (XPS) provide chemical identification of the adsorbed material but the studies are normally carried out ex-situ in a dry ambient after protein adsorption; thus, conformation of the proteins may differ from that in a wet ambient. Atomic Force Microscopy (AFM) can be used to monitor the adsorption in-situ or ex-situ. It does not allow chemical identification of the adsorbed material but it is possible to monitor the changes in surface morphology due to the adsorption.

In the present work, Ta₂O₅, Nb₂O₅ and TiO₂ thin films deposited on Si (100) substrates by Reactive Magnetron Sputtering were chosen as the study surfaces, mainly due to their potential as biocompatible coatings. Albumin (BSA) and Fibrinogen (Fib) were chosen as the study proteins. BSA is a small protein that readily adsorbs on surfaces and is the most abundant protein in serum; Fib is a bigger protein, highly abundant in blood and relevant for haemocompatibility.

The films were immersed in protein solutions and protein adsorption was monitored in-situ by DE during 2400 s; then, the protein layer adsorbed on the surface was studied using SE. After this, the films were rinsed and dried and the adsorbed protein layer was studied ex-situ using AFM and XPS.

The DE results showed adsorption occurring at different rates on the different surfaces, Ta₂O₅ showed the highest rate of adsorption for both proteins, leading to a surface mass density (Γ) of 0.9 and 1.2 mg/cm² for BSA and Fib, respectively. The lowest adsorption occurred on TiO₂ where Γ was 0.38 mg/cm² for BSA and 0.45 mg/cm² for Fib. The AFM results evidenced a change in the morphology and increasing of the roughness after protein adsorption; however, no trend, respect to the metal oxide films, was observed for these changes. The XPS results confirmed that the layer detected by SE was indeed adsorbed proteins. The analysis of the XPS spectra showed the same trend as SE; the highest N at. %, a signature of the protein adsorbed, corresponded to adsorption on Ta₂O₅, for BSA and Fib; while the lowest N at. % corresponded to TiO₂.

Acknowledgements to L. Huerta and to CONACyT posdoctoral fellowship for PSB

DP-6 Biocompatibility of the Plasma-polymerized Para-xylene Films, C.M. Chou, Feng Chia University; Taichung Veterans General Hospital, Taiwan, C.M. Yeh, Taichung Hospital, Department of Health, Executive Yuan, Taiwan, C.J. Chung (cjchung@seed.net.tw), Central Taiwan University of Science and Technology, Taiwan, J.L. He, Feng Chia University, Taiwan

Plasma-polymerized para-xylene (PPX), an alternative to biocompatible parylene coating for the surface treatment of medical devices has been

developed in the previous study by adjusting the process parameters: pulse frequency of the input power (ω_p) and para-xylene monomer flow rate (f_p). PPX has an amorphous structure. It exhibits hydrophobicity, higher film growth rate and better cell proliferation than conventional parylene coating. In this study, *in vitro* (cell compatibility and platelet adhesion) tests and *in vivo* animal studies were done comparing PPX films deposited on industrial-grade silicone substrates and medical-grade silicone sheets.

Experimental results reveal that the PPX films deposited on industrial-grade silicone substrates at higher ω_p exhibit better cell proliferation in comparison with the medical-grade silicone sheets. However, PPX films show poor cell attachment regardless of the ω_p and f_p because of their hydrophobicity. Water contact angle of the deposited PPX films ranges from 98.5° to 121.1°, depending on the ω_p and f_p . This enables the deposited PPX films to exhibit a comparatively lower platelet adhesion ability than medical-grade silicone sheets. In the animal study, PPX-coated industrial silicone substrates result in similar local effects at 28 days (short-term) and 84 days (long-term) after implantation subcutaneously in the abdominal wall of rodents compared to medical-grade silicone sheets. These results suggest that the obtained PPX films are basically bio-inert and can be considered for application in the surface modification of biomedical devices where tissue fluids or blood will be encountered.

Keywords: plasma-polymerized para-xylene; biocompatibility; *in vitro*; cell compatibility; platelet adhesion; *in vivo*; animal study

DP-7 Bioactive coating on anodized titanium substrate by a combination of micro-arc oxidation and electrophoretic deposition, P. Soares (pa.soares@pucpr.br), J.R. Negrelli, C.A.H. Laurindo, Mechanical Engineering Department, Pontificia Universidade Católica do Paraná, Brazil, R. Torres, Mechanical Engineering Department, Pontificia Universidade Católica do Paraná, Brazil

Titanium and its alloys have been used successfully in several biomedical implants. However, they have certain disadvantages, such as poor osteoinductive properties and low corrosive-wear resistance. Several surface treatment techniques have been developed to overcome these drawbacks, such as alkaline and heat treatments, and microarc oxidation. There are also several techniques involving the application of bioactive coatings, such as dip coating, electrophoretic deposition, hot isostatic pressing, ion-beam sputtering, plasma spraying, conventional flame spraying and high velocity oxy-fuel combustion spraying. Among them, plasma spraying is the most popular method for coating implants. However, the deposition of these bioactive coatings is limited to the lacks in uniformity, mainly on implants with complex geometries. It results also on a poor adhesion of the coating due to the thermal expansion mismatch. To solve this problem, it is necessary to combine the biocompatibility of such coatings with the mechanical benefits of metal alloys, but with a surface that will serve as an anchor to the bioactive coating. The electrophoretic deposition technique has been studied as an alternative for the deposition of osteoinductive films on complex surface geometries by applying an electric field. Microarc oxidation is a simple and effective method to modify the surfaces of titanium implants and produce porous bioactive TiO₂ films. Our aim was to study the combination of the two techniques for surface modification of titanium, microarc oxidation and electrophoretic deposition, in order to obtain a bioactive homogeneous surface with good adhesion to the substrate. Bioactive glass-ceramic particles were deposited by electrophoresis on a porous film produced by anodic oxidation using a Ca-P containing electrolyte. X-ray diffraction (XRD), scanning electron microscopy (SEM) and Fourier transform infrared spectroscopy (FTIR) have been used to investigate the microstructure and morphology of the coatings. The adhesive strength between the TiO₂ films and substrate has been assessed using scratch test. Results indicate that a combination of micro-arc oxidation and electrophoretic deposition can provide a relatively thick and well adhered TiO₂ layer, with pores filled with bioactive glass-ceramic particles.

DP-10 Influence of Unipolar and Bipolar Voltage Modes on Corrosion Resistance of Cp-Ti Alloy coated by using Micro-arc Oxidation Process, E. Demirci (e_ebrudemirci@hotmail.com), Ataturk University, Turkey, E. Arslan, College of Erzurum, Turkey, V.K. Ezirmik, Ataturk University, Turkey, Y. Totik, Turkey, İ. Efeoglu, Ataturk University, Turkey Ti and Ti alloys are widely used in many application. There are lots of studies about to improve their mechanical, structural, tribological and electrochemical properties e.g. by using Micro arc Oxidation (MAO) process. However, there is only a few study about improving the corrosion properties by using unipolar modes. In this study, MAO was used to produce oxide coatings on Cp-Ti alloy at both unipolar and bipolar voltage modes. The microstructure, surface morphology, phase composition and corrosion resistance of MAO films were analyzed by XRD, SEM and potentiodynamic polarization test unit. The results showed that the voltage mode is significantly influenced the microstructure and morphology. In

addition, it was observed that the voltage modes effected the corrosion resistance of the oxide coatings.

Key Words: Ti alloys, MAO process, Corrosion resistance

DP-11 Improvement of Corrosion Resistance and Biocompatibility of Ti-6Al-7Nb Alloy Using Electrochemical Anodization Treatment, H.H. Huang (hhhuang@ym.edu.tw), C.P. Wu, Y.S. Sun, National Yang-Ming University, Taiwan

The surface characteristics of the implant materials determine the biocompatibility. This study was to investigate the application of electrochemical anodization surface treatment to improve the corrosion resistance and biocompatibility of Ti-6Al-7Nb for implant application. An oxide layer with nanoscaled porosity was produced on the Ti-6Al-7Nb alloy surface through an electrochemical anodization treatment. Surface characterizations, including the topography, microstructure, chemistry, wettability and protein adsorption, of the test specimens were evaluated using various surface analysis techniques. The corrosion resistance of the test specimens was investigated using potentiodynamic polarization curve measurement in the simulated body fluid (SBF). The responses of human bone marrow mesenchymal stem cells on the test specimens were evaluated using various biological analysis techniques. Results showed that comparing to the untreated Ti-6Al-7Nb alloy, the presence of the nanoporous oxide layer on the anodized Ti-6Al-7Nb alloy increased the corrosion resistance (*i.e.* decreased the corrosion rate and passive current) in SBF. This nanotopography also improved the wettability, protein adsorption, cell adhesion, cell migration and cell proliferation on Ti-6Al-7Nb alloy. We would conclude that a fast and simple electrochemical anodization treatment can be used for the improvement of the corrosion resistance and biocompatibility of Ti-6Al-7Nb alloy surface for implant application.

DP-12 Corrosion based failure of silicon containing interfaces in diamond-like carbon coated Co-Cr-Mo joint implants, K. Thorwarth (kerstin.thorwarth@empa.ch), U. Müller, Empa, Switzerland, G. Thorwarth, Synthes GmbH, Switzerland, M. Stiefel, C. Flaub, R. Hauert, Empa, Switzerland

Delamination has been the key issue barring widespread use of diamond-like carbon layers on joint implants. Silicon-based interlayers, such as grown from PACVD of silanes or silazanes, have been successfully used as interlayers for DLC in industry, but reports of failures in-vivo are published.

We are presenting a systematic study on the stability of the CoCrMo/a-SiC/DLC interface with respect to oxygen contamination, such as may be encountered in a commercial reactor. Defined amounts of oxygen were introduced into the growth process and the resulting contamination levels monitored. Then, samples thus coated were subjected to stress-corrosion-cracking (SCC) tests based on the relation between delamination speed and layer stress. Finally, contaminated layers were subjected to simulator tests and the failures compared with the predictions from the previous tests. It is shown that for this material system, the failure predicted from the SCC curves is reproduced in the simulator results.

DP-13 Tribocorrosion resistance of CoCrMo alloys coated with TiAlN/TiAl Multilayers in simulated body fluid, M. Flores (martin.flores@red.cucei.udg.mx), G. Alemon, A. Aleman, Universidad de Guadalajara, Mexico, E. Andrade, UNAM, R. Escobar, Instituto de Ciencia de Materiales de Madrid (ICMM -CSIC), Spain

In the present work we investigate the tribocorrosion behavior CoCrMo alloys coated with TiAlN, TiAlPtN and TiAlPtN/TiAlPt/TiAl multilayers. The coatings were deposited on CoCrMo alloys by magnetron sputtering. The structure of multilayers was studied by means of XRD and the composition by RBS and GDOES techniques. The period size of the multilayers was 300 nm. The tribocorrosion was performed using a ball-on-flat reciprocating tribometer, the test was conducted in a simulated body fluid at 36.5 °C of temperature. The loads used were 1 and 5 N, the oscillating frequencies was 1Hz. The corrosion was studied using open circuit potential (OCP) measurements and potentiodynamic polarization in a simulated body fluid. The individual and synergistic effects of wear and corrosion on total wear loss were estimate. The surface topography and worn surface were studied by means of optical microscopy and profilometry. The Pt content in TiAlN films was 0.5 at. % and improve its tribocorrosion resistance. The results indicate that multilayers improve the tribocorrosion resistance and reduce de friction coefficient compare with monolayers.

DP-15 Electrochemical and Morphological Analysis on the Titanium Surface Modified by Shot Blasting and Anodic Oxidation Processes, E.M.S. Szesz, Neortho/Research Institute, Brazil, B.L. Pereira, C.E.B. Marino, Universidade Federal do Paraná, Brazil, G.B. Souza, Universidade Estadual de Ponta Grossa, Brazil, P. Soares, Pontificia Universidade Católica do Paraná, Brazil, N.K. Kuromoto (kuromoto@fisica.ufpr.br), Universidade Federal do Paraná, Brazil

In the last years many surface modification processes have been developed in order to induce the osseointegration on titanium surface and thus to improve the implants' biocompatibility. So in this work, Ti surface has been modified by shot blasting and anodic oxidation processes in order to associate the good surface characteristics of both processes to obtain a roughness and porous surface able to increase the titanium bioactivity. Otherwise the behavior and success of the implants can be evaluated by electrochemical measurements for a variety of reasons. Corrosion processes that occur at implant surfaces, the role of oxide films in the corrosion process, alloy biocompatibility and the electrochemical response of these biomaterials to mechanical and electrical transients.

Commercially pure titanium (grade 2) plates were ultrasonically cleaned with acetone, ethanol and water. The shot blasting was performed using Al₂O₃ particles with 280µm average diameter and air pressure of 20 bars during 6s. The anodic oxidation (AO) was carried out using NaOH electrolyte 0.1 mol/L and constant current density of 150 mA/cm² for a minute. After AO the specimens were dried at 40°C for 24h. The morphology of the films was analyzed using a scanning electronic microscopy (SEM) Jeol JSM-6360LV. Structural changes were studied by X-ray diffraction (XRD Shimadzu XRD-7000) using Cu radiation at 40 kV and 20 mA to verify the phases present on the anodic film after heat treatment (HT) at 600°C. The open-circuit potentials (OCP) were obtained using a conventional cell with SCE as reference electrode and Voltalab 40 (PGZ300) equipment. The electrolyte was a PBS (phosphate buffer solution) solution.

It can be observed an increase on the rugosity of the blasted surface and a roughness and porous surface after AO process. The anodic film produced is thin and followed the blasted surface topography. It can be observed small pores size with regular shape covering all the surface. X-ray diffraction results showed that after HT at 600°C/1h the presence of the anatase and rutile phases on the blasted and anodized surface.

Concerning to electrochemical measurements when the different samples were submitted to open-circuit conditions, the protective effect increases with the oxidation process, because the oxide layer. This protective effect could be evidenced by the open circuit potential (OCP) values: Shot blasted Ti surface: -0.728V, Polished Ti: -0.653 V and Blasted and oxidized Ti surface: -0.492 V. When the surface was blasted the OCP was more cathodic when compared with the Ti surface without surface treatments.

DP-16 Morphological and mechanical characterization of the titanium anodic film obtained with a mixture of sulphuric and phosphoric acid under potentiostatic mode, A. Rossetto, S. Blunk, Universidade Federal do Paraná, Brazil, C.E. Foerster, Universidade Estadual de Ponta Grossa, Brazil, P. Soares, Pontificia Universidade Católica do Paraná, Brazil, B.L. Pereira, C. Lepienski, N.K. Kuromoto (kuromoto@fisica.ufpr.br), Universidade Federal do Paraná, Brazil

Titanium (Ti) and Ti alloys are used for the manufacture of dental and orthopedic prostheses. These materials must have appropriate properties, such as zero toxicity, good mechanical properties and resistance to corrosion. In addition, a short time of osseointegration is also desired to promote the rapid recovery of the patient. The film deposition or surface modification can be employed to obtain or improve these characteristics in a biomaterial. So in this work titanium oxide films produced on Ti commercially pure by anodic oxidation technique using a mixture of sulphuric and phosphoric acid as electrolyte in different proportion were analysed. Anodic oxidation was carried out at room temperature using a platinum counter electrode, 1M H₂SO₄ plus 1M H₃PO₄ as electrolyte (proportion of (a) 1 H₂SO₄ : 0.5 H₃PO₄, (b) 1 H₂SO₄ : 1 H₃PO₄, and (c) 1 H₂SO₄ : 1.5 H₃PO₄, at 180V/60s. The morphology of the films were analysed with scanning electron microscopy and hardness and elastic modulus profiles were obtained by instrumented indentation following the Oliver and Pharr method. The maximum applied load was 400mN in eight successive loading/unloading cycles at increasing loads using a Berkovich diamond indenter. It was observed that porous titanium layers were formed irrespective of the electrolyte mixture. Initially the film is relatively uniform with small and round pores and with the increase of the content of the phosphoric acid the porosity and the pore size increased. The anodic film obtained with same proportion of H₂SO₄ plus H₃PO₄ (case b 1:1) shows an appearance of pores and craters formed on the relatively flat ground oxide surface. The larger porous size (craters) observed in this case is probably due to interconnection of some pores. The nanoindentation results showed that the anodic films obtained in different conditions present similar hardness values (3,3 GPa) and elastic modulus values (70,5 GPa) indicating

that the H of anodic films increased compared with Ti substrate (2,2GPa) while elastic modulus decreased (110GPa).

DP-17 Investigation of Wear, Corrosion and Tribocorrosion Properties of AZ91 Mg Alloy Coated by Micro arc Oxidation Process in the Different Electrolyte Solution. *E. Demirci (e_ebrudemirci@hotmail.com), Ataturk University, Turkey, E. Arslan, College of Erzurum, Turkey, V.K. Ezirmik, Ataturk University, Turkey, O. Baran, Erzincan University, Turkey, Y. Totik, Turkey, I. Efeoglu, Yildiz, Ataturk University, Turkey*

Micro arc oxidation (MAO) is an effective technique to improve the surface properties of light materials by forming ceramic films on the surface. A number of studies have been carried out for depositing on Mg and Mg alloys. However, only a few have focused on wear, corrosion or tribocorrosion properties. In this study, MAO process was carried out on AZ91 Mg alloy in two different electrolyte solution namely phosphate-silicate and potassium stannate. The microstructures, morphology and crystallographic structure were analyzed by SEM and XRD. The wear, corrosion and tribocorrosion properties of the coatings were investigated by pin-on-disc wear test, potentiodynamic polarization test and combining tribocorrosion test unit, respectively. The results showed that solution has an important role on the wear, corrosion and tribocorrosion resistance of MAO coating.

Key Words: Mg alloys, MAO process, wear resistance, corrosion resistance and tribocorrosion resistance.

DP-18 Effect of Nitrogen Plasma Immersion Ion Implantation Treatment on Corrosion Resistance and Cell Responses of Biomedical Ti and Ti-6Al-4V Metals. *H.H. Huang (hhuang@ym.edu.tw), S. Wang, C.H. Yang, National Yang-Ming University, Taiwan, W.F. Tsai, C.F. Ai, Institute of Nuclear Energy Research, Taiwan*

Ti and Ti-6Al-4V metals are widely used in biomedical applications. However, excessive surface corrosion of Ti and Ti-6Al-4V may lead to the biological side effects. In this study, nitrogen plasma immersion ion implantation (N-PIII) treatment was utilized to improve the surface mechanical properties, corrosion resistance and cell responses of biomedical Ti and Ti-6Al-4V metals. The N-PIII treatment with different applied voltages, 5 and 20 kV, were used. Various surface characteristics, including hardness, Young's modulus, chemical composition and topography were analyzed. The corrosion resistance of the test specimens was studied using the potentiodynamic polarization curve measurement in simulated body fluid. Human bone marrow mesenchymal stem cells were used for testing the cell responses, including cell adhesion, cell proliferation and cell mineralization. Results showed that the N-PIII treatment slightly increased the surface roughness of Ti and Ti-6Al-4V. Through N-PIII treatment, a thin TiN film (< 200 nm in thickness) could form on Ti and Ti-6Al-4V. The presence of TiN on Ti and Ti-6Al-4V increased the surface hardness, surface Young's modulus, corrosion resistance and cell responses (i.e. better cell spreading, cell proliferation and cell mineralization), especially at a higher N-PIII treatment voltage. We would conclude that the N-PIII treatment increased the corrosion resistance and cell responses of biomedical Ti and Ti-6Al-4V metals.

Tribology & Mechanical Behavior of Coatings and Engineered Surfaces

Room: Golden Ballroom - Session EP

Symposium E Poster Session

EP-1 About the identification of generic tribological parameters. *M.C. Fuchs (marcus.fuchs@s2003.tu-chemnitz.de), N. Schwarzer, Saxonian Institute of Surface Mechanics, Germany*

To obtain tribological parameters like Archards wear depth parameter k_d usually requires some severe effort in performing and analyzing complex tribological experiments. The poster features an approach where such parameters are extracted from effective interaction potentials [1], which themselves are built up and fed from more physical measurements like nanoindentation and physical scratch test [2]. By using such effective material potentials one can derive critical loading situations leading to failure (decomposition strength). A subsequent connection of these decomposition or failure states with the corresponding stress or strain distributions allows the development of rather comprehensive tribological parameter models applicable in wear and fatigue simulations as demonstrated in this work.

[1] N. Schwarzer: "Short note on the effect of pressure induced increase of Young's modulus". Phil. Mag., submitted July 2011

[2] N. Schwarzer et al.: "Optimization of the scratch test for specific coating designs". Surface & Coatings Technology, accepted 2011.

EP-2 Gradient of tribological and mechanical properties of diamond-like carbon films grown on Ti6Al4V alloy with different condition of interlayer preparation. *G. Martins, Clorovale Diamantes S.A., Brazil, C. Silva, J. Machado, E. Corat, V. Trava-Airoldi (vladimir@las.inpe.br), Institute for Space Research, Brazil*

Ti6Al4V alloy are used on advanced aerospace systems, as a biomaterials, etc., because of their properties like high strength to weight ratio and excellent corrosion resistance and biocompatibility compared to many other metal alloys. In order to improve such applications, it is necessary to improve its tribological and mechanical properties and a good choice is the deposition of diamond-like carbon (DLC) coating with very high adhesion. DLC films are well known for their low friction, high hardness and good wear resistance. The adhesion between a DLC coating and Ti6Al4V alloy can be enhanced by the application of an interlayer of diverse materials. In this work, it was used a silicon interlayer that was deposited with different controlled ion energy, generating singular ion subimplantation profiles on the titanium alloy substrate. The DLC films were deposited using a modified PECVD pulsed-DC discharge under controlled conditions to obtain maximum hardness, minimum stress and maximum deposition rate. Tribological and mechanical tests were made to observe the friction and wear gradient of the samples. The tribometer was adjusted for ball-on-plate mode, in the reciprocating manner, in a humidity of $26 \pm 2\%$ RH and a temperature of 25 ± 1 °C. The scratching tests were made in order to study the adhesion of DLC coatings on Ti6Al4V alloy as a function of silicon interlayer parameters of obtaining. The samples were also characterized by micro and nano-indentation to observe the hardness profile, and Raman spectroscopy to verify the structural arrangement of carbon atoms. It was observed that the adhesion between DLC film and substrate is strongly related to gradient of mechanical and tribological properties of the substrate from the bulk to the surface.

EP-3 Synthesis and characterization of high flatness diamond-like carbon films deposited by filtered cathodic arc deposition. *D.Y. Wang (jackaljr@mdu.edu.tw), S.W. Lin, W.C. Chen, MingDao University, Taiwan*

The diamond-like carbon (DLC) films have been widely applied to various areas for as protective coating for its superior properties of high hardness, low friction coefficient, high wear resistance, and chemical inertness.

In this study, the tetrahedral amorphous carbon (ta-C) films were synthesized by using a self-design filtered cathodic vacuum arc (FCVA) system. The effect of substrate bias (from -50V to -250V) on the surface morphology of the films were observed by scanning electron microscopy (SEM). The ta-C film shows a uniform and smooth surface morphology and a dense cross-section texture. The electron microscopy, atomic force microscopy and Raman spectroscopy were employed to characterize the microstructure and carbon bond properties of DLC coatings.

According to the results of Raman and X-ray photoelectron spectroscopy (XPS) we found that the sp^3 fractions between 70% ~ 80%. When substrate bias was -100V, the maximum hardness of the film was 32 GPa. The surface particle density was decreased 60% than unfiltered process and the particle size was less than 2nm.

Keyword : Filtered Cathodic-Arc Deposition, Diamond-Like Carbon, surface flatness

EP-4 Effect of oxygen and nitrogen content on mechanical and tribological properties of Mo-N-O thin films. *M. Hromadka, P. Novak, J. Musil (musil@kfy.zcu.cz), R. Cerstvy, Z. Soukup, University of West Bohemia, Czech Republic*

The paper reports on preparation of Mo-N-O thin films deposited by reactive magnetron sputtering in an argon-oxygen-nitrogen atmosphere. The effect of oxygen and nitrogen content in gas mixture on mechanical properties (hardness H, effective Young's modulus E^* , elastic recovery W_e) and tribological properties (coefficient of friction μ , wear rate k) of Mo-N-O films were investigated in detail. Correlations between the mechanical and the tribological properties of the Mo-N-O film were also investigated. It was found that (i) there is no significant difference between the tribological behaviour of the δ -MoN and γ -Mo₂N films (ii) the addition of oxygen in discharge results in increase of the coefficient of friction (from 0.3 to 0.5) (iii) hardness (H), effective Young's modulus (E^*) $E^*=E/(1-\nu^2)$ and the ratio H^3/E^{*2} , characterizing the resistance of film to plastic deformation, increases with increasing amount of nitrogen in film (iv) the deposition rate of the MoN film decreases with increasing partial pressure of N₂ from 283 to 140 nm/min.

EP-5 The effective Indenter concept applied to a comprehensive 3D infinitesimal wear model, N. Bierwisch (*n.bierwisch@siomec.de*), N. Schwarzer, Saxonian Institute of Surface Mechanics, Germany

A new sophisticated wear model has been developed on the basis of the effective indenter concept [1, 2] by using the extended Hertzian approach [3]. Fed properly from physically performed experiments like ordinary Nanoindentation and lateral Nanoindentation via effective interaction potentials the models do not only allow to analyze certain tribological experiments like the well known pin-on disk test, but also to forward simulate such tests and even give hints for better component life-time predictions. The work will show a few examples.

[1] N. Schwarzer, G. M. Pharr: „On the evaluation of stresses during nanoindentation with sharp indenters”, *Thin Solid Films*, Vol.469-470C pp. 194-200

[2] N. Schwarzer, T. Chudoba, G. M. Pharr: „On the evaluation of stresses for coated materials during nanoindentation with sharp indenters”, *Surf. Coat. Technol.*, Vol 200/14-15 pp 4220-4226

[3] N. Schwarzer: "The extended Hertzian theory and its uses in analysing indentation experiments", *Phil. Mag.* 86(33-35) 21 Nov - 11 Dec 2006 5153 – 5767, Special Issue: "Instrumented Indentation Testing in Materials Research and Development"

EP-6 Mechanical Characterization of RF-DC Plasma Nitrided Tool Steels, T. Aizawa (*taizawa@sic.shibaura-it.ac.jp*), Shibaura Institute of Technology, Japan, Y. Sugita, YS Electric Industry, Co. Ltd., Japan

Pulse-enhanced plasma nitriding has been widely utilized as an industrial surface treatment. Various types of steel parts and components with variety of dimensional geometry are plasma-nitrided with high qualification in the nitrided layers and with controllability of hardness profile; e.g. formation of white layers is disliked in the nitrided tool steels. The present paper aims at lower temperature nitriding; RF-DC plasma nitriding method is proposed to describe the inner nitriding behavior of tool steels with comparison to the conventional DC-plasma and pulse-enhanced plasma nitriding processes. This new nitriding system works around 2 MHz with automatic matching; RF and DC conditions are independently controlled and wide range of pressure is also utilized for nitriding. First, SKD-11 substrate is employed to investigate the effect of holding temperature, pressure and hydrogen to nitrogen gas ratio on the surface hardness. After pre-sputtering for 900 s, plasma nitriding is performed by RF (200 V) and DC (-500 V) for 7200 s at 753 K; the average hardness reaches to 1100 to 1300 in the dependent manner on the RF-volt and pressure. Uniform nitriding takes place after observation on the cross-sectional SEM and optical microstructure images. Fine distribution of CrN with less population of iron nitrides in the nitrided layer is responsible for relatively high hardness even by lower temperature nitriding.

EP-7 Patterned Film Effects on the Adhesion of Al/TiN Barrier using Fracture-Energy Based Finite Element Analysis, C.C. Lee (*changchunlee@cycu.edu.tw*), Department of Mechanical Engineering, Chung Yuan Christian University, Chungli, Taiwan, C. S. Wu, Department of Mechanical Engineering, Chung Yuan Christian University, Taiwan, B.F. Hsieh, S.T. Chang, Department of Electrical Engineering, National Chung Hsing University, Taiwan

Currently, TiN films in the nanoscale order are widely used as barriers in multi-level interconnect systems of semiconductor devices. However, when an external loading or thermal stress is applied, the adhesion capability between barriers and conductive metals increases the likelihood of the interfacial delamination of dissimilar thin films, which is one of the important reliability issues in advanced interconnect technology. To quantify the adhesion of Al/TiN thin film, finite element analysis based on the interfacial fracture theory is presented to estimate precisely the cracking energy of the thin film. Through a comparison of four-point bending test data with the predicted results, the proposed simulated methodology is validated to be highly reliable in estimating the interfacial energy release rate of Al/TiN stacked films. Furthermore, the analysis results also indicate that the thickness and Young's modulus of dielectrics within testing samples both have a significant effect on the interfacial cracking energy of Al/TiN thin film.

EP-8 Cyclic Creep and Fatigue Testing of Nanocrystalline Copper Thin Films, Y.T. Wang, C.J. Tong, W.T. Tseng, M.T. Lin (*mingtlin@nchu.edu.tw*), National Chung Hsing University, Taiwan

A microtensile testing for studying the cyclic fatigue mechanical properties of freestanding nanocrystalline copper thin film with thickness of sub-micrometer was performed to observe its mechanical response under tension-tension fatigue experiments with a variety of stress amplitude and mean stress conditions at cyclic loading frequencies up to 20 Hz. Tensile sample loading was applied using a piezoelectric actuator. Loads were measured using a capacitance gap sensor with a mechanical coupling to the

sample. The experiments were carried out with feedback to give load control on sputter deposited 300, 500 and 700 nm Cu thin films. Loading cycles to failure reached over 10^6 at low mean load with a trend of decreasing cycles to failure with increasing mean load and load amplitude as anticipated. The cyclic results provided clear evidence for a cyclic creep rate dependent and change in failure mechanism from crack formation to extended plasticity as the mean load and load amplitude are decreased. Moreover, the length scale dependence on fatigue mechanism and cyclic creep of tested films were observed.

EP-9 On the determination of coating toughness during nanoindentation, J. Chen (*Jinju.chen82@gmail.com*), Newcastle University, UK

The ceramic coatings have fulfilled a wide range of functions such as wear resistance, energy storage, and optical properties. Due to their low fracture toughness, however, they usually show complex crack characteristics when these ceramic coatings are in contact with foreign objects. Such local cracks can affect the integration of the entire component as well as the function of the coatings. In order to optimise the material selection, design and fabrication, it is essential to determine the fracture toughness. Nanoindentation tests have been widely used to evaluate fracture toughness of brittle materials. With decrease of the coating thickness and the introduction of complex composition and structure, the fracture morphology becomes more complicated. This increases the difficulty in determining fracture toughness. For the thin coatings, energy based models have been shown to be effective.

Based on determination of unloading curve at the start and end points of the crack induced pop-in, one can assess fracture toughness. However, the existing models give a loose bound of fracture toughness limits.

Therefore, an improved method has been proposed based on a refined approach to determine the unloading curve at the start and end points of the crack induced pop-in. The semi-analytical generalized expressions have been presented to determine the fracture toughness of coatings for nanoindentation tests performed under both load and displacement control. This has provided a valuable theoretical guideline to determine fracture toughness from the energy point of view. Furthermore, this approach has been validated by nanoindentation tests on various coatings.

EP-10 Scratch Test of Optimized TiSiN Coating Deposited Via A Combination of DC and RF Magnetron Sputtering, A.R.Bushroa, Abdul Razak (*bushroa@um.edu.my*), University of Malaya, Malaysia, B. Beake, Micro Materials Ltd, UK, M. Haji Hasan, University of Malaya, Malaysia, M.R. Muhammad, Multimedia University, Malaysia

An optimized magnetron sputtered TiSiN coating on a high speed steel substrate was fabricated using a combination of direct current (DC) and radio frequency (RF) power in a physical vapor deposition (PVD) technique. Controlled samples were also developed for a comparison, whereby the DC power was varied at 300 and 400 W. The optimized sample was coated at 500 W. A scratch test was performed to investigate wear resistant of the coating. The test was done with at least nine constant load wear cycles on the coating. The coating deposited with DC power of 300 and 400 W failed after 4th and 6th cycles, but the coating of 500 W resisted wear even after 9th cycle. This result was supported with the optical image of scratch track, whereby no evidence of chipping, delamination and total exposure of substrate were observed. Mechanical property of optimized coating was also investigated for tribological performance. The value of effective ratio of hardness to relative modulus (H/E^*) was discussed to relate with the wear resistance. Furthermore, failure mode of 3 distinguished stages of deposited coating was explored.

EP-11 Evaluation of Adhesion of TiAlN/CrN Multilayer Coatings Deposited by CFUBMS, H. ÇİÇEK (*hikmetcicek25@hotmail.com*), Ataturk University, Turkey, Ç. Laloğlu, Turkey, Ö. Baran, Erzincan University, Turkey, E. Demirci, V. EZİRMİK, İ. EFEÖĞLU, Ataturk University, Turkey

TiAlN/CrN multilayer films widely used to increase the life of the materials in industry especially cutting tools and machine parts which work high velocity and dry friction conditions. One of the important factors affecting the performance of coatings is the adhesion of film to the substrate. This work, TiAlN/CrN films were coated on M2 tool steels by CFUBMS according to the taguchi technique. Microstructure and mechanical properties of these films were characterized by X-ray diffraction, SEM and micro hardness tester. And adhesion properties of these films determined by scratch tester. The obtained results from the adhesion test evaluated with hardness, thickness and structure of the films.

EP-13 Adhesion tendency of polymers to hard coatings. *M. Rebelo de Figueiredo* (*marisa.figueiredo@unileoben.ac.at*), *C. Bergmann*, *C. Ganser*, *C. Teichert*, *C. Mitterer*, Montanuniversität Leoben, Austria

In micro-injection moulding of small, precise and complex-shaped polymer parts, adhesion between the mould and the polymer needs to be minimized to achieve the requested tolerances of the parts and sufficient lifetime of the mould. Therefore, friction and wear behavior of the coating materials TiN, CrN, Al₂O₃, CrAlN, TiAlN and TiCN as well as an uncoated high-speed steel were studied against the polymers of interest polyoxymethylene (POM), polyamide 6.6 (PA 6.6) and polyether ether ketone (PEEK). Ball-on-disk tests in ambient air were performed at half of the melting temperature for each polymer. For POM and PEEK, the lowest friction (~0.15) and counterpart wear volume ($7.8 \times 10^{-4} \text{ mm}^3$) were observed for CrN, whereas for PA 6.6 TiCN and TiAlN showed the lowest friction (~0.55) and CrN the lowest counterpart wear volume ($1.2 \times 10^{-3} \text{ mm}^3$). Ex-situ Raman analyses carried out on the wear tracks of both parties revealed that chemical changes in the contact were only observed for the high-speed steel, giving evidence of the presence of hematite and magnetite and most importantly transfer material of the polymer counterparts. Correlations between the Raman results as well as roughness and surface energy to the obtained friction and wear properties provided new insights regarding the understanding of the tribological behavior.

EP-14 Effect of Nitrogen content on the Microstructure and Residual Stress of Ternary Ta-Ti-N Thin Films Using Magnetron Sputtering. *C.K. Chung* (*ckchung@mail.ncku.edu.tw*), *Y.R. Lu*, *T.S. Chen*, *C.H. Li*, *Y.T. Lin*, National Cheng Kung University, Taiwan

Binary transition metal nitride of Ta-N and Ti-N film has been extensively applied as diffusion barriers for Cu interconnection and hard coatings for protective application. The combination of Ta-N and Ti-N is expected to extend and develop functional for promising application of films. However, the films' buckling and peel off from substrate may be observed due to high residual stress. In this paper, the ternary Ta-Ti-N thin films were fabricated by magnetron co-sputtering using various nitrogen flow ratios (FN2%) of 0-20% for studying the evolution of microstructure and residual stress of films. The microstructure, morphology, composition, and residual stress of Ta-Ti-N films were measured by grazing incident angle X-ray diffraction (XRD), scanning electron microscopy (SEM), energy dispersed spectrum, and surface profilometer with curve fitting by Matlab, respectively. XRD patterns showed that Ta-Ti film is body center cubic structure with three distinct (110), (200) and (211) diffraction peaks and the phase transforms to face center cubic (FCC) structure as over 5 FN2%. The SEM image showed that the particle was precipitated on the film's surface at 20 FN2% due to the over solubility of Ta-Ti-N. The tensile stress of 2.36 GPa was observed from the film at 0 FN2% while the compressive stress of 1.64 GPa was obtained at 10 FN2%. The relationship between the nitrogen flow ratios, microstructure and residual stress of ternary Ta-Ti-N thin films is discussed and established.

EP-15 A study of microstructures and mechanical properties of cathodic arc deposited ZrSiN coatings with silane gas. *S.H. Huang*, National Chiao Tung University, Taiwan, *T.C. Tseng*, *C.Y. Tong*, *Y.B. Lin*, *J.W. Lee* (*jefflee@mail.mcut.edu.tw*), Ming Chi University of Technology, Taiwan, *T.E. Hsieh*, Gigastorage Corporation, Taiwan, *J.G. Chen*, *H.W. Chen*, National Tsing Hua University, Taiwan

The ZrSiN coatings were deposited by cathodic arc deposition system. The silane gas (SiH₄) was added to the sputtering gas to deposit the ZrSiN coatings with different Si contents. The microstructures and mechanical properties of coatings were determined by grazing angle X-ray diffractometer. Microstructures of thin films were examined by a scanning electron microscopy (SEM) and transmission electron microscopy (TEM), respectively. A nanoindenter, scratch tester and pin-on-disk wear tests were used to evaluate the hardness, adhesion and tribological properties of thin films, respectively. It was found that the hardness and tribological properties were strongly influenced by the silane gas flow rate, i.e. the Si contents of the ZrSiN coatings. Optimal silicon content for the ZrSiN coating was proposed in this work.

EP-16 Effect of micro-droplets and surface morphology on the local residual stress field in thin hard coatings. *E. Bemporad* (*e.bemporad@stm.uniroma3.it*), *M. Sebastiani*, *M. Piccoli*, *F. Carassiti*, University of Rome "Roma Tre", Italy

The effect of surface defects on the residual stress distribution in thin coatings has been investigated by an innovative high resolution methodology, which mainly consists of incremental focused ion beam (FIB) ring-core milling (I_pRCM), combined with high-resolution in situ SEM-FEG imaging of the relaxing surface and a full field strain analysis by digital image correlation (DIC). The through-thickness profile of the residual stress can be obtained with sub-micron spatial resolution (both lateral and in-depth), by comparison of the experimentally measured surface strain with finite element modeling using Schajer's integral method.

Commercial Titanium Nitride (TiN) and Chromium Nitride (CrN) coatings were produced by Cathodic Arc Evaporation Physical Vapor Deposition (CAE-PVD) on tool steel substrate, which were prepared at three different roughness levels.

Preliminary characterization of coatings consisted on nanoindentation testing, FIB cross section microstructural analysis and XRD (sin²ψ) average residual stress measurement and micr-scratch testing on each coating.

Local residual stress were measured by the I_pRCM method nearby to droplets of different size, with the main aim of investigating the effect of such defect on the residual stress in-depth distribution. FIB cross section were also prepared in correspondence of each test, in order to investigate the changes of microstructure and growth mechanism due to the defect. Residual stress were also measured in correspondence of surface roughness defects (polishing scratches, wrinkles, asperities). A series of stress measurements were finally performed on the homogeneous defect-free coating

Significant differences were found in terms of residual stress and stress gradient in proximity of surface defects, in comparison with the residual stress measured in defect-free areas.

In case of micro-droplets, such differences were attributed to significant modification of growth mechanisms and microstructure of the coating. This assumption was supported by the microstructural FIB-SEM observation, which showed anomalous grain growth and changes in crystal orientation in correspondence of a droplet.

Finally, the observed surface residual stress local variation where correlated to the failure modes during scratch test, which could be affected by local residual stress peaks.

EP-17 Tribological Behaviour of Electrodeposited CoW-WC Nanocomposite Coatings. *S.K. Ghosh* (*sghosh@barc.gov.in*), *A.K. Suri*, BARC, India, *J.P. Celis*, KUL, Belgium

Research for alternatives to electroplated hard chromium coatings is continued because of their tremendous environmental and health hazard concern. Among the various possibilities, recently, electroplated Co-W alloys show promising results like abrasive wear and corrosion resistance close to and even better than electroplated hard chromium. In the present study, the Co-W alloy matrix is further strengthened by incorporating nano-size WC particle (500 nm) via electrochemical codeposition technique. The matrix cobalt helps in binding the WC particles and in return particles strengthen the matrix along with host tungsten as alloy element. A sulphate-tungstate based electrolyte was used to electrodeposit the Co-W alloys and Co-W-WC nanocomposites. In order to increase the particle-content within the alloy matrix, effect of current density and particle loading within the electrolyte were investigated in detail. Nanoindentation was used to evaluate the nanohardness and elastic modulus of the CoW alloys and CoW-WC nanocomposites deposited under identical current density conditions in order to study the strengthening performances. No drastic change in hardness was observed in case of nanocomposite as compared to alloy counterpart. On the other hand, a significant improvement in wear behaviour was noticed for CoW-WC nanocomposites in comparison to CoW alloy coatings. The fretting tests were performed at a normal load of 2-10N, keeping the total displacement amplitude at 200 μm, the frequency at 5 Hz for 10000-100000 cycles in humid air (50% RH) at 23 °C. A corundum (Al₂O₃) ball of 10 mm diameter was used as counter body. Typical wear volume measured in case of CoW-WC (deposited at 50mA.cm⁻²) under 3D optical profilometer was almost half of CoW alloy (deposited at 50mA.cm⁻²), after fretting test under identical conditions. Post deposition annealing of these coatings was done to found influence on hardness and wear rate. The observed wear rate data of coatings will be discussed in the light of microstructure, crystal structure and surface morphology of the as deposited coating and wear scar analysis. A special attention was given to correlate nanohardness, elastic modulus with the measured wear rate of these coatings.

EP-18 Duplex coating of DLC films for Al and Al alloys. *Y. Sakamoto* (*yukihiro.sakamoto@it-chiba.ac.jp*), Chiba Institute of Technology, Japan
Aluminum is one of light metals and thermal conductivity of aluminum and its alloy is excellent. However, tribological properties of aluminum and aluminum alloys are worse compared with iron based material.

On the other hand, "Duplex coating" is a one of hardening processing such as thin nitride film formation on the surface of nitrided layer. The adhesion strength was improved by introducing of the chemical bonding between the film and the substrate using this method.

In this study, duplex coating of Diamond Like Carbon coating on the nitride layer were studied to improve the tribological properties of aluminum and aluminum alloys.

AC8A and ADC12 were used as the substrates. The mixture of NH₃ and H₂ was used as a reaction gas of radical nitriding. DLC films were prepared on

the substrates directly or after radical nitriding. Evaluation of adhesion strength was performed by observation of peeling areas using SEM after Rockwell indentation test. Tribological properties were evaluated by a friction tester.

DLC peaks were observed in the Raman spectra of samples after DLC coating. The hardness of the sample of duplex coating was higher than that of direct coating. Surface SEM image of duplex coating sample showed no peeling off and the adhesion had been improved.

From the result of tribological estimation, friction coefficient of the DLC duplex coating samples was lower than that of Al alloys.

As a result, improvement of the hardness, adhesion strength, friction properties were confirmed for duplex coating.

EP-20 The effect of grooved surface texture on friction-induced vibration and noise, J.L.M. Mo (*jimo@swjtu.cn*), H.L.D. Dan, G.X. Chen, M.H. Zhu, Southwest Jiaotong University, China, T.M. Shao, Key Laboratory of Tribology, Tsinghua University, China, Z.R. Zhou, Southwest Jiaotong University, China

Grooved surface texture (30 μm in depth, 150 μm in width and 500 μm in pitch) was manufactured on the surface of compacted graphite iron samples (brake disc material) by electromachining. The difference of friction-induced vibration and noise properties between groove-textured and smooth surfaces was studied in a ball-on-flat configuration under different normal loads of 3, 5, 10, 20, 40 N. A Si_3N_4 10 mm diameter sphere was used as counterface ball. The dominant frequencies of the interface forces and noise were analyzed and the influence of grooved surface texture on friction-induced vibration and noise behaviors was investigated. The test results showed that the normal load had significant influence on the friction noise level of the smooth surface but little influence on that of the groove-textured surface. For the grooved surface texture adopted in this work, friction noise was prone to occur even under low normal load of 3 N. No friction noise occurred at the smooth surface until the normal load increased from 5 N to 10 N, but its level increased rapidly approaching to that of the groove-textured surface. The groove-textured surface adopted in this work exhibited higher coefficient of friction and wear resistance as compared to the smooth surface, but it made the friction system easier to generate multi-frequency friction vibration and friction noise with more complex frequency components. The existence of grooved surface texture changed the friction and wear behaviors as well as friction-induced vibration and noise properties of the frictional surfaces, further study will be performed to gain understanding for their corresponding relationship.

EP-21 Adhesion enhancement of polymers by an intermediate layer through photografting polymerization, J. Takahashi, A. Hotta (*hotta@mech.keio.ac.jp*), Keio University, Japan

In this paper, a new surface treatment method for adhesion improvement of polymers using photografting polymerization was introduced. Although polymers have been widely utilized due to their usability, few studies have been reported on the solutions of the low gas barrier property, low abrasion property, and low adhesion property of the polymers. In order to solve these problems, surface modification was introduced. Surface modification can bring in plenty of new functions to polymers for wider industrial applications. In addition, the surface modification causes no loss in the bulk property of the polymers with simplicity and easiness in the surface treatment. There are currently three major methods in the surface modifications. They are flame treatment, corona discharge treatment, and polymer coating. Flame treatment is a dangerous method using flame, and corona discharge treatment requires great care, while polymer coating is occasionally difficult to find an appropriate solvent. In this work, we investigated a new type of surface treatment by photografting polymerization. Photografting polymerization is one of the chemical surface modification methods by radical polymerization. The method introduces functional monomers onto materials as side chains with the reaction starting simply by irradiating UV. As compared with the current three methods, the photografting polymerization is an easier and safer method. It was found that the surfaces of various widely-used polymers, such as high density polyethylene (HDPE), low density polyethylene (LDPE), linear low density polyethylene (LLDPE), isotactic polypropylene (iPP), syndiotactic polypropylene (sPP), polystyrene (PS), polymethyl methacrylate (PMMA), polydimethyl siloxane (PDMS), polyurethane (PU), and polyethylene terephthalate (PET) were overall nicely modified to show a good adhesion to soft and hard substrates e.g. DLC after photografting acrylic acid (AA). Additionally, the adhesive strengths of the polymers were remarkably increased, which could be a new and effective way of treating the surface of polymers.

EP-22 Tool life and surface characterization of four commercial drills, S. Muhl (*muhl@unam.mx*), Universidad Nacional Autónoma de México - Instituto de Investigaciones en Materiales, Mexico, D. Garcia, A. Figueroa, SEPI, ESIME-Zacatenco, Instituto Politécnico Nacional, Mexico

Drilling is one of main machining procedures in industry and the quality of the drill plays a fundamental role in the productivity and efficiency of the process. The quality determines the useable tool life, the characteristics of the machined holes, the machining time and the electrical power needed. However, ascertaining this quality from a surface and tribological characterization of the drill bit is difficult. There are many different kinds of drills commercially available with variations in their cutting edge, the tool material, the surface treatment, etc. and these result in drill bits of a great variety of prices.

The object of this paper is to report the results of our study of the work performance of four readily available but very differently priced $\frac{1}{2}$ " diameter metal cutting drill bits. The study was designed to determine the life work of each drill and compare this with the measured surface and tribological characteristics. For this, each drill was used under control conditions, such as cutting speed, load, drilling depth and drill machine. The surface and tribological properties of each drill was measured by: ball-cratering, nano and micro-indentation, scratch testing and the chemical composition of the surface and bulk by EDS and RBS. The results show the relation between each drill performance (number of holes that could be made, the drilling time and the electrical energy used) and the results of the different tribological tests (hardness, wear resistance, scratch resistance and composition).

EP-23 Surface modification of cast iron substrates using radical nitriding, I. Sugiura (*s0721178TQ@it-chiba.ac.jp*), Graduate School, Chiba Institute of Technology, Japan, Y. Sakamoto, Chiba Institute of Technology, Japan

Though tribological property of cast iron is excellent and used as sliding parts and rotating parts, its hardness is not so high. To improve wear resistance and fatigue strength of cast iron, induction hardening and nitriding are usually used. However, induction hardening is rapidly heated and quenched over the transformation point of the steel. So, it needs to be considered as stress and dimensional changes. In contrast, nitriding is treated by under the transformation point of the steel. So, stress and dimensional changes after nitriding are smaller than those of induction hardening. However, formation of compound layer and holes formed on the surface are problems for conventional nitriding of cast iron. On the other hand, radical nitriding is one of the surface hardening methods and it is possible to keep surface roughness smooth like as initial surface to control the plasma state precisely. Investigation was carried out on the surface modification of cast iron substrates using radical nitriding.

The surface of substrates was cleaned by H_2 etching before radical nitriding. The condition of H_2 etching was follows: pressure; 133Pa, applied voltage; -380V and -600V, H_2 flow rate; 50SCCM, external heater temperature; 843K and processing time; 10min, respectively. The condition of radical nitriding was follows: pressure; 133Pa, applied voltage; -380V and -600V, NH_3 flow rate; 100SCCM, H_2 flow rate; 100SCCM, external heater temperature; 843K and processing time; 60min, respectively. The evaluations of the nitrided layer were carried out by surface profiler, micro vickers hardness tester and ball-on-disk friction tester. Measurements of friction coefficient were conducted by using of load; 0.5N, turning radius; 2.4mm, speed of sliding; 6.2mm/s and counterpart materials SUJ2 4.76mm in diameter, respectively.

Surface roughness of the substrate after nitriding was worse than that of the no-treated cast iron substrate, and it was depended on the radical nitriding conditions. The surface states were changed rough by higher applied voltage. Vickers hardness of the substrate after nitriding was depended on the conditions. Effects of the H_2 etching conditions were smaller than the radical nitriding conditions. As a result of estimation on the tribological properties, the harder specimens showed lower friction coefficient.

As a result of surface modification of cast iron substrates using radical nitriding, improvements of mechanical properties were recognized by treating at appropriate conditions.

EP-24 Mechanical and Tribological Properties of Duplex Stainless Steels Submitted to P13 Nitriding at Low Temperatures, C.E. Foerster (*carlosof@uepg.br*), Universidade Estadual de Ponta Grossa, Brazil, C. Lepiński, S. Blunk, A.M.C. Oliveira, Universidade Federal do Paraná, Brazil, A. Kolitsch, Institute of Ion Beam Physics and Material Research, Germany

Duplex Stainless Steels (DSSs) that are formed by a approximately equal content of ferritic and austenitic phases are employed in the petrochemical industry. In the present work we submitted SAF2101 and SAF2205 to ion nitriding process by plasma immersion ion implantation (PI3) at 300 °C and 380 °C during 1h and 4h. Nitriding at surfaces in longitudinal and

transversal directions to austenitic and ferritic grains orientation were compared. X-ray diffraction allowed identifying the surface microstructure after the nitriding. Nitriding at 300°C promotes only N in solid solution (expanded austenite and ferrite). Treatments at 380°C form iron nitrides at different stoichiometries in addition to N in solid solution. The thickness of N modified layers varies from 1 to 8 µm depending working P13 parameters. Mechanical properties were investigated by instrumented indentation at nanoscale, following the Oliver and Pharr method. Tribological behaviour was investigated by reciprocating sliding process at severe dry condition using WC(Co) and SiC balls as counter bodies. Nanoscratch tests were employed to investigate the surface brittle response under increasing loadings employing pyramidal stylus. The hardness at shallow depths is about 15 GPa and decreases to the bulk value (3-3.5 GPa) for both duplex steels. The highest hardness values are not modified at the surface by increasing the nitriding time as observed at shallow depths by nanoindentation tests. In addition, nitriding at surfaces oriented longitudinally to grains orientation or transversally to them did not cause modification in hardness measured profiles. The behaviors after nanoscratch tests for the steels nitrided at 300°C are compared to pristine surface to evaluate the effect of occurrence of plastic deformation and/or fractures on grain boundaries on austenitic and ferritic phases. The results of conventional tribological tests for the both steels were compared considering the nitriding conditions (300°C and 380°C). Even in the presence of thin N modified layers, as in the case of nitriding at 300°C by 1h, the wear resistance can improve by 10 times in respect to untreated sample. The effect of grain orientation in respect to nitriding and wear sliding test is discussed.

EP-26 Characterisation of TiCN and TiCN/ZrN Coatings for Cutting Tool Application. *P.C. Siow (pcsiow@eng.ukm.my), J. Abdul Ghani, M.J. Ghazali*, Universiti Kebangsaan, Malaysia, *T. Ria Jaafar*, Advanced Materials Research Centre SIRIM Berhad, Malaysia, *C.H. Che Haron*, Universiti Kebangsaan, Malaysia

It is well known that coating deposited on a cutting tool can improve the wear resistance of the tool, and hence prolongs the tool life. The performance of a coating is strongly depends on its mechanical and chemical properties. In machining process, the type of chosen coating depends on the cutting condition, due to properties of the applied coating material. In addition, there are also many factors that influence the performance of a coating, such as the coating thickness, the composition ratio, the sequences of layer in a multilayer coatings and the deposition method. In this paper, the properties of TiCN and TiCN/ZrN were characterised by using thermal shock and wear tests. The substrate material made from carbide-based cutting tool was also developed in house. From the characterisation analysis, it was found that the performance of TiCN and TiCN/ZrN coatings were comparable, and in some cases better than the commercial TiN coated carbide cutting tool.

EP-27 Quantification of tool coating effects on surface finish while dry cutting of glass/epoxy composite. *A. Ben-Soussia, A. Mkaddem (ali.mkaddem@enscm.fr), M. El Mansori, A. Meena*, Arts et Métiers ParisTech, France

This work aims to investigate the effects of coating type on the cutting induced damage and surface integrity when dry machining glass/epoxy composites at intermediate fibers' orientations. The wear rate mechanisms and the material removal process affecting the surface finish were analyzed on both the uncoated tungsten carbide (WC) insert and CVD and PCD multi-layers (ML) coated inserts using the Atomic Force Microscope (AFM). The developed cutting forces and the generated mechanisms of chip formation were also investigated and correlated with the AFM measurements. The experimental findings showed good performance of coating layers to alter tool wear with comparison to PCD tool. It was found also that the improved adhesive properties of coating layers of carbide coated tool are capable to dissipate the sequential shock due to alternation of phases within the material. The aspect of cut surface of fiber was also discussed in details in order to explain the effects of fiber orientation on accelerating the tool damage.

Keywords: Dry cutting; Glass/epoxy; ML Coatings; Wear; AFM.

New Horizons in Coatings and Thin Films Room: Golden Ballroom - Session FP

Symposium F Poster Session

FP-1 Pseudocapacitive Performance of Vertical Copper Oxide Nanoflakes. *Z. Endut (rg253c@yahoo.com), M.H. Abd Shukor*, Center of Advanced Manufacturing and Material Processing, Malaysia, *W.J. Basirun*, University of Malaya, Malaysia

Vertical copper oxide nanoflakes have been formed by oxidation in alkaline solutions. Their structural and surface morphology were characterized using X-ray diffraction (XRD) and field emission scanning electron microscopy (FE-SEM) while its pseudocapacitive properties were investigated using cyclic voltammetry, charge-discharge testing and electrochemical impedance spectroscopy. The structural and surface morphological studies showed the grown copper oxide nanoflakes is amorphous and vertically grown with high lateral aspect ratio. Electrochemical study exhibited significant specific capacitance and good cycling activity in 1.0 M KOH electrolytes making vertical copper oxide nanoflakes as a promising candidate in supercapacitor electrode application.

FP-2 Structural and Optical Properties of CdO Nanostructures Prepared by Atmospheric-pressure CVD. *T. Terasako (terasako.tomoaki.mz@ehime-u.ac.jp), T. Fujiwara*, Graduate School of Science and Engineering, Ehime University, Japan, *Y. Nakata, M. Yagi*, Kagawa National College of Technology, Japan, *S. Shirakata*, Graduate School of Science and Engineering, Ehime University, Japan

Cadmium oxide (CdO) with a cubic structure is an n-type semiconductor and shows a wide direct band gap of ~2.6 eV and a narrow indirect band gap of ~0.5 eV. Recently, CdO has attracted much attention because of its technological applications such as photodetectors, solar cells, gas sensors and nonlinear optics.

Chemical vapor deposition (CVD) methods utilizing the vapor-liquid-solid (VLS) mechanism are favorable for position- and size-controlled growth of nanostructures. In this paper, shape controllability and optical properties of CdO nanostructures grown by atmospheric-pressure CVD methods using Cd and H₂O as source materials and Au nanocolloids as a catalyst will be discussed in terms of substrate temperature, source supply ratio and growth time.

The catalytic solution of Au nanocolloids diluted with ethanol was coated on the *c*-plane Al₂O₃ substrates by the spin-coating technique (1500 rpm, 5 sec). Substrate temperature (*T_s*) was varied in the range from 825 to 975 °C. Source temperature of Cd (*T_{Cd}*) was kept at 500 °C. The vaporizer containing H₂O (*T_{H2O}*) was kept at 54 °C. The nitrogen carrier gas flow rates for Cd and H₂O (*F_{Cd}* and *F_{H2O}*) were changed in the range from 10 to 60 sccm.

Various shapes of nanostructures, such as nanorods (NRs), nanotrees (NTs) and nanobelts (NBs), were successfully grown. Especially, it was found that the shapes of the NRs change from the cylinders to the cones with increasing *T_s*, so-called "tapering". In general, two different types of growth mechanisms are in progress simultaneously during the CVD process; one is the axial growth due to the VLS mechanism through the catalyst and the other is the radial growth due to the film growth mechanism on the NR's side wall (VS growth). The tapering behavior is probably due to the rapid increase in radial growth rate with increasing *T_s*. Moreover, the appearances of Y- and T-shape NTs and their 3D network structures suggest that the catalytic particles split and migrate during the growth process. We believe that the simultaneous work of the VS and VLS mechanisms together with the splitting and migration of catalytic particles is the driving force of the morphological variety of nanostructures.

Photoacoustic measurements revealed that the absorption edge shifts towards lower energies and the absorption band below the absorption edge becomes larger with increasing *T_s*. This tendency is probably related to the increase in intrinsic defects introduced by the deviation from stoichiometric composition. Therefore, we must pay attention to the fact that the change in growth condition affects not only the structural shapes of the nanostructures but also their optical properties.

FP-3 Substrate texturing effect on the microstructural and electrochemical performance of the rf sputtered LiCoO₂ film cathodes. *J. Kumar, J. Babu*, Sri Venkateswara University, Thin Films Laboratory, India, *C. V. University of Texas at El Paso, US, O.M. Hussain (hussainsvu@gmail.com)*, Sri Venkateswara University, Thin Films Laboratory, India

LiCoO₂ in thin film form is identified as one of the best cathode materials by its high energy density, long cycle life and high capacity retention. Investigations are aimed to enhance the electrochemical performance of the

as-grown films using textured Si as a base substrates and compared the results with the films grown on polished Si substrate. Thin films of LiCoO_2 were prepared by rf magnetron sputtering technique on Au/Ti/SiO_2 /(polished)Si and Au/Ti/SiO_2 /(textured)Si maintained at a substrate temperature 300°C . Comprehensive investigation was performed on the growth, microstructure and electrochemical properties of thick LiCoO_2 films deposited at various reactive gas composition and rf powers. The as-grown LiCoO_2 films on polished Si metalized substrate at low O_2 to Ar gas composition ratio of 1:9 and rf power 150 W exhibited predominant (0 0 3) orientation representing partially ordered HT- LiCoO_2 structure with R3m crystalline space group. The average surface area fraction observed from SEM analysis is observed to be 4.1 %. The films exhibited first ordered phase transition during intercalation/de-intercalation reaction and demonstrated a discharge capacity of $53 \mu\text{Ahcm}^{-2} \mu\text{m}^{-1}$ with a higher capacity fading rate of 0.26 %. Where as, the films deposited on Au/Ti/SiO_2 /(textured)Si substrates represented predominant (0 0 3) orientation with relatively enhanced surface area fraction of 16.7 %. The surface of the film observed from SEM contains pyramidal shaped clusters composed of grains with an average size of 210 nm. These films exhibits improved electrochemical performance in terms of discharge capacity ($57.5 \mu\text{Ahcm}^{-2} \mu\text{m}^{-1}$), capacity retention (95.4% per 50 cycles) and lower capacity fade rate (0.07 % per cycle) which is demonstrated by the substrate texturing influence.

FP-4 The Grain Evaluation and Electrochemical properties of RF sputtered LiMn_2O_4 thin films., J. Babu, J. Kumar, O. Mahammad (*hussainsvu@gmail.com*), Sri Venkateswara University, Thin Films Laboratory, India, V. Ramana, University of Texas at El Paso, US
Abstract:

Lithium transition metal oxides have received a considerable attention in recent years as high voltage positive electrode materials in the fabrication of all solid state microbatteries. Among various lithium based cathode materials, LiMn_2O_4 is one of the most promising cathode material as it offers high energy density, high cell voltage, low cost, and low toxicity over the other electrode materials. In the present investigation, thin films of LiMn_2O_4 were prepared by radio frequency magnetron sputtering on gold coated silicon substrates in an Oxygen to Argon ratio of 1:6 and an oxygen partial pressure of 2×10^{-2} mbar. The films were deposited from different substrate temperatures ranging from 400 K – 700 K and RF power was varied from 50-125 W. The influence of substrate temperatures and RF power on growth, microstructure and electrochemical properties was studied. The XRD and SEM results revealed that with the increase of substrate temperature the film structure changed from amorphous to polycrystalline. The films deposited at $T_s = 673$ K with RF power 80 W exhibited predominantly (111) orientation representing cubic spinel structure of $\text{Fd}3\text{m}$ symmetry with an average grain size and lattice parameter of 275 nm and 8.23 \AA . Further increase in crystallinity and electrochemical performance was observed by annealing these films at 700°C . The films annealed at 973 K exhibited better electrochemical performance with initial discharge capacity of $53.5 \mu\text{Ah cm}^{-2} \mu\text{m}^{-1}$ in the aqueous media suggesting that the film can be used as binder free cathode in Li-ion battery application.

FP-5 Electrochemical Properties of V_2O_5 Thin Films Grown on Flexible Substrates using Plasma Assisted Activated Reactive Evaporation. K. Hari Krishna, University of Calabria, Italy, O.M. Hussain (*hussainsvu@gmail.com*), Sri Venkateswara University, India
Vanadium Pentoxide (V_2O_5) thin films have been deposited using home built plasma assisted activated reactive (ARE) evaporation on ITO coated flexible Kapton substrates and investigated their microstructural and electrochemical properties. X-ray diffraction pattern displayed predominant (001) orientation by designating the Orthorhombic structure of the films deposited at optimized growth conditions. The surface of the films is observed to be composed of vertical elliptically shaped nanosized grains of size 98 nm provided with an estimated rms roughness of 9 nm as evidenced from AFM studies. At room temperature, the as-deposited V_2O_5 films demonstrated a discharge capacity of $60 \mu\text{Ah}(\text{cm}^2 - \mu\text{m})$ for 10 cycles in the potential window of 4.0 V - 2.5 V. The influence of silver (Ag) inter-layer on electrochemical properties of V_2O_5 films is investigated and observed appreciable increment electrochemical performance of multi-layered ' $\text{V}_2\text{O}_5/\text{Ag}/\text{V}_2\text{O}_5$ ' films. The multi-layered ' $\text{V}_2\text{O}_5/\text{Ag}/\text{V}_2\text{O}_5$ ' films demonstrated a discharge capacity of $75 \mu\text{Ah}(\text{cm}^2 - \mu\text{m})$ provided with enhanced cyclicability.

FP-6 Bismuth thin films deposited by DC Magnetron Sputtering for electrochemical analysis electrodes. S.E. Rodil, P. Silva-Bermudez (*suriel21@yahoo.com*), J. Baron, O. Garcia-Zarco, Instituto de Investigaciones en Materiales, Universidad Nacional Autónoma de Mexico, México

In the last ten years, Bismuth-film electrodes (BiFEs), prepared by coating a suitable substrate with a metallic Bi thin film, have proved valuable tools for electroanalysis in the reductive potential regime, especially for anodic and adsorptive stripping analysis. They have been proposed as a green alternative to substitute Hg film electrodes.

In order to evaluate the physicochemical properties and the electrochemical behavior of Bi films produced by DC magnetron sputtering and to assess their feasibility to be used as BiFEs for detection of heavy metal traces in water, in the present work Bi films were deposited by DC magnetron sputtering onto glass substrates using a high purity Bi target (99.9 at. %, 4" in diameter), a working pressure of 4 Pa (Ar atmosphere), a current density of 0.2 A and deposition times of 5, 10 and 15 minutes.

The structural properties of the films were characterized by X-ray Diffraction, X-ray Photoelectron Spectroscopy and Raman Spectroscopy. The thickness, roughness and dielectric constant of the films were also characterized. The structure of the deposited films was basically the Bi-rhombohedral phase with a preferred orientation (012) & (104). The films were polycrystalline and have large deposition rates.

For the electrochemical tests of the films, a 1 cm^2 area was exposed to buffer solutions. First, the potential window of the films at which the electrode might be useful and their stability upon potentiostatic extreme conditions were characterized in buffer solutions of pHs 4.6, 7 and 10, in an electrochemical cell with a saturated calomel reference electrode and a Pt wire as the counter electrode. No strong variations in the potential windows with deposition time (film thickness) were observed. The oxidation potential became more negative as the pH increased, from -0.3 to -0.5 V. The potential windows were about 1 V for all the films in the 3 different pHs.

After determination of the potential window an electrochemical impedance spectroscopy test was performed; the spectra were very similar for the 3 pH values and the different film thickness, probably indicating similar interfacial effects. Then, the samples were subjected to a cyclic potential from -1.5 to 1.5 V; the films could support these extreme conditions without undergoing delamination. Finally, the performance of the films as BiFEs was evaluated by anodic adsorptive stripping analysis in water solutions containing either, Cu or Sn traces.

Acknowledgements to funding from the European Community Seven Framework Programme (FP7-NMP-2010-EU-MEXICO) and CONACyT under grant agreements n° 263878 and 125141; and to the ICyTDF postdoctoral fellowship for P. S-B

FP-7 SnO_2 -cored heteronanowires sheathed with metal shells and their application to gas sensors. H.W. Kim (*hyounwoo@hanyang.ac.kr*), Hanyang University, Republic of Korea

The current trend towards downsized integrated electronic and optical devices has strongly motivated the intensive study of various one-dimensional (1D) nanostructures. In particular, one attempt has been made to create coaxial 1D structures with a core/sheath geometry, which may assist in the realization of various tailor-made functions by assembling the different features of both nanowires (as cores) and nanotubes (as sheaths) with different chemical compositions in the radial direction. Indeed, the great potential has recently been demonstrated in nanodevice applications such as coaxial-gated transistors and laser diodes. SnO_2 is a well-studied functional material that has been extensively used in dye-based solar cells, transparent conducting electrodes, and gas sensors.

Pre-grown SnO_2 1D nanostructures are coated via a DC sputtering technique using a metal target. By carrying out the subsequent thermal annealing, we have generated the metal nanoparticles on the core nanowires. Metallic catalysts are known to functionalize the surface of nanomaterials. For example, noble metals anchored on semiconducting oxides facilitate the dissociation of oxygen molecules into oxygen species, including atomic oxygen, thereby enhancing the oxygen sensitivity. Accordingly, some research groups have attempted to functionalize the surface of oxide nanowires with nanosized noble metals using various methods. In the present work, we have investigated the effect of metal nanoparticles on the gas sensor properties of nanowires.

FP-8 Enhancement of electron-emission and long-term stability in tip-type carbon nanotube field emitters by lithium coating. J.S. Park, B.J. Kim, J.P. Kim, J.S. Park (*jinsp@hanyang.ac.kr*), Hanyang University, Republic of Korea

Recently, carbon nanotubes (CNTs) have been researched to develop a high resolution x-ray image system for medical applications such as early

diagnosis of cancers, using the superior properties of CNTs such as chemical stability, thermal conductivity, mechanical strength, and structural aspect ratio. For use of CNT-emitters as electron source for x-ray generation, a large number of investigations have been focused on how to enhance the emission current level and to reduce the turn-on field for electron-emission. Especially, to obtain high-resolution x-ray images, the diameter of the beam incident area must be tens of micrometers or less when the electron beam emitted from the CNT cold cathode collides against the x-ray generation target. For this purpose, some researchers have recently developed CNT emitters by growing them on very sharp tip-type substrate. In these tip-type CNT emitters, however, the long-term emission stability should be ensured due to a relatively low bonding force between the CNT and the substrate. In order to achieve desirable performances in emission current and stability, coating of CNTs with various materials, such as metal carbides like titanium carbide (TiC), metal nitrides like boron nitrides (BN), and metal oxides including magnesium oxide (MgO), have been studied.

In this work, the effects of coating of lithium (Li) thin layers with various thicknesses have been investigated for the purpose of enhancing the electron-emission current and the long-term stability of CNT-emitters. The CNTs were grown on metal-tip (tungsten, approximately 500 nm in diameter at the summit part) substrates via electrophoretic deposition (EPD). The Li layers were coated on CNTs using an electroplating method. The morphologies, microstructures, and chemical compositions of the Li-coated CNTs were analyzed as a function of the thickness of the Li layer. For all the fabricated Li-coated CNT-emitters, the electron-emission characteristic and the long-term (up to 20 h) stability of the emission current were measured, which were also compared with those of the conventional non-coated CNT-emitter. The experimental results showed that the electron-emission capacity was noticeably enhanced by coating Li layers on the surface of CNTs. This was attributed to the fact that the effective work function of CNTs was reduced by Li coating. It was also observed that the Li-coated CNT-emitters exhibited a more stable electron-emission characteristic than that of the non-coated one.

FP-9 Electron emission properties of carbon nanotubes grown on polymer substrates with high absorbency, B.J. Kim, H.B. Chang, J.S. Park (jinsp@hanyang.ac.kr), Hanyang University, Republic of Korea

Carbon nanotubes (CNTs) have much attraction for high-current density applications because of their superior properties, such as chemical stability, thermal conductivity, mechanical strength, and structural aspect ratio. Among the many promising applications of CNTs, the electron emitted source of cold cathode for miniature x-ray system is that which can be most immediately realized because CNT-based cold cathodes could overcome many problems with conventional thermionic cathodes, such as limited temporal resolution, a short lifetime, a high operating cost, and restricted miniaturization. Currently, in order to use CNTs as electron sources, many investigations have been focused on how to enhance the emission current level and to reduce the turn-on field for electron-emission. The CNT-based field emitters have been fabricated either by direct growth methods like chemical vapour deposition (CVD) or by indirect printing methods, with various types of substrates such as pin-type or flat type. In general, the pin-type substrates have some advantages for obtaining high resolution of emitted electron beams, but they are hard to meet the current level required for x-ray generation. On the other hand, the flat-type substrates may produce sufficient currents, but they have poor adhesion between the CNTs and the substrates due to the weak van der Waals force.

In this study, we present a novel method for fabricating CNT-based field emitters with high emission current level by using flat-type polymer substrates (such as cellulose and polyester) with high absorbency. The CNTs were grown using a dip-coating method by dipping the substrates in the CNT suspension. The CNTs attached on the substrates formed covalent and hydrogen bonds with the polymer surface that has hydrophilic groups (i.e., OH) after acid purification of CNTs. The morphologies and microstructures of polymer substrates and CNTs were monitored via field-emission scanning electron microscopy (FESEM) and high-resolution transmission microscopy (HRTEM). Fourier transform infrared spectroscopy (FTIR) was used to identify the covalent and hydrogen bonds between CNTs and substrates. These analyses indicated that the polymer substrate was chemically combined with a large number of CNTs with a strong adhesion. The electron emission properties of the fabricated CNT emitters were also measured at a pressure of below 10^{-5} Pa, with a distance of 1 mm between the cathode (CNTs) and the anode. The results showed that the CNT emitters fabricated with the polymer substrates produced more than 1 mA at 1 V/ μm of applied field.

FP-10 Structure and Electronic Properties of Sputter-Deposited LiFePO₄ Thin Films, V. Ramana (rvchintalapalle@utep.edu), M. Mares, G. Baghmar, University of Texas at El Paso, US

The successful commercialization of lithium ion batteries for electronics, automobiles, and technology has led to many research groups to invest

considerable amount of money in this battery technology that utilizes LiCoO₂, LiNiO₂, and LiMnO₂ cathodes. However, lower cost cathode materials are required for various applications. In addition, these materials limit the applications to small batteries due to the high cost, toxicity, and environmental harmful of the materials. LiFePO₄ has received significant attention and commercialized as a cathode for Li-ion batteries. The exceptional stability of LiFePO₄ at elevated temperatures enables safe, large lithium ion batteries for large scale applications such as electric vehicles or space applications. The present work was performed to understand the effect of temperature, an important thermodynamic variable, on the microstructure and electronic properties of LiFePO₄ films fabricated by radio-frequency (RF) magnetron sputtering. LiFePO₄ films were grown under varying deposition temperatures in the range of 25 to 400 °C. In addition, LiFePO₄ films were annealed in temperature ranges of 400 to 800 °C for 1 and 2 hours. The effect of growth temperature on the crystal structure, surface morphology, chemical quality and electronic properties is investigated in detail. Characterizations of the films were performed using X-ray diffraction (XRD), high resolution scanning electron microscopy (HRSEM), energy dispersive X-ray spectrometry (EDS), optical spectrophotometer, and electrical resistivity measurements. The grain size increased as the annealing temperature increased from 400 to 800 °C. The optical properties of the LiFePO₄ films indicate that, as the growth temperature is increased, the transmittance of the films increases. The band gap increases from 2.75 eV to 3.28 eV with increasing temperature from RT- 400 °C. When the films were annealing at 1 hour from 400-800 °C, the band gap increased from 3.12 eV to 3.7 eV. Annealing for 2 hours at temperatures from 400 to 800 °C showed an increase in band gap 3.12 eV to 3.75 eV showing the maximum value at 600 °C. The electrical conductivity indicates that with an increase in substrate temperature, the resistivity of the films also increases. The results will be presented and discussed.

FP-11 Development of thin film cathodes for lithium-ion batteries in the materials system Li-Mn-O by r.f. magnetron sputtering, J. Fischer (Julian.Fischer@kit.edu), C. Ziebert, C. Adelhelm, J. Ye, M. Rinke, J. Desaiques, M. Stüber, S. Ulrich, H. Seifert, Kit, Iam-Awp, Germany

In the last years there has been an increasing interest in electrical energy storage. The requirements of the industry are clear and unambiguous: the storage solutions should be powerful, compact and save. All these properties can be achieved with thin film lithium ion technology. The research on cathode materials plays a key role because the performance of a lithium ion cell is mostly limited by its cathode. Today the most commercially available lithium ion batteries are still based on the toxic and expensive LiCoO₂ as standard cathode material. Cheaper and environmentally friendlier are lithium manganese based cathode materials.

In this work LiMn₂O₄ spinel and orthorhombic LiMnO₂ thin films have been prepared by non-reactive r.f. magnetron sputtering from commercial ceramic LiMn₂O₄ and LiMnO₂-targets in a pure argon discharge. The deposition parameters target power and working gas pressure were optimized in combination with a post deposition furnace annealing with respect to microstructure and electrochemical behavior. The chemical composition was determined using inductive coupled plasma optical emission spectroscopy (ICP-OES) and inert gas fusion analysis (IGFA) and the results were compared with laser ablation mass spectroscopy (LA-MS) and high frequency glow discharge optical emission spectroscopy (HF-GDOES). The films crystal structure, phase evolution and microstructure were investigated by X-ray techniques, micro Raman spectroscopy and scanning electron microscope (SEM). Due to the fact that these thin films consist of the pure active material without impurities like binders or conductive additives like carbon black, they are particularly well suited for measurements of the pure intrinsic physical properties.

The electrochemical behavior of these films was investigated by galvanostatic methods in lithium half cells with a standard EC:DMC (1:1) liquid electrolyte containing 1 mol LiPF₆. Both the influence of the charging and discharging currents and of the voltage window was investigated. To get a deeper insight into the electrochemical reactions cyclic voltammetry was carried out. Finally both materials will be compared and some ideas for structural improvements will be given.

FP-12 The resistive switching characteristics in TaON films for nonvolatile memory applications, M.C. Chen (iro926@gmail.com), T.C. Chang, National Sun Yat-Sen University, Taiwan, Y.C. Chiu, National Chiao Tung University, Taiwan, S.C. Chen, National Tsing Hua University, Taiwan, S.Y. Huang, National Sun Yat-Sen University, Taiwan, S. Sze, National Chiao Tung University, Taiwan, F.S. Yeh(Huang), National Tsing Hua University, Taiwan, M.J. Tsai, Indian Institute of Science Bangalore, India

In this study, the bipolar resistive switching characteristics of the resistive random access memory (RRAM) device based on sputter-deposited TaON thin film was investigated. The resistive switching behavior of the Pt/TaON/TiN structure can be traced by dc voltage and pulse voltage. The

proposed memory device exhibits excellent resistance switching with a high resistance state/ low resistance state ratio of 2.5 order, write/erase endurance of about 2 order, and long retention time of 10^4 s at 85 °C. In addition, the device was investigated to achieve multilevel operation, which could increase storage density for next generation memory application. It was also found that the polarity of the forming process would not influence the resistive switching characteristic but influence the first reset process behavior. The switching behavior could be regarded as the oxygen redox near the TiN interface. However, the first reset behavior of negative forming process was related with the oxygen concentration gradients near the Pt electrode and the Joule heating enhanced oxidation.

FP-13 Switching mechanism transition induced by annealing treatment in ZnO/Ru/ZnO resistive memory, *L.C. Chang* (*lcchang@mail.mcut.edu.tw*), *Y.H. Wei*, Ming Chi University of Technology, Taiwan, *K.H. Liu*, Chang Gung University, Taiwan

ZnO/Ru/ZnO trilayer films sandwiched between Ru electrodes were prepared for nonvolatile resistive memory applications. These structures show resistance switching under electrical bias both before and after a rapid thermal annealing treatment, while it is found that the resistive switching effects in the two cases exhibit distinct characteristics. The ZnO devices after RTA treatment demonstrates remarkable device parameter improvements including lower threshold voltages and lower write current. Furthermore, the RTA treatment has triggered a switching mechanism transition from a carrier trapping/de-trapping type to an electrochemical-redox-reaction-controlled conductive filament formation/rupture process, as indicated by different features in current-voltage characteristics.

FP-14 Bismuth Oxide thin films grown by RF reactive magnetron sputtering, *P. Lunca Popa*, *P. Eklund* (*perek@ifm.liu.se*), Linköping University, Sweden

Bismuth oxide has five known crystalline phases: alpha, beta, gamma, delta and omega, each with its distinct properties and stability domains. The delta phase exhibits ionic conductivity 1-2 orders of magnitude higher than yttria-stabilized zirconia, the compound widely used in solid oxide fuel cells. In bulk, the delta-Bi₂O₃ phase is not stable at room temperature but from 750 C to 825 C, the melting point of bismuth oxide. Outside this temperature range, other phases are stable but their conductivities are up to three orders of magnitude lower than that of the delta phase. The stability of the delta phase stability can be extended to lower temperatures by doping, but this process yields a severe reduction in ionic conductivity.

In the present work, we have synthesized Bi₂O₃ films by RF reactive magnetron sputtering using a Bismuth target in an Ar/O₂ gas discharge. We investigate how the structure of the films is influenced by substrate temperature, source power, and oxygen flow rate/total gas flow rate ratio. As expected, the substrate temperature influences the initial nucleation process and growth kinetics. Deposition at ambient temperature yields mainly amorphous films while higher temperature yields crystalline films. Different stoichiometric compositions can be obtained by varying the source power and the oxygen flow ratio. By tuning all these parameters we obtain Bi₂O₃ with cubic structure, with thickness of hundreds of nanometers. XRD shows crystalline films with peaks around 27 and 55 two theta degrees corresponding to (111) and (222) planes for cubic structure. Pole figures XRD analysis was also performed for those peaks and diffractions rings were observed near phi angle of 70 degree which corresponds to the angle between (1 1 1) and (1 1 -1) planes in a cubic structure, consistent with the delta phase. SEM showed a columnar structure of our films with very good uniformity of the films. Electrical and optical measurements have also been performed; ellipsometry yields a value of the band gap around 2.5eV while for optical constants values of $n \approx 2.5$ and $k \approx 0.5$ are obtained for UV-Vis wavelength interval.

FP-15 Electromechanical reliability of ITO-coated polymer substrates after exposure to acrylic acid, *K. Burrows*, University of Birmingham, UK, *A. Hoover*, *D. Cairns*, *K. Sierrros*, West Virginia University, US, *S. Kukureka* (*s.n.kukureka@bham.ac.uk*), University of Birmingham, UK

This paper considers the electromechanical reliability of ITO-coated polymer substrates, for use in flexible display applications, after exposure to acrylic acid (a common constituent of display structures). Due to the mechanical mismatch of properties between the organic polymer substrate and the inorganic transparent conducting oxide, it is important to investigate the electro-mechanical response to a number of stresses commonly seen in general use.

Three films of varying ITO thicknesses were examined: sheet resistance and optical transmission were monitored and tensile testing performed before and after exposure to acrylic acid. Also the tribological properties of the coated films were examined under a specially-modified fretting rig.

It appears that even low concentrations of acrylic acid that would often go unnoticed, may cause failure to occur more readily. In both tensile testing

and the monotonic bending test where the film is subjected to tension, high concentrations of acrylic acid would normally be a cause of failure. Nevertheless, even low concentrations such as 0.1M can also cause the critical onset strain to occur more readily due to stress-corrosion cracking. However when the films are subjected to stresses in compression, the exposure to acrylic acid shows little or no effect.

FP-16 Observation of amorphous to crystalline phase transformation in Te substituted Sn-Sb-Se chalcogenide thin films for memory applications, *R. Chander* (*rcohri@yahoo.com*), *R. Thangaraj*, GNDU, India

Thin films of Sn Sb Se Te ($x = 10, 12, 14$) chalcogenide system were prepared by thermal evaporation technique using melt quenched bulk samples. The as-prepared thin films were found amorphous as evidenced from X-ray diffraction studies. Resistivity measurement showed an exponential decrease with temperature upto critical temperature (transition temperature) beyond which a sharp decrease was observed and with further increase in temperature showed an exponential decrease in resistivity with different activation energy. The transition temperature showed a decreasing trend with tellurium content in the sample. The resistivity measurement during cooling run showed no abrupt change in resistivity. The resistivity measurements of annealed films did not show any abrupt change revealing the structural transformation occurring in the material. The transition width showed an increase with tellurium content in the sample. The resistivity ratio showed two order of magnitude improvements for sample with higher tellurium content. The observed transition temperature in this system was found quite less than already commercialized Ge Sb Te system for optical and electronic memories.

FP-17 Investigating the degradation behavior under Hot Carrier Stress for InGaZnO TFT with symmetric and asymmetric structure, *M.Y. Tsai* (*baxiatwice@yahoo.com.tw*), NSYSU, Taiwan

This letter studies the hot-carrier effect in indium-gallium-zinc oxide (IGZO) thin film transistors with symmetric and asymmetric source/drain structures. The different degradation behaviors after hot carrier stress in symmetric and asymmetric source/drain device indicate that different mechanisms dominate the degradation. Since the C-V measurement is highly sensitive to the trap state compared with the I-V characteristics, thus, the C-V curves are utilized to analyze the hot carrier stress induced trap state generation. Furthermore, the asymmetric C-V measurements (gate-to-drain capacitance, gate-to-source capacitance) are useful to analyze the trap state location. For asymmetric device structure, different source/drain structure under hot carrier stress will induce asymmetric electrical field and cause different degradation behaviors. In this work, the on-current and subthreshold swing (S.S) degrade under low electrical field, whereas the apparent V_t shift occurs under large electrical field. The different degradation behavior indicates that the trap state generates under low electrical field and channel-hot-electron (CHE) effect occurs under large electrical field.

FP-18 Investigating the Drain Bias stress of InGaZnO TFTs under Dark and Light Illumination for AMOLED application, *S.Y. Huang* (*aramis88888@gmail.com*), *T.C. Chang*, *L.W. Lin*, *M.C. Yang*, National Sun Yat-Sen University, Taiwan, *K.H. Yang*, University of Toronto, Canada, *M.H. Wu*, *M.C. Chen*, National Sun Yat-Sen University, Taiwan, *F.Y. Jian*, National Tsing Hua University, Taiwan

The degradation mechanism of the drain bias stress for a-IGZO TFT under dark and light illumination are investigated in this paper. The current crowding effect, on current decreased of current-voltage, and a stretch-out of capacitance-voltage indicate that an additional barrier increased near the drain region by the oxygen molecules adsorbed model after the drain-bias stress under the dark (DBS). This result induces the carrier transport is impeded from source terminal to drain terminal. In addition, the recovery characteristics show that all degradation behaviors significant disappear, which can be regarded as the O₂ desorption from the active back channel. However, the unusual stretch-out phenomenon for the subthreshold capacitance after the drain bias stress under light illumination (DBIS) can not recover to the initial in the dark. This is attributed to the additional fix charge generated near the drain region by the photo-leakage current. Furthermore, an obvious negative threshold voltage shift after the DBIS indicates the charge trapping mechanism simultaneously occurred. Finally, this work also employs the gate and source floating conditions during the DBIS to further clarify the mechanism of degradation behaviors.

FP-19 Properties of Ge · SiC nanodots / SiC stacked structure, Y. Anezaki, T. Ootani, Nagaoka University of Technology, Japan, K. Satou, Department of Electrical, Electronic and Information Engineering, Japan, T. Kato, Nagaoka University of Technology, Japan, A. Kato, Department of Electrical, Electronic and Information Engineering, Japan, K. Yasui (kyasui@vos.nagaokaut.ac.jp), Nagaoka University of Technology, Japan

Semiconductor quantum dots can confine the carriers such as electrons and holes in three-dimensional directions and exhibit unique electronic and optical properties. For highly efficient IR light-emitting devices using germanium (Ge) dots, the Ge dots with high density and small size less than 10nm in diameter is required. As regards the density of dots, it has been reported that a density of $2 \times 10^{11} \text{ cm}^{-2}$ was achieved by the pregrowth of submonolayer carbon.¹⁾ In this case, carbon atoms were incorporated into a Si(001) substrate and surface strain was induced, leading to the formation of a Si(001) c(4x4) reconstruction structure at the surface layer, which changed the Ge growth mode from the Stranski-Krastanov (SK) mode to the Volmer-Weber (VW) mode, leading to high-density dot formation. As a strong repulsive interaction can operate between Ge and C, Ge atoms deposited on the SiC layer do not interdiffuse. The c(4x4) surface was expected as a template substrate for the formation of high-density Ge nanodots. In our previous study, it was found that the c(4x4) structure was formed by the reaction of monomethylgermane (MMGe) on Si(001) 2x1 surface. The Ge nanodots embedded in SiC structure is expected to strongly confine the carriers due to the difference in the band-gap between Ge and SiC. As a result of the experiment of the Ge nanodot formation using MMGe, SiC and Ge nanodots were formed after the appearance of the c(4x4) reconstructed surface. Using a pulse-controlled nucleation method, the formation of high-density ($1.3 \times 10^{11} \text{ cm}^{-2}$) and small size dots (6 nm) with small standard deviation (1 nm) was achieved.

In this study, surface structure of Ge and SiC nanodots fabricated using MMGe were investigated by reflection high-energy electron diffraction (RHEED) and scanning tunneling microscopy (STM). PL spectra of the Ge nanodots capped with SiC layer were also measured at a low temperature. The PL spectra obtained were deconvoluted into some components to consider the origin of each emission. The PL peaks around 1.01 eV and 1.07 eV, which are considered to be originated from the Ge nanodots, were observed. Eberl et al. have observed PL peak around 0.99 eV and 1.04 eV from Ge nanodots generated by a solid source molecular beam epitaxy (MBE) method. Blue shifts of the emission peaks observed in our sample were considered to be due to the difference in the chemical composition compared to that of the Ge dots formed by the solid source MBE or residual stress of nanodots.

Reference

1) M. Stoffel, L. Simon, J. L. Bischoff, D. Aubel, L. Kubler, and G. Castelein: Thin Solid Films **380** (2000) 32.

FP-20 Oxygen-Graded TiO_x ($x=1.5-1.9$) Produced by High Power Impulse Magnetron Sputtering and Its Thin Film Solar Cell Application, Y.H. Chen (tieamo2002@gmail.com), W.C. Yan, M.C. Lai, J.L. He, Feng Chia University, Taiwan

Thin film solar cells are currently demanded to be flexible with acceptable photovoltaic (PV) efficiency. Among a variety of PV materials, titanium-based oxide with low material cost, non-toxicity and most important, low crystal growth temperature, seemed to be a good candidate for PV material on flexible substrate. Strategies in this study is to produce oxygen-graded TiO_x ($x=1.5-1.9$) ($E_g=1.8 - 2.7 \text{ eV}$) layer as the absorption layer followed by depositing stoichiometric TiO_2 ($E_g=3.0 - 3.2 \text{ eV}$) as the window layer to form eventually a hetero-junction device on flexible polyimide (PI) substrate. This allows maximum light harvest of the device. To achieve low temperature deposition of titanium-based oxide on PI substrate, a high power impulse magnetron sputtering (HIPIMS) technique is employed, which is known to provide high density plasma to favor crystalline growth during deposition and hence a reduced substrate temperature.

Experimental results show that an oxygen-graded TiO_x can successfully deposited on PI substrate. Crystallography of the obtained TiO_x shows great dependence on the deposition conditions. Morphology of the TiO_x film presents flat surface with a columnar structure. Optical and electrical properties are strongly related to microstructure of the obtained TiO_x films. Results of photovoltaic measurements further established the feasibility of such PI/Ti/ TiO_x / TiO_2 /ITO hetero-junction device for thin film solar cell application.

FP-21 Time Evolution and the Gas Rarefaction of Long HIPIMS Pulses, C. Huo (chunqing@kth.se), KTH Royal Institute of Technology, Sweden, M.A. Raadu, Royal Institute of Technology, Sweden, D. Lundin, Université Paris-Sud 11, France, J.T. Gudmundsson, Shanghai Jiaotong University, China, A. Anders, Lawrence Berkeley National Laboratory, US, N. Brenning, Royal Institute of Technology, Sweden

Studies of long pulses of high power impulse magnetron sputtering (HIPIMS) have been reported, both by experiments and by modeling. The model used is based on IRM I, which referred to as IRM II here, is a time dependent plasma chemical discharge model developed for the ionization region in magnetron sputtering discharges. It is benchmarked against the experiments performed at Lawrence Berkeley National Laboratory, with square voltage pulses (330V to 1000V), 400 μ s long, applied to an Al target in Ar at 1.8Pa. The power is kept so low that the discharge does not go into the runaway self sputtering mode. The model uses two fitting parameters, the probability of ion back-attraction to the target, and the fraction of the electric discharge power, that goes to the electrons. Model calculations are found to give a close fit to an experimentally observed initial high current transient, as well as a later plateau value of constant lower current, but only within the limited parameters range. The following observations hold within all of this fitting parameter range. The peak in discharge current precedes a maximum in gas rarefaction. The time durations of the high current transient, and of the rarefaction maximum, are determined by the time it takes to establish a steady state diffusional refill of process gas from the surrounding volume. The dominating process for gas rarefaction is ionization losses, with only about a few percent due to the sputter wind, heating, and kick-out processes that dominate in dcMS. The plasma density peaks during the high current transient, and more than half of the sputtered metal ionized. During the whole plateau phase the electron density stays stable, while the degree of metal ionization is lower and almost constant. The electron temperature was steady throughout the pulse. The degree of self sputtering (here defined as the metal ion fraction of the total ion current to the target) varies during the pulse. It grows from zero at pulse start to a maximum some time later, coinciding in time with the maximum gas rarefaction. It then stabilizes during the plateau phase. This makes the degree of self-sputtering as an important parameter in the HIPIMS discharge. The part of the decrease in deposition rate that can be attributed to the back-attraction of the ionized sputtered species also varies during the pulse, in such a fashion that it is correlated to the momentary discharge current. It is low during the initial stage, then peaks during the current transient, and finally stabilizes during the plateau phase.

FP-22 Mass and energy spectrometry of a feedback controlled reactive Ti HIPIMS discharge in Ar/O₂, M. Audronis (martynas.audronis@gencoal.com), Gencoal Ltd, UK, Y. Gonzalvo, Hiden Analytical Ltd., UK, V. Bellido-Gonzalez, Gencoal Ltd, UK

This paper investigates the reactive High Power Impulse Magnetron Sputtering (HIPIMS) of Ti in Ar/O₂ discharge by means of a quadrupole mass spectrometer. Accurate process control (i.e. target oxidation level) was obtained using the recently developed fast closed loop process control system based on optical plasma monitoring [Surface & Coatings Technology 204 (2010) 2159–2164]. HIPIMS discharge (pulsed at 200 Hz) was operated at different set points between the ‘metal’ and ‘fully poisoned’ states, inclusive. Mass and energy of species present in the discharge were characterised at a distance that is a typical for locating substrates in industrial vacuum coating processes. Quantitative analysis results are presented in this paper. The presence and quantity and of negative ions and charged molecules is emphasised and the effect of them on coating properties is discussed.

FP-23 Progress in BIPOLAR sputtering technology – new approach to process control and its applications, W. Glazek

(wojciech.glazek@pl.huettinger.com), A. Klimczak, P. Ozimek, P. Rozanski, Huettinger Electronic, Poland

BIPOLAR sputtering is currently being implemented in progressing number of applications replacing older MF technology. Most important new feature of the technology is ability to react on changing parameters of the process and plasma very fast in order to enhance process and coating parameters.

New abilities of the BIPOLAR power supplies mainly result from ultra fast digital internal control system. Fast digital data processing, enables new BIPOLAR power supplies serve broad range of applications better than older MF technology. Faster and more precise digital control gives user enhanced control over the process, and enables power supply to react on process parameters in sophisticated way employing advanced algorithms.

Most importantly digital control platform enables new features supporting reactive sputtering with BIPOLAR technology. The solution enabled to deposit coatings with enhanced quality and at high deposition rate. Results of use of the solution will be presented and potential for industrial applications will be discussed.

FP-24 Effect of hydrogen addition on the residual stress of cubic boron nitride thin film deposited by UBM sputtering method. *J.-S. Ko, J.K. Park*, Korea Institute of Science and Technology, Republic of Korea, *J.-Y. Huh*, Unaffiliated, *Y.J. Baik* (*yjbaik@kist.re.kr*), Korea Institute of Science and Technology, Republic of Korea

The effect of hydrogen addition on the formation of cubic boron nitride thin film was investigated, especially focusing on the behavior of the residual stress of the film. The films were deposited by UBM (unbalanced magnetron sputtering) method. A boron nitride target of 3" diameter was used as a sputtering source, which was connected with 13.56 MHz RF (radio-frequency) electric power supply. The substrate holder was placed at 7.5 cm under the target and 200 KHz electric power supply was used as a substrate bias power supply. Either Si or Si wafer with nanocrystalline diamond thin film on it was used as a substrate. The chamber was evacuated down to 10^{-6} torr and a mixed gas of Ar-10% nitrogen was flowed into the chamber during deposition. The hydrogen was added to the mixed gas up to 5 sccm while maintaining the total gas flow rate at 20 sccm. The deposition pressure was maintained at 2 or 4 mtorr. The electric power of the target was 500 W and the substrate self bias voltage was -60 V. The residual stress was calculated by Stoney equation by using the curvatures of thin Si strip of (3 x 40) mm² measured during deposition. FTIR, SEM, TEM as well as RBS were used to analyze the phase, structure and composition.

It was observed that the residual stress was decreased with the increase of the hydrogen flow, while the cBN fraction was also decreased. The rate of the decrease, however, has shown different behavior. The former was faster than the latter at the initial stage of the added hydrogen amount, which implies that a little addition of the hydrogen could lessened the residual stress of the film to a much degree with only a trivial decrease of the cBN fraction. The reason of this behavior was discussed with the incorporation of Ar atoms into the film and its effect on the formation of the residual stress.

This research was supported by a grant from the Fundamental R&D Program for Core Technology of Materials funded by the Ministry of Knowledge Economy, Republic of Korea.

FP-25 Behavior of cubic boron nitride thin film formation according to the deposition pressure. *E.S. Lee, J.K. Park*, Korea Institute of Science and Technology, Republic of Korea, *T.Y. Seong*, Korea University, Republic of Korea, *Y.J. Baik* (*yjbaik@kist.re.kr*), Korea Institute of Science and Technology, Republic of Korea

The formation of cBN is known to be affected mainly by ion energy and flux. During sputtering process, both the ion energy and the ion flux are a function of substrate bias voltage and a mean free path of ions. In this study, the effect of deposition pressure on the formation was investigated to see the role of the mean free path length in the cBN formation. The films were deposited by UBM (unbalanced magnetron sputtering) method. A boron nitride target of 3" diameter was used as a sputtering source, which was connected with 13.56 MHz RF (radio-frequency) electric power supply. The substrate holder was placed at 7.5 cm under the target and 200 KHz electric power supply was used as a substrate bias power supply. Either Si or Si wafer with nanocrystalline diamond thin film on it was used as a substrate. The chamber was evacuated down to 1.2×10^{-6} Torr and a mixed gas of Ar-10% nitrogen was flowed at 20 sccm into the chamber during deposition. The deposition pressure was varied from 2 to 20 mTorr. For the system we used, the mean free path length was calculated to be around the range of the target to the substrate distance. The electric power of the target was 500 W and the substrate selfbias voltage was varied from -20 to -120 V. FTIR, SEM as well as TEM were used to analyze the phase and structure.

The formation of the cBN phase was affected both by the substrate bias voltage and the deposition pressure. There appeared a critical pressure above which only a hBN phase formed. With increasing the substrate bias voltage, the critical pressure increased. The cBN content in the FTIR spectrum was not varied in the range under the critical pressure. The critical substrate bias voltage was also increased with increasing deposition pressure. This behavior was discussed with a view point of ion energy and ion flux ratio relation curve for the cBN formation.

This research was supported by a grant from the Fundamental R&D Program for Core Technology of Materials funded by the Ministry of Knowledge Economy, Republic of Korea

FP-26 Effect of moisture adsorption inside the chamber on the formation of cubic boron nitride thin film. *E.S. Lee, J.K. Park*, Korea Institute of Science and Technology, Republic of Korea, *T.Y. Seong*, Unaffiliated, *Y.J. Baik* (*yjbaik@kist.re.kr*), Korea Institute of Science and Technology, Republic of Korea

It was reported previously that minor addition of either the oxygen or the hydrogen had inhibited the formation of cBN during the PVD process. It is, thus, expected that the moisture adsorbed inside the deposition chamber

could have a harmful effect on the deposition of the cBN film. Such possibility was investigated in this study. The chamber was open to the atmosphere before deposition for 1 h under the moisture content of about 30%. Then it was evacuated down to 3.5×10^{-6} Torr. It took 30 min to arrive the pressure and then a mixed gas of Ar-10% nitrogen at 20 sccm was flown and the deposition process was started. The films were deposited by UBM (unbalanced magnetron sputtering) method. A boron nitride target of 3" diameter was used as a sputtering source, which was connected with 13.56 MHz RF (radio-frequency) electric power supply. The substrate holder was placed at 7.5 cm under the target and 200 KHz electric power supply was used as a substrate bias power supply. Either Si or Si wafer with nanocrystalline diamond thin film on it was used as a substrate. The deposition pressure was 4mTorr. We deposited the films for 30 min. Then, the sample was changed via load lock chamber and the chamber was evacuated again down to 1.2×10^{-6} Torr with baking the chamber. The baking was done by heating the substrate heater whose temperature was adjusted between room temperature and 500 °C. It took 90 min to arrive the base pressure. It is believed that little moisture was involved into the chamber during this stage. We compared the FTIR spectra of these samples to see the effect of moisture contamination.

The first deposited sample has shown that only a hBN phase formed in the film. The cBN phase began to appear as the deposition batch proceeded. The number of batch forming the cBN phase was smaller as the baking temperature increased. The baking time also affected the formation of the cBN content. We measured the OES (optical emission spectra) during deposition and compared them from batch to batch to find the possible indicator of cBN formation. The variation of the intensity of main emission peak with the number of the batch was shown and their relation with the cBN formation was discussed.

This research was supported by a grant from the Fundamental R&D Program for Core Technology of Materials funded by the Ministry of Knowledge Economy, Republic of Korea

FP-27 Precise modulation of pore diameter of porous anodic alumina templates by hybrid pulse periods at room temperature. *C.K. Chung* (*ckchung@mail.ncku.edu.tw*), *H.C. Chang, S.L. Li, M.W. Liao*, National Cheng Kung University, Taiwan

In the applications of photonic crystal, optic, and photovoltaic, highly ordered porous anodic aluminum oxide (AAO) is one of famous nano-templates as etching mask for pattern transfer and synthesis of nanocomposite materials. The AAO structural characteristics i.e., pore size and thickness affected the optical and optoelectronic properties sensitively. In this article, we proposed a novel synthesis, namely hybrid pulse anodization (HPA) combined with positive (V+) and negative (V-) voltage in one pulse period, to fabricate effectively AAO templates using aluminum foils in 0.5 M oxalic acid at room temperature which is different from conventional direct-current anodization at low temperature 0-10 °C. The objective of our research was to study the influence of principal factors, such as pulse period and applied voltage, on modulating pore diameter (< 100 nm) precisely by HPA. Many researchers demonstrated that the relationship between voltage and interpore distance was positive. Therefore, HPA at suitable voltage with different pulse period could produced various pore diameters, because modulating V- time attracts more or less hydrogen ions for dissolution of electrolyte/oxide interface. High electrolyte temperature provides much Joule's heat for accelerating chemical reaction of surface, too. It was found that such a method could control mean pore diameters with difference of about 10 nm. The morphology of surface was investigated by field-emission scanning electron microscopy for pore size distribution and regularity analysis. Furthermore, we designed a statistical experiment using analysis of variance to quantify the effects of these factors mentioned above on pore diameter variation.

FP-28 Transparent Anti-fingerprint Protective Coatings Prepared by Duplex Plasma Polymerization. *S.W. Chang*, Feng Chia University, Taiwan, *C.M. Chen* (*harlem@pidc.org.tw*), Feng Chia University; Plastic Industry Development Center, Taiwan, *J.L. He*, Feng Chia University, Taiwan

Polymeric materials have been widely used as flexible substrates and housing parts of modern electronic wares. However, their low hardness and scratch resistance must be improved by additional protective surface coatings, which require not only mechanical durability but also additional functions such as surface hydrophobicity, oleophobicity as well as anti-fingerprint performance. To satisfy these, a power modulated plasma polymerization technique was designed to synthesize a transparent compositional gradient coating on polycarbonate (PC) substrate. Firstly, a constant flow rate of tetramethyldisiloxane (TMDSO) precursor was introduced where higher plasma power was employed to deposit a hard H-C-Si-O bottom layer. The plasma power was then decreased meanwhile admitting increased fluoromethane (CF₄) gas flow as the second precursor to obtain a top layer with low surface energy. The hard bottom layer acts as a

strong mechanical support and the top layer gives additional hydrophobicity and oleophobicity. Ultimately, the coating shows that a pencil hardness of 3H and Scotch-tape adhesion of 5B improves its protective function. A water contact angle of 105° and oil contact angle of 31.7° can be obtained. The coated specimen remains an optical transparency of 90% close to bare PC material. Comparing with commercialized screen protectors, the developed coating shows superior protective and anti-fingerprint performance.

Applications, Manufacturing, and Equipment Room: Golden Ballroom - Session GP

Symposium G Poster Session

GP-1 Effect of Pulse Frequency on Physical Properties of Diamond-Like Carbon Films Synthesized under Atmospheric Pressure, T. Sakurai (*t-s-0127@z8.keio.jp*), M. Noborisaka, T. Hirako, T. Suzuki, Keio University, Japan

Diamond-like carbon (DLC) films are generally synthesized at low pressure less than 10 Pa, but high cost for vacuum devices, long deposition time and a limited synthetic area have been pointed out as fundamental problems. Based on above reasons, DLC films synthesized under atmospheric pressure (AP-DLC) have attracted much attention in many fields. In our previous study, AP-DLC films were generally inferior to those synthesized at low pressure in surface smoothness and hardness.

In this study, we synthesized DLC films using C₂H₂ gas diluted with N₂ gas under atmospheric pressure and investigated the effect of applied pulse frequency of electric source on the physical properties. Changing the pulse frequencies at 2, 4, 6, 8, 10 kHz, the pulse width and applied voltage were fixed at 5 μs and 18 kV, respectively. The surface roughness and hardness were analyzed by atomic force microscope (AFM) and tribo scope nano-mechanical indentation tester, respectively. As the pulse frequency decreased from 10 to 2 kHz, the surface roughness decreased from 32.5 to 1.76 nm, and finally, the hardness increased from 0.5 to 1.2 GPa.

GP-2 Monte Carlo simulation of energy and particle distributions in the molybdenum disulfide sputtering process, B. Vierendeel (*Vierendeel@mfk.uni-erlangen.de*), S. Tremmel, S. Wartzack, Friedrich-Alexander-University Erlangen-Nuremberg, Germany

Recent studies indicated that the deposition process parameters exhibit strong dependence on crystal growth and stoichiometry of sputtered MoS₂. All the studies are focused on building highly oriented coatings without columnar crystal growth. There is a wide consensus that these films can be achieved mainly by low process pressures. Considering the different characteristics (mass) of the two species and models of film growth in which the energy flux is a main influence factor, the question arises how process parameters like working gas pressure affect the kinetic energy and the composition of particles arriving at the substrate.

In general, the sputter deposition process can be separated into three steps. The first one is the vaporization of the target caused by collision cascades of impacting ions. The second one is the transport of sputtered particles through the gas phase and the last one is film growth on the substrate. In this paper, results of a Monte Carlo simulation with TRIM considering the first two steps are presented. Within the first step the energy and angular distribution of the sputtered molybdenum and sulfur atoms were calculated when argon ions with varying kinetic energies impact the MoS₂ target perpendicularly. The varying argon ion energy represents different acceleration and cathode voltages respectively. To simplify matters, energy and angular distribution of the impacting argon ions were neglected.

Within the second step the transport through the gas phase in the vacuum chamber is calculated. The calculation is based on sputtered particles from the first step with equal angles and energies. In this step the pressure of the working gas, argon in this case, was varied. Finally, energy distribution and amount of particles are analyzed at different distances from the target. This enables to determine the effect of three process parameters namely cathode voltage, working gas pressure and distance to target on energy and amount of particles. To visualize the mutual interactions of parameters in response surface diagrams design of experiment methods were applied.

In short, this study gives a fundamental understanding for the sputtering process of MoS₂ and the energy distributions and composition of sputtered particles.

GP-3 Temperature-induced abnormal sub-threshold leakage current in amorphous Indium-Gallium-Zinc-Oxide thin film transistors, J.-C. Jhu, National Sun Yat-Sen University, Taiwan, G.W. Chang (*b922030049@gmail.com*), National Chiao Tung University, Taiwan, Y.E. Syu, National Sun Yat-Sen University, Taiwan

The electrical characteristics of amorphous Indium-Gallium-Zinc-Oxide Thin Film Transistors (a-IGZO TFTs) were investigated at different temperatures from 300K to 450K in order to analysis the behavior of the sub-threshold region. The transfer curve exhibits abnormal sub-threshold leakage current at high temperature. The abnormal electrical properties are explained by the energy band diagrams at both forward and reverse sweep. Above 400K, the hole could be generated from trap-assisted tunneling and drift to the source side that induced the source barrier lowering. The source side barrier lowering enhances electrons injection from the source to channel and causes an apparent sub-threshold leakage current. This phenomenon only appears at high temperature, above 400K, which is experimentally verified. Moreover, the device further was given negative bias stress at the different temperatures and under the different drain biases to confirm the proposed mechanism.

GP-4 Microstructural analysis of Zn-Sn interface with thin films based of Ta over Cu and Si substrates, S. Medrano, G. Ramirez, Instituto de Investigaciones en Materiales, Universidad Nacional Autónoma de México, Circuito Exterior s/n, CU, México D.F. 04510, México, S.E. Rodil, Instituto de Investigaciones en Materiales, Universidad Nacional Autónoma de México, México, S. Muhl, Universidad Nacional Autónoma de México - Instituto de Investigaciones en Materiales, Mexico, G. Gonzalez (*joseggr@unam.mx*), Instituto de Investigaciones en Materiales, Universidad Nacional Autónoma de México, Circuito Exterior s/n, CU, México D.F. 04510, México

Atomic diffusion, and later formation of intermetallic compounds, can become a serious problem in electronic joints. The growing of intermetallic compounds at the interface can affect the structural integrity of the joints, due the formation of cracks. This process hinders the use of some lead-free solders like Zn-Sn alloys. This alloy system is a good candidate to substitute high temperature solders based on lead. The joint failure between Zn-Sn and Cu comes from the formation of CuZn₅ and Cu₅Zn₈ intermetallic compounds. The use of a conductor thin film as a diffusional barrier coating can inhibit the formation of intermetallic compounds and consequently maintain the structural integrity of the joint.

In this work the atomic diffusion between Zn-Sn alloy into Cu and Si substrates was studied. Two different diffusional barrier coatings were used: tantalum - tantalum nitride and tantalum - tantalum nitride + 5% wt Silicon. The Ta/TaN thin film was deposited using a DC sputtering under Argon / Nitrogen atmosphere. The Ta/TaN+Si film was deposited under an Ar/Ni atmosphere, using two separate magnetrons, the first with a RF source and a Si target, and the second with DC source and a Ta target.

Standard XRD diffraction patterns were obtained from the coatings (using a grazing configuration), in order to analyze a structural change due the addition of Si. Samples were annealed at 423 K a different times, to evaluate the performance of the DBCs as a diffusion barrier coating. The elemental diffusion was obtained from EDX spectra (line scan), showing marginal Zn content into the coatings. The interfaces and epitaxies between coatings and substrates were discussed based on the observations made through FIB, SEM and TEM.

GP-5 Characterization of Polysilazane Based Sod Films As Function of Process Temperature and Thin Barrier used, G. Gulleri (*ggulleri@micron.com*), Micron Semiconductor Italia S.r.l., Italy, F. Fumagalli, Micron Semiconductor Italia S.r.l., Italy, C. Ricci, University of Cagliari, Physics Department, Italy

The main effort in the development of a new generation of metal-oxide-semiconductors (MOS) devices is toward the reduction of their dimension down to submicron values. The actual technology node is undergoing below 35 nm and became critical the oxide deposition technique and its effective characterization. Spin-on-Dielectric (SOD) materials have generated much interest for gap filling as alternative to chemical vapour deposition (CVD) and high density plasma deposited materials (HDP). In high aspect ratio (HAR) structures CVD technologies have difficulties in gap filling where SOD conversion to silicon oxide could be inhibited inside the pattern structure and by the presence of thin film barriers. In this direction the effects of the SOD conversion temperature as well as the different chemical composition of the amorphous liner, deposited between the Silicon wafer and the SOD layer, are studied on unpatterned wafers. Silicon oxide and silicon nitride liners via furnace and CVD deposition technique are provided.

Intrinsic stress induced on silicon wafer was studied and analysed by means of the Stoney's formula. Fourier Transform Infrared Spectroscopy (FTIR) was performed to compare SOD conversion degree. The quality of silicon

oxide obtained was correlated to the presence of 4-fold and 4/6-fold Si-O bonds that is an index of sub-stoichiometry of the bulk. This fact indicates a better amorphous conversion of SOD in presence of silicon oxide liners instead of silicon nitride or bare-silicon.

GP-6 A novel multilayer barrier film encapsulated plastics purely prepared by inductively coupled plasma chemical vapor deposition. *L.W. Lai* (lwilai@itri.org.tw), *M.H. Ko*, *K.W. Lin*, *J.T. Chen*, *C.H. Chang*, Industrial Technology Research Institute, Taiwan

Recently, transparent materials such as silicon oxide were widely used as gas barrier films. However, these inorganic oxide films often crack or peel as a result of the difference in thermal expansion coefficient between the substrate and the coated film. To overcome this problem, a multilayer barrier structure consisting of soft organic and hard inorganic films was commonly used, which benefiting in improving the water vapor barrier performance. However, these gas barrier films were prepared in various vacuum equipments, which resulted in significant inconvenience for multilayer coating deposition. Based on the above consideration, the development is necessary to prepare a gas barrier film with high reliability and low cost in a single-chamber process. Therefore, a novel thin-film encapsulation technology was developed using an organosilicon/silicon oxide multilayer barrier structure. The vapor barrier property of the inorganic SiO_x film deposited on the PES substrate prepared by an inductively coupled plasma chemical vapor deposition (ICP-CVD) using precursors of hexamethyldisiloxane (HMDSO) and oxygen gas mixture was firstly optimized. The water vapor transmission rate of a PES substrate was significantly decreased from 50 to 0.8 g/m²/day coated with a 250 nm-SiO_x prepared at room temperature. The WVTR of the PES substrate was further improved by inserting an organosilicon film plasma-polymerized using the same HMDSO monomer. Such organosilicon film abundant in hydrophobic C-H function group and cross-linking Si-C structure functioned to release the internal residual stress in the SiO_x film during deposition as a consequence of the improvement on the film adhesion. A lowest value of 0.07 g/m²/day can be obtained under the SiO_x film inserting the organosilicon layer. In addition, the developed organosilicon film characterized by hydrophobic C-H group was also able to modify the surface hydrophilicity of the multilayer barrier structure and thus minimized the adsorption of oxygen and water molecules on the substrate surface. Additionally, a more efficient method to improve the permeability was carried out by using a non-symmetrical double-sided coating of SiO_x (150 nm) and organosilicon(100 nm)/ SiO_x (250 nm) stacked films on the PES substrate. Because the double-sided coatings is to balance the stress and obtain a flat and noncurved barrier substrate, the WVTR can be decreased down to 0.001 g/m²/day, which is one order of magnitude lower than that of a single-sided barrier coating. Such simple and novel multilayer barrier structure is a promising candidate for the application on the encapsulation technology of the flexible optoelectronic devices.

GP-7 Surface modification using silane coupling agent for polypropylene with high gas barrier property. *H. Tashiro*, *A. Hotta* (hotta@mech.keio.ac.jp), Keio University, Japan

Polymer materials such as polypropylene (PP), polyethylene (PE), and polyethylene terephthalate (PET) are widely used as food packaging materials due to their lightness, low cost, and optical transparency. However, most of the polymer materials have low gas barrier property which may cause a great damage on the quality of food products. Thus the improvement of the low gas barrier property is widely desired.

Recently, thin solid coatings by diamond-like carbon (DLC) and silicon oxide (SiO_x) based on plasma technology have been prominent methods. Several researches have been reported on the gas barrier properties of polymers coated with DLC, eventually improving the gas barrier properties of certain types of polymers. However, most plasma systems used for the syntheses of DLC and SiO_x are operated under low pressure and, therefore, require an expensive and complicated vacuum system.

As a new thin coating method, silane coupling treatment was investigated. The silane coupling agent is a common adhesion promoter and is widely used in polymeric composites. In addition, the silane coupling agent possesses high transparency, and it can easily spread over polymer films since it is in a liquid state. Furthermore, the silane coupling treatment can solidify itself through hydrolysis, which can be an easier and faster way to produce a high gas barrier coating.

According to the results of the gas permeation test, it was found that the polymers coated with various types of silane coupling agents showed high gas barrier properties. Especially the silane coupling agents with an amino group showed a very low oxygen transmission rate which was comparable to the results of PET with high gas barrier property. Additionally, PP films remained transparent even after the coating. Such improvement in gas barrier property may be due to the formation of siloxane (-Si-O-Si-) networks through hydrolysis and condensation processes. It is also

considered that the siloxane networks had a dense molecular structure similar to that of SiO_x, which resulted in establishing an impermeable layer. The method could be applicable to several types of polymers including PE.

GP-8 Manufacturing of mode-conversion type microwave plasma CVD apparatus and applying for synthesis of carbon materials. *T. Kameshima* (tack_kameshima@yahoo.co.jp), Graduate School, Chiba Institute of Technology, Japan, *H. Tanaka*, Shutech Co., Ltd., Japan, *Y. Sakamoto*, Chiba Institute of Technology, Japan

For fabrication of thin film using microwave plasma CVD, mode-conversion type microwave plasma is expected to improve the deposition area and growth rate. By converting the TE₁₀ mode to the TM₀₁ mode for microwave, electric field component is changed from vertical direction of the rectangular waveguide into the circumference direction of the circular waveguide. And then, uniform electric field distribution can be obtained. So, larger deposition area and higher growth rate may be performed. Moreover, quality of deposits is improved because of the higher microwave density. On the other hand, carbon materials such as diamond and diamond like carbon (DLC) can be obtained by using microwave plasma CVD. So, investigation was carried out on the manufacturing of mode-conversion type microwave plasma CVD apparatus and applying for synthesis of carbon materials.

Different wavelengths microwave of 2.45 GHz and 915 MHz were applied to experimental apparatus. The mode of microwave was converted by using of mode convertor. It is important to discharge plasma at higher microwave density and higher pressure to obtain higher growth rate and high qualities for diamond growth.

Diamond synthesis using the apparatus applied 2.45 GHz microwave, CH₄-H₂ mixture gas system was used as the reaction gas. The flow rate of CH₄ and H₂ were set at 1 to 10 and 100, respectively. Pressure, microwave power and reaction time were unified at 20.0 kPa, 1.5 kW, and 3h, respectively. Si wafers scratched by diamond powders were used as substrates. The deposits were characterized by a scanning electron microscopy (SEM) for surface observation, and Raman spectroscopy was used for estimation of quality of deposits.

Results of the surface observation by SEM, deposits which has clear crystalline shape were observed in all the conditions. In addition, in the estimation of quality of deposits by Raman spectroscopy, diamond peak at 1333 cm⁻¹ was observed in their Raman spectra of all samples, and DLC peak at 1550 cm⁻¹ was observed.

In the case of the apparatus applied 915 MHz microwave, 915 MHz microwave apparatus is tried to set up the similar configuration. The deposition area will be larger by applying 915 MHz microwave because of longer wavelength.

In conclusion, diamond was synthesized from CH₄-H₂ reaction gas system using mode-conversion type microwave plasma CVD apparatus applied 2.45 GHz microwave.

GP-9 A novel technique to suppress self sputtering of radio-frequency electrode in capacitively-coupled glow discharge. *X.B. Tian* (Xiubotian@163.com), *Y.H. Ma*, *C.Z. Gong*, *S.Q. Yang*, Harbin Institute of Technology, China, *P. Chu*, City University of Hong Kong, Hong Kong Special Administrative Region of China

A novel technique to suppress self sputtering of radio-frequency electrode in capacitively-coupled glow discharge

*Xiubo Tian*¹, *Yinghe Ma*¹, *Chunzhi Gong*¹, *Shiqin Yang*¹, *Paul. K. Chu*²

¹State Key lab of Advanced Welding & Joining, Harbin Institute of Technology, Harbin, China

²Department of Physics & Materials Science, City University of Hong Kong

The capacitively-coupled Radio-frequency discharge (CCP) has been widely utilized in industry. The self-sputtering effect induced by self bias on the radio-frequency electrode inherently exists. This may produce the metal contamination to the generated plasmas. Although some measures including quartz covering have been taken and the sputtering effect was weakened, the self-bias does not be eliminated. In this paper we proposed a novel technique to decrease the self-bias and resultant self-sputtering effect. An external circuit was added into the radio frequency discharge circuit. The self bias on radio frequency electrode may be counteracted by external energy. Our experimental results have demonstrated that the self-bias on the electrode may effectively be eliminated. The positive and negative waveform of radio frequency current seems to be symmetric. The electrical circuit to weaken the self-bias is described and the waveform before and after the external circuit is coupled is compared and suppression effect of self sputtering is experimentally demonstrated.

GP-10 An experimental study on a large area multi-electrode discharge in the fabrication of microcrystalline thin film solar cell. *H. Seo* (shseo69@kaist.ac.kr), *S. Lee, Y. Chang*, Korea Advanced Institute of Science and Technology, Republic of Korea

Recently, there have been many research for higher deposition rate (DR) and good uniformity of $\mu\text{-Si:H}$ film in large-area discharge. Two factors should be the most important issues in the fabrication of the thin film solar cell. In order to solve these issues, several discharge conditions, including large area electrode (more than 1.1 m x 1.3 m), higher pressure (more than 1 Torr), and very high-frequency RF power (more than 40 MHz), have attracted. But, in the case of large-area capacitive discharges (CCP) driven at high frequencies, the effect caused by the standing wave should be important limitation. Furthermore, the ion damage on the thin film layer by the high sheath voltage can cause the defects, which degrade the film quality.

Here, we will propose new CCP electrode concept, which consists of a series of electrodes and grounds arranged by turns, and provide the processing results. The high DR (1 nm/s), the controllable crystallinity (~70%), and the relatively good uniformity can be obtained at the high frequency of 40 MHz in the large-area discharge (280 mm x 540 mm). And, we will show the TEM images of the $\mu\text{-Si:H}$ films at the various conditions of $\mu\text{-Si:H}$ films, and discuss the crystal formation compared to the case of VHF CCP. Finally, we will discuss the issues in expanding the multi-electrode to the 8G class large-area plasma processing (2.2 m x 2.4 m) and in improving the process efficiency.

GP-11 Advanced PVD coatings in a combination with a new intermetallic substrate for hobs - A major step forward in productivity. *P. Immich* (pimmich@lmt-fette.com), *U. Kretzschmann, U. Schunk, R. Fischer*, LMT Fette Werkzeugtechnik, Germany

The ever increasing demand for higher productivity in manufacturing gears requires advanced hard coatings and new substrate materials. Up to now in this field of gear manufacturing two different substrate materials are available for single-piece hobs: powder metallurgy high-speed steel (PM-HSS) and cemented carbide. Today PM-HSS has a market share around 70% offering limited cutting speeds for wet and dry conditions on labile machine conditions. On the other hand cemented carbide offers from the technical point of view strong performance related features like high cutting speeds up to 400 m/s on stable machine conditions.

But due to the fact, that hobs have a typical life cycle time of 10-15 recondition cycles— hobs are often demounted – packed and shipped – decoated- reground and coated again- could cause small handling or production damages that result in a shorter tool life time and less reliability of the production process. Additionally using cemented carbide hobs required often new hob machines with stable machine conditions.

To fill this gap, a new generation of substrate material was developed based on intermetallic phases. This cutting material offers compared to conventional PM-HSS higher hot hardness and as result from this higher cutting speeds. In fact today hobs are coated and e.g. dry gear cutting is only possible with coated tools due to the prevention of chip welding.

Today hob coatings that are available on the commercial market mainly based on TiAlN system applied by AIP and Sputter PVD processes.

Since the last years a strong development towards higher wear resistance coatings by adding e.g. silicon to the TiAlN-system can be observed. But these systems are limited. Now there is a significant switch in the market towards the system Cr-Al-N offering higher oxidation resistance and higher wear resistance. In this regard different state of the art coatings are applied on this new hob material and tested in laboratory scale and industrial filed tests. Especially a new developed AlCrN multilayer coating offers a higher wear resistance compared to state of the art coatings. As a result of these investigations it is possible to increase cutting speeds up to 50% compared to conventional coated PM-HSS hobs

GP-12 Adhesive-free gas adsorption joining of cycloolefin polymer film and glass sheet. *Y. Taga* (y-taga@isc.chubu.ac.jp), Thin film research Center, Chubu University, Japan

Attempt has been made to join glass and cycloolefin polymer (COP) film by gas adsorption method at low temperature. Gas coadsorption of water vapor in air atmosphere and silane coupling agent (SCA) gasses was carried out on both surfaces after sophisticated plasma treatment. SCA of glycidoxypropyltrimethoxysilane (GPS) was adsorbed on glass sheet and aminopropyltrimethoxysilane (APS) on COP. Thicknesses of glass sheet and COP film were both 100 μm . Joining was carried out by annealing at 130°C for 10 min after lamination. A necessary condition for joining of COP and glass is at first to make the contact surfaces clean, where surface cleanliness was evaluated by contact angle of water droplet. Surface functional group of O-H can be seen on glass after corona plasma treatment. On the other hand, XPS spectra of C1s from COP surface after plasma

treatment revealed the existence of complex functional group of O-H, CO, C=O, COO and CO₃. Joining force was found to be of more than 10MP corresponding to almost equal to COP bulk tensile strength. Thickness of joining layer was evaluated by XPS and found to be 2-5 nm. In addition, durability of strength thus joined remained unchanged over 2000 hrs even after exposure to the conditions of 60 °C and 95% RH. Joining mechanism can be explained in terms of epoxy reaction and amino reaction to form covalent bonding such as O-Si-O and O-Si-C. In conclusion, adhesive-free gas adsorption joining of glass and COP was carried out and established strong adhesion and durability at low temperature under ultimate joining thickness of 2-5 nm.

GP-13 Silicon oxide permeation barrier coating of PET in microwave plasmas with arbitrary substrate bias. *S. Steves* (steves@aept.rub.de), Electrical Engineering and Plasma Technology, Ruhr-Universität Bochum, Germany, *B. Oezkaya*, Technical and Macromolecular Chemistry, University of Paderborn, Germany, *M. Rudolph, M. Deilmann*, Electrical Engineering and Plasma Technology, Ruhr-Universität Bochum, Germany, *C.N. Liu*, Technical and Macromolecular Chemistry, University of Paderborn, Germany, *N. Bibinov*, Electrical Engineering and Plasma Technology, Ruhr-Universität Bochum, Germany, *O. Ozcan, G. Grundmeier*, Technical and Macromolecular Chemistry, University of Paderborn, Germany, *P. Awakowicz*, Electrical Engineering and Plasma Technology, Ruhr-Universität Bochum, Germany

Plastics such as PET offer poor barrier properties against gas permeation. For applications of PET in food packaging the shelf life is reduced compared to glass or metal containers. Barrier performance is enhanced by depositing a transparent plasma polymerized silicon oxide (SiO_x) coating on the inner surface of the PET bottle. A permeation barrier coating of the inner surface of PET bottles and PET foils is developed by means of a microwave driven low pressure plasma reactor based on a modified Plasmaline antenna. A substrate bias with arbitrary waveforms is applied. Thus, the substrate electrode voltage is feedback controlled using fast Fourier transformation. The influence of a substrate bias leading to variable ion energy distributions is investigated with respect to the characteristics of plasma and coating.

Properties of coating are correlated with plasma characteristics. Barrier properties are determined concerning oxygen permeation. The composition of the coatings regarding carbon and hydrogen content is analyzed by means of Fourier transform infrared spectroscopy (FTIR) and x-ray photoelectron spectroscopy (XPS). Good oxygen barriers are observed as carbon content in the film is reduced. Atomic oxygen etching of the coated substrate visualizes coating defects responsible for a residual permeation. Crack formation mechanisms are studied in-situ by means of atomic force microscopy (AFM) using an AFM-stage to apply a desired strain. In addition, the evaluation of water up-take in barrier films was performed. The results show how process parameters such as gas composition and substrate bias have an impact on properties of permeation barrier coatings.

The authors gratefully acknowledge the support provided by the Deutsche Forschungsgemeinschaft (DFG) within the framework of SFB-TR 87, the Ruhr-University Research School, Aurion Anlagentechnik Seligenstadt and the Center for Plasma Science and Technology – CPST (Ruhr-Universität Bochum).

GP-14 Fluidized Bed Machining (FBM) of thermally sprayed cobalt-chromium and chromium oxide coatings. *M. Barletta* (barletta@ing.uniroma2.it), *S. Guarino, V. Tagliaferri, F. Trovalusci*, Università degli Studi di Roma Tor Vergata, Italy

In the present paper, Fluidized Bed Machining (FBM) of thermally sprayed coatings is proposed. In particular, aluminium cylindrical components coated by High Velocity Oxy Fuel (HVOF) with Stellite 6 (cobalt-chromium alloy) and by Atmospheric Plasma Spraying (APS) with chromium oxide were exposed to the impact of suspended abrasives, while rotating at high speed within the fluidization column. The interaction between Al₂O₃ abrasive media and surfaces of the thermally sprayed coatings was studied, identifying the effect of the main process parameters, such as machining time, abrasive mesh size and rotational speed. The change in surface morphology as a function of the process parameters was evaluated by Field Emission Gun – Scanning Electron Microscopy (FEG-SEM) and contact gauge profilometry. The change in the size of the machined parts was measured by Coordinate Measuring Machine (CMM). The experimental findings emphasize an improvement in the finishing as well as in the dimensional accuracy of the processed surfaces was achieved whatever the setting of the operational parameters, showing FBM as a very promising technique in the reprocessing of thermally sprayed coatings.

Key words: Fluidized Bed; Abrasive; Grinding; Thermally Sprayed Coatings; Morphology; Dimensional Tolerance.

Post Deadline Discoveries and Innovations

Room: Golden Ballroom - Session PDP

PDP-1 Oxidation resistance coatings of Ir-Zr and Ir by double glow plasma. W.P. Wu, Z.F. Chen (zhaofeng_chen@163.com), X.N. Cong, Nanjing University of Aeronautics and Astronautics, China

Refractory metals have low coefficients of thermal expansion. The ability of refractory metals to withstand extreme temperatures without significantly expanding or softening makes them useful as nozzle inserts in solid or liquid rocket-motor environments. However, the oxidation resistance for refractory metals is poor. Iridium (Ir) has a high melting temperature, excellent chemical compatibility and stability, low oxygen permeability and good oxidation resistance. Many of features of Ir make itself suitable for protecting the refractory metals from higher temperature damage and then have a longer service life. However, Ir does not form a condensed oxide due to the vapor species. In order to provide enhanced high temperature protection over a wide range of operating conditions, the refractory metals could be improved by depositing a graded coating of Ir-Zr. In this article, the Ir-Zr and Ir coatings were produced on molybdenum substrate by double glow plasma technology. The structure and composition of the Ir-Zr and Ir coatings were confirmed by SEM, AFM, XRD and EDS. The adhesion between the coating and the substrate was evaluated by a scratch tester. Thermal stability and oxidation resistance of Ir-Zr and Ir coatings were evaluated at high temperature.

PDP-2 A comparative study on hot corrosion resistance of three types of thermal barrier coatings: YSZ, YSZ/normal Al_2O_3 and YSZ/nano Al_2O_3 . M. Daroonparvar (re_dr7@yahoo.com), M.S. Hussain, Universiti Teknologi, Malaysia

Hot corrosion is one of the principal destructive factors in thermal barrier coatings (TBCs) at high temperatures. Low quality fuels usually consist of impurities such as Na and V which can form Na_2SO_4 and V_2O_5 salts onto the turbine blades. Hence, hot corrosion resistance of three types of plasma sprayed TBCs was investigated: (a) normal YSZ (yttria-stabilized zirconia), (b) layer composite of (YSZ / normal Al_2O_3 as an outer layer) and (c) layer composite of (YSZ/ nano Al_2O_3 as an outer layer). Hot corrosion tests were done onto the coatings in molten salts ($45\%\text{Na}_2\text{SO}_4 + 55\%\text{V}_2\text{O}_5$) at 1000°C for 52 h. The cracking and the premature spallation were observed in normal YSZ coating. The formation of monoclinic ZrO_2 and YVO_4 large crystals as hot corrosion products caused the degradation of the mentioned TBC. Although monoclinic ZrO_2 and YVO_4 crystals had been considerably reduced in (YSZ / normal Al_2O_3) in comparison with normal YSZ, YVO_4 crystals had main role in creation of micro-cracks in (YSZ / normal Al_2O_3) coating. Nano alumina coating as an outer layer in YSZ/ nano Al_2O_3 significantly reduced the penetration of molten salts into the YSZ layer and resulted in the further resistance of TBC against hot corrosion, because the hot corrosion products had been substantially decreased in YSZ/ nano Al_2O_3 coating in comparison with YSZ/normal Al_2O_3 and usual YSZ coatings.

Key words: Hot corrosion; YSZ; TBC; nano Al_2O_3 layer; YVO_4 crystals; normal Al_2O_3 ; monoclinic ZrO_2

PDP-3 Determination of the local mechanical properties and residual stresses of an a-C:H coating system by nanoindentation and FIB milling. C. Schmid (christoph.schmid@ww.uni-erlangen.de), V. Maier, Schaufler, M. Göken, University Erlangen-Nuremberg, Germany, K. Durst, University Erlangen-Nuremberg, Germany

It is a common technique to enhance the adhesion of hydrogenated amorphous carbon (a-C:H) coatings on steel substrates by applying adhesion layers based on different elements like Cr or Si. They frequently show a complex assembly with distinct chemical and mechanical gradients on a length scale in the submicron range. Therefore a correlation between the local mechanical properties and the corresponding chemical composition of these layers is difficult. In this work a Si-based adhesion layer for a-C:H coatings with a thickness of about $1\ \mu\text{m}$ was investigated. The coating system was deposited by PECVD and the adhesion layer consists of a silicon rich layer followed by an adjacent ramp layer with a graded chemical composition. The adhesion layer was characterized in terms of microstructure, chemical composition and local mechanical properties by means of focused ion beam (FIB), auger electron spectroscopy and nanoindentations. Using the small-angle cross-section method detailed information on the local mechanical properties as hardness and Young's modulus as well as on the chemical composition of the adhesion layer was obtained. It was found that the mechanical properties are strongly influenced by the chemistry of the adhesion layer. In addition, residual stresses in the a-C:H coating were determined by means of FIB and digital image correlation (DIC). For this a H-bar was FIB milled in the a-C:H coating which causes the residual stresses to relax locally. By determining the resulting displacements with DIC and correlating them to an appropriate

finite element analysis the residual stresses can be quantified. For the a-C:H coating residual compressive stresses of about $-2\ \text{GPa}$ were found.

PDP-4 A simple FIB milling technique for residual stress measurements on thermally cycled NiAl bond coats. M. Krottenthaler (markus.krottenthaler@ww.uni-erlangen.de), C. Schmid, R. Webler, J. Schaufler, S. Neumeier, University Erlangen-Nuremberg, Germany, K. Durst, University Erlangen-Nuremberg, Germany, M. Göken, University Erlangen-Nuremberg, Germany

PDP-5 In-Situ TEM Observations of Indenting Deformation and Fracture of Bone Nanopillars. S.Y. Chang (shouyi@dragon.nchu.edu.tw), Y.T. Wang, Y.C. Huang, C.M. Chen, National Chung Hsing University, Taiwan

Clarifying the correlations among the structures, mechanical properties and deformation and fracture behaviors of hierarchical bone tissue at a nanometer scale will improve the research in bone nanomechanics and the development of biomedical coatings and implants. Thus in this study, the nanostructures of normal and osteoporotic mouse bone were characterized; nanoscopic deformation and fracture were examined by the in-situ observations of bone nanopillars under indentations in transmission electron microscopy. Normal mouse bone comprised densely-packed hydroxyapatite crystallites and plied collagen fibers, and presented a ductile fracture toughened by microcracking, crack deflections and ligament bridging. Lattice distortions and a large number of dislocations that formed in mineral crystals consumed applied strain energy additionally. Upon osteoporosis, mouse bone changed to a loose structure with dispersed mineral crystals in a matrix of ground substance. The loss of collagen fibers, the sliding and rotations of dispersed crystals and also the intergranular fracture along the weak matrix led to the brittleness of the osteoporotic bone tissue.

PDP-6 In situ deposition and characterization of B-C-N films. H. Alagoz, M.F. Genisel, E. Bengu (bengu@fen.bilkent.edu.tr), D. Inan, Bilkent University, Turkey

We have deposited and characterized coordination preference in B-C-N films as a function of deposition parameters using a new multi-chamber system which allows for the of deposition of coatings in a chamber not only kept under UHV ($\sim 10^{-10}$ mbar) conditions, but also enables *in situ* characterization. With the help of this system, contamination of freshly prepared surfaces due to exposure to ambient is eliminated prior to analysis with a monochromated XPS system (energy resolution $< 0.7\ \text{eV}$). Furthermore, the need for ion-etching for the removal of the contaminated layers prior to XPS analysis is also eliminated allowing for the direct access to pristine film surface.

Our results regarding B-C-N films indicated findings contrary to our earlier *ex situ* findings. XPS, Raman and FTIR data from depositions carried out under *ex situ* conditions suggested increasing the substrate bias and/or increasing N_2 flow rate during depositions triggered formation of an hexagonal network of well defined separate B-N and C-C dominated domains. This is generally considered as an evidence for phase segregation. On the other hand, *in situ* characterization of B-C-N films deposited with comparable deposition parameters in the multi-chamber system suggested the evidence of a significant C-N bonding component. In some cases, nitrogen coordinated carbon amount is even found to be more than carbon-carbon coordination.

Overall, we have encountered enough evidence to suggest that the local coordination of atoms in B-C-N films deposited in the UHV chamber and analyzed *in situ* are notably different than B-C-N films deposited in a HV chamber and analyzed *ex situ*. While our investigations are ongoing to uncover the possible root causes, we would like to raise the question regarding whether residual gases in a chamber is a significant player in defining the final chemistry and structure such as the long standing case of c-BN deposition.

Symposium TS Poster Session

Room: Golden Ballroom - Session TSP

TS Poster Session

TSP-1 A route to strong p-doping of epitaxial graphene on SiC. U. Schwingenschlögl (udo.schwingenschloegl@kaust.edu.sa), Y.C. Cheng, N. Singh, KAUST, Saudi Arabia

Epitaxial graphene on SiC shows n-type behavior due to interaction with the SiC substrate. However, for metal-oxide-semiconductor applications, it is important to induce p-type doping in graphene. Recent work has shown that an Au layer deposited on a graphene monolayer (GML) develops into an

intercalation layer between the GML and the Si-terminated SiC substrate when the system is annealed at 800°C for 5 min [1]. Within the GML, a p-doping effect is observed. Furthermore, it has been reported that by controlling the Au coverage level GMLs ranging from strongly n-doped to weakly p-doped can be formed [2]. However, it is still a problem to achieve a strongly p-doped GML by intercalation of an Au layer.

Using first principles calculations, we study the effect of Au intercalation on the electronic properties of epitaxial graphene grown on SiC substrates [3]. A GML on SiC restores the shape of the pristine graphene dispersion, where doping levels between strongly n-doped and weakly p-doped can be achieved by altering the Au coverage. In addition, we predict that Au intercalation between the two C layers of bilayer graphene grown on SiC makes it possible to achieve a strongly p-doped graphene state, where the p-doping is controlled the Au coverage.

References:

[1] B. Premal, M. Cranney, F. Vonau, D. Aubel, D. Casterman, M. M. De Souza, and L. Simon, *Appl. Phys. Lett.* 94, 263115 (2009).

[2] I. Gierz, T. Suzuki, R. T. Weitz, D. S. Lee, B. Krauss, C. Riedl, U. Starke, H. Hochst, J. H. Smet, C. R. Ast, and K. Kern, *Phys. Rev. B* 81, 235408 (2010).

[3] Y. C. Cheng and U. Schwingenschlögl, *Appl. Phys. Lett.* 97, 193304 (2010).

TSP-2 Nitrogen Introduced at Interface to Improve Resistance Switching Characteristics with SiGeO_x RRAM Device, Y.E. Syu (*syuyongen@gmail.com*), National Sun Yat-Sen University, Taiwan, G.W. Chang, National Chiao Tung University, Taiwan

In this study, the SiGeO_x film was taken as the resistive switching layer in Pt/SiGeO_x/TiN memory cells because germanium and silicon are extremely compatible with the prevalent complementary metal oxide semiconductor (CMOS) process. To enhance memory switching parameters, a compatible SiGeON layer between SiGeO_x and TiN is proposed to control the disruption length of filaments. Compared with Pt/SiGeO_x/TiN memory cells, the proposed Pt/SiGeO_x/SiGeON/TiN cells is effective improvement the characteristics of memory switching parameters including excellent characteristic with good endurance of more than 10⁷ times, long retention time of 10⁴ s in 125°C and more stable in resistance switching state. Because the nitrogen introduced can effective minimize the dispersions of oxygen. It is a simple method to enhance the resistance switching parameters which introduce only the gas of ammonia in the manufacturing process. The most merit of this method is that the bi-layer structure is composed of the unitary material.

TSP-3 Electroluminescence of ZnO nanocrystal in sputtered ZnO-SiO₂ nanocomposite light-emitting devices, J.T. Chen (*L7897106@mail.ncku.edu.tw*), National Cheng Kung University, Taiwan, W.C. Lai, J.K. Sheu, Y.Y. Yang, Unaffiliated

Recently, nanoscale materials have attracted considerable attention in the past few years due to their features and potential applications in various areas. ZnO nanoparticles are of great interest because of their three-dimensional quantum confinement, which strongly enhances the excitation radiative recombination. Nanoscale or submicron-sized ZnO materials have also been synthesized through various methods, such as sol-gel coating, sputtering technique, atomic layer deposition etc. In this study, we using a cosputtering technique to deposit ZnO-SiO₂ nanocomposite layer, the structure of ZnO nanoclusters embedded in the nanocomposite matrix can be fabricated. The sizes of the ZnO nanoclusters distributed from 2 to 7 nm in the ZnO-SiO₂ nanocomposite layer were examined using a high resolution transmission electron microscope (HRTEM). The mechanism of the electroluminescence emission peak at 376 and 427 nm from the Ga:ZnO/i-ZnO-SiO₂ nanocomposite/p-GaN n-i-p heterostructured light-emitting devices (LEDs) were attributed to the radiative recombination occurred from the ZnO clusters and the Mg acceptor levels in the p-GaN layer.

Key words: electroluminescence; ZnO-SiO₂ nanocomposite; light-emitting devices (LEDs); ZnO nanoclusters; sputtering

TSP-4 Sampling the local structure in γ-Al₂O₃ by XPS analysis of embedded Argon, M. Prenzel (*marina.prenzel@rub.de*), A. Rastgoo Lahrood, A. Kortmann, T. de los Arcos, A. von Keudell, Ruhr Universität Bochum, Germany

X-ray Photoelectron Spectroscopy (XPS) is a widely used technique for the chemical characterization of surfaces. In this work we would like to present evidence that XPS characterization of the Argon gas trapped within an oxide film deposited by magnetron sputtering can be used to determine the presence or absence of crystalline structure within the film.

It is known that, during sputter deposition, a certain percentage of noble gas can be trapped within the growing film. Although these embedded gases are not expected to interact chemically with their environment, their electronic structure has been shown to react to the characteristics of their host. The shifts in binding energy and their correlation to material characteristics can be successfully determined using XPS, particularly in metallic and semiconducting materials [1]. In the case of insulating materials, however, the interpretation of the energy shifts in core levels has not been so thoroughly investigated.

Aluminium oxide films were deposited by RF magnetron sputtering, driven by 13.56 MHz and 71 MHz. The films were deposited under different biasing and temperature conditions to ensure varying degrees of crystallinity, and characterized by X-ray diffraction. The Ar2p core level of the embedded Argon atoms was investigated by XPS.

In totally amorphous samples, the Ar2p peak was fitted using a single component at ~242 eV. However, in the cases of films with γ-crystalline phases, the Ar2p peak needed to be fitted with two different components at ~241 eV and ~242 eV, respectively. In order to confirm the association of the lower binding energy component to the crystalline phase, the samples were bombarded in-situ with Neon ions to destroy the crystallinity of the film without introducing additional Argon. The in-situ sputtering with Neon of crystalline samples resulted in the disappearance of the lower BE component in the Ar2p signal. This indicates that the embedded noble gas has the potential to provide a fingerprint for crystallinity that can be used during standard XPS characterization of the films.

The work is funded by DFG within SFB-TR 87.

[1] A. Rastgoo Lahrood *et al.* *Thin Solid Films* 520 (2011) 1625-1630

TSP-5 Deposition, Microstructure and Mechanical Properties of Mo-doped CeO₂ Films Prepared by Pulsed Unbalanced Magnetron Sputtering, I.W. Park (*ipark@mines.edu*), J. Moore, J. Lin, Colorado School of Mines, US, D. Hurley, M. Khafizov, Idaho National Laboratory, US, A. El-Azab, Florida State University, Florida, US, T. Allen, C. Yablinsky, M. Gupta, University of Wisconsin, Wisconsin, J. Gan, Idaho National Laboratory, US, M. Manuel, H. Henderson, B. Valderrama, University of Florida, US

A fission-reactor fuel assembly typically contains ceramic components (the fuel itself) and metallic components (the cladding that isolates the radioactive fuel from the coolant). The cumulative effect from fission-damage processes, high temperatures, and high thermal gradients is to cause severe degradation in the thermal and mechanical properties of the fuel assembly, limiting its lifetime and strongly affecting operational cost. In this work, metallic Mo was doped into the CeO₂ base materials to investigate the relationship between microstructural changes and mechanical properties of Ce-Mo-O films. The films were deposited on silicon wafer substrates in argon-oxygen atmosphere using pulsed unbalanced magnetron sputtering (P-UBMS) from pure Ce and Mo targets with a substrate heating capability system. The crystallinity of the samples was characterized by x-ray diffraction (XRD, PHILIPS, X'pert-MPD) using CuKα radiation. X-ray photoelectron spectroscopy (XPS, PHI XPS System, 5600LS) using a monochromatic Al source was also performed to determine the contents of Ce, Mo and O and to observe the bonding status of the annealed ceria samples. A MTS nano-indenter equipped with Berkovich diamond indenter will be used to perform depth sensing nanoindentation testing on the annealed Ce-Mo-O films and to obtain mechanical values of nanohardness and Young's modulus with a Poisson's ratio of 0.25.

TSP-6 Effect of stress on the electrical bistability of poly N-vinylcarbazole films, J.C. Wang, Y.S. Lai (*yslai@nuu.edu.tw*), National United University, Taiwan

In this work, the bistable switching of resistance memory devices on a flexible substrate is investigated. PVK films are deposited by spin coating on a polyethylene terephthalate (PET) substrate. The Al bottom and top electrodes are patterned through a hard mask to form an Al/PVK/Al/PET structure. The bending stress (i.e., tensile or compressive) and cyclic bending deformation are carried out to study the bistable switching of the device. The operation voltage and stability of memory states (retention) are also examined. The connection between the bistable behavior and material properties is also demonstrated.

TSP-7 Thin Film Bond and Mass Density Measurements Using Fourier Transform Infrared Spectroscopy, S. King (*sean.king@intel.com*), Intel Corporation, US

Fourier Transform Infrared (FTIR) Spectroscopy has long been utilized as an analytical technique for qualitatively determining the presence of various different chemical bonds in gases, liquids, and thin dielectric films. In some cases, quantitative measurements of the concentration or density of different

chemical bonds have also been achieved utilizing FTIR via cross calibration with other techniques. In this talk, we will demonstrate that transmission FTIR can be, in certain instances, further extended to quantitatively determine the full chemical bonding in a dielectric thin film. In turn, knowledge of the full bond concentrations allows accurate determination of the mass density and full elemental composition of the film. This capability is demonstrated for a-SiC:H thin films deposited by plasma enhanced chemical vapor deposition (PECVD). The resulting FTIR mass density and compositional analysis determined by this technique shows an excellent correlation to similar measurements by X-ray Reflectivity, X-ray Photoelectron Spectroscopy, and Scanning Ion Mass Spectroscopy Techniques.

TSP-8 Ordered thin film materials with ultra-low thermal conductivity. *C. Muratore* (chris.muratore@wpafb.af.mil), Air Force Research Laboratory, Thermal Sciences and Materials Branch, US, *V. Varshney*, UTC/Air Force Research Laboratory, Thermal Sciences and Materials Branch, US, *J.J. Gengler*, Air Force Research Laboratory, Thermal Sciences and Materials Branch, US, *J.J. Hu*, UDRI/Air Force Research Laboratory, Thermal Sciences and Materials Branch, US, *T.S. Smith*, Air Force Research Laboratory, Thermal Sciences and Materials Branch, US, *J.E. Bultman*, UDRI/Air Force Research Laboratory, Thermal Sciences and Materials Branch, US, *A. Voevodin*, Air Force Research Laboratory, Thermal Sciences and Materials Branch, US

Transition metal dichalcogenide (TMD) crystals are characterized by their distinct layered atomic structures, with strong covalent bonds comprising each layer, but weak van der Waals forces holding the layers together. The relationship between chemical bonding in a material and its thermal conductivity (k) is well-known, however the thermal properties of TMD thin films with such highly anisotropic chemical bonds have only recently been investigated with remarkable results, such as ultra-low k_z . Materials with very low thermal conductivity in the z-axis, but higher k_x and k_y have potential as next-generation thermal barrier or heat spreading materials. Molecular dynamics (MD) simulations predicted $k_x=k_y=4k_z$ for perfect TMD crystals (MoS_2 in this case). Experiments to determine $k_{x,y}$ and k_z were conducted by developing processes to grow crystalline TMD thin film materials with strong (002) (basal planes parallel to surface) or (100) (perpendicular basal planes) preferred orientation. Initially, no correlation between structure and thermal conductivity was apparent, as water intercalation and reactivity to ambient air resulted in a thermal “short-circuit” across basal planes, such that the time between deposition and k measurement had a stronger impact on thermal conductivity than film orientation. Experiments to measure intrinsic thermal conductivity of MoS_2 revealed values approximately one order of magnitude lower than those predicted using MD simulations, however, measurement of $k_x=k_y=4k_z$ was consistent with simulation results. Simulations to evaluate the dependence of thermal conductivity on grain size was evaluated, which correlated well to measured values. Comparison of measured k values for strongly (002) oriented MoS_2 , WS_2 , WSe_2 and other materials with analogous crystal structures are discussed in the context of the Slack Law, which accounts for intrinsic physical properties of the crystal, but not film microstructure.

TSP-9 Texture change and off-axis accommodation through film thickness in fcc structured nitrides. *A. Karimi*, *A. Shetty* (akshath.shetty@epfl.ch), EPFL, Switzerland

The control of texture in fcc nitride coatings by varying the film thickness was demonstrated on polycrystalline TiAlN coatings grown by pulsed DC magnetron sputtering. Development of off-axis texture with film thickness was observed. For this purpose the evolution of texture versus thickness was studied by a set of analytical x-ray diffraction (XRD) methods like θ - 2θ and pole figures, while scanning electron microscopy (SEM) and transmission electron microscopy (TEM) were used to observe the microstructure and changes in texture with thickness. The stresses along the (111) and (002) orientation were obtained by $\sin^2\psi$ method. Based on the results obtained, the texture formation mechanism is divided in three different stages of film growth. Films at low thickness lead to the development of (002) orientation due to the surface energy minimization. Meanwhile, the competitive growth promotes the growth of (111) planes parallel to film surface at higher thickness. However, contrary to the prediction of growth models, the (002) grains are not completely overlapped by (111) grains at higher thickness. Rather the (002) grains still constitute the surface, but are tilted away from the substrate normal showing substantial in-plane alignment to allow the (111) planes remain parallel to film surface. Intrinsic stress along (111) and (002) shows a strong dependence with preferred orientation. The stress level in (002) grains which was compressive at low thickness changes to tensile at higher thickness. This change in the nature of stress allows the (002) planes to tilt away in order to promote the growth of $\langle 111 \rangle$ parallel to film normal and to minimize the overall energy of system due to high compressive stress stored in the (111) grains. The change in surface morphology with thickness

was observed using SEM. An increase in surface roughness with film thickness was observed which indicates the development of (111) texture parallel to film surface. TEM observations support the XRD results regarding texture change. Film hardness was measured by nanoindentation and a correlation between (111) texture, stress and hardness is obtained. The results indicate that texture development is a complex interplay between thermodynamic and kinetic forces. An attempt is made to understand this phenomenon of off-axis accommodation of (002) at higher thicknesses, which is a new result not reported previously.

Hard Coatings and Vapor Deposition Technology Room: Royal Palm 4-6 - Session B3-1

Ion-Surface Interactions in Film Growth and Post-Growth Processes

Moderator: S. Fairchild, Air Force Research Laboratory, US, K. Sarakinos, Linköping University, Sweden

8:00am **B3-1-1 Tantalum Based Coatings Deposited by Pulsed DC Magnetron Sputtering and Highly Ionized Pulse Plasma Processes**, J. Barriga (*jbarriga@tekniker.es*), L. Mendizabal, U. Ruiz de Gopegui, R. Bayon, Tekniker, Spain

Transition metals and their nitrides are widely used in the industry as protective coatings because of their excellent tribological properties. Among them, tantalum (Ta) demonstrated to provide high wear protection [1] as well good corrosion resistance and biocompatibility [2]. However, there are only a few studies up to date about tribological analysis of coatings based on this metal. This could be due to the difficulty in evaporating Ta in Physical Vapor Deposition systems because its relatively low thermal and electrical conductivity and high fusion temperature.

In this work three different evaporation techniques are used and compared. All of them are varieties of Magnetron Sputtering: pulsed DC, HiPIMS (High Power Impulse MS) and MPP (Modulated Power Pulse). With these last two techniques there is a potential improvement on coating quality because during the evaporation process we have peaks of high power density increasing the ionization, density of the coating, adhesion and wear resistance [3].

We have seen that high power techniques (HiPIMS and MPP) enhance the hardness of TaN coatings compared to conventional Pulsed DC MS. The interface TaN with stainless steel is denser with MPP technique and better adhesion of the coating is achieved. In corrosion tests all samples show passive behavior and low corrosion currents in the anodic branch. TaN by HiPIMS showed the highest corrosion resistance which increased when increasing the immersion time due to its denser microstructure and the stable electrochemical behavior of its passive film formed in PBS solution.

[1] J. Esteve, E. Martínez, A. Lousa, F. Montalà, L.L. Carreras, "Microtribological characterization of group V and VI metal-carbide wear-resistant coatings effective in the metal casting industry", *Surf. Coat. Technol.* 133–134 (2000) 314–318.

[2] J. Black, "Biological performance of tantalum". *Clin. Mater.* 16 (3): 167–173. (1994). doi:10.1016/0267-6605(94)90113-9.

[3] A.P. Ehasarian, book chapter: "Fundamentals and Applications of High Power Impulse Magnetron Sputtering", *Plasma Surface Engineering Research and its Practical Applications*, p. 35 – 86 (2007), ISBN 978-81-308-0257-2.

8:20am **B3-1-2 Studies on plasma immersion ion implantation of nitrogen on titanium**, K. R. M. Rao (*rammohanrao.k@gmail.com*), Department of Engineering Chemistry, GITAM Institute of Technology, GITAM University, India, E. Richter, Institute of Ion Beam Physics for Materials Research, Helmholtz-Zentrum Dresden-Rossendorf, Germany, S. Mukherjee, FCIPT, Institute of Plasma Research, India, I. Manna, Central Glass and Ceramic Research Institute, India

Abstract

Formation of titanium nitride layer by following plasma immersion ion implantation (PIII) has been investigated at variable energies. For PIII experiments, square shaped commercially pure Ti samples of 1 mm thickness and 100 mm² area were mirror polished by standard metallographic techniques using 10-0.1 µm sized diamond paste. PIII was performed at variable negative bias without auxiliary heating. PIII chamber was first evacuated to 2×10^{-3} Pa, then back filled with dehumidified N₂ gas to 0.4 Pa pressure. Nitrogen plasma was created by a radio frequency (13.56 MHz) coupled generator operated at 400 W. N₂⁺ ion implantation from this RF coupled N₂⁺ with 10^{21} ions/m² was carried out at variable energy.

Post implanted specimens were examined by X-ray diffraction (XRD) and Scanning Electron Microscope (SEM) for phase analysis and surface topography respectively. X-ray diffraction (GAXRD) using Cu-*ka* radiation (0.154 nm). All of them reflected the signature of the usual peaks of Ti along with TiN₁₁₁. The volume fraction of TiN seems to be directly related to the implantation voltage.

Moreover, the surface modified samples were exposed to Hank's solution as the corrosive medium for the assessment of corrosion resistance properties.

These samples were subjected to potentiodynamic polarization tests at 1 mV/sec scan rate and compared with respect to their polarization characteristics. Since TiN phase has been found in almost all the treatment conditions the enhancement in corrosion resistance may be attributed to the presence of titanium nitride covered on the surface layer.

It has also been found that the corrosion resistance was higher at higher implantation voltage. The best condition of PIII for the corrosion resistance in Hank's solution was found to be at a dose 2.4×10^{21} ions/m².

8:40am **B3-1-3 On the role of ions during reactive magnetron sputtering**, D. Depla (*Diederik.Depla@ugent.be*), Ghent University, Belgium **INVITED**

Ions play an prominent role during reactive magnetron sputtering. Their influence can be quite explicit as for example when a substrate bias is applied during thin film growth. However, ions can also play a more hidden role. This paper aims to give an overview of the different processes in which ions play a key role.

The first, and most obvious during magnetron sputtering, is of course the sputter process as such. Although it seems straightforward to describe this, fundamental issues as the angular emission profile, compound sputter yield hampers a quantitative description of the deposition profile, and therefore the deposition rate at the substrate[1].

A similar question exists about the role of ions during the sustaining mechanism of the magnetron discharges. In recent years, substantial progress has been in the understanding of the behaviour of the electron emission yield when oxidizing the target[2]. As the latter behaviour also influences the emission of negative oxygen ions, a good understanding is needed because high energetic negative oxygen ions affect in an important way thin film growth. A few examples of this behaviour will be given[3].

As the ions bombard the target, they also become implanted. For inert gas atoms, their influence is minor. However, reactive ion implantation is an important pathway in the poisoning mechanism during reactive magnetron sputtering[4]. The paper will discuss the latest trends in the modelling of this process.

Finally, ions can be used as a tool to influence the thin film growth. As they are charged species, their energy can easily be influenced by biasing the substrate. Moreover, they can also be guided towards the substrate. This approach becomes even more interesting when most of the metal species are ionized as in HIPIMS plasmas. However, when studying thin film growth, one must realize that not only the ions are important, and other species play also their role. This will be discussed in the context of the characterisation of the different particle fluxes from the plasma towards the substrate [5].

[1] F Boydens, W P Leroy, R Persoons and D Depla, Submitting for publication to *Physica status Solidi a*

[2] D Depla, S Mahieu, R.De Gryse, *Thin Solid Films* 517 (2009) 2825

[3] S Mahieu, WP Leroy, K Van Aeken, D Depla, *JAP* 106 (2009) 093302

[4] D. Depla, X. Y. Li, S. Mahieu, K. Van Aeken, W. P. Leroy, J. Haemers, R. De Gryse, A. Bogaerts, *JAP* 107 (2010) 0113307

[5] S Mahieu, WP Leroy, K Van Aeken, M Wolter, J Colaoux, S Lucas, G Abadias, P Matthys, D Depla, *Solar Energy* 85 (2011) 538

9:20am **B3-1-5 In situ characterization of plasma-surface interactions with a quartz crystal microbalance**, C. Corbella (*carles.corbella@rub.de*), O. Kreiter, S. Grosse-Kreul, Ruhr Universität Bochum, Germany, D. Marinov, Ecole Polytechnique, France, T. de los Arcos, A. von Keudell, Ruhr Universität Bochum, Germany

Particle beam experiments were conducted in an ultra-high-vacuum (UHV) vessel and monitored in real time by means of a quartz crystal microbalance (QCM). Several atom and ion guns were focused to the QCM and sent controlled fluxes of particle beams constituted by different elements. The UHV was achieved by using a turbomolecular pump in combination with an ion-getter-pump. First, the study of ion-enhanced oxidation of aluminium targets during reactive magnetron sputtering was performed by bombarding an Al-coated QCM with argon ions and oxygen atoms. An effusion cell provided Al vapour to restore the metallicity of the QCM. Second, beams of argon ions, together with oxygen and hydrogen species, were used to investigate the chemical sputtering of diamond-like carbon (DLC) films during plasma etching processes. For this purpose, we deposited DLC thin films on the QCM. Finally, remote plasmas interacted with the QCM to promote the physisorption/chemisorption of nitrogen atoms on SiO₂ surfaces. The treated surfaces were studied by X-ray photoelectron spectroscopy (XPS). These experiments shed some light into fundamental plasma-surface processes taking place in industrial plasma applications.

9:40am **B3-1-6 Compressive stress generation and atom incorporation during growth of low-mobility materials**, **G. Abadias** (gregory.abadias@univ-poitiers.fr), A. Fillon, A. Michel, C. Jaouen, Institut P² - Université de Poitiers, France

The incorporation of growth-induced defects from energetic deposited particles during sputter-deposition, known as the “atomic peening” effect, is revisited in low-mobility material thin films by combining *in situ* and real-time wafer curvature and *ex situ* X-ray diffraction techniques.

A series of metastable $\text{Mo}_{1-x}\text{Si}_x$ solid solution films were deposited by magnetron sputtering at low pressure (0.12 Pa) in Ar plasma discharge onto crystalline (110) Mo template layers. Unbalanced magnetron configuration and substrate bias voltages up to -120V were used to increase the contribution of energetic ions to the total deposited energy. The stress evolution was monitored in real-time using a multiple-beam optical stress sensor (MOSS) designed by kSA and implemented in the deposition chamber. The stress-field was determined from XRD using the $\sin^2\psi$ technique adapted for the case of textured/epitaxial layers. Post-growth ion irradiation using 310 keV Ar^+ ions at low dose (< 0.2 dpa) were carried out to identify the nature of point-defects and associated stress field.

Compressive stress evolution due to atomic peening is observable only above a first critical energy threshold. The stress-field appears in that case fully biaxial. Grain-size dependence of stress confirms that defect creation is confined to the grain boundaries. Further increase of the deposited energy, above a second threshold, results in the creation of additional volume defects inside the grains, i.e. expansion of the unit cell. Examination of $\sin^2\psi$ plots evolution on irradiated films shows that defects incorporated in the grain boundaries are stable, while those created inside the grain are highly unstable.

In a deposited-energy/composition space diagram, these thresholds depict the existence of biaxial or hydrostatic stress domains related to these two distinct defect creation mechanisms. The strong variation of the critical energy thresholds with the Si content points out the sensitivity of defects creation to the intrinsic properties of the material.

10:00am **B3-1-7 Variation of substrate biasing and temperature and their influence on the crystal orientation of $\gamma\text{-Al}_2\text{O}_3$ films**, **M. Prenzler** (marina.prenzler@rub.de), A. Kortmann, A. von Keudell, Ruhr Universität Bochum, Germany

Temperature and substrate bias play a key role in the structural evolution of aluminium oxide (Al_2O_3) during the deposition process. On the one hand, crystallinity depends on the mobility of the particles in the growing film, which is influenced by the substrate temperature. On the other hand, correct tailoring of the substrate bias allows to selectively control the energy distribution function of the ions impinging on the substrate (IEDF). Thus, film characteristics such as hardness, adhesion, crystallinity, or wear resistance can be controlled. In this work, manipulation of the substrate bias is performed by variation of the frequency, amplitude and shape of the applied bias signal. We will show how different bias functions affect the shape of the IEDF while keeping the mean energy constant at 55 eV, and how this in turn has a clear influence on the crystallinity of the film.

The films are deposited in a RF magnetron discharge, driven by 13.56 MHz and 71 MHz. The target is mounted on the powered electrode and a silicon substrate is placed on a biased electrode at the opposite side.

Our previous experiments have already shown a preferred orientation in the film when using a rectangular pulsed bias with 1 MHz frequency and an on-time of 5 μs . Here, we will present a thorough investigation of how variations in frequency and duty cycle in the bias signal affect the IEDF and film properties for constant mean energy and an on-time of 5 μs . Additionally, the influence of growth temperature (500 °C, 550 °C and 600 °C) will be shown.

Film characterization is performed using FTIR and XRD to determine the orientation/crystallinity of the films. The measurements are correlated with the measured and simulated IEDFs in each case. We will show how the tailoring of the IEDF through bias shape manipulation is excellent tool for controlling film structure.

The work is funded by DFG within SFB-TR 87.

10:20am **B3-1-8 High-Voltage Positive Nanopulse Assisted Hot-Filament CVD Diamond Growth**, **M. Takashima**, **N. Ohtake** (ohtaken@mech.titech.ac.jp), Tokyo Institute of Technology, Japan

In this study, extremely short pulse, whose pulse width was about 50 ns and called “nanopulse”, assisted hot-filament chemical vapor deposition method was used for the diamond synthesis, and depositions at low substrate temperature below 500 °C were attempted decreasing filament temperature and using high-voltage nanopulse assist. In addition, characteristics of nanopulse plasma were investigated through optical emission spectroscopy (OES) analysis as well as time resolved optical emission spectroscopy (TROES) analysis. Spectrometer used was special and the time resolution of

10 ns was enough to trace nanopulse plasma and investigate the effects of nanopulse on diamond growth.

As a result, we had succeed in depositing diamond at the substrate temperature of 400 °C using 1500 °C filament and high-voltage nanopulse assist. Moreover, according to OES and TROES measurements of nanopulse plasma, the relations between diamond properties and deposition conditions were found. Atomic hydrogen played an important role on diamond growth and the diamond was able to be deposited with sufficient concentration of CH radicals at the afterglow of nanopulse plasma.

Coatings for Biomedical and Healthcare Applications Room: Sunset - Session D2-1

Coatings for Biomedical Implants

Moderator: R. Hauert, Empa, Switzerland, J. Piascik, RTI International, US

8:00am **D2-1-1 Functional plasma polymer films engineered at the nanoscale for biomaterial applications**, **K. Vasilev** (krasimir.vasilev@unisa.edu.au), University of South Australia, Australia
INVITED

Functional coatings presenting a variety of functional chemical groups can be readily prepared by plasma polymerisation in an easy one-step process. Applications of such films span over a range of fields from modification of biomaterials to protective coatings.

In my talk, I will present recent developments from our group on various biomaterial coatings prepared by plasma polymerisation which include chemical and biomolecular gradients, and antibacterial coatings based on silver nanoparticles and conventional antibiotics.

Surface gradients have become important tools for studying and guiding cellular responses such as migration, adhesion, differentiation, etc. We generate gradients of various surface chemistries via plasma co-polymerisation over a moving mask. We used these chemical gradients to direct differentiation of kidney (KSC) and embryonic stem cells. We found that KSC express proximal tubule markers at medium amine group surface concentration and adapt a podocyte-like morphology at high. We extended these surface chemical gradients to density gradients of bound ligands, proteins and nanoparticles. We developed gradients of two proteins because gradients of single protein (employed in cell studies up to now) are probably too simplistic to mimic natural biological processes. We also developed density gradients of nanoparticles to use as a tool to study the effect of nanoscale surface features on cell behaviour.

Antibacterial coatings are important for many biomedical applications. We developed unique coatings based on silver nanoparticles which allow control over the rate of release of silver ions. As we show, the rate of silver release can be tuned such that it allows normal adhesion and spreading of mammalian cell and preserves the antibacterial properties of the coatings. We also developed two platforms for release of conventional antibiotics such as vancomycin and levofloxacin. Delicate control over the rate of release was achieved by a plasma polymer overlayer of a controlled thickness.

References:

- K. Vasilev et al “Tunable antibacterial coatings that support mammalian cell growth” *Nano Lett* 10 (1), 202–207 (2010)
- K. Vasilev et al “A PEG-density gradient to control protein binding: creating gradients of two proteins”, *Biomaterials* 31, 392–397 (2010)
- S. Simovic, D. Losic and K. Vasilev “Controlled drug release from mesoporous materials by plasma polymer deposition” *Chem Commun* 46, 1317–1319 (2010)
- R.V. Goreham, R. D. Short and K. Vasilev “A Novel Method for the Generation of Surface-Bound Nanoparticle Density Gradients” *J Phys Chem C* 115 (8), 3429–3433 (2011)

8:40am **D2-1-3 Effect of the surface atom ordering on the protein adsorption**, **P. Silva-Bermudez** (surriel21@yahoo.com), L. Huerta, S.E. Rodil, Instituto de Investigaciones en Materiales, Universidad Nacional Autónoma de México, México

The study of the protein adsorption is relevant to understand the interactions biological media–foreign material since the adsorbed protein layer on the material surface mediates the interactions cell-material, greatly determining the biological response. The protein adsorption on solid surfaces is mainly driven by the surface properties; different studies have shown that properties such as hydrophobicity or roughness influence protein adsorption. Also, certain crystalline phases of a material have been

mentioned as to induce a more biocompatible response than other crystalline or amorphous phases of the same material. However, this is not fully understood and more studies are needed to get a deeper understanding of the processes occurring when surfaces of the same material but with different atom ordering interact with biological media.

In the present study titanium oxide, a potential material for biocompatible coatings for orthopaedic and dental implants, was chosen as the model material to study the influence of surface atom ordering on protein adsorption. Albumin (BSA) and Fibrinogen (Fib) were chosen as the model proteins. Quasi-amorphous and polycrystalline titanium oxide thin films (qa-TiO₂ and pc-TiO₂) were deposited on Si(100) substrates by Reactive Magnetron Sputtering. The atom ordering, wettability, surface energy, roughness, optical properties and chemical composition of the films were characterized. The films were immersed in BSA and Fib solutions and the protein adsorption was studied in-situ using dynamic and spectroscopic ellipsometry. Then, after 2400 s of immersion the adsorbed protein layer was studied ex-situ in a dried ambient using Atomic Force Microscopy and X-Ray Photoelectron Spectroscopy (XPS).

The results showed that the film roughness decreased with atom ordering; however, their water contact angle increased from 74° for qa-TiO₂ to 85° for pc-TiO₂. For both proteins a higher adsorption rate was observed on pc-TiO₂ characterized for a total Δ change 3 degrees higher compared to that one for qa-TiO₂. The surface mass density of the adsorbed protein layer was higher on pc-TiO₂. The N at. % calculated from XPS after protein adsorption evidenced a slightly higher protein adsorption on pc-TiO₂; for BSA adsorption on pc-TiO₂ the N at. % was \approx 5.3 while on qa-TiO₂ it was \approx 4.7%. For Fib adsorption the difference was more notorious with a N at. % \approx 8.2 on qa-TiO₂ and \approx 28% on pc-TiO₂. The Differences observed in the protein adsorption on the two films might be related to the changes in the films hydrophobicity induced by the different surface atom ordering.

Acknowledgments to the financial funding from the CONACyT project # 152995

9:00am **D2-1-4 Nanodiamond/DLC Composite Coating Deposited on Ti6Al4V for Orthopaedic Joint Applications.** C. Zhang, Q. Yang (qiaolin.yang@usask.ca), Y. Tang, Y. Li, University of Saskatchewan, Canada

Researches show that 90% of the population over the age of 40 suffers from some degree of degenerative joint disease. Surgeries to repair or replace damaged joints are increasingly needed in recent years. However, current artificial joints made of Ti6Al4V have limited service lifetime due to their low wear resistance. The debris caused by wear results in tissue inflammation, osteolysis, and loosening of the implants, which is the main failure mechanism of artificial joints. Diamond-like carbon (DLC) coatings exhibit low friction coefficient, high wear resistance, and excellent biocompatibility and thus they are very promising protective coatings for artificial joints to prolong their service lifetime. However, DLC often suffers from high internal stress and poor adhesion on Ti6Al4V due to their thermal expansion mismatch.

In this research, nanodiamond/DLC composite coatings were deposited on Ti6Al4V substrates. Initially, nanocrystalline diamond particles were deposited on Ti6Al4V substrates by microwave plasma enhanced chemical vapor deposition to enhance adhesion and wear resistance of DLC. DLC thin film was then deposited on the predeposited substrate by ion beam deposition. Scanning electron microscopy, Raman spectroscopy and X-ray diffraction were used to characterize the microstructure of the Diamond/DLC composite. Nanoindentation and scratch tests were used to study the hardness and adhesion property of the films. The friction and wear tests were conducted using both ball- and pin- on-disc techniques. The results show that the nanocrystalline diamond particles can significantly enhance the adhesion between DLC thin film and Ti6Al4V substrate as well as the hardness and wear resistance of DLC.

9:20am **D2-1-5 Effects of argon plasma treatment on controlling the drug release rate from biocompatible polymers.** K. Hagiwara, Keio University, Japan, T. Hasebe, Toho University Sakura Medical center, Japan, T. Suzuki, A. Hotta (hotta@mech.keio.ac.jp), Keio University, Japan
Argon plasma surface treatment was introduced for the modification of the surface of drug-eluting stent (DES) coated with polymers in order to prevent the initial burst release of the drug. Currently, the implantation of DES is the most powerful way to treat coronary artery disease. DES elutes anti-proliferative drugs that suppress the proliferation of smooth muscle cells in the stented segment of the artery. Despite the impressive reduction in restenosis, DES still has a disadvantage for not preventing restenosis at the implant site due to the relatively vast drug release from the stent surface in the early stage of the release.

To solve the problem, we focused on argon plasma treatment. Argon gas is an inert gas without the risk of damaging the surface of the stent by surface treatment. In this experiment, polymers were used as drug-reservoir

materials, where it was necessary to achieve the controllable and sustainable drug release from the polymers. Three biocompatible polymer films were selected as base drug-reservoir materials: hydrophilic 2-metacryloyloxyethyl phosphorylcholine (MPC), hydrophobic poly (ethylene-co-vinyl acetate) (EVA), and less hydrophobic polyurethane (PU). Structural analyses were carried out using scanning electron microscopy (SEM), atomic force microscopy (AFM), water contact angle measurements, and X-ray photon spectroscopy (XPS). By changing processing time of argon plasma from 5 sec to 45 sec, it was found that the initial burst release of drug, especially with EVA and PU films, was suppressed. These experimental results of the plasma treatment could provide a new and alternative approach to a controllable and sustainable drug release system.

9:40am **D2-1-6 In vitro biological response of plasma electrolytically oxidised and sprayed hydroxyapatite coatings on Ti6Al4V alloy.** W. Yeung, A. Yerokhin (A.Yerokhin@sheffield.ac.uk), G. Reilly, A. Matthews, University of Sheffield, UK

Plasma electrolytic oxidation (PEO) is a new branch of surface modification to attain bioactivity of Ti alloy implants, compared to conventional plasma spray method. Enhanced interfacial bonding between the PEO coating and the metal substrate reduces risk of coating delamination, which is highly desired for long term orthopaedic implants. The aim of this study is compare surface characteristics and biological effects of PEO and plasma spray coatings on human osteosarcoma cells (MG-63). The coating characteristics were examined by XRD, EDX, SEM, surface profilometry and wettability tests. The biological properties were determined by cell viability, calcium and collagen synthesis assays. PEO coatings showed a different morphology than the plasma sprayed coating. The results show that the PEO coatings are more hydrophilic and have a lower surface roughness than the plasma sprayed coating. At the same time, cellular behaviour is strongly dependent on the phase composition and surface distribution of elements in the PEO coatings. Thus MG-63 cell viability for the TiO₂-based PEO coating containing amorphous calcium phosphates it is significantly less than that for the coating containing crystalline hydroxyapatite as well as for the plasma sprayed coating. However, the collagen synthesis on both PEO coatings is significantly higher than the plasma sprayed coating after 14 days.

10:00am **D2-1-7 Biocompatibility and Anti-Microbial Properties of Silver Modified Amorphous Carbon Films.** A. Almaguer-Flores, Universidad Nacional Autónoma de México, Mexico, R. Olivares-Navarrete, Georgia Tech, US, G. Ramirez, Universidad Nacional Autónoma de México, Mexico, S.E. Rodil (ser42@iim.unam.mx), Universidad Nacional Autónoma de México, Mexico

Microbial infection on implant surfaces has a strong influence on healing and long-term outcome of implants. The prevention and control of biofilms can be achieved by reducing the initial bacterial adhesion on the surfaces of modified metallic implants. Amorphous carbon (a-C) films have been studied as a surface modification for implant materials. These films could be interesting due to the biocompatibility, corrosion resistance and antibacterial properties that have been reported. In this work, we proposed the modification of the a-C films by inclusions of silver nanoparticles in small percentages to prevent device-associated infections, since in a previous study our results showed no inhibition of the bacterial adhesion on a-C films. The a-C:Ag films were deposited by dual co-sputtering using graphite and silver targets under an Argon plasma, varying the power applied to the Ag target. The biocompatibility of the a-C:Ag samples containing up to 6 at% Ag was evaluated using osteoblast-like cells (MG63). The biological tests showed that a-C:Ag films allowing the osteoblast to proliferate and produce osteogenic local factors, demonstrating that the biocompatibility and the osteoinduction properties of the surfaces were not modified by the addition of small percentages of silver. Having this information, we evaluate the antibacterial properties of the a-C:Ag samples with Ag concentrations ranging from 0 to about 10 at%. The bacterial adhesion at 24 hours (counting the number of colony forming units) and the biofilm formation (observed by scanning electron microscopy, SEM and fluorescence microscopy) during incubation periods of 1, 3 and 5 days were evaluated for three bacterial strains: *Escherichia coli*, *Staphylococcus aureus* and *Pseudomonas aeruginosa*. The results shows a decrease in the number on bacteria found in samples with a-C:Ag films comparing with the samples in which no silver were added. The microstructure and composition of the a-C:Ag films was characterized by X-ray Diffraction, Energy Dispersive spectroscopy (EDS), Atomic Force Microscopy (AFM) and SEM.

10:20am **D2-1-8 Corrosion Resistance and Biocompatibility of Titanium Coated with Tantalum Pentoxide**, *Y.S. Sun, H.H. Huang* (hhuang@ym.edu.tw), National Yang-Ming University, Taiwan

Titanium (Ti) is commonly used as dental implant material because of its good corrosion resistance and biocompatibility. Nevertheless, corrosion process might still happen when Ti metal is implanted in the human body for long-term application. The tantalum pentoxide (Ta_2O_5) has superior corrosion resistance than the titanium dioxide (TiO_2) spontaneously formed on Ti surface. In this study, the Ta_2O_5 coating was produced on Ti surface using hydrolysis-condensation process. Surface characteristics, including chemical composition, microstructure, topography, wettability and substrate adhesion, of the coating were analyzed. The corrosion resistance of the test specimens was evaluated using potentiodynamic polarization curve measurement in simulated blood plasma. The *in vitro* biocompatibility, in terms of protein adsorption and cell adhesion, was evaluated. Experimental data were analyzed using Student's *t*-test with $\alpha=0.05$. Results showed that the Ta_2O_5 coating was successfully produced on Ti surface using a simple hydrolysis-condensation process. The Ta_2O_5 coating showed a good adhesion to Ti substrate, and enhanced the corrosion resistance (*i.e.* decreased the corrosion rate and anodic current) and biocompatibility (*i.e.* improved the protein adsorption and cell adhesion) of Ti surface. We would conclude that the Ta_2O_5 coating could be easily produced on Ti surface using a simple hydrolysis-condensation process. The Ta_2O_5 coating provided the Ti surface with better corrosion resistance and *in vitro* biocompatibility.

10:40am **D2-1-9 Mechanical Properties of Fluorinated DLC and Si Interlayer on a Ti Biomedical Alloy**, *C.C. Chou* (cchou@mail.ntou.edu.tw), Y.Y. Wu, National Taiwan Ocean University, Taiwan, J.W. Lee, Ming Chi University of Technology, Taiwan, J.C. Huang, Tungnan University, Taiwan, C.H. Yeh, Keelung Chang Gung Memorial Hospital, Taiwan

Fluorinated diamond-like carbon (F-DLC) films were deposited on Ti6Al4V substrates by radio frequency plasma enhanced chemical vapor deposition (rf PECVD) technique using a mixture of methane (CH_4) and tetrafluoromethane (CF_4) gases. A 100 nm Si interlayer was coated in advance by physical vapor deposition (PVD) process to improve the adhesion between F-DLC and Ti alloy. The structure and surface properties of F-DLC coatings, prepared by various fluorine flow ratios, were investigated by using Raman spectroscopy, Fourier transform infrared spectroscopy, X-ray photoelectron spectroscopy, scanning electron microscopy, and atomic force microscopy. The mechanical properties were evaluated by nano-indentation and the adhesion, by nano-scratch. As CF_4 flow ratio is promoted in the mixture, CF_x group and sp^2 carbon clusters in the amorphous microstructure increase. However, the etching mechanism attributed to the fluorine species in the plasma becomes significant when the CF_4/CH_4 ratio was higher than 4 in this study. F-DLC film's Young's modulus and hardness were reduced by the increased fluorine content, but the critical load from the scratch test revealed that the film's thickness is the only factor that determines its adhesion strength. The results showed that a moderate incorporation of the fluorine content in the DLC films can still maintain acceptable mechanical properties, which, on the other hand, obtains remarkable benefits of biomedical application.

Tribology & Mechanical Behavior of Coatings and Engineered Surfaces

Room: Tiki Pavilion - Session E2-3

Mechanical Properties and Adhesion

Moderator: M.T. Lin, National Chung Hsing University, Taiwan, D. Bahr, Washington State University, US, R. Chromik, McGill University, Canada

8:00am **E2-3-1 Mechanical properties evaluation of the magnetron sputtered Zr-based metallic glass thin films**, *C.Y. Chung*, Ming Chi University of Technology, Taiwan, *H.W. Chen, J.G. Duh*, National Tsing Hua University, Taiwan, *J.W. Lee* (jefflee@mail.mcut.edu.tw), Ming Chi University of Technology, Taiwan

Recently metallic glass thin films represent a class of promising engineering materials for structural applications. In this work, a series of Zr-based ZrNiAlSi metallic glass thin films were fabricated by sputtering process. Different amount of nitrogen gas was introduced during thin films sputtering. The amorphous structures of coatings were determined by a glancing angle X-ray diffractometer and transmission electron microscope (TEM), respectively. The surface and cross sectional morphologies of thin films were examined by a field emission scanning electron microscopy (FE-

SEM). The surface roughness of thin films was explored by atomic force microscopy (AFM). A nanoindenter, a scratch tester and pin-on-disk wear tests were used to evaluate the hardness, adhesion and tribological properties of thin films, respectively. The influences of nitrogen concentration on the mechanical and tribological properties of metallic glass thin films were discussed. A proper nitrogen content of metallic glass thin films was proposed to achieve an amorphous structure with adequate mechanical properties in this work.

8:20am **E2-3-2 Microstructure and mechanical properties of copper-tin shape memory alloy thin films deposited from an anionic liquid electrolyte**, *N. Moharrami* (noushin.moharrami@ncl.ac.uk), *S. Ghosh, S. Roy, S.J. Bull*, Newcastle University, UK

Shape memory alloys (SMA) are finding an increasing range of industrial applications owing to the fact that a change in shape produced by plastic deformation can be recovered by heating and the materials may show a superelastic effect (*i.e.* plastic deformation is recovered at even at very large strains). Such materials show great potential as actuators and there has been considerable interest in developing SMA coatings and assessing them using nanoindentation tests. Although most work has been done on NiTi and CuAlZn there remains an interest in developing cheaper, simpler to process materials for mass market applications. Copper-15%Sn shows the shape memory effect and may be deposited by electrodeposition on a range of substrates. Whereas it is difficult to get the correct chemical and phase composition by plating from aqueous electrolytes good results are obtained when plating from an ionic liquid. In this study the nanoindentation response of copper-tin coatings deposited from a Room Temperature Ionic Liquid (RTIL) has been measured and compared to that of coatings deposited from an aqueous electrolyte. The results show that the shape memory effect is enhanced when using the RTIL route.

8:40am **E2-3-3 Precipitation and Fatigue in Ni-Ti-Zr Shape Memory Alloy Thin Films by Combinatorial nanoCalorimetry**, *J. Vlassak* (vlassak@esag.harvard.edu), Harvard University, US **INVITED**

The parallel nano-scanning calorimeter (PnSC) is a novel silicon-based micromachined device for calorimetric measurement of nanoscale materials in a high-throughput methodology. The device contains an array of calorimetric sensors, each one of which consists of a silicon nitride membrane and a tungsten heating element that also serves as a temperature gauge. The small mass of the individual sensors enables measurements on samples as small as a few hundred nanograms at heating rates up to 10^4 K/s. This device was used to study thin-film samples of Ni-Ti-Zr shape memory alloys to evaluate the effects of high-temperature (900°C) heat treatments and low-temperature (450°C) thermal cycling on the characteristics of the martensite transformation. The response of the samples to heat treatments depends on composition and is controlled by a precipitation mechanism. Two precipitate types, a Ti_2Ni base phase at low Zr concentration and a $\text{Ni}_{10}\text{Zr}_7$ base phase at high Zr concentration, affect the martensite transformation characteristics by altering the composition and the stress state of the shape memory phase. Thermal fatigue behavior, induced by thermal cycling, is improved compared to previous results. The most stable sample demonstrates a transformation temperature reduction of just 11°C for 100 cycles. The improved stability of the samples is attributed to the very small grain size of approximately 5-20 nm. The high heating and cooling rates characteristic of nanocalorimeters allowed this study to be performed in a high-throughput manner with efficiencies not previously achieved.

9:20am **E2-3-5 Investigation of the elastic-plastic properties of thin films on polyimide substrate under controlled biaxial deformation**, *S. Djaziri*, Institut P' - Universite de Poitiers, France, *D. Faurie* (faurie@univ-paris13.fr), LSPM-CNRS, Université Paris13, France, *P. Renault, E. Le Bourhis*, Institut P' - Universite de Poitiers, France, *G. Geandier*, Institut Jean Lamour, France, *C. Mocuta, D. Thiaudière*, SOLEIL Synchrotron, France, *P. Goudeau*, Institut P' - Universite de Poitiers, France

This presentation reports the elastic-plastic behaviour of Au and W thin films deposited on Kapton® under controlled biaxial loadings thanks to a biaxial testing device developed on DiffAbs beamline at SOLEIL synchrotron (Saint-Aubin, France). In-situ tensile tests were carried out combining 2D synchrotron x-ray diffraction (XRD) and digital-image correlation (DIC) techniques. First, the elastic behaviour of the composite metallic film – polymeric substrate was investigated under equi-biaxial and non-equi-biaxial loading conditions. The results show that the strain measurements (in the crystalline film by XRD and the substrate by DIC) match to within 1×10^{-4} . This demonstrates the full transmission of strains in the elastic domain through the film-substrate interface and thus a good adhesion of the thin film to the substrate. The second part of the paper deals with higher strains response including plastic strains under equi-biaxial tensile tests. The elastic limit of the nanostructured thin films was

determined by using a criterion which is defined by the bifurcation point between strains obtained by XRD and those obtained by DIC technique.

9:40am **E2-3-6 Heat treating effects on the microstructure and mechanical properties of Ti-Cr-B-N thin films**, *L.W. Ho, J.W. Lee* (*jefflee@mail.mcut.edu.tw*), Ming Chi University of Technology, Taiwan, *H.W. Chen, J.G. Duh*, National Tsing Hua University, Taiwan

The Ti-Cr-B-N thin films with various boron contents were deposited by pulsed DC magnetron sputtering on silicon substrates and SUS420 stainless steel discs. Heat treatments were carried out in a vacuum furnace at 600, 800 and 1000°C for 1 hour, respectively. The crystalline structures and BN bonding nature of thin films before and after heat treating were characterized by grazing angle X-ray diffraction (XRD) and Fourier transform infrared spectroscopy (FTIR), respectively. The surface and cross sectional morphologies of heat treated thin films were examined by scanning electron microscopy (SEM) and transmission electron microscopy (TEM). A nanoindenter and nanoscratch tester were adopted to evaluate the mechanical properties of coatings before and after heat treating. It was found that a hardening effect occurred after heat treating. Evolution of microstructures and mechanical properties after heat treatment at different temperature was investigated. The possible hardening mechanism of Ti-Cr-B-N coatings was also proposed.

10:00am **E2-3-7 Innovative nanomechanical testing for coating optimisation in severe applications - experiments and modelling**, *B. Beake* (*ben@micromaterials.co.uk*), Micro Materials Ltd, UK, *N. Schwarzer*, SIO, Germany, *M. Davies*, Micro Materials Ltd, UK, *W. Helle*, LOT Oriel, *T. Liskiewicz*, Leeds University, UK

Optimising coating performance for applications such as (1) ultra-high speed machining of hard-to-cut materials (2) the severe conditions that occur in automotive engines, artificial joints or helicopter gears when solid-solid contact occurs requires the combination of advanced new experimental nanomechanical test techniques with improved analytical methods for interpreting the data produced.

This presentation will include three case studies:-

- 1) Improvements to the Oliver and Pharr approach to take account of time dependency in nanoindentation, as applied to nanoindentation at 750C
- 2) The importance of high temperature nanoindentation of DLC in accurate modelling of sliding contact
- 3) High-speed reciprocating nano-wear of DLC and metallic samples

In addition it will be demonstrated how the such extracted generic material parameters can be used for computer aided optimizing of coating systems.

10:20am **E2-3-8 A new method to measure mechanical properties of very thin top layers (<100nm)**, *G.G. Guillonnet* (*gaylord.guillonnet@ec-lyon.fr*), *J.L. Loubet*, *S.B. Bec*, *G. Kermouche*, Ecole Centrale de Lyon, France

Extraction of mechanical properties of thin layers from nanoindentation tests needs determination of the projected contact area. Different formulas and procedures can be used to calculate this indentation surface from the displacement measurement. However, material properties are more difficult to obtain for small penetration depths, below 100 nm. A new method based on second harmonic detection for dynamic nanoindentation testing is proposed. This technique permits to determine the Young modulus and the hardness of materials at small depths. With this new method, the measurement of the normal displacement is not used, avoiding needing precise contact detection. Moreover, the tip defect and thermal drift influence on the measurements are reduced. Results show that the amplitude of second harmonic can be correctly measured at small depths. The Young modulus and the hardness of the tested materials can be obtained from this measurement with rather good accuracy. The mechanical properties determined with this new method are in good agreement with values obtained with classical nanoindentation tests and extend their domain. Influence of indentation size effect at small penetration depths and the limitation of the technique are discussed.

10:40am **E2-3-9 Extending Thin-Film Mechanical-Property Measurement Techniques for New Applications**, *N. Barbosa* (*barbosa@boulder.nist.gov*), *L. Liew*, *D. Read*, National Institute of Standards and Technology, US

INVITED

Investigating the mechanical behavior of thin films, coatings, and small-scale structures to understand the unpredicted behavior associated with scale-related mechanisms has led to the development of specialized micro- and nano-scale techniques. Through this work and the application of these techniques, situations where property-changing effects must be considered have been defined. We will present a methodology where these techniques and insights were leveraged to explore the use of micro-scale methods to evaluate bulk materials. In the first case, a new approach to perform tests on

tensile specimens with ~300 µm long gauge sections will be discussed. A micro-fabricated support frame was used for specimen gripping, and to create a link between the specimens and the displacement actuators and the load sensor. A digital image correlation technique was applied measure strains. In the second case, a fully integrated, on-chip, bending-fatigue MEMS device will be discussed. The system utilized an electrostatic scheme for actuation and sensing. Optical methods were used to measure fatigue-crack growth. In both cases EDM or chemical etching was utilized to section specimens from bulk material prior to integration into the MEMS testing platforms. Tensile and fatigue results of several stainless steels and aluminum will be presented. Early results show promise for use of this methodology to extract mechanical property and fracture data from small sections of materials, potentially opening the door for more thorough investigations of materials where conventional techniques are not applicable.

11:20am **E2-3-11 Atomic Force Microscopy for Nanoscale Mechanical Mapping**, *B. Pittenger* (*bede.pittenger@bruker-nano.com*), *C. Su*, *S. Minne*, Bruker-Nano Inc., AFM Unit, US

Mechanical property characterization with spatial resolution of a nanometer was recognized as a grand challenge for nanotechnology a decade ago. Because atomic force microscopes (AFM) interrogate the samples mechanically and provide resolution down to the level of atoms, they are a natural candidate for nanomechanical mapping. However, factors such as tip geometry characterization, load and displacement calibration and control, and the models used to compute material properties substantially complicate the measurements. For industrial applications, throughput is an additional challenge.

In the last decade, much progress has been made. A series of calibration methods for force and tip geometry have been developed. Various tip-sample interaction models were developed and validated by comparison with bulk measurements. During material property mapping, the time scale of tip-sample interaction now spans from microseconds to seconds, tip sample forces can be controlled from piconewtons to micronewtons, and spatial resolution can reach sub-nanometer. AFM has become a unique mechanical measurement tool having large dynamic range (1kPa to 100GPa in modulus) with the flexibility to integrate with other physical property characterization techniques in versatile environments. The methods of mechanical mapping have also evolved from slow force volume to multiple-frequency based dynamic measurements using TappingMode™ and contact resonance.

Even more recently, high speed and real-time control of the peak force of the tip sample interaction has led to a fundamental change in AFM imaging, providing quantitative mapping of mechanical properties at unprecedented resolution. In addition, ease of use improvements and development of high speed AFM have led to faster, simpler, and more quantitative SEM like operation with the AFM. This presentation will review this recent progress, providing examples from a wide range of fields that demonstrate the dynamic range of the measurements and the speed and resolution with which they were obtained.

New Horizons in Coatings and Thin Films **Room: Royal Palm 1-3 - Session F3-1**

New Boron, Boride and Boron Nitride Based Coatings
Moderator: H. Högberg, Linköping University, A.
Inspektor, Kennametal Incorporated, US

8:00am **F3-1-1 Quantum-mechanically guided materials design of boron-based hard coatings**, *J. Emmerlich* (*emmerlich@mch.rwth-aachen.de*), *D. Music*, Materials Chemistry, RWTH Aachen university, Germany, *J. Schneider*, RWTH Aachen University, Germany **INVITED**

Quantum-mechanically guided materials design and selection enjoys increasing attention due to significantly reduced material development time compared to the conventional "trial-and-error" approach. This trend is enabled by a significant increase in computer performance allowing faster and increasingly complex electronic descriptions of structure and properties that are useful for materials selection and design. In the following this will be illustrated on boron-based hard coatings, especially on the nanolaminate Mo₂BC as well as on boride materials composed of complex B-icosahedra, e.g. MXB₁₄ (M, X = usually metals).

Boron-based hard coatings, due their outstanding properties of high stiffness and hardness, have been of interest for many years. Typical examples are TiB₂ and cubic BN (the second hardest phase known). Recently Mo₂BC has attracted attention: Electronic structure calculations of Mo₂BC predicted very high stiffness and moderate ductility [1]. This

property combination is attractive for protective coatings on cutting tools. Mo₂BC thin films were synthesized using DC magnetron sputtering. Nanoindentation experiments determined a high Young's modulus of 470 GPa. Topographical imaging of the residual indent did not reveal any crack formation but pile-up was measured confirming the combination of high stiffness and moderate ductility of Mo₂BC predicted by *ab initio* calculations.

MXB₁₄ (M, X = usually metals) is a class of materials with the crystallographic structure based on a framework of B-icosahedra and bestows these phases with excellent mechanical and wear properties. However, a serious challenge is to synthesize crystalline MXB₁₄ coatings. A quantum-mechanical description of XMgB₁₄ (X = Al, Ge, Si, C, Mg, Sc, Ti, V, Zr, Nb, Ta, Hf) [2] and a detailed charge analysis based on Bader decomposition revealed that these phases are stabilized by the transfer of electrons from the X-element to the B-icosahedron, reflected by the effective charge of B-icosahedron. Not only the element but also the configurations of the phases, investigated for Al_xY_yB₁₄ (x, y = 0.25, 0.5, 0.75, 1), influences the phase stability through the effective charge of the B-icosahedron [3]. Generally, the maximum phase stability was identified by approximately two electrons transferred and seems to be connected to electronegativity and ionization potential.

1. J. Emmerlich et al., *J. Phys. D-Appl. Phys.* **42** (2009) (18), p. 6.
2. H. Kolpin et al., *Phys. Rev. B* **78** (2008) (5), p. 6.
3. H. Kolpin et al., *J. Phys.-Condens. Matter* **21** (2009) (35), p. 6.

8:40am **F3-1-3 Hard and lubricious Ti-B-C-N nanocomposite coatings via magnetron sputtering**, *F.J. Li, S. Zhang (msyzhang@ntu.edu.sg)*, School of Mechanical and Aerospace Engineering, Nanyang Technological University, Singapore, *B. Li*, Central Iron and Steel Research Institute, China

Lubricant-free machining has become the goal of hard coatings for modern wear-resistant applications. Demonstrated are hard and low friction Ti-B-C-N nanocomposite coatings via co-sputtering of TiB₂ and C in an Ar/N₂ atmosphere. The surface morphology, microstructure, chemical composition and mechanical properties of the coatings are examined with increasing B content. The results show that up to five phases, TiB, TiB₂, TiN, TiC and BN exist in the coatings. The coating hardness varies from 10.78 GPa to 31.78 GPa as the power density on the TiB₂ target increases from 1.2 W/cm² to 3.6 W/cm². The incorporation of C gives rise to very low friction coefficient while sliding against steel ball. The hardening mechanism of B and the lubricating mechanism of C are also discussed.

9:00am **F3-1-4 Microstructural study of cubic boron nitride thin film deposited by UBM method with hydrogen addition**, *J.-S. Ko, J.K. Park*, Korea Institute of Science and Technology, Republic of Korea, *J.-Y. Huh*, Unaffiliated, *Y.J. Baik (yjbaik@kist.re.kr)*, Korea Institute of Science and Technology, Republic of Korea

Characteristics of microstructure of cubic boron nitride film, deposited with hydrogen containing Ar-nitrogen mixed gas were investigated. The films were deposited by UBM (unbalanced magnetron sputtering) method. A boron nitride target of 3" diameter was used as a sputtering source, which was connected with 13.56 MHz RF (radio-frequency) electric power supply. The substrate holder was placed at 7.5 cm under the target and 200 KHz electric power supply was used as a substrate bias power supply. Either Si or Si wafer with nanocrystalline diamond thin film on it was used as a substrate. The chamber was evacuated down to 10⁻⁶ torr and a mixed gas of Ar-10% nitrogen was flowed into the chamber during deposition. The hydrogen was added to the mixed gas up to 5 sccm while maintaining the total gas flow rate at 20 sccm. The deposition pressure was maintained at 2 or 4 mtorr. The electric power of the target was 500 W and the substrate self bias voltage was -60 V. FTIR, SEM, as well as TEM were used to analyze the phase and microstructure.

TEM observation has shown three layered structure of a-BN, t-BN and cBN on Si substrate, which was little affected with the addition of hydrogen. The high resolution TEM structure of t-BN, however, was shown to vary with the addition of hydrogen. The alignment of t-BN laminate was broken for samples with hydrogen, which is believed to correlate the residual stress formation. The microstructure variation of the cBN layer itself was also shown to be affected by the presence of the hydrogen in the reaction gas. The possibility of the codeposition of hBN and cBN phase was shown in the microstructure of the existence of the hBN phase within the cBN layer. The role of hydrogen in the formation of such a microstructure as well as the relation with the variation with the FTIR spectra was also discussed.

This research was supported by a grant from the Fundamental R&D Program for Core Technology of Materials funded by the Ministry of Knowledge Economy, Republic of Korea.

9:20am **F3-1-5 Effect of deposition temperature of cubic boron nitride thin film deposited by UBM method with nanocrystalline diamond buffer layer**, *E.S. Lee, J.K. Park*, Korea Institute of Science and Technology, Republic of Korea, *T.Y. Seong*, Unaffiliated, *Y.J. Baik (yjbaik@kist.re.kr)*, Korea Institute of Science and Technology, Republic of Korea

Diamond has the nearest lattice parameter to cubic boron nitride and been considered as an adequate substrate to deposit cubic boron nitride thin film without any t-BN like intrinsic buffer layer. In this study, the behavior of the intrinsic t-BN like buffer layer was investigated when the cBN films were deposited on nanocrystalline diamond (NCD) film at various temperatures. The films were deposited by UBM (unbalanced magnetron sputtering) method. A boron nitride target of 3" diameter was used as a sputtering source, which was connected with 13.56 MHz RF (radio-frequency) electric power supply. The substrate holder was placed at 7.5 cm under the target and 200 KHz electric power supply was used as a substrate bias power supply. Either Si or Si wafer with nanocrystalline diamond thin film on it was used as a substrate. The chamber was evacuated down to 10⁻⁶ Torr and a mixed gas of Ar-10% nitrogen was flowed at 20 sccm into the chamber during deposition. The deposition pressure was maintained at 2 or 4 mTorr. The electric power of the target was 500 W and the substrate selfbias voltage was -60 V. The deposition temperature was varied in the range between room temperature and 1000°C. FTIR, SEM and TEM RBS were used to analyze the phase and structure.

With increasing the deposition temperature, the hBN intensity of the FTIR spectrum decreased. No visible hBN peak was observed for the films deposited around 800°C under the above deposition condition. The high resolution TEM microscopy has shown very thin discontinuous hBN layers between the NCD and the cBN layer and epitaxial growth of the cBN on the NCD was also found. The films deposited at room temperature, however, showed typical three layered structure of a-BN, t-BN and cBN. It is thus believed that the hBN peak of the FTIR spectra was originated from the interfacial layer. Other behaviors such as stress variation was also discussed.

This research was supported by a grant from the Fundamental R&D Program for Core Technology of Materials funded by the Ministry of Knowledge Economy, Republic of Korea

9:40am **F3-1-6 Microwave-assisted surface synthesis of amorphous and crystalline boron-carbon-nitrogen foams for thermal physisorption applications**, *R. Paul*, Birck Nanotechnology Center, Purdue University, US, *A. Voevodin*, Birck Nanotechnology Center, Purdue University; Materials and Manufacturing Directorate, Air Force Research Laboratory, US, *A. Amama, S. Ganguli, A.K. Roy*, Air Force Research Laboratory, Materials and Manufacturing Directorate, US, *T.S. Fisher (tsfisher@purdue.edu)*, Birck nanotechnology Center, Purdue University; Air Force Research Laboratory, Materials and Manufacturing Directorate, US, *J.J. Hu*, University of Dayton Research Institute/Air Force Research Laboratory, US

A microwave assisted thermo-chemical surface treatment of highly porous carbon foams was developed to synthesize boron-carbon-nitrogen foams for thermal energy storage and release using adsorption/desorption cycle with lightweight hydrocarbons. Carbon foams provide a combined advantage of large surface area and high thermal conductivity critical for thermal energy storage, but they are prone to oxidation and have a low adsorption enthalpy for lightweight hydrocarbons. This report describes carbon foam surface modification to synthesize oxidation resistant and high thermal storage capacity B-C-N foams. Boron and nitrogen were incorporated in graphitic carbon foam through microwave-assisted thermo-chemical synthesis using boric acid and urea as boron and nitrogen sources respectively. A 400 W microwave treatment for 5-30 minutes was used to accelerate foam surface modification, which was followed by high temperature annealing in an inert atmosphere to complete carbon foam surface conversion to B-C-N and to remove excess oxygen content. The resultant B-C-N foams were characterized by XPS, XRD, FESEM and Raman measurements to quantify their stoichiometry, structure, and morphology. The results reveal the formation of hexagonal B-C-N on the surface of graphitic carbon foams, where B-N and C-N bonding arrangements were dominant and indicate a direct substitution of carbon atoms in graphite lattice with boron and nitrogen atoms. The boron and nitrogen content can be increased with the higher annealing temperature and saturate at approximately BC₄N stoichiometry at 1100°C. Foam thermal conductivity was measured by transient plane source and laser flash techniques. Methanol adsorption experiments on the B-C-N foam surface were done by a BET method. The adsorption-desorption enthalpy of methanol molecules on the B-C-N foam surface was measured by differential scanning calorimetry (DSC). The adsorption enthalpy was found to increase with a decrease of the residual oxygen content within the B-C-N foam. An enhancement of adsorption enthalpy was found for B-C-N foam in comparison to pure carbon foam, confirming the B-C-N foam benefits for adsorption cooling applications and

waste heat storage and utilization. The advantages of the microwave assisted B-C-N foam synthesis and surface modification for thermal storage enhancement are discussed.

10:00am **F3-1-7 B₄C thin films for neutron detection**, *C. Höglund* (*carina.hoglund@ess.se*), European Spallation Source ESS AB/ Linköping University, Sweden, *J. Birch*, Linköping University, Sweden, *K. Andersen*, European Spallation Source ESS AB, Sweden, *T. Bigault*, *J.-C. Buffet*, *J. Correa*, *P. van Esch*, *B. Guerard*, Institute Laue Langevin, France, *R. Hall-Wilton*, European Spallation Source ESS AB, Sweden, *J. Jensen*, Linköping University, Sweden, *A. Khaplanov*, European Spallation Source ESS AB, Sweden; Institute Laue Langevin, France, *F. Piscitelli*, Institute Laue Langevin, France, *C. Vettier*, European Synchrotron Radiation Facility ESRF, France, *W. Vollenberg*, CERN, Switzerland, *L. Hultman*, Linköping University, Sweden

Due to the very limited availability of ³He, neutron detectors based on other elements are urgently needed. Here we present a method to produce thin films of ¹⁰B₄C, with a maximized detection efficiency, intended to be part of a new generation of large area detectors for neutron scattering instrumentation. A full-scale detector could be in total ~1000 m² of two-side coated Al-blades with ~1 mm thick ¹⁰B₄C films. B₄C thin films have been deposited onto Al blade and Si wafer substrates by DC magnetron sputtering from ^{nat}B₄C and boron-10 enriched ¹⁰B₄C targets in an Ar discharge, using an industrial deposition system. The films were characterized with scanning electron microscopy, elastic recoil detection analysis, X-ray reflectivity, and neutron radiography. We show that the film-substrate adhesion and film purity are improved by increased substrate temperature and deposition rate. A substrate temperature of 400 °C results in films with a density close to bulk values, good adhesion to film thickness above 3 mm, and a boron-10 content of close to 80 atomic %. Neutron absorption measurements agree with Monte Carlo simulations and show that the layer thickness, number of layers, neutron wavelength, and amount of impurities are determining factors. Initial prototype performance measurements yield an efficiency of ca. 50%, which is in general agreement with the theoretical predictions.

Applications, Manufacturing, and Equipment Room: Sunrise - Session G6-1

Advances in Industrial PVD & CVD Deposition Equipment

Moderator: M. Rodmar, Sandvik Tooling, Sweden, K. Bobzin, Surface Engineering Institute - RWTH Aachen University, Germany

8:00am **G6-1-1 Source Technologies for Amorphous Carbon Hard Coatings**, *R. P. Welty* (*rw1@magplas.com*), Magplas Technik LLC, US
INVITED

Hard coatings comprising amorphous carbon have become widely commercialized during the last 2 decades in products including automotive components, razor blades, window glass, data disks and heads, water faucet valves, and machining and forming tools. The coatings are deposited by numerous techniques including sputtering, PECVD, cathodic arc evaporation with various degrees of macroparticle filtering, and ion beam deposition using various types of ion sources. Coating properties vary widely according to the deposition technique and process conditions, in particular the energy of the coating flux and the amount of hydrogen incorporated into the coating. The commercial viability of different coating types and processes for a particular application depends in part on the required coating thickness and production rate. In this presentation I will discuss several source technologies for hard amorphous carbon coatings, and factors relating to their use in industrial production equipment.

8:40am **G6-1-3 Broadening the application range of HiPIMS coatings in industrial cutting operations**, *W. Koelker* (*werner.koelker@camecon.de*), *O. Lemmer*, *C. Schiffrers*, *S. Bolz*, CemeCon AG, Germany

Since its introduction in the late 1990 years by Vladimir Kouznetsov HiPIMS sputter technology has gained for many years a growing interest in many research activities worldwide. Basic research by many groups on this new and promising high power sputter technology was very successful. It led to the understanding of many fundamental and specific aspects of the HiPIMS process and plasma conditions. Supported by this growing knowledge CemeCon as an industrial user and supplier of HiPIMS technology drove HiPIMS technology to marketability by developing a powerful and reliable HiPIMS coating machine. In 2010 CemeCon further

introduced into the cutting tool market the first HiPIMS coating, named HPN1. Today HPN1 shows promising market growth and offers higher productivity in a variety of applications especially ranging from medium alloyed steels to spheroidal cast iron and even to challenging materials like nickel-based superalloys. The acceptance of this product in the market shows the needs for further solutions of HiPIMS coatings for cutting tools. The talk will focus on the specific advantages of HiPIMS technology and HiPIMS coatings and gives a status report on the recent application research with respect to cutting operations. It deals with the machining of high performance materials, dedicated cutting edge preparation and optimized wear volume for roughing and finishing operations.

9:00am **G6-1-4 Technical challenges and solutions for scaling up of High Power Impulse Magnetron Sputtering (HIPIMS) technologies**, *J. Landsbergen* (*jlandsbergen@hauzer.nl*), *F. Papa*, *R. Tietema*, *M. Eerden*, *T. Krug*, Hauzer Techno Coating, BV, Netherlands

HIPIMS is a technology which has been developed for over the last ten years. Its main advantage being the ability to produce some degree of ionized metal in the plasma which is needed for depositing superior hard coatings. However, the path from laboratory investigation to full integration into large scale production equipment has not been an easy one. Due to the demands on the hardware and due to the generation of pulses into the megawatt range and the sustenance of the bias voltage during such high power pulses, hardware development and integration have taken much time. Specific challenges related to these developments for cathode sizes up to 1800 cm² will be discussed along with some unexpected problems which can occur during HIPIMS processes for certain target materials.

9:20am **G6-1-5 S3p™ the HIPIMS approach of Oerlikon Balzers**, *S. Krassnitzer* (*siegfried.krassnitzer@oerlikon.com*), *M. Lechthaler*, *H. Rudigier*, OC Oerlikon Balzers AG, Liechtenstein

High Power Impulse Magnetron Sputtering (HIPIMS) has reached a high level of knowledge and understanding, and this technology is now ready to be industrialized.

S3p™ - Scalable Pulsed Power Plasma - is the HIPIMS approach of Oerlikon Balzers, which offers full flexibility in terms of applied pulse power density and pulse duration. The degree of ionization can be balanced together with the deposition rate to achieve an optimum between coating properties and productivity.

With S3p™ very smooth and dense coatings can be obtained at reasonable batch time, and new options for flexible design of coating structures and materials compositions are opened up. The present work gives an overview on the evolution of coating properties of TiAlN, by a variation of sputter power density and pulse duration. Optical Emission Spectroscopy is used to investigate the plasma properties and to estimate the degree of ionization of the sputtered material.

Finally, tools coated with S3p™ coatings, are benchmarked against tools coated with best in class coatings deposited by arc evaporation, and show a remarkable performance.

9:40am **G6-1-6 Hybrid - PVD coatings: arc evaporation combined with HIPAC**, *J. Vetter* (*joerg.vetter@sulzer.com*), *J. Mueller*, *G. Erkens*, Sulzer Metaplas GmbH, Germany

A new class of advanced PVD-coaters, the METAPLAS-DOMINO series, for dedicated coating applications comprise both improved vacuum arc evaporators (APA, Advanced Plasma Assisted) and high power impulse magnetron sputtering sources (HIPAC - High Ionized Plasma Assisted Coating). The ion cleaning is based on the (AEGD, Arc Enhanced Glow Discharge) process. It's possible to run the processes in different modes, e.g. pure APA arc evaporation or pure HIPAC magnetron sputtering. However the combination of the two high ionized deposition processes to generate multilayer, nanomultilayers and nanocomposite layers opens new horizons in tailoring of coating.

The arc evaporation itself is limited to specific cathode material properties (mostly metal alloys). HIPAC magnetron sputtering processes can be used to atomize and ionize materials which are difficult to evaporate or not evaporable by cathodic arc, e.g. Si, SiC, WC, TiB₂ and others. Specific features of the PVD system equipped with APA arc evaporators and HIPAC magnetron sources will be shown. First results of hybrid coatings will be presented

10:00am **G6-1-7 Towards uniform coating on complex geometries by PVD techniques**, *T. Takahashi* (*takahashi@kcs-europe.de*), *R. Cremer*, *P. Jaschinski*, KCS Europe GmbH, Germany, *K. Yamamoto*, *S. Hirota*, Kobe Steel Ltd., Japan

Physical Vapor Deposition (PVD) methods such as sputter and cathodic arc processes are in general characterized as a line-of-sight deposition, and hence the uniform coating on substrates having complex geometries by

PVD is a challenging task. The present work demonstrates a fast and semi-quantitative method for evaluating the coating homogeneity over a large substrate area. Thin films are deposited using three different PVD techniques of cathodic arc, DC-sputtering, and High Power Pulsed Magnetron Sputtering (HPPMS), and compared in terms of the coating homogeneity and the deposition rate. While the cathodic arc provides a significantly higher deposition rate compared to the others, similar coating distributions are achieved among these deposition techniques. The method presented here contributes towards a fast and efficient optimization of process parameters for PVD coatings on complex geometries.

the "Deutsche Forschungsgemeinschaft" within the frame of the SFB-TR 87 and the "Ruhr University Bochum Research School".

10:20am **G6-1-8 LPPS hybrid Technologies: New Thermal Spray Processes for new emerging Energy Applications**, *H.-M. Hoehle* (*hans-michael.hoehle@sulzer.com*), Sulzer Metco Europe GmbH, Germany, *M. Gindrat*, *A. Barth*, Sulzer Metco AG (Switzerland), Switzerland

Recent developments in hybrid low pressure thermal spray technologies, such as Plasma Spray-Thin Film (PS-TF), PS-PVD, PS-CVD are being increasingly used to develop functional inorganic coatings and films for emerging high end energy applications. Such applications include protection layers and electrolytic films in SOFC, gas tight mixed electron and ion conducting membranes for gas separation and thin functional layers in photo-voltaic applications. This paper provides a brief overview of the status of developments of several high end emerging energy applications. Beside the applications the basics of these technologies will be described.

10:40am **G6-1-9 Development of metal strip cooling equipment for demands of high-rate vacuum coating**, *J.-P. Hei  * (*jens-peter.heinss@fep.fraunhofer.de*), *P. Lang*, Fraunhofer FEP, Germany

Metal strip coating is developing continuously and opens steadily new application fields. Solar heat and thin film photovoltaic are actual examples. From economical reasons the electron beam evaporation is predestined to fit the mass throughput and in the near past a lot of successful developments became known. Fraunhofer FEP is engaged in developments of vacuum coating as well as in additional and ambient processes.

High-rate vacuum depositions demand in few cases an effective cooling concept for scooping out their potential. Otherwise substrate or layer temperature exhibits the limiting factor. The technical challenge consists in realizing an effective heat transfer process under high vacuum conditions and was unsolved up to now. Therefore new cooling equipment for vacuum metal strip coating was developed. A description of adapted principles and developed design will be presented. The heat transfer coefficient was extended outgoing from common cooling drum with 50 up to 200 W/m²K for the new designed cooling equipment. We demonstrate several dependencies for the heat transfer coefficient and also first results of adaption of cooling equipment during electron beam deposition of steel strip.

The increased cooling efficiency opens new technical capabilities: utilization of very high deposition rates, deposition of thin metal strips and foils, increase of layer thickness, defining of strip temperature during deposition up to keeping it constant during high-rate deposition. We discuss these different performances also in connection with economical consequences.

11:00am **G6-1-10 Multiple frequency coupled plasmas for enhanced control of PVD processes**, *S. Bienholz* (*bienholz@aept.rub.de*), *E. Semmler*, *P. Awakowicz*, Ruhr-Universit   Bochum, Germany

Capacitively coupled plasmas are widely used in PVD processes over several years. Classical single radio frequency capacitively coupled plasmas for PVD processes are nowadays replaced by high rate DC-Magnetron sputter coaters. Nevertheless, both techniques do not allow a separate control of ion flux and its energy distribution at the target, which limits the control range of sputter processes. A possibility to overcome this constriction consists of exciting the plasma at two or even more different radio frequencies simultaneously. Whereas high electron densities and therefore a high ion flux can be achieved by using a very high frequency (VHF) excitation, a lower frequency (HF) excitation gives a certain control over the ion bombarding energy at the target. In this contribution we discuss the possibility of tuning electrical discharge quantities by using multiple excitation frequencies. Especially, the influence of the relative phase between one frequency and its second harmonic on the target voltage waveform and the self bias voltage is investigated, as well as the effect on relevant plasma quantities. Langmuir probe measurements and optical emission spectroscopy are performed to fully characterize the plasma. It is shown, that multiple frequencies capacitively coupled plasmas give an independent control over ion flux and the ion bombarding energy at the target over a wide range. The experiments show, that capacitively coupled multiple frequency plasmas are a promising complement to existing PVD processes. The authors would like to acknowledge the funding provided by

Authors Index

Bold page numbers indicate the presenter

— A —

Abadias, G.: B3-1-6, **129**; B7-1-1, 27; BP-12, 98;
BP-2, 97; BP-3, 97; BP-38, **103**
Abd El-Rahman, A.M.: E1-3-8, 56
Abd Shukor, M.H.: A3-1/F8-1-12, **72**; FP-1, **116**
Abdul Ghani, J.: EP-26, 116
Abdul Razak, A.R.Bushroa.: B4-1-8, **42**; EP-10,
113
Abdullah, S.: B4-2-4, 51
Abell, S.: F6-1-5, 7
Abendroth, B.: C4-1-8, 32
Abraham, B.: F2-2-4, 46
Abrasonis, G.: B1-2-10, **11**
Abrikosov, I.: B7-2-2, 43; B7-2-7, 43; B7-2-8, 43;
B7-2-9, 44; BP-31, 101; C5-1/F7-1-4, 88
Abusoglu, A.: C3-1-4, 13
Achenbach, L.: D3-1-3, 15
Adamiak, M.: G5-1-8, **49**
Adams, D.: F6-1-1, 7; TS3-1-5, **81**
Adelhelm, C.: FP-11, 118
Ageh, V.: E1-2-6, **34**
Ahlgren, M.: B4-3-1, 62
Ahmed, H.: B4-1-10, 42
Ai, C.F.: DP-18, 112
Aijaz, A.: F2-1-5, 35
Aizawa, T.: BP-29, 101; E4-1/G4-1-3, 66; EP-6,
113
Akimoto, K.: C2-2/F4-2-7, 12
Alagoz, H.: B1-3-5, **25**; B1-3-9, 26; PDP-6, 125
Alam, M.T.: TS1-1-2, 68
Alami, J.: F2-2-10, **47**
Alangaram, A.: BP-28, 101; G1-1-11, 58
Alcalá, A.: A1-3-5, 71
Aleman, A.: DP-13, 111
Alemo, G.: DP-13, 111
Alfano, P.: A1-2-10, **62**
Allen, M.W.: C4-1-1, 30
Allen, T.: TSP-5, 126
Alling, B.: B5-1-3, 53; B7-2-2, 43; B7-2-7, 43; B7-
2-9, 44; BP-32, 102; F1-1-3, **19**
Allred, D.: F1-1-11, 20
Almaguer-Flores, A.: D2-1-7, **130**
Almandoz, E.: E3-1/G2-1-2, **17**
Almer, J.: B4-1-6, 41
Alpas, A.T.: E3-1/G2-1-13, 18
Altfeder, I.: TS4-1-6, 59; TS4-1-9, 59
Alves, R.: E4-1/G4-1-6, 66
Amama, A.: F3-1-6, 133; TS1-1-9, **70**
Ambrosch-Draxl, C.: B4-1-1, 40
Anagnostopoulos, D.: B1-3-11, 26
Anders, A.: C4-1-2, 31; C4-2/F4-2-6, **12**; FP-21,
120
Andersen, K.: F3-1-7, 134
Anderson, C.: E2-2-2, 90
Ando, T.: TS3-1-9, 82
Andrade, E.: DP-13, 111
Andrich, M.: B6-1-10, 76
Anezaki, Y.: FP-19, 120
Anthopoulos, T.: TS4-1-4, **59**
Aouadi, S.: E1-3-5, **56**
Apatiga, L.: CP-10, **106**
Aperador, W.: AP-5, 94; PD-1-5, 92
Araki, K.: TS1-1-11, 70
Argarwal, A.: E3-2/G2-2-3, 44
Argon, A.S.: E2-2-5, 90
Ariga, T.: B4-1-8, 42
Armstrong, B.: AP-10, 95
Arndt, M.: B6-1-5, 75; E4-2/G4-2-11, 80
Arslan, E.: DP-10, 110; DP-17, 112; E2-1-7, 78
Arteaga, O.: C3-1-3, 13
Arzate-Vázquez, I.: E2-2-7, 91
Asakawa, R.: DP-4, 109
Asano, T.: C1-1-1, **3**
Asta, M.: B7-1-3, **27**
Atthipalli, G.: TS4-1-12, 60

Audronis, M.: C2-2/F4-2-1, **11**; FP-22, **120**
Austin, L.: E3-2/G2-2-10, 45
Awakowicz, P.: G6-1-10, 135; GP-13, 124; TS2-2-
7, 21
— B —
Babacan, Y.: CP-31, 109
Babu, J.: FP-3, 116; FP-4, 117
Bachmann, T.: B6-1-5, 75
Badger, R.: F1-1-11, 20
Bagcivan, N.: B1-2-8, 10; B4-1-9, 42; B4-3-2, 62;
B6-1-7, 76; B6-2-9, 88; BP-15, **99**; F2-1-8, 36
Baghmar, G.: CP-20, **107**; FP-10, 118
Bahr, D.: E2-1-1, **77**; F6-1-1, 7
Baik, Y.J.: B1-2-12, 11; F3-1-4, 133; F3-1-5, 133;
FP-24, 121; FP-25, 121; FP-26, 121
Baker, M.: BP-20, 100
Balmain, J.: AP-2, 94
Balmer, C.: C4-1-12, 33
Ban, Z.: B2-1-3, 73
Bandorf, R.: F2-1-4, **35**
Banerjee, I.: C2-3/F4-3-9, 30; D1-1-2, **5**
Bao, M.D.: E3-2/G2-2-3, **44**
Baquiao, D.: B2-2-5, 85
Baran, Ö.: B4-3-5, 63; BP-18, **99**; DP-17, 112; E2-
1-7, 78; EP-11, 113
Baránková, H.: G3-1-2, 67
BARAS, F.: TS3-1-4, 81
Barbosa, N.: E2-3-9, **132**
Bardos, L.: G3-1-2, **67**
Bareiss, J.C.: B2-2-4, **85**
Barhai, P.K.: C2-3/F4-3-9, 30; D1-1-2, 5
Barletta, M.: G1-1-12, **59**; GP-14, 124
Baron, J.: FP-6, 117
Barriga, J.: B1-3-4, **25**; B3-1-1, 128
Bartelt, N.: TS4-1-3, 59
Barth, A.: G6-1-8, 135
Basirun, W.J.: A3-1/F8-1-12, 72; FP-1, 116
Bayon, R.: B3-1-1, 128
Beake, B.: E2-3-7, **132**; EP-10, 113
Bec, S.B.: E2-3-8, 132
Begley, M.: A2-1-1, 23
Belliard, L.: B7-2-6, 43; BP-3, 97
Bellido-Gonzalez, V.: C2-2/F4-2-1, 11; FP-22, 120
Belous, V.: B1-3-8, 25
Bemporad, E.: EP-16, **114**; TS2-2-2, 20
Benaben, P.: F6-1-4, 7
Benaboud, R.: B2-1-7, 74
Bendavid, A.: F1-1-7, 20
Bengu, E.: B1-3-5, 25; B1-3-9, **26**; PDP-6, **125**
Benhamida, M.: BP-3, 97
Bensaid, B.: F6-1-4, 7
Ben-Soussia, A.: EP-27, 116
Bergmann, C.: EP-13, 114
Bertram, R.: B1-2-3, 9
Bertran, E.: C3-1-3, 13
Bewilogua, K.: B6-1-4, **75**; E3-2/G2-2-11, 45
Bhakhri, V.: B4-2-10, 53
Bibinov, N.: GP-13, 124
Bidev, F.B.: E2-1-7, 78
Bienholz, S.: G6-1-10, **135**
Biermann, D.: E4-2/G4-2-1, 79
Bierwisch, N.: E1-3-4, 55; E2-1-2, 77; E3-1/G2-1-
1, **17**; EP-5, **113**
Bigault, T.: F3-1-7, 134
Bijwe, J.: B6-1-10, 76
Bikowski, A.: C4-1-9, 32
Bilek, M.: C4-1-8, 32
Birch, J.: B2-2-7, 86; B7-1-6, 27; C5-1/F7-1-8, 89;
F3-1-7, 134
Birch, M.A.: D1-1-1, 5
Blanquet, E.: B2-1-7, 74
Blazek, J.: B1-1-1, **2**; B4-1-2, 40
Blomfield, C.: TS2-1-5, 8
Blondy, G.: E1-1-2, 6
Blunk, A3-2/F8-2-7, 84

Blunk, S.: DP-16, 111; EP-24, 115
Bobzin, K.: B1-2-8, 10; B4-1-9, 42; B4-3-2, 62;
B6-1-7, **76**; B6-2-9, 88; BP-15, 99; F2-1-8, 36
Boddaert, X.: F6-1-4, **7**
Bois, J.: F6-1-4, 7
Boisselier, G.: B2-2-3, 85
Böke, M.: F2-2-1, 46
Bolon, A.: A2-1-5, **23**
Bolz, S.: G6-1-3, 134
Bomas, H.: E4-1/G4-1-5, 66
Bonetti, L.: B2-2-5, 85
Borchert, D.: B2-1-8, 74
Boscher, N.D.: B2-1-10, 74
Bouamama, K.: B7-2-6, 43; BP-2, 97; BP-3, 97
Bousser, E.: B5-1-5, **54**
Bouzakis, E.: E4-2/G4-2-3, 79
Bouzakis, K.-D.: BP-30, **101**; E4-2/G4-2-3, **79**
Brahmandam, S.: E4-1/G4-1-1, 66
Bräuer, G.: F2-1-4, 35
Braun, R.: A1-3-4, 71
Brenning, N.: F2-2-2, 46; FP-21, 120
Brinkmann, R.P.: G3-1-7, 68
Brito, H.: C2-3/F4-3-7, 29
Brizuela, M.: A1-3-5, 71; E1-3-3, 55
Broitman, E.: B1-2-5, 9; B7-1-6, 27; C5-1/F7-1-10,
89
Brugnara, R.H.: B4-3-2, **62**
Buckley, J.: TS3-1-9, 82
Buffet, J.-C.: F3-1-7, 134
Bull, S.J.: B7-1-7, 28; D1-1-1, 5; E2-3-2, 131; F6-
1-3, **7**
Bultman, J.E.: TS1-1-3, 69; TSP-8, 127
Burkett, S.L.: G1-1-2, 57
Burrows, K.: FP-15, 119
— C —
Cabrera, E.: C3-1-3, 13
Cada, M.: F2-2-6, 47
Caicedo, J.: AP-5, 94
Caicedo, J.C.: PD-1-5, 92
Cairns, D.: F6-1-5, 7; FP-15, 119
Calderon V., S.: DP-3, 109
Camargo, H.: C2-3/F4-3-7, 29
Campbell, L.: B6-2-8, 87
Campiche, A.: F2-2-8, 47
Campo, M.: E3-1/G2-1-5, 17
Campos-Silva, I.: E1-2-12, 34; E2-2-6, 91; E2-2-7,
91
Camps, E.: B5-2-10, 65; BP-19, 99; BP-26, **101**
Camps, I.: BP-19, 99
Cano, M.F.: B4-2-3, 51
Canovic, S.: A1-2-5, 61; A3-1/F8-1-9, **72**
Capek, J.: F2-1-1, 35
Carassiti, F.: EP-16, 114; TS2-2-2, 20
Cardona, D.: BP-26, 101
Caro, M.: C5-1/F7-1-6, 89
Carvalho, S.: DP-3, **109**
Cassar, G.: B4-2-1, 51
Castañeda, I.: A1-3-5, 71
Castillo-Aranguren, F.: G1-1-1, **57**
Cavaleiro, A.: B6-2-3, **87**; DP-3, 109; E3-1/G2-1-
10, 18
Celis, J.P.: D3-1-4, 15; EP-17, 114
Cersty, R.: B1-1-1, 2; B4-1-2, 40; B5-1-10, 55;
EP-4, 112; F2-2-3, 46
Champagne, V.: G1-1-9, 58
Chan, C.C.: CP-15, 106
Chan, Y.C.: B5-1-1, 53
Chander, R.: C2-3/F4-3-11, **30**; FP-16, **119**
Chandross, M.: E1-3-9, **56**
Chang, C.C.: C3-1-7, 14; C3-1-9, 14; CP-1, 104;
CP-15, **106**
Chang, C.H.: GP-6, 123
Chang, C.J.: C2-2/F4-2-3, 12; F1-1-4, 19
Chang, C.K.: AP-11, **95**; BP-5, 97

- Chang, G.W.: C2-3/F4-3-3, **29**; GP-3, 122; TS2-2-10, 22; TSP-2, 126
- Chang, H.B.: FP-8, **117**; FP-9, 118
- Chang, H.C.: F1-1-6, 19; FP-27, 121
- Chang, J.: B5-2-11, 66
- Chang, J.J.: CP-2, 104
- Chang, J.L.: CP-22, 107
- Chang, K.C.: F1-1-5, **19**; TS2-2-12, 22
- Chang, L.C.: FP-13, 119
- Chang, L.W.: B2-1-12, 75
- Chang, S.T.: EP-7, 113
- Chang, S.W.: FP-28, 121
- Chang, S.Y.: BP-23, 100; PDP-5, **125**
- Chang, T.C.: C2-1/F4-1-4, 4; C2-3/F4-3-4, 29; C5-1/F7-1-5, 89; C5-1/F7-1-9, 89; CP-11, 106; CP-21, 107; F1-1-5, 19; FP-12, 118; FP-18, 119; TS2-2-12, 22
- Chang, Y.: GP-10, 124
- Chang, Y.L.: CP-19, 107
- Chang, Y.M.: CP-16, 106
- Chang, Y.Y.: BP-17, 99; BP-39, 103; DP-1, 109; DP-2, 109
- Chao, W.H.: C3-1-7, 14; C3-1-9, 14; CP-1, 104
- Charitidis, C.: BP-12, 98
- Charoenpanich, A.: D1-1-6, 5
- Chávez-Gutiérrez, E.: E2-2-7, 91
- Chawla, V.: B7-2-5, **43**
- Che Haron, C.H.: EP-26, 116
- Check, M.: TS1-1-7, 69
- Chellah, N.: A2-2-3, **39**
- Chen, C.: E2-2-3, 90
- Chen, C.C.: A3-2/F8-2-8, 85
- Chen, C.E.: C2-1/F4-1-2, **4**
- Chen, C.L.: A3-2/F8-2-8, 85
- Chen, C.M.: FP-28, **121**; PDP-5, 125; TS2-2-4, 21
- Chen, C.Y.: A3-2/F8-2-2, 84; BP-40, **103**; CP-2, 104
- Chen, C.-Y.: CP-12, **106**
- Chen, G.X.: EP-20, 115
- Chen, H.W.: B5-1-1, 53; E2-3-1, 131; E2-3-6, 132; EP-15, 114
- Chen, J.: D1-1-1, **5**; EP-9, **113**; TS3-1-9, 82
- Chen, J.T.: GP-6, 123; TSP-3, **126**
- Chen, L.H.: A3-2/F8-2-1, 84
- Chen, M.C.: C2-3/F4-3-4, **29**; FP-12, **118**; FP-18, 119
- Chen, S.C.: FP-12, 118
- Chen, S.M.: BP-9, **98**
- Chen, T.C.: C2-3/F4-3-4, 29; C5-1/F7-1-3, **88**; C5-1/F7-1-9, 89; CP-11, 106
- Chen, T.S.: C1-1-4, 3; CP-27, **108**; EP-14, 114
- Chen, W.C.: EP-3, **112**
- Chen, W.H.: C3-1-8, 14
- Chen, Y.C.: C2-3/F4-3-2, **29**; DP-1, **109**; DP-2, 109
- Chen, Y.H.: FP-20, **120**
- Chen, Y.I.: BP-9, 98
- Chen, Y.T.: C2-1/F4-1-3, **4**; C5-1/F7-1-9, 89; CP-11, 106
- Chen, Z.F.: PDP-1, **125**
- Cheng, S.: E1-3-9, 56
- Cheng, Y.C.: TSP-1, 126
- Cheng, Y.H.: BP-33, 102
- Cheng, Y.K.: BP-10, **98**
- Cheng, Y.L.: CP-16, 106; CP-19, **107**
- Cheng, Y.T.: A3-2/F8-2-3, 84
- Chhowalla, M.: TS4-1-4, 59
- Chiang, C.-Y.: CP-12, 106
- Chichignoud, G.: B2-1-7, 74
- Chien, H.: B2-1-3, 73
- Chiou, S.E.: CP-27, 108
- Chirita, V.: B7-1-10, 28; B7-1-8, **28**
- Chistyakov, R.: F2-2-4, 46
- Chiu, H.L.: C2-3/F4-3-1, **29**
- Chiu, T.J.: CP-16, 106
- Chiu, Y.C.: FP-12, 118
- Choi, C.K.: CP-17, **107**
- Choi, H.W.: CP-13, 106; CP-3, 104; CP-6, 105
- Choi, J.H.: BP-16, 99
- Chollon, G.: B4-2-7, **52**
- Choquet, A.: B2-1-10, 74; F2-2-5, **46**
- Chou, C.C.: D2-1-9, **131**
- Chou, C.M.: DP-6, **110**
- Chou, K.: E2-1-8, 78
- Chou, L.S.: C2-3/F4-3-1, 29
- Choudhary, N.: B5-1-8, 54; C3-1-13, **15**
- Chromik, R.: E1-2-3, **33**; E3-2/G2-2-1, 44
- Chu, J.: B1-3-10, 26; B5-2-7, 65; B5-2-8, **65**
- Chu, P.: BP-42, 103; D1-1-3, **5**; F2-1-11, 36; GP-9, 123
- Chuang, S.L.: TS2-2-11, **22**
- Chung, C.J.: DP-6, 110
- Chung, C.K.: C1-1-4, 3; EP-14, 114; F1-1-6, 19; FP-27, 121
- Chung, C.Y.: E2-3-1, **131**
- Chung, W.Y.: CP-16, **106**
- Chyrkin, A.: A1-2-9, 62
- ÇİÇEK, H.: EP-11, **113**
- Ciurea, C.: B4-2-10, **53**
- Clegg, W.: B5-1-9, 54; E2-2-1, 90; E3-2/G2-2-4, 44; TS2-2-3, **21**
- Clegg, W.J.: TS2-1-4, 8
- Colin, J.J.: BP-38, 103
- Colleaux, F.: TS4-1-4, 59
- Collins, E.: TS3-1-3, **81**
- Cong, X.N.: PDP-1, 125
- Contreras, A.: E1-3-3, 55
- Cooke, K.: A3-2/F8-2-6, 84; C1-1-7, 4
- Corat, E.: B2-2-5, 85; EP-2, 112
- Corbella, C.: B3-1-5, **128**
- Cordill, M.: F6-1-1, 7
- Corona, E.: F6-1-1, 7
- Correa, J.: F3-1-7, 134
- Coupeau, C.: AP-2, 94
- Covarel, G.: F6-1-4, 7
- Cozza, R.: E1-1-6, **6**
- Creatore, M.: C2-1/F4-1-5, **4**
- Cremer, R.: B6-1-1, **75**; F2-1-3, 35; G6-1-7, 134
- Cremona, M.: C2-3/F4-3-7, **29**
- Cui, Q.: TS3-1-9, 82
- Czettel, C.: B1-2-2, 9; B2-1-2, **73**
- **D** —
- Dadheech, G.: A3-2/F8-2-7, **84**
- Dahmen, U.: B7-1-3, 27
- Dai, C.H.: C2-1/F4-1-4, 4; CP-21, 107
- Dai, M.: BP-27, **101**
- Dallas, T.: E2-2-2, 90; TS3-1-3, 81
- Dan, H.L.D.: EP-20, 115
- Danek, M.: E3-1/G2-1-10, 18
- Daniel, R.: B6-2-1, **86**
- Darooparvar, M.: A1-2-11, 62; PDP-2, 125
- Das, A.K.: C2-3/F4-3-9, 30
- Davenport, J.: E3-2/G2-2-4, **44**
- Davies, M.: E2-3-7, 132
- Davis, R.: F1-1-11, 20
- De Gryse, R.: EX-1, **38**
- de los Arcos, T.: B3-1-5, 128; F2-2-1, 46; TSP-4, 126
- de Wit, J.H.W.: E2-1-6, 78
- DeHosson, J.T.: E1-2-7, **34**
- Deilmann, M.: GP-13, 124
- Demirci, E.: DP-10, **110**; DP-17, 112; EP-11, 113
- Depla, D.: B3-1-3, **128**; F2-2-11, 47
- Depner, U.: B1-2-8, 10; B6-2-9, 88
- Desaigues, J.: FP-11, 118
- Deshpande, R.: A3-2/F8-2-3, 84
- Dessarzin, P.: B6-2-7, 87; E4-2/G4-2-10, 80
- Ding, G.: C4-1-11, **32**; CP-4, **104**
- Ding, X.Z.: B5-1-9, 54
- Dixit, S.: E3-2/G2-2-2, **44**
- Diyatmika, W.: B1-3-10, **26**
- Djaziri, S.: E2-3-5, 131
- Djemia, P.: B7-2-6, **43**; BP-2, 97; BP-3, **97**
- Djouadi, A.: F2-1-12, 37
- Döbeli, M.: B6-2-4, 87
- Doisneau, B.: B2-1-7, 74
- Donohue, E.: A2-1-1, **23**
- Doumanidis, C.: TS3-1-9, 82
- Drache, S.: F2-2-6, 47
- Duday, D.: F2-2-5, 46
- Duffles, M.: G1-1-9, 58
- Duh, J.G.: B5-1-1, 53; E2-3-1, 131; E2-3-6, 132; EP-15, 114
- Durham, D.: E2-1-8, 78
- Durst, K.: E2-1-3, **77**; PDP-3, 125; PDP-4, 125
- **E** —
- E. Rodil, S.: BP-26, 101
- Edström, D.: B7-1-8, 28
- Eerden, M.: G6-1-4, 134
- Efeoglu, H.: C3-1-4, **13**; CP-31, **109**
- Efeoglu, I.: B4-3-5, 63; BP-18, 99; DP-10, 110; DP-17, 112; E2-1-7, **78**
- EFEÖĞLU, İ.: EP-11, 113
- Ehiasarian, A.P.: F1-1-1, **19**
- Ehiazarian, A.: F2-1-9, 36
- Eitzinger, G.: A3-2/F8-2-6, 84; C1-1-7, 4
- Eklund, P.: B1-1-5, 2; FP-14, **119**
- El Mansori, M.: E1-1-5, 6; E3-1/G2-1-11, **18**; E3-1/G2-1-12, 18; E4-2/G4-2-4, 79; EP-27, 116
- El-Azab, A.: TSP-5, 126
- Eldridge, J.I.: A2-1-2, **23**
- Ellermeier, J.: B1-2-8, 10; B6-2-9, **88**
- Ellmer, K.: C4-1-9, **32**
- Elsaesser, C.: C4-1-3, 31
- Elzwawi, S.: C4-1-1, 30
- Emmerlich, J.: AP-8, 95; B7-2-1, 42; F3-1-1, **132**
- Endler, I.: B2-1-6, **73**
- Endut, Z.: A3-1/F8-1-12, 72; FP-1, 116
- Englberger, G.: E1-2-11, 34
- Epaminonda, P.: BP-20, **100**
- Erdemir, A.: E1-3-13, 57; E3-2/G2-2-2, 44; E3-2/G2-2-7, **45**; G5-1-11, 49; G5-1-12, 49
- Erdeniz, D.: TS3-1-9, 82
- Eremin, D.: G3-1-7, 68
- Ericson, T.: C2-2/F4-2-9, 12
- Ericsson, B.: B4-3-1, 62
- Erkens, G.: G6-1-6, 134
- Eryilmaz, O.: E1-3-13, 57
- Eryilmaz, O.L.: E3-2/G2-2-2, 44; E3-2/G2-2-7, 45; G5-1-11, 49; G5-1-12, 49
- Escobar Galindo, R.: DP-3, 109
- Escobar, C.: AP-5, 94
- Escobar, C.A.: PD-1-5, 92
- Escobar, R.: DP-13, 111
- Escobar-Alarcon, L.: BP-19, **99**; BP-26, 101
- Escobar-Alarcón, L.: B5-2-10, 65
- Espindola, J.: CP-10, 106
- Esteve, J.: AP-5, 94; PD-1-5, 92
- Ewering, M.: B4-3-2, 62; B6-1-7, 76; BP-15, 99
- Ezirmik, K.: E1-3-13, **57**
- EZİRMİK, V.: EP-11, 113
- Ezirmik, V.K.: DP-10, 110; DP-17, 112
- **F** —
- Fadenberger, K.: BP-20, 100
- Fager, H.: B1-2-5, 9; B5-2-5, **65**
- Fajfrowski, M.: PD-1-6, **93**
- Falz, M.: B1-2-9, 10
- Fan, X.S.: BP-41, **103**
- Faria, G.: B2-2-5, 85
- Fasuba, O.: AP-3, **94**
- Faure, C.: B6-1-6, 76
- Faurie, D.: B7-2-6, 43; BP-2, **97**; BP-3, 97; E2-3-5, **131**
- Favaro, G.: B4-1-7, 41; E1-3-4, **55**; E2-1-2, 77
- Felderhoff, F.: E4-2/G4-2-5, **79**
- Fenker, M.: B5-2-2, **64**; F2-2-10, 47
- Fernandez, J.: E3-1/G2-1-2, 17
- Ferrarese, A.: E3-1/G2-1-8, 18; E3-1/G2-1-9, 18
- Ferre-Borrull, J.: C3-1-3, 13
- Ferrec, A.: F2-1-12, 37
- Feuerstein, A.: A2-2-1, **39**
- Field, M.R.: C4-1-1, 30
- Fietzek, H.: A2-2-6, 39
- Figuerola, A.: EP-22, 115
- Figuerola-Guadarrama, M.A.: E1-2-12, 34
- Fillon, A.: B3-1-6, 129; BP-38, 103

Fischer, A.: D3-1-10, 16
 Fischer, F.D.: B7-1-5, **27**
 Fischer, J.: FP-11, **118**
 Fischer, R.: GP-11, 124
 Fischer, S.: TS1-1-1, 68
 Fischer-Cripps, A.: E2-1-10, **79**
 Fisher, T.S.: F3-1-6, 133; TS1-1-4, **69**; TS1-1-9, 70; TS4-1-6, 59; TS4-1-9, 59
 Flaub, C.: DP-12, 111
 Fleischman, M.: G3-1-1, 67
 Flores, M.: DP-13, **111**
 Foerster, C.E.: DP-16, 111; EP-24, **115**
 Fok, A.: AP-6, 95
 Fontaine, J.: E1-3-1, **55**
 Forest, B.: D3-1-7, 16
 Forsén, R.: B7-2-9, 44
 Fouvry, S.: E1-1-2, **6**
 Fox-Rabinovich, G.: E4-2/G4-2-9, 80
 Franz, R.: B1-1-6, **2**
 Fratzl, P.: PL-1, **1**
 Friák, M.: BP-1, 96
 Fridrici, V.: E1-1-1, 6
 Friederichsen, N.: C4-1-2, 31
 Friedle, S.: A1-3-4, **71**
 Froitzheim, J.: A3-1/F8-1-9, 72
 Fu, R.: BP-42, 103
 Fuchs, M.C.: B1-2-6, **10**; EP-1, **112**
 Fuentes, G.G.: E1-3-11, **56**; E3-1/G2-1-2, 17
 Fuh, C.S.: CP-9, **106**
 Fujii, H.: B1-2-1, 9; G1-1-5, 57
 Fujiwara, T.: FP-2, 116
 Fukumasu, N.K.: E3-1/G2-1-8, 18; E3-1/G2-1-9, **18**
 Fumagalli, F.: GP-5, 122
 Funk, R.H.: D3-1-3, 15
 Furue, S.: C2-2/F4-2-7, 12
— G —
 Gabriel, B.: G1-1-9, 58
 Gadaud, P.: AP-2, 94
 Galaviz-Pérez, J.A.: PD-1-4, 92
 Gale, R.: E2-2-2, 90
 Galetz, M.: A1-1-4, 50
 Galicia, G.: B5-2-10, 65
 Gall, D.: B5-2-1, 64
 Gallardo-Hernandez, E.: E1-2-12, 34
 Gallian, S.: G3-1-7, 68
 Gan, D.S.: F1-1-5, 19; TS2-2-12, 22
 Gan, J.: TSP-5, 126
 Ganciu, M.: F2-1-12, 37
 Ganguli, S.: F3-1-6, 133
 Ganser, C.: EP-13, 114
 Gao, Y.: A2-1-8, 24; D3-1-9, **16**
 Garcia, D.: EP-22, 115
 Garcia, J.A.: E3-1/G2-1-2, 17
 Garcia-Bustos, E.: E1-2-12, 34
 García-Luis, A.: E1-3-3, 55
 Garcia-Zarco, O.: FP-6, 117
 Gay, P.-A.: E1-2-10, **34**
 Ge, F.: B5-1-11, 55
 Geandier, G.: E2-3-5, 131
 Geers, C.: A1-1-4, **50**
 Gehrke, K.: C4-1-3, 31
 Gell, M.: A2-2-9, **40**
 Gengler, J.J.: B4-2-8, 52; TS1-1-3, 69; TSP-8, 127
 Genisel, M.F.: B1-3-9, 26; PDP-6, 125
 Gentleman, M.: A2-1-5, 23
 Genvald, A.: B4-3-1, 62
 Geringer, J.: D3-1-7, **16**
 Ghafoor, N.: B1-2-5, 9; B5-1-3, **53**; B7-2-9, 44; TS2-1-3, 8
 Ghazali, M.J.: B4-2-4, **51**; EP-26, **116**
 Ghosh, S.: E2-3-2, 131
 Ghosh, S.K.: D3-1-4, **15**; EP-17, **114**
 Gibson, P.: BP-20, 100
 Gindrat, M.: G6-1-8, 135
 Gisario, A.: G1-1-12, 59
 Giuliani, F.: B4-2-10, 53
 Glavin, R.: TS1-1-7, 69
 Glazek, W.: FP-23, **120**

Gleeson, B.: A1-1-6, **50**
 Glukhoy, Y.: G3-1-8, **68**
 Gnoth, C.: B4-1-9, 42
 Go: A2-2-10, **40**
 Goeke, R.: E1-2-9, **34**; E1-3-12, 56
 Goedel, B.: E3-1/G2-1-11, 18; E3-1/G2-1-12, **18**
 Göken, M.: PDP-3, 125; PDP-4, 125
 Goltvyanytsya, S.: B1-3-8, 25
 Goltvyanytsya, V.: B1-3-8, **25**
 Gomez, H.: E2-1-8, 78
 Gómez, M.: AP-5, 94
 Gomez, M.E.: PD-1-5, 92
 Gong, C.Z.: F2-1-11, 36; GP-9, 123
 Gonzalez, G.: GP-4, 122
 Gonzalez, J.M.: B4-2-3, 51
 González-Reyes, J.G.: BP-37, 102
 Gonzalvo, Y.: FP-22, 120
 Gopikishan, S.: C2-3/F4-3-9, 30
 Gorokhovskiy, V.: G5-1-1, **48**
 Göthelid, E.: B4-3-1, **62**
 Gotzmann, G.: D3-1-3, **15**
 Goudeau, P.: B7-2-6, 43; E2-3-5, 131
 Gourmala, O.: B2-1-7, 74
 Goyal, V.: C3-1-6, **14**
 Grant, J.: TS1-1-9, 70
 Grasser, S.: B1-2-2, 9
 Gray, J.: TS4-1-12, **60**
 Greczynski, G.: F2-1-7, **36**
 Greene, J.E.: B1-2-5, 9; B5-1-3, 53; B5-2-5, 65; B7-1-6, 27; B7-1-8, 28; F2-1-7, 36
 Griesler, R.: TS2-2-1, 20
 Grosse-Kreul, S.: B3-1-5, 128
 Grossmann, B.: B6-1-3, 75
 Gruettner, H.: B1-2-3, 9
 Grundmeier, G.: B4-1-9, 42; GP-13, 124; TS2-2-7, 21
 Gu, Z.: TS3-1-9, **82**
 Guarino, S.: GP-14, 124
 Gudmundsson, J.T.: FP-21, 120
 Guenther, K.: B1-2-3, 9
 Guerard, B.: F3-1-7, 134
 Guillonnet, G.G.: E2-3-8, **132**
 Guller, G.: GP-5, **122**
 Gunduz, I.: TS3-1-8, 82; TS3-1-9, 82
 Gupta, M.: TSP-5, 126
 Gustavsson, F.: E3-1/G2-1-10, 18
— H —
 Habrard, F.: F6-1-6, 7
 Hadjiafrenti, A.: TS3-1-9, 82
 Hagiwara, K.: D2-1-5, **130**; DP-4, **109**
 Hagmann, J.: B6-1-5, 75
 Hah, D.: G1-1-8, 58
 Haji Hasan, M.: B4-1-8, 42; EP-10, 113
 Hala, M.: F2-1-1, 35
 Hall-Wilton, R.: F1-1-3, 19; F3-1-7, 134
 Halvarsson, M.: A1-2-5, **61**; A3-1/F8-1-9, 72
 Hamilton, P.: A3-2/F8-2-6, 84
 Hampshire, J.: C1-1-7, 4
 Hancock, M.: E3-2/G2-2-4, 44
 Hansen, R.: F1-1-11, **20**
 Haque, M.D.: TS1-1-2, 68
 Harbin, A.: E1-3-5, 56
 Hari Krishna, K.: FP-5, **117**
 Harig, T.: B2-1-8, 74
 Hartl, C.: E1-3-11, 56
 Hartmann, P.: B6-2-10, 88
 Hasebe, T.: D2-1-5, 130; DP-4, 109
 Hassan, F.: C4-1-11, 32; CP-4, 104
 Hattori, N.: BP-24, **100**
 Hauert, R.: DP-12, 111
 Haynes, J.: A1-2-4, **61**; AP-10, **95**
 He, J.L.: DP-6, 110; FP-20, 120; FP-28, 121; TS2-2-4, **21**
 Hecimovic, A.: F2-2-1, **46**
 Heeg, B.: A2-1-2, 23
 Heinhold, R.: C4-1-1, 30
 Heinß, J.-P.: G6-1-9, **135**
 Helle, W.: E2-3-7, 132
 Hellström, A.: A1-2-5, 61

Helmersson, U.: B1-2-7, 10; B7-1-1, 27; F2-1-5, **35**; F2-2-2, 46
 Henderer, W.: E4-2/G4-2-2, **79**
 Henderson, H.: TSP-5, 126
 Henry, A.: B2-2-7, 86
 Hernandez, M.: B6-2-8, **87**
 Herper, J.: E4-2/G4-2-1, 79
 Herrendorf, A.P.: F2-2-6, 47
 Herrera-Hernández, V.: PD-1-4, **92**
 Herrmann, M.: B2-1-6, 73
 Hetmanczyk, M.H.: AP-16, 96; AP-17, 96
 Hetzner, H.: B4-3-9, **63**
 Hierro, P.: A1-3-5, 71
 Hippler, R.: F2-2-6, 47
 Hirako, T.: GP-1, 122
 Hirano, T.: C2-2/F4-2-2, 11
 Hirose, A.: B4-3-7, 63; B5-1-4, 54
 Hirota, S.: F2-1-3, **35**; G6-1-7, 134
 Hlawacek, G.: TS4-1-13, 60
 Ho, L.W.: E2-3-6, 132
 Ho, W.Y.: BP-35, **102**
 Hodroj, A.: B6-1-6, 76
 Hodson, S.L.: TS1-1-4, 69
 Hoehle, H.-M.: G6-1-8, **135**
 Höfer, M.: B2-1-8, 74
 Hoffmann, F.: B4-2-11, 53
 Hofmann, D.: E3-2/G2-2-11, **45**
 Hofmann, T.: C3-1-1, **13**
 Högberg, H.: B6-1-11, **77**
 Höglund, C.: B2-2-7, 86; F1-1-3, 19; F3-1-7, **134**
 Höhn, M.: B2-1-6, 73
 Holec, D.: B1-1-2, 2; B7-1-9, **28**; B7-2-5, 43; BP-1, **96**
 Hollerweger, R.: B1-3-6, **25**
 Holzherr, M.: B1-2-9, **10**
 Holzschuh, H.: B2-2-1, **85**
 Hong, F.C.N.: C3-1-8, 14
 Hong, J.S.: CP-3, 104
 Hoover, A.: FP-15, 119
 Hosenfeldt, T.: E3-2/G2-2-5, **44**
 Hotta, A.: D2-1-5, 130; DP-4, 109; EP-21, 115; G1-1-7, 58; G5-1-5, 48; GP-7, 123
 Hou, H.: BP-27, 101
 Housden, J.: E1-3-11, 56
 Houska, J.: B1-1-1, 2; F2-2-3, 46
 Hovsepian, P.: F2-1-9, **36**
 Howe, B.M.: B1-2-5, 9; B5-2-5, 65; TS1-1-8, **69**
 Hromadka, M.: EP-4, **112**
 Hsiao, Y.C.: AP-11, 95; BP-5, 97
 Hsieh, B.F.: CP-23, **107**; EP-7, 113
 Hsieh, C.H.: BP-35, 102
 Hsieh, C.Y.: CP-19, 107
 Hsieh, J.H.: B1-3-1, **24**; CP-22, 107; CP-25, 108
 Hsieh, T.E.: B5-1-1, 53; EP-15, 114
 Hsieh, T.Y.: C5-1/F7-1-9, **89**; CP-11, **106**
 Hsieh, Y.T.: C3-1-7, 14; C3-1-9, 14; CP-1, 104
 Hsu, C.: E3-2/G2-2-8, 45
 Hsu, C.C.: TS2-2-4, 21
 Hsu, C.H.: BP-33, 102; BP-35, 102; C3-1-7, **14**; C3-1-9, 14; CP-1, 104; CP-15, 106
 Hsu, C.S.: CP-15, 106
 Hsu, Chan-Jung.: B2-1-9, 74
 Hsu, J.T.: DP-1, 109
 Hsu, M.H.: F1-1-4, **19**
 Hu, H.: E4-1/G4-1-7, 67
 Hu, J.J.: F3-1-6, 133; TS1-1-3, 69; TSP-8, 127
 Hu, M.: B4-2-12, 53
 Huang, F.: B5-1-11, **55**
 Huang, H.C.: F1-1-5, 19
 Huang, H.H.: D2-1-8, 131; DP-11, 111; DP-18, **112**
 Huang, H.L.: DP-1, 109; DP-2, 109
 Huang, J.: TS4-1-10, **60**
 Huang, J.C.: D2-1-9, 131
 Huang, J.H.: B4-3-6, **63**; BP-10, 98; BP-11, 98; BP-4, 97; BP-40, 103; E2-2-8, 91
 Huang, J.J.: C2-2/F4-2-11, **13**
 Huang, J.L.: C3-1-12, 14
 Huang, Jow-Lay.: B2-1-9, 74

Huang, K.H.: BP-33, **102**
Huang, P.H.: B4-3-6, 63
Huang, S.: C2-3/F4-3-10, 30
Huang, S.H.: B5-1-1, 53; EP-15, 114
Huang, S.Y.: C2-3/F4-3-4, 29; C5-1/F7-1-5, **89**;
FP-12, 118; FP-18, **119**
Huang, Y.C.: BP-23, 100; PDP-5, 125
Hubicka, Z.: F2-2-6, 47
Huerta, L.: D2-1-3, 129
Hufenbach, W.: B6-1-10, 76
Huh, J.-Y.: F3-1-4, 133; FP-24, 121
Hultman, L.: B1-1-5, 2; B1-2-5, 9; B5-1-3, 53; B5-2-5, 65; B7-1-10, 28; B7-1-6, 27; B7-1-8, 28; B7-2-7, 43; BP-32, 102; C5-1/F7-1-10, 89; C5-1/F7-1-8, 89; F1-1-3, 19; F2-1-7, 36; F3-1-7, 134; TS2-1-3, 8
Hung, F.Y.: A3-2/F8-2-1, 84
Hunter, N.: TS1-1-7, **69**
Huo, C.: FP-21, **120**
Hurley, D.: TSP-5, 126
Hussain, M.S.: A1-2-11, **62**; PDP-2, **125**
Hussain, O.M.: FP-3, **116**; FP-5, 117
Hussein, R.: G3-1-5, **67**
Hutchinson: A2-1-3, **23**
Hutton, S.: TS2-1-5, 8
— **I** —
Igarashi, M.: B2-1-5, **73**
Imamiya, M.: BP-14, **99**
Immich, P.: B2-1-1, **73**; GP-11, **124**
Inan, D.: PDP-6, 125
Ingemarsson, A.: A1-2-5, 61
Irissou, E.: E3-2/G2-2-1, 44
Ishikawa, T.: B1-1-3, **2**; F2-2-8, 47
Ishizuka, S.: C2-2/F4-2-7, 12
Ito, T.: G5-1-4, **48**
Iwai, Y.: B4-3-3, **63**; G1-1-5, 57
— **J** —
Jackson, R.W.: A2-2-5, **39**
Jacobson, N.: A2-2-11, 40
Jacobson, S.: E1-2-4, 33
Jang, B.K.: A2-1-6, 23
Jang, J.: AP-14, 96
Jankowski, A.: B4-1-10, **42**
Jansson, B.: B4-1-6, 41
Jansson, U.: B1-2-7, 10; E1-2-4, 33
Jaouen, C.: B3-1-6, 129; BP-38, 103
Jardret, D.: PD-1-6, 93
Jarvis, A.: B4-3-10, **64**
Jaschinski, P.: G6-1-7, 134
Jayaganthan, R.: A1-1-8, 50
Jennett, N.M.: B4-1-7, **41**
Jensen, B.: F1-1-11, 20
Jensen, J.: B1-1-5, 2; B2-2-7, 86; F2-1-7, 36; F3-1-7, 134
Jeong, Y.: D1-1-7, 5
Jespersen, M.: TS1-1-7, 69
Jeung, W.Y.: CP-17, 107
Jheng, Y.: A3-1/F8-1-11, 72
Jhu, J.-C.: GP-3, **122**
Jian, F.Y.: C2-3/F4-3-4, 29; C5-1/F7-1-9, 89; CP-11, 106; FP-18, 119
Jimenez, C.: B2-1-7, 74
Johansson, L.G.: A1-1-1, 50; A1-2-5, 61; A3-1/F8-1-9, 72
Johansson, M.: B4-2-9, 52; B7-2-9, 44; F2-1-7, 36
Johnson, L.: B5-1-3, 53; TS2-1-3, **8**
Jones, Jr., D.: TS3-1-5, 81
Jonsson, A.: A1-2-5, 61
Jordan, E.: A2-2-9, 40
Jouan, P.-Y.: F2-1-12, 37
Juez Lorenzo, M.: A1-3-3, 71; A2-2-6, 39
Jung, S.: A2-1-7, 23
Jung, S.B.: TS2-2-8, 21
Jung, Y.: A2-1-7, 23; A2-2-10, 40; AP-14, 96; E2-2-9, 91
— **K** —
Kahevcioğlu, O.: E3-2/G2-2-7, 45
Kahvecioğlu, O.: G5-1-11, 49; G5-1-12, **49**

Kalesaki: CP-28, 108
Kalss, W.: B6-1-5, 75
Kamal, S.: A1-1-8, **50**; A1-1-9, 51
Kamath, G.: F2-1-9, 36
Kameshima, T.: GP-8, **123**
Kamijo, A.: DP-4, 109
Kamiya, N.: C4-1-7, 32
Kamiya, S.: E2-2-3, **90**
Kang, I.K.: D1-1-7, 5
Kappl, H.: B5-2-2, 64
Kapsa, Ph.: E1-1-1, 6
Karacali, T.: C3-1-4, 13
Karakostas: CP-28, **108**
Karimi, A.: B6-2-7, **87**; TSP-9, **127**
Kartal, G.: E3-2/G2-2-7, 45; G5-1-11, 49; G5-1-3, **48**
Karvankova, P.: E4-2/G4-2-10, 80
Kassman-Rudolph, Å.: B1-2-7, 10
Katardjiev, I.: C5-1/F7-1-1, **88**
Kathrein, M.: B1-2-2, 9; B2-1-2, 73; C2-3/F4-3-8, 30
Katirtzoglou, G.: E4-2/G4-2-3, 79
Kato, A.: FP-19, 120
Kato, T.: B2-1-11, 74; BP-16, 99; FP-19, 120
Kaur, D.: B5-1-2, 53; B5-1-8, **54**; C3-1-13, 15; C3-1-6, 14
Kaur, N.: B5-1-2, **53**
Kawamura, K.: A3-1/F8-1-7, 71
Kazmanlı, K.: E1-3-13, 57
Ke: PD-1-3, 92
Keblinski, P.: TS1-1-6, 69
Keckes, J.: B4-1-1, 40; B5-1-7, 54; B6-2-1, 86
Keipert-Colberg: B2-1-8, 74
Keller, I.: A1-2-2, **61**
Kennedy, M.: F6-1-1, 7
Kermouche, G.: E2-3-8, 132
Kerzhner, T.: G3-1-8, 68
Keunecke, M.: B6-1-4, 75
Khafizov, M.: TSP-5, 126
Khaplanov, A.: F3-1-7, 134
Khatibi: B1-1-5, **2**
Khokhar, F.: TS4-1-13, 60
Khor, O.K.: F1-1-6, 19
Kilchenstein, G.: G1-1-9, 58
Kim: BP-21, 100
Kim, B.J.: FP-8, 117; FP-9, **118**
Kim, B.S.: BP-22, 100; E1-3-7, 56
Kim, C.Y.: CP-17, 107
Kim, D.E.: E1-2-2, 33
Kim, D.J.: BP-22, 100; E1-3-7, **56**
Kim, E.H.: E2-2-9, **91**
Kim, H.: A2-1-7, 23
Kim, H.-J.: E1-2-2, **33**
Kim, H.T.: A2-1-6, 23
Kim, H.W.: FP-7, **117**
Kim, H-S: C4-1-1, 30
Kim, J.H.: CP-30, **108**
Kim, J.P.: FP-8, 117
Kim, J.Y.: BP-22, **100**; E1-3-7, 56
Kim, K.H.: CP-13, 106; CP-3, **104**; CP-6, **105**
Kim, K.S.: TS2-2-8, **21**
Kim, M.: A2-1-7, 23
Kim, S.: A2-2-10, 40
Kim, S.W.: A2-1-6, 23
Kim, W.: CP-7, **105**; CP-8, 105
Kindlund, H.: B7-1-6, **27**
King, S.: B4-3-8, **63**; TSP-7, **127**
Kioseoglou, -: CP-28, 108
Kirchlechner, C.: B5-1-7, 54
Kiriakidis, G.: C4-1-3, 31
Kirschner, M.: E4-2/G4-2-1, **79**
Kiruykhansev-Korneev, Ph.V.: B4-1-3, 41
Kiruykhansev-Korneev, P.: AP-9, **95**; B5-1-12, **55**
Klaus, J.: TS2-2-1, 20
Klemberg-Sapieha, J.E.: B5-1-5, 54; F2-1-1, 35
Klenov, D.: B5-1-3, 53
Klever, C.: F1-1-12, 20
Klimczak, A.: FP-23, 120
Knaut, M.: B2-1-6, 73

Knutsson, A.: B4-1-6, **41**
Knutsson, P.: A1-1-1, 50
Ko, J.-S.: B1-2-12, 11; F3-1-4, **133**; FP-24, **121**
Ko, J.W.: CP-17, 107
Ko, M.H.: GP-6, 123
Kodambaka, S.: TS2-2-5, **21**; TS4-1-3, 59
Koelker, W.: B2-2-4, 85; G6-1-3, **134**
Köhler, B.: E4-1/G4-1-5, 66
Kohlscheen, J.: E4-1/G4-1-8, **67**
Kohout, J.: B5-1-10, **55**
Koiwa, K.: E2-2-3, 90
Kolarik, V.: A1-3-3, **71**; A2-2-6, 39
Kolitsch, A.: EP-24, 115
Kölker, W.: F2-1-7, 36
Komaki, H.: C2-2/F4-2-7, 12
Komendera, L.K.: AP-16, 96
Kominou: B7-1-11, **28**; CP-28, 108
Konitzer, D.: A2-2-4, 39
Konstantinidis, S.: F2-2-11, **47**
Koo, H.S.: C3-1-9, 14; CP-1, 104
Koo, T.H.: D1-1-7, 5
Korte, S.: B5-1-9, 54; E2-2-1, **90**; TS2-1-4, 8; TS2-2-3, 21
Kortmann, A.: B3-1-7, 129; TSP-4, 126
Köstenbauer, H.: C2-3/F4-3-8, **30**
Koster, A.: A2-1-9, 24
Kotula, P.: E1-2-9, 34; E1-3-12, 56
Koutsokeras, L.: BP-12, 98; C3-1-5, 14
Kovac, J.: E4-1/G4-1-5, **66**
Kovacs, G.: F6-1-6, 7
Krämer, S.: A2-1-8, 24
Krassnitzer, S.: B6-1-5, 75; G6-1-5, **134**
Kreiter, O.: B3-1-5, 128
Kretzschmann, U.: B2-1-1, 73; GP-11, 124
Krogstad, J.: A2-1-8, **24**
Krottenthaler, M.: PDP-4, **125**
Krug, T.: F2-2-8, 47; G6-1-4, 134
Kubart, T.: B6-2-3, 87; C2-2/F4-2-9, **12**; E1-2-4, 33
Kubiak, J.: E1-2-1, 33
Kuchenreuther, V.: A1-3-3, 71; A2-2-6, **39**
Kukureka, S.: F6-1-5, 7; FP-15, 119
Kumar, A.: E2-1-8, 78; TS1-1-4, 69; TS4-1-6, 59; TS4-1-9, **59**
Kumar, J.: FP-3, 116; FP-4, 117
Kunkel, S.: E3-2/G2-2-11, 45
Kunze, C.: B4-1-9, **42**
Kunze, K.: B6-1-10, 76
Kuo, C.C.: B5-1-1, 53
Kuo, Y.C.: AP-13, **96**; B4-3-11, **64**
Kuptsov, K.A.: B4-1-3, 41
Kurapov, D.: B6-1-5, **75**
Kurokawa, Y.: B1-2-1, 9
Kuromoto, N.K.: DP-15, **111**; DP-16, 111
Kwak, K.H.: A2-1-6, 23
— **L** —
Lackner, J.M.: B6-2-10, **88**
Laha, P.: C2-3/F4-3-9, 30
Lahiri, D.: E3-2/G2-2-3, 44
Lai, C.H.: DP-2, 109
Lai, D.W.: E3-2/G2-2-8, 45
Lai, H.: A1-1-1, 50
Lai, L.H.: B2-2-9, **86**
Lai, L.W.: GP-6, **123**
Lai, M.C.: FP-20, 120
Lai, W.C.: TSP-3, 126
Lai, Y.S.: A3-2/F8-2-8, **85**; TSP-6, **126**
Lai, Yan-Liang.: CP-25, **108**
Laloglu, C.: B4-3-5, **63**
Laloğlu, Ç.: EP-11, 113
Lambertini, V.: C4-1-3, 31
Lamy, T.: PD-1-1, 92
Landsbergen, J.: G6-1-4, **134**
Lang, P.: G6-1-9, 135
Lasanta, I.: A1-3-5, 71
Laukart, A.: B2-1-8, 74
Laurindo, C.A.H.: DP-7, 110
Lawal, J.: AP-12, **96**
Lawrence, S.: E2-1-1, 77

- Le Bourhis, E.: AP-4, 94; B7-2-6, 43; E2-3-5, 131
 Le Priol, A.: AP-4, **94**
 Le, M.: C4-1-11, 32; CP-4, 104; CP-5, 104
 Leadore, J.: G3-1-1, 67
 Lechthaler, M.: B1-1-2, 2; B1-1-6, 2; B1-3-6, 25; G6-1-5, 134
 Leckie, R.: A2-1-8, 24
 Lee: A3-2/F8-2-2, 84
 Lee, C.C.: EP-7, **113**
 Lee, E.S.: F3-1-5, **133**; FP-25, **121**; FP-26, 121
 Lee, J.: A2-2-10, 40; AP-14, 96; E2-2-9, 91
 Lee, J.J.: E1-3-7, 56
 Lee, J.W.: AP-13, 96; B1-3-12, 26; B4-3-11, 64; B5-1-1, 53; D2-1-9, 131; E2-3-1, 131; E2-3-6, **132**; EP-15, 114
 Lee, K.: A2-2-7, **40**; AP-14, 96
 Lee, K.M.: CP-17, 107
 Lee, M.H.: CP-23, 107
 Lee, S.: A2-1-7, 23; GP-10, 124
 Lee, S.H.: CP-7, 105; CP-8, **105**
 Lee, S.M.: A2-1-6, 23
 Lee, S.Y.: BP-21, **100**; BP-22, 100; E1-3-7, 56
 Lee, W.C.: C1-1-3, **3**; C2-2/F4-2-3, 12
 Lee, W.S.: BP-16, 99
 Lee, W.-S.: B1-2-12, 11
 Legoux, J.-G.: E3-2/G2-2-1, 44
 Lei, M.: F2-1-10, 36
 Leiste, H.: F1-1-12, 20
 Lejars, A.: F2-2-5, 46
 Lekka, C.: BP-12, 98
 Lemmer, O.: B2-2-4, 85; F2-1-7, 36; G6-1-3, 134
 Leonhardt, M.: B1-2-9, 10; B6-1-10, 76
 Lepienski, C.: DP-16, **111**; EP-24, 115
 Lepieski, C.: G5-1-13, 49
 Lepple, M.: A2-1-8, 24
 Leroy, W.: F2-2-11, 47
 Leson, A.: B6-1-10, 76; E1-2-11, 34
 Leu, J.I.M.: CP-16, 106
 Leu, M.S.: CP-2, 104
 Levashov, E.A.: AP-9, 95; B4-1-3, 41; B5-1-12, 55
 Levi, C.G.: A2-1-1, 23; A2-1-11, 24; A2-1-8, 24; A2-2-4, 39; A2-2-5, 39
 Lew, W.: B1-3-12, 26
 Lewin, E.: B5-2-6, **65**
 Leyens, C.: G1-1-3, **57**
 Leyland, A.: AP-12, 96; AP-3, 94; B4-2-1, **51**; B4-2-6, 52; BP-20, 100
 Li, B.: F3-1-3, 133
 Li, C.: B5-2-7, 65
 Li, C.H.: C1-1-4, **3**; EP-14, **114**
 Li, C.M.: C2-3/F4-3-1, 29
 Li, F.J.: F3-1-3, **133**
 Li, H.: AP-6, 95
 Li, J.: A3-2/F8-2-3, 84
 Li, L.: A2-2-1, 39
 Li, L. H.: BP-42, 103
 Li, S.: B5-1-11, 55
 Li, S.L.: FP-27, 121
 Li, Y.: B2-2-8, 86; B4-3-7, 63; B5-1-4, **54**; D2-1-4, 130
 Li, Z.Z.: CP-9, 106
 Liang, C.-J.: G3-1-6, 68
 Liao, M.W.: F1-1-6, **19**; FP-27, **121**
 Lichtenberg, J.: PD-1-2, 92
 Lidorikis, E.: CP-29, 108
 Liedtke, F.: D3-1-10, 16
 Liew, L.: E2-3-9, 132
 Lim, S.: C4-1-2, **31**; C4-1-8, 32; C4-2/F4-2-6, 12
 Lima, L.G.D.B.S.: E3-1/G2-1-8, **18**; E3-1/G2-1-9, 18
 Lin, C.: A3-2/F8-2-2, 84; B1-3-10, 26; BP-33, 102; E3-2/G2-2-8, **45**
 Lin, C.A.: BP-35, 102
 Lin, C.H.: A3-1/F8-1-10, **72**
 Lin, C.K.: C2-2/F4-2-3, 12; C3-1-7, 14; CP-12, 106; F1-1-4, 19
 Lin, C.L.: BP-35, 102
 Lin, H.H.: C3-1-8, **14**
 Lin, J.: B5-2-1, 64; F1-1-8, 20; F2-1-10, **36**; F2-2-4, 46; TSP-5, 126
 Lin, K.W.: GP-6, 123
 Lin, L.D.: B2-1-12, 75
 Lin, L.W.: FP-18, 119
 Lin, M.T.: A3-1/F8-1-10, 72; A3-1/F8-1-11, 72; A3-2/F8-2-5, **84**; EP-8, **113**
 Lin, S.: BP-27, 101
 Lin, S.W.: EP-3, 112
 Lin, S.Y.: BP-23, **100**
 Lin, Y.B.: B5-1-1, 53; EP-15, 114
 Lin, Y.T.: C1-1-4, 3; EP-14, 114
 Lind, H.: B7-2-9, **44**
 Liou, Y.Y.: BP-17, **99**
 Lipkin, D.: A2-1-8, 24
 Liskiewicz, T.: E1-2-1, **33**; E2-3-7, 132; E3-2/G2-2-10, 45
 Liu, C.N.: GP-13, 124; TS2-2-7, 21
 Liu, J.: TS1-1-6, 69
 Liu, K.H.: FP-13, 119
 Liu, K.Y.: AP-11, 95; BP-5, 97
 Liu, P.T.: CP-9, 106
 Liu, S.: B5-1-9, **54**
 Liu, S.J.: CP-22, 107
 Liu, Y.: B2-1-3, 73; B4-2-12, 53
 Lo, S.S.: C2-2/F4-2-3, 12
 Lo, W.H.: C2-1/F4-1-4, **4**; CP-21, **107**
 Lobo, E.: D1-1-6, 5
 Löffler, J.: F2-2-10, 47
 Lopez, J.: B2-2-10, 86
 Lopez, A.: E3-1/G2-1-5, **17**
 Lopez-Hirata, V.: A1-1-5, 50
 Loubet, J.L.: E2-3-8, 132
 Löwenberg, L.: B4-3-1, 62
 Lu, C.W.: BP-11, **98**
 Lu, J.: B1-1-5, 2; B7-1-6, 27; F2-1-7, 36
 Lu, P.: E2-1-8, **78**
 Lu, Q.Y.: BP-42, **103**
 Lu, W.S.: C5-1/F7-1-9, 89
 Lu, X.J.: AP-6, **95**
 Lu, Y.C.: CP-2, 104
 Lu, Y.R.: EP-14, 114
 Lu, Z.: AP-14, 96
 Luchaninov, A.: B1-3-8, 25
 Lui, T.S.: A3-2/F8-2-1, 84
 Lukitsch, M.J.: E2-1-8, 78; E3-1/G2-1-13, 18
 Lunca Popa, P.: FP-14, 119
 Lundin, D.: F2-1-5, 35; F2-2-2, **46**; FP-21, 120
 Luo, J.Y.: C3-1-9, 14; CP-1, 104
 Lusth, J.C.: G1-1-2, 57
 Lyo, I.W.: BP-34, 102
- M —**
- Ma, Y.H.: GP-9, 123
 Macdonald, D.: D3-1-7, 16
 Machado, J.: EP-2, 112
 Magerl: TS3-1-10, 82
 Magnfält, D.: B7-1-1, 27
 Mahammad, O.: FP-4, **117**
 Mahapatra, S.K.: C2-3/F4-3-9, **30**; D1-1-2, 5
 Maier, V.: PDP-3, 125
 Major, L.: B6-2-10, 88
 Makino, H.: C2-2/F4-2-4, 12; C4-1-5, 31; C4-1-6, **31**
 Makowski, S.: E1-2-11, 34
 Makrimalakis, S.: E4-2/G4-2-3, 79
 Maliaris, G.: BP-30, 101; E4-2/G4-2-3, 79
 Malic, B.: C4-1-3, 31
 Malzer, M.: F2-2-10, 47
 Manaia, A.: E4-1/G4-1-6, **66**
 Manakhov, A.: B2-1-10, 74
 Manap, A.M.: B7-1-2, **27**
 Manaud, J.-P.: B6-1-6, 76
 Manna, I.: B3-1-2, 128
 Manoharan, M.P.: TS1-1-2, 68
 Manuel, M.: TSP-5, 126
 Mao, S.: C4-2/F4-2-6, 12
 Mares, M.: FP-10, 118
 Maric, Z.: F2-2-10, 47
 Marinin, V.: B1-3-8, 25
 Marino, C.E.B.: DP-15, 111
 Marinov, D.: B3-1-5, 128
 Mark, G.: F2-2-10, 47
 Mark, M.: F2-2-10, 47
 Marques, C.: BP-13, **98**
 Martin, P.: F1-1-7, **20**
 Martinez-Trinidad, J.: E2-2-6, 91; E2-2-7, 91
 Martini, A.: E1-1-3, **6**
 Martins, G.: EP-2, 112
 Martins, R.: C4-1-3, 31
 Martinu, L.: B5-1-5, 54; F2-1-1, **35**
 Maruyama, T.: A3-1/F8-1-7, 71
 Mastorakos, I.: E2-1-1, 77
 Mat Kamal, E.: B4-2-4, 51
 Matenoglou, M.: C3-1-5, 14
 Mathew, M.T.: D3-1-10, 16; D3-1-5, 16
 Mato, S.: A1-3-5, 71
 Matsubara, K.: C2-2/F4-2-7, 12
 Matsubara, T.: B4-3-3, 63
 Matsushita, N.: CP-3, 104
 Mattei, M.: F6-1-4, 7
 Mattes, W.: AP-15, **96**
 Mattevi, C.: TS4-1-4, 59
 Matthews, A.: AP-12, 96; AP-3, 94; B4-2-1, 51; B4-2-6, 52; B4-3-10, 64; BP-20, 100; D2-1-6, 130; D3-1-9, 16; G3-1-6, 68
 Matumoto, T.: G5-1-4, 48
 Maurel, V.: A1-2-8, 62; A2-1-9, **24**
 Maury, F.: B2-2-3, **85**
 Maushart, J.: E4-2/G4-2-7, 80
 Mavrin, B.: B5-1-12, 55
 May, C.: TS3-1-7, 81
 Mayes, E.H.: C4-1-1, 30
 Mayrhofer, P.H.: B1-1-2, 2; B1-3-6, 25; B4-2-10, 53; B4-2-8, 52; B5-1-7, 54; B6-1-3, **75**; B7-1-9, 28; B7-2-5, 43; BP-1, 96; BP-20, 100
 McCarty, K.: TS4-1-3, 59
 McCulloch, D.G.: C4-1-1, 30
 McDonald, P.: TS3-1-5, 81
 McKenna, D.: F1-1-11, 20
 McKenzie, D.: C4-1-8, 32
 Médard, J.: PD-1-1, 92
 Medina, V.: BP-19, 99
 Medrano, S.: GP-4, **122**
 Meena, A.: E4-2/G4-2-4, **79**; EP-27, **116**
 Mei, A.: B1-2-5, **9**; B5-2-5, 65
 Melo, L.: A1-1-5, 50
 Melo-Máximo, D.: A1-1-3, 50
 Mendala, B.M.: AP-16, 96; AP-17, 96
 Mendelsberg, R.: C4-1-2, 31; C4-2/F4-2-6, 12
 Mendez, N.: CP-10, 106
 Mendizabal, L.: B1-3-4, 25; B3-1-1, **128**
 Meneses-Amador, A.: E2-2-6, **91**
 Meng-Burany, X.: E3-1/G2-1-13, 18
 Meyer, C.-F.: B1-2-9, 10
 Mezghani, S.: E1-1-5, **6**
 Michael, S.: TS2-2-1, 20
 Michailidis: BP-30, 101
 Michalke, T.: E4-2/G4-2-11, **80**
 Michel, A.: B3-1-6, 129; BP-38, 103
 Michely, T.: TS4-1-1, **59**
 Michotte, C.: B2-1-2, 73; B4-1-5, 41
 Midgley, P.A.: TS2-1-4, 8
 Milhet, X.: AP-2, **94**
 Minami, T.: C2-2/F4-2-2, 11; CP-18, 107
 Minea, T.: F2-2-2, 46
 Minne, S.: E2-3-11, 132
 Minor, A.: E2-2-10, **91**
 Mitterer, C.: B1-1-6, 2; B1-2-2, 9; B2-1-2, 73; B4-1-1, **40**; B4-1-5, 41; B6-2-1, 86; EP-13, 114
 Miyata, T.: C2-2/F4-2-2, **11**; CP-18, 107
 Mkaddem, A.: EP-27, 116
 Mo, J.L.M.: B4-2-6, **52**; EP-20, **115**
 Mocuta, C.: E2-3-5, 131
 Moharrami, N.: E2-3-2, **131**
 Mohseni, H.: E1-2-6, 34
 Mok, H.S.: TS4-1-3, **59**
 Mol, J.M.C.: E2-1-6, 78
 Monkman, P.: C2-3/F4-3-5, **29**

Moody, N.R.: F6-1-1, **7**
Moon, S.: D1-1-7, **5**
Moore, J.: F1-1-8, 20; F2-1-10, 36; F2-2-4, 46; TSP-5, 126
Moreno-Couranjou, M.: B2-1-10, **74**
Mori, T.: BP-24, 100
Morishita, K.: BP-8, **97**
Morris, C.: TS3-1-7, **81**
Morstein, M.: B6-2-7, **87**; E4-2/G4-2-10, **80**
Moskal, G.M.: AP-16, 96; AP-17, 96
M'Saoubi, R.: B4-2-9, 52
Mücklich, F.: TS2-1-1, **8**; TS3-1-8, 82
Mudgal, D.: A1-1-8, 50; A1-1-9, **51**
Mueller, J.: G6-1-6, 134
Muhammad, M.R.: B4-1-8, 42; EP-10, 113
Muhl, S.: B2-2-10, **86**; B4-1-11, 42; B4-2-3, 51; B5-2-10, 65; B6-1-9, 76; DP-5, 110; EP-22, **115**; GP-4, 122
Mühlbacher, M.: B1-1-6, 2; B4-1-1, 40
Mühle, U.: C2-3/F4-3-8, 30
Mukherjee, S.: B3-1-2, 128
Muller, K.H.: F1-1-7, 20
Muller, P.: AP-4, 94
Müller, U.: DP-12, 111
Mulligan, C.: B5-2-1, **64**
Munemasa, J.: G1-1-5, **57**
Murata, Y.: TS2-2-5, 21; TS4-1-3, 59
Muratore, C.: E1-3-5, 56; TS1-1-2, **68**; TS1-1-3, 69; TSP-8, **127**
Musayev, Y.: E3-2/G2-2-5, 44
Music, D.: F3-1-1, 132
Musil, J.: B1-1-1, 2; B4-1-2, 40; EP-4, 112
Mussenbrock, T.: G3-1-7, **68**
Myoung, S.: A2-1-7, **23**; A2-2-10, 40; AP-14, **96**
Myung, W.R.: TS2-2-8, 21
— **N** —
Nagasawa, T.: E2-2-3, 90
Nagatomi, E.: B2-1-11, 74
Nagelli, C.: D3-1-10, **16**
Najafi, H.: B6-2-7, 87
Nakamura, T.: E2-2-3, 90
Nakata, Y.: FP-2, 116
Naumenko, D.: A1-2-2, 61; A1-2-9, **62**
Nayak, PramodaKumar.: B2-1-9, **74**
Neder: TS3-1-10, 82
Negrelli, J.R.: DP-7, 110
Neumeier, S.: PDP-4, 125
Neville, A.: E3-2/G2-2-10, **45**
Ngugen, M.: C4-1-11, 32; CP-4, 104 CP-5, **104**;
Ni, N.: B4-2-10, 53
Ni, W.: B4-2-12, 53
Niakan, H.: B5-2-4, **64**
Nie, S.: TS4-1-3, 59
Nie, X.: AP-1, 94; E2-1-5, **78**; E4-1/G4-1-7, 67; G3-1-5, 67
Nieher, M.: B1-2-3, 9
Nießen, N.: A1-3-4, 71
Niki, S.: C2-2/F4-2-7, **12**
Nikumaa, M.: A3-1/F8-1-9, 72
Nishi, Y.: CP-18, **107**
Nishida, M.: E2-2-3, 90
Nishioka, K.: G5-1-4, 48; TS1-1-11, **70**
Nivot, C.: F2-1-12, 37
Noborisaka, M.: BP-24, 100; GP-1, 122
Noda, S.: C1-1-1, 3
Nohava, J.: E4-2/G4-2-10, 80
Nokuo, T.: E2-2-3, 90
Nomoto, J.: C2-2/F4-2-2, 11
Norrby, N.: B4-2-9, **52**
Northwood, D.: G3-1-5, 67
Novak, P.: EP-4, 112
Nunes, L.C.S.: E3-1/G2-1-8, 18
Nyberg, H.: E1-2-4, 33
Nyberg, T.: E1-2-4, 33
Nygren, K.: B1-2-7, **10**
— **O** —
O'Reilly, E.: C5-1/F7-1-6, 89
O'Brien, P.: TS1-1-6, **69**

Oden, M.: B1-2-5, 9
Odén, M.: B4-1-6, 41; B4-2-9, 52; B5-1-3, 53; B7-2-8, 43; B7-2-9, 44; BP-31, 101; TS2-1-3, 8
Oechsner, M.: B1-2-8, 10; B6-2-9, 88; TS1-1-1, 68
Oezer, D.: B4-1-11, 42; BP-43, 104
Oezkaya, B.: GP-13, 124
Ogawa, K.: B7-1-2, 27
Oh, Y.S.: A2-1-6, **23**; BP-34, **102**
Ohtake, N.: B3-1-8, 129; G3-1-3, **67**
Oila, A.: B7-1-7, **28**
Okabe, T.: B7-1-2, 27
Olivares-Navarrete, R.: D2-1-7, 130
Oliveira, A.M.C.: EP-24, 115
Olmsted, D.: B7-1-3, 27
Olovsson, W.: B7-2-7, **43**
Omiya, M.: E2-2-3, 90
Ootani, T.: FP-19, 120
Ophus, C.: B7-1-3, 27
Opila, E.: A2-2-11, **40**
Osada, A.: B2-1-5, 73
Oseguera, J.: A1-1-3, **50**; A1-1-5, 50
Oseguera-Peña, J.: G1-1-1, 57
Osés, J.: E1-3-11, 56
Oshima, M.: C4-1-7, 32
Ota, Y.: TS1-1-11, 70
Ou, K.: BP-33, 102; E3-2/G2-2-8, 45
Ozcan, O.: GP-13, 124; TS2-2-7, 21
Ozimek, P.: FP-23, 120
Özkanat, Ö.: E2-1-6, **78**
Ozkaya, B.: TS2-2-7, **21**
Özkucur, N.: D3-1-3, 15
— **P** —
Page, S.: TS2-1-5, 8
Paik, U.: A2-2-10, 40; AP-14, 96
Pallier, C.: B4-2-7, 52
Palomar-Pardavé, M.: PD-1-4, 92
Pan, K.Y.: B2-1-12, **75**
Panda, A.B.: C2-3/F4-3-9, 30; D1-1-2, 5
Panier, S.: E2-2-6, 91
Pantke, K.: E4-2/G4-2-1, 79
Pantoya, M.: TS3-1-3, 81
Paolini, T.: C2-3/F4-3-7, 29
Papa, F.: F2-2-8, **47**; G6-1-4, 134
Papi, P.: B5-2-1, 64
Pappa, M.: BP-30, 101
Pappas, D.: G3-1-1, **67**
Parfenov, E.: G3-1-6, 68
Park, I.W.: TSP-5, **126**
Park, J.K.: B1-2-12, **11**; F3-1-4, 133; F3-1-5, 133; FP-24, 121; FP-25, 121; FP-26, **121**
Park, J.S.: CP-7, 105; CP-8, 105; FP-8, 117; FP-9, 118
Park, S.J.: BP-34, 102
Park, W.S.: BP-16, **99**
Parlinska-Wojtan, M.: B5-2-6, 65
Parra Maza, E.: F2-2-10, 47
Parreira, N.M.G.: B6-2-3, 87
Partridge, J.G.: C4-1-1, **30**
Pascual, E.: C3-1-3, 13
Patsalas, P.: B1-3-11, 26; BP-12, **98**; C3-1-5, **14**; CP-29, 108
Patscheider, J.: B5-2-6, 65; F6-1-6, **7**
Paul, R.: F3-1-6, **133**; TS4-1-6, 59; TS4-1-9, 59
Paulitsch, J.: B1-1-2, 2; B1-3-6, 25; B5-1-7, 54
Pedersen, H.: B2-2-7, **86**
Pellier, J.: D3-1-7, 16
Pena-Rodriguez, Y.: B2-2-10, 86
Peng, X.: A1-3-1, **71**
Peng, Z.J.: AP-1, **94**
Penoy, M.: B2-1-2, 73; B4-1-5, 41
Pereira, B.L.: DP-15, 111; DP-16, 111
Pereira, L.: C4-1-3, 31
Perez, D.: B7-2-3, **43**
Pérez, J.: A1-3-5, **71**
Perrinet, O.P.: E3-2/G2-2-9, **45**
Petorak, C.: A2-2-1, 39
Petrov, I.: B1-2-5, 9; B5-1-3, 53; B5-2-5, 65; B7-1-6, 27; B7-1-8, 28; F2-1-7, 36; F2-1-9, 36; TS2-2-5, 21

Petrova, V.: TS2-2-5, 21
Pezoldt, J.: TS2-2-1, 20
Pham, T.: B7-2-6, 43
Philips, N.: A2-1-1, 23
Piascik, J.: D1-1-6, **5**
Piccoli, M.: EP-16, 114
Piehler, L.: G3-1-1, 67
Pinedo, C.: BP-36, 102
Pingree, L.: E3-1/G2-1-3, **17**
Pint, B.: A1-2-3, **61**; A1-2-4, 61; AP-10, 95
Pireaux, J.J.: B2-1-10, 74
Piscitelli, F.: F3-1-7, 134
Pitonak, R.: B2-1-1, 73
Pittenger, B.: E2-3-11, **132**
Platzer-Björkman, C.: C2-2/F4-2-9, 12
Poelsema, B.: TS4-1-13, 60
Pogozhev, Yu.: AP-9, 95
Pohler, M.: B1-1-2, 2
Polcar, T.: B6-2-3, 87; E3-1/G2-1-10, **18**
Polcik, P.: B1-1-2, 2; B1-1-6, 2; B1-2-2, 9; B1-3-6, 25; B6-1-3, 75
Politano, O.: TS3-1-4, **81**
Pollet, B.: A3-2/F8-2-6, 84
Polychronopoulou, K.: BP-20, 100
Pons, M.: B2-1-7, **74**
Popov, M.: B4-1-1, 40
Poppleton, A.: C4-1-8, **32**
Portal-Marco, S.: C3-1-3, **13**
Potoczny, G.: F6-1-5, 7
Poulon-Quintin, A.: B6-1-6, **76**
Pourzal, R.P.: D3-1-10, 16
Prakash, B.: BP-18, 99
Prakash, S.: A1-1-8, 50; A1-1-9, 51
Prasad, S.: E1-2-9, 34; E1-3-12, **56**
Prenzel, M.: B3-1-7, **129**; TSP-4, **126**
Prichard, P.: B2-1-3, 73
Prieto, P.: AP-5, **94**; PD-1-5, **92**
Proksova, S.: B4-1-2, 40
Prskalo, A.-P.: PD-1-2, **92**
Psyllaki, P.: BP-12, 98
Putnam, S.: TS1-1-7, 69
— **Q** —
Qi, Y.: E3-1/G2-1-13, 18
Qin, Y.: E1-3-11, 56
Quadackers, W.J.: A1-2-2, 61; A1-2-9, 62
— **R** —
Raadu, M.A.: FP-21, 120
Rachbauer, R.: B4-2-8, **52**; B6-1-3, 75
Radetic, T.: B7-1-3, 27
Radhakrishnan, R.: D3-1-5, 16
Rafaja, D.: C2-3/F4-3-8, 30
Ramachandran, G.: E2-2-2, **90**
Ramana, V.: B6-2-8, 87; CP-20, 107; FP-10, **118**; FP-4, 117
Ramanath, G.: TS1-1-6, 69
Ramirez, G.: D2-1-7, 130; GP-4, 122
Ramírez, G.: B4-1-11, 42; B5-2-10, **65**; B6-1-9, 76; BP-37, **102**
Ramm, J.: B1-1-2, 2; B6-2-4, **87**; E1-3-4, 55; E2-1-2, 77
Rams, J.: E3-1/G2-1-5, 17
Randall, N.X.: E1-3-4, 55
Randeniya, L.: F1-1-7, 20
Rao, K. R. M.: B3-1-2, **128**
Rao, M.: G1-1-2, **57**
Rastgoo Lahrood, A.: TSP-4, 126
Raumann, L.: B7-2-1, 42
Read, D.: E2-3-9, 132
Rebello de Figueiredo, M.: EP-13, **114**
Rebholz, C.: BP-20, 100; TS3-1-8, 82; TS3-1-9, 82
Rechberger, J.: E4-2/G4-2-7, **80**
Reed, A.N.: TS1-1-3, 69
Reedy, E.D.: F6-1-1, 7
Reeves, R.: TS3-1-5, 81
Reeves, R.J.: C4-1-1, 30
Reichelt, R.: A1-1-3, 50
Reichert, J.: C4-2/F4-2-6, 12
Reilly, G.: D2-1-6, 130

Reisse, G.: B1-2-3, 9
 Remmert, J.: TS4-1-6, 59; TS4-1-9, 59
 Rémy, L.: A1-2-8, 62; A2-1-9, 24
 Renault, P.: AP-2, 94; AP-4, 94; E2-3-5, 131
 Resch, K.: B4-2-8, 52
 Reshetnyak, E.: B1-3-8, 25
 Restrepo, J.S.: B4-2-3, **51**
 Rezek, J.: F2-2-3, 46
 Rhee, S.W.: CP-13, **106**
 Ria Jaafar, T.: EP-26, 116
 Ricci, C.: GP-5, 122
 Richter, E.: B3-1-2, 128
 Rinke, M.: FP-11, 118
 Ritter, M.: TS2-1-4, **8**
 Rivera, M.: B4-1-11, 42; B6-1-9, 76; DP-5, 110
 Roberts, A.: TS2-1-5, 8
 Rocha, L.A.: D3-1-1, **15**
 Rockett, A.: B1-2-5, 9
 Rodil, S.E.: B4-1-11, 42; B5-2-10, 65; B6-1-9, **76**;
 BP-37, 102; D2-1-3, 129; D2-1-7, 130; DP-5,
 110; FP-6, **117**; GP-4, 122
 Rodrigo, J.: E1-3-11, 56
 Rodrigo, P.: E3-1/G2-1-5, 17
 Rodriguez, M.: TS3-1-5, 81
 Rodriguez, R.J.: E3-1/G2-1-2, 17
 Rodriguez, R.J.: E1-3-11, 56
 Rodriguez-Castro, G.A.: E1-2-12, **34**; E2-2-6, 91;
 E2-2-7, 91
 Rodriguez-Santiago, V.: G3-1-1, 67
 Rogachev, TS3-1-10, 82
 Rogström, L.: B4-1-6, 41
 Rohrer, S.: B2-1-3, **73**
 Rommel, M.: B2-1-1, 73
 Rossetto, A.: DP-16, 111
 Rossi, C.: TS3-1-1, **81**
 Rost, D.: B1-2-3, 9
 Roth, J.: A2-2-9, 40
 Roussel, R.: A1-3-3, 71
 Roy, A.K.: F3-1-6, 133; TS1-1-2, 68; TS1-1-3, 69
 Roy, S.: D1-1-1, 5; E2-3-2, 131
 Royhman, D.: D3-1-5, **16**
 Rozanski, P.: FP-23, 120
 Rudigier, H.: B6-1-5, 75; B6-2-4, 87; G6-1-5, 134
 Rudolph, M.: GP-13, 124
 Ruiz de Gopegui, U.: B1-3-4, 25; B3-1-1, 128
 Rullyani, C.: B5-2-7, **65**
 Ryaboy, A.: G3-1-8, 68

— S —

Sabitzer, C.: B1-2-2, 9
 Sabri, L.: E3-1/G2-1-11, 18; E3-1/G2-1-12, 18
 Sachdev, A.: E2-1-8, 78
 Sachitanand, R.: A3-1/F8-1-9, 72
 Sachkova: TS3-1-10, 82
 Saeed, Y.: B7-2-10, 44
 Sakamoto, Y.: B1-3-3, 24; B2-2-6, 85; BP-14, 99;
 E1-2-5, 34; EP-18, **114**; EP-23, 115; GP-8, 123
 Sakurai, T.: C2-2/F4-2-7, 12; GP-1, **122**
 Salas, O.: A1-1-3, 50; A1-1-5, **50**
 Sallot, P.: A1-2-8, **62**
 Samuelsson, M.: B1-2-7, 10
 Sánchez, J.: A1-3-5, 71
 Sánchez-López, J.C.: E1-3-3, **55**
 Sandström, P.: C5-1/F7-1-10, 89
 Sandu, C.S.: BP-43, 104
 Sangiovanni, D.: B7-1-10, **28**; B7-1-8, 28
 Sanjines, R.: B4-1-11, **42**; BP-43, **104**
 Sarakinos, K.: B7-1-1, **27**; F2-1-5, 35
 Sardela, M.: B1-2-5, 9
 Sarhammar, E.: E1-2-4, **33**
 Sarkar, A.: G1-1-8, **58**
 Sartwell, B.D.: G1-1-9, **58**
 Sasaki, T.: C4-1-6, 31; F2-1-6, **36**; F2-2-8, 47
 Sato, H.: E2-2-3, 90
 Satomoto, S.: B2-1-11, 74
 Satou, K.: FP-19, 120
 Scano, A.: E1-3-11, 56
 Schaaf, P.: TS2-2-1, **20**
 Schäfer, L.: B2-1-8, **74**
 Schalk, N.: B4-1-5, **41**

Scharf, T.: E1-2-6, 34; E1-2-9, 34
 Schaufler: PDP-3, 125
 Schaufler, J.: PDP-4, 125
 Scheerer, H.: TS1-1-1, 68
 Scheibe, H.-J.: B1-2-9, 10; B6-1-10, **76**
 Schiffers, C.: B2-2-4, 85; G6-1-3, 134
 Schlögl, M.: B5-1-7, **54**
 Schmauder, S.: PD-1-2, 92
 Schmid, C.: PDP-3, **125**; PDP-4, 125
 Schmidt, J.: B2-1-6, 73
 Schmidt, T.: B1-2-9, 10
 Schmied, S.: B6-1-4, 75
 Schnabel, V.: TS2-2-3, 21
 Schneider, J.: AP-8, 95; B4-1-9, 42; B6-2-5, **87**;
 B7-2-1, 42; F3-1-1, 132
 Schoeppner, R.L.: E2-1-1, 77
 Scholtalbers, M.: F2-1-4, 35
 Scholz, S.: B2-1-6, 73
 Schreiber, G.: C2-3/F4-3-8, 30
 Schuh, C.: B2-1-5, 73
 Schulz, C.: C4-1-12, **33**
 Schulz, S.: C5-1/F7-1-6, **89**
 Schulz-von der Gathen, V.: F2-2-1, 46
 Schunk, U.: B2-1-1, 73; GP-11, 124
 Schuster, F.: B2-2-3, 85; F2-1-12, **37**
 Schütze, M.: A1-1-4, 50; A1-3-4, 71
 Schwarzer, N.: B1-2-6, 10; E1-3-4, 55; E2-1-2, 77;
 E2-1-9, **78**; E2-3-7, 132; E3-1/G2-1-1, 17; EP-
 1, 112; EP-5, 113
 Schwingschlogl, U.: B7-2-10, 44; TSP-1, 126
 Scragg, J.J.: C2-2/F4-2-9, 12
 Sebastiani, M.: EP-16, 114; TS2-2-2, **20**
 Seemann, K.: F1-1-12, 20
 Seifert, H.: FP-11, 118
 Semmler, E.: G6-1-10, 135
 Sen, F.G.: E3-1/G2-1-13, **18**
 Seo, H.: GP-10, **124**
 Seong, T.Y.: F3-1-5, 133; FP-25, 121; FP-26, 121
 Sequeda, F.: B4-2-3, 51
 Setsuhara, Yuichi.: CP-25, 108
 Shamberger, P.: TS1-1-9, 70
 Shang, L.: AP-8, 95
 Shao, T.M.: EP-20, 115
 Shashkov, P.: B4-3-10, 64
 Shemet, V.: A1-2-9, 62
 Sheng, J.: B4-2-4, 51
 Shenogin, S.V.: TS1-1-2, 68; TS1-1-3, **69**; TS1-1-
 6, 69
 Shetty, A.: TSP-9, 127
 Sheu, J.K.: TSP-3, 126
 Sheveiko, A.N.: B4-1-3, 41
 Sheveyko, A.: B5-1-12, 55
 Shibata, H.: C2-2/F4-2-7, 12
 Shibata, T.: C4-1-6, 31
 Shieh, T.M.: DP-2, 109
 Shieu, F.S.: BP-23, 100
 Shih, C.C.: CP-2, 104
 Shih, H.C.: B2-1-12, 75
 Shih, S.-J.: CP-12, 106
 Shih, Y.T.: A3-2/F8-2-1, **84**
 Shimomura, H.S.: B2-2-6, **85**
 Shine, J.W.: BP-4, **97**
 Shirakata, S.: C2-2/F4-2-4, 12; FP-2, 116
 Shiroya, T.S.: B1-3-3, **24**
 Shishido, N.: E2-2-3, 90
 Shiue, S.T.: B2-2-9, 86; CP-27, 108
 Shiyu, L.: E2-2-1, 90
 Shkodich, N.: TS3-1-10, **82**
 Shockley, J.M.: E3-2/G2-2-1, **44**
 Shtansky, D.V.: AP-9, 95; B4-1-3, **41**; B5-1-12, 55
 Siddle, D.: E4-1/G4-1-1, 66
 Sierros, K.: F6-1-5, 7; FP-15, **119**
 Sik, H.: AP-4, 94
 Silva Junior, L.: B2-2-5, 85
 Silva, C.: EP-2, 112
 Silva-Bermudez, P.: D2-1-3, **129**; DP-5, **110**; FP-6,
 117
 Singh, N.: B7-2-10, **44**; TSP-1, **126**
 Singh, S.: A1-1-9, 51; B4-1-8, 42

Singheiser, L.: A1-2-2, 61; A1-2-9, 62
 Siow, P.C.: EP-26, 116
 Siozios, A.: B1-3-11, **26**; CP-29, **108**
 Sista, V.: E3-2/G2-2-7, 45; G5-1-11, **49**; G5-1-12,
 49
 Sivakumar, G.: E2-2-2, 90
 Sivakumaran, S.: BP-28, **101**; G1-1-11, **58**
 Skarmoutsou, A.: BP-12, 98
 Slomski, E.M.: TS1-1-1, **68**
 Smith, T.S.: TSP-8, 127
 Snyders, R.: F2-2-11, 47
 Soares, M.: G5-1-13, 49
 Soares, P.: DP-15, 111; DP-16, 111; DP-7, **110**;
 G5-1-13, 49
 Sobiech, M.: E2-1-2, **77**
 Solis-Casados, D.: B5-2-10, 65; BP-19, 99
 Song, H.-P.: C2-2/F4-2-4, 12; C4-1-5, **31**; C4-1-6,
 31
 Sopcisak, J.: TS4-1-12, 60
 Sortais, P.: PD-1-1, **92**
 Soukup, Z.: EP-4, 112
 Souza, G.B.: DP-15, 111
 Souza, P.: G5-1-13, 49
 Souza, R.M.: A1-1-5, 50; E3-1/G2-1-8, 18; E3-
 1/G2-1-9, 18; G5-1-13, 49
 Speaks, D.: C4-2/F4-2-6, 12
 Spielmann, J.: C3-1-10, **14**
 Spitaler, J.: B4-1-1, 40
 Spitsberg, I.: E4-1/G4-1-1, **66**
 Sproul, W.: B5-2-1, 64; F2-1-10, 36; F2-2-4, **46**
 Sprute, T.: B4-2-11, **53**
 Stamm, W.: A2-2-6, 39
 Stearn, R.: E2-2-1, 90; E3-2/G2-2-4, 44; TS2-2-3,
 21
 Steidl, P.: B5-1-10, 55
 Stein, S.: E4-2/G4-2-11, 80
 Steneteg, P.: B7-2-2, **43**
 Stephan, P.: TS1-1-1, 68
 Steves, S.: GP-13, **124**; TS2-2-7, 21
 Stiefel, M.: DP-12, 111
 Stiller, K.: A1-1-1, **50**; TS2-1-3, 8
 Stock, H.-R.: E4-1/G4-1-5, 66
 Stone, S.: E1-3-5, 56
 Stoner, B.: D1-1-6, 5
 Stoyanov, P.: E1-2-3, 33
 Stranak, V.: F2-2-6, **47**
 Strauss, H.: E1-2-3, 33; E3-2/G2-2-1, 44
 Strel'nitskij, V.: B1-3-8, 25
 Strunk, K.: TS4-1-12, 60
 Stubenrauch, M.: TS2-2-1, 20
 Stüber, M.: FP-11, 118; F1-1-12, 20
 Stupka, P.: B1-1-1, 12
 Su, C.: E2-3-11, 132
 Su, J.F.: E4-1/G4-1-7, **67**
 Su, Y.T.: CP-22, **107**
 Sugita, Y.: EP-6, 113
 Sugiura, I.: EP-23, **115**
 Sukotjo, C.: D3-1-5, 16
 Sun, H.: A3-2/F8-2-6, **84**
 Sun, X.W.: C1-1-5, **3**
 Sun, Y.: B5-2-11, **66**
 Sun, Y.S.: D2-1-8, **131**; DP-11, **111**
 Sun, Z.: C4-1-11, 32; CP-4, 104
 Sundberg, J.: E1-2-4, 33
 Suneson, M.: A1-1-10, 51
 Sung, JamesC.: B2-1-9, 74
 Suri, A.K.: EP-17, 114
 Surman, D.: D1-1-6, 5; TS2-1-5, **8**
 Suzuki, T.: BP-24, 100; D2-1-5, 130; DP-4, 109;
 GP-1, 122
 Suzuki, T.S.: E2-2-3, 90
 Svensson, J.-E.: A1-2-5, 61; A3-1/F8-1-9, 72
 Svoboda, J.: B7-1-5, 27
 Swadzba, L.S.: AP-16, 96; AP-17, 96
 Swadzba, R.: A1-2-1, **61**; AP-16, 96; AP-17, **96**
 Syu, Y.E.: C2-3/F4-3-3, 29; F1-1-5, 19; GP-3, 122;
 TS2-2-10, **22**; TS2-2-12, 22; TSP-2, **126**
 Szala, C.: BP-38, 103
 Sze, S.: FP-12, 118

Szeremley, D.: G3-1-7, 68
 Szesz, E.M.S.: DP-15, 111
 Szpunar, J.A.: B5-2-4, 64
 Szyszka, B.: C4-1-12, 33; C4-1-3, **31**

— T —

Taga, Y.: GP-12, **124**
 Tagliaferri, V.: GP-14, 124
 Tahara, M.: B2-1-11, 74
 Tai, Y.H.: C2-3/F4-3-1, 29
 Takahashi, J.: EP-21, **115**; G1-1-7, **58**
 Takahashi, M.: BP-24, 100
 Takahashi, T.: BP-24, 100; G6-1-7, **134**
 Takashima, M.: B3-1-8, **129**
 Tamura, K.: TS1-1-11, 70
 Tanaka, H.: GP-8, 123
 Tanaka, I.: E1-2-5, **34**
 Tang, Y.: B2-2-8, 86; B4-3-7, 63; D2-1-4, 130
 Tang, Z.: A1-1-6, 50
 Tanifuji, S.: B1-2-1, **9**; E4-2/G4-2-9, 80
 Tashiro, H.: G5-1-5, **48**; GP-7, **123**
 Tasnádi, F.: B7-2-8, **43**; B7-2-9, 44; BP-31, **101**;
 BP-32, 102; C5-1/F7-1-4, 88; C5-1/F7-1-8, 89
 Tatat, M.: AP-2, 94
 Taylor, T.A.: A2-2-1, 39
 Teichert, C.: B6-2-10, 88; EP-13, 114; TS4-1-13, **60**
 Tejero, M.: A1-3-5, 71
 Teng, L.F.: CP-9, 106
 Terada, N.: C2-2/F4-2-7, 12
 Terasako, T.: C2-2/F4-2-4, **12**; FP-2, **116**
 Terryn, H.: E2-1-6, 78
 Teule-Gay, L.: B6-1-6, 76
 Teyssandier, F.: B4-2-7, 52
 Thangaraj, R.: FP-16, 119
 Theiss, S.: B1-2-8, 10; B4-1-9, 42; B6-2-9, 88; F2-1-8, **36**
 Thiaudière, D.: E2-3-5, 131
 Tholander, C.: BP-32, **102**; C5-1/F7-1-4, **88**; C5-1/F7-1-8, 89
 Thomas, J.: B6-2-4, 87
 Thorwarth, G.: DP-12, 111
 Thorwarth, K.: DP-12, **111**
 Thuvander, M.: TS2-1-3, 8
 Tian, X.B.: F2-1-11, **36**; GP-9, **123**
 Tietema, R.: E3-2/G2-2-10, 45; F2-2-8, 47; G6-1-4, 134
 Tillmann, W.: B4-2-11, 53; E4-2/G4-2-1, 79
 Timur, S.: E3-2/G2-2-7, 45; G5-1-11, 49; G5-1-12, 49; G5-1-3, 48
 Ting, J.-M.: PD-1-3, **92**
 to Baben, M.: AP-8, **95**; B4-1-9, 42; B6-2-5, 87; B7-2-1, **42**
 Tolpygo, V.K.: A2-1-11, 24
 Tong, C.J.: EP-8, 113
 Tong, C.Y.: B5-1-1, **53**; EP-15, 114
 Tonisch, K.: TS2-2-1, 20
 Torres, B.: E3-1/G2-1-5, 17
 Torres, R.: A1-1-5, 50; DP-7, 110; G5-1-13, **49**
 Torres-Hernández, A.: E2-2-6, 91; E2-2-7, 91
 Totik, Y.: B4-3-5, 63; DP-10, 110; DP-17, 112; E2-1-7, 78
 Trava-Airoldi, V.: B2-2-5, **85**; EP-2, **112**
 Tremmel, S.: B4-3-9, 63; E3-1/G2-1-6, 17; GP-2, 122
 Tricoteaux, A.: F2-1-12, 37
 Troßmann, T.: B1-2-8, 10; B6-2-9, 88; TS1-1-1, 68
 Trovalusci, F.: GP-14, **124**
 Trube, J.: B2-1-8, 74
 Tsai, C.H.: BP-35, 102
 Tsai, C.Y.: BP-39, **103**
 Tsai, J.Y.: C2-1/F4-1-1, **4**
 Tsai, M.J.: FP-12, 118
 Tsai, M.T.: DP-1, 109
 Tsai, M.Y.: C5-1/F7-1-11, **90**; C5-1/F7-1-9, 89; CP-11, 106; FP-17, **119**
 Tsai, T.M.: F1-1-5, 19; TS2-2-12, **22**
 Tsai, W.F.: DP-18, 112
 Tsai, Z.Z.: C3-1-12, **14**

Tsay, C.Y.: C2-2/F4-2-3, **12**; CP-12, 106; F1-1-4, 19
 Tschiptschin, A.: BP-36, **102**
 Tseng, H.C.: C2-2/F4-2-12, **13**
 Tseng, H.Y.: CP-2, 104
 Tseng, T.C.: EP-15, **114**
 Tseng, W.T.: EP-8, 113
 Tsou, Y.: C2-3/F4-3-10, 30
 Turner, B.: TS1-1-7, 69
 Turner, G.C.: C4-1-1, 30

— U —

Uddin, N.: B1-3-5, 25
 Ueda, M.: A3-1/F8-1-7, **71**
 Ugras, M.: B1-3-5, 25; B1-3-9, 26
 Uhm, H.S.: CP-7, 105; CP-8, 105
 Ullbrand, J.: B4-1-6, 41
 Ulrich, S.: F1-1-12, **20**; FP-11, 118; PD-1-2, 92
 Unocic, K.: A1-2-3, 61
 Ürgen, M.: G5-1-6, **49**
 Ürgen, M.: E1-3-13, 57
 Uzun, E.: B1-3-5, 25; B1-3-9, 26

— V —

V, C.: FP-3, 116
 Vadchenko: TS3-1-10, 82
 Valderrama, B.: TSP-5, 126
 van Esch, P.: F3-1-7, 134
 van Gastel, R.: TS4-1-13, 60
 Van Sluytman, J.S.: A2-1-11, **24**
 Vanfleet, R.: F1-1-11, 20
 Varela, L.B.: BP-36, 102
 Vargas-García, J.R.: PD-1-4, 92
 Varshney, V.: TSP-8, 127
 Vasilev, K.: D2-1-1, **129**
 Vasilevskiy, M.: B6-2-3, 87
 Vasyliov, V.: B1-3-8, 25
 Venettaci, S.: G1-1-12, 59
 Veprek, S.: E2-2-5, **90**
 Veprek-Heijman, M.: E2-2-5, 90
 Verbrugge, M.: A3-2/F8-2-3, **84**
 Vesco, S.: G1-1-12, 59
 Vetter, J.: G6-1-6, **134**
 Vettier, C.: F3-1-7, 134
 Viana, A.: BP-13, 98
 Viana, C.: AP-15, 96
 Vidal-Sétif, M.H.: A2-2-3, 39
 Vieira, M.T.: E4-1/G4-1-6, 66
 Viernusel, B.: E3-1/G2-1-6, **17**; GP-2, **122**
 Vijayasai, A.: E2-2-2, 90; TS3-1-3, 81
 Vitelaru, C.: F2-2-2, 46
 Vlassak, J.: E2-3-3, **131**
 Vlcek, J.: AP-9, 95; B5-1-10, 55; F2-2-3, **46**
 Voevodin, A.: B4-2-8, 52; E1-3-5, 56; F3-1-6, 133; TS1-1-2, 68; TS1-1-3, 69; TS1-1-4, 69; TS1-1-7, 69; TS1-1-9, 70; TS4-1-6, **59**; TS4-1-9, 59; TSP-8, 127
 Vollenberg, W.: F3-1-7, 134
 von Keudell, A.: B3-1-5, 128; B3-1-7, 129; TSP-4, 126
 Vozniy, O.: F2-2-5, 46

— W —

Wagner, P.: BP-1, 96
 Waldhauser, W.: B6-2-10, 88
 Walter, C.: B4-1-1, 40; TS2-2-3, 21
 Walukiewicz, W.: C4-2/F4-2-6, 12
 Wan, C.H.: A3-1/F8-1-10, 72; A3-1/F8-1-11, **72**;
 A3-2/F8-2-5, 84
 Wang, A.N.: E2-2-8, **91**
 Wang, C.J.: AP-13, 96; B4-3-11, 64; C3-1-8, 14
 Wang, C.K.: C3-1-12, 14
 Wang, C.W.: A3-2/F8-2-2, **84**
 Wang, D.Y.: EP-3, 112
 Wang, H.: B5-1-11, 55; F1-1-8, **20**
 Wang, J.C.: TSP-6, 126
 Wang, M.J.: C3-1-7, 14
 Wang, S.: DP-18, 112
 Wang, S.C.: B2-1-9, 74; C3-1-12, 14
 Wang, Y.: A1-1-10, **51**; B1-3-12, **26**
 Wang, Y.T.: EP-8, 113; PDP-5, 125

Wang, Z.J.: AP-1, 94
 Wartzack, S.: B4-3-9, 63; E3-1/G2-1-6, 17; GP-2, 122
 Weaver, L.: A1-2-10, 62
 Webler, R.: PDP-4, 125
 Wei, C.: BP-27, 101
 Wei, R.: B5-1-4, 54; E1-3-8, **56**
 Wei, Y.H.: FP-13, **119**
 Weigand, M.: B2-2-4, 85
 Weigel, K.: B6-1-4, 75
 Weihnacht, V.: E1-2-11, **34**
 Weihs, T.: TS3-1-7, 81
 Weimar, U.: C4-1-3, 31
 Weirather, T.: B1-2-2, **9**
 Weisbecker, P.: B4-2-7, 52
 Weiß, R.: B1-2-8, **10**; B6-2-9, 88
 Weißenbacher, R.: B2-1-1, 73
 Weissmantel, S.: B1-2-3, **9**
 Welty, R. P.: G6-1-1, **134**
 Welzel, T.: C4-1-9, 32
 Wen, M.H.: C3-1-7, 14; C3-1-9, 14; CP-1, **104**
 Weng, J.C.: DP-2, **109**
 Werner, C.: D3-1-3, 15
 Wessels, K.: A2-2-4, **39**
 Wetzel, C.: D3-1-3, 15
 Widrig, B.: B6-2-4, 87; E1-3-4, 55; E2-1-2, 77
 Wilkins, P.: TS3-1-7, 81
 Wimmer, M.: D3-1-10, 16; D3-1-5, 16
 Wingqvist, G.: C5-1/F7-1-10, 89; C5-1/F7-1-8, 89
 Winkler, J.: C2-3/F4-3-8, 30
 Winter, J.: F2-2-1, 46
 Wirtz, T.: F2-2-5, 46
 Witala, B.W.: AP-16, **96**; AP-17, 96
 Wittorf, R.: E3-2/G2-2-11, 45
 Woll, K.: TS3-1-8, **82**
 Wong, M.: B5-2-11, 66; C1-1-3, 3
 Wong, P.: TS3-1-9, 82
 Woo, J.K.: CP-17, 107
 Woo, T.: A2-1-7, 23
 Wu, C. S.: EP-7, 113
 Wu, C.H.: A3-2/F8-2-1, 84; A3-2/F8-2-2, 84
 Wu, C.L.: C3-1-12, 14
 Wu, C.P.: DP-11, 111
 Wu, F.B.: AP-11, 95; BP-5, **97**
 Wu, J.B.: CP-2, **104**
 Wu, J.Y.: BP-40, 103
 Wu, M.H.: C2-3/F4-3-4, 29; FP-18, 119
 Wu, M.K.: C3-1-7, 14; C3-1-9, 14; CP-1, 104; CP-15, 106
 Wu, W.: A3-1/F8-1-10, 72; A3-2/F8-2-5, 84; C2-3/F4-3-10, **30**
 Wu, W.P.: PDP-1, 125
 Wu, Y.R.: C3-1-7, 14; C3-1-9, **14**; CP-1, 104
 Wu, Y.Y.: D2-1-9, 131
 Wu, Z.: F2-1-10, 36
 Wu, Z.Z.: F2-1-11, 36
 Wulff, H.: F2-2-6, 47

— X —

Xiao, P.: AP-6, 95
 Xiao, X.: A3-2/F8-2-3, 84; E2-1-8, 78
 Xing, Z.C.: D1-1-7, **5**
 Xu, F.: E4-2/G4-2-2, 79

— Y —

Yablinsky, C.: TSP-5, 126
 Yagi, M.: FP-2, 116
 Yamada, A.: C2-2/F4-2-7, 12
 Yamada-Takamura, Y.: F1-1-9, **20**
 Yamaguchi, M.: TS1-1-6, 69
 Yamamoto, K.: B1-2-1, 9; B4-3-3, 63; E4-2/G4-2-9, **80**; F2-1-3, 35; G1-1-5, 57; G6-1-7, 134
 Yamamoto, N.: C4-1-5, 31; C4-1-6, 31
 Yamamoto, T.: C2-2/F4-2-4, 12; C4-1-5, 31; C4-1-6, 31
 Yan, W.C.: FP-20, 120
 Yang, C.H.: DP-18, 112
 Yang, J.: E1-1-1, **6**
 Yang, J.B.: C2-2/F4-2-10, **13**
 Yang, K.H.: C2-3/F4-3-4, 29; FP-18, 119

Yang, L.: B2-2-8, 86	Yoshino, K.: C4-1-7, 32	Zhang, C.: B2-2-8, 86; BP-41, 103; D2-1-4, 130 ; E3-2/G2-2-3, 44
Yang, M.C.: C2-3/F4-3-4, 29; FP-18, 119	Young, N.: C4-1-3, 31	Zhang, L.L.: B2-2-8, 86; B4-3-7, 63
Yang, Q.: B2-2-8, 86 ; B4-3-7, 63; B5-1-4, 54; B5- 2-4, 64; D2-1-4, 130	Young, T.F.: F1-1-5, 19	Zhang, S.: B1-3-12, 26; F3-1-3, 133
Yang, S.Q.: GP-9, 123	Yu, G.P.: B4-3-6, 63; BP-10, 98; BP-11, 98; BP-4, 97; BP-40, 103; E2-2-8, 91	Zhang, X.: C1-1-7, 4
Yang, Y.H.: BP-34, 102	Yu, K.M.: C4-1-2, 31; C4-2/F4-2-6, 12	Zhang, Z.: C1-1-7, 4
Yang, Y.Y.: TSP-3, 126	Yukawa, S.: BP-29, 101	Zhao, S.: C4-2/F4-2-6, 12
Yang, Z.G.: BP-41, 103	— Z —	Zhou, K.: BP-27, 101
Yantchev, V.: C5-1/F7-1-1, 88	Zabeida, O.: F2-1-1, 35	Zhou, Z.R.: EP-20, 115
Yasui, K.: B2-1-11, 74 ; FP-19, 120	Zaidat, K.: B2-1-7, 74	Zhu, L.: B4-2-12, 53
Ye, J.: FP-11, 118	Zakharov, D.: TS4-1-6, 59; TS4-1-9, 59	Zhu, M.H.: B4-2-6, 52; EP-20, 115
Yeager, J.: F6-1-1, 7	Zaleski, E.: A2-2-5, 39	Zhu, P.: B5-1-11, 55
Yeh(Huang), F.S.: FP-12, 118	Zalnezhad, E.: BP-7, 97	Zhu, Y.: C4-2/F4-2-6, 12
Yeh, C.H.: D2-1-9, 131	Zandvliet, H.: TS4-1-13, 60	Zhu, Y.K.: C4-1-2, 31
Yeh, C.M.: DP-6, 110	Zbib, H.: E2-1-1, 77	Zhuk, N.: G1-1-6, 57
Yerokhin, A.: AP-3, 94; B4-3-10, 64; D2-1-6, 130; D3-1-9, 16; G3-1-6, 68	Zeman, P.: B4-1-2, 40	Ziebert, C.: FP-11, 118; PD-1-2, 92
Yeung, W.: D2-1-6, 130	Zemlyanov, D.: TS4-1-6, 59; TS4-1-9, 59	Zoch, H-W.: E4-1/G4-1-5, 66
Yildiz: DP-17, 112	Zeng, Q.Z.: G5-1-11, 49	Zukauskaite, A.: C5-1/F7-1-10, 89; C5-1/F7-1-8, 89
Yoon, K.H.: CP-30, 108	Zeng, X.T.: B5-1-9, 54	
	Zenker, R.: B6-1-4, 75	

NOTES

R. F. Bunshah Award Laureates

2007: Wolf-Dieter Munz, SHU, UK, and Systec SVS, Germany

2008: Steve Rossnagel, IBM, USA

2009: Ivan Petrov, University of Illinois, USA

2010: Helmut Holleck, Karlsruhe Institute of Technology, Germany

2011: Stan Veprek, Technical University of Munich, Germany

2012: Sture Hogmark, Uppsala University, Sweden

Protocol for the R. F. Bunshah Award and ICMCTF Lecture

Purpose

This Award is intended to recognize outstanding research or technological innovation in the areas of interest to the Advanced Surface Engineering Division (ASED) of the AVS, with emphasis in the fields of surface engineering, thin films, and related topics.

Eligibility

The nominee shall have made pioneering contributions to the science or technology of surface engineering, thin films, or related fields of interest to ASED. The Award shall be granted without further restriction except that the current ICMCTF General and Program Chairs and current members of the ASED Executive and Awards Committees are not eligible.

Nomination Procedure

A nomination may be made by anyone qualified to evaluate, highlight, and validate the nominee's accomplishments. Any individual may submit one nominating or seconding letter for the award in any given year. The nomination packages **MUST** include the following.

Nomination Letter: The letter nominating an individual for an award must describe the work for which the award is proposed and indicate the role the work has played in solving particular scientific or technological problems. The significance of these problems and the impact of the nominee's accomplishments in the field should be discussed. If the work was performed in collaboration with others, the contributions of the nominee should be clearly stated. A proposed citation, a one-sentence synopsis of the reason for selecting the nominee, and a list of individuals sending supporting letters, must also be included. The nominating letter should not exceed two pages in length, but should be as detailed as possible to allow the Award Committee to evaluate the nominee's contributions.

Supporting Letters: A minimum of two and a maximum of five supporting letters must be arranged by the nominator. Typically, the letters should not exceed one page. Their main purpose is to endorse the nomination and to provide additional evidence of the nominee's accomplishments. The supporting letters should be written by individuals at institutions other than that of the nominee.

Description of Research Highlights: A two-page summary of research accomplishments citing key papers and patents must be included. The purpose of the material is to document the scope of a nominee's technical career, placing in context the specific work being nominated for the award.

Biographical Materials: A Curriculum Vitae or biographical sketch of the nominee and a list of publications and patents must be submitted.

Nominations remain active for three years.

Nature of the Award:

The award consists of a \$1500 cash award, an engraved statuette stating the nature of the award, and an honorary lectureship at the ICMCTF conference at which the award is presented. This award is conferred annually, subject to availability of suitable candidates. The Award Recipient shall receive complimentary meeting registration, travel expenses up to \$1500, and up to six nights lodging at the Town and Country Hotel.

Nomination Submission and Deadline: October 1, 2012

All nomination materials must be compiled by the nominator and submitted as one package. The **complete** nomination package is to be sent **electronically** to the current Chair of the ASED Awards Committee (asedawards@avs.org) such that it is received by **October 1, 2012**. Late or incomplete application packages will not be evaluated.

ASED Awards website:

<http://www2.avs.org/divisions/ased/>

Protocol for the ICMCTF Graduate Student Awards

Purpose

These Awards are intended to honor and encourage outstanding graduate students in fields of interest to the Advanced Surface Engineering Division (ASED) of the AVS. ASED seeks to recognize students of exceptional ability who show promise for significant future achievement in ASED-related fields.

Eligibility

The nominee must be:

- a graduate student in science or engineering who is in good standing at a University with a recognized graduate degree program
- the presenting author of an oral presentation at the annual ICMCTF conference.

Nominees who receive their final research degree after the ICMCTF Abstract Submission deadline are still eligible for that year. However, previous Graduate Student Award winners are ineligible.

Nomination Procedure

The Student's Advisor must submit the following items to the current Chair of the ASED Awards Committee by the **Abstract Submission and Nomination Deadline, October 1, 2012** for the upcoming annual ICMCTF Conference (late or incomplete applications will not be evaluated):

- a completed application form can be downloaded from the ASED website: <http://www2.avs.org/divisions/ased/>
- one copy of the abstract that has been submitted separately to the ICMCTF Conference
- a two-page description of research associated with the abstract to be considered for the award, including a clear, concise description of the:
 - aim of the work and its relationship to the status of the field
 - a summary of the applicant's specific contributions and how they demonstrate exceptional ability and future promise
 - a summary of significant results of the work and how they relate to the specific research area
 - a list of any publications authored by the applicant that are relevant to this research.
- a resume which includes a list of publications with complete citations; a list of fellowships, scholarships, and/or other honors received; a list of past employment with dates; a list of technical/professional organizations, including AVS, in which you are a member; other activities or relevant information
- an Advisor's Student Evaluation Form completed by the student's advisor; please download the form from the ASED website: <http://www2.avs.org/divisions/ased/>
- a recommendation letter from the student's advisor(s).

Selection Process:

Graduate Student Award Applications are accepted from graduate students who authored or co-authored a submitted abstract that is accepted for the current ICMCTF Conference. Applications are reviewed by the ASED Awards Committee and up to three finalists are selected. At the ICMCTF Conference, the finalists will present oral presentations which will be scheduled in an appropriate symposium on Monday, Tuesday, or Wednesday of the Conference week. The Awards Committee will meet and have discussions with the finalists. The committee will attend

their presentations in order to evaluate for the Gold, Silver, and Bronze ASED Graduate Student Awards based upon: (1) the quality of their application materials and (2) the quality and professionalism of their presentation and discussion.

Selection Criteria:

In the selection of finalists and award recipients, the judges look for evidence of:

- Excellence in scholarly research, including
 - thoroughness of the applicant's work
 - originality and independence of the applicant's contributions
 - depth of understanding of the research topic, the methodologies used, and the relationship of the results to the specific research area and the broader field
 - scholarship and ingenuity shown by the student in attacking the research project
- Promise for future substantial achievement in research fields of interest to ASED.

Nature of the Award:

The finalists receive Gold, Silver, or Bronze ASED Graduate Student Awards, a cash prize, and a certificate. In addition, they also receive travel support of up to \$500 to attend the ICMCTF conference, complimentary meeting registration, and up to six nights lodging at the Town and Country Hotel. The Awards are presented at the ICMCTF Conference and announced in the *AVS Newsletter* and on the ASED website. The cash prizes consist of \$400, \$300, and \$250 for the Gold, Silver, and Bronze recipients.

Nomination Submission and Deadline: October 1, 2012

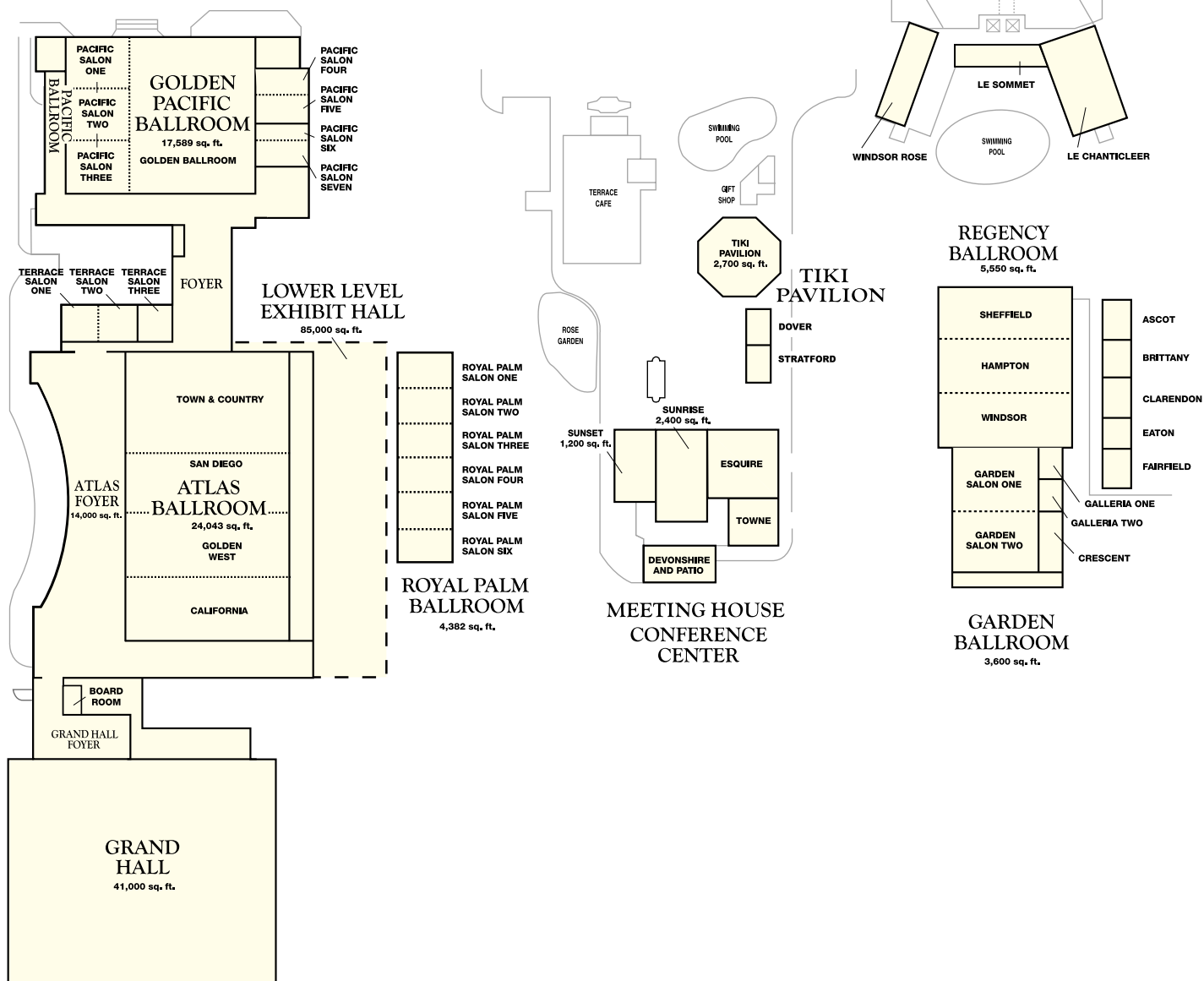
All nomination materials must be compiled by the nominee's advisor and submitted as one package. The **complete** nomination package is to be sent **electronically** to the current Chair of the ASED Awards Committee (asedawards@avs.org) such that it is received by the ICMCTF Abstract Submission Deadline, October 1, 2012. Late or incomplete applications will not be evaluated.

ASED Awards website:

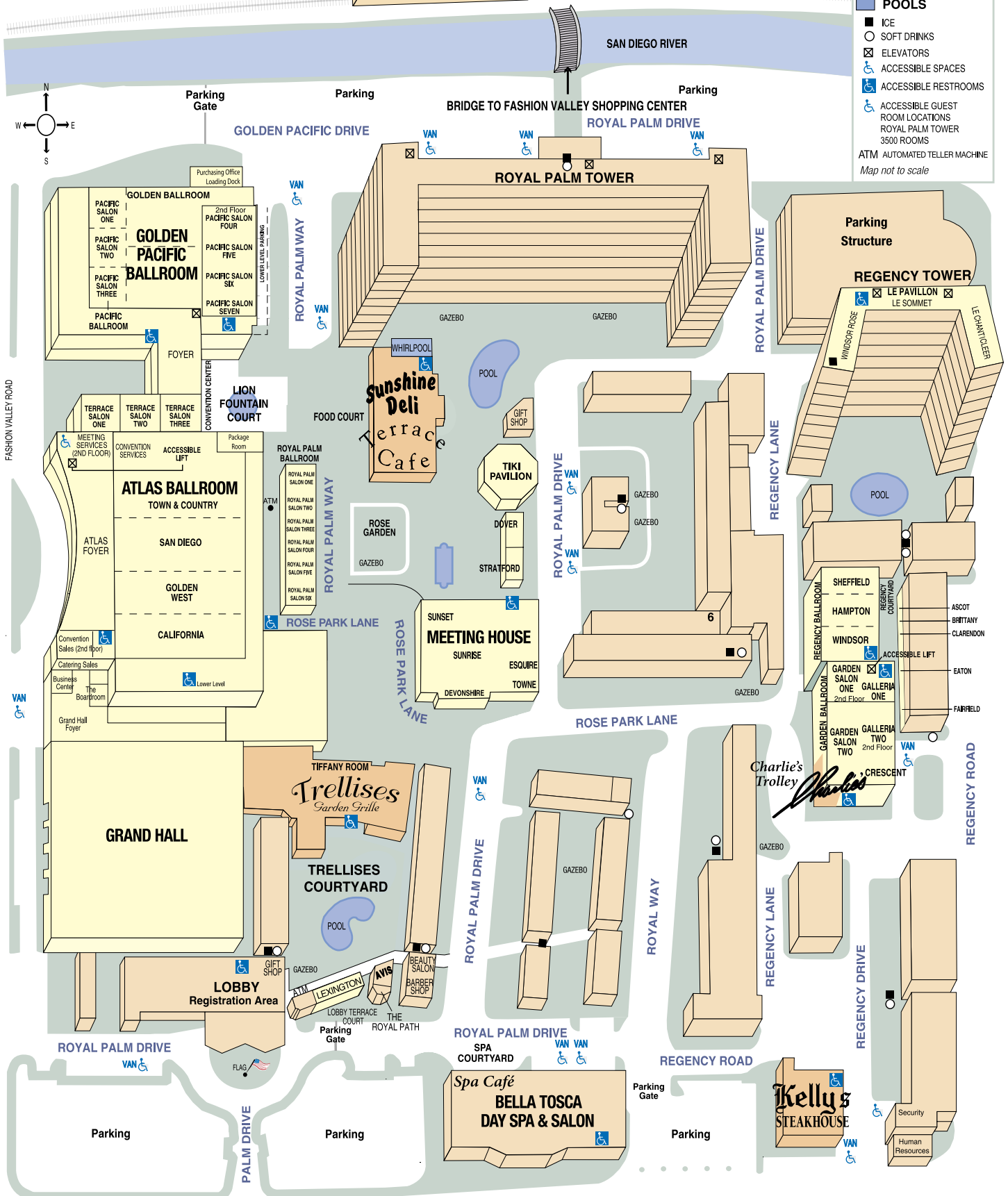
<http://www2.avs.org/divisions/ased/>

NOTES

NOTES



- RESTAURANTS
 - MEETING ROOMS
 - GUESTROOMS
 - POOLS
 - ICE
 - SOFT DRINKS
 - ELEVATORS
 - ACCESSIBLE SPACES
 - ACCESSIBLE RESTROOMS
 - ACCESSIBLE GUEST ROOM LOCATIONS
 - ROYAL PALM TOWER 3500 ROOMS
 - ATM AUTOMATED TELLER MACHINE
- Map not to scale





R.F. Bunshah Award and ICMCTF Lecture and the ICMCTF Graduate Student Awards

You are invited to submit nominations for the prestigious ASED Awards to be presented at the 2013 ICMCTF. The Awards were established to recognize outstanding research and/or technical innovation and to honor exceptional graduate students.

Deadlines: October 1, 2012

Award protocols and nomination procedures are available at:

<http://www2.avs.org/divisions/ASED/>

MARK YOUR CALENDAR FOR ICMCTF 2013!

**International Conference on Metallurgical
Coatings and Thin Films (ICMCTF)**

**April 29 – May 3, 2013
Town & Country Hotel
San Diego, California, USA**

**Sponsored by:
Advanced Surface Engineering Division of AVS**



For Additional Information, Contact:

General Chair 2013:

Paul Mayrhofer
Montanuniversitaet Leoben
Dept. of Physical Metallurgy & Materials Testing
Franz Josef Strasse 18
A- 8700 Leoben, Austria
Ph: +43-384-2402-4211, Fax: +43-384-2402-4202
paul.mayrhofer@unileoben.ac.at



Program Chair 2013:

Yip-Wah Chung
Dept. of Materials Science & Engineering
Northwestern University
2220 N. Campus Drive
Evanston, IL. 60208-3108, USA
Ph: 847-491-3112, Fax: 847-491-7820
ywchung@northwestern.edu

Web Address:

<http://www2.avs.org/conferences/icmctf>

ICMCTF Future Dates:

2014: April 28 – May 2, 2014
2015: April 20 – 24, 2015

2013 Deadlines:

ABSTRACT SUBMISSION:
Oct. 1, 2012

AWARD NOMINATIONS:
Oct. 1, 2012

MANUSCRIPT SUBMISSION:
March 1, 2013

EARLY PRE - REGISTRATION:
March 23, 2013

[illegible]

Now Invent.™

**AMERICAN
ELEMENTS**®

The World's Manufacturer of Engineered & Advanced Materials

photovoltaics

Nd:YAG

catalog: americanelements.com

© 2001-2011. American Elements is a U.S. Registered Trademark.

